UNCLASSIFIED

AD NUMBER

AD822827

NEW LIMITATION CHANGE

TO

Approved for public release, distribution unlimited

FROM

Distribution authorized to U.S. Gov't. agencies and their contractors; Administrative/Operational Use; Oct 1967. Other requests shall be referred to Aero Propulsion Laboratory, Attn: APFL, Wright-Patterson AFB, OH 45433.

AUTHORITY

AFAPL ltr, 12 Apr 1972

THIS PAGE IS UNCLASSIFIED

AFAPL-TR-67-114
Part I

AD822827

VAPORIZING AND ENDOTHERMIC FUELS FOR ADVANCED ENGINE APPLICATION

Part I. Studies of Thermal and Catalytic Reactions, Thermal Stabilities, and Combustion Properties of Hydrocarbon Fuels

A.C. Nixon, G.H. Ackerman, L.E. Faith, R.D. Hawthorn, H.T. Henderson, A.W. Ritchie, L.B. Ryland

Shell Development Company,
A Division of Shell Oil Company

TECHNICAL REPORT AFAPL-TR-67-114, Part I

October 1967

STATEMENT #2 UNCLASSIFIED

This document is subject to special export controls and each transmittal to foreign governments or foreign nationals may be made only with prior approval of Aero Propulsion Lab, attn: APFL, W-P AFB, Ohio 45433

DDC
RECEIVED
NOV 24 1967
C

Aero Propulsion Laboratory
Air Force Systems Command
Wright-Patterson Air Force Base, Ohio

BEST

AVAILABLE

COPY

NOTICES

When Government drawings, specifications, or other data are used for any purpose other than in connection with a definitely related Government procurement operation, the United States Government thereby incurs no responsibility nor any obligation whatsoever; and the fact that the Government may have formulated, furnished, or in any way supplied the said drawings, specifications, or other data, is not to be regarded by implication or otherwise as in any manner licensing the holder or any other person or corporation, or conveying any rights or permission to manufacture, use, or sell any patented invention that may in any way be related thereto.

Copies of this report should not be returned to the Research and Technology Division unless return is required by security considerations, contractual obligations, or notice on a specific document.

FOREWORD

This report was prepared by Shell Development Company, Emeryville, California, under U.S. Air Force Contract No. AF 33(615)-3789. The contract was initiated under Project No. 3048, Task No. 304801. The work was administered under the direction of the AF Propulsion Laboratory, Mr. H. L. Lander, Project Engineer, AFPL.

This report covers work for June 1966 to June 1967.

A. C. Nixon was principal investigator and project supervisor for Shell Development Company. The professional staff participating in the investigation was comprised of: G. H. Ackerman, L. E. Faith, R. D. Hawthorn, H. T. Henderson, A. W. Ritchie, and L. B. Ryland.

This report was submitted by the authors 1 August, 1967.

This report has been reviewed and is approved.

Arthur V. Churchill

ARTHUR V. CHURCHILL, Chief
Fuels, Lubrication and Hazards Branch
Support Technology Division

ABSTRACT

Investigation of the feasibility of using endothermic reactions to augment the latent and sensible heat of fuels for cooling engines operating under a high mach number regime is continuing. Studies in the literature continue to maintain the desirability and feasibility of producing vehicles with hypersonic flight speeds and suggest some areas of advantage of hydrocarbons.

Laboratory studies on the dehydrogenation over Pt/Al_2O_3 of a number of mixtures of naphthenes have been made including methyl-Decalin and dicyclohexyl as well as the pure components, with additional studies on Decalin.

About 220 dehydrogenation catalysts have been prepared using a variety of metals and supports. Most of these have been tested in our micro-scale reactor and a number of these have shown activity somewhat superior to our standard Pt/Al_2O_3 catalyst in MCH dehydrogenation. The results have been confirmed in our bench scale equipment. Attempts are being made to develop vapor (or dispersed) phase catalysts for the dehydrogenation of naphthenes; a number of compounds have shown some indications of activity when tested with MCH.

Propane and an advanced jet fuel were tested as possible heat sink fuels in our fuel system simulation test reactor under thermal cracking conditions. A maximum heat sink of 1300 Btu/lb was achieved at space velocities to 400 and pressures to 900 psi with maximum conversions of about 60%. The effect of increasing tube size from 3/8 to 3/4 inch has been checked using the $MCH-Pt/Al_2O_3$ system. Conversions of up to 95% at 80 LHSV were obtained with anticipated heat sinks.

Our packed bed reactor program included herein, has been rewritten and simplified resulting in a considerable saving in both human and computer time. With this program we have been able to extrapolate analytically to a variety of configurations extending far beyond fuel flow and heat fluxes presently possible in the FSSTR. A short high heat flux section has been designed for this unit to allow experimental verification of calculations. Operation at 900 psi pressure, LHSV of 1600, conversion of 65% at a heat flux of 3.6×10^5 Btu/hr/sq ft was achieved with MCH over R-8 catalyst.

The thermal stability of MCH, Decalin and a naphthenic jet fuel were all critically, but uniquely, dependent on O_2 concentration in the region below about 10 ppm. A new apparatus for assessing thermal stability of endothermic type fuels was designed, constructed and brought into successful initial operation.

The ignition delay behavior of both ethane and ethylene was found to be considerably different from other hydrocarbons in the shock tube, the ignition delay reaching a minimum in the region of $E/R = 0.5$ with two different temperature coefficients which are dependent upon total reactives concentration. Additional data have also been obtained on normal dodecane, Decalin, methyl-Decalin, methane, tetramethylbutane and neopentane. The benefit of utilizing infrared detection for measuring ignition delays was

established. The essential identity of combustion of propane and toluene when premixed hot with hot air was determined in a small subsonic burner.

Included in this report are: the physical properties of the MCH system to 1600°F and 5000 psi; a bibliography of papers and reports of interest in this field; a computer program for simulating reactions in a packed bed; a summary table on the evaluation of candidate fuels.

TABLE OF CONTENTS

	PAGE
Introduction	1
Summary	4
Considerations Affecting Applications	9
Laboratory Reaction Studies	17
Monocyclic Naphthenes	18
Dehydrogenation of 1,2,4,5-Tetramethylcyclohexane	18
Catalyst Stability Tests With Methylcyclohexane	20
Bench-Scale Catalyst Evaluation Tests With Methylcyclohexane	27
Thermal Reaction of Methylcyclohexane Over Alumina	27
Thermal Reaction of Ethylcyclohexane	30
Dicyclic Naphthenes	38
Dicyclohexyl	38
Reaction Rates for Dehydrogenation of Dicyclohexyl and Phenylcyclohexane	38
Dehydrogenation Over UOP-R8 Catalyst	41
Decalin	45
Reaction Rates and Equilibrium Constants for Dehydrogenation of Decalin and Tetralin	45
Relative Stabilities of Laboratory Platinum on Alumina and UOP-R8 Catalysts	54
Dehydrogenation Over 1% Platinum on UOP-R8 Alumina: No Halogen	56
Extended Dehydrogenation Test With Laboratory Catalyst	62
Dehydrogenation of F-111 Decalin Over UOP-R8 Catalyst	62
Dehydrogenation and Isomerization of Decalin Isomers	65
Summary: Dehydrogenation of Decalin	73
1-Methyldecalin	73

TABLE OF CONTENTS (Contd)

PAGE

Effect of Pore Size on Catalyst Stabilities for the Dehydrogenation of Naphthenes 77

Dehydrogenation of Naphthene Mixture 78

Dicyclohexyl-Methylcyclohexane 78

Effect of Temperature 80

Effect of Space Velocity and Conversion 80

Effect of Pressure 80

Thermal Reaction 88

Decalin-Methylcyclohexane 88

Dicyclohexyl-Decalin 93

Thermal Reaction of Dicyclohexyl-Decalin Mixture 109

Dicyclohexyl-Methyldecalin 113

Propane Cracking 113

Thermal Reaction 116

Catalytic Reaction 118

Conventional Catalysts: Preparation and Testing 121

Catalyst Preparation 121

Exploratory Preparations 121

Larger Scale Preparations 121

Catalyst Evaluation 122

Supported Platinum 122

Various Supported Metals 128

Catalysts on Shaped Supports 128

Nonconventional Catalyst Systems: Homogeneous Catalysis 130

Thermal Stability 134

TABLE OF CONTENTS (Contd)

PAGE

Effect of Oxygen Concentration on the Thermal Stability of Napnthenes 134

Thermal Stability of Reaction Products 146

Preliminary Tests 146

Catalyst and Fuel System Test Rig (CAFSTR) Design 147

CAFSTR Testing 152

Calorimetric Tuberator 154

Fuel System Simulation Test Rig 155

Thermal Cracking of Fuel F-71 158

Catalytic Dehydrogenation of MCH in 3/4" Reactor 166

Thermal Cracking of Propane 175

Catalytic Dehydrogenation of Propane 186

High Heat Flux Section 186

Dehydrogenation of MCH Over UOP-R8 in the High Heat Flux Reactor Section 190

Development of Analytical Models of Catalytic Reactors 193

Simulations of FSSTR Experiments 194

Heat Transfer to a Packed Bed Reactor 196

Influence of Thermal Conductivity of Catalyst Particles 200

Exploratory Calculations 203

One Side Heating of Reactor Tubes 205

High-Flux Test Section for FSSTR 207

Shock Tube Studies of Ignition Delays of Hydrocarbons 207

Ethane and Ethylene 209

n-Dodecane 213

trans-Decahydronaphthalin 213

TABLE OF CONTENTS (Contd)

PAGE

Methane 213

Examination of Experimental Method and Equipment 218

Infrared Equipment 218

Limitations of the Experimental Method 220

Detection of Ignition by Infrared Emission 221

Determination of Concentration Histories of Molecular Species . . 227

Ignition Delays of Paraffins With Unusual Structures 228

Small-Scale Subsonic Combustion Tests 234

Physical Properties Program 238

Methylcyclohexane-Toluene-Hydrogen System 239

Description of Methods Used for Extending or Estimating Pure Component Data 240

Present Status and Future Projections 242

Appendix 247

References 344

Bibliography 348

Subject Index for Bibliography 381

ILLUSTRATIONS

FIGURE		PAGE
1.	Characteristics of Supersonic Aircraft	11
2.	Environments of Supersonic Aircraft	12
3.	Typical Reaction Profile for Hypersonic Transports	13
4.	Hypersonic Interceptor Test Bed	15
5.	Thermal Reaction of 1,2,4,5-Tetramethylcyclohexane. Temperature Coefficient	22
6.	Dehydrogenation of Methylcyclohexane, Catalyst Life Tests	26
7.	Thermal Reaction of Methylcyclohexane Over Alumina	33
8.	Thermal Reaction of Ethylcyclohexane, Temperature Coefficient	36
9.	Relative Rates and Energies of Activation for Thermal Reaction of Naphthenes	37
10.	Temperature Coefficient for the Dehydrogenation PCH $\longrightarrow$ DP + $3H_2$	40
11.	Equilibrium Constants for DHN $\rightleftharpoons$ THN + $3H_2$ $\rightleftharpoons$ N + $5H_2$	46
12.	Equilibrium Composition of DHN-THN-N System	47
13.	Total Conversion of Decalin as a Function of cis-Decalin in Feed	50
14.	Dehydrogenation of Various Decalins. Temperature Coefficients	51
15.	Dehydrogenation of Various Decalins. Effect of Temperature on Conversion	52
16.	Dehydrogenation of Tetralin to Naphthalene. Temperature Coefficient	55
17.	Dehydrogenation of Decalin Over UOP-R8 and Laboratory Pt/Al_2O_3 Catalysts	60
18.	Isomerization of Decalin: cis-trans Equilibrium	66
19.	Dehydrogenation of cis and trans Decalin. Temperature Coefficient	70
20.	Dehydrogenation of DCH-MCH Mixture. Effect of Temperature on Conversion of DCH	82
21.	Dehydrogenation of DCH-MCH Mixture. Effect of Conversion on Selectivity for DP	84

ILLUSTRATIONS (Contd)

FIGURE		PAGE
22.	Dehydrogenation of DCH-MCH Mixture at 842°F. Effect of Pressure on DCH Conversion and Selectivity for Diphenyl	86
23.	Dehydrogenation of DCH-MCH Mixture at 1022°F. Effect of Pressure on DCH Conversion and Selectivity for Diphenyl	87
24.	Thermal Reaction of DCH-MCH Mixture. Temperature Coefficient	90
25.	Dehydrogenation of Decalin and Methylcyclohexane at 1022°F. Effect of MCH on Component Reaction Rates	95
26.	Dehydrogenation of DCH-DHN Mixture. Effect of Temperature on Conversion	100
27.	Dehydrogenation of DCH-DHN Mixture. Temperature Coefficient	102
28.	Dehydrogenation of DCH-DHN Mixture. Effect of DCH Conversion on Selectivity for DP	105
29.	Dehydrogenation of DCH-DHN Mixture. Effect of Pressure on Selectivity for Naphthalene	108
30.	Thermal Reaction of DCH-Decalin Mixture. Temperature Coefficient	111
31.	Dehydrogenation of 1-MDHN-DCH Mixture. Temperature Coefficient	115
32.	Influence of Surface Area on MCH Dehydrogenation Activity	124
33.	Influence of Platinum Content on MCH Dehydrogenation Activity	125
34.	Temperature Coefficient for MCH Dehydrogenation With Improved Pt/Al_2O_3 Catalyst	127
35.	Low Pressure Drop Catalyst Supports	129
36.	Typical Vaporization and Expansion Curve	132
37.	Effect of Dissolved O_2 on MCH Thermal Stability	137
38.	Effect of O_2 Partial Pressure on SD Coker Ratings of Decalin	138
39.	Effect of Temperature on Thermal Stability of Decalin	140
40.	Effect of Temperature on Thermal Stability of MCH	141
41.	Effect of Temperature on Thermal Stability of Decalin	142

ILLUSTRATIONS (Contd)

FIGURE		PAGE
42.	Effect of Temperature on Thermal Stability of Naphthenic Jet Fuel	143
43.	Effect of Dissolved O_2 on Thermal Stability of Naphthenes	144
44.	Catalyst and Fuel System Test Rig (Schematic)	150
45.	Catalyst and Fuel System Test Rig (Photo)	151
46.	Calorimetric Tuberator	156
47.	Flow Sketch of Fuel System Simulation Test Rig	157
48.	FSSTR-Thermal Cracking of Fuel F-71: Total Heat Sink	163
49.	FSSTR-Thermal Cracking of Fuel F-71: Effect of Temperature on Reaction Products	164
50.	FSSTR-3/4" OD Reactor Tube	167
51.	FSSTR-Dehydrogenation of MCH Over UOP-R8 in a 3/4" Reactor: Temperature Profile for Run 10018-9-14:00	171
52.	FSSTR-Heat Transfer to MCH in Empty 3/8" Tube: Dittus-Boelter Correlation	173
53.	FSSTR-Thermal Cracking of Propane: Effect of Reaction Conditions	180
54.	FSSTR-Thermal Cracking of Propane: Total Heat Sink	181
55.	FSSTR-Thermal Cracking of Propane: Temperature Profile for Run 10018-27-15:50	182
56.	FSSTR-Thermal Cracking of Propane: Section III Temperature Profiles for Series 10018-27	183
57.	FSSTR-Heat Transfer to Propane in Empty 3/8" Tube: Dittus-Boelter Correlation	184
58.	FSSTR-Heat Transfer to Propane: Physical Properties of Propane	185
59.	FSSTR-Dehydrogenation of Propane Over Chromia on Alumina Catalyst: Catalyst Deactivation	188
60.	FSSTR-High Heat Flux Section	189
61.	FSSTR-High Heat Flux Study: Catalyst Bed Exit Fluid Temperature	192

ILLUSTRATIONS (Contd)

FIGURE		PAGE
62.	Calculated Temperature and Conversion Profiles for Conditions of Run 10018-9-1500	197
63.	Calculated Temperature and Conversion Profiles for Conditions of Run 10018-9-1400	198
64.	Calculated Temperature and Conversion Profiles for Conditions of Run 8915-198-1420	199
65.	Comparison of Experimental Heat Transfer Coefficients at Tube Wall With Correlation	202
66.	Calculated Axial Temperature Profiles for Dehydrogenation of Methyl Cyclohexane at High Heat Flux	206
67.	Comparison of Ethylene Ignition Data With White's Correlation	210
68.	Ignition Delays for Ethylene	212
69.	Correlation of Ignition Delays for Very Lean and Dilute Ethane Mixtures	214
70.	Correlation of Ignition Delays for Lean Ethane	215
71.	Correlation of Ignition Delays for Near Stoichiometric Mixtures With Ethane	216
72.	Comparison of Ignition Delays for MCH and Decalin	217
73.	Ignition Delays for Methane-Oxygen-Argon	219
74.	Comparison of Ignition Delays Detected by Two Methods for a Propane-Oxygen-Argon Mixture	222
75.	Ignition Delays for Propane-Oxygen-Argon With Temperature Corrected for Shock Wave Attenuation	223
76.	Oscilloscope Traces Showing IR Emission From CO_2 and CO Calibration Mixtures, and Comparison of CO_2 and Visible Light Emission at Ignition	225
77.	Oscilloscope Traces Showing CO_2 and CO IR Emission for Ignition of Two Propane Mixtures	226
78.	Oscilloscope Traces at High Sweep Rates for Observation of IR Emission at 2350 cm^{-1}	229
79.	Ignition Delay Times for n-Octane	231

ILLUSTRATIONS (Contd)

FIGURE		PAGE
80.	Ignition Delay Times for 2,2,3,3-Tetramethylbutane	232
81.	Ignition Delay Times for Neopentane	233
82.	Rate Constants for Post-Ignition Appearance of CO_2 for n-Octane Mixtures	235
83.	Assembly of Redesigned Combustion Chamber	236
84a.	Contact Time for MCH Dehydrogenation: 100% Conversion	249
b.	Contact Time for MCH Dehydrogenation: 75% Conversion	250
c.	Contact Time for MCH Dehydrogenation: 50% Conversion	251
d.	Contact Time for MCH Dehydrogenation: 25% Conversion	252
e.	Contact Time for MCH Dehydrogenation: 0% Conversion	253
85.	Inner Furnace Liner for Pulse Reactor System	255
86.	Schematic Diagram of Pulse Reactor System	256
87.	Micro-Catalyst Test Reactor (Schematic)	257
88.	Micro-Catalyst Test Reactor (General View)	258
89.	Micro-Catalyst Test Reactor (Detail)	259
90.	Details of Heat Exchanger	268
91.	Annular Heat Exchanger From CAFSTR	269
92.	Diagram of Bench-Scale Reactor System	338
93.	Dual Catalytic Reactor	339
94.	Dual Catalytic Reactor Showing Product Sampling System	340

TABLES

TABLE		PAGE
1.	Dehydrogenation of 1,2,4,5-Tetramethylcyclohexane	19
2.	Thermal Reaction of 1,2,4,5-Tetramethylcyclohexane	21
3.	Dehydrogenation of MCH Over UOP-R8 Catalysts: Life Test	23
4.	Dehydrogenation of MCH Over 1% Pt on Al_2O_3 Catalyst: Life Test	24
5.	Dehydrogenation of MCH Plus IONOL Over UOP-R8 Catalyst: Life Test	25
6.	Evaluation of Various Catalysts: Dehydrogenation of MCH	28
7.	Thermal Reaction of Methylcyclohexane	31
8.	Thermal Reaction of Methylcyclohexane: Gas Phase Production Distribution	32
9.	Thermal Reaction of Ethylcyclohexane	34
10.	Thermal Reaction of Ethylcyclohexane: Gas Phase Product Distribution	35
11.	Comparison of Reaction Rates for DCH ⟶ PCH and PCH ⟶ DP	39
12.	Dehydrogenation of Dicyclohexyl Over UOP-R8 Catalyst: Effect of Temperature	42
13.	Dehydrogenation of Dicyclohexyl Over UOP-R8 Catalyst: Effect of Pressure	43
14.	Dehydrogenation of Dicyclohexyl Over UOP-R8 Catalyst: Effect of Conversion on Selectivity for Diphenyl	44
15.	Dehydrogenation of Decalin: Various Feedstocks	48
16.	Reaction Rates and Equilibrium Constants for the Decalin/Tetralin/Naphthalene/H_2 System	53
17.	Dehydrogenation of Decalin Over UOP-R8 Catalyst - Effect of Temperature and Conversion	57
18.	Dehydrogenation of Decalin Over UOP-R8 Catalyst - Effect of Pressure	58
19.	Dehydrogenation of Decalin Over Laboratory Platinum Catalyst	59
20.	Dehydrogenation of Decalin: Test of Platinum on UOP-R8 Base With no Halogen	61
21.	Dehydrogenation of Decalin: Extended Catalyst Test	63

TABLES (Contd)

TABLE		PAGE
22.	Dehydrogenation of F-111 Decalin Over UOP-R8 Catalyst	64
23.	Dehydrogenation and Isomerization of cis-Decalin	67
24.	Dehydrogenation and Isomerization of trans-Decalin	68
25.	Rate Constants for Dehydrogenation and Isomerization of Decalin	72
26.	Dehydrogenation of 1-Methyldecalin at Various Pressures	75
27.	Pore Distribution of Two Platinum on Alumina Catalysts	79
28.	Dehydrogenation of DCH-MCH Mixture: Effect of Temperature	81
29.	Dehydrogenation of DCH-MCH Mixture: Effect of DCH Conversion on Selectivity for Diphenyl	83
30.	Dehydrogenation of DCH-MCH Mixture: Effect of Pressure	85
31.	Thermal Reaction of DCH-MCH Mixture	89
32.	Thermal Reaction of DCH-MCH Mixture: Cracked Liquid Product Distribution	91
33.	Thermal Reaction of DCH-MCH Mixture: Gas Phase Product Distribution	92
34.	Dehydrogenation of Decalin-Methylcyclohexane Mixtures	94
35.	Dehydrogenation of DCH-Shell DHN Mixture: Effect of Temperature	96
36.	Dehydrogenation of DCH-DHN Mixture: Effect of Temperature	98
37.	Dehydrogenation of DCH-DHN Mixture: Effect of Conversion on Selectivities for Diphenyl and for Naphthalene	103
38.	Dehydrogenation of DCH-DHN Mixture: Effect of Pressure	106
39.	Thermal Reaction of Dicyclohexyl-Decalin Mixture	110
40.	Thermal Reaction of Dicyclohexyl-Decalin Mixture: Gas Phase Product Distribution	112
41.	Dehydrogenation of 1-Methyldecalin-Dicyclohexyl Mixture	114
42.	Thermal Reaction of Propane	117
43.	Propane Cracking Over Houdry M46 Catalyst	119
44.	Catalytic Cracking of Propane Over Various Catalysts	120

TABLES (Contd)

TABLE		PAGE
45.	MCH Dehydrogenation With Platinum on Type 1 Supports of Varying Surface Area	123
46.	MCH Dehydrogenation Rates Over Reference and Improved Pt/Al_2O_2 Catalysts	126
47.	Dehydrogenation of MCH Over Shaped Support	130
48.	Homogeneous Catalysis: Dehydrogenation of MCH With Organometallic Compounds	133
49.	Thermal Stability Test	135
50.	Description of F-71 Jet Fuel	148
51.	SD Coker Ratings of F-71 Jet Fuel Thermal Reaction Products From the FSSTR	149
52.	FSSTR-Thermal Cracking of Fuel F-71: Summary of Operating Conditions	159
53.	FSSTR-Thermal Cracking of Fuel F-71: Data Summary	160
54.	FSSTR-Thermal Cracking of Fuel F-71: Product Recovery and Analyses	162
55.	Description of Jet Fuels	165
56.	FSSTR-Dehydrogenation of MCH Over UOP-R8 in a 3/4-Inch Reactor: Summary of Operating Conditions	169
57.	FSSTR-Dehydrogenation of MCH Over UOP-R8 in 3/4-Inch Reactor: Data Summary	170
58.	FSSTR - Dehydrogenation of MCH Over UOP-R8 in a 3/4-Inch Reactor: History of Catalyst Charge	172
59.	FSSTR-Heat Transfer Correlation: MCH in Empty 3/8-Inch Tube	174
60.	FSSTR-Thermal Cracking of Propane: Range of Operating Conditions	176
61.	FSSTR-Thermal Cracking of Propane: Data Summary	177
62.	FSSTR-Thermal Cracking of Propane: Product Analyses	179
63.	FSSTR-Dehydrogenation of Propane Over Chromia on Alumina Catalyst: Data Summary	187
64.	FSSTR-High Heat Flux Study: Data Summary for Series 10018-50	191

TABLES (Cont'd)

TABLE		PAGE
65.	Comparison of Computer Calculations With Experimental Results for Dehydrogenation of MCH in 3/4-Inch Tube	195
66.	Components of Measured Temperature Differences in Reaction Section	201
67.	Predicted Effect of Mass Velocity and Heat Flux in Constant Flux Reactors	204
68.	Comparison of Performances Calculated for Several High Output Conditions for MCH Dehydrogenation	204
69.	Effect of Bed Thickness on Performance of Flat-Plate Catalytic Reactor for Dehydrogenation of MCH	205
70.	Predicted Performance of High Heat Flux Test Section for Two Sets of Conditions	208
71.	Stability Limits in Modified Small-Scale Combustor	237
72.	Radiation Measurements for Small-Scale Combustor: LR 9669-28	238
73.	MCH Dehydrogenation With Various Catalysts in MICTR (LHSV = 100).	261
74.	MCH Dehydrogenation With Various Catalysts in MICTR (LHSV = 200).	266
75.	Shell Development Packed Bed Reactor Program	280
76.	Ignition Delays for Ethylene-Oxygen-Argon Mixtures	297
77.	Ignition Delays for Ethane-Oxygen-Argon Mixtures	299
78.	Ignition Delays for Decalin-Oxygen-Argon Mixtures	302
79.	Ignition Delays for α-Methyl Decalin-Oxygen-Argon Mixtures	303
80.	Ignition Delays for n-Dodecane-Oxygen-Argon Mixtures	304
81.	Ignition Delays for Propane-Oxygen-Argon Mixtures	305
82.	Ignition Delays for Methane-Oxygen-Argon Mixtures	306
83.	Ignition Delays for n-Dodecane-Oxygen-Argon Mixtures	307
84.	Ignition Delays for Toluene/$3H_2$-Oxygen-Mixtures	308
85.	Ignition Delays for MCH-Oxygen-Argon Mixtures	309
86.	Ignition Delays for Propane-Oxygen-Argon Mixtures	311

TABLES (Contd)

TABLE		PAGE
87.	Ignition Delays for 2,2,3,3-Tetramethyl Butane-Oxygen-Argon Mixtures	313
88.	Ignition Delays for Neopentane-Oxygen-Argon Mixtures	314
89.	Ignition Delays for 2,2,3-Trimethyl Butane-Oxygen-Argon Mixtures	315
90.	Ignition Delays for n-Octane-Oxygen-Argon Mixtures	316
91.	Property Values for Methylcyclohexane (Gas and Liquid)	317
92.	Property Values for Toluene (Gas and Liquid)	318
93.	Property Values for Hydrogen (Gas)	319
94.	Physical Properties of Methylcyclohexane-Toluene-Hydrogen Mixtures	322
95.	Summary Table: Evaluation of Vaporizing and Endothermic Fuels	336
96.	Thermodynamic Heats of Reaction	342
97.	Latent Plus Sensible Heats of Various Naphthenes	343

Introduction

The objective of this study is to provide the information necessary for specifying nonhydrogen fuels which will be capable of providing cooling and propulsion for engines powering aircraft in the speed range above Mach 3. The fuel will provide cooling by giving up its latent and sensible heat and by undergoing endothermic reactions before it is fed into the engine in vapor form. This could be in the temperature range up to about 1400°F. In order for the fuel to function in this manner, it must have excellent thermal stability up to the temperature at which reaction occurs and also in the post-reaction portion of the heat exchanger, to avoid fouling problems. Work under early Air Force contracts served to establish many of the parameters which obtain in delineating the boundaries of the problem. Work was done under our previous contract[1-3] to define more closely the advantages and limitations for the application of hydrocarbon fuels. In that contract the goal was to develop specifications for a fuel or fuels which could be utilized for advanced engine application and to design methods and equipment for testing the properties of such a fuel.

In order to allow precise definition of the fuel, we studied various problems that could arise in several parts of the fuel-combustion system. These included thermal stability problems which could originate in the fuel tanks or in the various metering devices and fuel lines; deposition or coking problems which could affect the efficiency of heat exchanger-reactor devices and catalysts, or plug fuel nozzles; and combustion parameters which could affect the design or operation of the combustion chambers. In order to provide a sound basis for the selection or rejection of fuels, we endeavored to relate the various phenomena observed to the physical and chemical properties of the fuels studied.

The problem areas and approaches used were broken down in the following manner: we improved a previously designed coker apparatus for use in studying the thermal stability of possible fuels and components at temperatures up to 900°F. We studied possible thermal and catalytic reactions in laboratory scale equipment in order to test the reactivity of fuels and the suitability of selected catalysts. The heat sinks available in the hydrocarbons tested were calculated from thermodynamic properties of the reactants and products. A fuel system simulation test rig (FSSTR) was constructed and used to provide data on hydrocarbon systems. A computer program for simulating the behavior of a packed bed reactor was modified to accept and correlate the results obtained in the fuels system simulator. The subsonic combustion properties of selected fuels and reaction products were observed in a small scale combustor while the ignition-delay behavior of the same fuels and products was studied in a single-diaphragm shock tube to give an indication of supersonic combustion properties.

Studies done under the previous contract indicated the general feasibility of the endothermic reaction approach, particularly the utilization of catalytic dehydrogenation reactions. Our best results were

1) See References.

achieved with the methylcyclohexane-platinum/alumina combination. With this combination, the possibility of achieving the original goal of 2000 Btu per pound of fuel total heat sink seems possible. The importance of restricting the oxygen content to very low levels to reduce heat exchanger problems was also indicated. Operations with the fuel system simulation test unit (FSSTR) have provided valuable data for heat exchanger design calculations and demonstrated the possibility of high space velocity and long catalyst life with the MCH system. The limitation of thermal cracking of hydrocarbons to a relatively low heat sink of about 300 Btu per pound due to hydrogen transfer reaction was demonstrated. The mathematical model for the cylindrical axial flow reactor was found to be adequate to the extent of its development. The combustion studies suggest that the possibilities of burning the proposed feed materials and the products of their dehydrogenation under both subsonic and supersonic combustion conditions are promising.

Under our present contract we are continuing and extending the work done under the previous contract, with some changes in emphasis: We are continuing to survey the pertinent literature and will issue bibliographies from time to time. We will continue to consider various feed materials which might be useful in this application and assess the probability of their being successful candidate materials. Such candidates are screened in our small scale equipment for reactivity and effect on catalyst life and their thermal stability under heat exchanger conditions. Successful candidate materials will be tested with improved catalysts and also under larger scale conditions as represented by our fuel system simulation test rig.

In the previous contract only a limited number of catalysts, selected for their probable activity, were tested with a variety of feed materials. The reactions of interest in that program included dehydrogenation, dehydrocyclization and depolymerization. In the present program we are conducting an intensive catalyst development program for new catalysts for these types of reactions. This involves the small scale preparation of a wide variety of catalysts in which catalytic elements (e.g., transition metals) are deposited on substrates and modified by a variety of noncatalytic elements such as the alkalies, alkaline earths, and halogens. Other catalysts are prepared containing metallic oxides and acidic sites. Such catalysts are tested initially in a small scale apparatus (the "micro-scale catalyst test reactor", MICTR) which allows rapid screening with standard feed materials such as methylcyclohexane, dimethylhexane and tetraisobutylene. In addition to the attempt to prepare superior conventional type catalysts in which catalytic materials are mounted on substrate granules, attempts are being made to prepare nonconventional catalysts in which the catalytic material is mounted on specially shaped supports (designed to minimize pressure drop), or is previously dispersed in the feed material, or is formed by decomposition in the heated zone. Such nonconventional catalysts are to be tested with the appropriate standard feed materials prior to being used with other feed materials developed as a result of the program mentioned above.

The computerized mathematical model mentioned above has been carried to the point where good representation of the FSSTR experimental results is possible. Further development of this model undertaken under the present contract allows the inclusion of different size tubes and catalyst dispositions and variable heat flux and temperatures along the tube length. It will eventually include latent and sensible heat sinks both before and

after the reaction zone, and the mating of a reaction exchanger with a heat source such as a combustor or a leading edge. This latter [illegible] will require collaboration with engine manufacturers who are working on the combustor design part of the overall program.

Extension of the program towards an aircraft system requires that considerably more work be done on the supersonic combustion characteristics of the candidate fuels. This phase might include an analytical program involving different modes of controlling flames within the combustor, analysis of nozzle expansion, an experimental small scale and large scale effort which would put the combustion end of the problem on a sound basis. In this program, our own efforts will be directed towards maintaining collaboration and liaison with other programs and with other contractors in the hydrocarbon scramjet program. We have been continuing our studies in the shock tube with high molecular weight fuels and infrared study of naphthenic dehydrogenation systems. We have also undertaken to complete our work on the examination of subsonic combustion in the small burner developed under the previous contract with the additional feature of obtaining quantitative data on the radiation emitted, as a function of fuel composition and burner conditions.

An important consideration in any system which attempts to use the fuel for cooling is the thermal stability of the fuel in the exchanger portions of the fuel system. In our previous contract we used the Shell Development Coker for evaluating the thermal stability both of feed material and of products produced by both thermal and catalytic reactions. Examination of the products suffers from the serious deficiency that inevitably a time lapse and some handling has to occur, before the products of reaction are tested. We have therefore constructed a new piece of equipment under the present contract for establishing a standard test for both catalysts and fuels. This unit, called the Catalyst and Fuel Stability Test Rig (CAFSTR), will permit simulation of the thermal environment and representative contact times all the way from the fuel tank to the engine inlet. Fuels will be tested using a standard catalyst, while catalyst will be tested using a standard fuel.

Specific support is also being furnished to contractors in the cooling program. This support consists of consultation with respect to problems encountered in the study programs, the furnishing of technical data required for the solution of design problems or for the carrying out of experimental investigations. We also expect to perform some mutually specified tests in our laboratory equipment to solve specific problems encountered by the other contractors.

Summary

Examination of the literature during the past year has revealed a continuing interest in the possibility of developing aircraft capable of achieving flight speeds up to about Mach 12. It appears that sound technological reasons exist that lend optimism to hopes of overcoming the formidable cooling and propulsion problems that still stand in the way of being able to achieve such speeds utilizing hydrocarbons as fuels. Some of the more important of the papers and reports that have appeared are analyzed below.

During this year considerable attention has been given to the effect of mixed feed components on the dehydrogenation reaction and catalyst stability. Thus, in both the DCH/MCH (dicyclohexyl/methylcyclohexane) and DHN/MCH (Decalin/methylcyclohexane) systems the effect of mixtures under both thermal and catalytic conditions is to increase the rate of reaction of the dicyclic compound and decrease the rate of reaction of MCH. Contrary to previous results, the presence of MCH with DHN either increased catalyst deactivation or did not improve it. This differs from previous results with a different sample of DHN where the addition of MCH improved the catalyst stability. Attention has also been given to the possibility of utilizing mixed feeds with dicyclohexyl and Decalin as components as well as further investigations of the dehydrogenation of the pure components. The dehydrogenation of Decalin over Pt/Al_2O_3 is complicated by the presence of the geometric isomers and by the fact that the reaction goes in two steps. Studies with the pure isomers have given insight into the course of the 3 parallel reactions which proceed simultaneously. Pure 1,2,4,5-tetramethylcyclohexane was tested (bench scale) under both thermal and catalytic (Pt/Al_2O_3) conditions. This compound reacted considerably faster than MCH, but in the case of the catalytic reaction deactivation occurred rapidly. The effect of two alumina carrier materials on the thermal reaction of MCH was tested in comparison to the usual quartz chips used in the small-scale reactor to fill the catalyst space. Both increased the rate by about 50 to 100%. Although this is probably not tremendously important, it does suggest a possibility for improving catalysts supports by decreasing their acidity.

Our standard laboratory catalyst (1% Pt/Al_2O_3) and the UOP R-8 catalyst have been compared for their efficacy in the dehydrogenation of Decalin (DHN). The two catalysts are equivalent at high (30 atm) pressures, but the R-8 catalyst is less active and shows a tendency to deactivate at low pressures (somewhat at 20 atm but markedly at 10 atm). This probably can be ascribed to the presence of acidic sites in the R-8 catalyst due to the presence of chloride in the formulation. The dehydrogenation of dicyclohexyl (DCH) also proceeds in two steps; first, to phenylcyclohexane and then to diphenyl. The first order rate constants and energies of activation for both steps have been determined using the method of Wheeler. The initial reaction is faster at low temperature but slower at high temperature than the second reaction, the apparent energies of activation being 8 and 43 kcal/mole. The addition of an equal volume of DCH to DHN resulted in some modification of the rates of reaction of each component, but the effects were not large. The presence of the DCH reduced the tendency of DHN to deactivate the catalyst. Stability tests with both the lab and the UOP catalysts have

been done in the laboratory reactor over a 10-hour processing period. Both catalysts declined at a rate of about 0.5% conversion per hour after an initial drop of about 2% in the first hour. The presence of a phenolic antioxidant reduced both the activity and the catalyst stability to some extent. MCH was used as the test fluid in the tests.

Comparison of results with both DCH and DHN over Pt/Al_2O_3 catalysts suggests that stability is related to the pore size of the catalyst. Stability increases as pore size decreases, due it is thought, to the increasing surface to volume ratio, which results in an increasing H_2 partial pressure in the pores. As the pores decrease in size, however, a point will be reached where the rate will be diffusion rather than surface limited and further decrease in pore size will result in decreased stability.

Analysis of results with decalin over Pt/Al_2O_3 indicates that while cis isomer dehydrogenates only moderately faster than trans, its rate of isomerization is almost an order of magnitude faster than the trans.

Attempts to achieve catalysis of the thermal reaction of propane (hopefully to CH_4 and C_2H_4) by the introduction of free radical sources (e.g., Me I, allylchloride, hydrogen) failed to achieve its goal (at 1295°F, 1 atm, LHSV of 25). Little additional conversion, except to coke, was observed. However, some additional experiments will be done on this system with other free radical sources in the future.

Further work on the catalytic cracking of propane in an attempt to achieve the reaction to ethylene and methane using a hydrocracking catalyst and several modified zeolite catalysts was unsuccessful; little reaction occurred at a block temperature of 1022°F, atmospheric pressure, and a LHSV of 20. Apparently, the propane reacts almost instantaneously to form coke which precludes catalysis of the reaction of interest. Dehydrogenation of methyl Decalin over the laboratory catalyst was also tested. It reacts at about the same rate as Decalin but has a somewhat more adverse effect on catalyst stability. Previously, we indicated that the Decalin/R-8 catalyst combination had somewhat less stability than the Decalin/standard laboratory catalyst combination. This was previously attributed to the presence of halogen in the R-8 catalyst. However, catalyst prepared on the R-8 base in the absence of halogen also is somewhat less stable indicating that this is probably, in part at least, a specific effect of the base used. Similarly, dehydrogenation of DCH over R-8 catalyst indicated that this catalyst, under laboratory conditions, shows less stability with this feed also. However, catalyst stability is generally improved by operation at higher pressures.

Recheck of previous runs using very pure ethylcyclohexane has brought the results of previous work into line with those obtained with other naphthenes, indicating that for this naphthene impurities in the feed were affecting our results.

The catalyst development program designed to produce conventional type catalysts of superior activity and thermal indifference has been continued. A total of about 220 dehydrogenative catalysts have been made, and have been tested in the microscale catalyst test reactor (MICTR) using MCH as a test fluid. Most of the catalysts are inferior to our standard laboratory catalyst or the R-8 catalyst, but about a dozen have been found

which are of superior activity. These have been tested further in the small scale reactor setup and their activity generally confirmed. The best catalyst increased the specific reaction rate by about 50%.

Some success has been achieved in placing an active catalyst on a low pressure drop fused alumina shape after initially affixing a highly active alumina on the surface.

Attempts have also been made to develop disperse or vapor phase catalysts by utilizing metallo-organics. Some activity has been noted with a number of compounds in screening tests.

Modifications to the fuel system simulation test rig (FSSTR) were made and a 3/4-in. by 10-ft section packed with R-8 catalyst was installed. Smooth operation with the modified equipment ensued and 95% conversion at 80 LHSV was obtained. The observed temperature profiles, conversions, and pressure drops were well represented by our packed bed reactor computer program.

Study of the thermal cracking of an advanced state-of-the-art paraffinic jet fuel (F-71) begun under the previous contract was completed. Studies indicate a maximum endothermic heat sink of about 300 Btu/lb and maximum allowable fluid temperature of operation of about 1200°F. The results observed are not very sensitive to operating conditions except temperature. The upper temperature limitation occurred because of coking which caused plugging of the pressure control valve.

The catalytic dehydrogenation of propane using a K-promoted Cr_2O_3-Al_2O_3 catalyst was examined in the FSSTR using a 10' x 3/8" diam bed. Two series of tests have been made at a feed rate of 10 lb/hr (LHSV = 75). In the first series, bed inlet temperature was maintained at 900°F. Variables were inlet pressure of 430 and 590 psig and catalyst section exit temperature of 1100 and 1200°F. Maximum conversion measured was 7.7%. Conversion declined rapidly and after about 5 hours of operation the catalyst was almost completely deactivated. Following this test, 10.7 g of carbon was burned from the catalyst bed.

For the second test series, nominal inlet and exit temperatures of 1000°F and 1250°F respectively and an inlet pressure of approximately 500 psig were maintained for the entire operating period (ca 4 hours). Propane conversion started at ca 23% and declined to ca 5% after 250 minutes of operation. Pressure drop increased from about 300 to 465 psi during the first 25 minutes, then increased at 5 psi per hour through the rest of the run to a maximum of 490 psi. Coke was not burned from the catalyst after this test. A weight increase of 15 grams due to coke deposit was measured after dumping the catalyst charge. It had been hoped that more satisfactory results would be achieved in the FSSTR because of the better temperature control and the higher linear velocity achieved in this equipment compared to the bench scale apparatus.

A two-foot long (by 3/8" diam) high flux section capable of accepting about 600,000 Btu/hr/sq ft has been constructed and put into operation during the year. It has been used for the dehydrogenation of MCH on R-8 Pt/Al_2O_3 at an LHSV of 1600 with a maximum heat sink of ca 360,000

Btu/hr/sq ft. Some catalyst deactivation was noted at the most severe conditions (fluid temperature, ca 1100°F). Conversions under high heat flux conditions were generally higher than predicted by our mathematical model indicating a need to reexamine the parameters used in the program.

The mathematical model of a packed bed reactor system, developed under our previous contract, has been modified and completely rewritten in order to economize on both human and machine time. It has been used successfully to represent the results obtained in the FSSTR and to extrapolate to condition inaccessible to experimentation. It has indicated, for instance, that increasing the thermal conductivity of the catalyst particles (even by a factor of 1000) would have no beneficial effect on the heat sink capabilities of a reacting system. Also that supplying the heat from one side only of a catalyst bed, such as would be encountered in a regeneration type application, can be represented by the model.

Flat plate configuration shows that the basic features of the results are similar to those obtained with the axisymmetric cylinder model. It appears that the average flux over a 2' length is about 0.5 to 0.7 x 10^6 Btu/hr/sq ft. Some compromise between maximum heat flux and the degree of reaction of the fuel must be made. With the flat plate configuration, the dimension of the layer compared to the particle diameter is more critical. The region of dimension which appears to be most favorable is a thickness of only 2 to 4 particle diameters. Also, we can calculate the relative advantages of a series of adiabatic reactors compared to a single bed. We find that a five-bed reactor (with intermediate heat absorption) with a total length of 2-1/2 feet and a maximum fluid temperature of 1150°F can absorb about 8 x 10^7 Btu/hr/square foot cross-section area with a flow rate of 120,000 lb/hr/square foot and a pressure drop of 400 psi, while a single continuous bed under the same conditions can take up somewhat more heat. Thus we conclude there is no benefit to this scheme except it might allow better matching with the radiation flux in an engine.

Considerations of the changes that must be made in the mathematical model to represent the dehydrogenation of dicyclonaphthenes such as Decalin and DCH are proceeding. Attempts will be made in the first instance to apply the kinetic results obtained in the bench scale reactors to this calculation. The application is difficult in this case because of the uncertainty in our knowledge of fluid temperatures in this configuration of equipment, as well as the complexities of the kinetics.

Work that has been done on the effect of oxygen on the thermal stability of naphthenes has been brought together and summarized with particular reference to the pure naphthenes, MCH and decalin, and to a highly naphthenic jet fuel (RAF 163). All hydrocarbons show improved thermal stability when oxygen is removed at least down to 1 ppm, generally by about 200°F improvement in SD coker breakpoint. This effect has been related to the fundamental response of hydrocarbons to oxygen concentration during oxidation. The effect varies with the composition of the feed, with the lowest oxygen content to which the fuel is sensitive decreasing in the order: decalin, MCH, naphthenic jet fuel.

A new piece of equipment, the CAFSTR (catalyst and fuel system test rig) was designed, manufactured, and put into operation during the year.

This equipment, which is intended to provide a standardized test for either fuels or catalysts, consists of 3 preheaters, internally heated by rod type heaters; an externally heated packed reactor; and a final preheater similar to the first three; followed by an orifice plate (to simulate a fuel nozzle). Preliminary runs have been made with an advanced jet fuel and with MCH at 3 and 6 lb/hr flow rate, 1000 psig, temperatures up to 1200°F, with and sans Pt/Al_2O_3, catalyst. The equipment has performed according to design.

However, the question of how to rate the preheater tubes must be resolved since visual ratings with the Eppi Tuberator are far less meaningful than before. At high temperatures, the presence of a blue coloration of the tube metal, plus some shades of yellow and tan which may also be the metal itself (Inconel 600), make the visual evaluation of thermal stability both difficult and uncertain. In some cases, the change in ΔT (T metal surface - T fluid) over the course of the run (where flow and heat input were constant) may give a more reliable indication of true deposit lay-down. Not enough data has been accumulated to date to assess the usefulness of this measure. The possibility of developing a calorimetric tuberator is being explored. Calculations indicate that significant results should be obtained if reasonable stability and accuracy in the test equipment is achieved.

Tests have been done in the modified small scale subsonic combustor with both propane and toluene/$3H_2$ using a Rayotube to monitor the total radiation, at E. R. values of 0.9-1.4 and 0.95-1.3, respectively. The results indicate radiation fluxes for propane for 5000-7000 Btu/hr and 6000-8000 for toluene/$3H_2$. The lowest fluxes were associated with the richest mixtures in both cases, presumably because of lower flame temperature and lower production rates of the emitting species CO_2 and H_2O. There was no indication of radiation from carbon particles with either fuel.

Shock tube studies of the effect of environment on ignition delay of ethylene and ethane were done. Both compounds show behaviors different from those observed with higher hydrocarbons or with methane. Ignition delay decreases with increasing E/R down to about 0.5 and then increases. Under otherwise constant conditions, increasing pressure, concentration, and temperature decrease delay times. Both compounds under lean conditions give two different temperature coefficients, varying with total reactant concentration (18 kcal below 10^{-5} m/l and 36 kcal above). Studies of ignition delays of dodecane, Decalin, and methyl Decalin have been extended to higher partial pressures. The behavior of all compounds is quite similar to that of MCH. The behavior of methane has been studied over a wider range of conditions. Temperature coefficients were found to vary with E/R, activation energies being 25-30 kcal in lean mixtures and 45-55 in rich. Under otherwise constant conditions, increasing E/R increases delay time while increasing pressure decreases it.

It has been found that utilization of the infrared emission from CO_2 gives considerably better definition of ignition delay time in the shock tube than utilizing either visible light (as used in the past) or CO infrared emission. This is particularly true in the region of very short ignition delays where apparently the superior collimation of the infrared system and decreased reflection affords sharper reception. CO_2 emission is superior to that from CO because of the higher signal-to-noise ratio even at the same species concentration.

The study of the effect of hydrocarbon structure on ignition delay has been extended to include a number of highly branched paraffins utilizing the infrared detection technique in the single diaphragm shock tube. The hydrocarbons examined were 2,2,3 trimethyl butane, 2,2,3,3 tetramethylbutane and neopentane (tetramethyl methane). Normal octane was included for comparative purposes. Experiments were concentrated over a fairly narrow range of operating conditions, at low equivalents ratios and pressures of 9,15 and 25 psia. Because of the improvement in detection techniques, the compounds were studied over a wider range of temperature (ca 1100-1500°K) than was previously possible. The results indicate that although the more highly branched paraffins do have a somewhat longer delay (ca a factor of 2 in the mid-temperature range) the effect of structure is not very large. The effect of pressure and equivalence ratio was not great over the range studied while the effect of temperature is reasonably represented by an activation energy of about 40 kcal per mole. The effect of oxygen concentration appeared to be somewhat less than first order.

By comparing the output obtained with argon and CO_2 in the tube with that obtained with a reacting mixture some indication of the rate of combustion in the mixture could be estimated. The apparent rate constant has a value of about 10^3 sec^{-1} in the middle of the temperature range studied and is relatively insensitive to the effect of temperature (7 kcal per mole) and oxygen concentration. This would suggest a time for complete combustion of several milliseconds. However, the values obtained are for low equivalence ratios (0.1 and 0.2) and it will be worthwhile to extend the study over the entire equivalence ratio range of interest and to get similar data for the MCH system.

As part of our program to support work done by others in attempts to utilize hydrocarbons for fueling and cooling sub- and supersonic combustion ramjets, and also for our own calculations, we have been attempting to systematize and extend the physical data for hydrocarbons over the temperature and pressure ranges of interest (up to 1600°F and up to 3000 psia). Considerable difficulty was encountered in reconciling various existing correlation programs but concordance was finally achieved, for the MCH system at least. Data are included delineating data for this system at 0, 25, 50, 75, and 100% conversion to toluene/$3H_2$.

We have also calculated equilibrium compositions for the Decalin/ tetralin/ naphthalene/H_2 system from the data of Allam and Vlugter[4] at 10, 30, and 60 atmospheres as a function of temperature over the range 600 to 1100°F. A consistent set of data was obtained which indicates that at the three pressures mentioned a 95% conversion of Decalin to naphthalene would be possible at 775, 925 and 1075°F respectively.

We have attempted to maintain continuing surveillance of the literature of interest in this area. A bibliography comprising 337 references is appended.

Considerations Affecting Applications

A recent group of articles in Astronautics and Aeronautics[5] (October, 1966) on the hypersonic transport (the HST) highlighted some of

the opportunities and the problems in the development of aircraft designed to operate in the range of Mach 6 to Mach 12. It is proposed that a hydrocarbon fuel would be the optimum selection for a flight regime up to about Mach 7 or 8 with hydrogen becoming necessary at higher speeds. Miller's[5a] article suggests that the penalty associated with the use of hydrocarbon fuels stem largely from the losses in the propulsion system due to dissociation phenomena resulting from the inability of the carbon dioxide fragments to recombine sufficiently rapidly in the nozzle to achieve the full specific impulse potential. This range could possibly be extended somewhat if it turns out that our development of a dispersed "throwaway" catalyst leads to a situation where we will also have a catalyst for recombination of carbon dioxide fragments because of the presence of metal or metal oxide particles in the exhaust.

The article by Ferri[5b] also endorses the idea of using a hydrocarbon fuel up to about Mach 8 (Figure 1) using the latent and sensible heat capacity of the fuel for cooling the aircraft, without however mentioning the possibility of using endothermic reactions to give additional heat sink. It would appear that this might be a more economical way to cool the air required for cooling the structure rather than the use of expansion turbines to absorb the energy of the air as proposed by Ferri in his article. The article by Laidlaw and Johnston[5c] discusses the structural technology required for HST's in the Mach 6 and the Mach 12 range, assigning methane as a fuel to the Mach 6 aircraft and recommending hydrogen for Mach 12 as a consequence of the environments encountered by such aircraft (Figure 2). Here again, they have not given any consideration to the possibility of achieving higher heat sinks with endothermic reactions. This lack of consideration is probably not due to any lack of knowledge of the possibilities involved but simply reflects the fact that a great deal of work remains to be done before the potential heat sink available can be translated into meaningful proven concepts. The article by Simpson and Hursch[5d] gives an interesting estimate of the mission profile of a M-12 aircraft (Figure 3). We have amended the figure slightly to also show how a Mach 7 aircraft would behave.

A recent paper by Stroud and Miller[6] on the design of hypersonic inlets emphasizes the importance of cooling in obtaining improved inlet pressure recovery. For instance, they show that at Mach 8 cooling the inlet surfaces to 2000°F provides for optimization of the inlet design system at a fineness ratio between 2 and 3, thus, achieving near maximum efficiency at a relatively low weight penalty. It is apparent from their analysis of the problem that better cooling would result in still higher inlet efficiency.

Similarly, an investigation of flow separation in aerodynamic controls at hypersonic speeds by Kaufman et al.[7] reveal the extremely high heating rates associated with most types of controls and suggests that the provision of cooling at critical points when the controls are to be used may alleviate the severe problems associated with this application.

Another interesting article involving hypersonic aircraft was by Peterson et al[8] in which they presented the results of a launch vehicle mission analysis for a hypersonic first stage which accelerated up to Mach 7 before launching the second stage. They assumed that the air frame and leading edges were cooled by radiation but used regenerative cooling for the

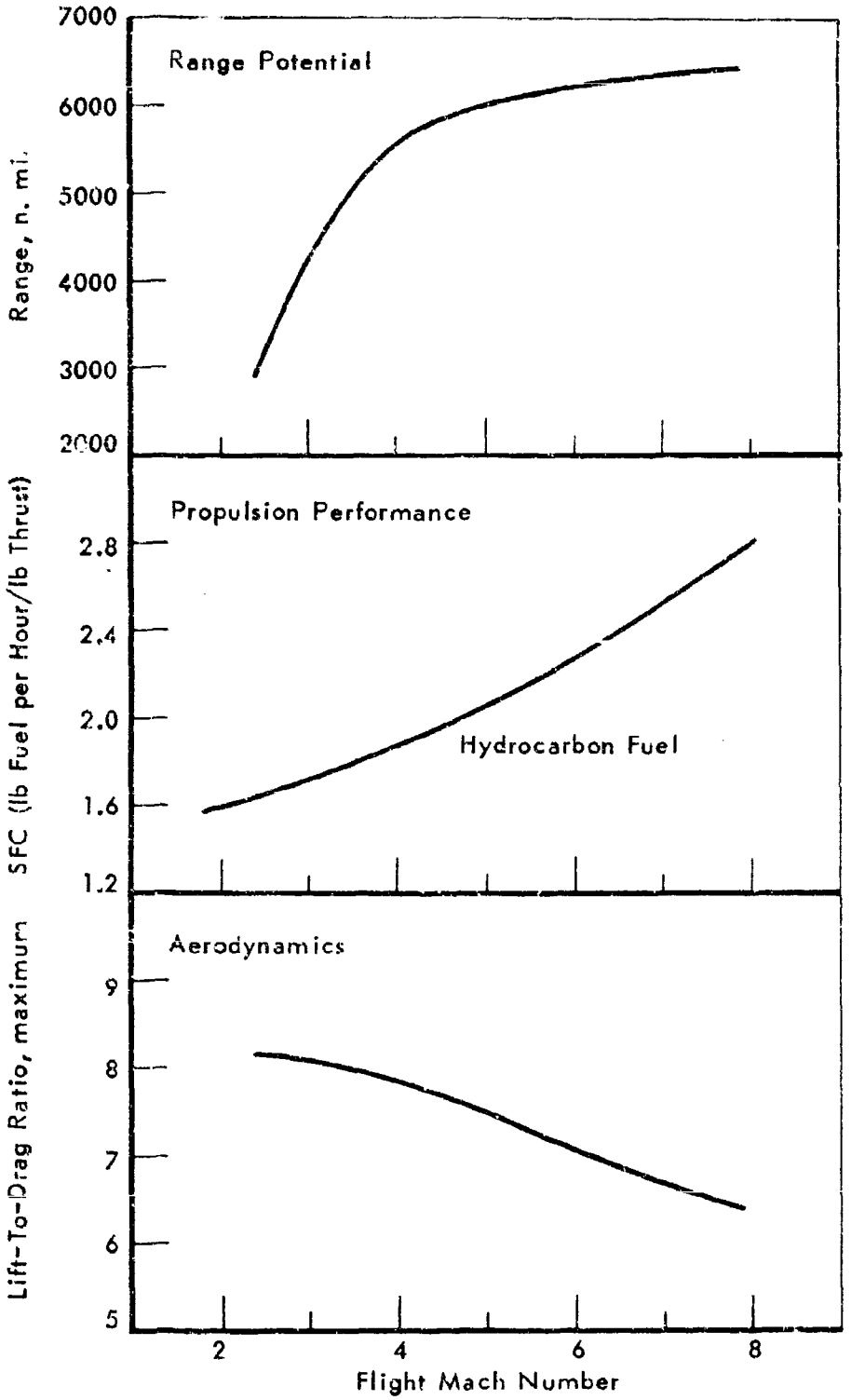


Figure 1. CHARACTERISTICS OF SUPERSONIC AIRCRAFT

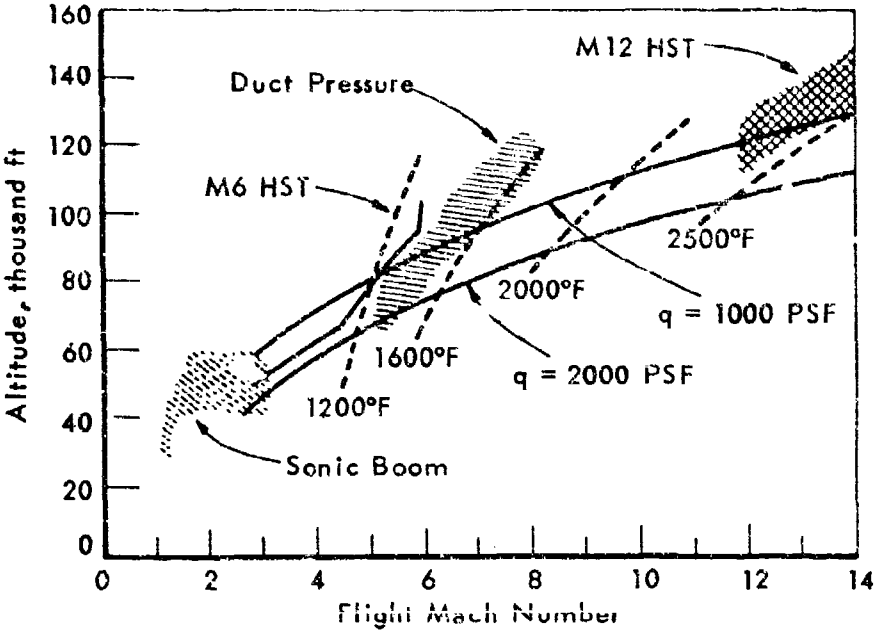


Figure 2. ENVIRONMENTS OF SUPERSONIC AIRCRAFT

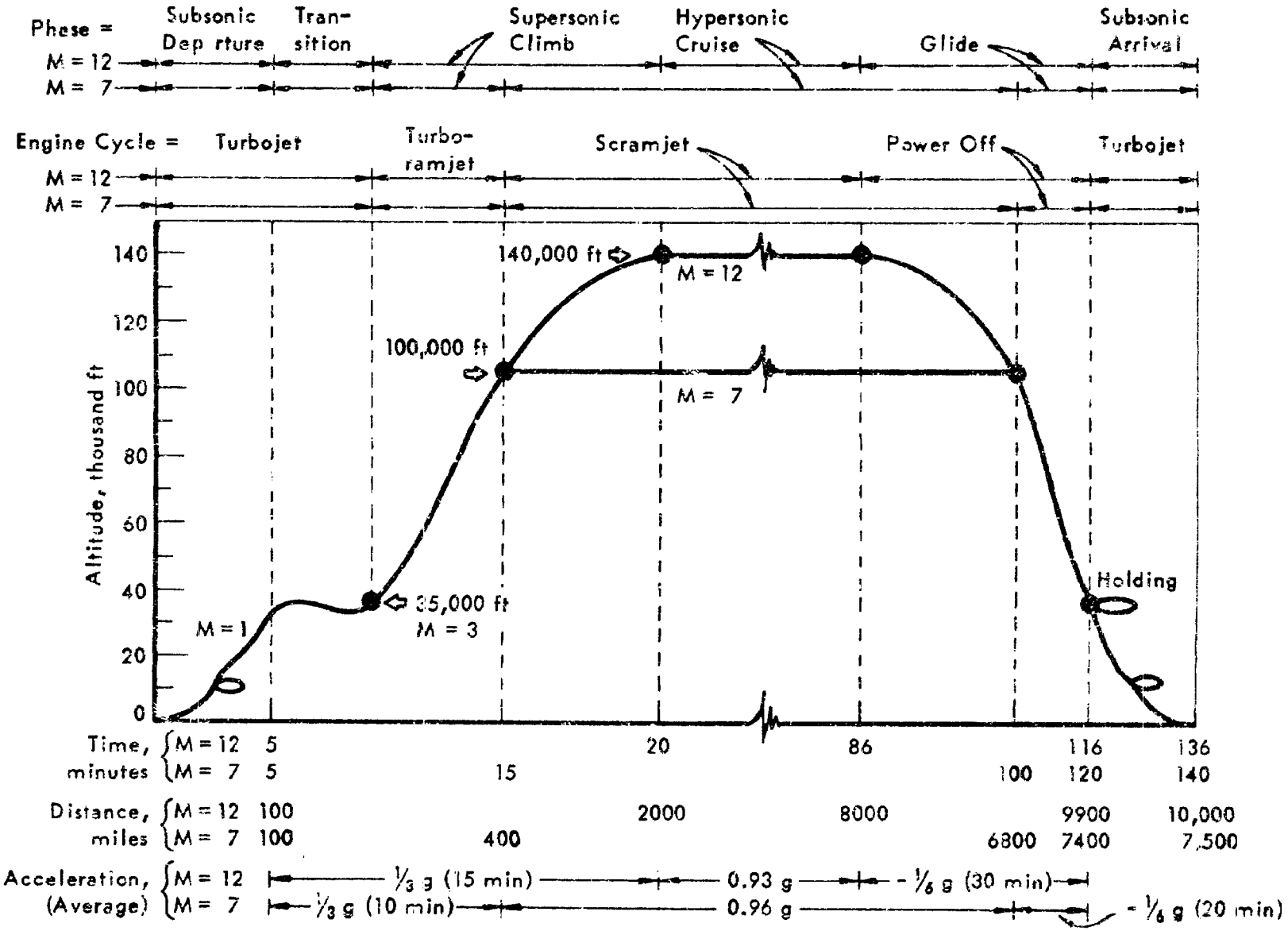


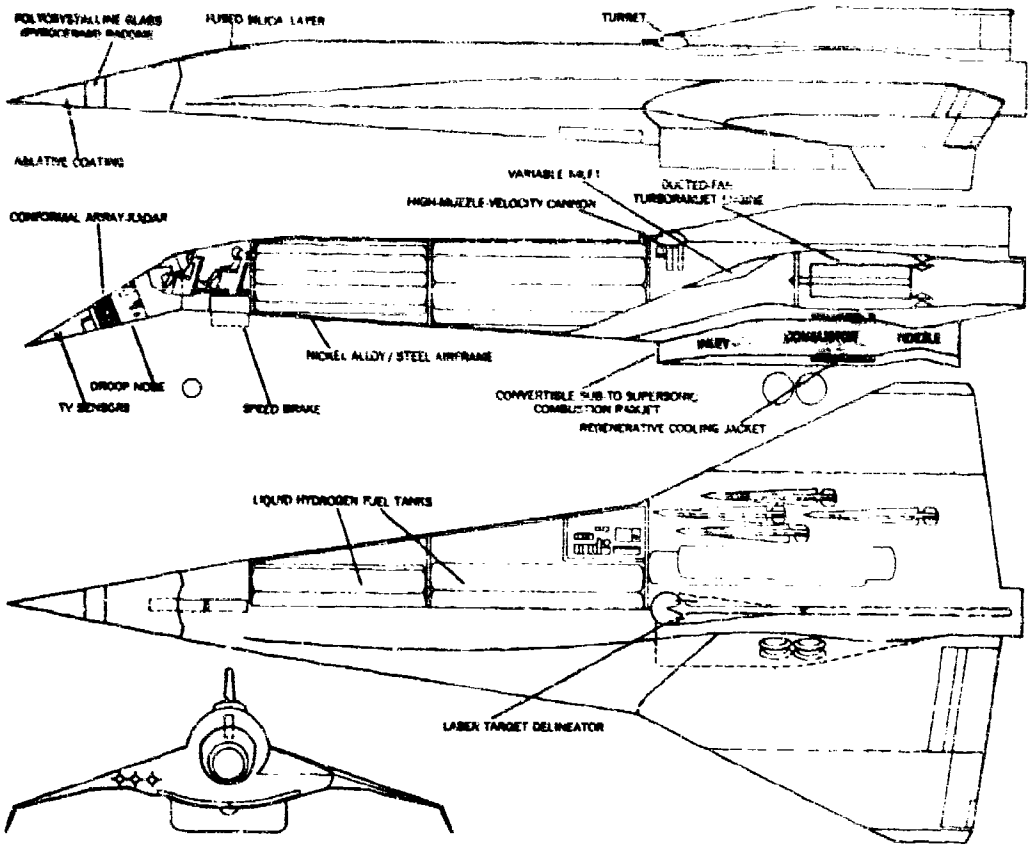
Figure 3. TYPICAL MISSION PROFILES FOR HYPERSONIC TRANSPORTS

internal surfaces of the propulsion system. They assumed that the engines were hydrogen-fueled subsonic burning turbo ramjets. They made a parametric investigation of the vehicle characteristics and trajectory. The first-stage parameters that were varied included wing loading, fusilage slenderness ratio, wing thickness, and aspect ratio. Their optimum vehicle cruising at about Mach 6 delegated 35% to the airframe and about 25% to the fuel using liquid hydrogen fuel. For a launch vehicle of 500,000 lb with a 2000-nautical mile lateral range, about 13,500 lb could be placed in orbit. In view of the favorable volume ratio for hydrocarbons of about one third that required for liquid hydrogen it would be interesting to determine if the weight of the airframe could be reduced sufficiently to overcome in combination with reduced drag the unfavorable weight ratio of hydrocarbon to liquid hydrogen of 2-1/2 to 1.

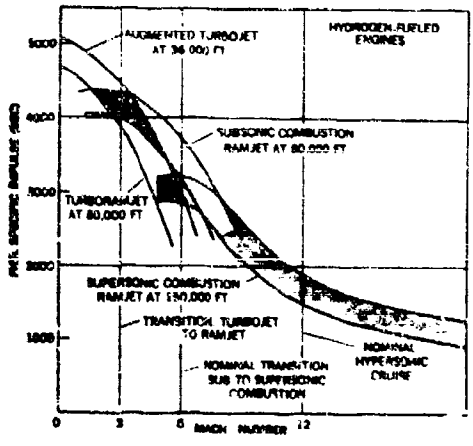
It would appear that a low-weight, high-efficiency catalytic heat exchanger could be constructed on the basis of the high surface area heat exchanger introduced by du Pont.[9] Our concept would utilize a multiplicity of thin-walled tubes of an appropriate metal having, say, an OD of 0.1 inch and a wall thickness of 0.01 inch. The circulating fluid (e.g., hydrogen or helium) would be pumped from the primary heat exchange surface (i.e., the engine or leading edge) through the inside of the small tubes to heat exchange with the fuel which would be circulated on the outside of the tubes. Catalysts would be deposited on the outside of the tubes in the bundle. Latent and sensible heat would be utilized initially for cooling the circulating fluid; but as the temperature of the coolant fluid increased, reaction would occur. This construction should provide about 200 sq ft of heat transfer area per cubic ft of shell volume; and if a modest heat transfer coefficient of only 200 is assumed with an average approach of 400°F, it may be calculated that the 2×10^8 Btu/hr required to provide 3000 Btu/lb for 100,000 lb/hr fuel flow could be provided in 12.5 cu ft of volume (in the FSSTR we have actually measured heat transfer coefficients of 1200). This would appear to provide the promise of a highly efficient device having a low pressure drop. Its success as a reactor/heat exchanger will depend on our ability to deposit a sufficiently active catalyst on the surface of the heat exchanger tubes. This is presently being investigated.

A recent paper by Ashby and Stone,[10] analyses the effect of volume addition on L/D_{max} for configurations suitable for a cruise type vehicle. This indicates that a reduction in drag loss is achieved equivalent to about 40% reduction in the loss in L/D_{max} for a typical hydrocarbon fuel compared to the volume required for liquid hydrogen (assuming that a volume increase of 92% would be necessary in the latter case). However, it is realized this potential benefit from the use of hydrocarbons may become less as Mach numbers increase because the increasing capture area necessary for the inlet system will shadow a considerable volume which could be utilized for fuel storage.

The editorial in Space/Aeronautics for November 1966 by John B. Campbell[11] is entitled "The Hypersonic Era" and concludes"...and, if events do not force a faster pace, we well may see an operational hypersonic interceptor by the early 1980's". This is accompanied by an article by L. H. Delberger[12] on "Advanced Interceptor Aircraft" in which he discusses the possibility of production of hypersonic aircraft. This article shows an illustration (cf Figure 4) of a LH_2 fueled hypersonic interceptor test bed







HYPERSONIC INTERCEPTOR TESTBED

By extrapolating presently evolving technology, a hypersonic-cruise interceptor-testbed configuration may be postulated, and could be constructed and tested by the late 1970s. Nominal cruise speed at 140,000 ft would be Mach 12, although actual intercepts would depend on long-range maneuverable air-to-air missiles. To provide firepower within missile minimum-range limitations, the aircraft, built of steel with a nickel alloy skin, would be stressed for close-in maneuverability in the supersonic regime and outfitted with cannon firing high-speed projectiles. Target identification might be augmented by a laser target-delineator at high altitudes or in clear weather. Forward vision for the pilot, with droop-nose up in hypersonic forward flight, is afforded by a tv camera system. Two engines, each capable of dual-mode operation, are aboard: a turbo-ramjet for flight Mach numbers from zero to about Mach 6, equipped with a shutter to close off its inlet above Mach 3; and a convertible sub-to-supersonic combustion ramjet (scramjet) operating from Mach 3 to 12+. Redundant capability of one of the engines in the Mach 2 to 6 range would be abrogated in an operational version. Liquid hydrogen fuel, used with both engines, could provide regenerative cooling of the scramjet's combustors, a heat exchange which preheats the -423 F fuel for more efficient burning. The fuel might also be circulated to cool the wing leading-edges and nose surface which may reach 1800-2400 F. As an alternate, an ablative coating might be used. The low-density of liquid hydrogen militates for a large aircraft weighing at least 200,000 lb with a length of over 100 ft. Use of integrated microwave circuit modules could permit design of a conformal array-radar wrapped around the nose for target search-and-track and missile guidance. A speed-brake for deceleration is required, due to the aircraft's low-drag configuration.

Figure 4. HYPERSONIC INTERCEPTER TESTBED
Courtesy Space-Aeronautics Magazine

which would operate in the range of Mach 3 to 12+. It is described as a large aircraft weighing at least 200,000 pounds with a length of over one hundred feet in which leading edges and nose surfaces may reach 1800-2400°F. It is stated that, "there is intense effort to develop a more manageable fuel with higher density to permit reducing storage tank volume and thus aircraft size and to avoid the temperature problems of raising -423°F fuel to combustion temperature in the supersonic combustor. Ideally a fuel as easy to handle as JP-4 is sought, but hydrocarbons because of low flame speed, kinetic energy, and storage temperature limitations, are presently unattractive".

A paper presented at the AIAA Third Annual Meeting (December 1966) by A. Ferri[13] discusses scramjet propulsion technology. In this Ferri reviews the present status and some of the important considerations on the use of supersonic combustion breathing engines as propulsion systems for hypersonic vehicles. The author concludes that good progress is being made toward solutions of the many problems that exist but that considerable work remains to be done.

In a study issued by the Rand Corporation last year, T. F. Kirkwood[14] comments on future air transportation systems. The author considers that in the future ranges up to 9000 nautical miles nonstop will be a desirable feature and that under these circumstances an aircraft capable of cruising at Mach 8 is not out of the question.

Recent studies[3] have emphasized the desirability of achieving higher heat sink capability in hydrocarbon fuels. Under otherwise equivalent conditions it appears that in a system utilizing endothermic cooling with MCH, the maximum sustained speed achievable would only be about 2/3 of that possible with liquid hydrogen at a heat sink equivalent ratio of one. Matching LH_2 would involve achieving reaction heat sinks above about 1400 Btu/lb. On paper there are a number of ways that this could be achieved with hydrocarbon fuels. Preliminary calculations indicate that a number of polycyclic structures should fall in this category if maximum dehydrogenation can be achieved. Other reactions in this category include the clean catalytic cracking of even-numbered paraffins to ethylene and hydrogen (if ethane production can be avoided). The catalytic cracking of butadiene to acetylene will yield about 2700 Btu/lb (if ethylene and acetylene are formed, the value is about 1300). The dehydrogenation of methylamine to cyanogen would yield over 2000 Btu/lb (with some loss in heat of combustion). However, whether catalysts exist which will give good selectivity in these reactions is a matter still to be established.

Two articles[15][16] in Industrial Engineering Chemistry emphasized the importance of a good understanding of the behavior of fixed bed catalytic bed reactors. Both articles discussed the problem of building models for such reaction systems and stressed the value of the computer in choosing optimum operating conditions. It appears on the basis of these articles that the mathematical model we have developed is more useful than anything available in the literature.

Rubins and Bauer point out in a recent article[17] that a scramjet may be required to utilize several combustion methods to traverse a desired flight path and, further, that in this flight path envelope regions will

exist which produce combustor inlet air flow conditions in which the chemical reactions are relatively slow and for which more accurate knowledge of reaction chemistry is necessary than now available. They point out that in this region premixing of the fuel may shorten the combustor length and that shock-induced combustion may be necessary or at least desirable. They further state that, in spite of the advances that have been made in the past few years, more research on mixing and combustion will be needed before results can be applied with confidence to scramjet engines.

Laboratory Reaction Studies

The bench-scale laboratory studies of candidate endothermic fuels and their catalyst systems, that were initiated under the previous contract, are being continued under the present contract. Tests were conducted in the apparatus that was developed under the previous contract, and which was described in detail in other reports[1)2)3)] and in the Appendix.

Extending the work with monocyclic naphthenes, 1,2,4,5-tetramethylcyclohexane (TeMCH) was tested for catalytic dehydrogenation and for thermal reaction. The effect of the alumina catalyst support on the thermal decomposition of MCH was tested using a Harshaw 0104 alumina (the support for our standard 1% Pt on Al_2O_3, catalyst) and a UOP alumina that was the support for the UOP-R8 catalysts. Extended catalyst life tests (10 hr) for the dehydrogenation of methylcyclohexane were done with both the laboratory and commercial platinum on alumina catalysts. The effect of IONOL[®a)] on catalyst stability was determined. A number of new catalysts were evaluated for the dehydrogenation of methylcyclohexane.

Continuing the work with dicyclic naphthenes, the commercial UOP-R8 platforming catalyst was tested for the dehydrogenation of dicyclohexyl. Rate constants and activation energies were calculated for the dehydrogenations of dicyclohexyl to phenylcyclohexane and for the latter to diphenyl, using data obtained in earlier work. The dehydrogenation and isomerization of cis and trans Decalin isomers were studied over the laboratory platinum on alumina catalysts. The relative rates for the various reaction processes were computed. 1-Methyl Decalin was tested with the platinum on alumina catalysts. Factors influencing the relative stabilities of platinum on alumina catalysts for the dehydrogenation of dicyclic naphthenes were studied.

Mixtures of methylcyclohexane with dicyclohexyl and with Decalin and of dicyclohexyl with Decalin and with 1-methyldecalin were tested for dehydrogenation and for thermal reaction.

Some exploratory work was done on the thermal and catalytic cracking of propane.

Procedures for carrying out the runs and analyzing the products for the thermal and catalytic experiments and for computing the conversions, selectivities and first order rate constants have been described in previous reports.[1)2)3)] In this respect it should be noted that these reactions were treated as being first order. Although this is not strictly kinetically accurate, the calculated k-values are useful in comparing different fuels and catalysts.

a) 2,6-Ditertiarybutyl-4-methylphenol.

Monocyclic Naphthenes

Dehydrogenation of 1,2,4,5-Tetramethylcyclohexane

1,2,4 5-Tetramethylcyclohexane (TeMCH) was tested for catalytic dehydrogenation and for thermal reaction at 10 atm pressure and 842-1292°F. This material was prepared by hydrogenation of the corresponding tetramethylbenzene (TeMB) and contained at least four of the six 1,2,4,5-TeMCH cis-trans species. Identification of the individual species was not made due to lack of GLC reference compounds.

The catalytic dehydrogenation was carried out over our standard 1% Pt on Al_2O_3 catalyst at 842-1022°F and LHSV[a] of 100. Under these conditions, this naphthene showed the same instability that was observed previously with trimethylcyclohexane[4] (TMCH), namely, that catalyst deactivation occurred during all of the runs. This was shown by the increase in catalyst bed temperature during the 30-minute reaction periods (Table 1); and the magnitude of the temperature increase was taken as a measure of catalyst deactivation. The deactivation was small at 842 and 932°F (ΔT = 18 to 39°F), but was considerable at 1022°F where increases in bed temperatures of over 200°F were observed. This deactivation occurred rather rapidly with over 95% taking place during the first 15 minute reaction period (Table 1). Based on this criteria the TeMCH was less stable than TMCH feeds where the increase in catalyst bed temperatures were 90 to 140°F at 1022°F (cf Table 10).[3]

Product material was principally TeMB (85-90% selectivity), with possible small amounts of benzene and toluene. Our analysis system did not differentiate between benzene and one of the TeMCH isomers. Consequently, the benzene yield was taken as the increase in this feed component during reaction. However, isomerization during the run would also increase this feed component. Thus, the values of selectivities in Table 1 should be considered as minimum.

First order rate constants were computed at 842 and 932°F based on total feed conversion. These are minimum values due to catalyst deactivation during the run. Based on the rate constant of 0.98 sec^{-1} at 842°F, this feed was about 1.5 times more reactive than MCH ($k = 0.62$ sec^{-1}). A minimum apparent activation energy of 5.4 kcal/mole was calculated for the temperature range of 842-932°F.

As in the study of TMCH, no attempt was made to identify the deactivating reaction. Presumably deactivation was due to a hydrocracking-type reaction that affects naphthenes with three or more substituted alkyl groups. Gas products were mainly hydrogen but did contain 0.1% to 0.2% methane. The small amount of methane produced indicates that deactivation of the catalyst requires the production of only a small amount of dealkylated naphthene. This suggests that modification of the catalyst need not be profound to eliminate this effect. Best heat sink was 429 Btu/lb (about 70% of theoretical) which corresponds to a total heat sink of 1379 Btu/lb at 1340°F.

Under the conditions of thermal reaction (1022-1293°F, LHSV = 20), 1,2,4,5-TeMCH was the most reactive of all the naphthenes tested. With this feedstock at 1202 and 1293°F conversions of 53.0% and 72.2%, respectively.

a) Liquid Hourly Space Velocity = volumes of feed/volume of catalyst/hour.

TABLE 1
DEHYDROGENATION OF 1,2,4,5-TETRAMETHYLCYCLOHEXANE

Pressure: 10 atm

Reaction	Feed	Thermal				Catalytic			
Run Number 9645-		110	111	112-1	112-3	107	108	109-1	109-3
Catalyst		Quartz Chips				1% Pt on Al_2O_3			
Catalyst Vol, ml		20				?			
LHSV		20				100			
Temperature, °F									
Block		1022	1112	1202	1293	842	932	1022	1022
Wall		1017	1101	1175	1244	730-29	812-03	903-90	990-1013
Catalyst Bed		995	1065	1114	1157	626-44	693-732	808-993	993-1002
						617-19	686-89	768-975	975-1002
						650-44	716-12	795-916	916-1000
						671-62	745-34	830-66	866-997
Reaction Period, min		20				30	30	15	15
Product Analysis, %w									
Cracked[a]	-	0.9	4.5	8.4	8.4	-	-	-	0.3
Heptane	-	0.1	0.5	1.1	1.9	-	-	-	-
MCH	-	0.3	0.6	1.3	1.6	-	-	-	-
DMCH	-	0.2	2.1	1.7	1.7	-	-	-	-
Tri-MCH	-	0.2	0.3	1.8	2.2	-	-	-	-
U_1[b]	-	-	-	0.5	0.5	-	-	-	-
U_2[b]	-	0.1	0.7	1.1	0.8	-	-	-	-
U_3[b]	-	0.2	1.2	2.2	1.4	-	-	-	0.4
Feed + Benzene[c]	0.3	1.6	2.1	2.4	3.6	10.5	6.9	2.9	1.7
Feed	40.8	42.3	42.6	25.9	9.2	21.6	18.4	19.4	35.1
U_4[e]	-	-	-	2.9	3.1	-	-	-	-
Feed	9.4	8.5	6.7	4.1	1.7	3.6	2.3	3.1	8.3
Feed + Toluene[d]	48.9	44.0	30.2	16.1	13.3	5.6	3.1	6.7	34.4
U_5[e]	-	0.5	1.3	1.9	1.0	-	-	0.5	5.0
Xylene	-	1.0	2.0	7.3	12.3	-	-	0.1	0.5
Xylene	-	0.1	0.1	1.4	2.0	-	-	-	-
Tri-MB	-	-	0.2	1.1	2.4	-	0.6	2.9	1.2
U_6[e]	-	-	-	0.1	0.5	-	0.5	1.2	-
1,2,4,5-TeMB	-	-	-	-	-	58.7	68.2	63.2	12.5
Light Gas	-	-	5.0	18.8	32.6	-	-	-	-
1,2,4,5-TeMCH Conversion, % w	-	4.9	19.6	53.0	72.2	68.3	75.3	69.9	21.3
Selectivity for 1,2,4,5-TeMB, % w	-	-	-	-	-	85.9	90.6	90.4	58.7
k, sec^{-1}	-	0.010	0.049	0.177	0.312	0.981	1.273	-	-
E, act, kcal/mole	-	49.0				5.4			
Heat Sink, Btu/lb									
Reaction	-	7	29	80	78	376	429	391	78
Total at Block Temp	-	672	794	892	998	926	1044	1076	763
Total at 1340°F	-	957	979	1010	1028	1326	1379	1341	1029

a) C_6 and lighter paraffins and olefins.
b) Unidentified; presumed to be partially dehydrogenated naphthenes.
c) Feed = 0.9%, the rest taken as benzene as feed isomer and benzene not separable.
d) Not separable on our column; assume no toluene formed.
e) Unidentified.

were observed (Table 1). Product material was liquid and gaseous cracked material and alkyl aromatics. Product distribution of the light gas fraction is shown in Table 2. Heat sinks due to reaction were 60 Btu/lb and lower due to hydrogen transfer reactions.

First order rate constants were calculated from the overall feed conversions based on the wall temperatures, from which an apparent activation energy of 49.0 kcal/mole was computed. An Arrhenius plot of the data did not give a straight line (Figure 5) and the activation energy value was based on the best straight line drawn through the points. Actually, from the plot of the data it appears that the activation energy decreases with increasing temperature (or conversion) which suggests that at higher temperatures reactions with lower activation energies are becoming more predominant.

Based on a comparison of first order rate constants at 1202°F, the reactivity of 1,2,4,5-TeMCH ($k = 0.18$ sec^{-1}) was greater than all other naphthenes tested. (cf Table 16)[3]

Catalyst Stability Tests With Methylcyclohexane

Bench-scale tests on the dehydrogenation of methylcyclohexane over both the laboratory 1% Pt on Al_2O_3 and over the UOP-R8 catalysts showed a loss in activity of about 2% over a 90-minute reaction period (ca 1.3%/hr) when the reactor was operated at high MCH conversion.[2] While this activity decline rate could be tolerable for our intended catalyst application, it was germaine to see if catalyst stability improved or declined with further use. At the same time it was of interest to investigate the effect of a feed antioxidant (IONOL) on catalyst stability (earlier tests had indicated no gross effect).

Three extended series of runs were carried out over a ten-hour period at 10 atm pressure, 1022°F, and at LHSV of 50. These tests were done with pure MCH over the 1% Pt on Al_2O_3 catalyst and over the UOP-R8 catalyst, and with MCH feed containing 50 ppm IONOL over the UOP-R8 catalyst. In these experiments the dehydrogenations were interrupted for 15 minutes after 6 hours reaction in order to refill the liquid feed reservoir. During this time the catalyst was contacted with hydrogen at the reaction temperature. In these tests the change in MCH conversion was taken as a measure of the change in catalyst activity. The data are tabulated in Tables 3, 4, and 5.

In all three tests the change in catalyst stability appeared to follow the same pattern (see Figure 6). Catalyst activity declined rather rapidly initially and then more slowly and at a constant rate after 1-2 hours reaction time. Hydrogen treatment enhanced the activity temporarily.

In the tests conducted with pure MCH feed, the activity and stability of the 1% Pt on Al_2O_3 catalyst was greater than the UOP-R8 (see Figure 6). Thus, after three hours' reaction time the constant activity decline of the Pt on Al_2O_3 catalyst was 0.44%/hour compared to 0.58% per hour for the UOP-R8 catalyst. With IONOL both activity and catalyst stability (UOP-R8) were lower than with the pure MCH feed (0.83%/hr). Thus it appears that IONOL in concentrations of 50 ppm is deleterious to both catalyst activity and catalyst stability.

TABLE 2
THERMAL REACTION OF 1,2,4,5-TETRAMETHYLCYCLOHEXANE

Gas Phase Product Distribution

Pressure: 10 atm
LHSV: 20

Run Number	111	112-1	112-3
Block Temperature, °F	1112	1202	1293
Conversion to Light Gas, %w	5.0	18.8	32.6
Product Analysis, %v			
H_2	9.8	11.5	11.4
CH_4	73.8	65.8	61.3
C_2H_4	2.8	3.5	4.4
C_2H_6	6.1	6.8	7.0
C_3H_6	5.5	7.8	8.8
C_3H_8	0.8	1.5	1.8
C_4H_8	-	0.2	0.3
C_4H_6	0.8	2.0	3.4
C_4H_{10}	-	0.2	0.3
Higher than C_4	0.4	0.7	1.3

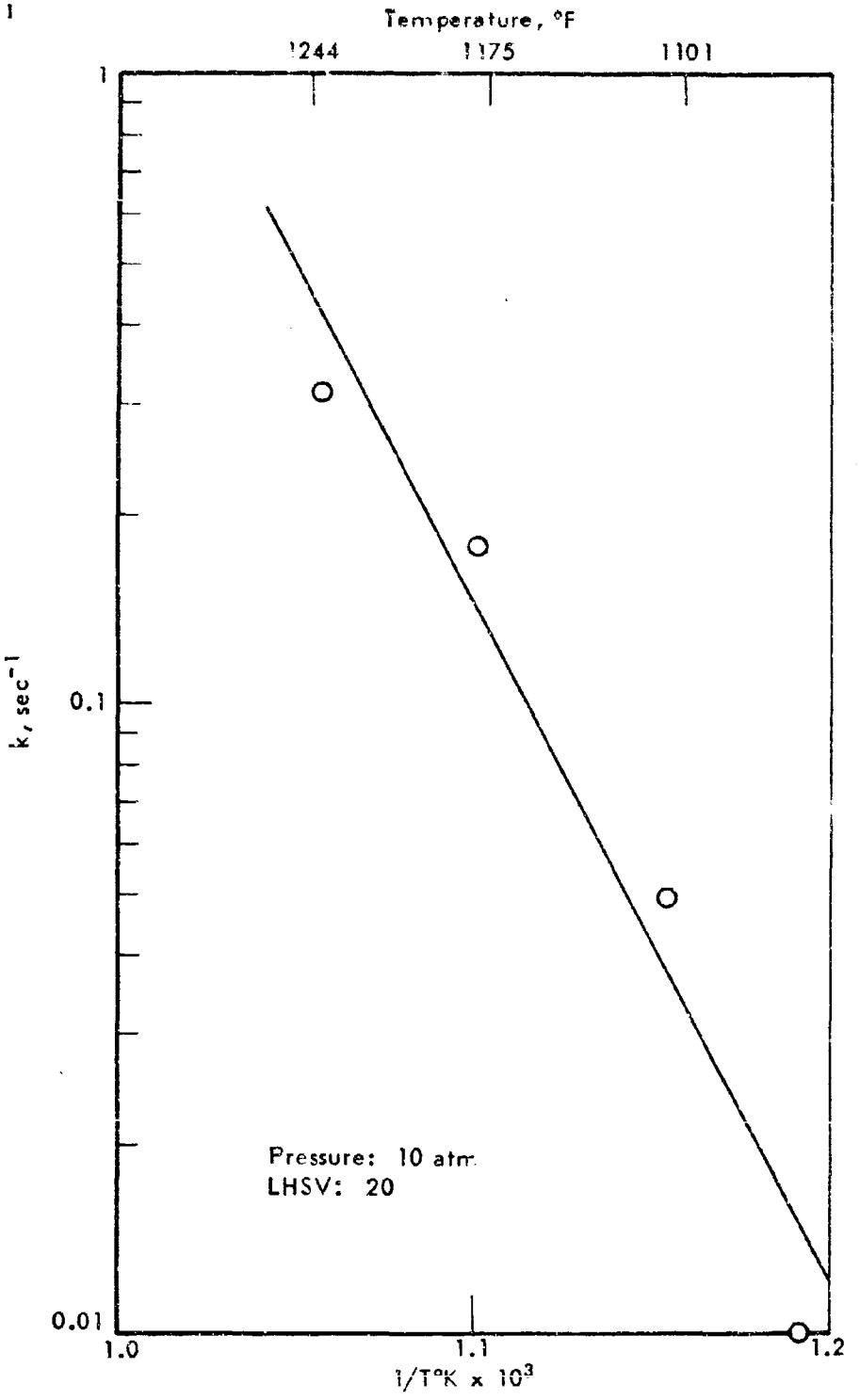


Figure 5. THERMAL REACTION OF 1,2,4,5-TETRAMETHYLCYCLOHEXANE TEMPERATURE COEFFICIENT

Table 3. DEHYDROGENATION OF MCH OVER UOP-R8 CATALYST: LIFE TEST

Feed: Pure MCH Catalyst volume: 7 ml
Pressure: 10 atm Block temperature: 1022°F
LHSV: 50

Run No. 934T-	Reaction Time, hr	Temperature, °F		Product Analysis, %					MCH Conv., %
		Wall	Catalyst	Cracked	MCH	Methyl-Cyclohexane	Benzene	Toluene	
111-1	0.25	887	694	0.2	4.8	0.0	0.5	94.5	95.2
111-2	0.5	878	691	0.2	5.6	0.0	0.3	93.9	94.4
111-3	1.0	873	686	0.2	6.5	0.0	0.3	93.0	93.5
111-4	1.5	871	682	0.2	7.2	0.0	0.3	92.3	93.8
111-5	2.0	871	680	0.2	7.9	0.0	0.2	91.7	92.1
111-6	2.5	869	680	0.2	8.9	0.0	0.2	90.7	91.1
112-1	3.0	869	678	0.2	9.1	0.0	0.2	90.5	90.9
112-2	3.5	869	678	0.2	9.0	0.0	0.2	90.6	91.0
112-3	4.0	869	676	0.2	9.6	0.0	0.2	90.0	90.4
112-4	4.5	873	678	0.2	9.5	0.0	0.2	90.1	90.5
112-5	5.0	869	676	0.2	9.7	0.0	0.3	89.8	90.3
112-6	5.5	864	676	0.2	10.6	0.2	0.3	88.7	89.4
113-1	6.0	869	676	0.1	10.5	0.1	0.2	89.2	89.5
113-2[a]	6.25[a]	880	705	0.3	8.4	0.1	0.4	90.8[a]	91.6[a]
113-3	6.5	880	698	0.3	9.4	0.1	0.2	90.0	90.6
113-4	7.0	880	694	0.3	10.5	0.1	0.2	88.9	89.5
114-1	7.5	878	691	0.2	11.5	0.1	0.2	88.0	88.5
114-2	8.0	876	689	0.2	11.0	0.1	0.2	88.5	89.0
114-3	8.5	871	689	0.2	11.5	0.1	0.2	88.0	88.5
114-4	9.0	874	689	0.2	12.4	0.1	0.2	87.1	87.6
114-5	9.5	873	686	0.2	12.3	0.0	0.2	87.3	87.7
114-6	10.0	878	686	0.2	12.7	0.1	0.1	86.9	87.3

a) Catalyst hydrogen treated at 1022°F for 15 minutes before this run.

Table 4. DEHYDROGENATION OF MCH OVER 1% Pt ON Al_2O_3 CATALYST: LIFE TEST

Feed: Pure MCH Catalyst volume: 7 ml
Pressure: 10 atm Block temperature: 1022°F
LHSV: 50

Run No. 9347-	Reaction Time, hr	Temperature, °F		Product Analysis, %				MCH Conv., %
		Wall	Catalyst	Cracked	MCH	Benzene	Toluene	
123-1	0.25	860	707	0.1	1.4	0.8	97.7	98.6
123-2	0.5	855	704	0.1	1.9	0.2	97.8	98.2
123-3	1.0	853	698	0.1	3.9	0.3	95.1	96.1
123-4	1.5	851	698	0.1	4.1	0.3	95.5	95.9
123-5	2.0	851	696	0.1	5.2	0.2	94.5	94.8
123-6	2.5	849	693	0.1	5.0	0.2	94.7	95.0
124-1	3.0	849	693	0.1	6.0	0.2	93.7	94.0
124-2	3.5	849	693	0.1	6.0	0.2	93.7	94.0
124-3	4.0	847	691	0.1	6.3	0.2	93.4	93.7
124-4	4.5	847	689	0.1	6.0	0.2	93.7	94.0
124-5	5.0	842	686	0.1	6.9	0.2	92.8	93.1
124-6	5.5	847	689	0.1	6.4	0.2	93.3	93.6
125-1	6.0	846	689	0.1	7.3	0.2	92.4	92.7
125-3	6.25[a]	866	711	0.1	3.9[a]	0.3	95.7	96.1
125-4	6.50	867	709	0.1	4.2	0.3	95.4	95.8
126-1	7.0	869	707	0.1	4.4	0.3	95.2	95.6
126-2	7.5	867	707	0.1	5.2	0.3	94.4	94.8
126-3	8.0	858	702	0.1	6.2	0.4	93.3	93.8
126-4	8.5	853	696	0.1	7.5	0.2	92.2	92.5
126-5	9.0	851	696	0.1	7.9	0.2	91.8	92.1
127-1	9.5	849	689	0.1	8.2	0.2	91.5	91.8
127-2	10.0	849	689	0.1	8.7	0.2	91.0	91.3

a) Catalyst hydrogen treated at 1022°F for 15 minutes before this run.

Table 5. DEHYDROGENATION OF MCH PLUS "IONOL" OVER UOP-R8 CATALYST: LIFE TEST

Feed: MCH + 50 ppm IONOL Catalyst volume: 7 ml
Pressure: 10 atm Block temperature: 1022°F
LHSV: 50

Run No. 9347-	Reaction Time, hr	Temperature, °F		Product Analysis, %					MCH Conv., %
		Wall	Catalyst	Cracked	MCH	Methyl-cyclohexane	Benzene	Toluene	
117-1	0.25	890	694	0.2	6.8	0.1	0.5	92.4	93.2
117-2	0.5	890	691	0.2	7.2	0.1	0.3	92.2	92.8
117-3	1.0	887	686	0.2	8.8	0.1	0.2	90.7	91.2
117-4	1.5	887	680	0.2	9.2	0.1	0.2	90.3	90.8
117-5	2.0	882	680	0.2	9.5	0.1	0.2	90.1	90.5
117-6	2.5	880	680	0.2	10.3	0.1	0.2	89.2	89.7
118-1	3.0	884	678	0.2	10.8	0.1	0.2	88.7	89.2
118-2	3.5	880	678	0.2	11.0	0.2	0.3	88.3	89.0
118-3	4.0	885	678	0.2	11.6	0.1	0.2	87.9	88.4
118-4	4.5	878	676	0.2	11.9	0.1	0.2	87.6	88.1
118-5	5.0	884	678	0.2	12.1	0.1	0.2	87.4	87.9
118-6	5.5	876	676	0.2	12.8	0.1	0.2	86.8	87.2
119-1	6.0	884	676	0.2	13.1	0.1	0.2	86.4	86.9
119-2[a]	6.25[a]	887	698	0.2	8.7	0.2	0.4	90.5	91.3
119-3	6.5	882	696	0.3	12.6	0.2	0.2	87.6	87.4
119-4	7.0	882	693	0.2	12.8	0.2	0.2	86.6	87.2
120-1	7.5	880	691	0.2	13.4	0.1	0.2	86.1	86.6
120-2	8.0	880	689	0.2	14.2	0.1	0.2	85.3	85.8
120-3	8.5	876	689	0.2	14.1	0.1	0.2	85.4	85.9
120-4	9.0	878	689	0.2	15.5	0.1	0.1	84.2	84.5
120-5	9.5	876	687	0.2	14.6	0.1	0.1	85.0	85.4
120-6	10.0	876	685	0.2	15.4	0.2	0.1	84.1	84.6

a) Catalyst hydrogen treated at 1022°F for 15 minutes before this run.

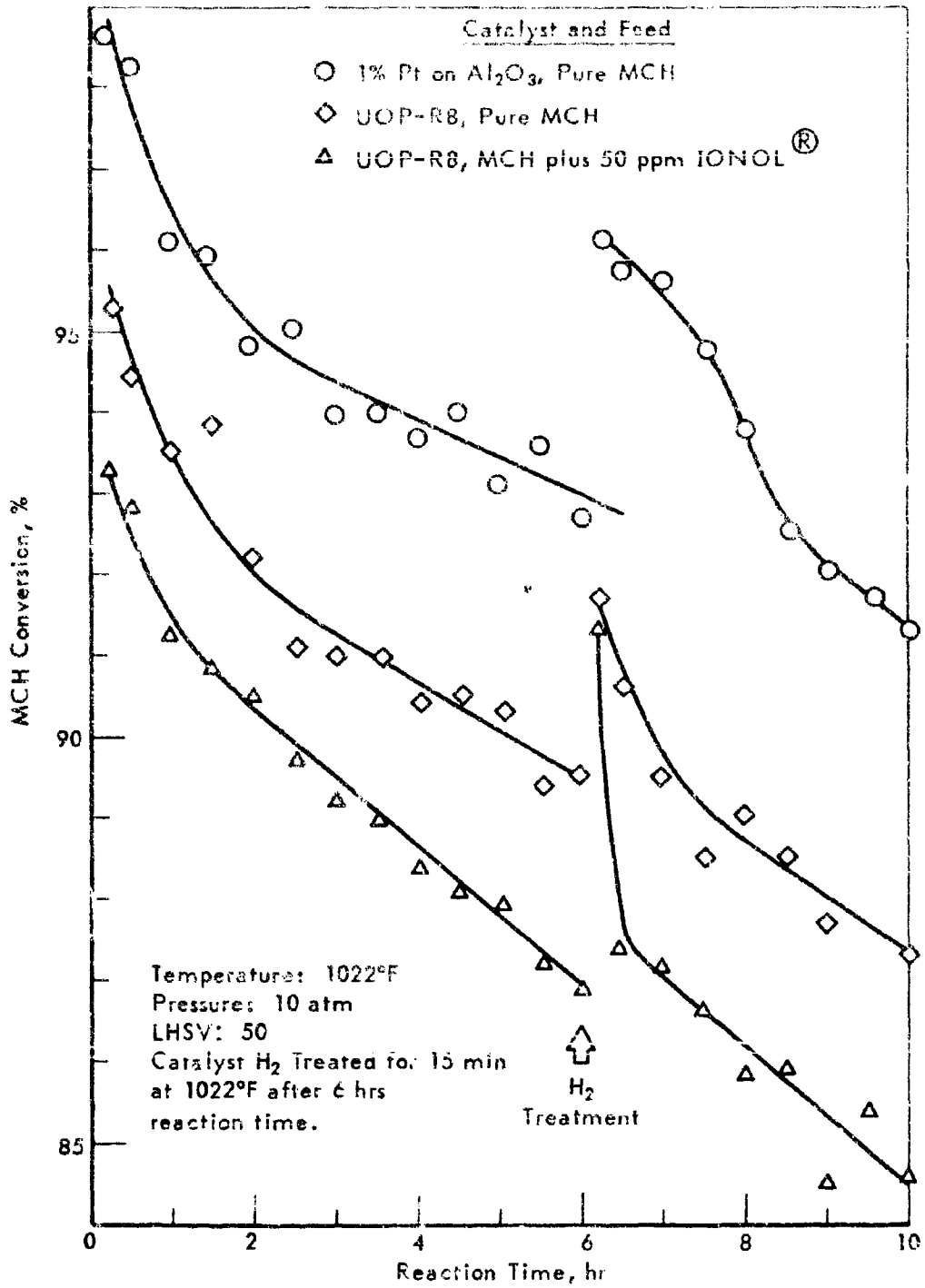


Figure 6. DEHYDROGENATION OF METHYLCYCLOHEXANE CATALYST LIFE TESTS

Bench-Scale Catalyst Evaluation Tests With Methylcyclohexane

The present contract calls for a catalyst development program in which candidate catalysts are rapidly screened in a micro-scale reactor (MICTR), and then the most promising are further evaluated in bench-scale tests. A bench-scale test procedure for dehydrogenation catalysts using methylcyclohexane feedstock has been devised, which gives a measure of the effect of temperature, pressure, space velocity (i.e., contact time) and catalyst stability over a three-hour test period using a single charge of catalyst. This test involves making a series of runs at 842 and 1022°F, 10 and 30 atm, and LHSV's of 50 and 100.

A number of catalysts that appeared promising under micro-scale testing were evaluated in our bench-scale test reactor. These catalysts contained varying amounts of active materials mounted on various supports. The tests were done in two groups with a test with the standard laboratory catalyst done in each group for reference. During the interval between the first and second series of tests, the Meehanite furnace liners warped and had to be replaced. The new liners made better contact with the reactor tube than did their predecessors. Presumably this better metal-to-metal contact enhanced the heat conductivity of the system and resulted in the higher MCH conversions for a given block temperature that was observed in the second series of runs.

The results of the tests, the conditions of each run, and the order in which the runs were made are shown in Table 6. Each catalyst was rated as to "Relative Performance". This rating was designed to show how the catalyst was performing at the end of the test, relative to the standard catalyst and quantitatively was taken as the ratio of the first order rate constant with the catalyst (k_c) to that with the standard catalyst (k_s) calculated from the MCH conversion of Run No. 7. Based on this criteria several of the catalysts tested appeared to be 25% to 50% better than the standard catalyst. Activation energies for the various catalysts ranged from 10 to 17 kcal/mole. These values were calculated from the first order rate constants obtained from the data of Runs 1 and 2. Generally, there was a parallelism between the ratio of the rate constants and the ratio of the activation energies (E_c/E_s) indicating that the better catalysts would be even more superior than the standard catalyst at higher temperatures. However, factors such as catalyst stability, effect on side reactions, and regenerability remain to be investigated. This will be studied in the course of future work.

Thermal Reaction of Methylcyclohexane Over Alumina

It was of interest to test the reaction of MCH over the aluminas that were used as supports for our platinum catalysts. These tests were carried out in the same manner as the thermal reaction tests, with alumina substituted for quartz chips (pages 20-22, reference 2, for detailed run procedures). Both Harshaw 0104 alumina and UOP RS Base alumina were tested at 10 atm pressure, 1022-1293°F and at LHSV of 20 (20 ml alumina; 10-20 mesh).

Methylcyclohexane reacted readily over both aluminas to give cracked and dehydrogenated products. The liquid products were identified by GLC

Table 6. EVALUATION OF VARIOUS CATALYSTS: DEHYDROGENATION OF MCH

Feed: Pure Methylcyclohexane
Reaction Time: 20 min

Run No.	1	2	3	4	5	6	7	E_{act}, kcal/mole	Ratio E_o/E_i	Relative Performance, k_o/k_i
Block Temp. °F	842	<--			902		-->			
Pressure, atm	10	10	30	10	10	10	10			
LHSV	100	100	100	100	50	100	100			
MCH Conversion, %w, for Catalyst No.										
	First Series									
9374	43.4	67.4	61.2	69.3	94.8	66.5	65.1	11.0	1.0	1.00
8A	43.7	66.9	61.1	68.2	93.4	64.0	64.5	11.7	0.99	1.01
8B	43.4	67.2	61.6	69.6	95.1	66.7	66.6	11.4	0.97	1.06
10A	42.6	65.5	60.7	67.7	94.6	65.6	66.2	11.8	1.0	1.00
10B	42.6	64.2	60.0	63.6	92.6	62.8	63.0	10.8	0.96	0.96
13A	43.5	63.9	60.1	69.3	95.1	64.8	65.3	10.9	0.93	1.01
13B	41.9	59.6	58.8	62.6	87.5	61.2	56.5	8.1	0.69	0.82
9A	36.0[c]	47.2[c]	49.7[c]	47.5[c]	69.0[c]	42.1[c]	39.7[c]	-	-	0.58
9B	34.0[c]	13.4[c]	<--		(b)		-->	-	-	(b)
35	35.2[c]	40.8[c]	42.7[c]	37.4[c]	46.7	(b)	(b)	-	-	(b)
95A	45.6	72.8	64.9	74.2	97.8	72.1	72.6	15.2	1.28	1.28
65B	41.1	66.3	58.2	68.4	95.9	63.9	66.6	11.7	0.99	1.07
108A	47.7	80.9	68.6	80.8	99.5	78.2	78.0	13.7	1.16	1.52
73	47.1	76.1	66.4	75.8	97.9	74.9	74.6	13.0	1.10	1.32
18D	46.2	69.9	65.2	70.3	99.0	67.6	67.8	9.9	0.84	1.00
117B	46.8	78.3	65.7	79.0	99.4	75.8	75.6	13.6	1.16	1.35
130	44.3	73.6	62.4	74.4	98.7	72.3	71.9	13.1	1.11	1.32
193B	48.6	78.9	67.4	78.0	97.6	77.1	77.1	13.4	1.24	1.04
197A	48.2	77.9	65.4	77.7	97.7	75.3	75.3	12.7	1.18	1.27
197B	47.6	76.9	67.7	79.1	98.5	77.6	77.4	13.1	1.21	1.35

a) Standard 1% Pt on Al_2O_3 Catalyst.
b) Catalyst Inactive
c) Catalyst Deactivating During the Test.

(Continued)

Table 6 (Contd). EVALUATION OF VARIOUS CATALYSTS: DEHYDROGENATION OF MCH

Feed: Pure Methylcyclohexane
Reaction Time: 20 min

Run No.	1	2	3	4	5	6	7	Eact, kcal/mole	Ratio, E_c/E_s	Relative Performance, k_c/k_s
Block Temp, °F	842	←		1022			→			
Pressure, atm	10	10	30	10	10	10	10			
LHSV	100	100	100	100	50	100	100			
MCH Conversion, %w, for Catalyst No.										
					Second Series					
9874- 7a)	52.3	78.0	72.6	80.1	97.0	75.2	75.5	11.9	1.0	1.00
161B	51.6	84.9	76.1	86.1	99.5	84.4	84.8	16.4	1.38	1.31
163A	44.8	68.0	65.9	66.1	75.5	40.8	(b)	(c)	-	(c)
165B	46.5	74.7	69.2	76.2	94.2	72.4	72.1	7.54c)	0.62	0.33c)
172B	46.9	67.0	68.1	70.2	88.7	58.0	46.0	4.12c)	0.35	0.18c)
186A	48.5	71.9	67.2	74.8	93.6	71.9	71.8	6.8	0.58	0.31
189A	52.4	82.5	75.9	85.4	99.0	78.8	78.8	17.2	1.44	1.07
156B	50.3	82.1	74.5	83.6	98.7	81.1	81.1	16.5	1.39	1.13
121B	60.7	83.4d)	80.9	24.8e)	-	-	-	9.1	-	-
10280- 16A	50.0	78.7	72.9	81.4	97.7	76.6	77.1	12.4	1.04	1.04
10280- 24C	50.6	80.7	73.0	82.2	99.3	79.9	79.1	12.3	1.04	1.11
9874-121A	56.8	84.3c)	81.7c)e)	(b)	-	-	-	10.1	0.84	-

a) Standard 1% Pt on Al_2O_3 Catalyst.
b) Catalyst Inactive.
c) Catalyst Deactivating During the Test.
d) Selectivity for Toluene = 64.4%.
e) Selectivity for Toluene = 63.5%.

analysis as methylcyclohexenes, methylcyclohexadienes,[a] benzene, toluene, and cracked material (Table 7). Analysis of the light gas products are shown in Table 8. At 1203°F (block temperature) extensive reaction occurred with about 60% of the MCH converted. Under these reaction conditions 100-150°F temperature differences were observed between the block and catalyst bed temperatures. Heat sinks were low however due to exothermic hydrogen transfer reactions between the products. Lower conversions and heat sinks were observed at lower temperatures. MCH was more reactive over the Harshaw 0104 than over the UOP support. The data are presented in Table 7, which also includes data obtained previously,[2)3)] with quartz chips.

First order rate constants were computed from the conversion of MCH. Based on these values at 1202°F the reactivity of MCH was 1.6/1.5/1 over Harshaw alumina, UOP alumina, and quartz chips. Further, the yields of dehydrogenated products and light gas products obtained with the aluminas were greater than those obtained with quartz chips. This enhanced reactivity of MCH over alumina could be a diffusion effect reflecting the greater pore volumes, and hence holding time, of the aluminas. Activation energies were computed from the first order rate constants and were 44.9 and 40.3 kcal/mole for Harshaw and UOP alumina, respectively, compared to 46.1 kcal/mole for the quartz chips. Figure 7 is an Arrhenius plot of the data for all three systems. It is doubtful that the differences in E values are significant. Although it is evident that the aluminas are weak catalysts for the cracking reaction, the effect in the temperature region of interest for catalytic reactions (i.e., below 1050°F) is probably unimportant.

Thermal Reaction of Ethylcyclohexane

The thermal reaction of ethylcyclohexane(ECH) was studied briefly under the previous contract.[2)] This naphthene appeared to be considerably less stable than the other monocyclic naphthenes that were subsequently tested. The ECH feedstock was a commercial product, "Practical" grade and was passed over silica gel prior to use. Because the reactivity of this material was so much greater than that of the other monocyclic naphthenes, it was suspected that impurities present might be acting as "initiators" for the thermal reaction. Consequently a high purity ECH feedstock was prepared by the hydrogenation of ethylbenzene. This feed was tested at 10 atm pressure, 1022-1239°F, at LHSV of 20. The data are tabulated in Table 9.

The reactivity of this lot of ECH was lower than that of the "Practical" grade and was the same as that of MCH under the above test conditions. For example, at 1202°F a first order rate constant of 0.08 sec^{-1} was observed for both MCH and high purity ECH compared to 0.26 sec^{-1} for the "Practical" grade ECH (Table 15).[2)] With the high purity ECH the reaction was highly exothermic due to hydrogen transfer reactions and had a calculated exothermic heat of reaction of 500 Btu/lb at complete conversion. The product distribution for the light gas products is shown in Table 10. From the first order rate constants an activation energy of 48.7 kcal/mole was calculated compared to 47 kcal/mole with the "Practical" ECH. Figure 8 is an Arrhenius plot of the data. Figure 9 shows the relative reaction rates and activation energies for the thermal reaction of various naphthenes. This includes the data for high purity ECH and replaces Figure 9 in a previous report.[3)]

a) See footnote (a), page 22 of reference 2.

TABLE 7
THERMAL REACTION OF METHYLCYCLOHEXANE

Pressure: 10 atm LHSV: 20
Catalyst Volume: 20 ml Reaction Time: 20 min

Catalyst	Quartz Chips			Harshaw Alumina-0104				UOP Alumina R8 Base			
Run Number	8277-			9645-				9645-			
	57	51	52	98	99	100-1	100-3	103-1	103-3	104	105
Temperature, °F											
Block	1112	1202	1295	1022	1112	1202	1293	1022	1112	1202	1293
Wall	-	1188	1256	1013	1100	1175	1247	1010	1094	1175	1245
Catalyst Bed	1067	1152	1191	962	1064	1107	1161	970	1033	1083	1136
Product Analysis, %w											
MCH	86.8	79.1	52.3	98.1	89.5	66.8	37.4	94.9	86.6	69.2	40.2
Methylcyclohexenes and Methylcyclohexadienes	2.8	7.7	10.5	1.3	3.3	5.3	5.1	0.7	1.8	3.7	5.2
Benzene	0.1	0.7	3.1	-	0.4	2.1	6.6	0.1	0.6	1.6	4.6
Toluene	0.2	0.4	2.2	-	1.1	7.6	20.8	2.2	5.0	7.8	12.5
Heavier Than Toluene	-	-	0.6	-	-	0.3	0.9	-	-	0.8	0.9
Cracked, Liquid[a]	8.2	7.3	13.6	0.6	2.5	7.9	10.4	1.6	3.9	8.5	12.4
Cracked, Light Gas	-	4.6	17.7	-	3.1	10.0	30.6	0.5	2.0	8.4	21.8
MCH Conversion	11.2	20.6	47.7	1.9	10.5	33.2	62.5	5.1	13.4	30.8	59.8
First Order Rate Constant, sec^{-1}	0.04	0.08	0.22	-	0.035	0.130	0.329	0.015	0.044	0.188	0.306
E, act, kcal/mole	<—— 46.1 ——>			-	<—— 44.9 ——>			-	<—— 40.3 ——>		
Heat Sink, Btu/lb											
Reaction	4	8	34	1	12	22	65	1	9	35	31
Total at Block Temp	924	1003	1104	848	932	1017	1135	843	929	1030	1101
Total at 1340	1124	1128	1157	1121	1132	1144	1185	1121	1129	1155	1151

a) Lighter than MCH.

TABLE 8
THERMAL REACTION OF METHYLCYCLOHEXANE

Gas Phase Product Distribution

Pressure: 10 atm
LHSV: 20
Catalyst Volume: 20 ml
Reaction Time: 20 min

Run Number	8277-58-2	9645-			
		100-1	100-3	104	105
Catalyst	Quartz Chips	Harshaw 0104 Alumina		UOP-R8 Base Alumina	
Block Temperature, °F	1293	1202	1293	1202	1293
Conversion to Light Gas, %w	21.5	10.0	30.6	8.4	21.8
Product Analysis, %v					
H_2	18.6	62.7	37.8	65.3	43.7
CH_4	39.4	21.6	31.1	21.4	30.4
C_2H_4	16.0	5.2	9.2	4.4	7.5
C_2H_6	11.0	4.8	8.9	4.0	7.5
C_3H_6	9.5	2.9	6.2	2.5	5.0
C_3H_8	2.1	1.2	2.6	1.0	2.2
C_4H_8	1.0	0.2	0.7	0.2	0.5
C_4H_6	2.6	1.1	2.4	0.9	2.0
C_4H_{10}	0.2	0.1	0.4	0.1	0.3
C_5H_{10}	-	0.1	0.3	0.1	0.3
C_5H_{12}	-	-	0.1	-	0.1
Higher than C_5	0.1	0.1	0.3	0.1	0.3

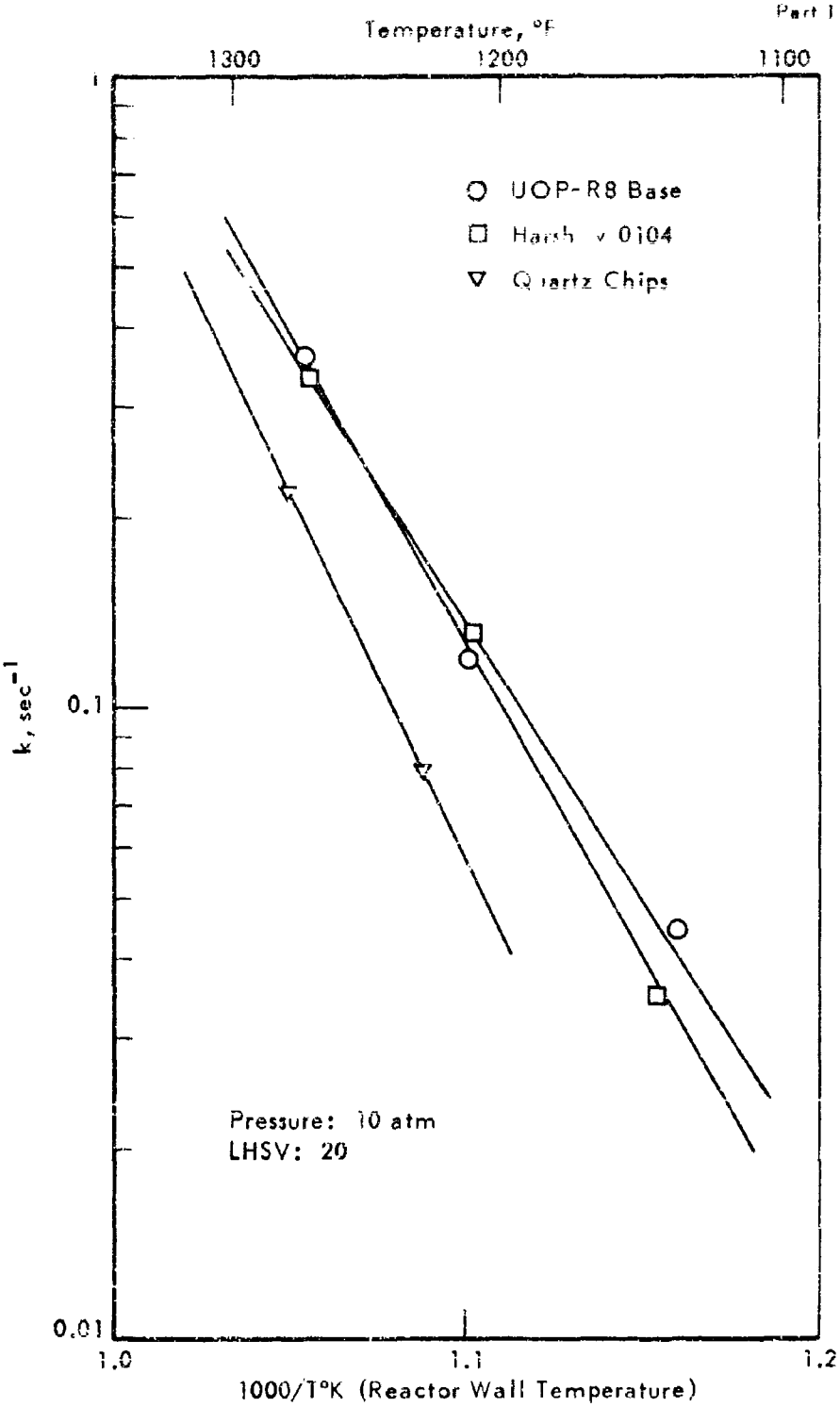


Figure 7. THERMAL REACTION OF METHYLCYCLOHEXANE OVER ALUMINA
Temperature Coefficient

Table 9. THERMAL REACTION OF ETHYLCYCLOHEXANE

Pressure: 10 atm
LHSV: 20
Catalyst: Quartz Chips

Reaction Time: 20 min
Catalyst Vol: 20 ml

Run No. 10100-	12	13	14-1	14-3
Temperature, °F	1022	1112	1202	1295
Block	1022	1112	1202	1295
Wall	1013	1101	1180	1247
Catalyst Bed	986	1072	1130	1175
Product Analysis, %w				
MCH	0.2	0.5	1.3	3.0
U_1 [a]	0.4	2.1	5.0	9.6
ECH	99.0	92.0	77.2	42.5
U_2 [a]	0.0	0.0	0.0	0.4
Benzene	0.0	0.3	0.9	4.8
U_3 [a]	0.0	0.2	0.5	1.0
Toluene	0.0	0.0	0.1	1.4
Ethylbenzene	0.0	0.0	0.0	0.4
Heavier Than Ethylbenzene	0.0	0.0	0.0	0.5
Cracked, liquid	0.4	2.0	5.0	11.0
Light Gas	0.0	3.0	10.0	26.3
ECH Conversion, %w	1.0	8.0	22.8	57.5
k, Overall, sec^{-1}	-	0.025	0.081	0.278
E, act, kcal/mole		← 48.7 →		

a) Unidentified.

Table 1C. THERMAL REACTION OF ETHYLCYCLOHEXANE: GAS PHASE PRODUCT DISTRIBUTION

Pressure: 10 atm
LHSV: 20

Run No. 10100-	13	14-1	14-3
Block Temperature, °F	1112	1202	1295
ECH Conversion, %w	8.0	22.8	57.5
Conversion to Light Gas, %w	3.0	10.0	26.3
Gas Product Analysis, %v			
H_2	12.6	11.5	12.8
CH_4	42.3	34.6	34.3
C_2H_4	21.1	23.3	21.3
C_2H_6	17.5	20.4	19.2
C_3H_6	2.7	5.1	6.4
C_3H_8	1.5	1.9	2.2
C_4H_6	0.5	1.0	1.0
C_4H_8	0.7	1.9	2.2
C_4H_{10}	0.0	0.0	0.1
C_5H_{10}	0.0	0.3	0.3

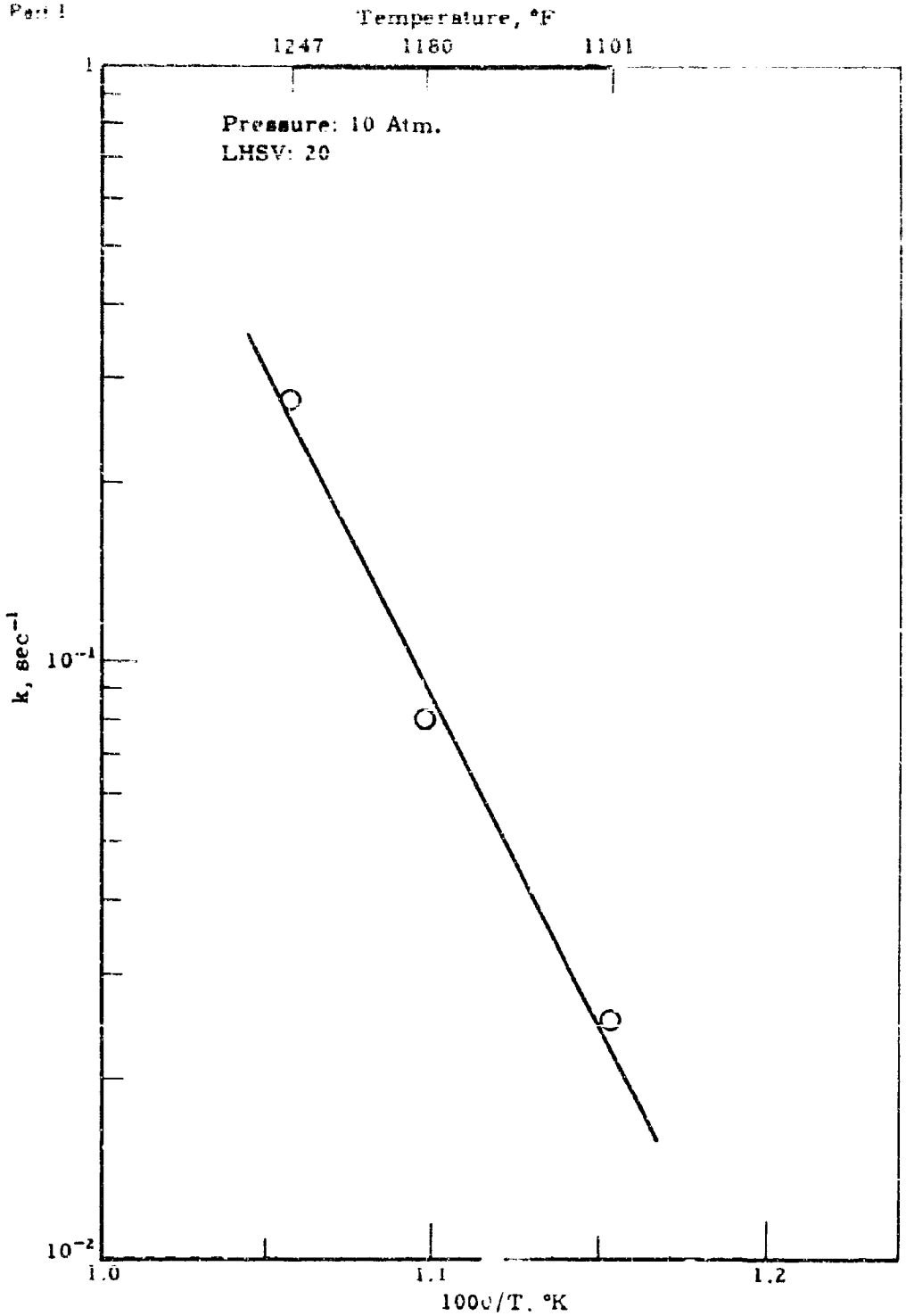


Figure 8. THERMAL REACTION OF ETHYLCYCLOHEXANE, TEMPERATURE COEFFICIENT

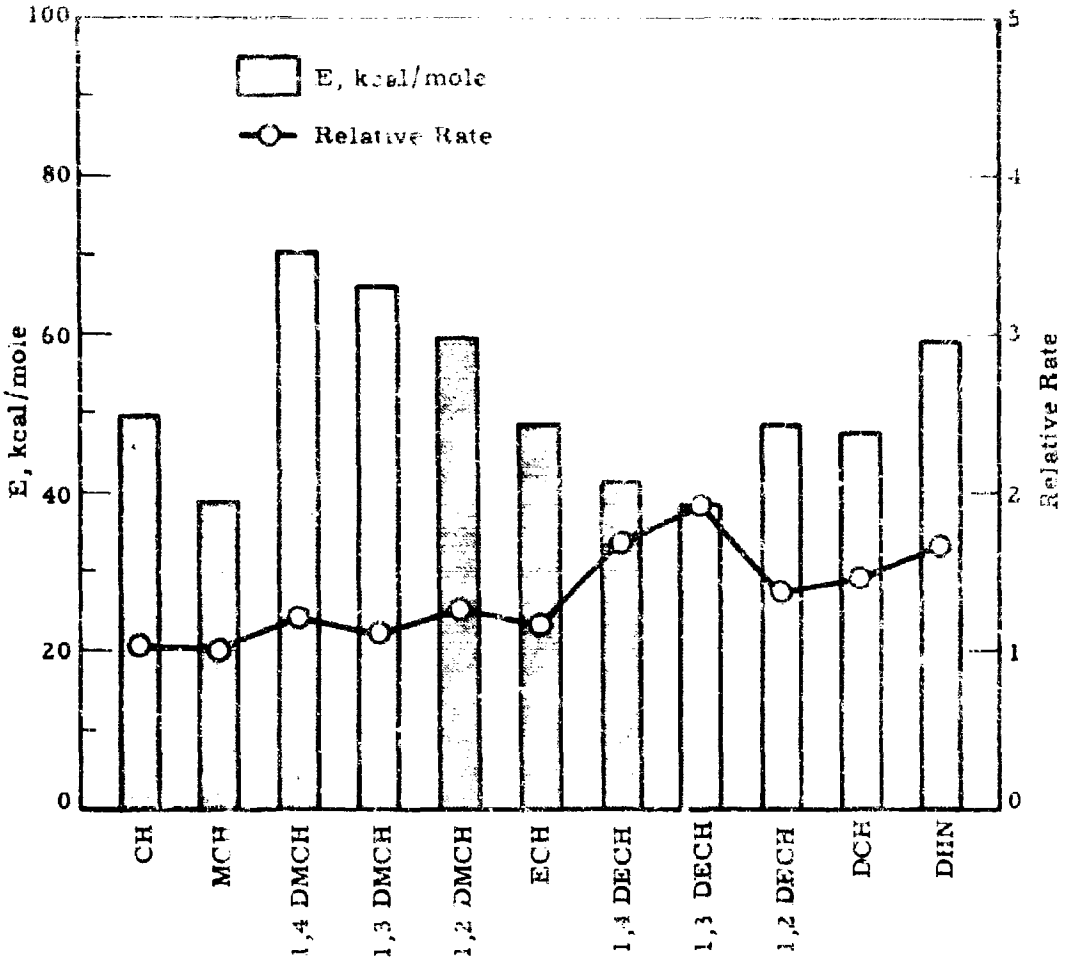


Figure 9. RELATIVE RATES AND ENERGIES OF ACTIVATION FOR THERMAL REACTION OF NAPHTHENES

If the employment of thermal cracking as a heat sink reaction becomes attractive, it will be worthwhile to investigate in more detail the nature of the impurities in the "Practical" grade of ECH that were responsible for the enhanced rate of reaction. However, it will also be necessary to determine if it is possible to simultaneously control the exothermic H-transfer reactions which reduce or destroy the endothermicity of the overall reaction.

Dicyclic Naphthenes

Dicyclohexyl

Reaction Rates for Dehydrogenation of Dicyclohexyl and Phenylcyclohexane

The dehydrogenation of dicyclohexyl (DCH) to dephenyl (DP) was shown to proceed in two detectable steps, in which phenylcyclohexane (PCH) was an intermediate product.[3] In this earlier work first order rate constants and apparent activation energies were calculated for the dehydrogenation reaction, based on the rate of disappearance of starting material. Presumably these values were for the first reaction step, namely DCH $\longrightarrow$ PCH + $3H_2$. Using the data of this earlier work, the rate constants and apparent activation energies now have been calculated for the second reaction step, PCH $\longrightarrow$ DP + $3H_2$, following the method of Wheeler.[18] In his treatment of a system using a porous catalyst, the fraction of DCH converted to PCH(α_B) in terms of the fraction of DCH reacted (α_A) and the selectivity factor S, is given by:

$$\alpha_B = \frac{S}{S-1}\left[(1-\alpha_A)^{\frac{1}{\sqrt{S}}} - (1-\alpha_A)\right] \qquad (1)$$

where $S = \frac{k_1}{k_2} = \frac{\text{rate constant for DCH} \longrightarrow \text{PCH}}{\text{rate constant for PCH} \longrightarrow \text{DP}}$

This equation is a rearrangement of Wheeler's Equation 92. By trial and error a value of S was obtained that satisfied equation (1) using values of α_B, α_A and k_1 obtained in previous work. It was then possible to obtain k_2 from S.

The results of these calculations with two different sets of data are presented in Table 11. At low temperature (842-932°F) the dehydrogenation of DCH to PCH was faster than the dehydrogenation of PCH to DP, and the overall reaction was more selective for PCH than DP. At 1020°F and higher the dehydrogenation of PCH to DP was faster and high selectivities for DP were obtained. The apparent activation energy for the reaction PCH $\longrightarrow$ DP, calculated from the rate constants (k_2), was 43 kcal/mole compared to 8 kcal/mole for DCH $\longrightarrow$ PCH. Figure 10 is an Arrhenius plot of the data. This suggests that the change in DP selectivity with temperature is at least in part, a kinetic effect.

When we study this reaction in the FSSTR where considerable pressure drop, higher linear velocities and different temperature profiles through the catalyst bed, it will be interesting to see if the

Table 11. COMPARISON OF REACTION RATES FOR DCH ——> PCH AND PCH ——> DP

Pressure: 10 atm
Feed: 98.4% DCH
1.6% PCH

Run No. 9426-	62-1	62-3	63	93-1	93-3	94-1
Temperature, °F						
Block	932	1022	1112	842	932	1022
Wall	819	880	963	756	824	891
α_A	0.590	0.664	0.761	0.530	0.592	0.665
α_B	0.220	0.138	0.082	0.314	0.216	0.134
S	1.8	0.6	0.38	5.0	1.5	0.6
First Order Rate Constant for, sec^{-1}						
k_1 = DCH ——> PCH	0.79	1.01	1.40	0.61	0.76	0.97
k_2 = PCH ——> DP	0.44	1.44	3.68	0.12	0.51	1.62

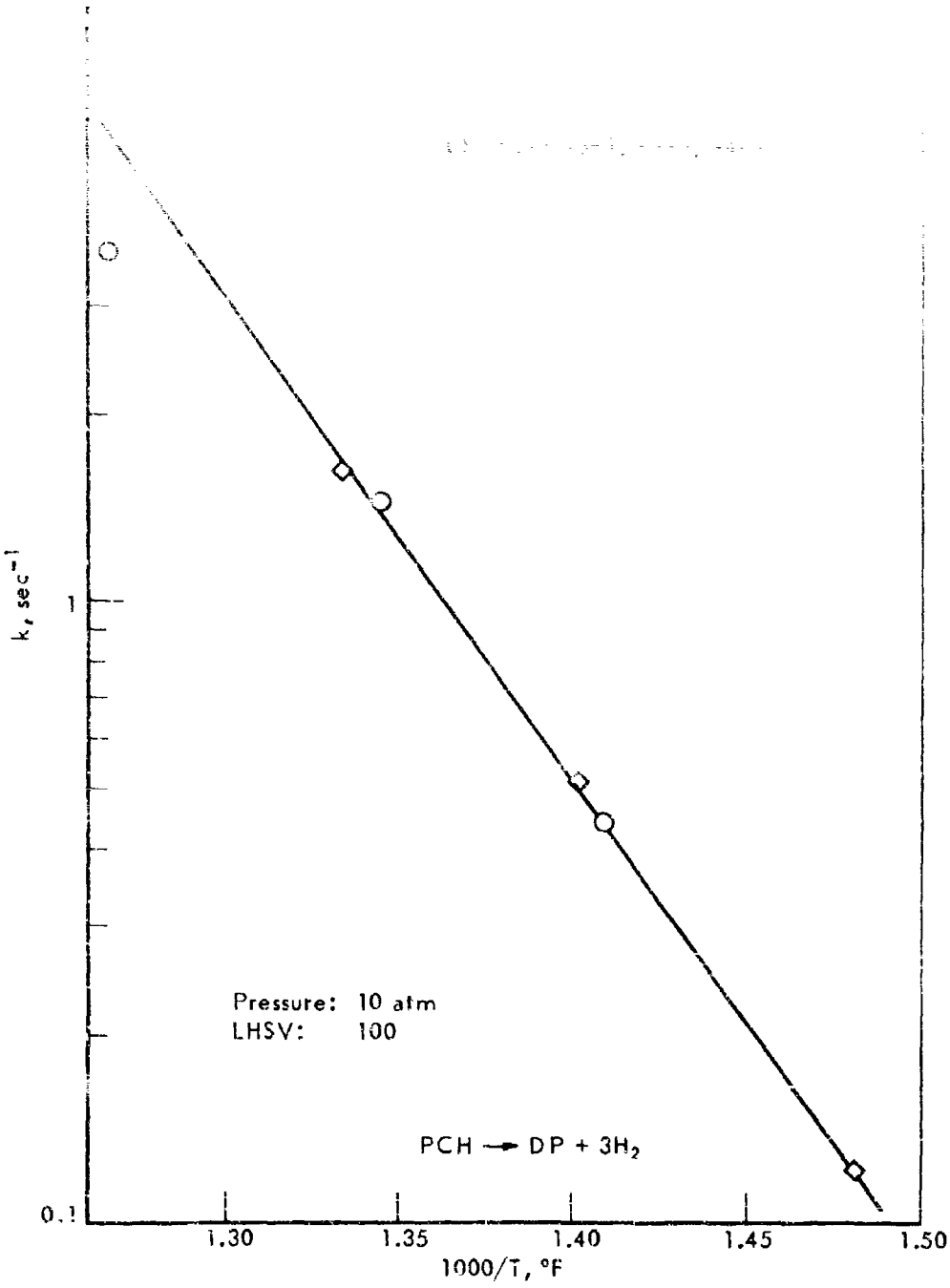


Figure 10. TEMPERATURE COEFFICIENT FOR THE DEHYDROGENATION OF PHENYL CYCLOHEXANE

additional complications introduced by the consecutive reactions can be handled by our packed bed reactor program.

Dehydrogenation Over UOP-R8 Catalyst

Good catalyst stability for the dehydrogenation of dicyclohexyl (DCH) was observed with our standard laboratory platinum on alumina catalyst.[3] For the dehydrogenation of decalin, moderately good stability was observed with this catalyst and poor stability with the UOP-R8 platinum catalyst.[3] Thus it was of interest to test this commercial catalyst for the dehydrogenation of dicyclohexyl.

The tests were done at 10 and 30 atm pressure, 842-1022°F at LHSV's of 30-100. The test procedures and the method of analyzing the reaction products were the same as used in the experiments with the laboratory catalyst.[3]

At 10 atm pressure, good catalyst stability was observed at 842°F. At higher temperatures, however, catalyst bed temperatures increased during the run, signifying catalyst deactivation (Table 12). At 1022°F the deactivation was considerable and the DCH conversion at this temperature was less than that observed at 932°F (Table 12). In these experiments the magnitude of the catalyst bed temperature increase was taken as a measure of catalyst deactivation. DCH conversions at 842 and 932°F observed with this catalyst were slightly higher than were observed with the laboratory catalyst; which suggests that initially the commercial catalyst was slightly more active. However, selectivities for diphenyl at a given conversion were slightly higher with the laboratory catalyst (Table 12; values obtained with the laboratory catalyst are shown in parentheses). These were abstracted from Table 22 of a previous report.[3]

Increasing the pressure appeared to stabilize the catalyst (Table 13). Also, operating the catalyst at elevated pressure appeared to stabilize the catalyst for operation at 10 atm pressure. For example, at 10 atm pressure and 1022°F an increase in catalyst bed temperature of only 41°F was observed after operation at 30 atm (842°F, Table 13) compared to an increase of 108°F after operation at 10 atm (842°F, 932°F, Table 12).

The effect of pressure on conversion and selectivity for diphenyl was about the observed with the laboratory catalyst. The data are recorded in Table 13 where the values obtained with the laboratory catalyst are shown in parentheses. These values were abstracted from Table 25 of a previous report.[3]

Operating the reactor at high conversion also appeared to stabilize the catalyst. Thus at 83.9% and 94.1% conversion increases in catalyst temperatures of only 26°F and 16°F, respectively, were observed (Table 14) compared to a temperature increase of 108°F at 60-65% conversion (Table 12; 10 atm pressure; 1022°F). The complete data for the runs a high conversion are shown in Table 14, which also shows the effect of space velocity on conversion and the effect of conversion on selectivity. The data obtained with the laboratory catalyst are shown in parentheses for comparison, and were abstracted from Table 24 of a previous report.[3]

Table 12. DEHYDROGENATION OF DICYCLOHEXYL OVER UOP-R8 CATALYST: EFFECT OF TEMPERATURE

Pressure: 10 atm
LHSV: 100
Catalyst Volume: 7 ml
Feed Composition: 97.2% DCH, 2.8% PCH

Run No. 10100-	24-1	24-2	25
Temperature, °F			
Block	842	932	1022
Wall	712	815-24	921-42
Catalyst Bed	663	671-87	781-878
	626	657-66	752-860
	628-6	658-50	727-63
	617-2	646-44	707-12
ΔT_{max} °F, catalyst bed	-5	+16	108
Product Analysis, %w			
Cracked	0.6	0.6	2.0
DCH	42.2	34.2	37.3
U_1 a)	0.0	0.3	3.0
PCH	37.9	30.0	16.6
U_2 a)	0.3	0.0	0.0
DP	19.0	34.9	41.1
DCH Conversion, %w	56.5	64.8	61.6
	(52.2)	(58.3)	(65.4)
Yield PCH, %w	35.1	26.7	13.6
Selectivity for, %w			
PCH	66.2	41.2	22.1
DP	33.3	55.4	69.6
	(40.8)	(63.5)	-
k, Overall, sec^{-1}	0.66	0.91	-

a) Unidentified.

Table 13. DEHYDROGENATION OF DICYCLOHEXYL OVER UOP-R8 CATALYST: EFFECT OF PRESSURE

LHSV: 100 Feed Composition: 97.2% DCH
Catalyst Volume: 7 ml 2.8% PCH

Run No. 10100-	33-1	33-2	34	35
Pressure	10	30	30	10
Temperature, °F				
Block	842	842	1022	1022
Wall	753-59	794-92	932-34	934-48
Catalyst Bed	648-44	691-93	750-52	747-88
	637-35	868	736-40	723-58
	61?-19	682	721	676-96
	617	684	727-25	682-91
ΔTmax, °F, catalyst bed	+2	+2	+4	41
Product Analysis, %w				
Cracked, liquid	0.5	1.2	2.7	0.8
DCH	42.8	54.4	23.0	27.5
U[a]	0.0	0.0	1.2	0.3
PCH	38.7	37.8	41.2	19.2
DP	18.0	6.6	31.9	52.2
DCH Conversion, %w	56.0	44.0	76.3	71.7
	(52.2)	(38.5)	(75.3)	(70.3)
Yield PCH, %w	35.9	35.0	38.4	16.4
Selectivity for, %w				
PCH	64.1	79.6	50.4	22.9
DP	33.3	15.5	43.0	75.0
	(38.4)	(16.9)	(40.5)	(74.2)
k, Overall, kcal/mole	0.680	0.230	0.454	1.206

a) Unidentified.

Table 14. DEHYDROGENATION OF DICYCLOHEXYL OVER UOP-R8 CATALYST: EFFECT OF CONVERSION ON SELECTIVITY FOR DIPHENYL

Pressure: 10 atm
Catalyst Volume: 7 ml
Feed Composition: 97.2% DCH, 2.8% PCH

Run No. 10100-	27-1	27-2	28-1	28-3
LHSV	50	30	50	30
Temperature, °F				
Block	842	842	1022	1022
Wall	774	779	936-38	948-54
Catalyst Bed	653	686-82	800-26	882-96
	633-35	622	772-92	810-26
	653	650-48	729-30	763-70
	658-55	655-53	738-29	781-771
ΔT_{max}, °F, Catalyst Bed	+2	-4	26	16
Product Analysis, %w				
Cracked	0.3	0.3	1.2	2.0
DCH	22.6	10.0	15.6	5.7
U[a)]	0.0	0.0	0.9	3.6
PCH	37.4	27.1	10.3	4.9
DP	39.7	62.6	72.0	83.8
DCH Conversion, %w	76.7	89.7	83.9	94.1
	(78.3)	(93.2)	-	(93.8)
Yield PCH, %w	34.6	24.3	7.5	2.1
Selectivity for, %w				
PCH	45.1	27.1	8.9	2.2
DP	53.4	71.6	88.3	91.6
	(57.0)	(79.0)	-	(95.4)
k, Overall, sec^{-1}	0.61	0.57	0.86	0.81

a) Unidentified.

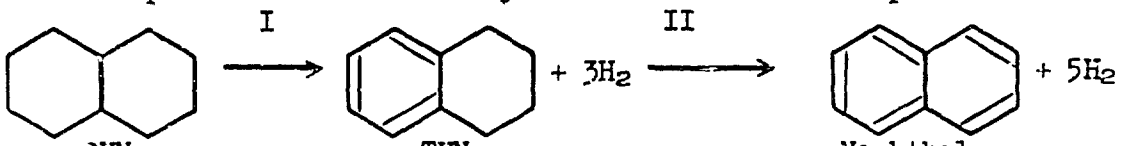
In summary then for the dehydrogenation of DCH, the commercial UOP-R8 catalyst was less stable and slightly less selective for diphenyl than the laboratory platinum catalyst. The effect of pressure and space velocity on conversion and on selectivity for diphenyl appeared to be the same with both catalysts. The commercial catalyst was stabilized by operating the reactor at a) higher pressures (20 to 30 atm); b) high conversion; c) 30 atm pressure prior to operation at 10 atm pressure. The effect of high pressure is generally favorable for the intended use since it is anticipated that the fuel will enter the reaction zone at several hundred pounds pressure. The effect of pressure and high conversion on catalyst stability during the dehydrogenation of naphthenes is discussed in detail in a later section.

Decalin

Reaction Rates and Equilibrium Constants for Dehydrogenation of Decalin and Tetralin

The study of the dehydrogenation of Decalin (DHN), initiated under the previous contract[2)3)] has been continued. Using data obtained in the previous work,[3)] data appearing in the literature,[4)19)] and data obtained from our laboratory experiments, equilibrium constants and first order reaction rate constants were calculated for the reactions DHN ⟶ Tetralin (THN) + $3H_2$ and THN ⟶ Naphthalene (N) + $2H_2$; relative rates of cis DHN to trans DHN and trans to cis isomerization and cis and trans DHN dehydrogenation were determined; and a series of experiments to determine the effect of reaction variables on two different platinum on alumina catalysts were carried out.

Under our test conditions the dehydrogenation of DHN to naphthalene (N) was a two-step process with tetralin (tetrahydrenaphthalene; THN) as an intermediate product. Schematically the reaction can be represented:



The heat of reaction to form THN is 670 Btu/lb.

Both reactions were equilibrium limited at high conversions and in the lower temperature region at both 10 and 30 atm pressure. Reaction II was faster than I and the back reaction was significant for II but not for I. Figure 11 shows the thermodynamic equilibrium constants for Reactions I (Kp_1) and II (Kp_2) as functions of temperature. Kp_2 was obtained by extrapolating the equilibrium data of Allam and Vlugter.[4)] Kp_1 was obtained using the data of Miyazawa and Pitzer[19)] and the calculated Kp_2. Figure 12 shows equilibrium concentrations of DHN, THN, and N at 10 and 30 atm pressure as a function of temperature using the calculated Kp_1 and Kp_2.

Comparative test data for the six feedstocks at 10 atm pressure and 842-1112°F are recorded in Table 15. At this pressure the decalin reactivities varied with each feedstock. Further, the reactivity (i.e., conversion) appeared to increase with increasing fraction of cis isomer in

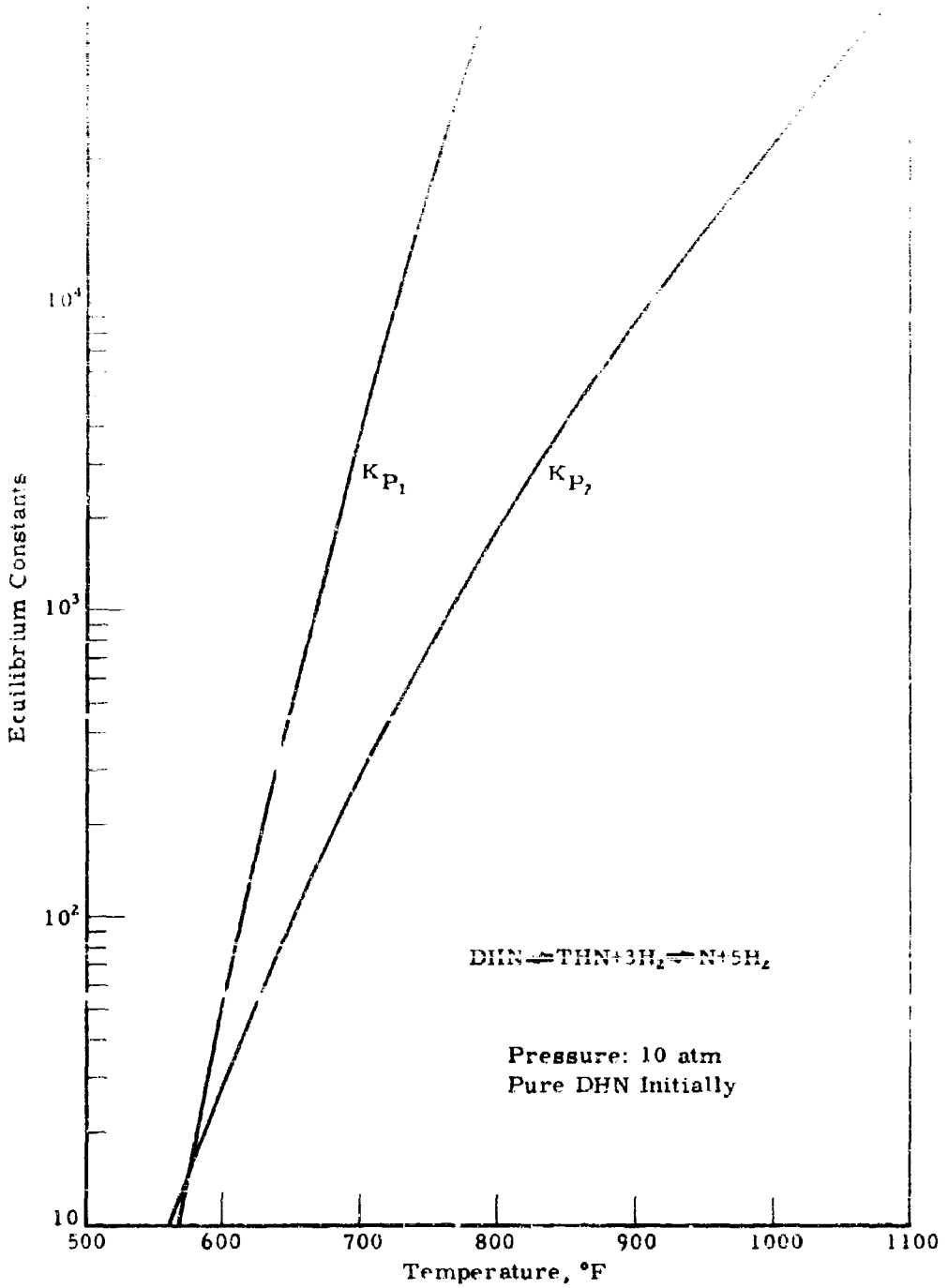


Figure 11. EQUILIBRIUM CONSTANTS FOR DECALIN SYSTEM

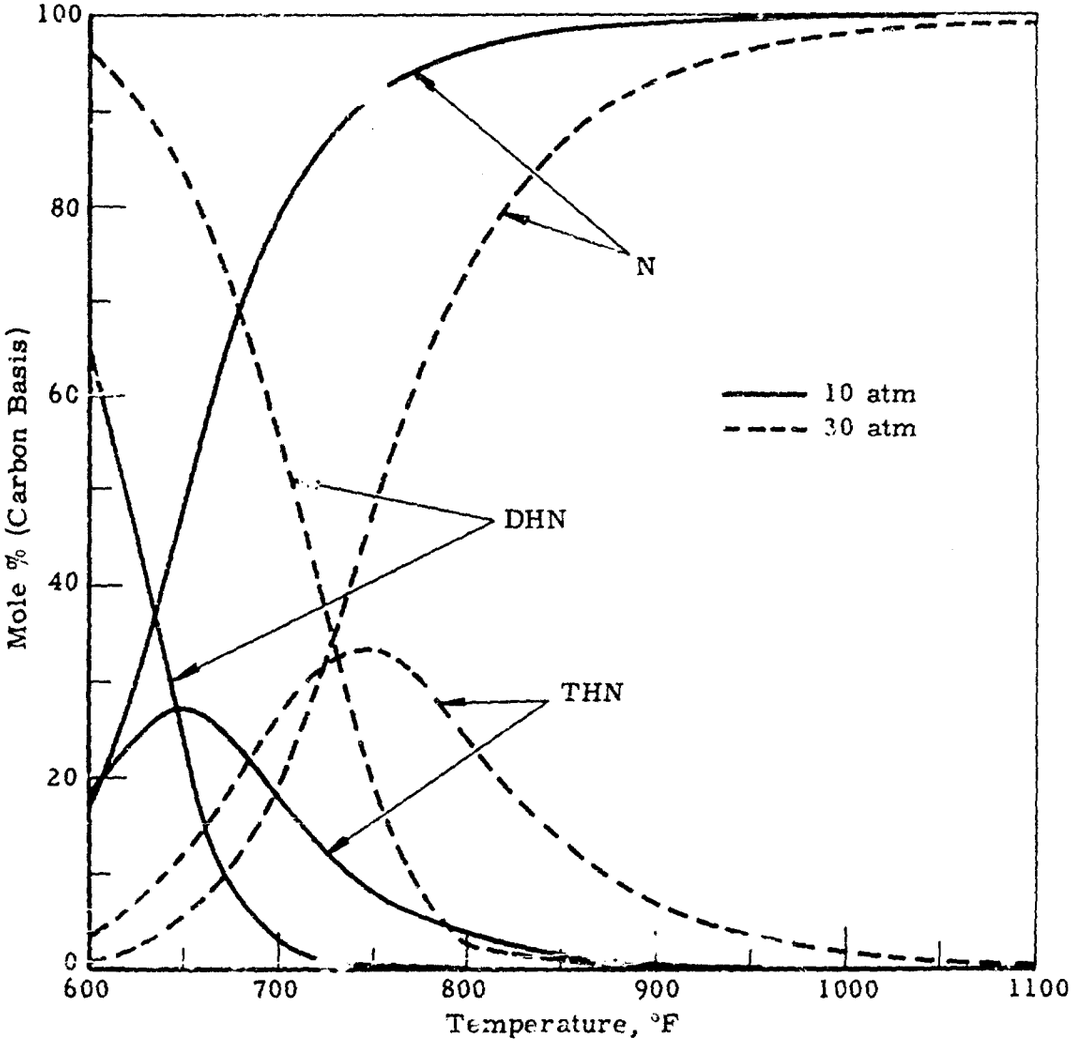


Figure 12. EQUILIBRIUM COMPOSITION OF DECALIN SYSTEM

Table 15. DEHYDROGENATION OF DECALIN: VARIOUS FEEDSTOCKS

Catalyst: 1% Pt on Al_2O_3
Catalyst Volume: 7 ml
Pressure: 10 atm
LHSV: 100
Reaction Time: 30 minutes

Run No.	9426-			9645-			9426-														
	199-1[a]	199-3	200	6-1[a]	6-3	7	104-1[a]	104-3	105	106	182-1[a]	182-3	183	184	186-1[a]	186-3	123-1[a]	123-3	124	119[a]	120-1	120-3
Feed	F-111			F-113			Shell DHN				EK P1905, Lot A						EK P1905, Lot B			EK 1905		
Feed Composition, %																						
trans-DHN	← 57.5 →			← 25.1 →			← 91.2 →				← 37.9 →						← 37.7 →			← 41.8 →		
cis-DHN	← 42.1 →			← 74.5 →			← 8.8 →				← 57.6 →						← 60.1 →			← 58.2 →		
THN	← 0.4 →			← 0.4 →			← 0.0 →				← 4.5 →						← 2.2 →			← 0.0 →		
Temperature, °F																						
Block	842	932	1022	842	932	1022	842	932	1022	1112	842	932	1022	1112	1062	1112	842	932	1022	932	1022	1112
Wall	738-45	815-24	887-90	740-43	802-08	874-80	756-58	806-15	874-85	943-68	756-61	824-29	878-87	948-68	832	961-86	729	849	914	794-99	853-58	9[illegible]
Catalyst Bed Profile	653-60	675-95	716-48	640-58	684-711	732-92	662-69	691-716	727-84	765-938	659-57	676-98	716-59	779-963	718-68	779-998	640-53	714-46	761-819	694-729	738-802	[illegible]
	635-42	673-80	711-19	628-35	666-75	709-18	664-71	693-705	729-48	722-828	637-48	673-80	707-18	753-812	707-18	756-810	632-37	702-07	750-61	662-73	698-711	752-[illegible]
	653-53	689-91	732-34	644-50	686-91	738	671-76	704-711	745-50	792-806	655-62	693-98	729-34	779-92	726	777-88	65[illegible]-41	732	763	676	712-16	769-[illegible]
	696-71	711-13	759	662-668	707-11	763	680-82	716-23	761-63	813-15	671-73	711-16	752-56	810-06	752	810	653-58	745	806	689	734	[illegible]
ΔT_{max}, °F, catalyst bed[d]	15	18	32	18	27	50	7	25	57	173	18	22	43	184	50	219	13	22	58	35	64	[illegible]
Product Analysis, %																						
trans-DHN	37.9	33.0	[illegible]	28.9	25.2	20.6	71.4	63.1	55.6	48.0	37.8	33.6	29.6	23.4	29.4	23.9	38.9	30.8	21.8	37.4	32.[illegible]	29.7
cis-DHN	24.6	20.2	17.0	30.5	25.2	22.5	3.6	3.4	2.9	2.9	24.2	19.8	17.0	16.2	17.4	17.5	27.3	18.8	14.6	20.7	17.6	2[illegible].0
[b]	0.0	0.2	0.2	0.0	0.1	0.5	0.1	0.5	0.9	1.5	0.0	0.0	0.0	0.9	0.1	0.6	0.0	0.1	0.4	0.0	0.0	[illegible]
THN	9.8	7.4	4.8	11.6	8.2	5.1	4.7	4.0	3.0	2.5	9.7	7.1	5.1	3.7	5.1	4.2	10.9	5.8	3.6	8.2	5.7	[illegible]
Naphthalene	27.5	39.2	50.7	29.0	41.4	51.2	20.1	29.0	37.6	45.0	28.3	39.5	[illegible]2	55.5	47.9	53.5	22.9	44.6	52.4	33.7	44.3	[illegible]
Cracked[c]	0.0	0.0	0.0	0.0	0.0	0.1	0.1	0.0	0.0	0.0	0.0	0.0	0.1	0.3	0.1	0.3	0.0	0.0	7.2[c]	0.0	0.0	[illegible]
DHN Conversion, %	56.9	46.4	55.3	40.2	49.2	56.5	25.0	33.5	41.5	49.1	35.1	44.2	52.3	55.9	48.7	54.1	31.6	48.4	61.4	41.9	50.0	[illegible]
k, sec^{-1}	0.447	0.646	0.879	0.498	0.693	0.930	0.284	0.419	0.580	0.774	0.402	0.569	0.750	1.081	0.729	0.904	0.36	0.696	1.060	0.555	0.737	-
E, act, kcal/mole	← 8.2 →			← 7.7 →			← 12.2 →			-	← 9.1 →			-	-	-	← 9.3 →		-	← 9.3 →		-
Selectivity for, %																						
THN	25.5	15.1	8.0	27.8	15.8	8.3	18.8	11.6	7.2	5.1	15.5	6.2	[illegible].2	-	1.2	-	27.3	7.5	2.8	19.6	[illegible].4	[illegible].0
Naphthalene	74.5	84.3	90.8	72.2	84.1	90.6	80.4	86.6	90.6	91.6	84.5	93.8	96.6	97.8	98.4	98.3	72.3	90.3	85.4	80.4	88.6	[illegible]
Heat Sink, Btu/lb																						
Reaction	327	422	514	353	484	530	222	302	377	444	304	393	474	528	456	514	276	446	510	375	455	280
Total at Block Temp	1037	1202	1364	1063	1228	[illegible]70	932	1082	[illegible]27	1364	1014	1173	1324	1448	1306	1434	986	1298	1450	1155	1308	[illegible]
Total at 1340°F	1392	1487	1579	1418	1513	[illegible]84	1287	1362	1442	1509	1369	1458	1539	1593	1521	1579	1283	1389	1503	1440	1523	[illegible]

a) Fresh catalyst.
b) Unidentified; heavier than decalin but lighter than tetralin.
c) Liquid products except for Run 9426-124 in which cracked component was 0.2% liquid and 7.0% light gas.
d) Maximum change in catalyst bed temperature during the run.

the feed (Figure 13). There appeared to be some cis to trans isomerization during the runs (cf 9426-199-1 and 9654-6-1) hence the relative reaction rates of the cis and trans species could not be quantitatively determined from these data.

Some catalyst deactivation occurred during the 30 minute runs with all six feedstocks. This conclusion is based on the observation that the temperature of the catalyst bed increased during the run (Table 15). The magnitude of the temperature increase was taken as a measure of catalyst deactivation. Curiously enough, poorest catalyst stability was observed with one of the purest decalin feeds, namely, EK 1905 where at 1022°F the catalyst bed temperature increased 64°F during the run, compared to an increase of 43°F with the "Practical" grad EK P1905. (At 1112°F the bed temperature increased over 300°F with the EK 1905 feed.) This suggested that trace impurities in the P1905 were moderating the catalyst to suppress the deactivating reactions.

Rate constants and apparent activation energies were calculated from decalin conversion. Because of the concurrent deactivation during dehydrogenation these values were minimal. For the six decalins tested, the activation energies ranged from 7.7 to 12.2 kcal/mole (Table 15). Presumably this variation in E_{act} was an isomer effect as the feeds with the highest and lowest E_{act} had the highest and lowest concentration of trans DHN, respectively. Indeed, it will be shown later that the apparent activation energy for dehydrogenation of trans isomer is greater than that for the cis species. Figure 14 is an Arrhenius plot of the data for the six decalins.

Figure 15 shows conversions as a function of furnace block temperature at 10 atm pressure. The slopes of the curves are reasonably parallel although conversion at a given temperature vary considerably between the decalins.

Selectivity for naphthalene was high and increased with increasing temperature. This was a kinetic effect that depended upon the relative ratio of Reactions I and II.

The first order rate constants for Reaction I were calculated from the rate of disappearance of DCH and are shown in Table 15. The rate constants for Reaction II for F-111 and F-113 DHN were computed following the method of Wheeler[18] and are shown in Table 16.[a] In both of these calculations, the effect of the back reaction was neglected.

---

a) In a system using a porous catalyst, the fraction of DHN converted to THN, in terms of the fraction of DHN converted, α_A, and the selectivity factor, α_B, S, is given by:

$$\alpha_B = \frac{S}{S-1}\left[(1-\alpha_A)^{\frac{1}{S}} - (1-\alpha_A)\right] \qquad (2)$$

where $S = \dfrac{\text{rate constant for DHN} \longrightarrow \text{THN}}{\text{rate constant for THN} \longrightarrow \text{N}} = \dfrac{k_1}{k_2}$

This equation is a rearrangement of Wheeler's Equation 92. By trial and error a value of S was obtained that satisfied Equation 2. k_2 then, was obtained from S.

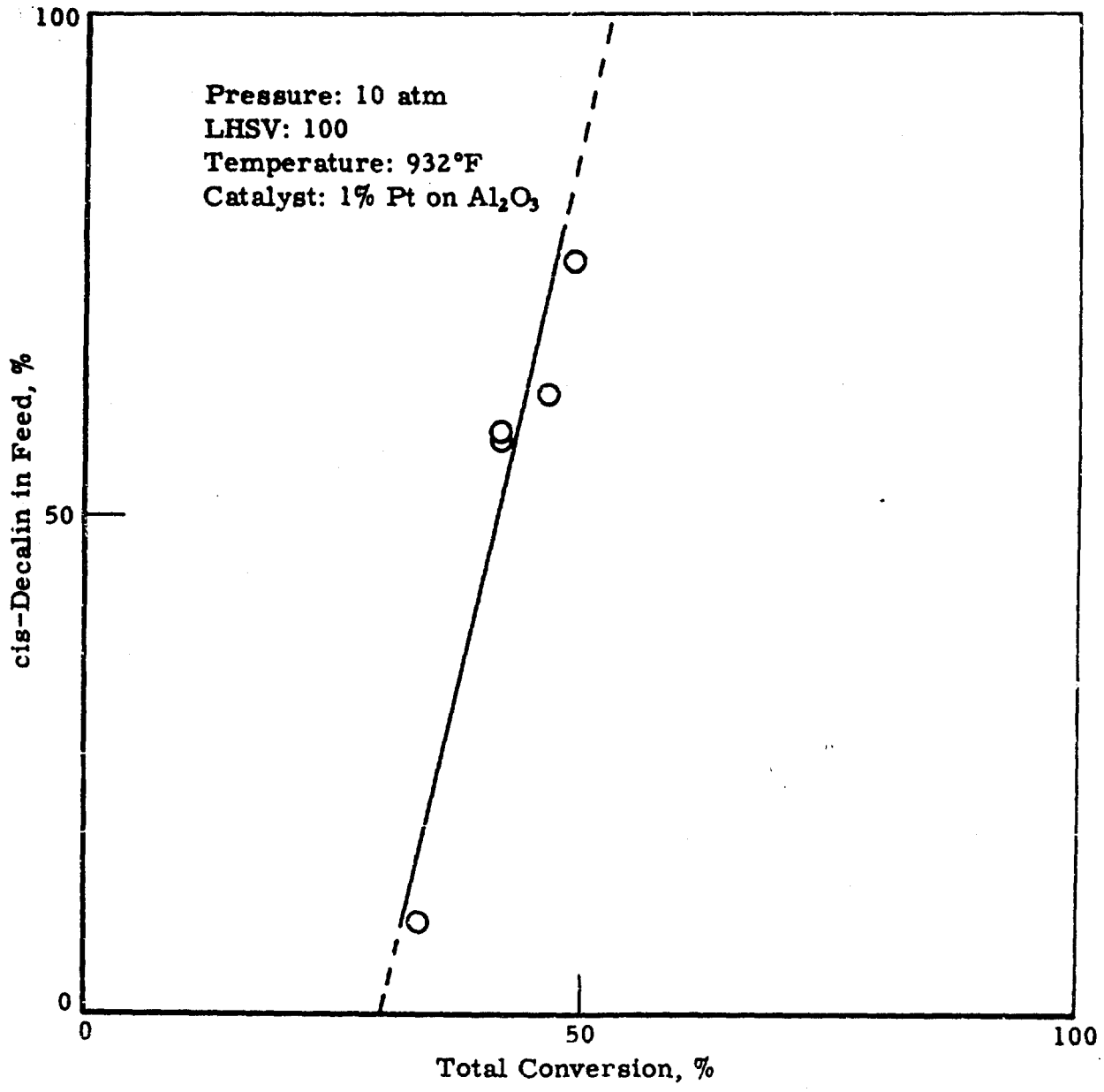


Figure 13. TOTAL CONVERSION OF DECALIN AS A FUNCTION OF cis-DECALIN IN FEED

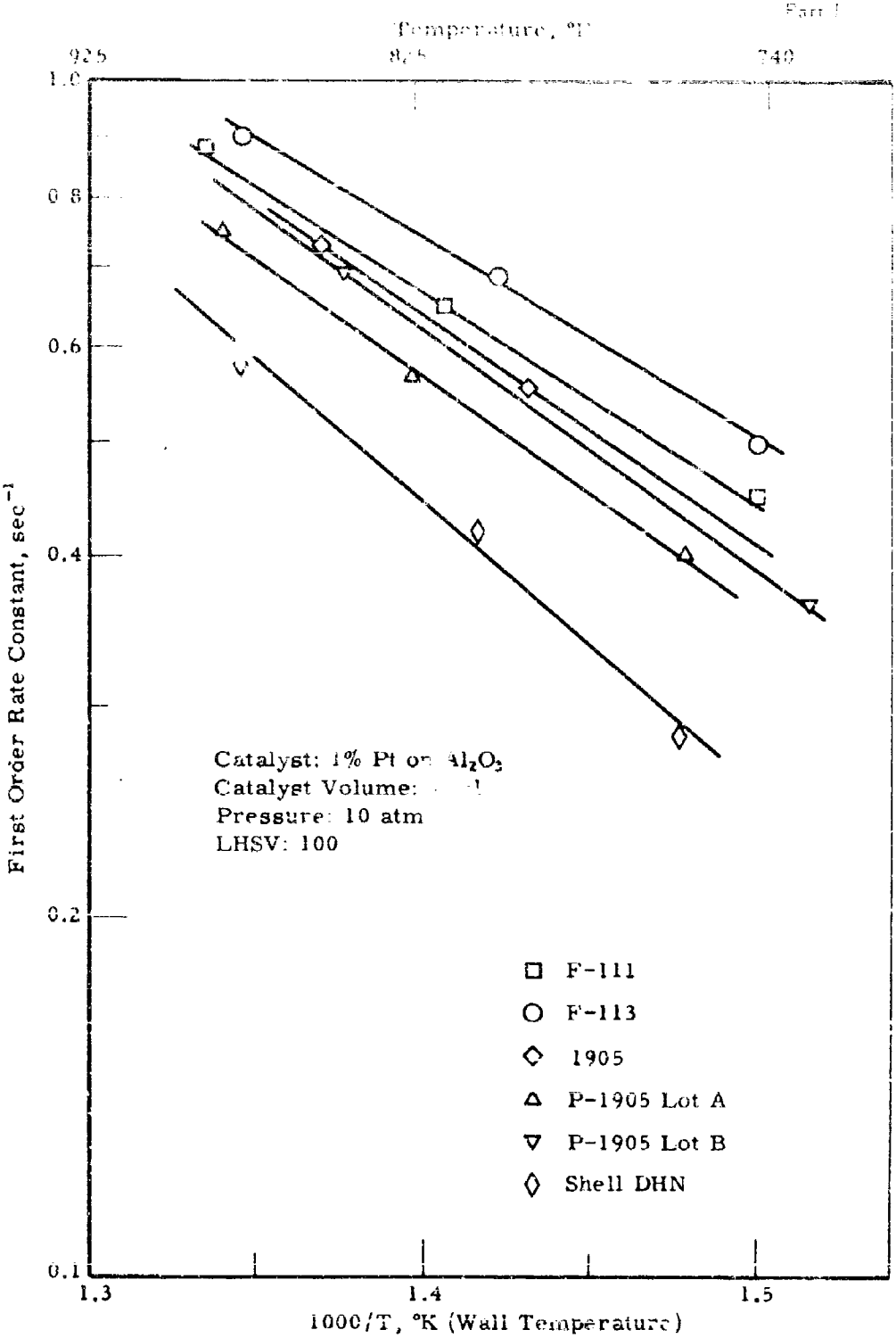


Figure 14. DEHYDROGENATION OF VARIOUS DECALINS
Temperature Coefficient

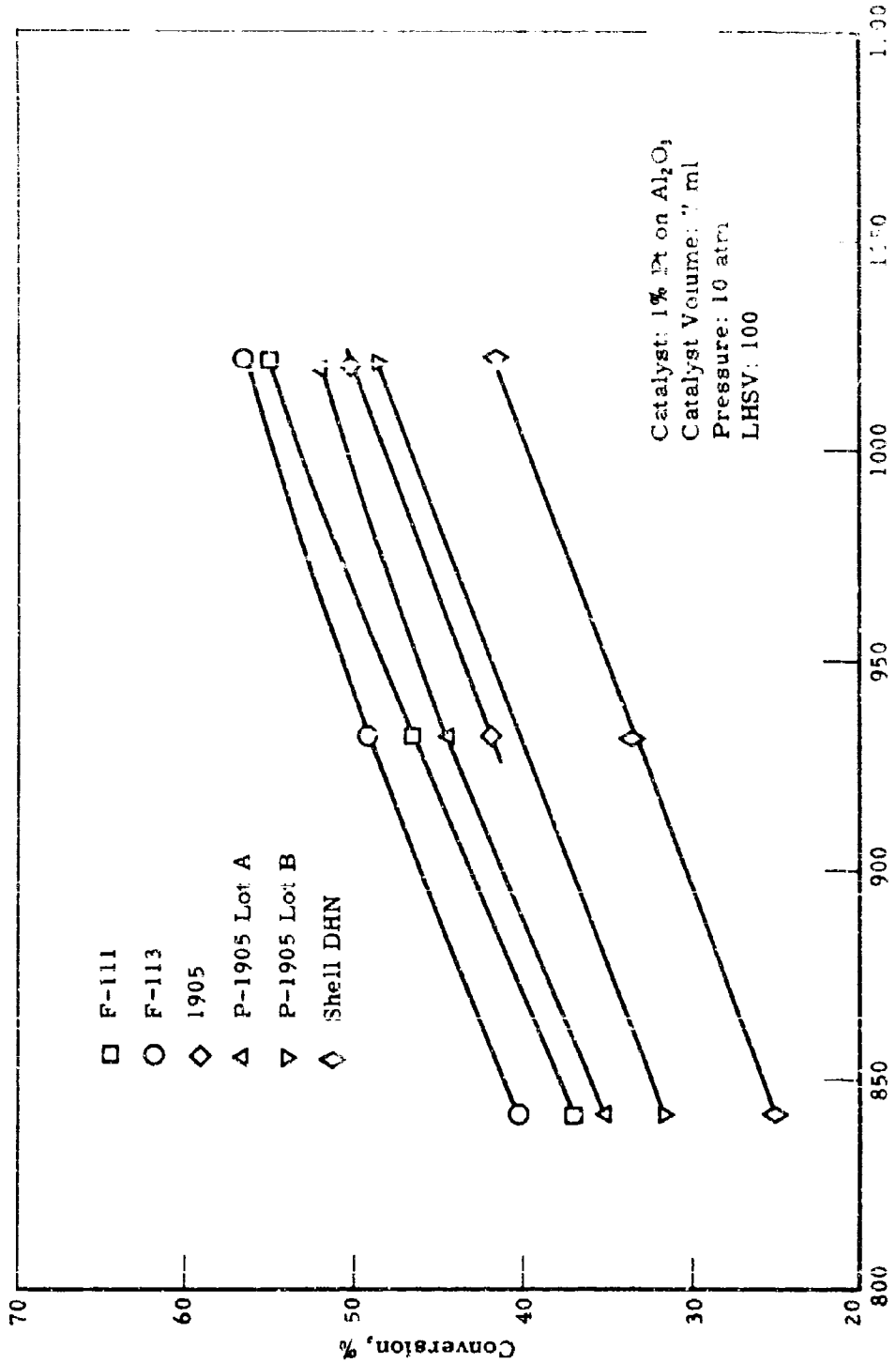


Figure 15. DEHYDROGENATION OF VARIOUS DECALINS
Effect of Temperature on Conversion

Table 16. REACTION RATES AND EQUILIBRIUM CONSTANTS FOR DHN → THN + $3H_2$ AND THN → N + $2H_2$

Pressure: 10 atm

Decalin	F-111			F-113		
Run No.	9425-			9645-		
	199-1	199-3	200	6-1	6-3	7
Temperature, °F						
Block	842	932	1022	842	932	1022
Wall	738-43	815-24	887-90	740-43	802-08	874-80
Gas Exit	670	712	759	665	709	763
Liquid Product Analysis, %w						
DHN	62.7	53.2	44.3	59.4	50.4	43.1
THN	9.8	7.4	4.8	11.6	8.2	5.1
N	27.5	39.2	50.7	29.0	41.4	51.2
α_A	0.370	0.464	0.553	0.402	0.492	0.565
α_B	0.094	0.070	0.044	0.112	0.078	0.047
S	0.42	0.20	0.10	0.45	0.22	0.12
Product Analysis, %m						
DHN	22.3	15.8	11.3	20.1	14.6	10.9
THN	3.6	2.3	1.3	4.1	2.5	1.4
N	10.5	12.6	13.9	10.7	12.9	14.0
H_2	63.6	69.4	73.5	65.1	70.0	73.8
Equilibrium Constant						
DHN → THN + $3H_2$						
K_p'	42	49	47	55	59	52
K_p	1,150	5,800	33,500	950	5,400	38,000
K_p'/K_p	0.037	0.008	0.001	0.058	0.018	0.001
THN → N + $2H_2$						
K_p'	108	264	578	111	253	544
K_p	160	382	930	157	365	1000
K_p'/K_p	0.675	0.692	0.622	0.707	0.693	0.544
First Order Rate Constants, sec^{-1}						
k_1 = DHN → THN + $3H_2$	0.45	0.65	0.88	0.50	0.67	0.90
k_2 = THN → N + $2H_2$	1.07	3.25	8.30	1.17	3.14	7.50
Corrected First Order Rate Constants, sec^{-1}						
k_1	0.46	0.65	0.88	0.54	0.68	0.90
k_2	3.29	10.65	23.3	3.78	10.2	16.5
E_a, est, kcal/mole[a]						
DHN → THN + $3H_2$	← 8.2 →			← 6.4 →		-
THN → N + $2H_2$	← 23.7 →			← 24.5 →		-

a) Based on corrected rate constants.

The extent to which the backward reaction affects the overall reaction rate can be determined by comparing the thermodynamic equilibrium constant K_p, with an equilibrium constant calculated from the experimental data K_p'. This was done for F-111 and F-113 DHN and the values for the various K_p and K_p' are shown in Table 16. For Reaction I the K_p' values were 0.06 to 0.001 times K_p while for Reaction II, the K_p' values were 0.71 to 0.54 times K_p. Thus the backward reaction had little effect on the overall rate of Reaction I, but had an appreciable effect on the overall rate of Reaction II.

The calculated rate constants were corrected for the effect of the backward reaction in the following manner. Near equilibrium, the rate of a first order reaction can be expressed by:

$$R = k P \left(1 - \frac{K_p'}{K_p} \right) \qquad (3)$$

where k is the first order rate constant for the forward reaction and P is the reactant pressure. Thus the rate constants calculated from rate of disappearance of P (i.e., from R) will be low by a factor of

$$\frac{1}{1 - \frac{K_p'}{K_p}}$$

This correction has been applied to our calculated constants and the corrected values are tabulated in Table 16. Apparent activation energies were calculated from the corrected rate constants (Table 16) and Figure 15 is an Arrhenius plot of the data for Reaction II. Appreciable catalyst deactivation was observed with F-113 DHN at 1022°F (Table 15), hence with this feed the activation energy was for the temperature range 842-932°F. Thus Reaction II was 2.2-3.4 times faster, and had an apparent activation energy 2.9-3.7 times greater than Reaction I.

Relative Stabilities of Laboratory Platinum on Alumina and UOP-R8 Catalysts

In a previous section of this report it was shown that the commercial UOP-R8 platforming catalyst was less stable than the laboratory platinum catalyst for the dehydrogenation of dicyclohexyl. In previous work with decalin, similar results were observed.[3] It was of interest now to extend this work and to compare relative stabilities of these two catalysts for the dehydrogenation of decalin under a variety of reaction conditions.

Decalin F-113 feedstock was tested with both the laboratory and commercial UOP-R8 platinum on alumina catalysts at LHSV of 30-100, 842-1022°F at 10-30 atm pressure. This feed was the most reactive in previous tests[3] and contained 74.5% cis DHN, 25.1% trans DHN and 0.4% tetralin (THN). Product material was analyzed by GLC from which conversions and selectivities were calculated. First order rate constants were calculated from the rate of disappearance of starting materials.

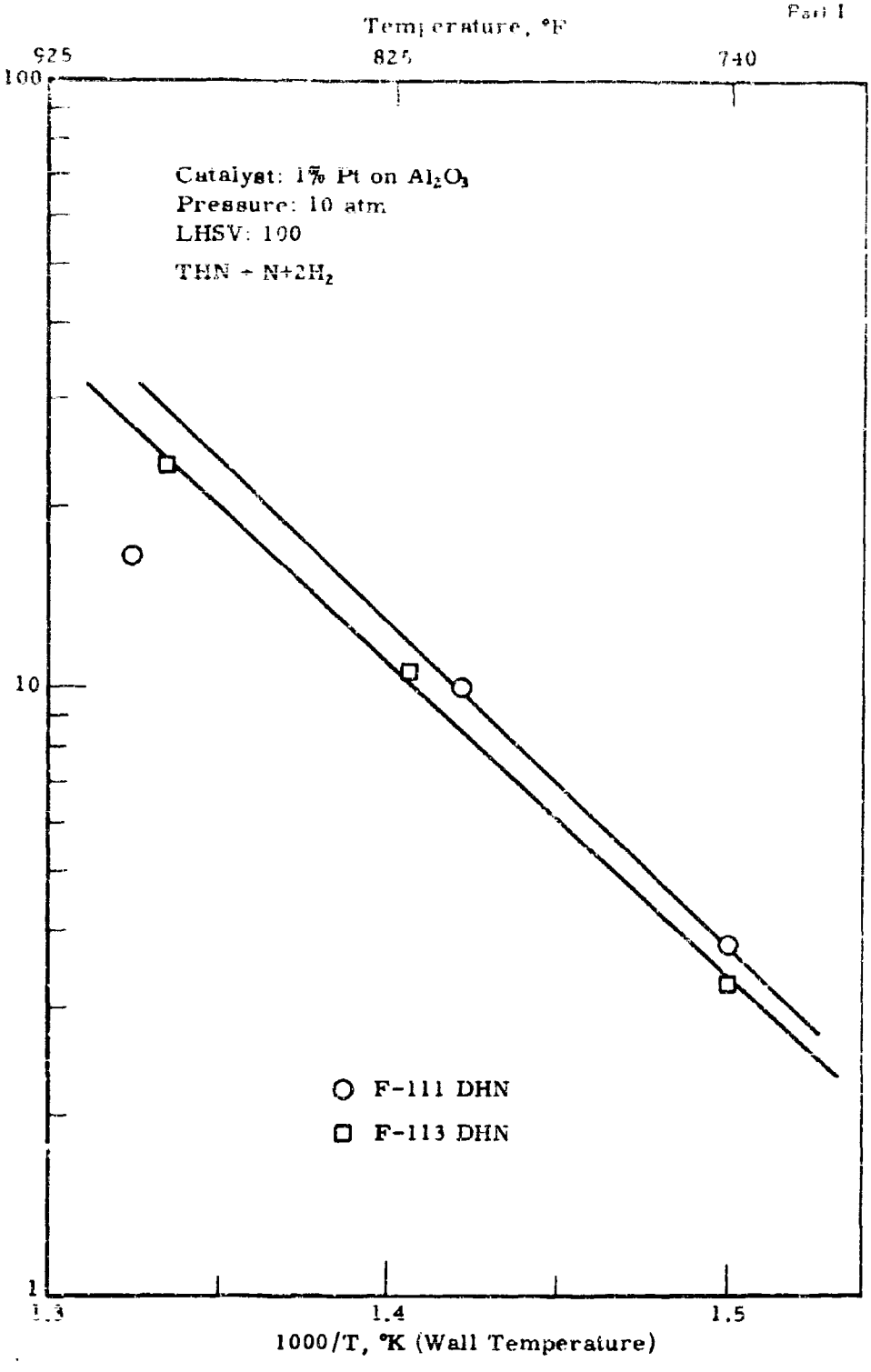


Figure 16. TEMPERATURE COEFFICIENT FOR DEHYDROGENATION OF TETRALIN

In series of runs on single charges of catalyst at 10 atm pressure, the R-8 catalyst was considerably less stable and less active than the laboratory catalyst. For example, an increase in catalyst bed temperature of 192°F was observed with the R-8 catalyst (Table 17), compared to only 60°F with the laboratory catalyst (Table 19). (The magnitude of the temperature increase during reaction was taken as a measure of catalyst deactivation.) Further at 932°F, DHN conversions of 43.7% and 49.2% were obtained with the R-8 and laboratory catalysts, respectively. However, with both catalysts at 10 atm pressure, increasing the conversion reduced the catalyst deactivation markedly. Thus with the UOP-R8 catalyst, an increase in catalyst bed temperature of only 40°F was observed at 83% DHN conversion compared to 192°F at 48% conversion (Table 17; 1022°F). A similar effect was observed with the laboratory catalyst (Table 19). Increasing the pressure also decreased catalyst deactivation and with both catalysts no deactivation was observed at 30 atm pressure; but at 20 atm slight deactivation (25°F) was noted for the R-8 catalyst (Table 18).

Activation energies were calculated from the first order rate constants. At 10 atm pressure an activation energy of 7.6 kcal/mole was obtained with the laboratory catalyst, compared to only 4.8 kcal/mole with the R-8 catalyst. Presumably this low value with the R-8 catalyst was due to the rather extensive catalyst poisoning which occurred at 1022°F (Table 18). Indeed at 30 atm pressure where no catalyst deactivation was observed, an activation energy of 7.2 kcal/mole was obtained with the R-8 catalyst. Figure 17 shows Arrhenius plots of the data.

Possible reasons for the variation in stabilities of the two catalysts are discussed in a later section (pg 77).

Dehydrogenation Over 1% Platinum on UOP-R8 Alumina: No Halogen

In previous work on the dehydrogenation of Decalin (DHN), it appeared that the UOP-R8 platinum catalyst was considerably less stable than the laboratory platinum on alumina catalyst.[3] As this latter catalyst was halogen-free while the commercial catalyst contained 0.76% halogen, it was thought that the instability of the commercial catalyst might be due to the halogen. Accordingly, a 1% platinum on UOP-R8 alumina base was prepared under halogen-free conditions and was tested for the dehydrogenation of F-113 Decalin (74.5% cis-DHN), at 10 atm pressure and at 842-1022°F. This catalyst had about one-half the weight of platinum per 7 ml volume as did the laboratory catalyst. The procedure for making the runs and analyzing the products was the same as the previous work.[3]

Under the above test conditions, this catalyst was less active and less stable than the laboratory 1% platinum on alumina catalyst. Thus at 842 and 932°F conversions and first order rate constants were lower, and increases in catalyst bed temperatures were greater than those obtained with the laboratory catalyst (Table 20). Further, at 1022°F the conversion was less than was observed at 932°F indicating severe catalyst deactivation at the higher temperature (Table 20). This was not observed with the laboratory catalyst (Table 28 of a previous report[3]). No differences in selectivities for naphthalene were observed with the two catalysts.

Table 17 DEHYDROGENATION OF DECALIN OVER UOP-[illegible]
CATALYST - EFFECT OF TEMPERATURE AND CONVERSION

Catalyst: 0.6% Pt on Al_2O_3 Feed: [illegible]% Decalin
Catalyst Vol: 7 ml 25.1% trans-DHN
Pressure: 10 atm 74.5% cis-DHN
0.4% THN

Run No. 9645-	171-1	171-3	172	134	135-1	135-2	139
LHSV	100	100	100	50	30	50	30
Temperature, °F							
Block	842	932	1022	842	842	1022	1022
Wall	752-4	835	909-38	752	761-85	905-14	923-28
Catalyst Bed	635-48	689-722	776-968	640-49	650-60	770-851	838-76
	617-22	662- 69	709-828	635-39	633-56	746- 66	779-97
	620-24	666- 68	702- 47	649-51	675-82	768	802-10
	626-30	671- 73	722- 29	668-21	700-07	600-795	853-56
ΔT_{max}, °F, catalyst bed[a]	13	33	192	9	10	81	40
Product Analysis, %w							
trans-DHN	35.9	29.8	24.1	32.2	25.7	17.3	9.9
cis-DHN	26.0	26.2	27.7	3.8	7.1	13.6	7.0
U	0.1	0.1	1.7	0.4	0.4	4.6	7.5
THN	16.6	11.1	6.5	14.8	11.3	4.2	2.8
Naphthalene	21.4	32.8	39.9	38.5	54.9	59.8	71.7
Cracked, liquid	0.0	0.0	0.1	0.0	0.1	0.4	0.5
Yield THN, %w	16.2	10.7	6.5	14.4	10.9	3.8	7.1
DHN Conversion, %w	37.8	43.7	48.2	53.8	67.0	69.9	83.0
k, sec^{-1}	0.46	0.60	0.74	0.38	0.33	0.65	0.60
E, act, kcal/mole	←		4.6	→	-	-	-
Selectivity for, %w							
THN	42.9	24.5	13.5	25.8	16.3	6.1	3.4
Naphthalene	56.6	75.3	83.7	72.7	83.3	80.5	78.8
Heat Sink, Btu/lb							
Reaction	312	383	423	465	598	594	700
Total at Block Temp	1022	1163	1273	1175	1308	1444	1550
Total at 1340°F	1377	1448	1488	1530	1663	1659	1768

a) Maximum change in catalyst bed temperature during the runs.

Table 18. DEHYDROGENATION OF DECALIN OVER UOP-R8 CATALYST - EFFECT OF PRESSURE

Catalyst: 0.76% Pt on Al_2O_3
Catalyst Vol: 7 ml
LHSV: 100

Feed: F-113 Decalin
25.1% trans-DHN
74.5% cis-DHN
0.4% THN

Run 9645-	174-1	174-3	175	177-1	177-3	178
Pressure, atm	10	20	30	10	20	30
Temperature, °F						
Block	← 842 →			← 1022 →		
Wall	722-7	732	736-8	902-12	908-12	912
Catalyst Bed	632-44	642-38	653	722-887	867-92	876
	622-28	637-35	653	694-740	734-45	744-40
	628-33	646-44	658	702- 16	720-22	725-23
	637-40	655-53	668-66	716- 18	725-25	730-28
ΔT_{max}, °F, catalyst bed[a]	12	16	-2	165	25	-4
Product Analysis, %w						
trans-DHN	35.1	44.8	54.8	24.3	27.4	29.8
cis-DHN	26.8	16.8	12.4	23.9	20.6	17.1
U	0.0	0.1	0.0	1.2	1.4	0.6
THN	14.8	24.2	23.9	7.1	16.3	25.2
Naphthalene	23.3	14.1	8.9	43.5	34.0	27.0
Cracked, liquid	0.0	0.0	0.0	0.0	0.3	0.3
Yield THN, %w	14.4	24.3	23.5	6.7	15.9	24.6
DHN Conversion, %w	57.8	38.6	32.4	51.6	51.8	52.9
k, sec^{-1}	0.46	0.23	0.14	0.81	0.41	0.28
E, act, kcal/mole	7.2 using data at 30 atm pressure					
Selectivity for, %w						
THN	38.1	63.0	72.6	13.0	30.7	46.9
Naphthalene	61.9	36.8	27.4	84.7	66.0	51.4
Heat Sink, Btu/lb						
Reaction	317	297	243	458	430	422
Total at block temp	1027	1007	953	1308	1280	1272
Total at 1340°F	1382	1362	1308	1423	1495	1487

a) Maximum change in catalyst bed temperature during the run.

Table 12. DEHYDROGENATION OF DECALIN OVER LABORATORY PLATINUM CATALYST

Catalyst: 1% Pt on Al_2O_3 Feed: F-113 Decalin
Catalyst Volume: 7 ml 25.1% trans-DHN
74.5% cis-DHN
0.4% THN

Run	9645-			10100-				9645-	
	6-1	6-3	7	137	138-1	138-2	180-1	180-3	181-1
Pressure, atm	← 10 →			← 10 →			10	30	30
LHSV	← 100 →			30	50	100	← 100 →		
Temperature, °F									
Block	842	932	1022	← 1022 →			← 1022 →		
Wall	740-49	802-08	874-80	925-21	902-900	891-80	894-98	902-08	898-89
Catalyst Bed	640-58	684-711	732-92	761-61	752-56	770-88	720-50	748-41	741-37
	628-36	666-75	709-18	786-84	756-56	743-50	705-12	728-16	724-20
	644-50	686-91	738-38	848-40	795-94	763-66	7..-84	736-38	741-39
	668-85	709-11	763-63	896-87	833-33	792-94	784-86	768-66	770-70
ΔT_{max} °F, catalyst bed	14	21	60	-9	+4	+18	30	-4	-4
Product Analysis, %w									
trans-DHN	28.9	25.2	20.6	6.6	16.6	19.9	21.6	24.6	27.1
cis-DHN	30.5	25.2	22.5	2.9	16.7	34.1	21.3	16.9	13.2
U[a]	0.0	0.1	0.5	1.5	0.6	0.7	0.0	0.0	0.0
THN	11.6	8.2	5.1	6.0	3.1	8.3	5.5	10.5	10.4
Naphthalene	28.9	41.4	51.2	82.4	62.2	36.4	50.6	48.0	48.7
Cracked, liquid	0.0	0.0	0.1	0.2	0.2	0.3	0.0	0.0	0.0
U[a]	-	-	-	0.4	0.6	0.3	-	-	-
Yield THN, %w	11.2	7.8	4.7	5.6	2.7	7.9	5.1	10.1	10.0
DHN Conversion, %w	40.2	49.2	56.5	90.5	66.6	48.5	55.9	58.3	58.9
k, sec^{-1}	0.498	0.693	0.900	-	-	-	0.839	0.479	0.328
E, act., kcal/mole	← 7.6 →								
Selectivity for, %w									
THN	27.9	15.7	8.8	6.2	4.1	17.3	9.1	21.1	35.5
Naphthalene	72.1	84.1	90.6	91.4	94.1	79.8	90.9	78.9	64.2
Heat sink, Btu/lb									
Reaction	353	445	520	820	608	399	514	518	521
Total reaction temp	1063	1228	1370	1670	1458	1294	1364	1369	1360
Total at 1340°F	1418	1513	1585	1885	1673	1464	1579	1573	1566

a) U = Unidentified.

AMAPL-TR-77-118

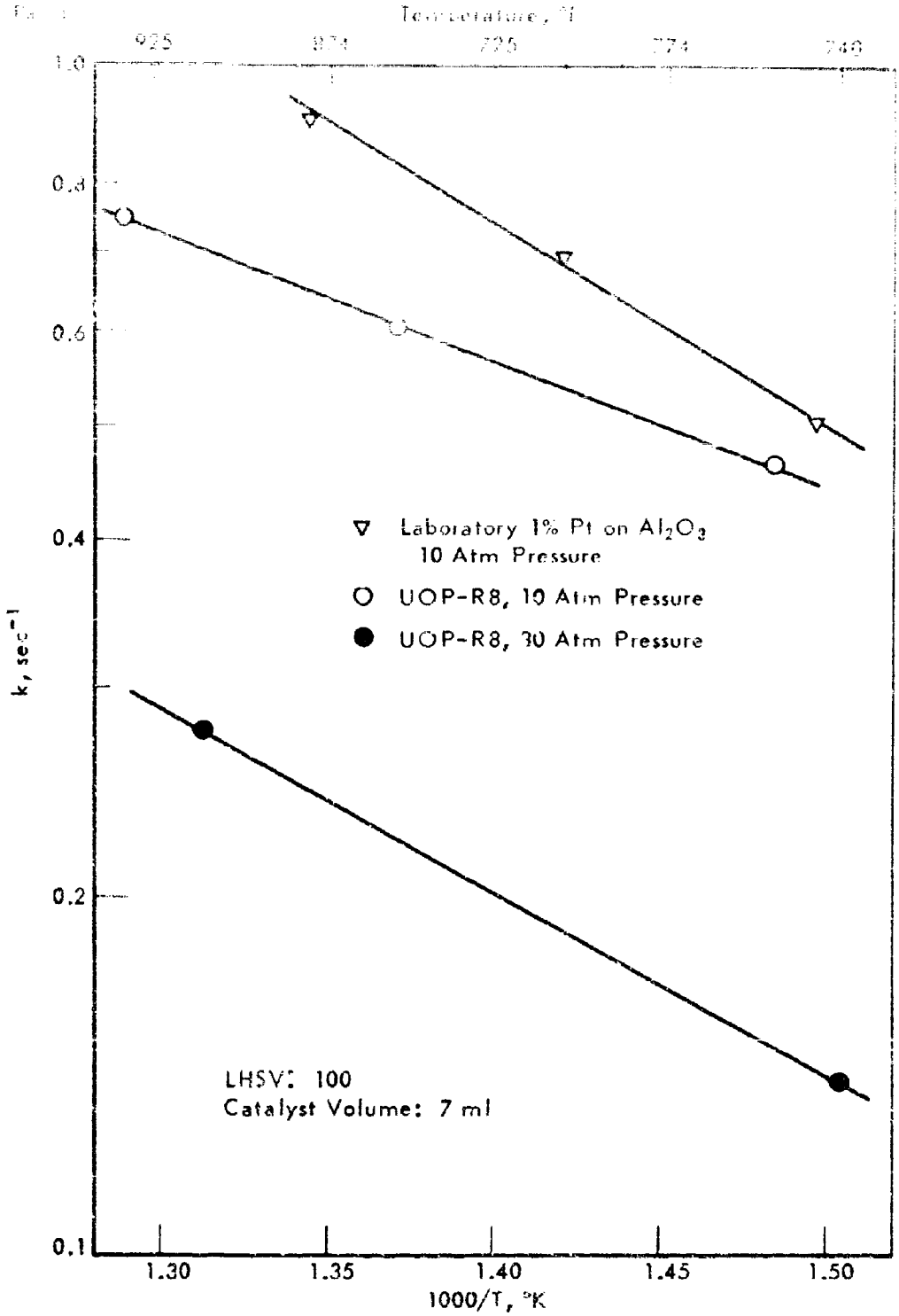


Figure 17. DEHYDROGENATION OF DECALIN OVER UOP-R8 AND LABORATORY Pt/Al_2O_3 CATALYSTS
Temperature Coefficient

62731

Table [illegible]. DEHYDROGENATION OF DECALIN: TEST OF PLATINUM ON OCT-RE BASE WITH NO HALOGEN

Pressure:	10 atm	Catalyst:	1% Pt on commercial alumina base
LHSV	150		
Decalin:	F-113	Feed:	25.1% trans-DHN
Catalyst Vol:	7 ml		74.5% cis-DHN
			0.4% THN

Run No. 10100	21-1	21-2	22
Temperature, °F			
Block	842	932	1022
Wall	747-48	883-42	934-99
Catalyst Bed	655-66	702-47	885-982
	637-44	676-93	790-970
	542-48	684-89	765-948
	650-53	694-98	770-932
T_{max}, °F, catalyst bed[d]	11 (18)[c]	45 (27)[c]	183 (40)[c]
Product Analysis, %			
Cracked	0.0	0.0	1.9
trans-DHN	30.2[a]	27.1[a]	23.0
cis-DHN	35.9	31.1	41.1
U[b]	0.4	0.3	7.2
THN	10.8	7.5	6.4
U[b]	0.0	0.0	0.6
Naphthalene	22.7	34.0	19.7
Yield THN, %	10.4	7.1	5.1
Total DHN Conversion, %	33.9 (40.2)[c]	41.6 (49.2)[c]	35.6 (56.5)[c]
Selectivity for, %			
THN	30.7	17.1	14.3
Naphthalene	66.6	81.0	55.0
k, overall, sec^{-1}	0.41 (0.50)[c]	0.57 (0.69)[c]	- (0.90)[c]

a) trans-DHN concentration in product higher than in feed due to cis-to trans-isomerization during dehydrogenation.
b) Unidentified.
c) Values obtained with laboratory catalyst.
d) Maximum change in catalyst bed temperature during the run.

Both the laboratory catalyst and the catalyst used in this test were prepared in the same manner. Both the alumina support used for the laboratory catalyst (Harshaw 0104) and the UOP-R8 alumina are high purity aluminas. While it is possible that the greater instability of the platinum on UOP-R8 alumina catalyst was due to lower platinum content, it appears more likely that the observed differences in catalyst performance are due to physical rather than chemical properties of the catalyst.

Extended Dehydrogenation Test With Laboratory Catalyst

In previous work on the dehydrogenation of various Decalin feedstocks, catalyst deactivation was observed during all of the runs.[3] These runs were of short duration (30 min) and it was of interest to see if the catalyst became stabilized with continued use. An extended run has now been carried out with F-113 Decalin (74.5% cis-DHN) over a four-hour period at 10 atm pressure, LHSV of 100 and at 1022°F using the standard laboratory 1% platinum on alumina catalyst. The test was interrupted for 15 minutes after three hours to refill the feed reservoir, during which time the catalyst was hydrogen treated at the reaction temperature. The data are recorded in Table 21.

There appeared to be no stabilization of the catalyst during the four-hour test. Thus, during this time, conversion declined from 56.1% to 43.2% or about 8%/hour; and the catalyst bed temperature increased progressively from 694°F to 959°F with the "cold spot" moving down the catalyst bed (Table 21). Hydrogen treatment reactivated the catalyst temporarily. This suggests that the catalyst might be stabilized by the addition of hydrogen to the feed; or possibly by operating the reactor at higher conversion which would increase the partial pressure of hydrogen over the catalyst during the run.

Dehydrogenation of F-111 Decalin Over UOP-R8 Catalyst

In previous work it was observed that the laboratory 1% platinum on alumina catalyst was moderately stable with Decalin F-113 (74.5% cis) and showed good stability with Decalin F-111 (62.1% cis).[3] The UOP-R8 catalyst was considerably less stable than the laboratory catalyst with Decalin F-113,[3] and it was of interest to test the stability of this catalyst with Decalin F-111. The tests were carried out at 10 atm pressure, LHSV of 100 over the temperature range of 842-1022°F following the same procedure that was used for previous tests.[3]

With this feedstock lower conversions and rate constants and greater increases in catalyst bed temperatures during the runs were observed with the UOP-R8 catalyst compared to the laboratory catalyst (Table 22; the values obtained with the laboratory catalyst are shown in parentheses for comparison). At the highest temperature tested (1022°F) the increase in catalyst bed temperature was 137°F which was about four times the temperature increase observed with the laboratory catalyst (Table 22). Further, at this temperature, DHN conversion was less than was obtained at 932°F which indicates severe catalyst deactivation at 1022°F. At the lower temperatures, however, conversions and catalyst bed temperature increases were comparable to those observed with the laboratory

Table 21. DEHYDROGENATION OF DECALIN: EXTENDED CATALYST TEST

Pressure:	10 atm	Catalyst:	1% Pt on Al_2O_3
LHSV:	100	Catalyst Vol:	7 ml
Temperature:	1022°F	Feed:	25.1% trans-DHN
Decalin:	F-113		74.5% cis-DHN
Run No.:	9347-184		0.4% Tetralin

Total Reaction Time, min	0	30	60	90	120	150	180[a]		210	240
Temperature, °F										
Wall	896	891	891	892	896	902	910[a]	892	902	918
Catalyst Bed[b]	694	711	725	752	795	858	932	835	918	959
	705	711	716	723	729	743	770	727	756	799
	738	743	745	748	748	752	759	738	747	759
	761	765	766	768	770	770	768	744	756	761
ΔT_{max}, °F, catalyst bed[c]		17	14	27	43	63	74	-97	73	43
Product Analysis, %w										
trans-DHN	-	21.1	21.1	-	-	-	20.6	-	20.9	20.6
cis-DHN	-	22.8	25.5	-	-	-	35.2	-	32.7	36.0
THN	-	5.4	5.3	-	-	-	4.7	-	5.2	5.0
Naphthalene	-	50.7	48.1	-	-	-	39.5	-	41.2	38.4
Total DHN Conversion, %w	-	56.1	53.2	-	-	-	44.0	-	46.2	43.2

a) Catalyst H_2 treated for 15 minutes after this run.
b) Cold spot moved down the catalyst bed with increased reaction time.
c) Maximum change in catalyst bed temperature during the run.

Table 22. DEHYDROGENATION OF F-111 DECALIN OVER UOP-R8 CATALYST

Pressure:	10 atm	Catalyst:	1% Pt on Al_2O_3
LHSV:	100	Feed:	37.5% trans-DHN
Decalin:	F-111		62.1% cis DHN
Catalyst Vol:	7 ml		0.4% Tetralin

Run No. 9347-	168	169-1	169-2
Temperature, °F			
Block	842	932	1022
Wall	729-36	819-30	928-984
	689-98	752-72	864-972
	639-49	704-11	804-941
	639-44	700-05	776-880
	646-49	704-68	768-824
ΔT_{max}, °F; catalyst bed	10 (15)[d]	20 (18)[d]	137 (32)[d]
Product Analyses, %w			
Cracked	0.0	0.0	0.5
trans-DHN	40.7[a]	34.1	29.4
cis-DHN	20.8	22.6	27.5
U[b]	0.1	0.4	4.1
THN	13.5	7.9	5.6
U[b]	0.0	0.0	0.2
Naphthalene	24.9	35.0	32.7
Yield THN, %w	13.1	7.5	5.6
Total DHN Conversion, %w	38.3 (36.9)[d]	43.1 (46.4)[d]	42.9[c] (55.3)[d]
Selectivity for, %w			
THN	34.2	17.4	13.1
Naphthalene	65.8	82.6	86.9
k, overall, sec^{-1}	0.47 (0.45)[d]	0.59 (0.65)[d]	– (0.88)[d]

a) trans-DHN concentration in product higher than in feed due to trans to cis isomerization during dehydrogenation.
b) Unidentified.
c) Conversion low presumably due to catalyst deactivation.
d) Values obtained with laboratory 1% Pt on Al_2O_3 catalyst.

catalyst. Possible reasons for differences in behavior between the UOP-R8 and the laboratory catalyst are discussed in a later section of this report (pg 77).

Dehydrogenation and Isomerization of Decalin Isomers

In previous work on the dehydrogenation of Decalin (DHN) the cis species appeared more reactive than the trans.[3] This conclusion was based on comparison of overall reaction rates of different feedstocks that contained different concentrations of the cis and trans species. We have since prepared two DHN feedstocks, one with a high concentration of the cis isomer, and the other with a high concentration of the trans isomer, and these feeds have been dehydrogenated over our standard 1% platinum on alumina catalyst. The dehydrogenations were carried out at both low and moderate conversions in order to study rates of isomerization and rates of dehydrogenation.

The experiments were carried out at 662-1112°F and at 10-30 atm pressure. The catalyst was 2 ml of 1% Pt on Al_2O_3 that was diluted with 5 ml of quartz chips. Product material was analyzed by GLC, from which conversions and selectivities were calculated. First order rate constants for DHN dehydrogenation were calculated from the rate of disappearance of starting material. The cis DHN and trans DHN feedstocks were prepared by fractional distillation and had the following compositions:

	cis-DHN	trans-DHN
% cis-DHN	95.0	4.9
% trans-DHN	4.1	95.1
% Tetralin	0.9	0.0

These compositions were nonequilibrium compositions over the temperature range of our study (Figure 18). Both feedstocks were tested at LHSV of 200, 842-1112°F and at 10-30 atm pressure. In addition the cis-DHN was tested at LHSV of 400, 662-842°F, 10-30 atm pressure. The data for the cis and trans feeds are tabulated in Table 23 and Table 24, respectively.

For dehydrogenation the reactivity of cis-DHN was greater than that of trans-DHN but not by a factor of two as was estimated in the previous work.[3] As an example at 10 atm pressure and 842°F, 37.5% cis-DHN conversion was observed compared to 29.7% trans-DHN conversion ($k_{cis} = 0.935$; $k_{trans} = 0.706$ sec^{-1}). Similar higher cis-DHN reactivities were observed at higher temperatures and pressures (cf runs 129 and 130, Table 23; and Runs 193 and 194, Table 24). No isomer effect on selectivity for naphthalene was observed with these feedstocks.

Apparent activation energies for DHN dehydrogenation were calculated from the first order rate constants and presumably are for the reaction DHN $\longrightarrow$ THN. Under similar reaction conditions E_{act} for trans-DHN was about 30% greater than E_{act} for cis-DHN. Further, the E_{act} for cis-DHN were greater for this isomer at lower temperatures and conversions (Table 23). This change in E_{act} with temperature or conversion might be a kinetic effect (i.e., the reaction changing kinetic order) or a heat transfer effect.

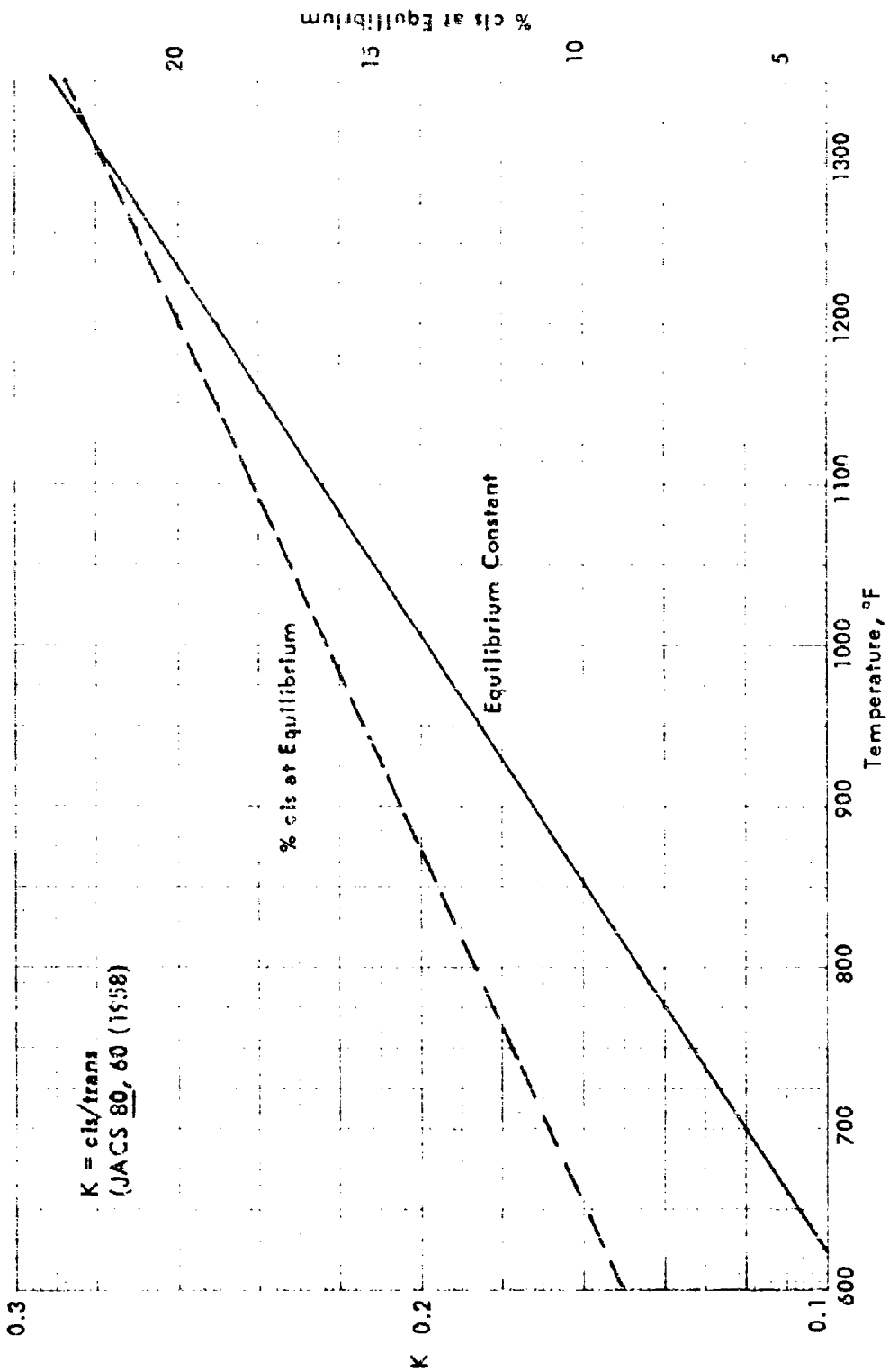


Figure 18. ISOMERIZATION OF DECALIN: cis-trans EQUILIBRIUM

60997

Table 23. DEHYDROGENATION AND ISOMERIZATION OF cis-DECALIN

trans/cis Ratio in Feed: 0.043
Catalyst: 1% Pt on Al_2O_3
Catalyst Volume: 2 ml
Catalyst diluted with 5 ml quartz chips

Feed: 4.1% trans-DHN
95.0% cis DHN
0.9% THN

Run No. 9347-	140	138	137-1	141	139	137-2	129-1	129-3	130	131	133-1	133-2	134	135
LHSV	← 40 →						← 200 →							
Pressure, atm	← 10 →			← 30 →			← 10 →				← 30 →			
Temperature, °F														
Block	662	752	842	662	752	842	842	932	1022	1112	642	932	1022	1112
Wall	614	694	765	639	686	740	770	842	912	1020	788	864	934	1017
Catalyst (cold spot)	585	651	704	619	653	678	694	745	815	997	673	728	772	846
ΔT, Catalyst	0	7	11	0	0	0	12	13	25	90	2	0	2	8
Product Analysis, %														
trans-DHN	9.5	8.1	8.1	24.6	22.9	19.2	9.6	7.6	4.8	3.1	26.5	16.8	11.4	6.0
cis-DHN	80.6	75.7	66.8	67.8	60.2	55.4	52.0	44.7	40.4	40.5	29.4	26.7	22.3	16.8
THN	6.6	6.0	7.1	7.0	14.3	18.3	8.9	6.9	5.4	5.5	27.1	24.7	17.0	7.4
Naphthalene	3.3	10.2	18.0	0.6	2.6	7.1	29.5	40.6	49.2	48.9	16.9	31.4	48.4	62.8
Others[a]	0.0	0.0	0.0	0.0	0.0	0.0	0.0	0.2	0.2	2.0	0.1	0.4	0.9	7.0
DHN Conversion, %w	9.0	15.3	24.2	6.6	16.0	23.5	37.5	46.8	53.8	53.6	42.3	55.4	65.0	76.3
E, act, kcal/mole (dehydrogenation)	← 12.1 →				← 14.1 →		← 8.5 →				← 9.3 →			
Yield THN, %	5.6	5.1	6.2	6.0	13.4	17.4	8.0	6.0	4.5	4.6	26.2	23.8	16.1	6.5
Selectivity for, %w														
THN	62.9	33.3	25.6	90.9	83.7	74.0	21.3	12.8	8.4	8.6	60.6	43.0	24.6	8.5
Naphthalene	37.1	66.7	74.4	9.1	16.3	26.0	78.7	87.2	91.6	91.4	39.2	56.6	74.4	81.4
Yield trans-DHN, %w	5.4	4.0	4.0	20.5	18.8	15.1	5.5	3.5	0.7	-1.0	25.6	15.9	12.5	5.1
% cis to trans	5.7	4.2	4.2	21.6	19.8	15.9	5.8	3.7	0.7	-1.1	26.9	16.7	13.1	5.3
% trans at Equilibrium (basis wall temp)	90.7	89.3	88.0	90.3	89.5	88.5	89.1	88.0	86.8	85.0	87.8	86.2	85.0	83.5
Trans/cis Ratio in Product	0.117	0.108	0.122	0.302	0.379	0.345	0.185	0.170	0.119	0.076	0.902	0.628	0.511	0.357
Rate Constants, sec^{-1}														
Dehydrogenation	0.33	0.63	1.10	0.08	0.22	0.34	0.94	1.18	1.72	2.21	0.38	0.58	0.74	1.16
cis trans isomerization	0.24	0.21	0.31	0.34	0.39	0.31	0.30	0.29	0.20	0.10	0.50	0.41	0.36	0.28
trans cis isomerization	0.023	0.025	0.043	0.036	0.045	0.041	0.041	0.036	0.045	0.020	0.072	0.066	0.066	0.056

a) Cracked and heavier than naphthalene.

Table 24. DEHYDROGENATION AND ISOMERIZATION OF trans-DECALIN

LHSV: 200 trans/cis Ratio in Feed: 18.55
Feed: 95.1% trans DHN Catalyst: 1% Pt on Al_2O_3
4.9% cis DHN Catalyst Volume: 2 ml
Catalyst diluted with 5 ml quartz chips

Run 9645-	193	194-1	194-3	195	197-1	197-3	198	199
Pressure, atm	← 10 →				← 30 →			
Temperature, °F								
Block	842	932	1022	1112	842	932	1022	1112
Wall	781	848	914	1029	782	847	918	993
Catalyst	716	763	813	1013	712	770	820	905
ΔT, Catalyst	9	11	13	108	0	0	4	13
Product Analysis, %w								
trans DHN	67.5	56.8	46.2	44.6	64.3	54.3	43.4	32.4
cis DHN	2.8	2.4	2.0	3 3	3.2	2.3	1.8	1.4
THN	3.7	3.6	3.6	3.9	15.3	13.0	9.6	5.9
Naphthalene	25.9	37.0	47.6	45.2	17.2	30.3	44.8	56.3
Others[a]	0.1	0.2	0.6	3.0	0.0	0.1	[illegible]	4.0
DHN Conversion, %w	29.7	40.8	51.8	52.1	32.5	43.4	54.8	66.2
k, sec^{-1}, dehydrogenation	0.71	1.09	1.62	-	0.27	0.40	0.60	0.85
E, act, kcal/mole (dehydrogenation)	← 11.9 →			-	← 11.1 →			
Yield THN, %w	3.7	3.6	3.6	3.9	15.3	13.0	9.6	5.9
Selectivity for, %w								
THN	12.5	8.8	7.0	7.5	47.1	30.0	17.5	8.9
Naphthalene	87.3	90.7	91.7	86.8	52.9	69.8	81.7	85.0
Yield cis DHN, %w	-2.1	-2.5	-2.9	-1.6	-1.7	-2.6	-3.1	-3.5
trans/cis Ratio in Product	24.1	23.7	23.1	13.5	20.2	23.6	24.1	24.5
% cis-DHN at Equilibrium (Basis Wall Temperature)	8.2	9.9	11.6	14.2	8.2	10.0	11.7	13.6

a) Cracked and heavier than naphthalene.

Arrhenius plots of the data for cis and trans-DHN at moderate conversion (LHSV = 200) and for cis-DHN at low conversion (LHSV = 400) are shown in Figure 19.

Catalyst deactivation occurred during dehydrogenation with both feedstocks. The increase in catalyst bed temperature was taken as a measure of catalyst deactivation, and the maximum temperature increase during each run is recorded in Tables 23 and 24. Deactivation was slight at 1022°F,10 atm pressure, and lower temperatures but was appreciable at 1112°F where the overall DHN conversions were about that observed at 1022°F. However, as in other cases, the effect was less at the higher pressure.

Rate constants for isomerization were calculated using the equations set down by Benson.[20] These show that for a reversible reaction:

$$A \underset{k_2}{\overset{k_1}{\rightleftharpoons}} B$$

that

$$-(k_1 + k_2)t = 2.3 \log \frac{AK - B}{A_oK - B_o}$$

where k_1 and k_2 are the rate constants for the forward and backward reaction, respectively,

A_o and B_o are the concentrations of cis and trans-DHN, respectively, in the feed

A and B are the concentrations of cis and trans-DHN, respectively, in the product

K is the equilibrium constant and = k_1/k_2

t is the reaction time which in a flow system is the residence time or Apparent Contact Time (ACT)[a]

Interpretation of the isomerization rate data was complicated by the fact that the rate of dehydrogenation of cis-DHN was greater than that of the trans species. The method used to calculate the isomerization rate constants did not take into account the relatively higher rate of disappearance of cis-DHN during dehydrogenation. Thus the calculated isomerization rate constants for cis to trans will be maximum values while those for trans to cis will be minimum values.

a) The Apparent Contact Time is related to the LHSV in the following manner:

$$ACT = \frac{3600 \times 273\ P_R \times MW}{LHSV \times T_R \times \rho \times 22{,}412}$$

where P_R = reactor pressure in atmospheres
T_R = reaction temperature in °K
MW = molecular weight of feed
ρ = liquid density of the feed.

(This equation neglects the volume change during reaction).

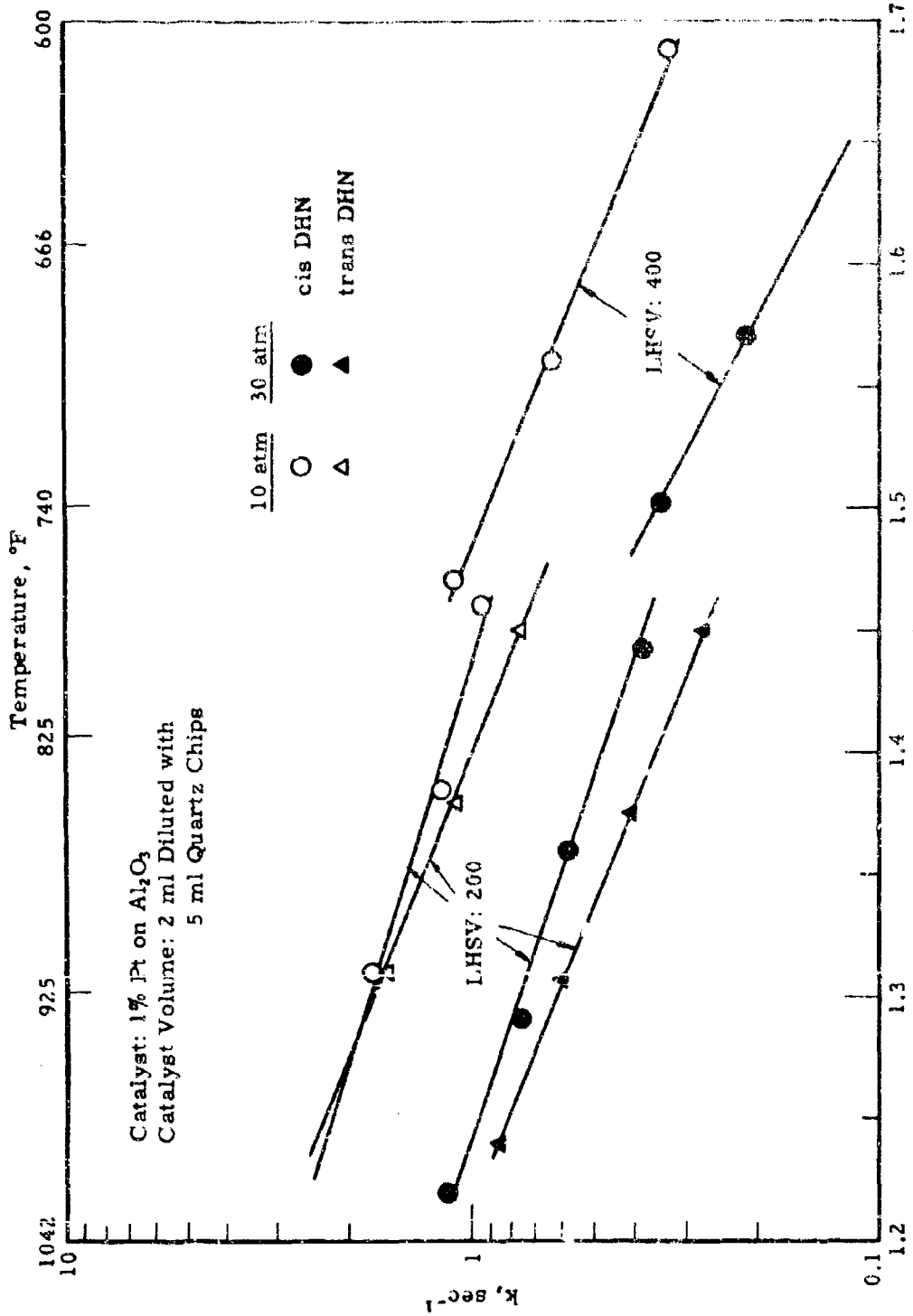


Figure 19. DEHYDROGENATION OF cis AND trans DECALIN
Temperature Coefficient

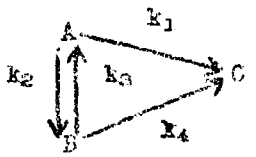
62731

With cis-DHN feed at the higher space velocity (LHSV = 400) the rate of cis to trans-isomerization was 7-10 times greater than the rate of trans to cis, at both 10 and 30 atm pressure (Table 23). No clear cut temperature effect was observed which suggests that the activation energy for isomerization was very low. The isomerization rates at 30 atm pressure were greater than those at 10 atm (662-752°F), which may have been because there was less dehydrogenation at the higher pressure.

At the lower space velocity (LHSV = 200) the rate of cis to trans was 4.5 to 6 times greater than the rate of trans to cis (Table 24). At both 10 and 30 atm pressures the rates appeared to decline with increased temperature, possibly due to the increased rate of the competing dehydrogenation reaction. As at the higher space velocity, isomerization rates were greater at the higher pressure.

No overall trans to cis-isomerization was observed with the trans-DHN feed. Thus no quantitative conclusion regarding the relative isomerization and dehydrogenation rates were obtained from these experiments. Qualitatively, however, it appeared that the rate of isomerization of trans to cis-DHN was lower than the rate of cis to trans-isomerization and lower than the dehydrogenation rates; since during reaction there was a net loss in the cis component of the feed even at up to 50% DHN conversion (Table 24).

The reactions of the DHN isomers for dehydrogenation and for isomerization can be represented by:



where A = cis-DHN
B = trans-DHN
C = THN

The relative rates of the various reactions can be obtained by comparing the calculated rate constants. For convenience these have been collected on Table 25. The cis isomer was more reactive than the trans for both dehydrogenation and isomerization. At 30 atm pressure, dehydrogenation was faster at 932°F and higher temperatures, but below 932°F isomerization was faster; presumably due to a combined effect of equilibrium and activation energy on the dehydrogenation reaction. For isomerization the rate of cis-DHN was five to ten times faster than the rate of trans. For dehydrogenation the rate of cis was 6-30% faster than the rate of trans.

In summary, during the dehydrogenation of a mixture of cis and trans-decalin isomers at 842-1112°F, 10 to 30 atm pressure, the cis isomer will dehydrogenate more rapidly than the trans; no trans to cis-isomerization will occur; some cis to trans-isomerization will occur; and the relative concentration of the trans to cis in the product will decrease with increased temperature due to the increase in rate of dehydrogenation of the trans isomer relative to that of the cis isomer.

Table 25. RATE CONSTANTS FOR DEHYDROGENATION AND ISOMERIZATION OF DECALIN

Catalyst: 1% Pt on Al_2O_3

Block Temp, °F	10 atm				30 atm			
	k_1	k_2	k_3	k_4	k_1	k_2	k_3	k_4
	LHSV = 200							
842	0.94	0.30	0.041	0.71	0.38	0.50	0.072	0.27
952	1.18	0.29	0.036	1.09	0.58	0.41	0.066	0.40
1022	1.72	0.20	0.045	1.62	0.74	0.36	0.066	0.60
1112	-	-	-	-	1.16	0.28	0.056	0.85
	LHSV = 400							
662	0.33	0.24	0.023	-	0.08	0.34	0.036	-
752	0.63	0.21	0.025	-	0.22	0.39	0.045	-
842	1.10	0.31	0.043	-	0.34	0.31	0.041	-

Summary: Dehydrogenation of Decalin

The dehydrogenation of decalin occurred in two discernible steps with tetralin as the intermediate product. In the region of 842-1022°F the second step (THN $\longrightarrow$ N + $2H_2$) appeared to be faster by 1 to 1.5 orders of magnitude and had an activation energy about three times greater than that of the first step (DHN $\longrightarrow$ THN + $3H_2$). The cis DHN species was slightly more reactive than the trans.

Isomerization of the cis and trans species occurred concurrently with dehydrogenation. Compared to rates of dehydrogenation the rate of trans-isomerization was lower by about an order of magnitude while that of the cis-isomerization was lower by a factor of about four. This suggests that if isomerization does play a role in the dehydrogenation mechanism, it is not the rate determining step.

Selectivity for naphthalene was governed by equilibrium and was favored by high temperature, high conversion, and low pressure.

The highest heat sink obtained thus far with decalin was 1688 Btu/lb, of which 838 Btu/lb was due to heat of reaction (10 atm, 1022°F, LHSV = 30). This corresponded to a total heat sink of 1903 Btu/lb at 1340°F. The adverse effect of pressure on selectivity for naphthalene at pressures greater than 10 atm would be expected to decrease heat sinks only slightly. For example, at complete DHN conversion a decline in selectivity for naphthalene of 20% would lower the heat of reaction by only about 7% and the total heat sink by about 4%.

The laboratory platinum on alumina catalyst was somewhat unstable at 10 atm pressure; a commercial platinum catalyst was even more unstable. Stability of both catalysts was improved at higher pressures and at high conversions.

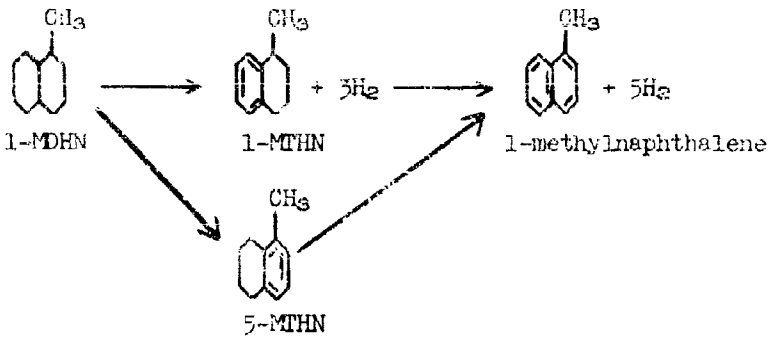
1-Methyldecalin

A brief study of the dehydrogenation of the 1-and 2-methyldecalins (MDHN) was made under the previous contract.[3] Using a platinum on alumina catalyst it was observed that at 10 atm pressure the catalyst was unstable with both isomers over the temperature range of 842-1022°F. This work now has been extended to higher pressures and conversions to study principally, the effect of these variables on catalyst stability.

The feed was 1-methyldecalin and contained 11.7% trans and 88.3% cis species.[a] This feed was prepared by hydrogenation of the corresponding methylnaphthalene. Vapor phase dehydrogenation was studied with our standard 1% platinum on alumina catalyst at 10-30 atm pressure, LHSV of 30-100 over the temperature range of 842-1022°F. Product material was analyzed by GLC using a five foot, 1/4-in. OD stainless steel column packed with 5% Carbowax 1000 on Chromosorb W.

a) This is a nominal value. Actually, there are 4 geometric isomers for each positional isomer (not counting optical isomers) cis-cis, cis-trans, trans-cis, trans-trans.

Under the above reaction conditions, the dehydrogenation of 1-MDHN to 1-methylnaphthalene was a two-step process with two methyltetralin isomers (MTHN) as intermediate products. Schematically the reaction can be represented:



The heat of reaction to form MTHN is 600 Btu/lb; and to form methylnaphthalene is 900 Btu/lb.

At 10 atm pressure, 842 and 932°F considerable catalyst deactivation was observed with this feedstock. This was shown by the fact that the catalyst bed temperature increased during the run by 68-108°F and 185-207°F at 932°F. Further, in these experiments no increase in MDHN conversion occurred when the reaction temperature was increased from 842°F to 932°F (cf Runs 180-1 and 180-2; and Runs 142 and 143; Table 26).

Increasing the reactor pressure appeared to stabilize the catalyst. Thus, increases in catalyst bed temperatures of only 9°F or less were observed when the pressure was increased to 20 and 30 atm (842-1022°F; Table 26). Also operating the reactor at elevated pressures (20 and 30 atm) appeared to stabilize the catalyst somewhat for subsequent operation at 10 atm pressure. This is shown by Run 189-3, Table 26 in which the catalyst deactivation at 1022°F after operation at 30 and 20 atm, was less than that observed either at 842 or 932°F at 10 atm with fresh catalyst (Runs 180-1 and 180-2; 142-143, Table 26).

The complete data are recorded in Table 26. Runs 183-1 to 189-3 were made on the same charge of catalyst in the order tabulated (left to right). Runs 180-1 and 142 were made on fresh catalyst. First order rate constants were calculated from the rate of disappearance of MDHN and were for the reaction MDHN ——→ MTHN.

At 20 and 30 atm pressure, the reaction products were mainly 1- and 5-MTHN and methylnaphthalene. Selectivity for the sum of these products was high (90-99%) at both moderate and high conversions. As was observed with Decalin, selectivity for the completely dehydrogenated product (methylnaphthalene) was favored by high temperature and high conversion. Presumably this was an equilibrium rather than a kinetic effect. For the two MTHN isomers, the 5-MTHN appeared to be favored by high pressure and lower temperature (cf 5-MTHN/1-MTHN ratio, Table 26).

At these pressures, the reactivities and selectivities for methylnaphthalene were about comparable to those observed with Decalin. Heat sinks were slightly lower than was observed with Decalin primarily due to the greater molecular weight of the MDHN.

Table 86. DEHYDROGENATION OF 1-METHYLDECALIN AT VARIOUS PRESSURES

Catalyst: 1% Pt on Al_2O_3 Feed: 11.7% trans-1-MDHN
Catalyst Volume: 7 ml 88.3% cis-1-MDHN
Reaction Time: 30 min

Run No. 9347-	183-1	183-3	184	185-1	185-3	186	187-1	188-1
Pressure, atm	← 30 →					← 20 →		
LHSV	100	100	100	50	30	100	100	100
Temperature, °F								
Block	942	932	1022	1022	1022	842	932	1022
Wall	745-47	874	950-54	959-57	970	741-43	819-26	894-900
Catalyst Bed	646-51	689-86	734	740-42	758-59	676-78	711-16	752-61
	650-53	698-93	732	754-56	799-801	674-76	707	743
	662-63	716-11	754-52	794	858-62	691-94	729	765
	680-82	736-32	781-79	835-37	912-16	712-14	756	795
ΔT_{max}, °F - catalyst bed	+5	-5	-2	+2	+4	+3	+5	+9
Product Analysis, %w								
trans-1-MDHN	22.3	16.4	13.4	10.0	3.9	14.1	13.2	11.8
cis-1-MDHN	38.8	36.9	30.2	9.7	2.1	56.8	46.4	34.8
U_1 [a]	0.0	0.0	0.0	0.4	1.9	0.0	0.0	0.0
1-MTHN	7.3	5.2	3.7	2.1	0.8	2.6	2.4	2.2
U_2 [a]	0.1	0.1	0.1	0.1	0.0	0.0	0.0	0.0
5-MTHN	15.9	10.7	7.3	4.1	1.4	4.9	4.3	3.7
U_3 [a]	0.0	0.0	0.1	0.5	2.6	0.0	0.0	0.1
Methylnaphthalene	15.6	30.7	45.2	71.6	82.4	21.6	33.7	47.4
Cracked	0.0	0.0	0.0	1.5	4.9	0.0	0.0	0.0
Conversion, %w	38.9	46.7	56.4	80.3	94.0	29.1	40.4	53.4
5-MTHN/1-MTHN	2.18	2.06	1.97	1.95	1.75	1.89	1.79	1.68
Selectivity for, %w								
MTHN	59.6	34.1	19.5	7.6	2.3	25.8	16.6	11.1
Methylnaphthalene	40.2	65.8	80.2	89.2	87.7	74.2	83.4	88.8
k, sec^{-1}	0.146	0.212	0.289	0.309	0.297	0.153	0.246	0.385
Heat Sink, Btu/lb								
Reaction	279	371	473	681	745	239	343	461
Total at Block Temp	989	1151	1323	1531	1595	949	1125	1311
Total at 1340°F	1379	1471	1572	1781	1845	1339	1443	1561

a) Unidentified.

(Continued)

Table 26 (Contd). DEHYDROGENATION OF 1-METHYLDECALIN AT VARIOUS PRESSURES

Run No. 9347-	188-3	189-1	189-3	180-1	180-2	142	143
Pressure, atm	← 20 →		10	10	10	10	10
LHSV	50	30	100	100	100	100	100
Temperature, °F							
Block	1022	1022	1022	842	932	842	932
Wall	916-18	936-38	972-92	729-50	823-923	741-68	797-823
Catalyst Bed	756	763-66	957-74	651-725	783-903	664-772	806-907
	761	795-97	860-920	648-80	718-903	646-689	711-912
	799-801	855-60	833-78	662-73	718-890	653-675	700-907
	842-44	910-12	853-78	680-91	748-872	671-684	720-887
ΔT_{max}, °F - catalyst bed	+2	+5	+68	+74	+189	108	207
Product Analysis, %w							
trans-1-MDHN	9.4	4.6	10.1	13.4	11.7	13.5	11.7
cis-1-MDHN	15.5	4.2	58.0	55.8	58.2	54.5	60.2
U_1 [a]	0.3	1.1	1.9	0.0	0.0	0.0	0.0
1-MTHN	1.4	0.7	4.2	2.0	2.6	2.2	5
U_2 [a]	0.0	0.0	0.0	0.0	0.0	0.0	0.0
5-MTHN	2.2	0.9	2.4	3.1	2.5	3.8	2.2
U_3 [a]	0.5	1.8	0.2	0.0	0.0	0.0	0.0
Methylnaphthalene	70.2	84.3	23.2	25.7	25.2	26.0	23.4
Cracked	0.5	2.4	0.0	0.0	0.8	0.0	0.0
Conversion, %w	75.1	91.2	31.9	30.8	30.1	32.0	29.1
5-MTHN/1-MTHN	1.57	1.29	0.57	1.55	0.89	1.73	0.88
Selectivity for, %w							
MTHN	4.8	1.7	20.7	16.6	16.3	18.8	19.6
Methylnaphthalene	93.4	92.4	72.8	83.5	82.8	81.2	80.4
k, sec^{-1}	0.354	0.419	0.412	0.329	0.337	0.342	-
Heat Sink, Btu/lb							
Reaction	654	768	249	262	262	270	239
Total at Block Temp	1504	1618	1099	972	1042	980	1019
Total at 1340°F	1754	1868	1349	1362	1352	1370	1339

a) Unidentified.

Effect of Pore Size on Catalyst Stabilities For the Dehydrogenation of Naphthenes

In the dehydrogenation of dicyclics decalin and decylcyclohexyl at 10 atm pressure, poor catalyst stability was observed with the commercial platinum on alumina catalyst, while better catalyst stability was observed with the laboratory platinum on Harshaw 0104 alumina catalyst. Further, poor catalyst stability was observed with a halogen-free platinum on the commercial alumina-base catalyst, prepared in the same manner as the laboratory catalyst. Stability of both catalysts was improved, however, at higher pressures and at high conversions. These results suggested the following explanation as to why naphthenes can be dehydrogenated without added hydrogen over a platinum on alumina catalyst with good catalyst stability.

For the dehydrogenation of MCH over our laboratory platinum on alumina catalyst it was observed that good catalyst stability was obtained when the partial pressure of hydrogen in the exit gas was about 0.75 atm; but that the catalyst became inactive when the partial pressure was less than about 0.7 atm. Presumably the hydrogen formed by dehydrogenation reacted with and removed the coke precursors, and this maintained a "clean" catalyst surface. Since this reaction occurred in the catalyst pores, the actual "effective" partial pressure of hydrogen in the pore may have been greater than 0.75 atm.

At a given overall naphthene conversion the "effective" hydrogen partial pressure is determined by the concentration of hydrogen in the pore. This hydrogen concentration will be greater in smaller pores, since the surface-to-volume ratio is greater and hence the fraction of naphthene in the pore that is converted will be greater. Further, the transport rate of hydrogen out of the pore may also be a factor in maintaining catalyst stability, as for a given conversion this rate will determine the "residence" time and hence effective partial pressure of hydrogen in the pore. Conceivably then, for the dehydrogenation of MCH with a catalyst having a smooth, nonporous surface the partial pressure of hydrogen needed for maintaining good catalyst stability may be greater than 0.75 atm. Thus the pore diameter of the catalyst will be a factor in maintaining good catalyst stability.

For the dehydrogenation of DHN and DCH at 10 atm pressure good catalyst stability was observed with the laboratory platinum catalyst. With the commercial catalyst, however, the following results were obtained:

a. Poor catalyst stability was obtained at 10 atm pressure at 50% conversion and lower.

b. Increasing the reactor pressure to 20 or 30 atm stabilized the catalyst.

c. Operating the reactor at 90% conversion stabilized the catalyst at 10 atm pressure.

Most of the pores in the laboratory catalyst are of smaller diameter than those of the commercial catalyst. For example, with the laboratory catalyst 72% of the pore volume was in pores of diameter 204 A or less, while with the commercial catalyst only 46% was in pores of 235 A or less diameter

(see Table 27). Thus for the commercial catalyst the partial pressure of hydrogen in the pores was lower than that in the laboratory catalyst and the hydrogen concentration was not greater enough to maintain good catalyst stability. When the partial pressure of hydrogen was enhanced by increasing the total reactor pressure or by operating the reactor at high conversion, good catalyst stability was obtained.

These views predict that a catalyst with smaller pore diameters than our laboratory catalyst would be more stable for the dehydrogenation of DHN. Also that the stability of the commercial catalyst would be improved by reducing the pore size of this catalyst. However, it would be expected that as pore size is continually decreased, a point will be reached at which the relative diffusion rate of hydrogen out of the pore will be greater than that of toluene and hence the "effective" hydrogen concentration in the pore will begin to decrease and catalyst instability will occur.

Dehydrogenation of Naphthene Mixture

Methylcyclohexane (MCH), dicyclohexyl (DCH) and decalin (DHN) are readily dehydrogenated over platinum on alumina catalysts to give heat sinks of 1800+ Btu/lb. With dicyclic naphthene, however, intermediate dehydrogenation products are formed, which can reduce the heat sink of reactions appreciably. With dicyclohexyl and decalin selectivity for the completely dehydrogenated aromatic was favored by high temperature, high conversion and low pressure. In earlier work it was shown that in a mixture of naphthenes, the reactivities of the components were different from those of the pure compounds.[2] Thus it was of interest to study the dehydrogenation of naphthene mixtures, particularly with respect to reactivity, selectivity for the completely dehydrogenated product, and to catalyst stability. For these studies mixtures of MCH with DCH and with DHN, and DCH with DHN and 1-methyldecalin were used.

Dicyclohexyl-Methylcyclohexane

In this series of experiments the effect of added methylcyclohexane (MCH) was studied on the reactivity of dicyclohexyl (DCH) for catalytic dehydrogenation and for thermal reaction, and on the selectivity of the dehydrogenation reaction for diphenyl (DP). The feed mixture was 75.5% DCH; 2.2% phenylcyclohexane (PCH) and 22.3% MCH.

The catalytic reaction was studied at 10-30 atm pressure, 842-1022°K LHSV of 30-100 using a 1% platinum on alumina catalyst. Compared to reaction of pure DCH[a] and MCH[3] the DCH-MCH feed gave:

1. Enhanced reactivity of the DCH component but lower reactivity of MCH at a given temperature and pressure.

2. Enhanced selectivity for DP at a given conversion, temperature and pressure.

Heat sinks were slightly lower for the DCH-MCH mixture than for pure DCH under the same reaction conditions.

a) The complete data for dehydrogenation of pure DCH were reported previously.[3]

Table 27. PORE DISTRIBUTION OF TWO PLATINUM ON ALUMINA CATALYSTS

1% Pt on Harshaw 0104 Alumina			UOP-R8		
Pore Diameter A	Cumulative Volume		Pore Diameter A	Cumulative Volume	
	cc/g	% of Total		cc/g	% of Total
24	0.001	0.4	24	0.003	0.4
50	0.013	4.9	35	0.024	3.4
109	0.095	35.7	52	0.050	7.0
204	0.192	72.2	82	0.091	12.8
850	0.266	100	147	0.186	26.1
			235	0.328	46.1
			419	0.599	84.1
			850	0.712	100

Effect of Temperature

The effect of temperature on conversion and reaction rate was studied at 10 atm pressure over the range of 842-1022°F. The data are tabulated in Table 28 and Figure 20 shows a comparison of conversion as a function of temperature for the DCH-MCH mixture (points) and pure DCH (solid line). Over this temperature range the DCH conversions obtained with the DCH-MCH mixture were about 10% greater than those obtained with pure DCH. First order rate constants were calculated from the component conversions and are recorded in Table 28. The values obtained previously with pure components[1)2)3)] are shown in parenthesis for comparison. Based on the rate constants, the reactivity of DCH in the mixture was about 1.2 times greater than that of pure DCH while the reactivity of MCH was about one fourth that of pure MCH. Activation energies were computed from the rate constants and were lower for DCH and higher for MCH compared to the pure components. Heats of reaction for the mixture (Table 28) were lower by 3-8% than those obtained with pure DCH (Table 28, values in parentheses).

Effect of Space Velocity and Conversion

The effect of space velocity on conversion of DCH and MCH and the effect of conversion of DCM on selectivity for DP were studied in a series of "bracketed" runs at 842 and 1022°F. There was some decline in catalyst activity during these runs as in each series the conversions observed in the final runs were always slightly lower than those in the initial runs. The data are recorded in Table 29. Figure 21 shows selectivity for DP as a function of DCH conversion for pure DCH (solid lines) and in the mixture (points) at 842 and 1022°F. At both temperatures for a given conversion the selectivity for DP appeared to be greater for the feed containing MCH. As was observed with pure DCH, higher selectivity was obtained at the higher temperature for a given DCH conversion.

Effect of Pressure

The effect of pressure on reactivity and selectivity for DP was studied at 842 and 1022°F over the pressure range of 10-30 atm. At the higher temperature, DCH conversion appeared to increase slightly with increased pressure while at the lower temperature the reverse was true (Table 30). Selectivity for DP was quite pressure sensitive (as was observed with pure DCH)[3)] particularly at the lower temperature where the selectivity declined by a factor of about 2.5 when the pressure was increased for 10 to 30 atm. In general selectivities for DP were higher with the DCH-MCH mixture. Figures 22 and 23 show DCH conversions and selectivities for DP as a function of pressure at 842 and 1022°F, respectively, for pure DCH (solid lines) and for the DCH-MCH mixture (points). Heats of reaction of the DCH-MCH generally were up to 10% lower than those obtained with pure DCH (Table 30, values in parentheses are for pure DCH), under comparable conditions due to the low conversion of MCH.

From the experiments carried out this far with DCH-MCH mixture it appears that diluting a DCH feed will enhance the reactivity of the DCH and the selectivity of the reaction for diphenyl. Slight loss in heat sink will occur, however, that appears to be due to the low reactivity of the MCH component. Presumably DCH or more probably the product diphenyl is more

TABLE 28
DEHYDROGENATION OF DCH-MCH MIXTURE

Effect of Temperature

(Values for Pure DCH and Pure MCH in Parentheses)
Catalyst: 1% Pt on Al_2O_3 Catalyst Volume: 7 ml
Feed: 75.7% DCH LHSV: 100
2.3% PCH Pressure: 10 atm
22.0% MCH

Run 9645-	122	123	124
Temperature, °F			
Block	842	932	1022
Wall	749	814	880
Catalyst Bed	608	640	680
Product Analysis, %w			
MCH	19.4	18.0	16.2
Benzene	0.0	0.1	0.1
Toluene	2.6	3.8	5.7
DCH	31.2	26.4	21.4
PCH	26.9	17.6	9.6
DP	19.9	34.1	47.0
Yield PCH, %w	24.6	15.3	7.3
Conversion, %w			
DCH	58.8	65.1	71.7
MCH	11.8	18.2	26.4
Selectivity for, %w			
PCH	44.8	34.0	17.0
DP	55.2	66.0	83.0
k, sec^{-1}			
DCH	0.730 (0.609)	0.910 (0.762)	1.148 (0.972)
MCH	0.151 (0.62)	0.252 (1.00)	0.406 (1.45)
E, act, kcal/mole			
DCH	← 6.4 →		
	← (7.8) →		
MCH	← 14.0 →		
	← (11.8) →		
Heat Sink, Btu/lb			
Reaction Mixture	396	480	593
Pure DCH	406	523	644

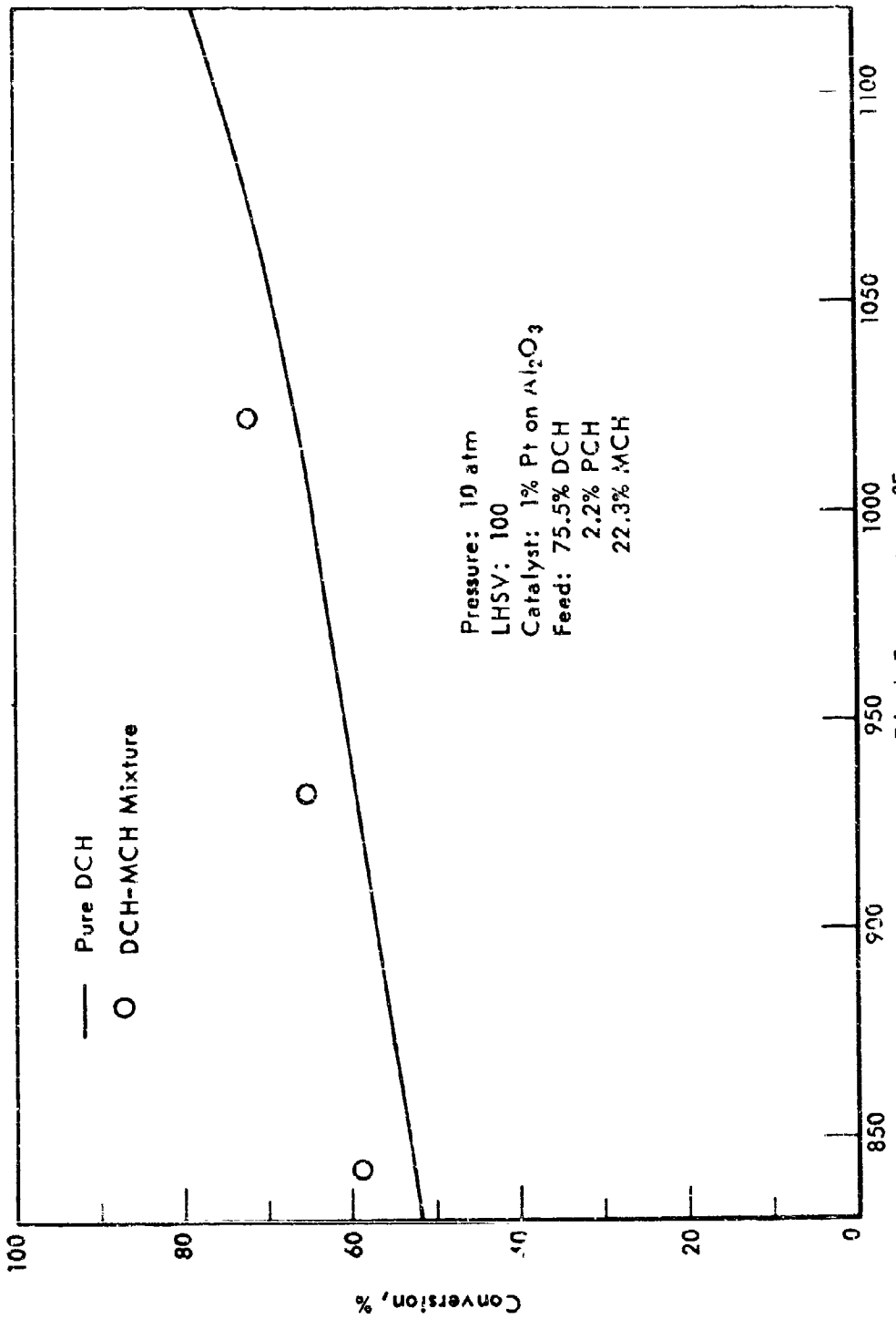


Figure 20. DEHYDROGENATION OF DCH-MCH MIXTURE
Effect of Temperature on Conversion of DCH

62392

TABLE 29
DEHYDROGENATION OF DCH-MCH MIXTURE

Effect of DCH Conversion on Selectivity for Diphenyl

(Values for Pure DCH and Pure MCH in Parentheses)
Catalyst: 1% Pt on Al_2O_3 Feed: 75.7% DCH
Catalyst Volume: 7 ml 2.3% PCH
Pressure: 10 atm 22.0% MCH

Run 9645-	126-1	126-3	127-1	127-3	128	129-1	129-3
Temperature, °F							
Block	← 842 →				← 1022 →		
Wall	741	750	761	747	887	900	892
Catalyst Bed	604	615	632	614	669	686	682
LHSV	100	50	30	100	100	50	100
Product Analysis, %w							
MCH	20.0	18.5	15.1	20.0	17.3	12.1	17.9
Benzene	-	0.2	0.2	0.1	0.3	0.5	0.2
Toluene	2.0	3.5	6.5	1.9	4.4	9.4	4.2
DCH	31.8	17.1	7.1	36.2	20.9	4.9	4.6
PCH	26.2	24.0	10.7	21.3	11.8	3.2	10.5
DP	20.0	36.7	60.4	20.5	45.3	69.9	43.6
Yield PCH, %w	23.9	21.7	8.4	19.3	9.5	1.4	8.2
Conversion, %w							
DCH	58.0	77.4	90.7	52.2	72.4	94.6	67.5
MCH	9.1	16.9	30.5	9.1	21.4	40.5	20.0
Selectivity for, %w							
PCH	54.4	37.2	12.0	48.5	17.3	2.0	15.8
DP	45.6	62.8	88.0	51.5	82.7	98.0	84.2
k, sec^{-1}							
DCH	0.707 (0.609)	0.610 -	0.590 -	0.604 -	1.177 (0.972)	1.345 -	1.030 -
MCH	0.114 (0.62)	0.111 -	0.132 -	0.115 -	0.320 (1.45)	0.348 -	0.296 -
Heat Sink, Btu/lb							
Reaction Mixture	-	-	-	-	-	851	-
Pure DCH						978	

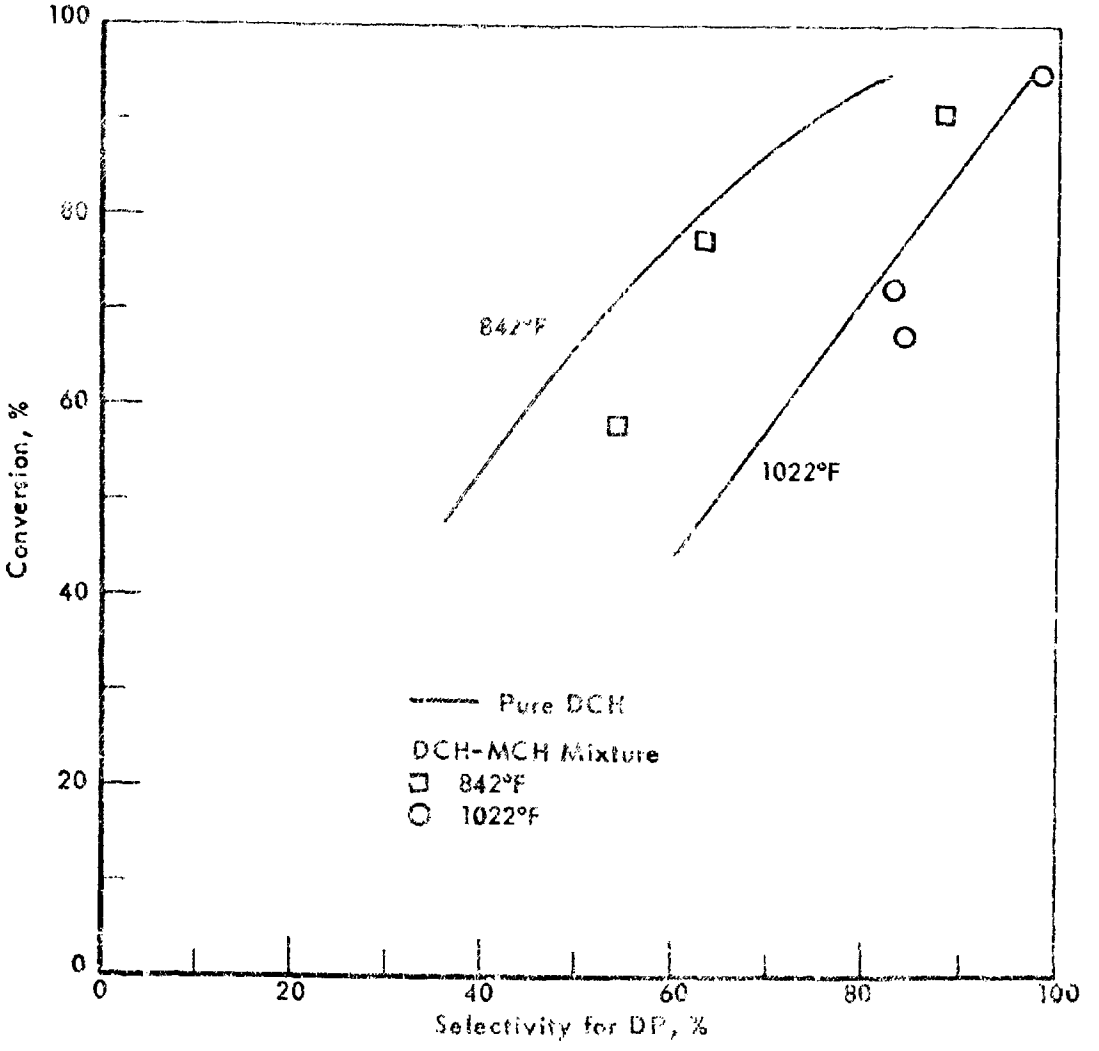


Figure 21. DEHYDROGENATION OF DCH-MCH MIXTURE
Effect of Conversion on Selectivity for DP

TABLE 30
DEHYDROGENATION OF DCH-MCH MIXTURE

Effect of Pressure

(Values for pure DCH and pure MCH in parentheses)

Catalyst: 1% Pt on Al_2O_3
Catalyst Volume: 7 ml
LHSV: 100
Feed: 75.5% DCH
2.2% PCH
22.3% MCH

Run No. 9645-	134	135-1	135-3	131-1	131-3	132
Temperature, °F						
Block	←	842	→	←	1022	→
Wall	734	745	752	873	874	882
Catalyst Bed	608	639	663	673	691	709
Pressure, atm	10	20	30	10	20	30
Product Analysis, %w						
MCH	19.8	19.4	19.9	17.0	16.5	16.4
Benzene	-	-	-	0.3	0.3	0.2
Toluene	1.9	2.5	2.1	4.7	5.4	5.2
DCH	31.8	31.9	39.9	19.5	16.3	16.9
PCH	26.0	34.1	31.6	9.3	21.8	31.8
DP	20.5	12.1	6.5	49.2	40.0	29.5
Yield PCH, %w	23.8	31.9	29.4	7.3	19.5	29.5
Conversion, %w						
DCH	57.9	57.7	47.2	74.2	78.5	77.7
MCH	11.3	13.1	10.8	22.8	25.0	25.5
Selectivity for, %w						
PCH	53.7	72.5	81.9	12.9	32.8	50.0
DP	46.3	27.5	18.1	87.1	67.2	50.0
k, sec^{-1}						
DCH	0.700	0.352	0.175	1.225	0.695	0.454
MCH	0.141	0.061	0.046	0.341	0.189	0.089
Heat Sink, Btu/lb						
Reaction Mixture	371	329	290	616	560	530
Pure DCH	390	294	242	672	619	565

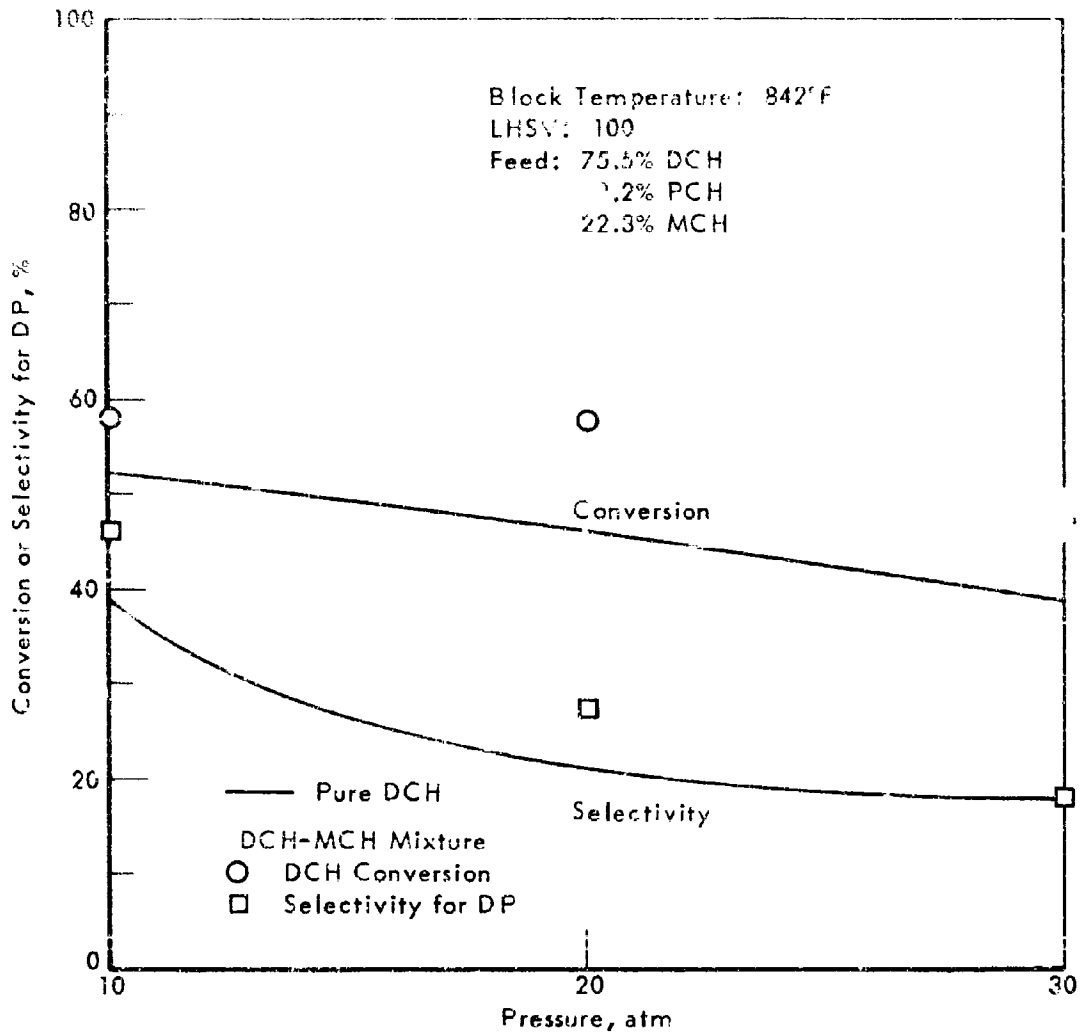


Figure 22. DEHYDROGENATION OF DCH-MCH MIXTURE AT 842°F
Effect of Pressure on DCH Conversion and Selectivity for Diphenyl

62392

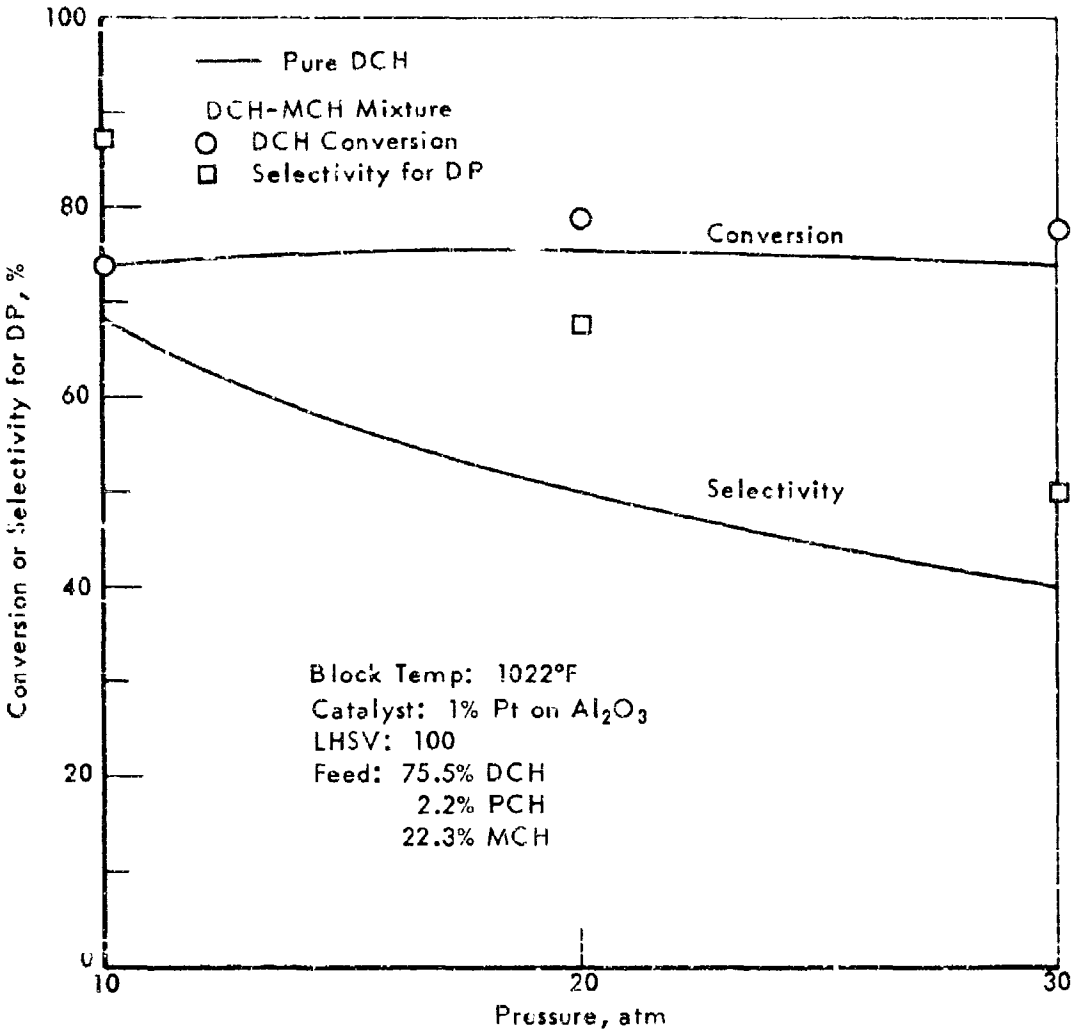


Figure 23. DEHYDROGENATION OF DCH-MCH MIXTURE AT 1022°F
Effect of Pressure on DCH Conversion and Selectivity for Diphenyl

strongly adsorbed on the catalyst surface than the MCH and hence inhibits the reactivity of this latter component. No further laboratory work with the DCH-MCH system is planned at this time. It is possible that results will be different under FSSTR conditions. If this appears likely by calculation, such a mixture may be tested under the larger scale conditions.

Thermal Reaction

The thermal reaction was studied at 40 atm pressure over the temperature range of 1022-1293°F. Under these conditions the reactivity of DCH was greater, and the reactivity of MCH was less than that of the pure components. For example, at 1293°F with the DCH-MCH mixture conversion of 86.2% and 54.7% were observed for DCH and MCH, respectively, compared to 67.7% and 47.7% for the pure components[a] (Table 31). Based on first order rate constants that were calculated from the conversion of the two components, the reactivity of DCH was greater by a factor of 1.6 to 1.8 and the reactivity of MCH less by a factor of 0.7 to 0.8 compared to the pure components. The apparent activation energy for DCH in the mixture was 45.6 kcal/mole compared to 47.0 kcal/mole for pure DCH. With MCH the apparent activation energy in the mixture was 60.1 kcal/mole compared to 39.3 kcal/mole for pure MCH. Figure 24 is an Arrhenius plot of the data obtained with the mixture. The values observed for DCH are certainly the same within the accuracy of measurement, but the values for MCH are probably significantly different. The cause of this effect is not known. The larger value for MCH is about the same as was observed by Fabuss et al of Monsanto[21,22] for naphthenes generally, while thermal decomposition of DCH at 800°F is 0.18 hr^{-1} which corresponds to ca 0.56 sec^{-1} at 1100°F using an E value of 60 kcal, compared to a value of 0.023 found here. If the 46 kcal value of E is used, k at 1100°F would be 0.027. Product material consisted of cracked liquid and light gas and dehydrogenated products. The dehydrogenated materials consisted of cyclohexenes, cyclohexadienes, benzene, toluene, and unidentified material heavier than toluene that was presumed to be alkyl aromatics. At the higher temperatures considerable light gas was formed that was principally methane, ethene, ethane, and hydrogen. The product distribution and yields of the cracked liquids are shown in Table 32. The light gas product distribution is shown in Table 33.

Heat sinks were estimated to be not greater than those obtained with pure DCH. This was based upon the fact that most of the products came from the reactions of DCH and that the products obtained were not very different from those obtained with pure DCH. (More conversion to light gas was observed with the mixture than with pure DCH.) Thus the heat of reaction for the mixture is estimated to be not greater than 65 Btu/lb.

Decalin-Methylcyclohexane

In earlier work on the dehydrogenation of MCH over a platinum on alumina catalyst,[2] it was shown that addition of 22% Decalin (decahydronaphthalene; DHN; 68% cis DHN) to the MCH feed reduced the reaction rate of the MCH by about a factor of two. In later work on the dehydrogenation of DHN addition of 10% MCH to one of the feeds appeared to retard the catalyst

a) The thermal reaction of DCH was reported in detail in reference 3 and, of MCH in reference 2.

TABLE 31
THERMAL REACTION OF DCH-MCH MIXTURE

(Values for pure DCH and pure MCH in parentheses)

Pressure: 10 atm
LHSV: 20
Catalyst: Quarts Chips
Feed: 75.5% DCH
2.2% PCH
22 3% MCH
Catalyst Volume: 20 ml

Run No. 9645-	137	138	139-1	139-3
Temperature, °F				
Block	1022	1112	1202	1293
Wall	1022	1110	1193	1267
Catalyst Bed	1011	1085	1139	1190
Product Analysis, %w				
MCH	21.5	21.4	17.3	10.1
Cyclohexenes	1.0	7.0	12.5	8.3
Cyclohexadienes	0.0	0.2	1.7	2.2
Benzene	0.0	0.3	2.7	9.2
Toluene	0.0	0.2	1.6	5.0
DCH	74.1	61.9	33.8	10.4
PCH	2.2	2.1	1.5	0.8
DP	0.0	0.0	0.0	0.0
Cracked, liquid	1.2	7.4	14.8	20.6
Cracked, light gas	0.0	0.0	14.1	34.1
Conversion, %w				
DCH	1.9	18.0	55.2	86.2
MCH	3.6	4.0	22.4	54.7
First Order Rate Constants, sec^{-1}				
DCH	-	0.043	0.180	0.465
(pure)	-	(0.023)	(0.111)	(0.255)
MCH	-	0.009	0.057	0.185
(pure)	-	(0.04)	(0.08)	(0.22)
E, act, kcal/mole				
DCH		←	45.6 (47.0)	→
MCH		←	60.1 (39.3)	→

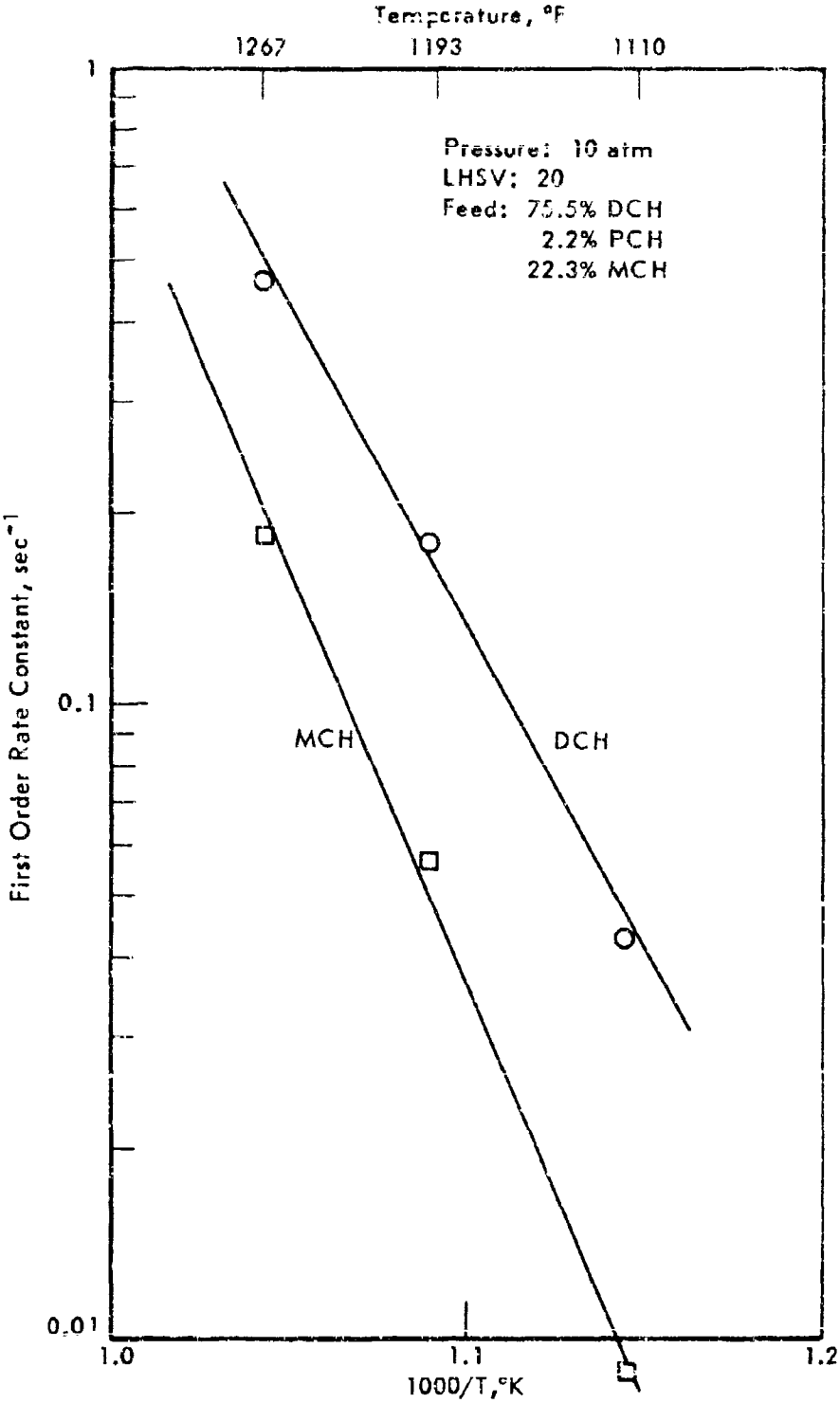


Figure 24. THERMAL REACTION OF DCH-MCH MIXTURE
Temperature Coefficient

TABLE 32
THERMAL REACTION OF DCH-MCH MIXTURE

Cracked Liquid Product Distribution

Feed: 75.5% DCH
2.2% PCH
22.3% MCH

Product	Product Analysis, %w				Yield, %w			
Run No. 9645-	137	138	139-1	139-3	137	138	139-1	139-3
Block Temperature, °F	1022	1112	1202	1293	1022	11.2	1202	1293
Lighter than C_6	-	6.8	10.1	14.6	-	0.5	1.5	3.0
Hexane	33.3	31.0	31.1	22.8	0.4	2.3	4.6	4.7
CH	41.7	17.0	20.9	10.2	0.5	2.0	3.1	2.1
U[a)]	-	1.4	6.8	3.4	-	0.1	1.0	0.7
U[b)]	25.0	28.4	25.0	35.0	0.3	2.1	3.7	7.2
U[c)]	-	5.4	6.1	14.0	-	0.4	0.9	2.9

a) Heavier than benzene but lighter than toluene.
b) Heavier than toluene but lighter than DCH.
c) Heavier than PCH.

TABLE 33
THERMAL REACTION OF DCH-MCH MIXTURE

Gas Phase Product Distribution

Feed: 75.5% DCH
2.2% PCH
22.3% MCH

Run No. 9645-	139-1	139-3
Block Temperature, °F	1202	1293
% Feed to Light Gas, %w	14.1	34.1
Product Analysis, %v		
H_2	19.9	16.5
CH_4	31.8	31.5
C_2H_4	22.2	20.6
C_2H_6	13.5	14.6
C_3H_6	7.0	9.1
C_3H_8	2.7	2.9
C_4H_8	0.8	1.0
C_4H_8	1.7	2.9
C_4H_{10}	0.0	0.2
C_5H_{10}	0.1	0.3
Higher than C_5	0.3	0.4

deactivating reaction. These effects have now been investigated further using DHN-MCH mixtures and studying the effect of MCH concentration on the reactivities of the feed components and on the catalyst deactivating reaction. In these tests DHN-MCH mixtures with 9%, 23%, 47% and 71% MCH were dehydrogenated over the 1% Pt on Al_2O_3 catalyst at 10 atm pressure and 842-1022°F. The DHN was a Shell plant preparation and contained 91.2% trans and 8.8% cis-DHN. The results are summarized in Table 34.

Based on the first order rate constants the reactivities of both DHN and MCH generally increased with increasing MCH concentration (Figure 25). However, the rates of reaction for DHN were greater, and those for MCH smaller, than for the pure compounds. Thus with the 29% DHN-71% MCH mixture, the reactivity of the DHN component was about double that of pure DHN, while the reactivity of MCH was about one half that of pure MCH (k_{MCH} = 1.45 sec^{-1} at 1022°F). The addition of MCH had no appreciable effect on the selectivity for naphthalene. Similar results with a different DHN feed, addition of 9% or 23% MCH to this DHN feed enhanced catalyst deactivation, while addition of 47% or 71% MCH reduced the deactivation only slightly. The magnitude of the increase in catalyst bed temperature during the run was taken as a measure of catalyst deactivation. These results suggest that factors influencing catalyst deactivation with DHN may be effected by the isomer composition of the DHN feed.

Dicyclohexyl-Decalin

Two mixtures of 50% DCH-50% DHN were tested at 842-1022°F, 10-30 atm pressure, at LHSV's of 30-100. One feedstock was made up with a Decalin containing a high concentration of the cis isomer (F113; 74.5% cis DHN) and the other with a Decalin containing a high concentration of the trans isomer (Shell DHN; 91.5% trans DHN). Complete compositions of the two feedstocks were:

	50% DCH Plus 50% of	
	F-113 DHN	Shell DHN
% DCH	49.2	49.5
% trans-DHN	12.3	44.8
% cis-DHN	36.9	4.3
% PCH	1.4	1.4
% THN	0.2	0.0

Reaction products were analyzed by GLC from which conversions and selectivities were calculated. First order rate constants were calculated for each naphthene component based on its rate of disappearance. Activation energies were computed from the first order rate constants, based on the reactor wall temperatures.

The effect of temperature on conversion was studied over the temperature region of 842-1022°F (10 atm, LHSV = 100). Tests with both feedstocks showed that addition of DHN to DCH lowered the reactivity of DHN; increased the reactivity of DCH when the DHN had high trans content (Table 35, Figure 36); and did not appreciably affect the DCH reactivity when the DHN had high cis isomer content (Table 36, Figure 26).

Activation energies (E_{act}) for the dehydrogenation of DCH and DHN were calculated from the first order rate constants (Tables 36 and 35) and

TABLE 54
DEHYDROGENATION OF DECALIN-METHYLCYCLOHEXANE MIXTURES

Pressure: 10 atm
LHSV: 100
Catalyst: 1% Pt on Al_2O_3
Catalyst Volume: 7 ml

Run Number 9645-	104-1	104-3	105	115	116-1	116-3	145	146-1	146-3	149	150-1	150-3	153	154-1	154-3
Feed Composition, %															
trans-DHN	91.2			83.1			70.5			48.7			26.0		
cis-DHN	8.8			8.0			6.8			4.7			2.5		
MCH	0.0			8.9			22.7			46.6			71.4		
Temperature, °F															
Block	842	932	1022	842	932	1022	842	932	1022	842	932	1022	842	932	1022
Wall	756-58	806-15	875-85	752-54	815-19	878-91	764	827-28	894-901	756-58	830	895	764-65	808	874-78
Catalyst Bed	662-69	691-716	727-84	664-96	716-63	751-874	676-93	726-61	765-876	653-67	689-718	734-83	664-80	707-27	754-90
	664-71	695-705	729-48	657-71	696-712	732-66	662-75	697-712	734-61	653-62	689-700	729-43	660-67	666-93	727-36
	671-76	704-711	745-59	671-78	707-16	750-61	676-80	711-18	750-61	666-71	704-09	748-52	659-62	694-700	743-47
	680-82	716-23	961-63	684-89	725-30	770-76	689-93	729-34	774-79	680-86	722-27	770-74	673-66	723-720	771-72
Product Analysis, %w															
MCH	-	-	-	7.3	5.6	6.1	18.5	16.4	14.7	35.9	31.9	27.3	54.7	49.9	39.4
Toluene	-	-	-	1.6	2.3	2.6	4.2	5.7	6.7	10.2	13.8	16.8	19.0	21.3	32.9
trans-DHN	71.4	65.1	55.6	63.7	57.0	49.3	54.5	47.4	41.1	35.3	30.3	24.9	16.3	13.2	10.4
cis-DHN	3.6	3.4	2.9	3.4	2.8	2.4	2.6	2.1	2.0	1.6	1.1	1.0	0.7	0.4	0.4
?[a]	0.1	0.5	0.9	0.1	0.1	0.6	0.0	0.2	0.5	0.0	0.1	0.5	0.0	0.0	0.2
THN	4.7	4.0	3.0	4.1	3.2	2.6	3.0	2.7	2.3	2.7	2.2	1.7	1.8	1.0	0.9
Naphthalene	20.1	29.0	37.6	19.7	28.0	36.2	17.2	25.5	32.7	14.3	20.5	27.7	9.2	13.1	17.1
Cracked	0.1	0.0	0.0	0.0	0.0	0.0	0.0	0.0	0.0	0.0	0.1[b]	0.1[b]	0.0[b]	0.1[b]	0.1[b]
Conversion, %w															
trans-DHN	24.8	30.8	39.0	23.4	31.4	40.7	22.4	32.8	41.7	27.6	37.8	48.8	36.6	49.1	60.0
cis-DHN	59.1	61.4	67.0	53.5	65.0	70.0	61.7	69.1	70.5	46.0	77.7	78.7	73.1	84.8	84.6
Total DHN	25.0	33.5	41.0	28.3	34.3	43.2	26.1	36.0	44.2	30.0	41.2	52.0	39.9	52.0	62.2
MCH	-	-	-	18.0	25.8	31.4	18.5	27.8	35.2	23.0	31.3	41.4	26.2	35.7	44.8
Selectivity for, %w															
THN[c]	18.8	11.6	7.3	17.2	10.2	6.6	14.9	9.5	6.6	13.9	9.6	5.7	13.4	10.2	5.9
Naphthalene[c]	80.4	86.6	90.6	80.4	89.5	91.8	85.1	89.7	92.1	84.1	89.2	93.2	85.6	89.1	93.4
First Order Rate Constants, sec^{-1}															
DHN	0.284	0.419	0.580	0.301	0.433	0.618	0.301	0.465	0.644	0.365	0.584	0.736	0.479	0.764	1.041
MCH	-	-	-	0.230	0.376	0.502	0.247	0.414	0.582	0.314	0.479	0.727	0.368	0.574	0.792
Pure MCH	0.62	1.00	1.49	-	-	-	-	-	-	-	-	-	-	-	-

a) Unidentified.
b) Benzene.
c) Based on DHN converted.

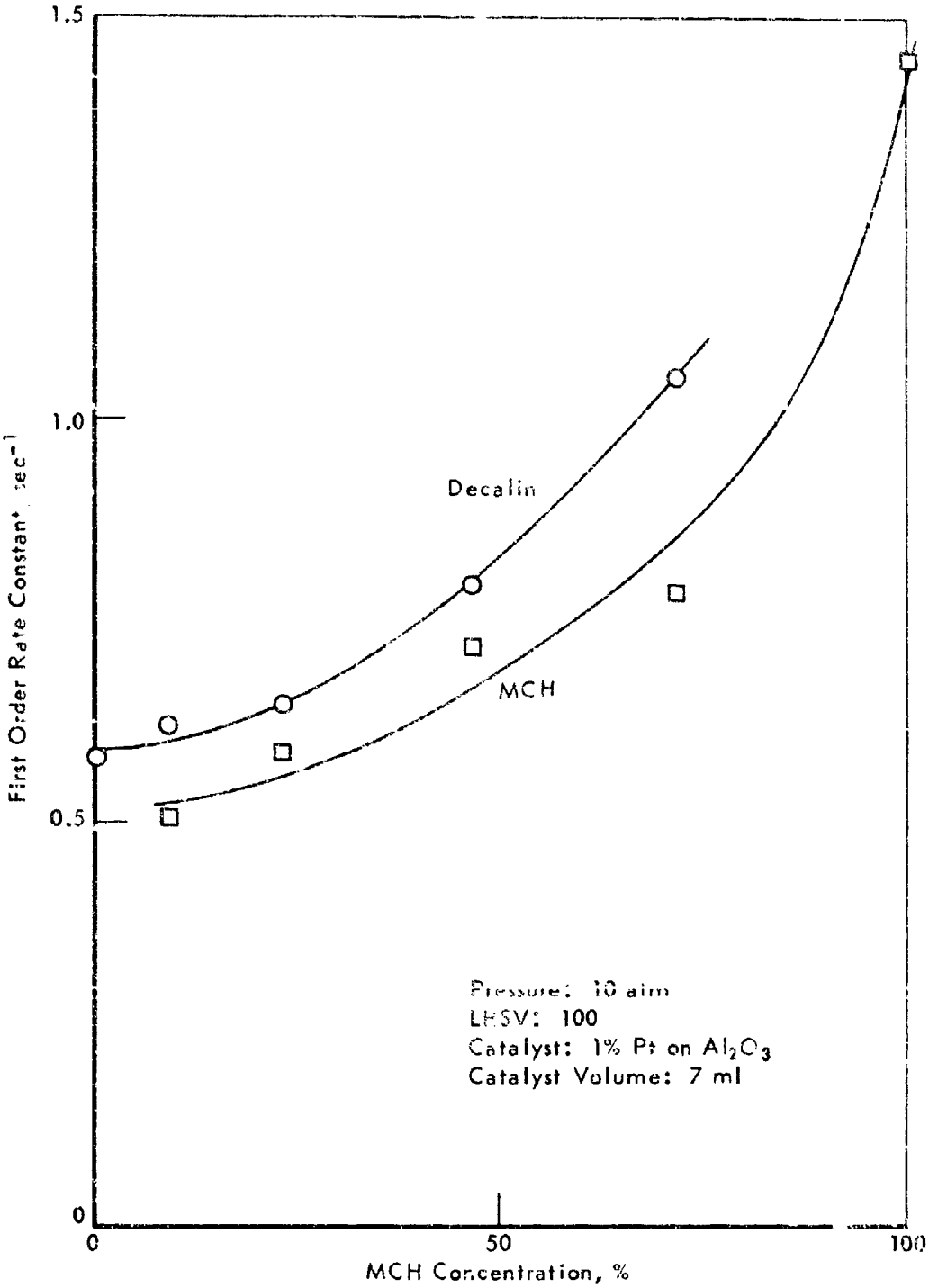


Figure 25. DEHYDROGENATION OF DECALIN-METHYL-CYCLOHEXANE AT 1022°F
Effect of MCH Concentration on Component Reaction Rates

Table 35. DEHYDROGENATION OF DCH-SHELL DHN MIXTURE: EFFECT OF TEMPERATURE

Values for pure DCH and pure DHN in parentheses.

Catalyst:	1% Pt on Al_2O_3	Feed:	44.6% trans-DHN
Catalyst Volume:	7 ml		4.3% cis-DHN
LHSV:	100		49.5% DCH
Pressure:	10 atm		1.4% PCH

Run No. 9645-	187	188-1	188-2
Temperature, °F			
Block	842	932	1022
Wall	738	802	862
Catalyst Bed	639	682	741
ΔT Catalyst Bed, °F	11	7	16
Product Analysis, %w			
trans-DHN	39.2	36.0	30.3
cis-DHN	2.5	2.3	2.4
DCH	20.0	15.2	11.8
THN	3.0	2.3	2.1
PCH	14.3	10.4	8.3
Naphthalene	5.1	8.8	14.5
DP	15.9	25.0	30.6
Yield PCH, %w	13.3	9.1	7.0
Conversion, %w			
DCH	59.7 (51.2)	69.7 (58.3)	76.3 (65.4)
DHN	15.1 (25.0)	22.0 (33.5)	33.4 (41.5)
Selectivity for, %w			
PCH	45.2	26.4	18.4
DP	54.8	73.6	81.6
THN	36.6	20.6	12.5
Naphthalene	63.4	79.4	87.5

(Continued)

Table 35 (Contd). DEHYDROGENATION OF DCH-SHELL DHN MIXTURE: EFFECT OF TEMPERATURE

Run No. 9645-	187	188-1	188-2
k, sec^{-1}			
DCH	0.739	1.022	1.231
	(0.609)	(0.762)	(0.872)
DHN	0.161	0.254	0.435
	(0.284)	(0.419)	(0.580)
Overall	0.398	0.577	0.812
E, act, kcal/mole			
DCH	←	7.8	→
	←	(7.8)	→
DHN	←	13.9	→
	←	(12.2)	→
Heat Sink Reaction, Btu/lb			
Mixture	454	583	637
Pure DCH	532	705	781
Pure DHN	128	196	306

TABLE 3(5). DEHYDROGENATION OF DECALIN MIXTURES: EFFECT OF TEMPERATURE

Values of pure cis and pure DCH in parentheses.

Catalyst:	1% Pt on Al_2O_3	Feed:	49.2% DCH
Catalyst Volume:	7 ml		32.3% trans DHN
LHSV:	100		16.9% cis DHN
Pressure:	10 atm		1.4% PCP
Decalin:	F-115		0.2% THN

Run 9645-	158	159	160
Temperature, °F			
Block	642	932	1022
Wall	718	844	889
Catalyst Bed	644	687	748
ΔT Catalyst Bed, °F	9	9	25
Product Analysis, %w			
trans-DHN	15.9[a]	12.7[a]	11.2
cis-DHN	20.7	18.0	15.1
DCH	25.4	20.3	17.1
THN	5.1	4.0	2.7
PCH	12.7	10.2	8.1
Naphthalene	10.2	14.8	19.8
DP	12.1	20.0	25.0
Yield PCH, %w	11.3	8.8	6.7
Conversion, %w			
DCH	51.2	58.7	65.0
	(52.2)	(58.3)	(68.4)
DHN	29.7	37.6	44.5
	(40.2)	(49.2)	(56.5)
Selectivity for, %w			
PCH	51.7	30.6	21.1
DP	48.3	69.4	78.9
THN	33.4	21.3	22.0
Naphthalene	66.6	78.7	88.0

a) cis to trans-isomerization occurred during dehydrogenation.

(Continued)

Table 36 (Contd). DEHYDROGENATION OF DCH-DHN MIXTURE: EFFECT OF TEMPERATURE

Run 9645-	158	159	160
k, sec^{-1}			
DCH	0.573	0.780	0.960
	(0.609)	(0.762)	(0.972)
DHN	0.357	0.497	0.642
	(0.498)	(0.693)	(0.900)
Overall	0.487	0.602	0.762
E, act, kcal/mole			
DCH	5.3		
	(7.8)		
DHN	6.6		
	(7.7)		
Heat Sink Reaction, Btu/lb			
Mixture	333	437	533
Pure DCH	406	523	644
Pure DHN	276	448	510

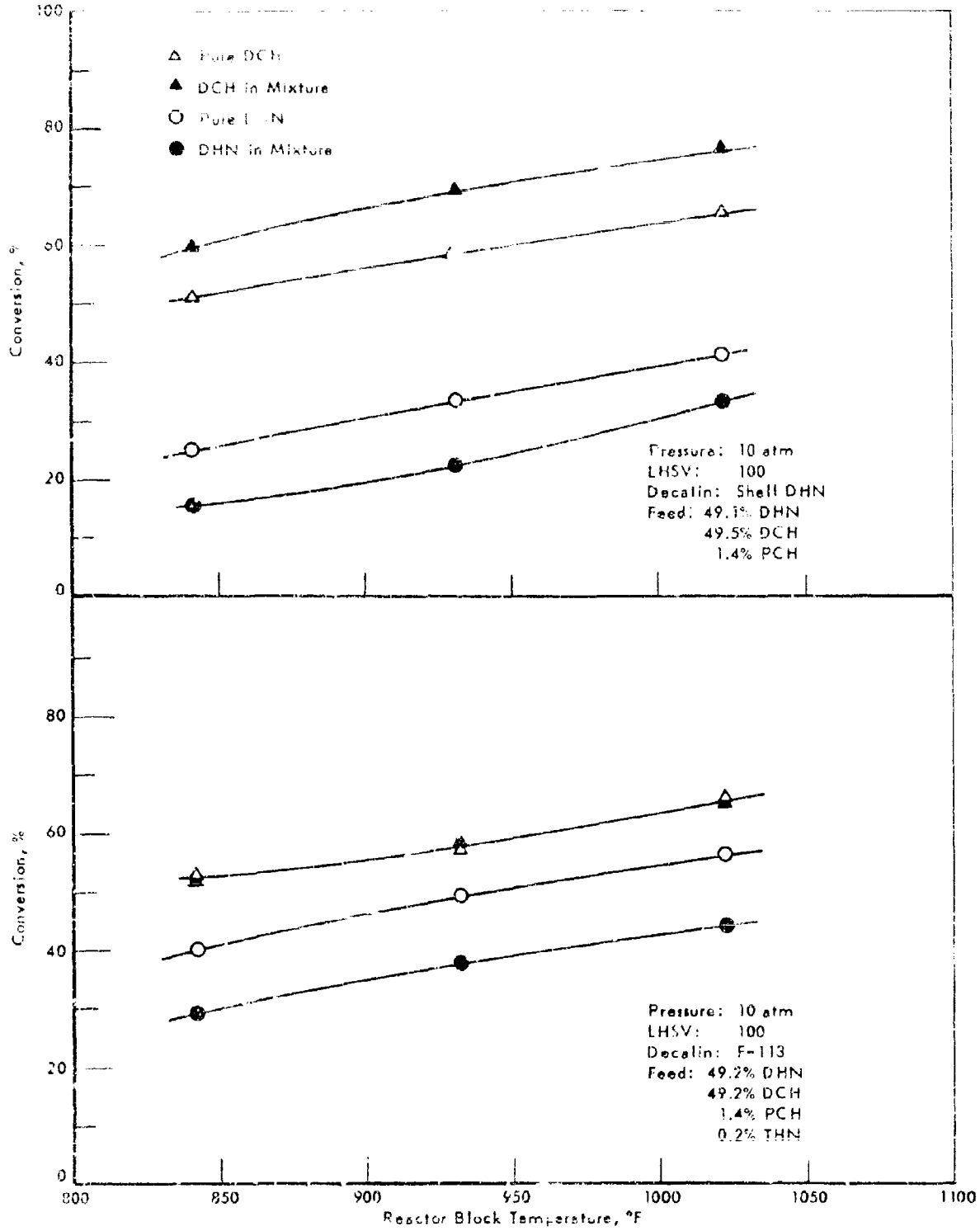


Figure 26. DEHYDROGENATION OF DCH-DHN MIXTURE
Effect of Temperature on Conversion for Different Decalins

63294

were different with the two feedstocks. Thus with the high cis-DHN feed, E_{act} for DCH and DHN were lower than those observed for the pure components (Table 36); while with the high trans-DHN feed, E_{act} for DCH equalled that of pure DCH and E_{act} for DHN was higher than that of pure DHN (Table 35). Figure 27 shows Arrhenius plots of the data for the DCH-DHN mixtures. As the activation energies were calculated from the first order rate constants, they represent activation energies for the first dehydrogenation step.

With pure DHN, catalyst deactivation was observed during dehydrogenation.[3] Mixing DCH and DHN reduced this catalyst deactivation considerably. For example, during dehydrogenation of pure F-113 DHN and pure Shell DHN increases in catalyst bed temperatures of 140°F and 57°F, respectively, were observed at 1022°F.[3] With the DCH-DHN feeds temperatures increases of only 23°F and 16°F were observed with the DCH-F-113 DHN (Table 36) and the DCH-SHELL DHN (Table 35), respectively.

Reaction heat sinks calculated for the DCH-DHN mixtures were lower than those obtained with pure DCH but higher than those obtained with pure DHN.

The effect of conversion on selectivity was studied in a series of experiments at 842° and 1022°F (LHSV 50 and 30; 10 atm pressure) using the DCH-F-113 DHN feedstock (i.e., high cis DHN concentration). With this mixture DCH conversions were about that observed with pure DCH (Table 37). Selectivities for DP at a given conversion were higher than was observed with pure DCH, more so at 842°F than at 1022°F (Figure 28). Comparison of the results for DHN with the mixture to that of pure DHN are not possible now as pure F-113 DHN has not been tested as yet under these reaction conditions. Heat sinks of reaction obtained with the DCH DHN mixture were somewhat lower than those observed with pure DCH.

The effects of pressure on conversions and selectivities were studied in a series of experiments at 10 and 20 atm pressure and 842° and 1022°F (LHSV = 100). In general, at a given pressure and compared to the pure components, conversions of the naphthenes in the mixture were slightly lower (Table 38); while selectivities for DP were slightly higher, and those for naphthalene slightly lower (Figure 29) than was observed with the pure components.[a] Heat sinks of reaction with the mixture were lower, general than those obtained with pure DCH but higher than those obtained with pure DHN.

In summary then, addition of 50% DHN to DCH reduced the reactivity of DHN; enhanced the reactivity of DCH if the trans isomer content of the DHN was high (90%); and did not effect the reactivity of DCH if the cis isomer content of the DHN was high (75%). No reason for this isomer effect on the DCH reactivity is immediately evident.

---

a) The DHN conversions and selectivities for naphthalene were compared to those obtained with EK P1905 DHN.[3] This Decalin was less reactive than F-113 DHN hence the DHN conversions and naphthalene selectivities shown in Table 9 and Figure 29 for pure DHN could be slightly higher for the F-113 decalin.

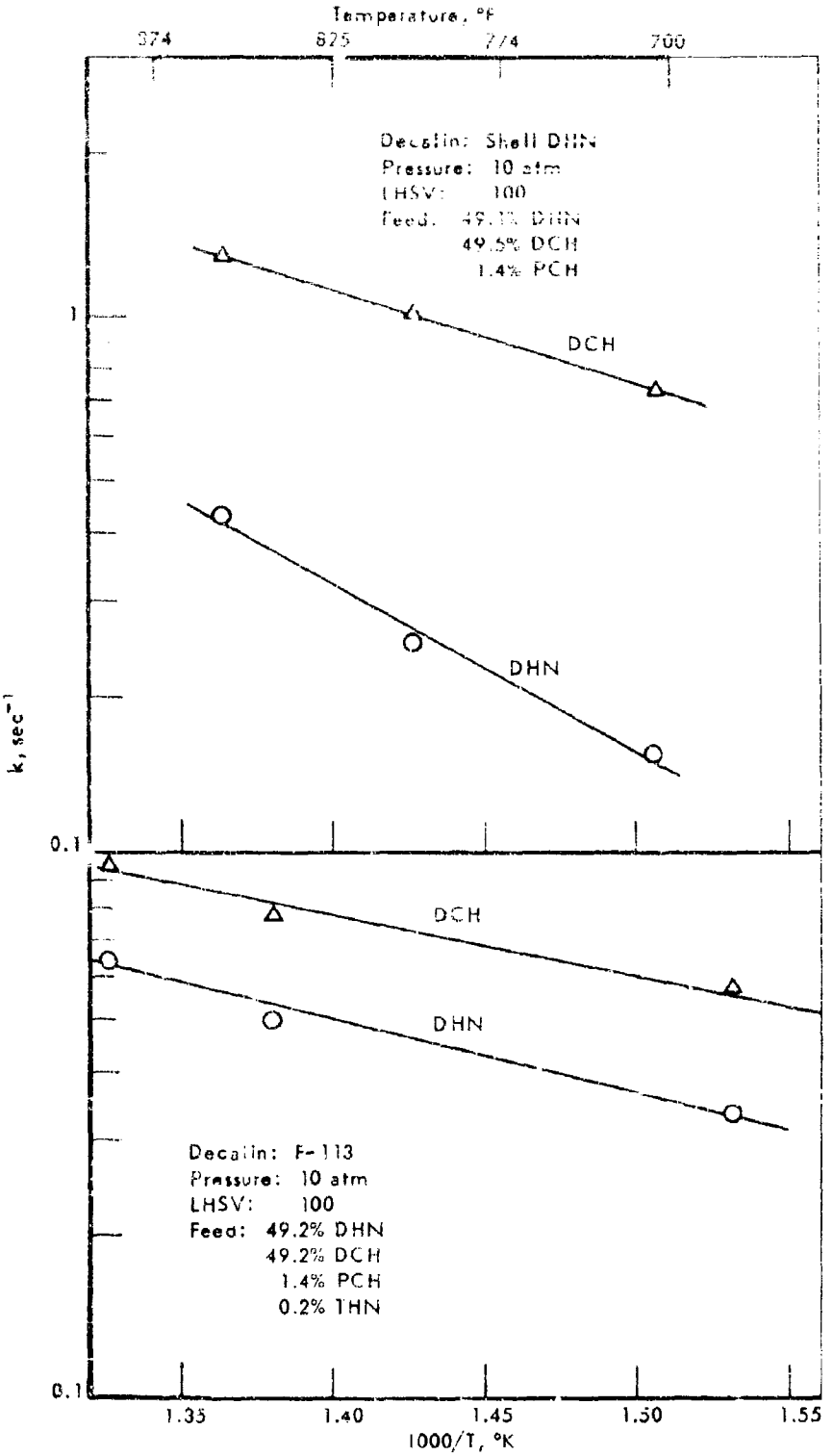


Figure 27. DcHYDROGENATION OF DCH-DHN MIXTURE
Temperature Coefficient

Table 37. DEHYDROGENATION OF DCH-DHN MIXTURE: EFFECT OF CONVERSION ON SELECTIVITIES FOR DIPHENYL AND FOR NAPHTHALENE

Values for pure DCH and pure DHN in parentheses.

Catalyst:	1% Pt on Al_2O_3	Feed:	49.2% DCH
Catalyst Volume:	7 ml		12.3% trans-DHN
Pressure:	10 atm		36.9% cis-DHN
Decalin:	F-113		1.4% PCH
			0.2% THN

Run 9645-	162-1	162-2	163-1	163-2
Temperature, °F				
Block	← 842 →		← 1022 →	
Wall	725	741	925	941
Catalyst Bed	635	640	720	732
LHSV	50	30	50	30
Product Analysis, %w				
Cracked	0.0	0.0	0.0	0.3
Benzene	0.0	0.0	0.1	0.4
Toluene	0.0	0.0	0.1	0.2
trans-DHN	14.9[a]	13.9[a]	7.5	2.7
cis-DHN	9.9	5.4	4.2	1.0
U[b]	0.0	0.0	0.1	0.4
DCH	11.3	5.0	3.3	0.4
THN	5.7	4.3	1.3	0.5
PCH	11.9	6.5	2.3	0.4
Naphthalene	19.2	26.9	36.5	44.8
DP	27.0	38.0	44.6	48.9
Conversion, %w				
DCH	78.6	89.9	93.3	99.2
	(78.3)	(93.2)	(93.8)	(-)
DHN	49.2	60.8	76.6	92.5
	(41.3)	(58.9)	(65.4)	(87.9)

a) cis to trans isomerization during the run.
b) Unidentified.

(Continued)

Table 37 (Contd). DEHYDROGENATION OF DCH-DHN MIXTURE: EFFECT OF CONVERSION ON SELECTIVITIES FOR DIPHENYL AND FOR NAPHTHALENE

Run 9645-	162-1	162-2	163-1	163-2
Selectivity for, %w				
PCH	28.0	11.8	2.0	0.0
DP	72.0	88.2	98.0	99.9+%
THN	22.2	13.2	2.9	0.4
Naphthalene	77.8	86.8	97.1	99.6
k, sec^{-1}				
DCH	0.587	0.560	0.761	-
DHN	0.325	0.273	0.813	0.880
Heat Sink, Btu/lb				
Reaction, Mixture	574	736	862	976
Reaction, Pure DCH	656	895	978	1050
Reaction, Pure DHN	383	552	618	825

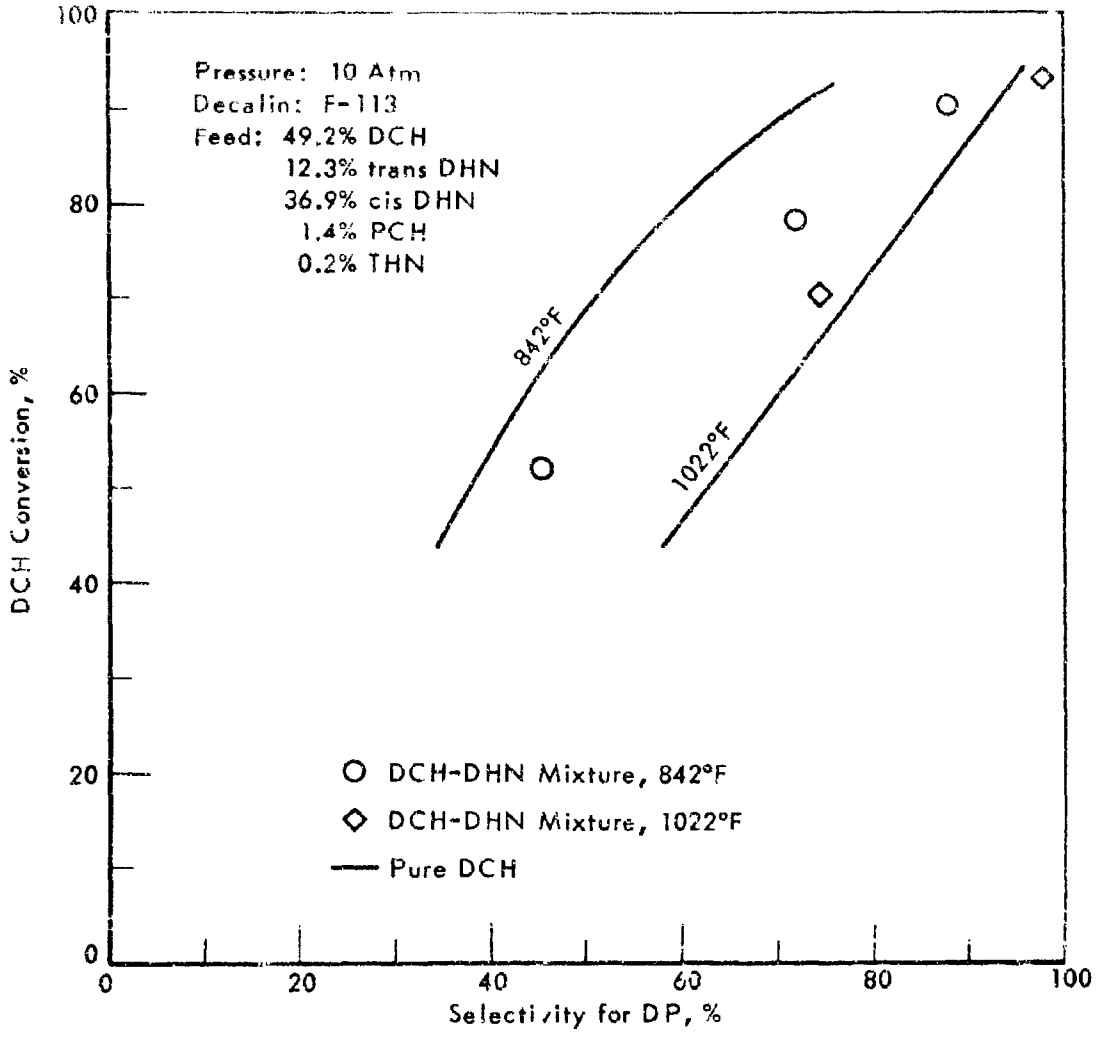


Figure 28. DEHYDROGENATION OF DCH-DHN MIXTURE
Effect of DCH Conversion on Selectivity for DP

Table 38. DEHYDROGENATION OF DCH-DHN MIXTURE: EFFECT OF PRESSURE

Values of pure DCH and pure DHN in parentheses.

Catalyst:	1% Pt on Al_2O_3	Feed:	49.2% DCH
Catalyst Volume:	7 ml		12.3% trans DHN
LHSV:	100		36.9% cis DHN
Decalin:	F-113		1.4% PCH
			0.2% THN

Run 9645-	165-1	165-3	166	168-1	168-3	169
Temperature, °F						
Block	←	842	→	←	1022	→
Wall	720	716	729	882	885	889
Catalyst Bed	624	635	660	703	702	711
Pressure, atm	10	20	30	10	20	30
Product Analysis, %w						
trans-DHN	14.8[a]	18.9[a]	23.6[a]	12.4[a]	14.2[a]	15.4[a]
cis-DHN	19.0	14.0	10.0	13.1	9.5	7.1
DCH	24.8	27.6	31.3	14.6	13.9	14.7
THN	6.1	10.6	12.2	4.2	9.6	13.5
PCH	14.2	17.6	17.0	10.2	16.5	20.7
Naphthalene	9.5	6.3	4.4	19.9	16.4	13.7
DP	11.6	4.9	1.5	25.6	19.8	14.6
Cracked	0.0	0.1	0.1	0.0	0.1	0.3
Yield PCH	12.8	16.2	15.6	8.8	15.1	19.3
Conversion, %w						
DCH	50.0	43.5	35.8	70.1	71.5	69.6
	(52.2)	(46.0)	(38.5)	(71.0)	(75.5)	(74.6)
DHN	31.7	32.5	31.1	47.8	51.4	54.1
	(31.5)	(33.1)	(32.6)	(52.9)	(54.0)	(55.5)
Selectivity for, %w						
PCH	53.1	76.8	91.3	25.6	43.3	56.9
DP	46.9	23.2	8.7	74.4	56.7	43.1
THN	38.4	62.3	75.2	16.7	36.4	49.2
Naphthalene	61.6	37.7	24.8	83.3	63.6	50.8

a) cis to trans-isomerization occurred during dehydrogenation. (Continued)

Table 38 (Contd). DEHYDROGENATION OF DCH-DHN MIXTURE: EFFECT OF PRESSURE

Run 9645-	165-1	165-3	166	168-1	168-1	169
k, sec^{-1}						
DCH	0.554	0.228	0.119	1.100	0.558	0.366
DHN	0.364	0.187	0.119	0.706	0.393	0.283
Heat Sink, Btu/lb						
Reaction, Mixture	333	273	220	547	530	491
Reaction, Pure DCH	390	294	211	661	625	567
Reaction, Pure DHN	288	242	230	503	495	485

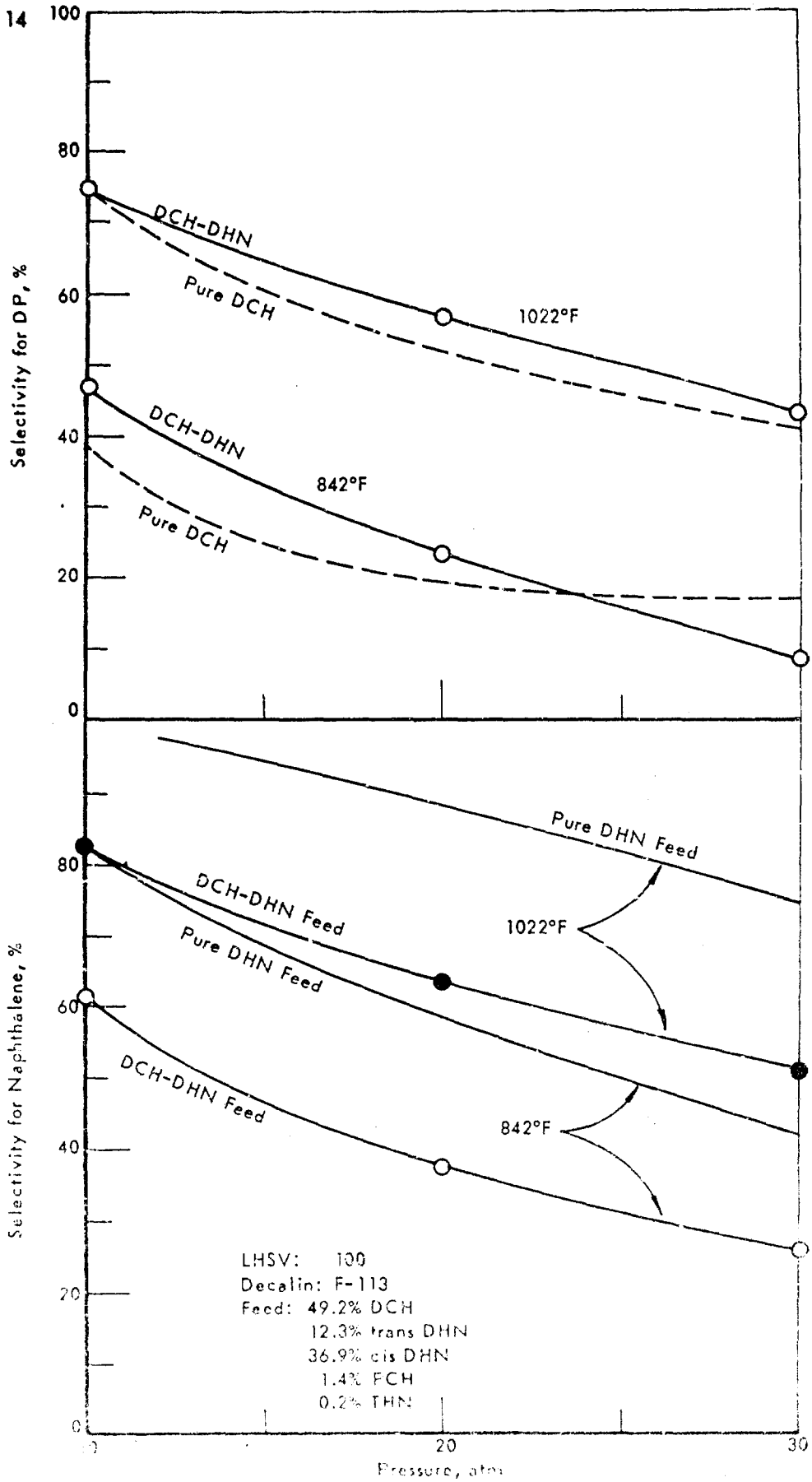


Figure 19. DEHYDROGENATION OF DCH-DHN MIXTURE
Effect of Pressure on Selectivity for Naphthalene and DP

Activation energies for the first dehydrogenation step were lower than those observed for the pure components with the 50% DCH-50% DHN (75% cis) but with the 50% DCH-50% DHN (90% trans) E_{act} for DCH was unchanged and E_{act} for DHN was higher than those obtained with the pure components.

At 842°F and a given DCH conversion (80-90%) there was a marked increase in selectivity for DP when DHN (75% cis) was added to DCH. A similar but less marked effect also was observed at 1022°F.

With increased pressure (10-30 atm) addition of DHN (75% cis) generally reduced the reactivity of both DCH and DHN; and at a given conversion gave a slight increase in selectivity for DP and a considerable decrease in selectivity for naphthalene. As was observed with pure DCH and pure DHN, at 842-1022°F conversions were essentially independent of pressure except for DCH at 842°F where conversion did decline somewhat with increased pressure.[1)]

Very little catalyst deactivation was observed during dehydrogenation of the 50% DCH-50% DHN mixtures.

With the dehydrogenation of 50% DCH-50% DHN the reaction heat sink was less than that of pure DCH, but greater than that of pure DHN. This was primarily because the total reaction heat sink available from DCH is 1080 Btu/lb and from DHN is 950 Btu/lb. Although an increase in selectivity for DP was obtained when DHN was added to DCH, the gain in reaction heat sink due to this enhanced selectivity was not enough to compensate for the loss in heat sink by diluting DCH with DHN. Thus it appears that no gain in reaction heat sink over that of pure DCH will be obtained by adding DHN to a DCH feedstock.

Thermal Reaction of Dicyclohexyl-Decalin Mixture

The 50% DCH-50% DHN mixture was also tested for thermal reaction at 10 atm pressure, 1022-1293°F at LHSV of 20. In these tests quartz chips (10-20 mesh) filled the reaction zone in the reactor.

With this mixture the reactivity of DCH was slightly greater than the overall reactivity of DHN. For example, at 1293°F DCH conversion of 69.9% was observed compared to 62.2% for DHN (Table 39). For the two DHN isomers the cis species was more reactive than the trans (cf rate constants Table 39). Apparent activation energies ranged from 44.2 kcal/mole (cis DHN) to 54.2 kcal/mole (trans DHN). Figure 30 is an Arrhenius plot of the data. Reaction products were mainly liquid cracked material (Table 39) with lesser amounts of gas products. Gas products were mainly methane, ethylene and hydrogen (Table 40). Heats of reaction were less than 230 Btu/lb due to hydrogen transfer reactions between the reaction products.

Conversions, first order rate constants and activation energies obtained with the pure components are shown in Table 39 in parentheses for comparison. In the mixture the reactivity of DCH was comparable to that of pure DCH while the overall reactivity of DHN was slightly less than that of pure DHN (cf rate constants, Table 39); while activation energies obtained with the mixtures were slightly greater than those obtained with the pure components.

Table 39. THERMAL REACTION OF DICYCLOHEXYL-[illegible] MIXTURES

Pressure: 10 atm
LHSV: 20
Reaction Time: 20 min
Catalyst: Quartz Chips
Catalyst Vol: 20 ml

Feed: 12.3% trans-DHN
36.6% cis-DHN
49.2% DCH
0.2% THN
1.4% PCH

Run No. 10100-	17-1	17-3	18	19
Temperature, °F				
Block	1022	1112	1202	1295
Wall	1009	1084	1175	1240
Catalyst Bed	972	1056	1119	1155
Product Analysis, %w				
Benzene	0.0	0.4	1.7	5.5
U_1 [b]	0.1	1.3	2.3	3.0
Toluene	0.0	0.1	1.2	4.6
U_2 [b]	0.0	0.4	1.5	2.8
trans-DHN	12.4	12.2	10.0	6.7
U_3 [b]	0.1	0.3	0.6	1.0
cis-DHN	36.1	32.3	22.8	11.9
U_4 [b]	0.0	1.4	3.5	4.6
DCH	49.0	44.1	30.1	14.8
U_5 [b]	0.0	0.0	0.6	0.8
THN	0.1	0.1	0.4	0.6
PCH	1.4	1.4	1.1	0.8
Naphthalene	0.0	0.0	0.0	0.5
Cracked, liquid	0.8	6.0	17.2	21.3
Cracked, light gas	0.0	0.1	8.2	21.5
Conversion, %w				
trans-DHN	0.0	0.8	18.7	45.6
cis-DHN	2.2	12.5	38.2	67.7
Total DHN [a]	1.5	9.6	33.4	62.2
		(14.6)	(46.2)	(78.2)
DCH	0.5	10.4	38.8	69.9
	(3.7)	(10.3)	(39.2)	(66.7)
First Order Rate Constant, sec^{-1}				
trans-DHN	-	-	0.065	0.167
		(0.018)	(0.119)	(0.348)
cis-DHN	-	0.034	0.127	0.361
		(0.055)	(0.201)	(0.492)
Total DHN	-	0.025	0.108	0.267
		(0.039)	(0.116)	(0.425)
DCH	-	0.023	0.109	0.277
		(0.023)	(0.111)	(0.255)
E, Act Energy, kcal/mole				
trans-DHN			← 54.2 →	
cis-DHN		← 44.2 →		
Total DHN		← 47.0 →		
			(45.3)	
DCH		← 48.0 →		
			(47.0)	
Heat Sink, Btu/lb				
Reaction	0.0	35	124	228
Total at Block Temp	769	866	1038	1206
Total at 1340°F	1015	1050	1139	1243

a) Values for pure components shown in parentheses.
b) Not identified.

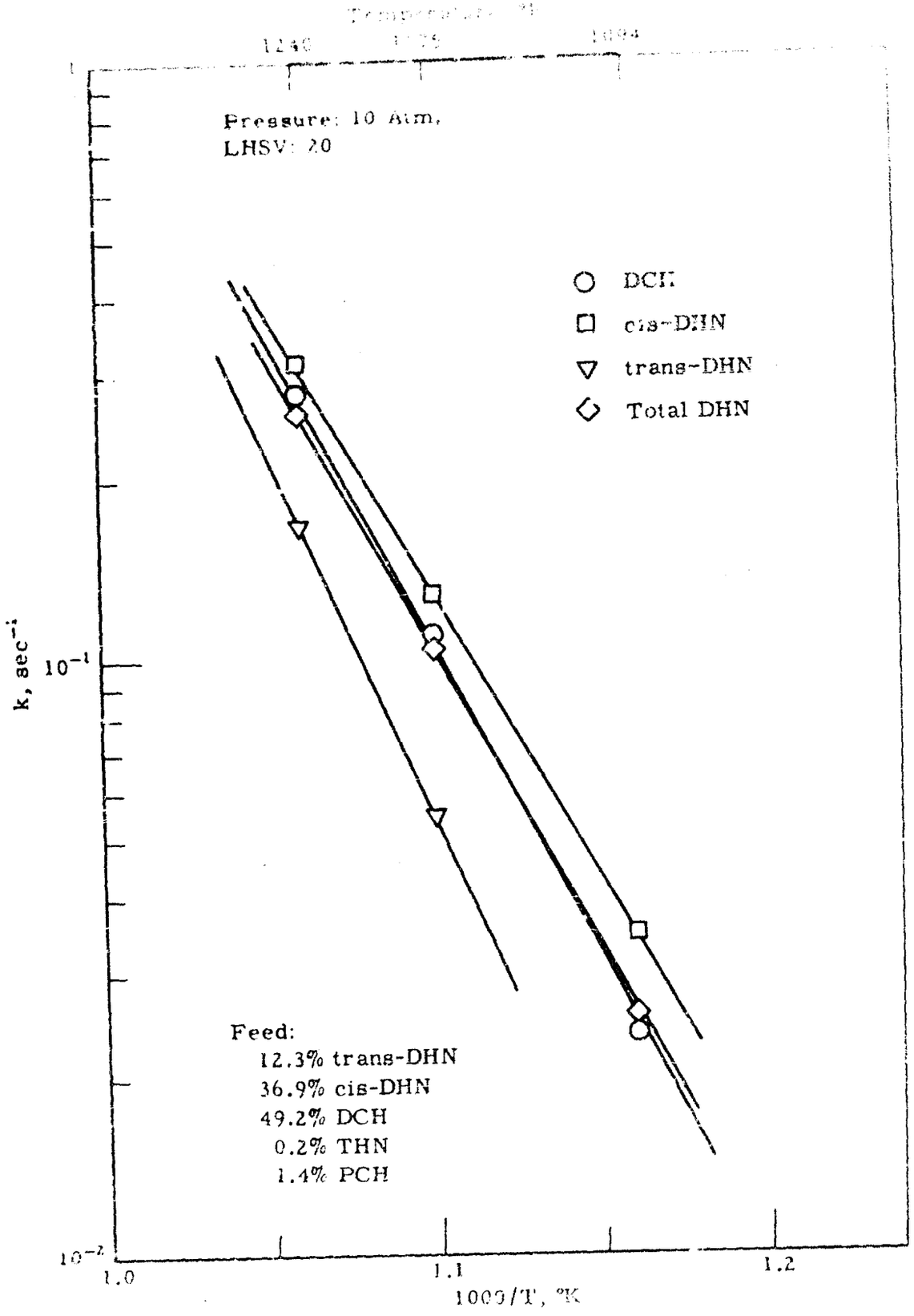


FIGURE 30. THERMAL REACTION OF DCH-DECALIN MIXTURE TEMPERATURE COEFFICIENT

Table 40. THERMAL REACTION OF DICYCLOHEXYL-DECALIN MIXTURE: GAS PHASE PRODUCT DISTRIBUTION

Pressure: 10 atm
LHSV: 20
Feed: 12.3% trans-DHN
36.9% cis-DHN
49.2% DCH
0.2% THN
1.4% PCH

Run No. 10100-	18	19
Block Temperature, °F	1202	1295
Total Conversion, %w	33.4	62.2
Conversion to Light Gas, %w	8.2	21.5
Gas Product Analysis, %v		
H_2	22.2	18.4
CH_4	30.2	29.8
C_2H_4	21.8	21.5
C_2H_6	12.8	14.3
C_3H_6	7.4	8.7
C_3H_8	2.7	3.8
C_4H_6	0.5	0.8
C_4H_8	1.3	2.3
C_4H_{10}	0.1	0.2
C_5H_{10}	0.0	0.2

Dicyclohexyl-Methyldecalin

These experiments were done with a 50% DCH-50% 1-MDHN mixture that analyzed to be:

6.1% trans-1-MDHN
43.9% cis-1-MDHN
49.4% DCH
0.6% PCH

The experiments were done at 10 atm pressure, LHSV of 100, at 842-1022°F using our laboratory 1% platinum on alumina catalyst. The procedure for carrying out the experiments was the same as that used for studying the DCH-Decalin system. Product material was analyzed by GLC, using a five-foot 1/4-in stainless steel column packed with 5% Carbowax on Chromosorb W. With this column the 5-MTHN and PCH emerged as one component. Hence these components were obtained by a separate analysis using a two-foot, 1/8-inch diameter column packed with 20% tricyanoethoxypropane on 100-200 Chromosorb W. The data are recorded in Table 41; values obtained with pure components are shown in parentheses.

Addition of DCH to 1-MDHN stabilized the catalyst. For example, at 932°F an increase in catalyst bed temperature of only 49°F was observed compared to an increase of over 200°F with pure 1-MDHN (Table 41). Further, the overall reactivity of 1-MDHN was enhanced, presumably because of catalyst stabilization (cf rate constants Table 41). Selectivity for methylnaphthalene was considerably lower in the mixture, however. The reactivity was enhanced, but the selectivity for DP was virtually that of the pure component (Table 41).

Activation energies were computed from first order rate constants and are recorded in Table 41. Figure 31 is an Arrhenius plot of the data. Heat sinks with the mixture were lower than those obtained with pure DCH but greater than those for pure 1-MDH (Table 41).

In summary then addition of DCH to 1-MDHN:

1. Stabilizes the catalyst for dehydrogenation of the naphthene mixtures.

2. Enhances the reactivities of both DCH and 1-MDHN.

3. Lowers the selectivity for methylnaphthalene but does not effect the selectivity for DP.

4. Gave a heat of reaction that was lower than that obtained with pure DCH but greater than that obtained with pure 1-MDHN.

Propane Cracking

The reaction of propane to give ethylene and methane has an endothermic heat of 740 Btu/lb. For this reaction the equilibrium propane conversion is 95% at 10 atm pressure and 1340°F. This would give a total

Table 41. DEHYDROGENATION OF 1-METHYLDECALIN-DICYCLOHEXYL MIXTURE

Values obtained with pure components shown in parentheses

Catalyst: 1% Pt on Al_2O_3
Catalyst Volume: 7 ml
LHSV: 100
Pressure: 10 atm

Feed: 6.1% trans-1-MDHN
43.9% cis-1-MDHN
49.4% DCH
0.6% PCH

Run No. 10100	9-1	10-1	10-2
Temperature, °F			
Block	842	932	1022
Wall	705-12	763-70	855-78
Catalyst Bed	640-67	698-747	777-925
	610-22	650-60	698-743
	615-20	657	707
	626-28	671-69	730-18
ΔT_{max}, °F, catalyst bed	27	49	148
Product Analysis, %w			
trans-1-MDHN	9.3	7.6	6.5
cis-1-MDHN	18.9	18.3	17.1
DCH	19.7	15.0	12.2
1-MTHN	2.3	1.5	1.1
5-MTHN	5.9	3.3	1.7
PCH	18.2	12.1	7.8
1-Methylnaphthalene	14.0	19.1	23.6
DP	11.7	23.1	30.0
Yield PCH, %w	17.6	11.5	7.2
Conversion, %w			
DCH	60.1	69.6	75.3
MDHN	43.6	48.2	52.8
Overall	51.8	58.9	64.0
Selectivity for, %w			
PCH	60.0	33.2	18.4
	(59.2)	(36.5)	(20.2)
DP	40.0	66.8	81.6
	(40.8)	(63.5)	(79.8)
MTHN	36.4	17.6	10.7
Methylnaphthalene	63.6	82.4	89.3
	(83.5)		
k, sec^{-1}			
DCH	0.731	0.993	1.249
	(0.609)	(0.762)	(0.872)
1-MDHN	0.498	0.598	0.729
	(0.329)	(0.367)	
Overall	0.606	0.775	0.953
E_{act}, kcal/mole			
DCH	← 8.6 →		-
	←(7.8)→		
1-MDHN	← 4.6 →		-
Overall	← 6.5 →		-
Reaction Heat Sink, Btu/lb			
Mixture	374	481	555
Pure DCH	448	662	732
Pure MDHN	300	340	378

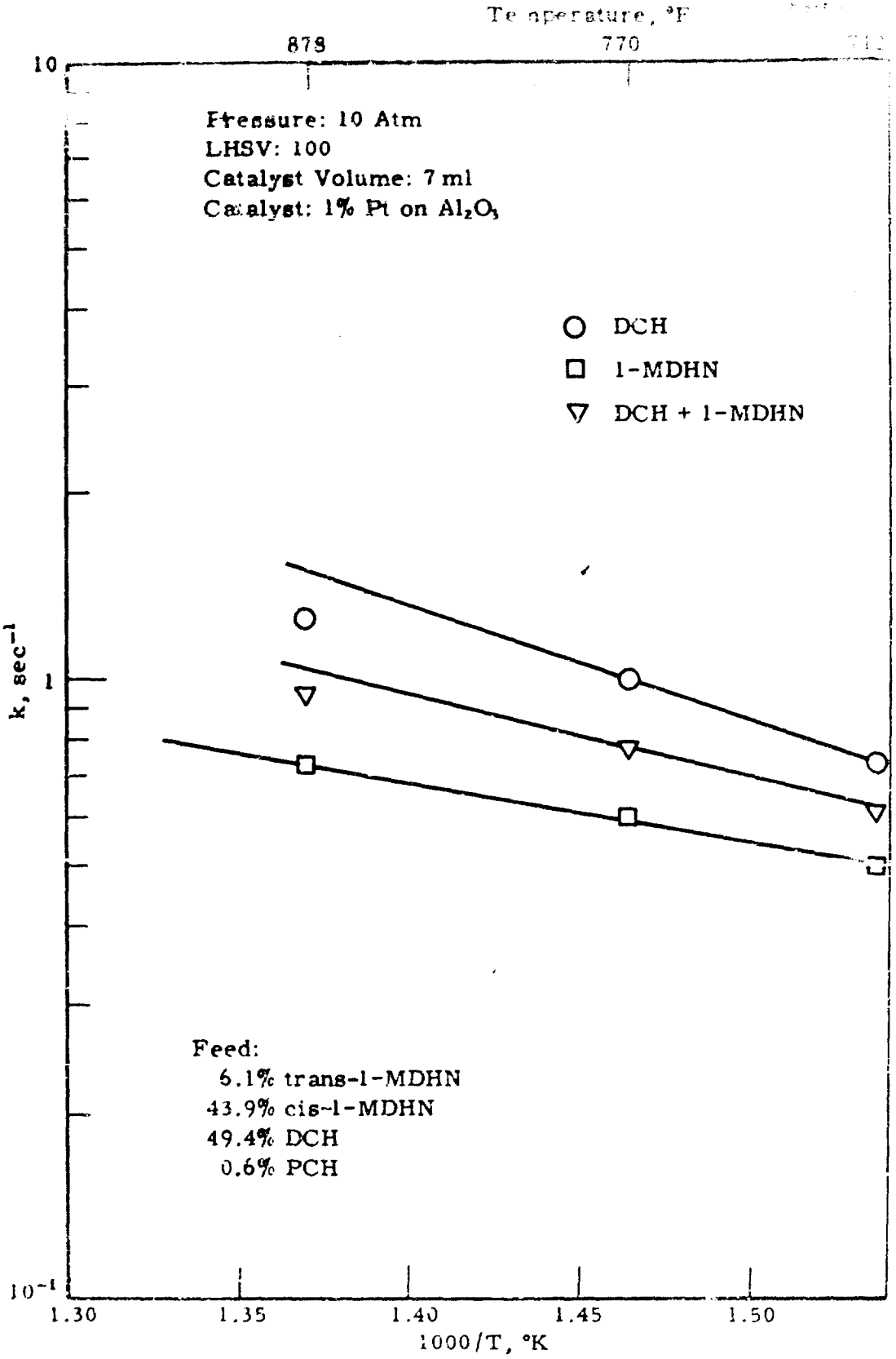


Figure 31. DEHYDROGENATION OF 1-MDHN-DCH MIXTURE TEMPERATURE COEFFICIENT

heat sink of about 1950 Btu/lb. Under conditions of thermal reaction about equal selectivities for the dehydrogenation of propane to propylene and the cracking of propane to ethylene and methane are reported in the literature. A few exploratory experiments were carried out under conditions of thermal reaction using free-radical initiators, and also at lower temperatures with various catalysts, to test the reactivity and selectivity of propane for the cracking reaction.

Thermal Reaction

The thermal reaction was tested in both the standard laboratory reactor (1/2" IPS; 5/8" ID) and in a modified apparatus using a 1/4" OD reactor tube.

The tests in the standard reactor were done at 10 atm pressure, 1022-1295°F at LHSV of 20, with 20 ml of quartz chips (10-20 mesh) in the reaction zone. Under these reaction conditions propane conversions were considerably higher then were observed previously at lower pressure. For example, at 1295°F about 20% propane conversion was observed at 10 atm pressure (Table 42) compared to only % at 1 atm pressure (see Table 16 of a previous report).[1] Presumably higher conversions were due to longer contact times at the higher pressure. Dehydrogenation and cracking were the principal reactions during propane pyrolysis. Thus at 1295°F selectivity for the dehydrogenation reaction (product propylene) was about 40% while that for cracking (products ethylene and ethane and methane) was about 53% (10 atm; Table 42). The reactivity of propane for thermal reaction was about one half that of methylcyclohexane (MCH) based on the first order rate constants. Thus at °F $k_{C_3H_8} = 0.04$ sec^{-1} compared to 0.08 sec^{-1} for MCH. Activation energy for propane pyrolysis was 51.4 kcal/mole over the temperature range of 1202°-1295°F (Table 42). Heat sink of reaction was only 175 Btu/lb (129) due to low conversion.

Thermal reactions proceed via a free-radical mechanism. A few experiments were carried out to explore the possibility of enhancing the rate of thermal reaction by the use of free-radical initiation. These experiments were done at 1 atm pressure, 1295°F, and as a propane LHSV of about 22. Allyl chloride (1%), methyl iodide (10%), and hydrazine (1%) were tried as initiators. To carry out an experiment, propane flow was started through the reactor and then liquid initiators were forced into the propane streams at the top of the reactor by a syringe pump. The flow rates were such that the initiator vaporized completely into the propane stream. These experiments were carried out in a modified apparatus using a 1/6" OD reactor tube and which is described in detail in the Appendix. The data for the experiments are shown in Table 42.

Very little enhanced reactivity was observed with 1% added allyl chloride. With 10% added methyl iodide the overall conversion was increased by a factor of three (cf runs 108 and 110-1, Table 42). Considerable coke accumulated during the runs with allyl chloride and methyl iodide, although the reactor was contacted with 4% O_2 in argon at 1022°F for 16 hrs between runs.

Table 42. THERMAL REACTION OF PROPANE

Catalyst: Quartz chips
Catalyst Volume: 20 ml

Run No. 10100-	72[a]	73[a]	74-1[a]	74-2[a]	110-1[b]	110-4[b]	108[b]
Initiator	← none →				none	1% allyl chloride	10% methyl iodide
LHSV	← 20 →				22 based on 2.3 cc volume		
Pressure, atm	← 10 →				← 1 →		
Temperature, °F							
Block	1022	1112	1202	1293	← 1295 →		
Wall	1018	1108	1197	1274			
Catalyst Bed	995	1090	1168	1240			
Product Analysis, %m							
H_2	0.0	0.4	2.6	9.2	2.3	2.0	4.6
CH_4	0.1	0.7	3.7	10.5	1.4	1.5	6.1
C_2H_4	0.0	0.6	3.2	6.5	1.4	1.6	3.5
C_2H_6	0.0	0.0	0.4	2.1	0.0	0.0	0.1
C_3H_6	0.0	0.5	2.6	6.7	1.4	1.6	5.5
C_3H_8	99.9	97.8	87.5	64.8	93.5	93.3	80.2
C_4H_8	0.0	0.0	0.0	0.2	0.0	0.0	0.0
C_3H_8 Conversion, %m	>0.1	1.1	6.6	19.2	2.9	3.4	10.6
Yield C_3H_6, %m	-	0.5	2.8	8.0	4.45	1.7	6.1
Yield $C_2H_4 + C_2H_6$, %m	-	0.6	3.8	10.6	1.45	1.7	4.0
First Order Rate Constant, sec^{-1}	-	-	0.040	0.134			
E_{act}, kcal/mole			← 51.4 →				

a) Carried out in the standard 5/8" ID reactor tube.
b) Carried out in the modified reactor with the 1/4" OD reactor tube.

From the results obtained thus far it did not appear that addition of small amounts of free-radical initiators would enhance the propane pyrolysis rate appreciably. No further experiments are presently planned although the idea has not been discarded completely since the effect on the rate would be critically related to the properties and abundance of the free-radical species generated. Here we have barely scratched the surface.

Catalytic Reaction

A few exploratory experiments were done on the catalytic cracking of propane using various types of off-the-shelf catalysts. The purpose of the work was to see if propane could be converted catalytically to ethylene and methane at temperatures lower than those needed by thermal reaction. Seven different catalysts were tested, including two platinum on aluminas, two commercial platinum catalysts, two commercial zeolites, and one zeolite upon which platinum had been highly dispersed. One of the catalysts was tested in our standard laboratory reactor, all of the catalysts were tested in the modified apparatus with the 1/4" OD reactor tube. This latter apparatus is described in detail in the Appendix. Product analyses were carried out by GLC and mass spectrometry.

A Houdry cracking catalyst (M46; 20 ml volume; 10-20 mesh) was tested in the standard laboratory reactor (1/2" IPS) at 932-1202°F, 1 and 10 atm pressure at LHSV of 20. At the highest temperature only 3.5% to 4.1% propane conversion was obtained at both pressures (Table 43). The catalyst was inactive at 1022°F and only slightly active at 1112°F (conversion 1%).

The catalysts were tested in the 1/4" reactor at 572°-1022°F, 1 and 5 atm pressure, at LHSV of 20. Catalyst of 2 ml diluted with 5 ml of quartz chips (10-20 mesh) were used in these tests. The data are tabulated in Table 43 in which the product distributions shown are from the mass spectrometric analyses.

The 1% platinum on alumina (our standard dehydrogenation catalyst) and the UOP-R8 platforming catalyst (0.76% Ptm Al_2O_3) were the most active of the catalysts tested. With these catalysts 15 to 24% conversion was observed at 1022°F. Dehydrogenation was the principal reaction and selectivities of 79 to 89% for this reaction (i.e., propylene) were obtained. Both catalysts were quite active and 5 atm pressure and 1022°F the propylene product concentrations were about the equilibrium values. The activity of both catalysts were about the same at 5 atm but at 1 atm pressure the UOP-R8 appeared somewhat more active (1022°F).

All of the other catalysts tested were less active than the platinum on aluminas. Based on propane conversion at 5 atm and 1022°F the catalysts in order of decreasing activity were: Zeolon (Mordenite) NH_4 form; Shell Hydrocracking catalyst; 0.08% Pt on Mordenite; Houdry M46; and Zelon (Mordenite) H form. With these catalysts propane conversions ranged from 6 to 0.6% (5 atm, 1022°F; Table 44). None of the catalysts showed activity at 572°F except UOP-R8 with which about 0.5% conversion was obtained at 5 atm pressure.

From the exploratory tests conducted with these catalysts it appeared that cracking catalysts and reforming catalyts do not catalyze the

propane cracking reactions with even a moderate degree of selectivity. It might be possible to develop a catalyst more selective for this reaction but we have no plans to do this at present.

Table 43. PROPANE CRACKING OVER HOUDRY M46 CATALYST[a)]

Catalyst Volume: 20 ml
LHSV: 20

Run No. 10100	75	76	77-1	77-2	79-1	79-2	79-3	79-4	80-1	80-2	81-1	81-2
Pressure, atm	←		1	→	←			10			→	
Temperature, °F												
Block	932	1022	1112	1202	932	932	1022	1022	1112	1112	1202	1202
Reaction Time, min	←		20	→	2	15	2	15	2	15	2	15
Product Analysis, %												
H_2	-	-	0.3	1.8	-	-	-	-	0.3	0.6	2.9	2.3
CH_4	-	-	0.2	1.6	-	-	-	-	0.5	0.5	2.5	2.4
C_2H_4	-	-	0.0	1.5	-	-	-	-	0.5	0.3	1.9	1.8
C_2H_6	-	-	0.0	0.0	-	-	-	-	0.0	0.0	0.3	0.2
C_3H_6	-	-	0.5	1.9	-	-	-	-	0.4	0.4	1.7	1.7
C_3H_8	100	100	99.5	93.2	100	100	100	100	98.3	98.2	90.7	91.6
C_3H_8 Conversion, %	0.0	0.0	0.5+	3.5	0.0	0.0	0.0	0.0	0.9	0.7	4.1	3.8
C_3H_8 Converted to C_3H_6, %	-	-	0.5	2.0	-	-	-	-	0.4	0.4	1.8	1.7
C_3H_8 Converted to $C_2H_4 + CH_4$, %	-	-	0.0	1.5	-	-	-	-	0.5	0.3	2.3	2.1

a) Carried out in the standard 5/8" ID reactor tube.

Table 44. CATALYTIC CRACKING OF PROPANE OVER VARIOUS CATALYSTS[a)]

Run No. 10100-	129-1	129-2	117	118	119-1	119-3	131-1	131-2	133-1	133-2	126-1	126-2	124-1	122-1
Catalyst	1% Pt on Al_2O_3	←	UOP-R8	→			Houdry M46		Zeolon NH_4 form		Zeolon H form		0.08% Pt on Mordenite	Shell Hydro-cracking Catalyst
Block Temperature, °F	← 1022 →		842	572	←						1022	→		
Pressure, atm	1	5	5	1	1	5	1	5	1	5	1	5	1	1
Product Analysis, %m														
H_2	14	11.4	4.0	1.7	18.9	12.1	0.4	1.1	1.6	3.6	-	-	1.4	9.2
CH_4	1	4.2	0.6	0.0	1.9	2.8	0.0	0.2	1.8	4.1	1.6	0.5	1.1	0.6
C_2H_4	0	0.2	0.0	0.0	0.2	0.0	0.0	0.3	0.8	2.3	1.3	0.4	0.8	0.0
C_2H_6	0	1.9	0.5	0.0	1.1	1.9	0.2	0.3	0.5	0.8	0.3	0.2	0.2	0.0
C_3H_6	12	10.5	3.8	0.5	17.2	11.4	0.0	0.4	0.5	1.4	0.0	0.0	0.7	1.1
C_3H_8	73	71.7	91.0	97.8	60.3	71.5	99.4	97.7	93.2	87.0	97.8	98.9	95.3	89.1
Higher than C_3	0	0.1	0.1	0.0	0.4	0.3	0.0	0.0	1.0	0.8	0.0	0.0	0.3	0.0
C_3H_8 Conversion, %m	14	15.6	4.6	0.5	24.0	15.8	0.2	1.0	2.8	6.0	1.6	0.6	1.7	1.8
C_3H_8 Converted to $C_3H_6 + H_2$, %m	12	12.3	4.0	0.5	21.8	13.4	0.2	0.4	0.5	1.5	0.0	0.0	1.0	1.1
C_3H_8 Converted to $C_2H_4 + CH_4$, %m	0	3.3	0.6	0.0	1.4	2.2	0.0	0.6	1.3	3.4	1.6	0.6	0.7	0.0

a) Analysis made on hydrogen-free basis.
b) Carried out in the modified reactor with 1/4" OD reactor tubes.

Conventional Catalysts: Preparation and Testing

An extensive catalyst preparation program has been carried out with the object of discovering catalysts more useful for endothermic reactions. Specifically, for naphthene dehydrogenation, this means such catalysts must be more active, or have other desirable attributes such as greater stability than the present reference catalyst 9874-24 (1% Pt/UOP R-8 Al_2O_3). Many catalysts (224) of different types have been prepared or obtained and rapidly screened for activity for MCH dehydrogenation at 10 atm pressure, LHSV 100, and at 662, 792 and 842°F, in the microscale test rig (MICTR).[a] The purpose of the screening tests has been to obtain a quick comparison with the reference catalyst and to eliminate catalysts with activities too low to be of practical importance. After the initial screening, some of the more active catalysts have been further evaluated in the bench scale reactor with MCH. If warranted, some of these catalysts will be later evaluated for dehydrogenation of other naphthenes (e.g., decalin), for dehydrocyclization (with 2,5-dimethylhexane) and for depolymerization (with tetraisobutylene).

Catalyst Preparation

Exploratory Preparations

The majority of catalysts have been prepared by impregnating various supports with one or more metal salt or metal complex solutions, followed by drying, and reduction in situ. Typically, only small quantities of any particular catalyst have been prepared, 10-50 g. The amounts of metals employed are within the broad limits of 0.5 to 30%, and most commonly within the limits of 1 to 5%. Virtually all of the individual metals in the periodic system that are known or can be expected to have dehydrogenating activity have been studied as well as bimetallic and a few trimetallic combinations. The active Group VIII metals have been given particular attention. Ten different types of supports have been employed. These are, commercial aluminas of many types, charcoal, graphite, ferric oxide, silica, zirconia, amorphous alumina-silica, three crystalline alumino-silicates (molecular sieves), and diatomaceous earth (celite). In addition, a number of commercially available catalysts have been included, and Shell catalysts available from earlier proprietary investigations.

Larger Scale Preparations

Two catalysts were prepared in relatively large quantities. Both consisted of Pt mounted on Harshaw 0104 alumina. The first preparation (5 lbs) duplicated our standard laboratory catalyst (1% Pt on 1/8" pellets) and had comparable activity; most of this was supplied to the Fuels, Lubricants, and Hazards Branch of AFAPL, Wright-Patterson AF Base for in-house studies.

The pellets were broken, sieved to 10-20 mesh size and tested in the bench-scale reactor at 10 atm pressure, 842-1022°F and LHSV of 100. The activity of this catalyst was slightly higher than that of the standard laboratory catalyst (9874-7) and at block temperatures of 842°, 932°, and

---

a) See Appendix.

1022°F MCH conversion of 44.6%, 57%, and 73.2% were obtained, compared to 40.8%, 54.8%, and 66.6% with the standard catalyst. With this catalyst a temperature increase of 16°F was observed during a 30-minute run at 1022°F. However, in another 4-hour test (1022°F) no catalyst bed temperature increase was observed, duplicating the behavior of other preparations of this catalyst. The reasons for this difference in behavior is not known.

The second preparation (1 lb) consisted of 0.76% Pt on 50-60 mesh alumina and was supplied to United Aircraft Research Labs (E. Hartford) for asymmetric heating studies. Because of the fine particle size, the catalyst was tested by forming into 1/8" pellets and fracturing. It had a high bulk density (0.88 vs 0.52 for the MICTR reference catalyst) and somewhat higher activity (1.1 x the standard). The enhanced activity was probably due to the larger amount of Pt in the reaction zone.

Catalyst Evaluation

Supported Platinum

Of the many different catalytic metals and metal combinations so far tested on various supports for dehydrogenation of methylcyclohexane to toluene, the most active system appears to be platinum supported on a number of high surface area aluminas. Some of the other supports (types 5,6 and 7) lead to active but not quite competitive catalysts. The results with a possible alternate support (type 7) are discussed below. In general, at relatively constant total platinum content the dehydrogenation activity rises rapidly with increasing surface area of the support and then tends to level off (cf Table 45 and Figure 32). Activity usually does not rise much beyond a total platinum content of 4% for the higher surface area supports. A typical example is shown in Figure 33 for a Type 1 support. The limiting factor is undoubtedly the amount of platinum which can be highly dispersed, a function of the extent of surface area of a particular support. Activity can diminish if the support is overloaded with Pt. This is shown in Figure 33 for a type 7 support (this is a dense support, so the two curves are not on a comparable basis). Optimum activity is obtained with a platinum content of 2%. The high activity is partly a result of the high catalyst charging weight per unit volume (cf catalysts 9874-111, 119A, and 119B; runs 49, 144, 145, respectively).

Table 46 shows the first order rate data obtained at various temperatures and LHSV 100 for the reference catalyst (9874-24) and for one of the better experimental catalysts (9874-200A) at LHSV 50, 100, and 200. The test conditions were closely controlled and the average temperatures between the block and the reactor tube wall have been used. The instruments had just been calibrated. The difference between the two series measurements did not exceed 45°F at the highest conversion, unlike bench scale results where differential temperatures of ~170°F or more are observed. At the highest temperature employed, the experimental catalyst has about twice the rate of dehydrogenation at LHSV 100 as the reference catalyst. Figure 34 shows a log k sec^{-1} vs 1/T plot. The apparent activation energies calculated from this relation are 19.3 and 15.2 kcal/mole, respectively. The differ-

Table 45. MCH DEHYDROGENATION WITH PLATINUM ON TYPE 1 SUPPORTS OF VARYING SURFACE AREA

Conditions: LHSV = 100, 10 atm pressure, temperatures indicated in block. Other details are in Table 73 of the Appendix

Surface Area, a) m^2/g	Pore Volume, c) ml/g	Pt, %w	Catalyst No. 9874-	Run No.	Conversion of MCH to Toluene, %w d)		
					662°F	752°F	842°F
437 b)	~0.6	2	108A	44	31	63	82
316 b)	~0.5	2	107	45	32	63	81
~278	~0.4	2	118A	70	34	61	88
~230	~0.45	2	132A	84	38	67	86
~188	~0.5	2	96	31	30	57	74
~175	~1.3	4	131	80	35	58	73
~165	~0.4	2	132B	83	37	66	86
164 b)	~0.8	1	ref 24	avg of 11 tests	28 ± 4	52 ± 3	72 ± 7
~100	0.8	1	7	111	29	53	77
~20	-	2	112	48	30	49	67
~0	hollow	2	116	50	0	0	1

a) Measurement on similar sample.
b) Measurement made on support.
c) Estimated from density.
d) Average of 8 and 13 minute samples.

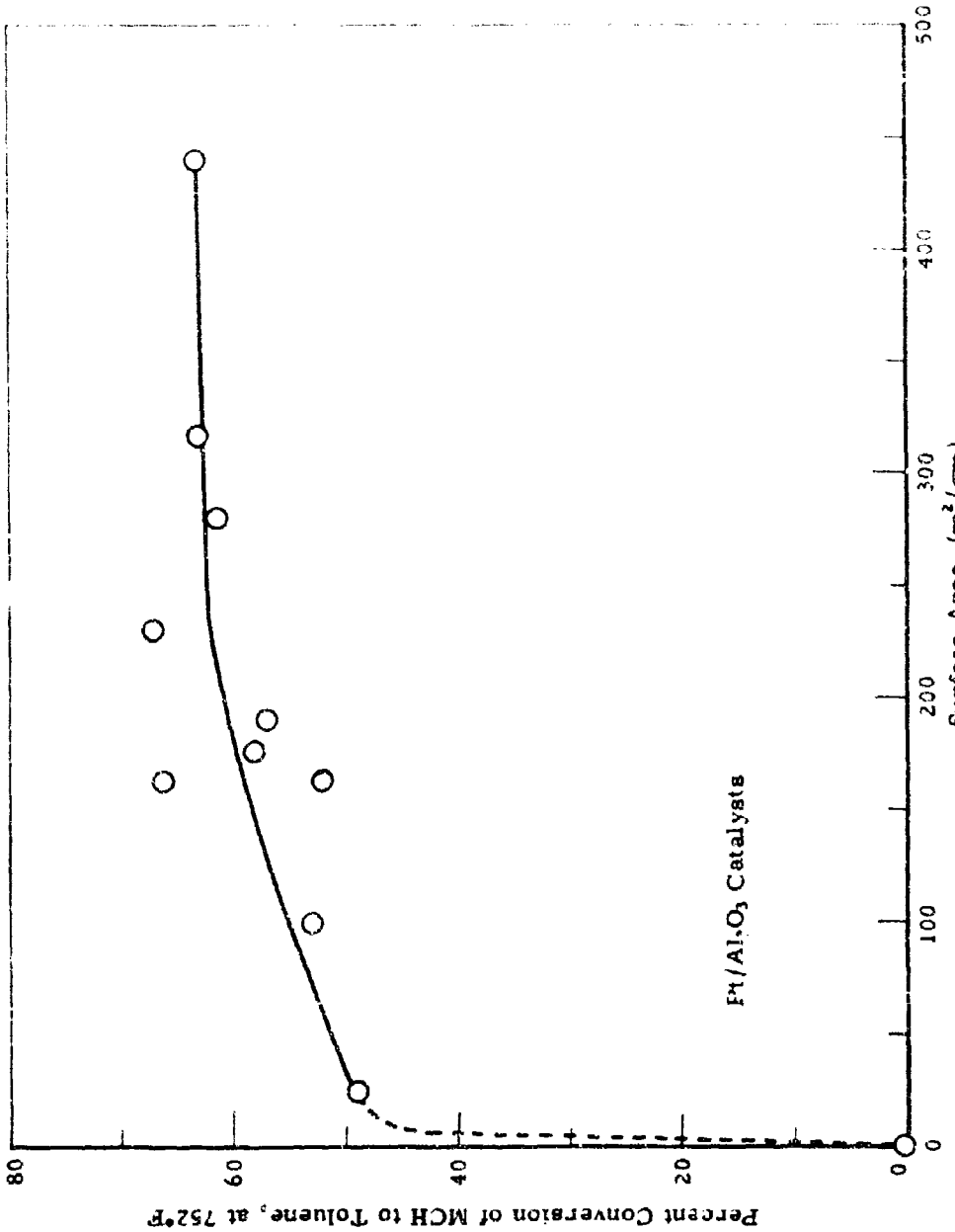


Figure 32. INFLUENCE OF SURFACE AREA ON MCH DEHYDROGENATION ACTIVITY

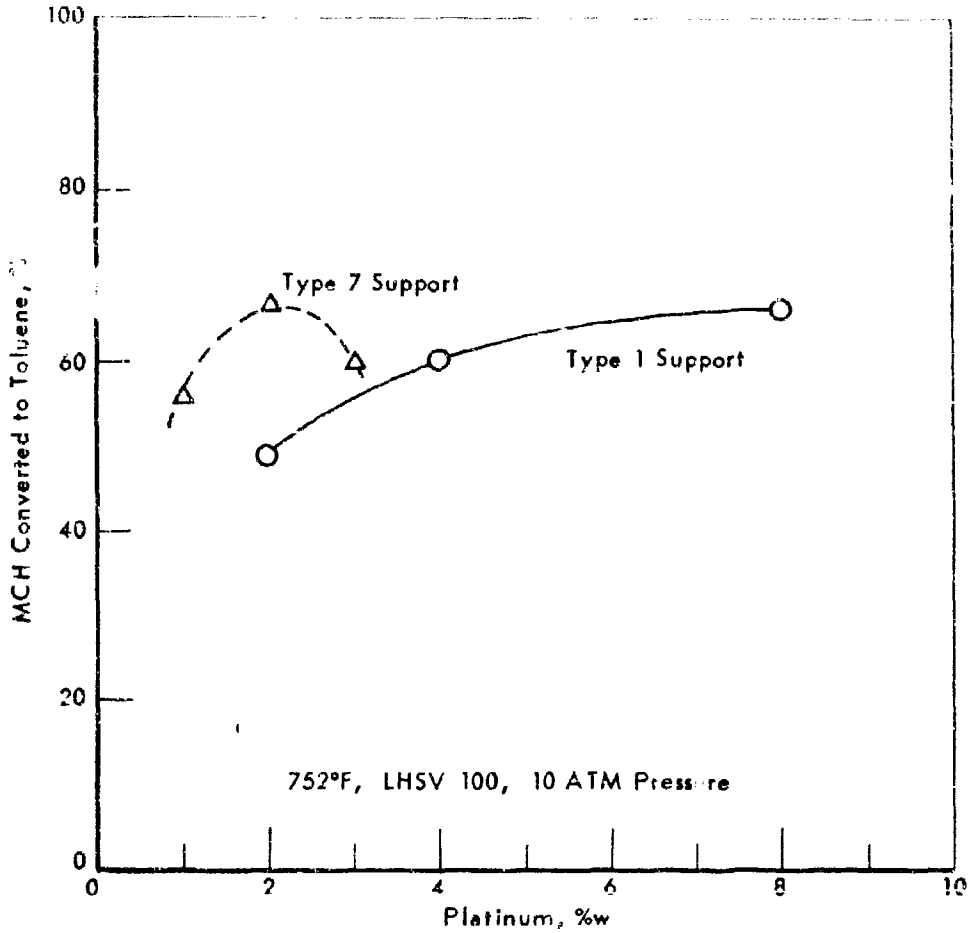


Figure 33. INFLUENCE OF PLATINUM CONTENT ON MCH DEHYDROGENATION ACTIVITY

Table 46. MCH DEHYDROGENATION RATES OVER REFERENCE AND IMPROVED Pt/Al_2O_3 CATALYSTS

Conditions: 10 atm pressure
Temperature variable
LHSV 50, 100, or 200

Cat. No. 9874	LHSV	Block Temp, °F	Avg Temp, °F[a]	% Mch Conv	k_f, Sec^{-1}	% of Equilibrium[b]
24 (reference)[c]	100	662	649	24	0.302	48
	100	752	729	49	0.792	55
	100	842	815	68.(5	1.46	69
200A[d]	50	662	649	37	0.256	60
	50	752	732	69	0.688	77
	50	842	812	94	1.7	95
	100	662	649	30	0.391	60
	100	752	732	63	1.17	70
	100	842	812	87	2.58	88
	200	662	649	30	0.781	48
	200	752	732	54	1.53	60
	200	842	817	70	2.85	71

a) Average of block temperature and lowest temperature measured.
b) cf, APL TDR 64-100, Part II, Figure 8, p. 21 (Ref. 2).
c) 1% Pt/R-8 Al_2O_3, Surface Area 180 m^2/g.
d) 4% Pt/H151 Al_2O_3, Surface Area 350 m^2g.

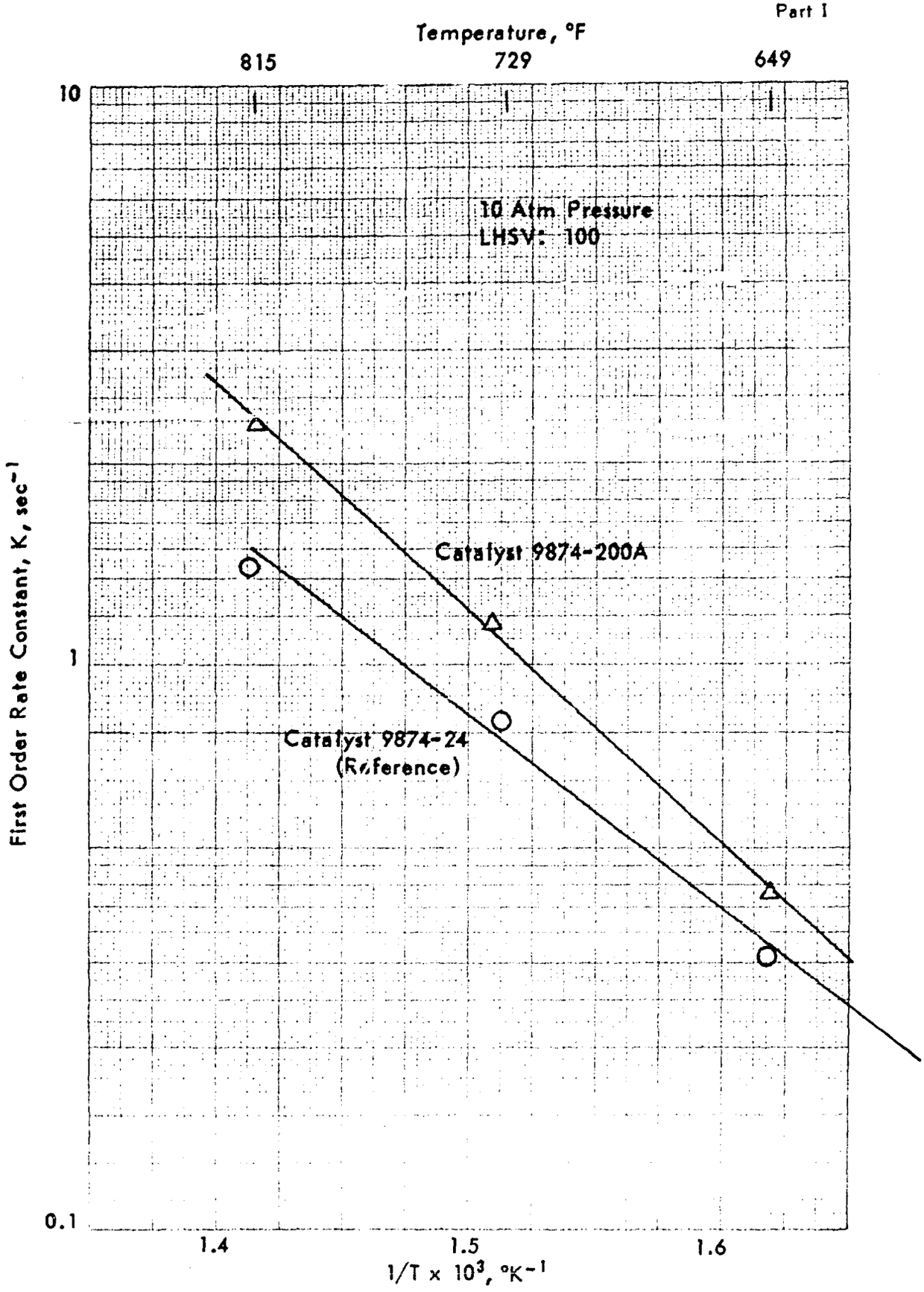


Figure 34. TEMPERATURE COEFFICIENT FOR MCH DEHYDROGENATION WITH IMPROVED Pt/Al_2O_3 CATALYST

ences between the E values calculated for this data and for the rates observed in the bench scale equipment is undoubtedly due to the different bed and furnace arrangements in the two apparatuses.

Various Supported Metals

A number of metals for promoting the activity of platinum on alumina and other supports have been studied. In general the dehydrogenation activity is only that induced by the platinum metal itself. Small improvements from incorporating a second metal oxide in alumina support (i.e. catalysts, 188A, 189A, 190A, 192A and 194A; runs 226, 233, 235, 241, and 256).

Most of the single metals or bimetallics on alumina or other supports ranged from inactive to moderately active. One of the more interesting metals on alumina gives activities similar to that of platinum although at higher metal content (i.e.,121A and 121B; runs 156 and 157, respectively). However, particularly at the higher temperature (842°F) such catalysts form benzene as well as toluene, and also hydrocarbon fragments (i.e.,CH_4). An exothermic reaction develops at the outlet end of the catalyst reactor tube. This reaction would detract from the total heat sink available. Such a catalyst was found to deactivate in a relatively short time during the bench scale test and this is probably a result of coking (cf page 29 , of this report). This metal on several other supports gives about the same activity as the reference catalyst, without the aforementioned side reactions (i.e., 140A, and 160B, runs 90 and 140, respectively).

A number of nonplatinum bimetallics on alumina are about as active as the reference catalysts but no means have been found to increase their activity further.(i.e.,155C, 156A, 157B, and 177A; runs 123, 128, 138, and 187, respectively).

A short study was made of materials which could be used to coat the surfaces of nonconforming catalyst shapes so that platinum could be replaced (i.e.,honeycomb structures).[a] Sauereisen cement impregnated with platinum gives an inactive catalyst. On the other hand fibrous acetate stabilized alumina (du Pont "Baymal") is a good support for active catalysts and adheres well to aluminum oxide honeycomb structures.

Catalysts on Shaped Supports

Pressure drop through packed beds can be reduced by utilizing geometric shapes designed to minimize resistance to flow. This possibility has been explored briefly by using a du Pont "Torvex" honeycomb shape as a catalyst support. It has longitudinal parallel hexagonal cellular passages. (See upper portion of Figure 35.) The cell size was 1/8" (cross-sectional area/hole = 0.007 $in.^2$), and the cell walls were 0.03" thick. The overall open area of the catalyst support was 60%, and the bulk density was about 40 lbs/ft^3 (d = 0.64). This configuration provides a geometric surface area of 384 ft^2 per cubic foot, with a surface roughness of ca 100 microns.

A catalyst consisting of a coating of Baymal on the mullite honey-

a) Desirable to minimize pressure drop at high space velocity and MCH conversion.

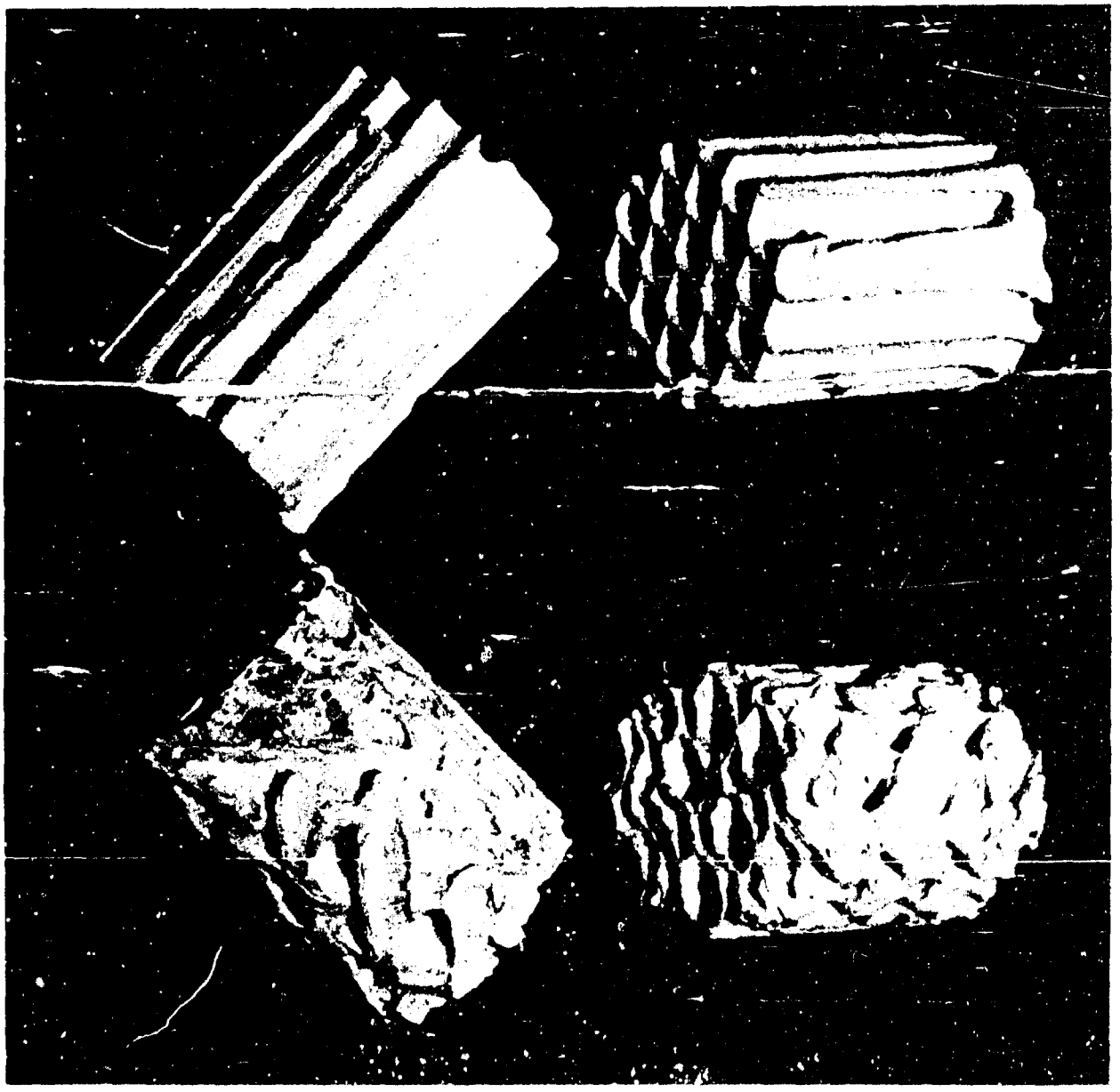


Figure 35. LOW-PRESSURE DROP CATALYST SUPPORTS
Upper: Straight, Parallel Cells
Lower: Crossflow Cells (Approx 45°)

comb support and impregnated with platinum to give 0.8%w was tested in a 5/8" ID tube at 18, 50, and 100 LHSV. Results for these tests are shown in Table 47. Typical conversions with a standard laboratory catalyst are also shown for comparison.

Table 47. DEHYDROGENATION OF MCH OVER SHAPED SUPPORT

Nonconventional Catalyst #9874-145

Run No.: 10100-J89
Pressure: 10 atm
Block Temp: 1022°F
Reaction Time: 10 min each condition
Apparatus: Bench-scale Reactor

LHSV =	18		50	100
Product Analysis, %w				
Cracked	1.7	1.9	0.1	Trace
MCH	23.2	23.9	54.3	66.3
Benzene	0.5	0.7	0.1	Trace
Toluene	74.6	73.5	45.5	33.7
MCH Conversion, %w	76.8	76.1	45.7	33.7
Conversion with Pellet Cat.,[a] %w	-	-	97.0	78.0

a) Standard laboratory catalyst = 1%w Pt on Al_2O_3; 1/16" pellets in an annular bed.

These lists show moderate conversions for the shaped catalysts, but less than with the pellet catalyst. The two catalysts were not tested under strictly comparable conditions, however, since the heat transfer path for the shaped catalyst was of the order of 10 times the distance of that in the pellet bed. Thus, the temperature near the center of the shaped catalyst might have been comparatively cold. The true surface area of the honeycomb catalyst was not determined.

The catalyst support shown in the bottom half of Figure 35 will be tried next, and this configuration should be more effective since the cell passages follow a zig-zag pattern from wall-to-wall which will improve the heat transfer. Further tests are planned to evaluate other configurations, and on a comparable tube diameter basis with the packed bed.

Nonconventional Catalyst Systems: Homogeneous Catalysis

Excellent conversions have been obtained on the dehydrogenation of MCH and other naphthenes over packed beds of solid catalysts. However, the use of packed beds can result in high pressure drops at high gas velocities. Although considerable improvements can be made by suitable selection of tube diameter and certain catalyst shapes, the problems of pressure drop, catalyst handling, and catalyst rejuvenation are always present.

Despite the difficulties associated with solid bed catalysts, alternative schemes are not simple, and no proven ones are available. However, one possible approach we have suggested is to use a "throw-away" catal-

yst in the form of an organometallic compound. Such a catalyst should best be fuel-soluble and stable in low temperature fuel environments. The effective catalyst agent might be the organometallic compound itself, but considering the temperatures required for high equilibrium conversion, would generally be a decomposition product, i.e., the finely dispersed metal or metal oxide.

Although we know of no literature precedence for dehydrogenation by homogeneous catalysis, the approach offers sufficient advantages to warrant investigation.

The first question to be answered was whether organometallic compounds could be found having dehydrogenation properties. To determine this, a small autoclave screening test has been set up. The autoclave is of a simple stainless construction, about 200 ml liquid capacity, and equipped with a Magna-dash stirrer. The maximum operating temperature was at first limited to 900°F due to the use of an aluminum heat transfer block. Temperature is controlled by a WEST Guardsman Indicating Pyrometric Controller, which is a taper or proportional type.

The method of test has been to place liquid MCH and 1%w[a] catalyst in the autoclave, which is then tightly sealed. Oxygen is then removed by seven repeated pressurings with helium to 200 psig. The pressure is then reduced to atmospheric, the valve is closed, and the Magna-dash and heater are turned on. The average heating rate to 900°F is about 3°F/min. Upon reaching 900°F the temperature is leveled out and held steady for some convenient length of time, usually under three hours.

Pressure and temperature are read versus time. The plot of P vs T is compared with a reference plot obtained with the same amount of MCH and no catalyst (see Figure 36). A fixed amount of MCH is charged each time. The amount selected, 7.41 g, was calculated to give about 150 psig pressure at 900°F when no reaction has occurred. Since a nonreactive run shows a vaporization curve followed by a nearly perfect gas law expansion line, moderate amounts of reaction can readily be observed by deviation from the reference pressure-temperature curve during the run. However, absolute conversions are determined by GLC analysis of the reaction products.

Table 48 shows the results with 19 organometallic catalysts which have been tried thus far. For comparison, an additional run was made using R-8 Pt/Al_2O_3 catalyst of the type used in the other laboratory dehydrogenation studies. A small amount of reaction occurs, of course, with no catalyst, as shown.

Although none of the organometallics showed large conversions, most did give some dehydrogenation reaction activity. LR-8527-92 gave the greatest conversion to toluene (1.8%) and the largest total conversion (4.0%). The catalyst compounds, except ferrocene, were decomposed during the test.

a) Basis weight of metallic element and MCH charged.

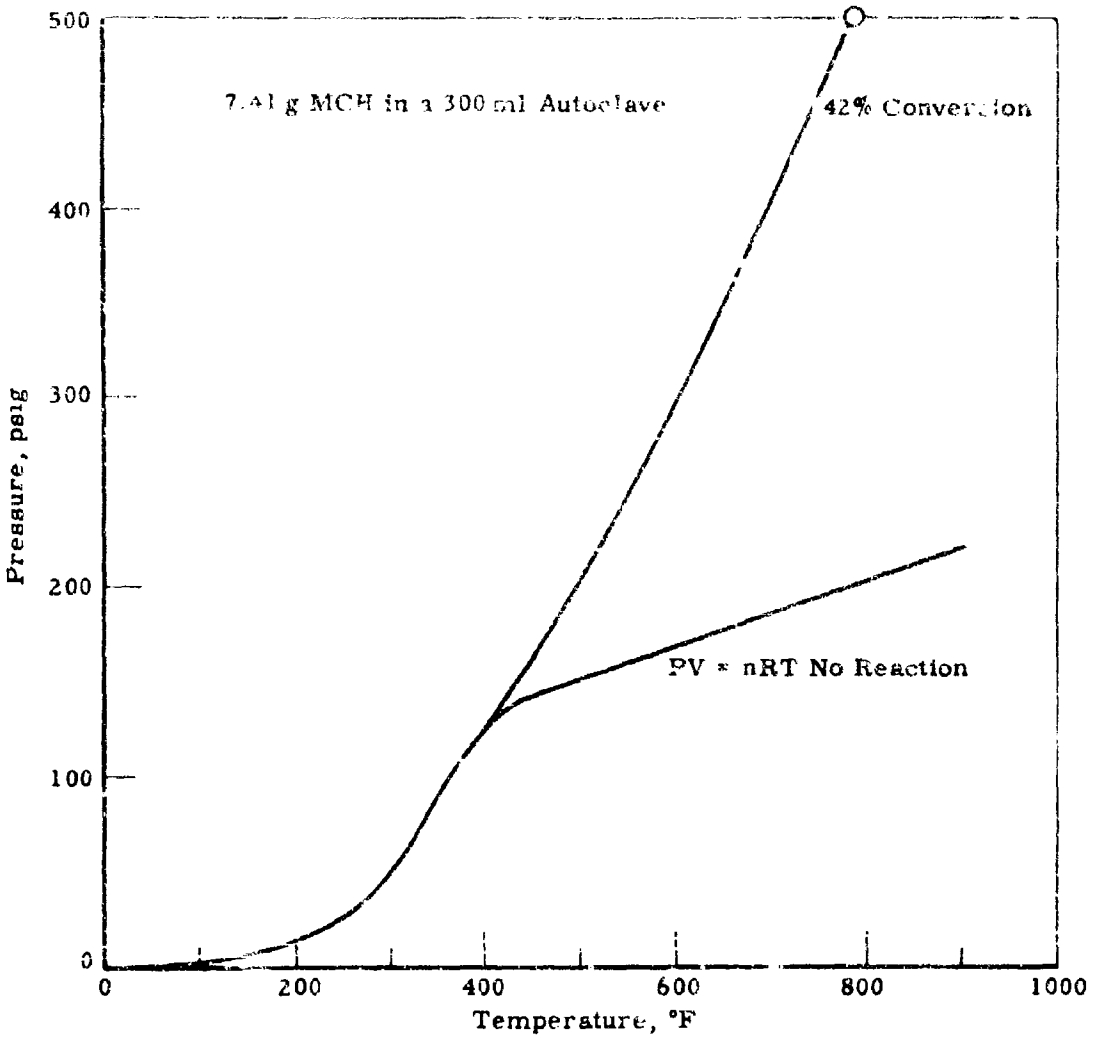


Figure 36. TYPICAL VAPORIZATION AND EXPANSION CURVE

While the results are not very impressive, there is at least encouragement to continue the investigation. A number of other compounds are on hand and are being tested; higher temperatures will be explored; and the effect of the presence of oxygen will be examined.

Table 48. HOMOGENEOUS CATALYSIS: DEHYDROGENATION OF MCH WITH ORGANOMETALLIC COMPOUNDS

Steady-State Temp = ca 900°F

Organometallic Catalyst[a] Code Number	Composition of Products, %				
	Toluene	Benzene	Methyl Cyclo-Hexadiene	Light[b] Products	Total[c]
LR 8527-87	0.1	-	0.1	0.2	0.4
-88	0.1	-	0.1	0.4	0.6
-89	0.3	0.1	0.5	0.2	1.1
-92	1.8	-	0.5	1.7	4.0
-93	0.5	0.2	0.2	0.3	1.2
-96	1.1	Trace	0.9	0.4	2.4
-97	0.5	-	0.7	0.5	1.7
-98	1.3	0.1	0.5	0.2	2.1
-100	0.4	Trace	0.7	0.2	1.3
-101	0.1	-	3.0	0.6	3.7
-102	0.1	-	0.6	0.2	0.9
-103	0.1	-	0.1	0.2	0.4
-104	0.1	-	0.3	0.2	0.6
-105	0.1	-	0.2	0.2	0.5
-106	0.1	-	0.3	0.2	0.6
-107	0.1	-	0.1	0.2	0.4
-108	0.4	0.4	0.1	0.2	1.1
-109	0.4	0.1	0.4	0.5	1.4
-110	0.1	Trace	0.1	0.2	0.4
None	0.1	Trace	0.1	0.2	0.4
R-8 Pt/Al_2O_3	41	-	0.5	0.5	42

a) Organometallic compounds added in an amount to give 1.0% metal, basis weight of MCH charged.
b) Light products were unidentified, but were lower mol wt than MCH.
c) Where catalyst ligands obviously contributed to the products, the theoretical amounts of these ligand products have been substracted from the totals determined by GLC analysis.

Thermal Stability

Effect of Oxygen Concentration on the Thermal Stability of Naphthenes

While the thermal stability quality of current jet fuels appears to be under control, we anticipate that higher speed jet aircraft[1] will bring with them a new round of fuel stability problems. Moreover, whenever cooling demands become such as to require endothermic fuels, we may assume that every possible means will be necessary to meet the severe thermal stability conditions of their use. This will entail consideration not only of the properties of the major fuel hydrocarbons themselves, but also of trace components, contaminants, and dissolved oxygen.

The role of oxygen in fuel thermal degradation has certainly been widely recognized,[23] and various investigators have reported its effect on the thermal stability of jet fuels.[24-28] However, work with specific pure hydrocarbons, at high temperatures, and particularly at dissolved oxygen contents extending below 1 ppm appears not to have been done.

We have consequently studied two naphthenes, methylcyclohexane and decalin, as well as a high naphthene content jet fuel, under conditions where dissolved oxygen concentrations ranged from air saturation down to the ppb level. (Properties for these fuels are shown in Table 49.)

The tests were made using the SD Coker, which we have previously described.[2][3][24]

For fuels and operating conditions such as used in the present work, vaporization usually takes place in the preheater, the vapor then passes through the filter (usually without significant pressure drop), cools and condenses in a water-cooled heat exchanger, and finally passes through a Grove pressure regulator and back into the glass reservoir for recycle. The SD Coker was operated at temperatures up to 900°F, usually at 250 psig. Preheater tube ratings were judged in an Eppi tuberator, using an extended color code scale (8 max) for each inch of tube. The maximum rating is the greatest value observed at any area on the tube, while the total rating is the sum of all 13 areas. In some instances we present the total as well as the maximum ratings. We have now built and are testing a calorimeter by means of which we hope to replace these arbitrary color ratings with heat transfer coefficient measurements.

To vary the dissolved oxygen content of the test fuels, several gas supplies of fixed and known oxygen concentration were previously prepared by suitable partial pressure blending of pure oxygen and nitrogen in standard nitrogen cylinders. Accurate O_2 concentration measurements were then made chromatographically.

Prior to beginning a run, the fuel was thoroughly sparged with the proper equilibrating gas. Simultaneously, the coker was flushed for at least an hour with a large flow of nitrogen. Since the SD coker was used in a fuel recycle mode, dissolved oxygen was continuously diminished by reaction in the test section, but was resaturated by gas sparging in the fuel reservoir. Saturation was ensured by following the dissolved O_2 content of the fuel effluent from the reservoir while increasing the sparge gas flow until the

Table 49. THERMAL STABILITY TEST

Fuel Properties

Fuel	Naphthene Purity, %	Naphthene Conc, mol/l	Sulfur, ppm	Copper, ppm	MW	Density, g/ml	bp, °F	Tc, °F	Pc, psi
Methylcyclohexane	100[a]	7.8	<0.2	<0.02	98.2	0.769	213.8	574.7	504
Decalin	100[b]	6.3	2	-	138.3	0.872	370.4	772.1	422
Jet Fuel RAF - 163-60	90[c]	4.5[d]	40	<0.02	190[d]	0.863	396-504[e]	831[d]	402[d]

a) MCH contained trace amounts of cyclohexane and unidentified heavy ends. MCH was passed through a silica gel column prior to use.

b) 91.2% trans.; Contained 0.1% IONOL® as received, which was reduced to <1 ppm by passing over silica gel.

c) Mass spec analysis: 11% paraffins, 2% olefins, 15% 1-ring, 51% 2-ring, 18% 3-ring, 3% 4-ring naphthenes.

d) Properties estimated using the paraffin/naphthene split, UOP characterization factor, 100°F kinematic viscosity, and API gravity.

e) ASTM D86 distillation; 50% pt = 450°F.

dissolved oxygen concentration no longer increased with further increase in gas flow rate. After the run was started and the test sections had reached thermal equilibrium, the reservoir oxygen content was again checked, and the sparge gas flow further increased, if required, to maintain equilibrium dissolved oxygen concentration.

Where dissolved oxygen levels below 100 ppb were desired, helium was used as the sparge gas (O_2 ca 6 ppm). Dissolved oxygen determinations were made using a chromatographic technique similar to that of Elsey,[28] and described in a previous report.[3] Although base line stability becomes limiting at high sensitivity, dissolved oxygen detection at concentrations below 50 ppb were found possible with 1 ml liquid samples. Readout was on a 1 mv recorder, and peak areas were determined by integrator count or by planimeter, although we favor the latter method for better precision at low oxygen levels. Oxygen was easily resolved from nitrogen since the ratio of emergence times was about $N_2/O_2 = 3$.

To make a dissolved oxygen determination, a liquid hydrocarbon sample of up to 1 ml was injected into a Vigreux column, where helium carrier gas quickly removed the air from the liquid.

Calibration of the analyzer was accomplished by using 1-10 µl samples of hydrocarbon of known dissolved oxygen content. Such standard solutions were obtained by saturating liquid samples at a known temperature.

A minor problem was the danger of contamination with air in sampling and transferring. Even the tip of the hypodermic needle could not be allowed to come in contact with air, particularly when measuring dissolved oxygen concentrations below 1 ppm.

In the figures presented in this section the preheater code ratings represent averaged values of two or more replicate determinations per set of conditions. Repeatability of coker ratings was generally within ± 1 for maximum code, and to within ± 5 for total ratings.

Dissolved oxygen determinations were repeatable to within 5% above 1 ppm. At lower levels the error was greater, partly because of the great difficulty of avoiding adventitious contamination on sampling.

In determining the effect of oxygen on deposit tendency, a series of runs was made at a selected set of conditions, with various oxygen contents. Figures 37 and 38 are typical of the type of data that were obtained. Figure 37 shows that at 550°F, MCH is most responsive to O_2 in the range from 1 to 4 ppm, becoming less so at higher values. The code ratings at 16.3 ppm is uncertain since the color was darker than 8, the upper limit of the scale. Also the possibility exists that the curve should sweep sharply upward at about 3 ppm, since we have insufficient data to know whether the point at 3.1 ppm is high or the point at 4.4 is low. However, with coker ratings at low O_2 contents it is easier to err towards higher ratings.

In Figure 38 we see that the thermal stability of decalin, at 550°F, remains constant over the entire range of 15 to 300 ppm oxygen, which corresponds to equilibration with gases of increasing oxygen-content-in-N_2 from 5%

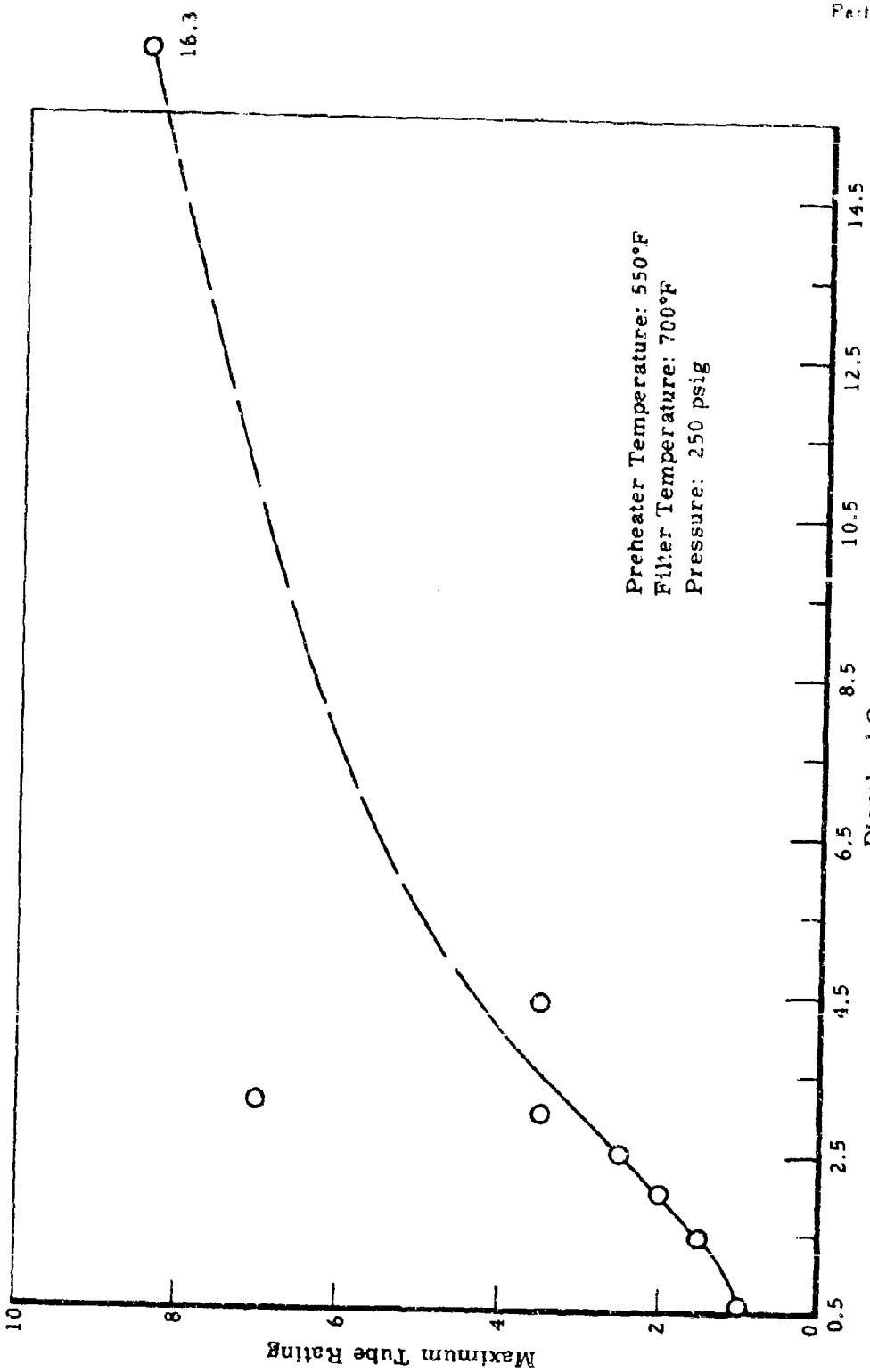


Figure 37. EFFECT OF DISSOLVED OXYGEN ON MCH THERMAL STABILITY
Averaged Data Points

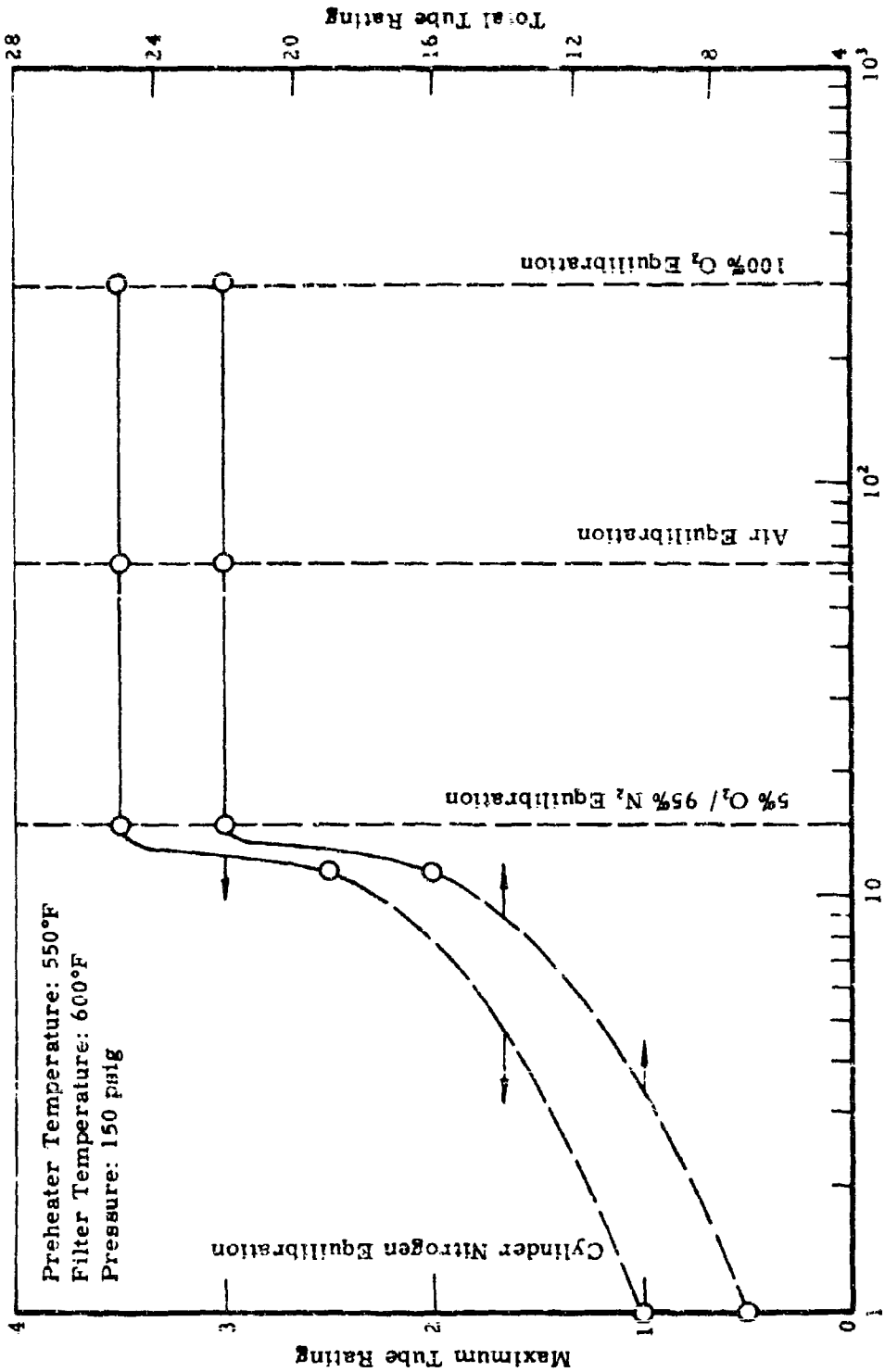


Figure 38. EFFECT OF OXYGEN PARTIAL PRESSURE ON SD COKER RATINGS OF DECALIN
Averaged Data Points

62698

to 100%. Below 15 ppm, improvement in thermal stability is marked, but tends to level out towards 1 ppm. A critical concentration region exists between 4 and 14 ppm.

Figure 39 shows the large temperature gradient effect on decalin when the dissolved oxygen content is only 0.6 ppm.

With good control of oxygen concentration, pure hydrocarbons demonstrate a sharp deposit-temperature breakpoint. This is illustrated by the behavior of MCH, shown in Figure 40, for two oxygen concentrations. The breakpoint for MCH is increased from 325 to 500°F by reducing the dissolved O_2 content from 80 to 3 ppm. The divergent slopes of the curves demonstrate the fact that oxygen content becomes increasingly important as the temperature rises. At and below the temperature of the air-saturation breakpoint (325°F, 80 ppm), oxygen concentration is of little importance. It would appear from this, that there would be little to be gained from controlling O_2 content, during flight, with subsonic jets: but with supersonic and, particularly, with hypersonic aircraft, handsome dividends would ensue from rigorous removal of O_2 from the fuel prior to takeoff.

In Figure 41 a similar sharp breakpoint is shown for Decalin, even at air saturation conditions. This is a temperature effect; the previous breakpoint shown (Figure 38) for Decalin was at constant temperature and was due to oxygen concentration change.

In contrast to these sharp breakpoints the naphthenic jet fuel displays a gradual change in deposit tendency with temperature (Figure 42), which may be characteristic of hydrocarbon mixtures. This broader breakpoint may be related to the existence of a spectrum of reaction rates and mechanisms. Differences in sharpness of breakpoint have also been noted by Zengel.[30]

From the table below we can see that Decalin can be increased in thermal stability by as much as 200°F by reducing the dissolved O_2 level from 64 down to 0.6 ppm. The improvement found for MCH was 175°F, and with the jet fuel, about 275°F, with the ultimate effect not yet in hand.

Fuel	Dissolved Oxygen, ppm			$T_{2.5}$ Breakpoint, °F		
	High	Low	Δ	High	Low	Δ
MCH	80	3	77	325	500	175
Decalin	64	0.6	63.4	500	700	200
Jet Fuel (F-1)	40	0.4	39.6	500	775	275

As exposure to temperature is increased, the level to which O_2 may have to be reduced is indicated by the curves shown in Figure 43 for all three fuels. The response of the naphthenic jet fuel, although uncertain in the interval 500-725°F, shows increasing thermal stability with decreasing O_2 content up to the lowest level tested. At higher O_2 contents, its stability falls below that of decalin. Mass spectrometric analysis of the

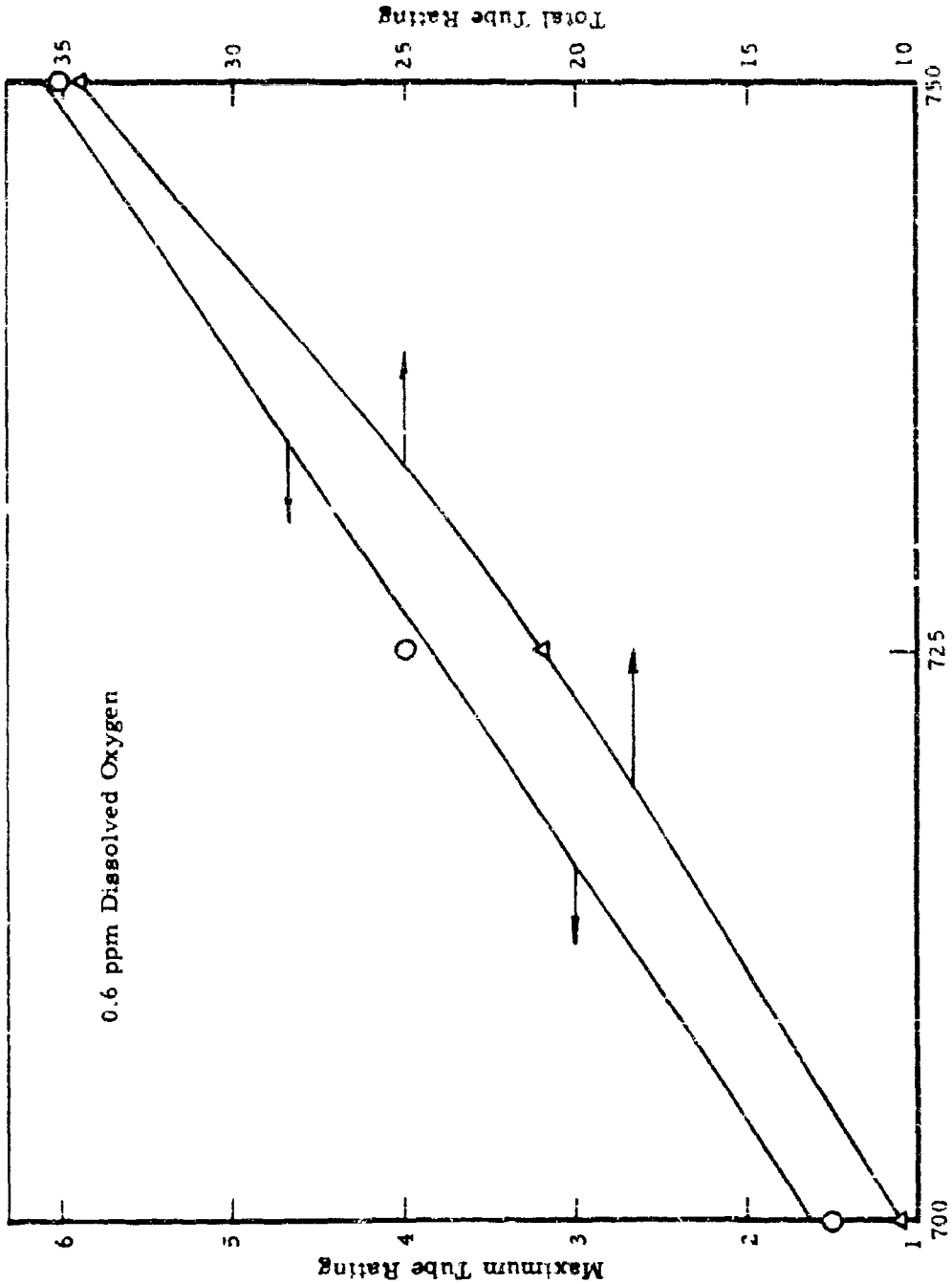


Figure 39. EFFECT OF TEMPERATURE ON THERMAL STABILITY OF DECALIN
Averaged Data Points

62698

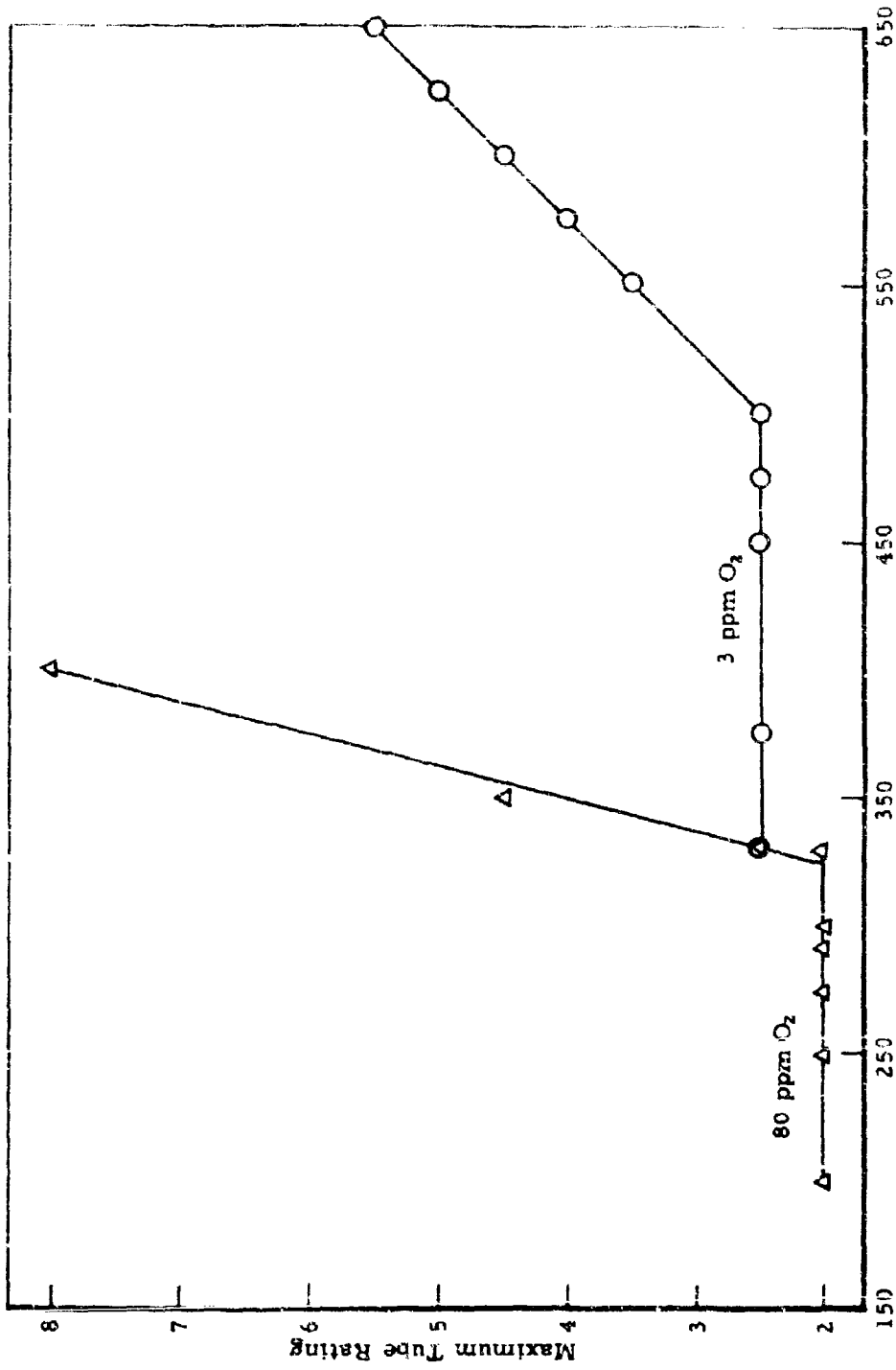


Figure 40. EFFECT OF TEMPERATURE ON THERMAL STABILITY OF MCH

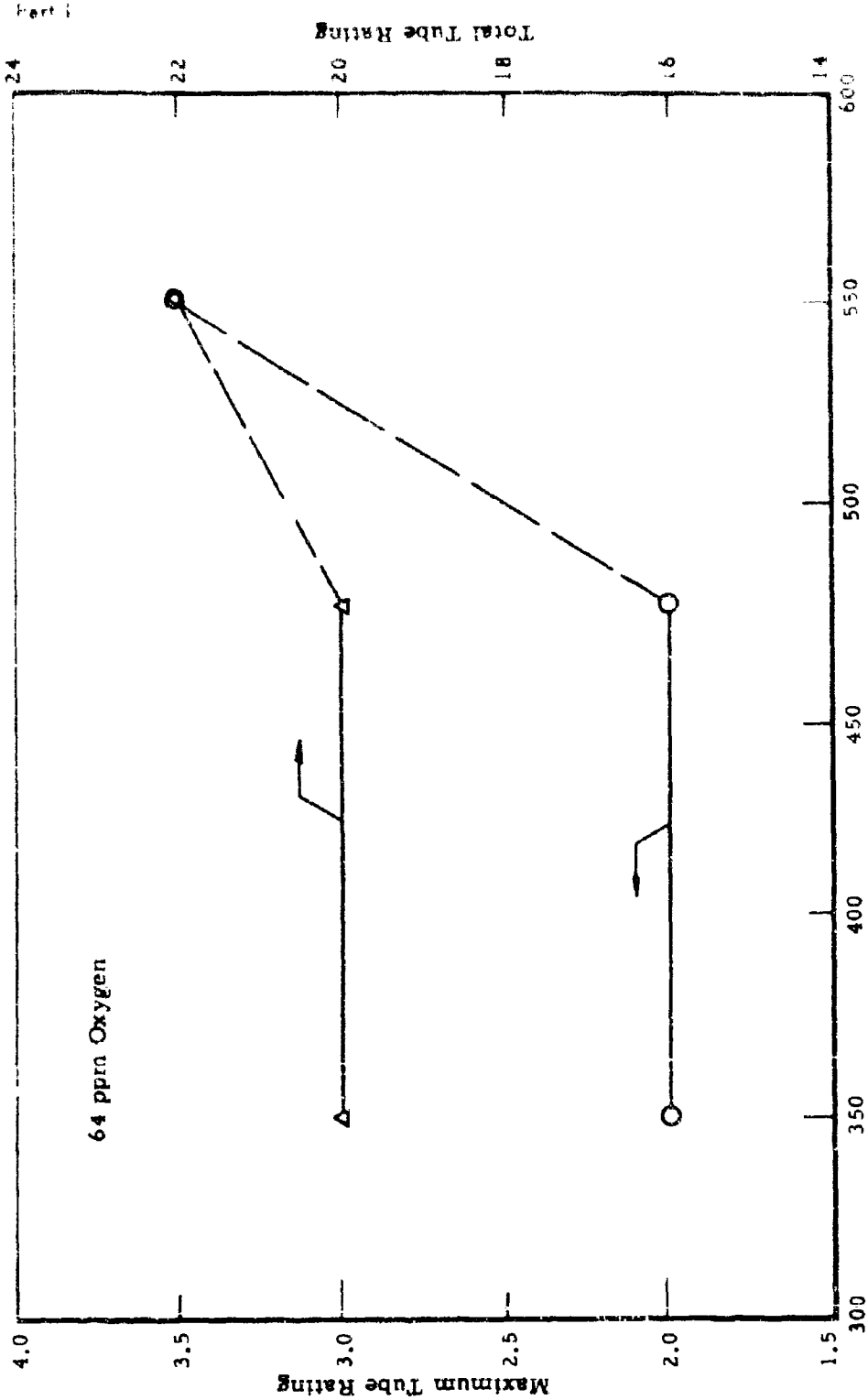


Figure 41. EFFECT OF TEMPERATURE ON THERMAL STABILITY OF DECALIN
Averaged Data Points

62698

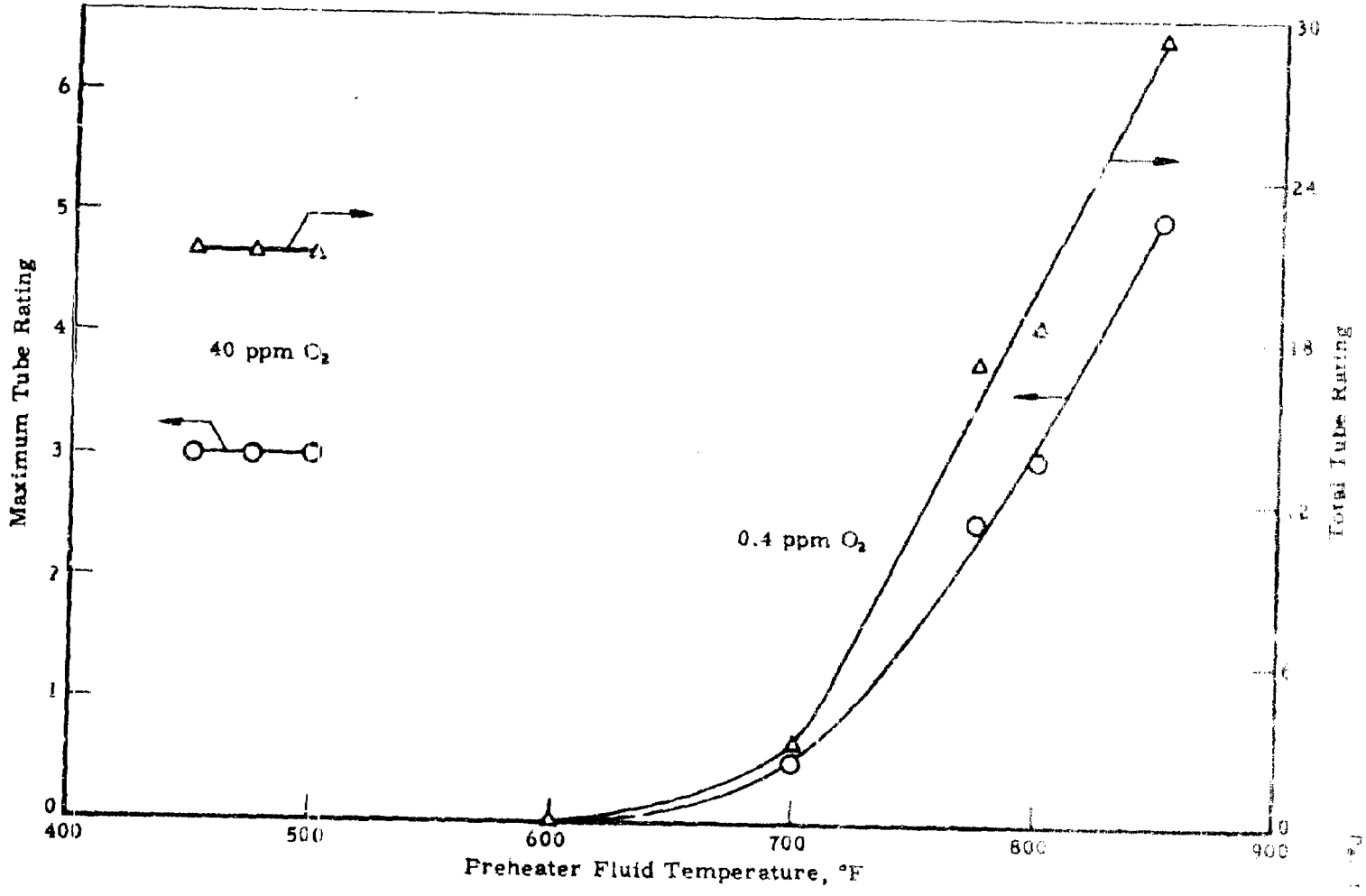


Figure 42. EFFECT OF TEMPERATURE ON THERMAL STABILITY OF NAPHTHENIC JET FUEL (F-1)

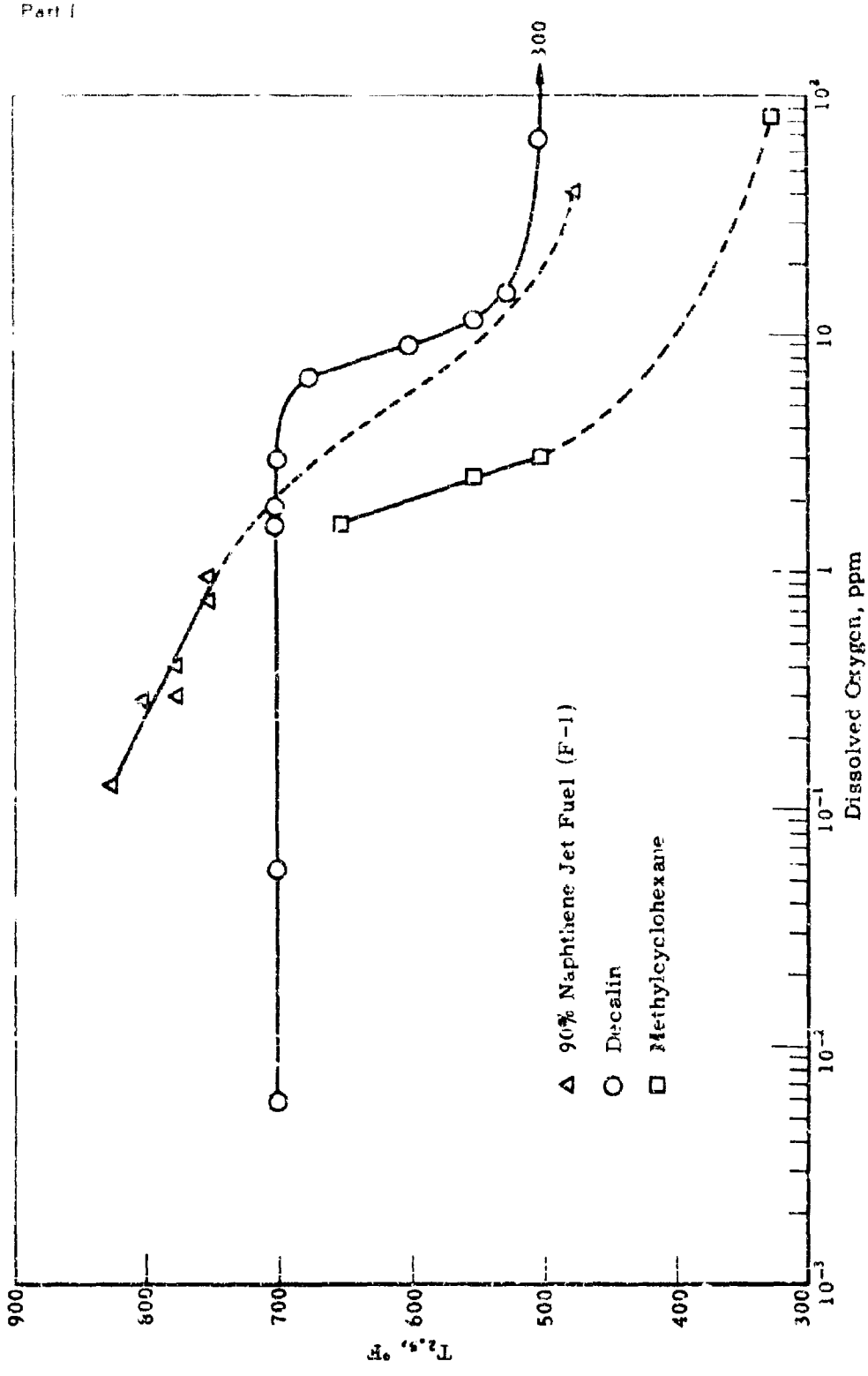


Figure 43. EFFECT OF DISSOLVED OXYGEN ON THERMAL STABILITY OF NAPHTHENES

62698

jet fuel revealed that it contains a broad spectrum of 1, 2, 3 and 4-ring cyclics. The possible significance of this on its behavior is discussed below.

It is interesting to consider the effect of oxygen concentration in the light of our previous efforts to tie the deposit forming reaction to the initial reaction of oxygen with hydrocarbons. If the initial reaction is assumed to be the interaction of a free radical with a dissolved oxygen molecule, leading to the formation of a chain propagating peroxide, the disappearance of O_2 may be represented by[23]

$$\text{Rate} = \frac{-d\,O_2}{d\,t} = \frac{k_a\,(RH)\,(ROOH)}{1 + \frac{k'(RH)}{P_{O_2}}}\,, \tag{4}$$

where (RH) is the hydrocarbon concentration, (ROOH) is the concentration of peroxide formed, P_{O_2} is the partial pressure of oxygen, and k_a and k' are empirical constants. Under our conditions, (RH) is substantially constant for each hydrocarbon and will be approximately 7.8 for MCH, 6.3 for decalin and about 4.5 for the jet fuel (m/l).

Under high oxygen concentrations the partial pressure of oxygen could be large, and the rate expression would tend to approach:

$$\text{Rate} = k_a\,'(RH)\,(ROOH) \tag{5}$$

$$\text{Rate} = k_a\,''(ROOH) \tag{5a}$$

being proportional to the peroxide concentration for any particular hydrocarbon. On the other hand at very low oxygen concentrations the expression would approach:

$$\text{Rate} = k_a\,'''(ROOH)\,P_{O_2}\,. \tag{6}$$

If the assumption we made regarding the role of the initial oxidation reactions is valid, then the results we have obtained are in general agreement with this thesis. For instance, at high concentrations of oxygen the tendency to form deposits appears to be independent of O_2 partial pressures (following Eq. 5a), while as the oxygen content is lowered, the rate (or deposit tendency) decreases (following Eq. 6), i.e., giving higher $T_{2.5}$ values. Also, rates would be expected to decrease with increasing molecular weight for similar type compounds since they have lower molar concentrations. Tendency to form peroxides would be very important, also.

The failure of decalin to follow the expected behavior below 3 ppm suggests that another mechanism, independent of oxygen content, is coming into play. Why this should be true for decalin at this particular oxygen concentration, but not true for the jet fuel, can only be conjectured at the present time. It is remarkable that the naphthenic jet fuel proved to be more stable than decalin at low oxygen concentrations, since the jet fuel undoubtedly contains C_{5-}, as well as C_6-ring naphthenes. The C_5-rings have been indicated to be less stable than the C_{6-} under conditions where substantial amounts of oxygen are present[3)24)32)]. This may not be true under low oxygen conditions. It may be that each compound has a characteristic

temperature at which it becomes indifferent to decreasing oxygen content, as suggested by the behavior of decalin. When the fuel consists of a large number of compounds, as does the jet fuel, the threshold temperature will gradually rise with decreasing O_2 as successive compounds abandon their dependence on oxygen concentration. In this case, it would be expected that at still lower oxygen levels the jet fuel would also become indifferent to changes in this parameter. It might also be expected that the proportion of oxygen in the deposits would decrease. Another expectation would be that comparable behavior could be achieved by a mixture of pure components. Both of these expectations will be tested in future work. It will be interesting to observe if such mixtures display synergy.

We have previously reported the effect of structure on the thermal stability of a wide variety of compounds.[3)24] It was found that naphthenes are generally more stable than aromatics or paraffins of comparable mol weight and that thermal stability increases with carbon number (and so also with molecular weight and with boiling point). The greater stability of naphthenes over aromatics is surprising, and it will be relevant to determine if this persists at very low O_2 concentrations. In the ultimate utilization of naphthenic fuels for endothermic cooling of high speed aircraft the naphthenes will be catalytically dehydrogenated to aromatics (and H_2). Under these conditions, the oxygen concentration will be vanishingly small. Results obtained with the CAFSTR (see below) should evaluate the thermal stability of such mixtures under more realistic conditions.

The thermal stability of naphthenes is strongly dependent on oxygen concentration, being independent at high levels, improving with decreasing content at intermediate levels (1-10 ppm) and then indifferent again at low levels.

Complete removal of oxygen increases the thermal stability breakpoint by about 200°F.

At constant O_2, thermal stability increases with molecular weight and perhaps with mixture complexity.

Naphthenes are generally more stable than aromatics or paraffins of comparable molecular weight.

Dissolved oxygen content, which has been perhaps of little importance to thermal stability with subsonic jets, will have to be rigidly controlled to a level below 1.0 ppm in fuels for future hypersonic aircraft. This procedure may also be beneficial with supersonic aircraft.

Thermal Stability of Reaction Products

Preliminary Tests

Fuel stability problems of endothermic jet fuels involve more than merely properties of the tank fuels. Where heat sink capacity is abetted by endothermic reactions (e.g., dehydrogenation), the characteristics of the reaction products must also be considered. Moreover, interactions between catalyst and fuel systems may produce integrated effects not discernible from the separate properties of either. For example, fuel composition

changes or admixture of chemicals for the purpose of improving fuel thermal stability can have seriously harmful effects on catalyst life and reactivity. In reverse, variations in catalyst properties might seriously impair thermal stability of reaction products.

As a first step in the assessment of reaction product thermal stabilities we looked at SD coker ratings of several pure aromatic hydrocarbons, as shown for example in Figure 8 of reference 24 and as discussed in previous reports.[1)2)3)]

In a second step, SD coker tests at 675°F were made on thermal reaction products taken from FSSTR runs with F-71 jet fuel (properties shown in Table 50). Coker data for runs at three different sets of FSSTR operating conditions are shown in Table 51. Results of these tests show satisfactory thermal stability of F-71 product exposed to FSSTR temperatures up to ca 1000°F fluid. However, product material from the 1200°F maximum fluid temperature run gave the heaviest deposits ever observed here in a coker test. Moreover, most of this deposit material was hard and unwipable, as shown by the ratings in Table 51. These tests were conducted at a standard dissolved oxygen level of 0.45-0.50 ppm. Higher oxygen concentrations would probably have resulted in even poorer thermal stability ratings.

Catalyst and Fuel System Test Rig (CAFSTR) Design

To be adequate, an evaluation test for endothermic fuel thermal stability must permit examination of the reaction products under actual exchanger conditions and with minimum time lapse. Conventional fuel cokers are inadequate for this purpose, since reaction products, on sampling and cooling, may further react to form condensation products of decreased thermal stability. Conventional coker results are also suspect with respect to evaluating reaction products at meaningful conditions of reaction and use.

To meet these peculiar requirements, a Catalyst and Fuel System Test Rig (called the CAFSTR) has been designed and built. The equipment schematic is shown in Figure 44 and the completed unit photograph in Figure 45.

Fuel flowing at a design rate of three pounds per hour is heated in a series of three annular heat exchangers, then passed through a tube reactor, and the product effluent further heated to a final temperature of upwards to 1300°F. Design operating pressure is to 1500 psig.

Each heat exchanger has a specific function and may be operated within closely defined liquid temperature ranges. Beginning with E_1 (see Figure 44), the first exchanger may be limited to sensible liquid heat transfer only. If the operating pressure is sufficiently low for boiling to occur, E_2 becomes a vaporizer and will convert all liquid to vapor. At low pressure, E_3 sees only vapor which it will heat to the predetermined reaction temperature. E_4 then heats the product fluid from the reactor to some higher temperature limited by thermal stability. The reactor may be operated either thermally or catalytically and consists of a simple straight tube, heated in an electric furnace.

Table 50. DESCRIPTION OF F-71 JET FUEL

Properties	F-71
Gravity, °API at 60°F	50.7
Specific Gravity, 60/60	0.777
ASTM Distillation, °F	
IBP	402
10%	409
20%	410
50%	420
90%	467
E.P.	543
Recovery, %v	98.5
Residue, %	1.5
Vapor Pressure, psia	
300°F	2.6
500°F	44.0
Flash Point, °F, P.M.C.C.	180
Freezing Point, °F	-51
Color, Saybolt	30+
Kinematic Viscosity at -30°F, cs	13.6
Aniline Cloud Point, °F	185
Aniline Gravity Constant	9805
Sulfur, %w	0.003
Mercaptan Sulfur, %w	0.0001
Cu Strip Corrosion at 212°F	1B
Luminometer	104
Gum, Existent (Steam Jet), mg/100 ml	1
Heat of Combustion, BM/16 (Net)	18,929
Water Separometer Index (Modified)	100
Thermal Stability, CFR Research Coker (650/650°F, 250 psig)	
Pressure Drop, in. Hg	0.2
Preheater Deposit Rating (as is/wiped)	2/1
Hydrocarbon Analysis, %v	
Paraffins	82.9
Naphthenes	10.6
Olefins	5.1
Aromatics	1.4
Thermal Stability, SD Coker, 450/500°F, 5 hr,	
Preheater Deposit (Maximum/Total Rating)	1.5/16
Pressure Drop, in. Hg	0

TABLE 51
SD COKER RATINGS OF F-72 JET FUEL THERMAL REACTION PRODUCTS FROM THE FSSTR

Preheater conditions: 675°F, 250 psig; dissolved oxygen content, 0.45-0.50 ppm

FSSTR Operating Conditions			SD Coker Preheater, Rating, Max/Total	
Max Fluid Temp, °F	Pressure, psig	Space Velocity, LHSV	Wiped	Unwiped
855	890	398	0.5/ 1	3 / 7
1076	766	256	0/ 0	2 / 7
1200	770	255	7 /74.5	8.5/87.5

Following the product heat exchanger, E-4, the fluid passes through an orifice to simulate a fuel nozzle. Pressure drop across this unit is detected by a Foxboro d/p cell and read out on a recorder.

Direct helium drive is used to establish fuel pressure while fuel flow is controlled by a needle valve-operated Foxboro pneumatic controller. A five-gallon stainless steel, unheated cylinder is used for the fuel supply reservoir. System pressure is controlled by the helium drive pressure regulator.

Temperature control of each preheater is by thermocouple in the effluent fluid temperature of each particular unit. Temperatures of the heat transfer surface and of the liquid adjacent to it are measured at inlet and outlet points of each preheater, and surface temperatures, every three inches along the reactor. Static pressures are read at a point upstream of preheater E-1 and downstream of the test orifice.

Further design details may be found in the Appendix of this report.

Tentatively, the test length has been set at about four hours, but this may be varied if desired.

Evaluation procedures for the tests likewise have not been finalized. However, the following kinds of data are being obtained directly from the CAFSTR.

A. At steady-state test conditions,

1. Pressure drop across the combined heat exchangers and reactor is noted. If this item proves to be significant, instrumentation for ΔP measurements across individual units may later be installed.

2. Fluid and heat transfer surface temperatures are recorded, and any changes in ΔT which reflect change in heat transfer coefficient are noted.

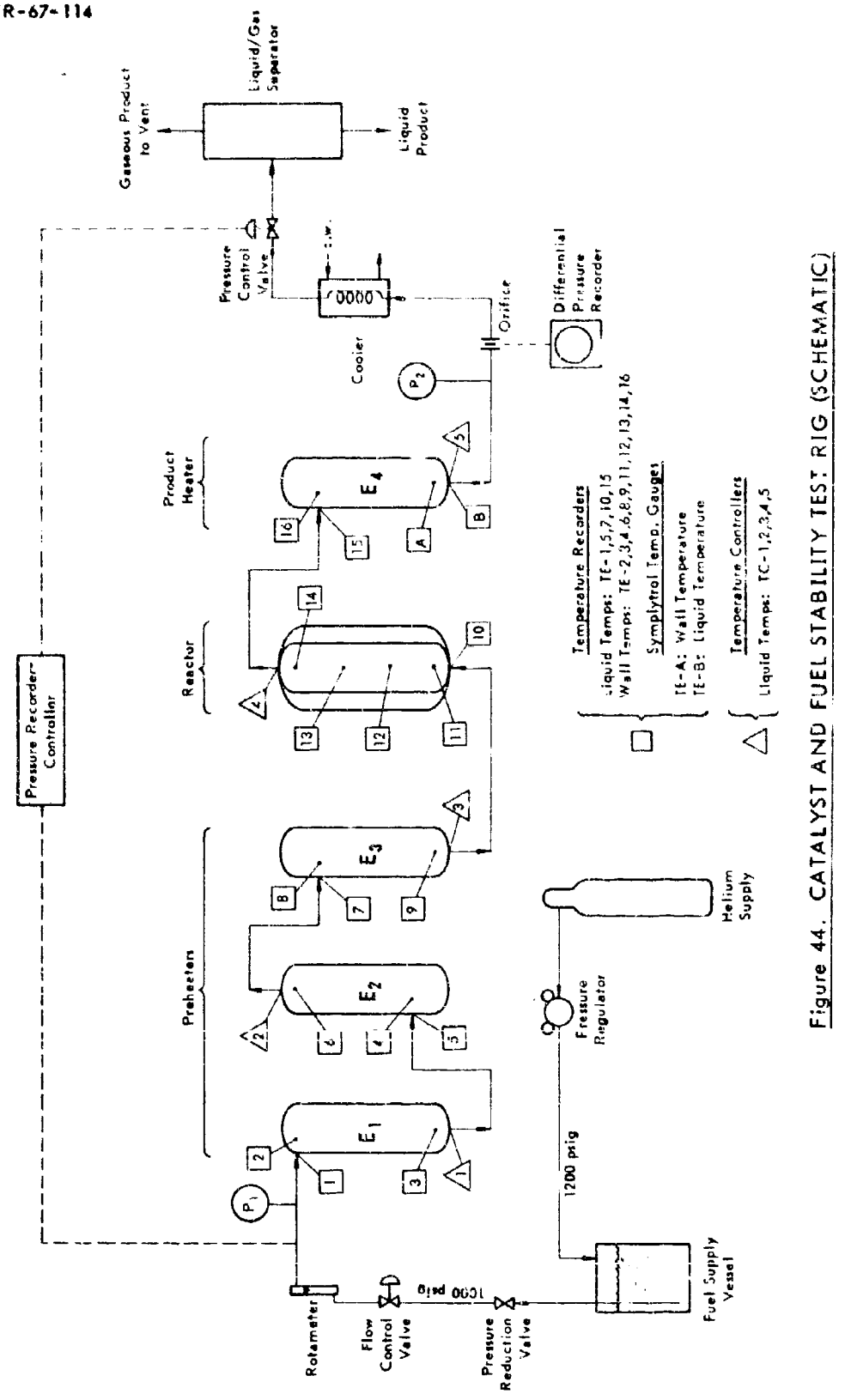


Figure 44. CATALYST AND FUEL STABILITY TEST RIG (SCHEMATIC)

62392

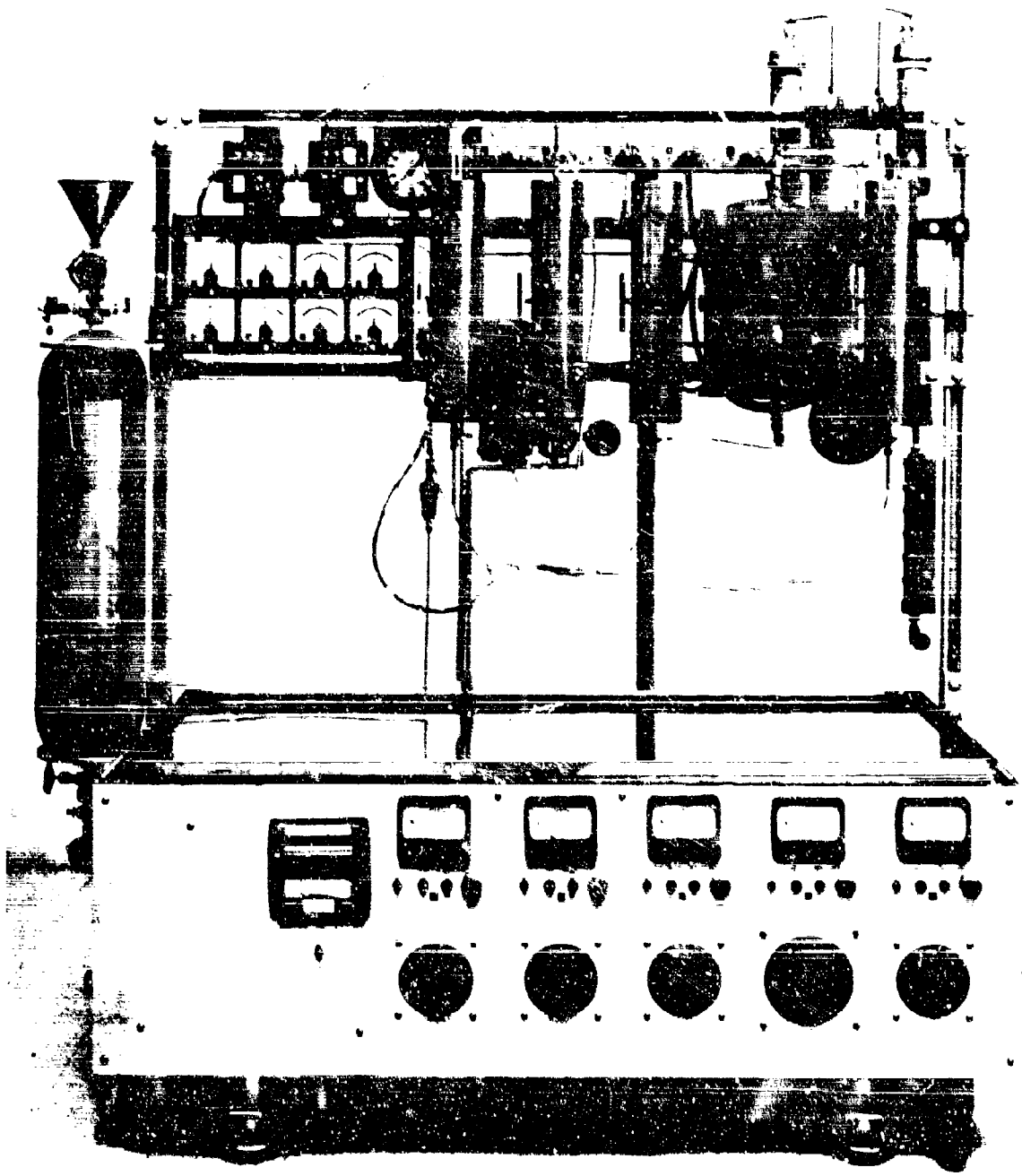


Figure 45. CATALYST AND FUEL SYSTEM TEST RIG

3. Total rate of power input to each unit is controlled and recorded. For comparative fuel testing, these rates are pre-estimated and preset, based upon the operating pressure and the desired temperature profile.

4. Changes in pressure drop across the test orifice are also continuously recorded. The size of the orifice has been set at .042 inches, but will require additional experience before a final selection can be made. Changes in ΔP may reflect either deposit formation or changes in conversion.

5. The temperature profile of the reactor wall is observed to indicate loss in catalyst activity with time.

6. Periodic samples of the product gas and liquid effluent are taken and liquid samples are tested for refractive index. Both liquid and gas are analyzed for composition by GLC. A continuous material balance on liquid and gaseous product is available since gaseous products are measured continuously through a wet test meter. Hence, catalyst life and change in selectivity can be observed over the time of test.

B. At conclusion of the test,

1. The inner tube of each heat exchanger is removed from the CAFSTR for inspection and rating. Although semi-quantitative visual ratings based on ASTM color codes have been made, construction of a calorimeter is now complete where heat transfer coefficients can be measured. If significant changes in liquid-heated surface temperature difference are observed during the actual CAFSTR test, this data may also be used. Detailed discussion of the calorimeter/tuberator is given below.

2. The reactor tube is opened for inspection. Carbon deposits or other physical effects can be observed.

3. The orifice is inspected for deposit formation. If appreciable, such deposits can be measured gravimetrically since the orifice plate is small.

CAFSTR Testing

The CAFSTR has been completed, debugged, and is operating according to design. Only minor problems requiring simple adjustments were encountered.

Preliminary runs were made on two fuels (F-7' Jet Fuel and MCH) at 1000 psig, at temperatures up to 1200°F (metal surface temperature), at both 3 and 6 lb/hr flow rate, and with and without R-8 platinum on alumina catalyst.

All runs were 4 hours duration and were made at a calculated dissolved oxygen level of a few parts per billion (ppb) obtained by sparging with helium of less than 10 ppm O_2 content while the reservoir was placed under 23 in. Hg vacuum.

In the first two runs with F-71 jet fuel, at 3 lb/hr flow and 446 and 500°F maximum temperatures in all heat exchangers (without catalyst) the

product fuel became amber in color, but no deposits were formed on any of the preheater tubes.

On further testing, F-71 jet fuel gave no visible deposits at temperatures up to a tube surface temperature of 950°F. No catalyst was charged with this fuel.

With MCH at 3 lb/hr flow, heavy carbonaceous deposits occurred in the third preheater where surface temperatures of 1104 to 1121°F and fluid temperatures of 1067 to 1092°F were reached. Some streaks of carbon appeared at 1024°F/972°F (surface/fluid). However, a 6-lb/hr run at 1024°F/972°F gave a virtually clean surface.

In preheater No. 1 and No. 2, no distinct effect of flow rate was seen. Black-brown color appeared on preheater tube No. 2 when surface temperatures ranged from 651 to 728°F, but whether this color originated entirely from a deposit film or in part from the tube surface itself could not be determined. A similar, but much lighter, color was observed at surface temperatures of 392 to 419°F in No. 1 preheater. Changes in ΔT (metal-fluid) were observed in some instances, but further experience will be necessary to know whether these differences were significant.

Preheater No. 4, which follows the reactor, was exposed to surface temperatures in the range of 1150-1200°F and products containing up to 43 mol percent toluene plus small amounts of cracked hydrocarbons. No deposit formation occurred; the light yellow colors observed were apparently due to the metal.

The question of how to rate the preheater tubes must now be answered, since visual ratings with the Eppi Tuberator are far less meaningful than before. At high temperatures, the presence of a blue coloration of the tube metal, plus some shades of yellow and tan which may also be the metal itself (Inconel 600), make the visual evaluation of thermal stability both difficult and uncertain.

An experiment was run on the CAFSTR in an attempt to clarify the meanings of the colors observed, since the tubes often appeared clean despite coloration. In this run the CAFSTR was operated with helium only, at a flow low enough to provide negligible heat transfer to the gas, but sufficient to prevent the presence of air. Results of this test are summarized in the following chart. Evidently, with the situation shown here, color code ratings are meaningless, and visual ratings of any sort are quite unreliable. Moreover, the "helium" colors cannot be assumed to be the colors which would occur with a nondegrading hydrocarbon, so that in the F-71 and MCH runs which were made it is impossible to know whether the colors observed were due to purely temperature effects on the metal, interaction effects between the fuel and the metal, or to thin deposits formed from the fuel.

CAFSTR HEAT EXCHANGER TUBE COLORATION DUE TO TEMPERATURE IN HELIUM[a] ENVIRONMENT

Preheater No.	Max Tube Skin Temp, °F	Tube Color Description	Approx Color Code
1	327	Very light yellow	1.5
2	543	Tan	3.0
3	931	Assorted colors = copper-pink, light and dark grey, dull blue, and dull blue-pink	3.0-3.5
4	97	Light copper tan with soft light grey overlay	0-3.5

a) Helium contained <10 ppm O_2.

Calorimetric Tuberator

There has been a long-recognized deficiency in the rating of coker tubes by assignment of an arbitrary color code number using the Eppi Tuberator. Although coker fuel "break points" have shown remarkably good agreement with the minex heat exchanger test,[30] the following weaknesses in color-code ratings have been recognized:

1) Deposit colors often do not match any of the standard code colors, and are, at best, subject to operator interpretation and hence, large error.

2) Deposit color is not necessarily a measure of deposit thickness or of its resistance to heat flow.

3) At high temperatures (particularly with metals other than aluminum) the tubes themselves may display a wide variety of colors due to oxide, sulfide, or other metal reaction product films.

4) Code ratings do not reflect the total area covered by deposits, but rather the maximum color density within an area.

Desirable features of a tube deposit rating test would include:

1) Repeatability and sensitivity
2) Simplicity and speed
3) Meaningfulness.

Thus, one might wish to rate tube deposits in terms of heat-transfer coefficients, which not only provide relative values but also would find direct usefulness in design work. Unfortunately, even heat-transfer coefficient measurement is a function of temperature, flow velocity, and system

geometry, so that the best one can probably be is to come up with a sensitive, rapid test which will reflect in a relative way how the total deposits affect heat-transfer rates.

Our concern with this problem has led us to a direct calorimetric approach. The apparatus, now nearing completion, (see Figure 46) consists of a stainless steel Dewar flask in which the preheater tube is immersed to above the heated zone in water, and the top of the flask is closed by a split styrofoam stopper. Thermocouple and power leads enter through tightly fitting holes in the stopper, through which also passes a motor-driven stirrer.

One thermocouple, welded to the inside of the preheater tube shell, will be used to control constant metal temperature by use of a Barber-Colman controller, while a second thermocouple opposite the first in the liquid gives the water temperature, which will be read out on a Honeywell strip recorder. Power to the preheater tube will be supplied through a SOLA constant voltage regulator and a variac.

As planned, the test will consist of holding the tube shell at a constant temperature of about 200°F and measuring the time elapsed while heating the stirred water (ca 2 quarts) from about 70 to 170°F. Average overall heat transfer coefficients will be calculable, but the time measurement is expected to be more sensitive for relative ratings. Therefore, it is proposed to define the deposit rating as,

$$\frac{\text{Time elapsed with dirty tube}}{\text{Time elapsed with clean tube}} \times 100.$$

In this way, ratings above 100 will represent loss in heat transfer due to the deposits. Time of the test is expected to be of the order of 3600 seconds. Calculations indicate an expected lower limit of deposit thickness detection of about 0.0002 in. Evaluation tests on clean tubes will be made first, followed by tests on tubes coated with aerosol sprayed lacquers.

Fuel System Simulation Test Rig

The Fuel System Simulation Test Rig (FSSTR) has been described in detail in the three annual reports associated with the preceding contract on this subject,[1)2)3)] therefore no description of the unit will be included here. However, a flow scheme is repeated as Figure 47 for convenience.

During the past year five different studies have been conducted in the FSSTR. These tests, which are reported here, were carried out in the following sequence:

Thermal Cracking of Fuel F-73
Catalytic Dehydrogenation of MCH in 3/4" Reactor
Thermal Cracking of Propane
Catalytic Dehydrogenation of Propane
High Heat Flux Study (in progress)

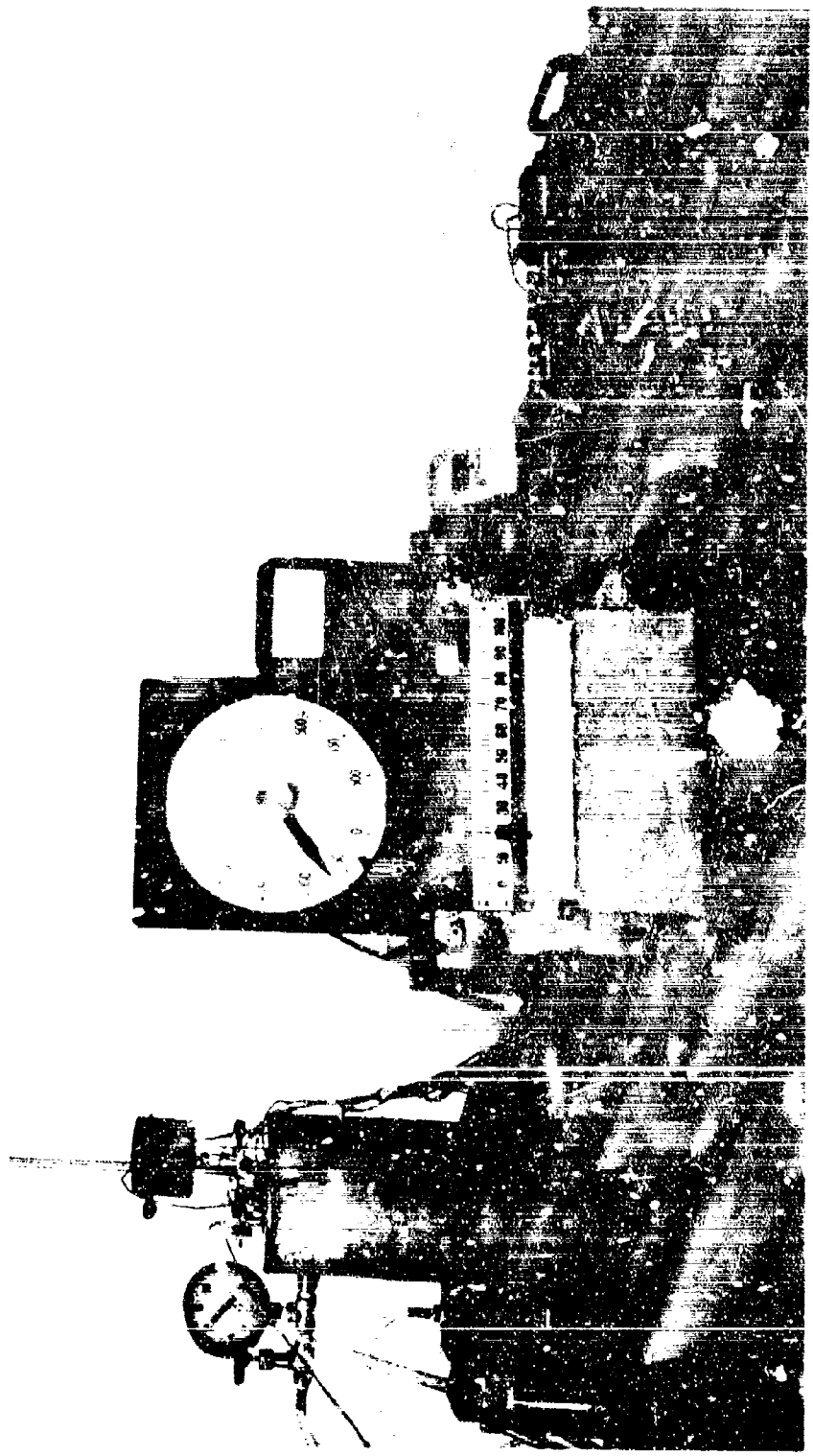


Figure 46. CALORIMETRIC TUBERATOR

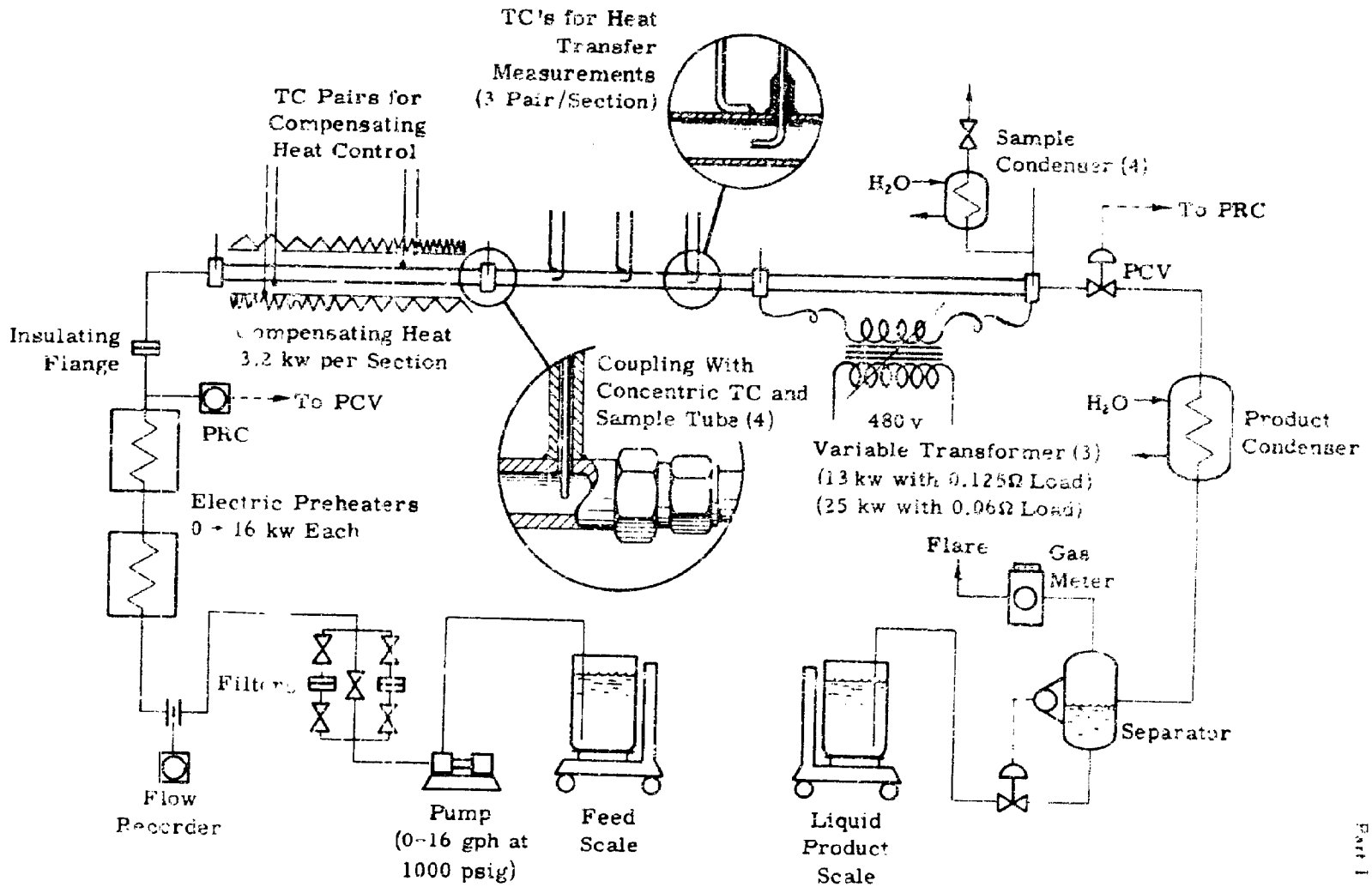


Figure 47. FSSTR - FLOW SKETCH OF FUEL SYSTEM SIMULATION TEST RIG

No modifications to the unit were made prior to the first of these tests. There were changes made during subsequent operations, however, which are described later in the appropriate sections.

Thermal Cracking of Fuel F-71

The program of tests for studying the thermal reaction of the highly paraffinic jet fuel F-71 (see Table 54 and Table 55 of this report for characteristics of this fuel) has been completed. The range of variables covered during these tests is outlined in Table 52.

Tables 53 and 54 present the operating data summary and product recovery and analytical data for the previously unreported tests. Previous work on this system was covered in Tables 73 and 74 of Reference 3. No further work using this fuel is presently anticipated.

Inspection of the product distribution data of Table 54 clearly shows that increasing pressure and decreasing flow rate, both tending to increase residence time, result in cracking larger fractions of the feed to gaseous products. However, it is also apparent that, over the ranges studied, these variables have only minor effect on total heat sink availability at a given fluid temperature. As illustrated in Figure 48, changing LHSV[a]) from 360 to 139 increased the heat sink by <10%. Pressure variation (from 500 to 900 psig) had even less effect. Heat-transfer coefficients did not show any unexpected characteristics, varying from about 85 to 450 Btu/hr/sq ft/°F.

The change in reaction with temperature and flow rate is shown in Figure 49 where the gas produced and change in paraffin content of the product liquid is presented as a function of temperature at the three space velocities tested. This indicates that the maximum conversion of the original feed material is about 60% at the highest temperature employed.

Coke formation resulted in very erratic operation during the 900 psig, 1200°F runs at both 360 and 130 LHSV. It appeared that, periodically, coke particles would partially plug the pressure control valve and then break free when the valve would open to maintain the set pressure. This resulted in fluctuating pressure and flow which in turn caused temperature cycling. During the previously reported tests, operation had been satisfactory at 1200°F at 750 psig and 255 LHSV but serious coke formation occurred at 1248°F. Thus, while we have been unable to determine any loss in heat-transfer coefficient resulting from coke deposition, it would appear that a realistic upper limit of ca 1150°F resulting in a total heat sink of 1000 to 1050 Btu/lb seems to be indicated. This would be some 200 Btu/lb above the heat sink available from sensible and latent heat only.

Our results have been compared qualitatively with those obtained by Kutzko in his hot air heated calorimeter.[33]) Although insufficient data were given in the reference to make an unambiguous quantitative comparison it appears that the heat sinks obtained by him with a special JP fuel (cf Table 55) are entirely concordant with ours. The composition of the cracked gases is also generally the same.

a) Calculated on the volume of one 10-foot section.

TABLE 52
FSSTR-THERMAL CRACKING OF FUEL F-71:
SUMMARY OF OPERATING CONDITIONS

Section III inlet temperature 970-1010°F
LHSV based on Section III volume only

Nominal LHSV	Nominal Pressure, psig	Section III Exit Fluid Temp, °F
130	500	1090-1196
130	750[a)]	1099-1174
130	900	1085-1214[b)]
265	750[a)]	1122-1200-1248[b)]
360	500	1067-1201
360	750	1068-120[illegible]
360	900	1068-1215[b)]

a) Previous work.
b) Coke formation seriously affected these runs.

TABLE 53
FSSTR-THERMAL CRACKING OF FUEL F-71 - DATA SUMMARY

Run No. 0915-	F-71 Feed Rate		Press., psig		Reactor Section	Fluid Temp at Coup-lings, °F		Heat Transfer[b]					Total Heat to Fluid, Btu/lb
								Temperature, °F			Btu	Btu	
	GPH	LHSV[a]	In	Out		In	Out	Fluid[b]	ΔT[c]	Avg[c]			
100-13:30	12.3	382	800	800	I	77	399	(180)	747	781	20,800	85	
								215	700	133	20,600	403	
								320	478	615	20,600	617	492
								480	135	528	20,100	149	
					II	399	648	512	126	575	20,100	180	
								586	112	642	20,100	180	381
								807	85	745	19,100	225	
					III	648	949	746	76	784	19,100	251	
								800	75	938	19,100	255	537
Burned coke from reactor. Measured 0.4 g carbon													
100-12:30	11.3	380	802	800	I	80	800	(285)	647	509	50,300	112	
								480	320	644	50,200	153	
								(663)	259	793	50,200	194	492
								853	58	884	21,100	264	
					II	800	897	895	56	923	21,100	327	
								951	61	982	21,100	344	702
								1015	33	1032	12,800	380	
					III	997	1067	1034	28	1048	12,800	450	
								1052	33	1069	12,600	380	828
100-13:30	11.3	380	781	750	I	80	810	(264)	450	511	50,300	112	
								484	334	651	50,300	150	
								(659)	270	794	50,300	186	492
								870	65	899	21,100	324	
					II	810	1001	913	62	944	21,100	340	
								968	61	997	21,100	346	706
								1020	37	1038	14,500	380	
					III	1001	1068	1038	30	1054	13,500	450	
								1054	33	1071	13,500	410	840
100-13:30	11.3	380	802	800	I	70	805	(285)	446	508	49,200	110	
								481	335	643	49,200	147	
								(650)	275	788	49,200	178	487
								868	89	903	21,100	306	
					II	805	1001	913	65	946	21,100	325	
								968	64	1000	21,100	330	697
								1020	37	1039	14,200	380	
					III	1001	1068	1037	32	1053	14,200	440	
								1053	37	1072	14,200	380	837
100-14:30 (Flow and pressure fluctuating badly)	11.3	380	(800)	(805)	I	71	815	(287)	450	512	49,200	109	
								485	335	653	49,200	147	
								(659)	273	796	49,200	180	487
								874	70	909	21,100	300	
					II	814	1004	919	54	951	21,100	328	
								977	53	1004	21,100	334	662
								1072	105	1125	42,900	808	
					III	1004	1215	1129	59	1174	43,800	491	
								1163	102	1214	42,900	420	1124
100-15:30	11.3	380	758	746	I	77	812	(281)	442	502	48,900	113	
								490	337	654	49,000	159	
								(665)	270	798	49,300	184	490
								873	65	908	21,200	328	
					II	812	1010	919	59	949	21,200	359	
								972	57	1001	21,200	372	701
								1075	97	1124	40,100	415	
					III	1010	1203	1130	82	1171	40,100	490	
								1162	83	1208	40,100	432	1104
100-16:30	11.3	380	484	466	I	73	802	(288)	442	510	50,100	113	
								484	322	645	50,100	158	
								(671)	251	797	50,100	200	480
								851	54	878	21,300	305	
					II	802	995	893	55	921	21,300	388	
								951	52	977	21,300	410	705
								1071	91	1117	38,300	428	
					III	999	1201	1134	74	1171	38,300	518	
								1165	86	1209	38,300	445	1083
Burned coke from reactor. Measured 0.5 g carbon													

a) LHSV based on single 10-in long reactor section.

b) Fluid temperatures in ( ) calculated from power input and fuel heat capacity. T.C. readings at these points were out of line. Heat-transfer coefficients for these locations were based on these calculated temperatures.

c) ΔT and Avg temperatures are calculated inside tube wall temperatures (T_{iw}).

$$\Delta T = T_{iw} - T_f \text{ and Avg Temp} = \frac{T_{iw} + T_f}{2}$$

(Continued)

TABLE 53 (CONTD)
FSSTR-THERMAL CRACKING OF FUEL F-71 - DATA SUMMARY

Run No. 8915-	F-71 Feed Rate		Press., psig		Reactor Section	Fluid Temp at Coupling, °F		Heat Transfer[b]					Total Heat to Fluid, Btu/lb
								Temperature, °F			Btu/(hr)(ft²)	Btu/(hr)(ft²)(°F)	
	GPH	LNSV[a]	In	Out		In	Out	Fluid[b]	ΔT[c]	Avg[c]			
191-13:40	4.08	130	894	892	II	70	993	(387)	243	508	24,600	102	
								659	167	743	24,900	149	
								862	157	941	24,900	158	691
					III	993	1085	1018	47	1042	8,700	185	
								1042	43	1064	8,700	202	
								1070	46	1093	8,700	189	928
191-15:00	4.08	130	490	489	II	70	987	(383)	242	505	25,300	104	
								652	153	729	25,300	165	
								858	139	928	25,300	182	691
					III	987	1090	1018	48	1042	8,500	177	
								1050	39	1070	8,500	218	
								1076	46	1099	8,500	185	9[illegible]
191-16:00	4.08	130	497	495	II	70	985	(380)	242	501	24,700	102	
								651	156	729	24,700	158	
								852	141	923	24,700	175	674
					III	985	1196	1058	93	1105	17,200	185	
								1121	78	1160	17,200	221	
								1156	88	1120	17,200	196	1150
191-16:40 (Flow and pressure fluctuating badly) (Port 4 sampler plugged)	4.08	130	(850)	(850)	II	70	984	(384)	245	507	24,700	101	
								655	169	740	24,700	146	
								859	156	938	24,700	158	674
					III	984	1214	1053	94	1100	17,200	183	
								1214	84	1151	17,200	205	
								1153	89	1198	17,200	193	1150
192-13:20	12.5	399	892	889	I	73	402	(150)	258	279	20,800	81	
								239	200	339	20,800	104	
								333	176	421	20,800	118	186
					II	402	653	467	131	532	20,300	155	
								519	125	591	20,300	162	
								591	114	648	20,300	178	369
					III	653	850	700	65	82	18,900	223	
								750	71	69	18,900	266	
								801	74	72	18,900	255	537

Burned coke from reactor. Measured 0.8 g carbon

TABLE 54
FSSTR-THERMAL CRACKING OF FUEL F-71: PRODUCT RECOVERY AND ANALYSES

Run Number 0815-	Feed[a]	189-12:30	188-13:10	188-13:50	188-14:30	188-15:50	188-16:50	191-15:00	185-[e] 14:40	191-13:40	191-16:00	185-[e] 16:00	191-16:30	General Electric Studies[d][e]
Operating Conditions														
LHSV[b]		360	360	360	360	360	360	130	129	130	130	129	130	900
Inlet Press., psig		502	761	902	494	750	900	490	762	894	497	765	(850)	300 (exit)
Max Fluid Temp, °F		1067	1068	1068	1201	1203	1215	1090	1099	1095	1196	1174	1214	1200
Heat to Fuel, Btu/lb		828	840	837	1083	1104	1124	928	981	929	1150	1131	1150	1100
Product Recovery, %		(101)[c]	(102)[c]	95	100	102	104	98	108	103	101	104	107	NR
Product Distribution, %														
Gas		(6)[c]	(9)[c]	10	29	33	37	17	20	21	43	42	51	NR
Liquid		94	91	90	71	67	63	83	80	79	57	58	49	NR
Product Gas Composition														
Mass Spec Analysis, %														
N_2				1.6	2.2	2.3	2.6	1.7	1.4	1.7	2.4	1.7	1.7	2.7
CH_4				21.2	22.1	23	24.8	19.3	20.4	19.6	22	21.8	24	15.1
C_2H_4				10.6	16.2	11	9.9	13.5	10.3	8.6	12	10	9	13.1
C_2H_6				17.1	14.4	15	15.4	15.7	16.2	15.9	15	16	15	13.8
C_3H_6				16.5	17.3	18.5	15.6	17.2	17.4	16.0	18	17	16	22.8
C_3H_8				13.9	9.1	10.6	11.4	11.9	13.0	13.8	9.4	12	11	17.3(+ C_2H_2)
C_4H_8				8.0	10.0	9.3	9.7	10.5	9.3	11.7	11	10	10	1.4
nC_4H_{10}				2.9	1.8	2.1	2.6	2.8	3.6	4.0	2	3.1	3	1.0
IC_4H_{10}				3.9	1.7	2.5	2.7	2.2	2.7	3.2	2.9	3	2	-
C_5				2.4	3.6	3.7	4.2	4.0	4.6	5.2	3.7	5.3	5.2	-
$>C_5$				.9	.8	.8	.8	.9	1.1	1.1	1.3	1.5	1.5	-
Product Liquid Composition														NR
GLC Analysis, %														
C_1														
C_2									Tr			0.1		
C_3		0.1	Tr	Tr			0.5	Tr	0.6	Tr	Tr	.4	0.1	
C_4		1.0	0.4	0.8	0.2	0.2	2.7	0.5	2.3	1.4	0.7	2.0	1.8	
C_5		1.4	1.4	1.8	1.2	1.4	5.4	2.6	4.2	4.2	4.4	4.0	2.1	
C_6	0	2.8	4.2	4.2	5.8	6.3	7.7	5.3	5.5	6.1	7.7	6.4	8.0	
C_7	Tr	2.3	2.9	3.4	5.6	7.3	7.8	3.1	7.1	5.5	8.1	10.6	11.4	
C_8	0	2.5	3.8	4.4	6.7	9.2	9.7	4.6	6.9	7.1	10.6	10.0	11.4	
C_9	0	2.4	3.2	4.0	5.9	8.0	7.9	4.3	5.4	6.1	7.6	8.1	12.2	
C_{10}	0.1	1.8	2.7	3.0	4.3	5.5	5.6	3.4	4.2	4.6	5.3	5.5	8.0	
C_{11}	16.5	15.4	14.7	14.7	13.3	12.7	10.1	22.3	15.1	16.2	16.0	12.5	9.9	
C_{12}	39.6	34.8	27.4	31.0	24.2	21.0	17.2	22.3	23.1	19.8	17.7	17.0	11.6	
C_{13}	22.8	19.4	14.3	16.8	16.5	12.9	7.9	16.4	13.1	12.0	10.8	9.1	7.9	
C_{14}	12.4	9.8	13.2	8.6	6.4	4.7	5.0	8.3	6.6	6.5	6.0	5.1	5.9	
C_{15}	4.8	3.6	6.3	2.9	4.5	4.0	2.8	3.2	3.2	3.2	2.1	2.5	3.4	
C_{16}	2.0	1.4	2.9	1.4	2.2	2.3	1.5	1.4	1.1	1.7	1.1	1.6	1.9	
C_{17}	.9	.7	1.0	1.0	1.1	.9	1.9	1.0	.6	1.4	.7	1.2	1.4	
C_{18}	.6	.4	.6	.5	.9	.7	1.5	.6	.3	.9	.6	1.1	1.0	
C_{19}	.2	.2	.4	.4	.6	.4	1.3	.5	.2	.9	.3	.9	.8	
$>C_{19}$	.1	.1	.6	.6	.7	.6	3.1	.7	.7	2.6	.4	1.9	1.1	
Mass Spec Analysis, %														NR
C_nH_{2n-2}	81.7	81.0	75.9	73.2	61.5	50.1	43.8	74.5	64.0	63.7	54.1	45.7	33.3	
C_nH_{2n}	3.4	13.2	17.7	19.8	25.7	28.5	26.9	16.7	22.3	21.8	21.4	25.3	22.0	
C_nH_{2n-6}	3.1	3.8	4.3	4.7	6.9	9.3	10.5	5.2	7.2	7.3	9.0	10.6	12.3	
C_nH_{2n-8}					1.2	3.3	4.5	.4	1.5	2.1	3.9	4.7	7.0	
C_nH_{2n-8}	1.3	1.5	1.7	1.9	3.5	6.2	8.2	2.3	3.6	3.6	7.2	8.9	5.5	
C_nH_{2n-8}				.2	.6	1.4	2.1	.4	.8	.8	2.4	2.5	4.7	
C_nH_{2n-10}					.1	.6	1.0		.2	.2	1.2	1.4	3.2	
C_nH_{2n-12}	.5	.4	.4	.4	.4	.6	.9	.1	.4	.4	.9	.9	2.0	

a) Data repeated from previous work.
b) LHSV based on single 10-ft reactor section.
c) Calculated assuming NR of product gas similar to other runs.
d) NR = not reported.
e) cf Reference ASD-TDR-62-920 Part II, January 1964, Ashland Special JP-6.

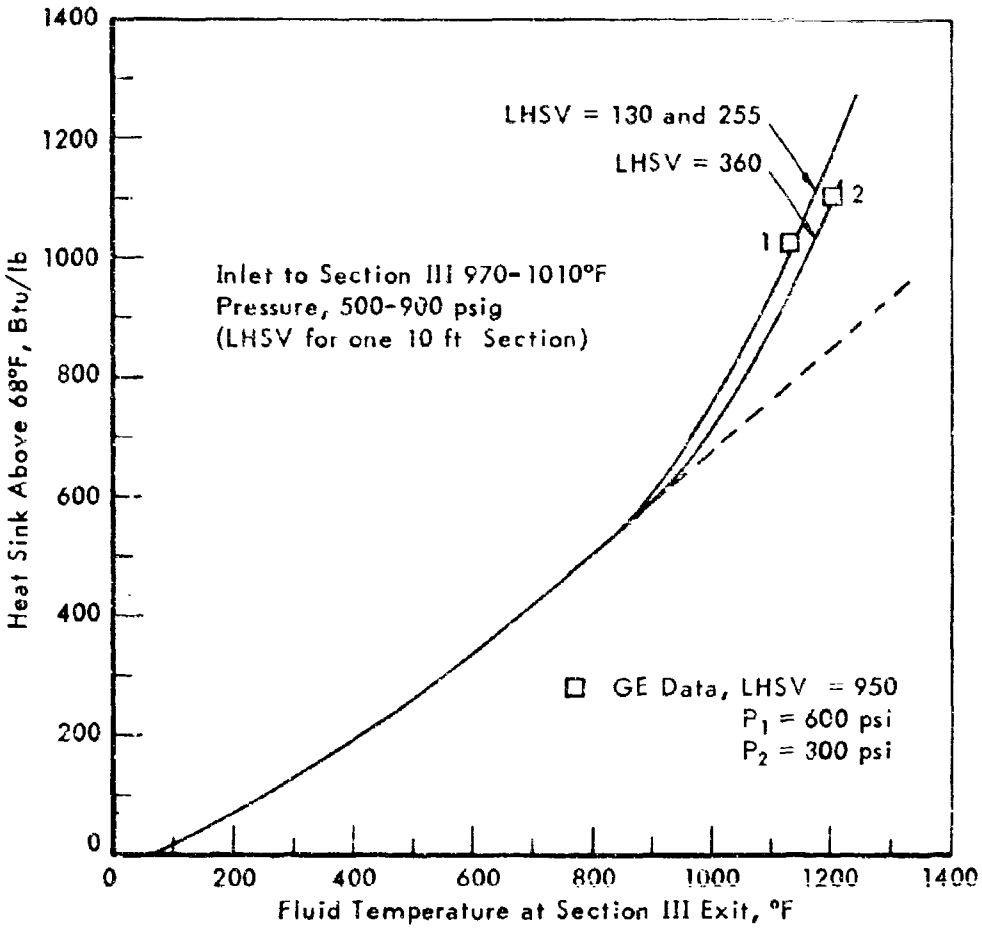


Figure 48. FSSTR - THERMAL CRACKING OF FUEL F-71: TOTAL HEAT SINK

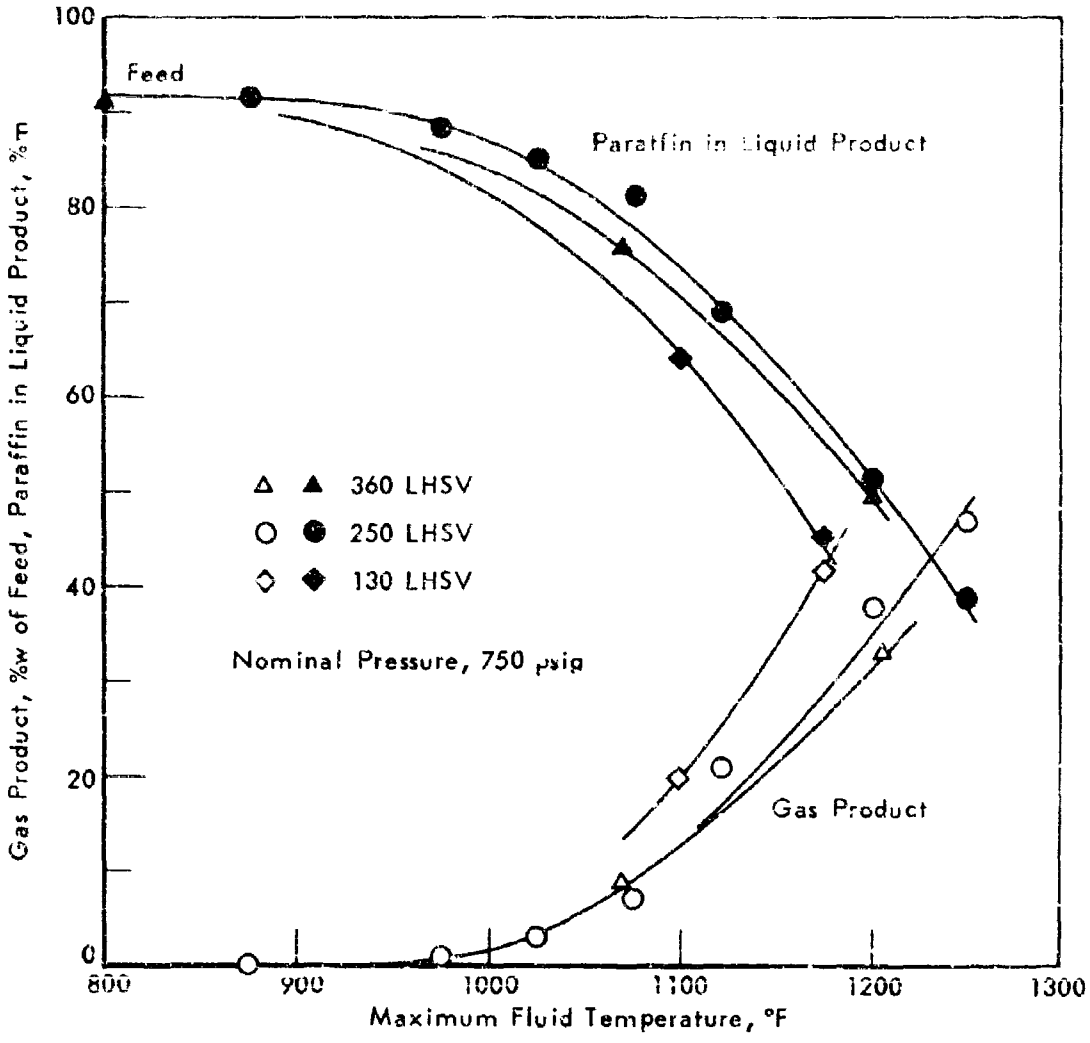


Figure 49. FSSTR - THERMAL CRACKING OF FUEL F-71: EFFECT OF TEMPERATURE ON REACTION PRODUCTS

62392

TABLE 55
DESCRIPTION OF JET FUELS

Properties	F-71	Ashland Special JP-6
Gravity, °API at 60°F	50.7	46.4
Specific Gravity, 60/60	0.777	0.796
ASTM Distillation, °F		
IBP	402	335
10%	409	342
20%	410	-
50%	420	352
90%	467	370
E.P.	543	400
Recovery, %v	98.5	99.0
Residue, %v	1.5	1.0
Vapor Pressure, psia		
300°F	2.6	
500°F	44.0	
Flash Point, °F, P.M.C.C.	180	122
Freezing Point, °F	-51	-80
Color, Saybolt	30+	-
Kinematic Viscosity at -30°F, cs	13.6	6.24 (-40)
Aniline Cloud Point, °F	185	135.5
Aniline Gravity Constant	9805	6287
Sulfur, %w	0.003	0.03
Mercaptan Sulfur, %w	0.0001	<0.001
Cu Strip Corrosion at 212°F	1B	1A
Luminometer	104	-
Gum, Existent (Steam Jet), mg/100 ml	1	0.6
Heat of Combustion, BM/16 (Net)	18,929	18,600
Water Separometer Index (Modified)	100	-
Thermal Stability, CFR Research Coker[b]		
Pressure Drop, in. Hg	0.2	
Preheater Deposit Rating (as is/wiped)	2/1	
Hydrocarbon Analysis, %v		
Paraffins	82.9	-
Naphthenes	10.6	-
Olefins	5.1	2.3
Aromatics	1.4	10.8
Thermal Stability, SD Coker, 450/500°F, 5 hr,		
Preheater Deposit	1.5/16	0[a]
ΔP	0	0

a) Erdco Coker, 450/550.
b) cf Table 50.

Catalytic Dehydrogenation of MCH in 3/4" Reactor

Prior to beginning this study the following changes were made in the Fuel System Simulation Test Rig (FSSTR):

1. A 24-point temperature recorder was substituted for the 16- and 6-point instruments which had been used previously. This allows all reactor temperature profile points to be printed out on a single chart.

2. A 3/4"-OD reactor tube was installed in reactor section III.

3. Power cables to Section III were doubled and heavier bus bars were welded to the reactor couplings to handle the anticipated heavier electrical load.

4. Thermocouples were attached to the four bus bars to monitor those temperatures.

5. Thermocouples were also wired on the necked-down adapter ends of the 3/4"-reactor section where tube wall temperatures would be expected to be the highest.

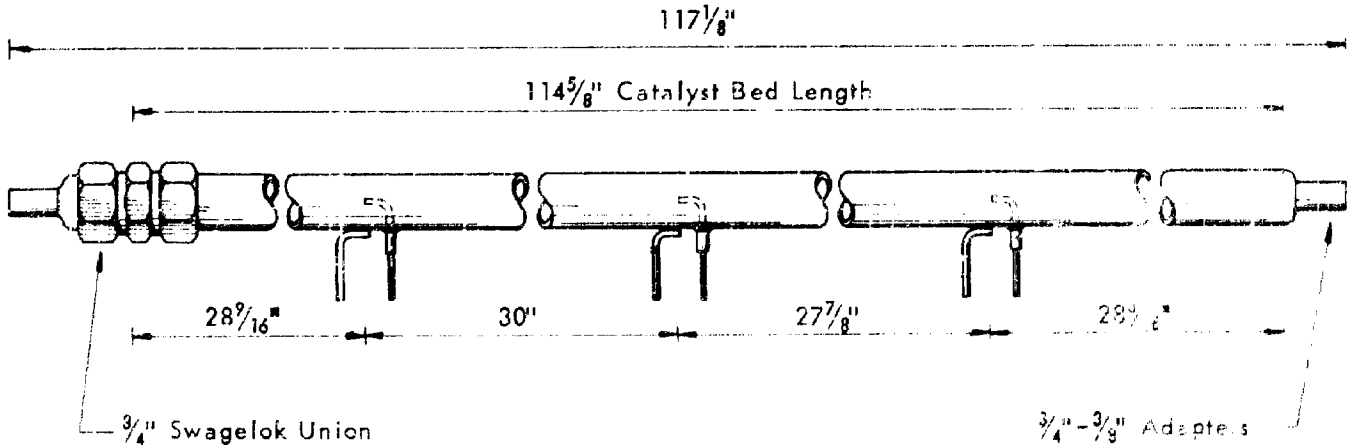
In order to provide an extension of the experimental data used to develop the computer program for predictions of reactor performance a program of test runs has been carried out using the MCH/UOP-R8 system in a 3/4"-OD x ca 10-foot long reactor tube. A sketch of the reactor section is given in Figure 50.

A total of seven runs were performed covering the range of operating conditions outlined in Table 56. The target for these tests was set at attaining a conversion of 95% at about 75 LHSV. Nominal bed inlet conditions were set at 900 psig and 900°F. For the bed volume used (627 cm^3 or 0.1657 gal) this required a feed rate of ca 12.5 gph and on the basis of 1000 Btu/lb heat sink in the catalyst section a power input of 80,300 Btu/hr or 23.5 KW was required. For the 0.60 ohm reactor resistance this corresponds to a current of 627 amps. While the rated output of the welding machine used as a power supply was 650 amps, the first series of runs showed the low efficiency of the transformer (ca 45% at maximum rated load) would prevent reaching this goal without first providing an increased primary current supply.

Series 8915-198 was, therefore, limited to a power input of ca 8 kw or 27,000 Btu/hr to the catalyst section. For the second series (10018 5) a Hunterdon Variable Reactance Transformer was used as the power supply. The superior efficiency of this transformer permitted operation at a maximum of ca 40,000 Btu/hr which gave 98% conversion at 37 LHSV and 62% at 72 LHSV. Installation of a larger circuit breaker (125 amp at 480 v) and heavier primary wire to the welding machine was then completed and the final series of runs was made reaching the desired conditions (97% conversion at 80 LHSV).

A complete data summary for all runs is presented in Table 57.

To minimize the current through the bus bar leading to the coupling between Sections II and III no power was supplied to Section II. Typical



Tube: 3/4" OD x 0.049" Wall Hastelloy "C"
Thermocouples: 1/16" OD Inconel Sheathed
Scale: None

Figure 50. FSSTR - 3/4" OD REACTOR TUBE

operations then had the preheaters raising the feed temperature to ca 600°F and Section I further heating to about 900°F. Figure 51 shows the temperature profile for the final run of the program (highest power input).

Experimental results were much as predicted by the computer program. A full analysis of the comparison of predicted and experimental data is presented in a later section of this report.

Dehydrogenation of MCH to toluene was quite clean, selectivity ranging from 92 to 98.5% and, as pointed out in the following tabulation, selectivity increased with extent of reaction.

LHSV	MCH Conversion, %	Selectivity for Toluene, %
37	64	92
37	98	96
77	43	95
72	62	96
80	77	98
80	97	99

(Bed inlet conditions ca 900 psig and 900°F for all above tests)

Liquid products formed other than toluene were predominantly C_7H_{14} isomers of MCH. Gas product samples from each run were analyzed by mass spectrometer and, except for Run 10018-5-13:20, were all pure H_2 (plus noncondensed MCH and toluene). In that run, the low feed rate-high conversion case, ca 0.2% CH_4 and 0.1% C_2H_6 were found in the samples.

A single catalyst charge which had been initially activated by heating in a N_2 stream at 1100°F for two hours was used for these tests during which a total of 1028 vol of feed/vol of catalyst was processed. No evidence of catalyst deactivation was noted. A summary of the catalyst charge operating history is given in Table 58.

In the course of these tests some additional data points were obtained from Section I on heat transfer to MCH in an empty 3/8"-OD x 0.049"-wall tube. A comparison of these points with the Dittus-Boelter correlation

$$N_{Nu}/N_{Pr}^{0.4} = 0.023\ N_{Re}^{0.8}$$

is shown in Figure 52. A tabulation of the dimensionless numbers calculated for the various data points is included in Table 59. (Previous data on this correlation was reported in reference 3, Figure 66 for fuel F-71 and Figure 70 for MCH.)

Other than the power supply problem described above, the unit operated satisfactorily during these tests. However, we have about reached a limit on power which can be supplied to the 3/4" reactor section as it is presently constructed. At the maximum power used (Run 10018-9-14:00) the tube wall temperature at the necked-down tube entrance reached 1235°F as measured

by a wired-on thermocouple. While this is not an unsafe condition, the temperature level at this location was increasing rapidly with power input and further power increase seems unwarranted.

Table 56. FSSTR- DEHYDROGENATION OF MCH OVER UOP-R8 IN A 3/4-INCH REACTOR: SUMMARY OF OPERATING CONDITIONS

LHSV	Nominal Inlet Press., psig	Catalyst Bed Exit Temp., °F	Total Power Input, Btu/lb
37	900	825	1110
37	900	1013	1600
80	500	682	840
77	900	782	930
72	900	838	1150
80	900	872	1300
80	900	1034	1640

a) Catalyst bed inlet temp 894-905°F. LHSV based on catalyst bed volume only. ID = 0.652 .

Table 57. FSSTR - DEHYDROGENATION OF MCH OVER UOP-R8 IN 3/4-INCH REACTOR: DATA SUMMARY

Run No.	Catalyst Charge	MCH Feed Rate[a]		Press., psig		Reactor Section[c]	Fluid Temp at Coolings, °F		Heat Transfer					Total Heat to Fluid, Btu/lb	MCH Converted, %	Selectivity for Toluene, %
									Temperature, °F			Btu/(hr)(ft²)	Btu/(hr)(ft²)(°F)			
		gph	LHSV[b]	In	Out		In	Out	Fluid	ΔT[d]	Avg[d]					
8915-198-15:00	I	12.8	77	913	809	PH			698	64	730		450	370		
						I	654	895	750	71	796	27,600	590			
									835	67	867		410	610		
						II	895	895				0				
						III	895	782	732	24	744		670			
									750	22	761	16,000	730			
									764	24	776		670	930	[illegible]	[illegible]
8915-198-14:20	I	13.2	80	488	419	PH								510		
						I	573	893	640	92	686		490			
									764	93	771	30,100	345			
									811	85	853		385	580		
						II	893	894				0				
						III	394	682	687	22	698		650			
									687	21	698	14,200	680			
									684	24	696		590	840	44	99
10018-5-12:00	I	6.2	37	902	871	PH								180		
						I	410	900	558	136	626		174			
									678	117	737	23,600	202			
									807	83	849		284	610		
						II	900	898				0				
						III	898	825	746	26	759		480			
									777	24	789	12,500	520			
									800	27	814		490	1110	64	92
10018-5-15:20	I	6.2	37	904	860	PH								180		
						I	411	902	555	142	626		168			
									679	123	741	23,800	193			
									811	84	853		283	610		
						II	902	900				0				
						III	900	1013	773	51	799		470			
									824	47	848	24,000	510			
									872	52	898		410	1000	98	96
10018-5-16:20	I	11.9	72	907	790	PH								340		
						I	601	902	674	88	718		347			
									748	88	792	30,600	347			
									835	70	870		437	620		
						II	902	900				0				
						III	900	858	749	56	767		690			
									777	33	794	25,000	760			
									798	35	816		710	1150	[illegible]	96
10018-9-15:00	I	13.2	80	886	720	PH								350		
						I	610	904	679	86	722		365			
									752	81	793	31,400	388			
									838	74	875		424	610		
						II	904	904				0				
						III	904	839	758	47	782		760			
									797	43	814	35,600	830			
									817	47	841		760	1500	77	98
10018-9-14:00	I	13.2	80	854	690	PH								350		
						I	615	907	713	84	755		365			
									795	82	796	30,700	374			
									841	70	876		439	610		
						II	907	905				0				
						III	905	1014	777	39	812		750			
									824	62	855	39,000	840			
									866	72	902		720	1540	97	99

a) Feed 99.4% MCH, 0.1% Toluene, 0.1% Cyclohexane.
b) LHSV based on volume of catalyst section in 3/4" OD reactor.
c) PH = preheater; heat input from PH based on heat content of MCH at Section I inlet temperature.
d) ΔT and Avg temperatures are calculated inside the wall temperature, T_{in}: $\Delta T = T_{out} - T_{in}$ and avg temp. $= T_{in} + T_{\Delta T}/2$.

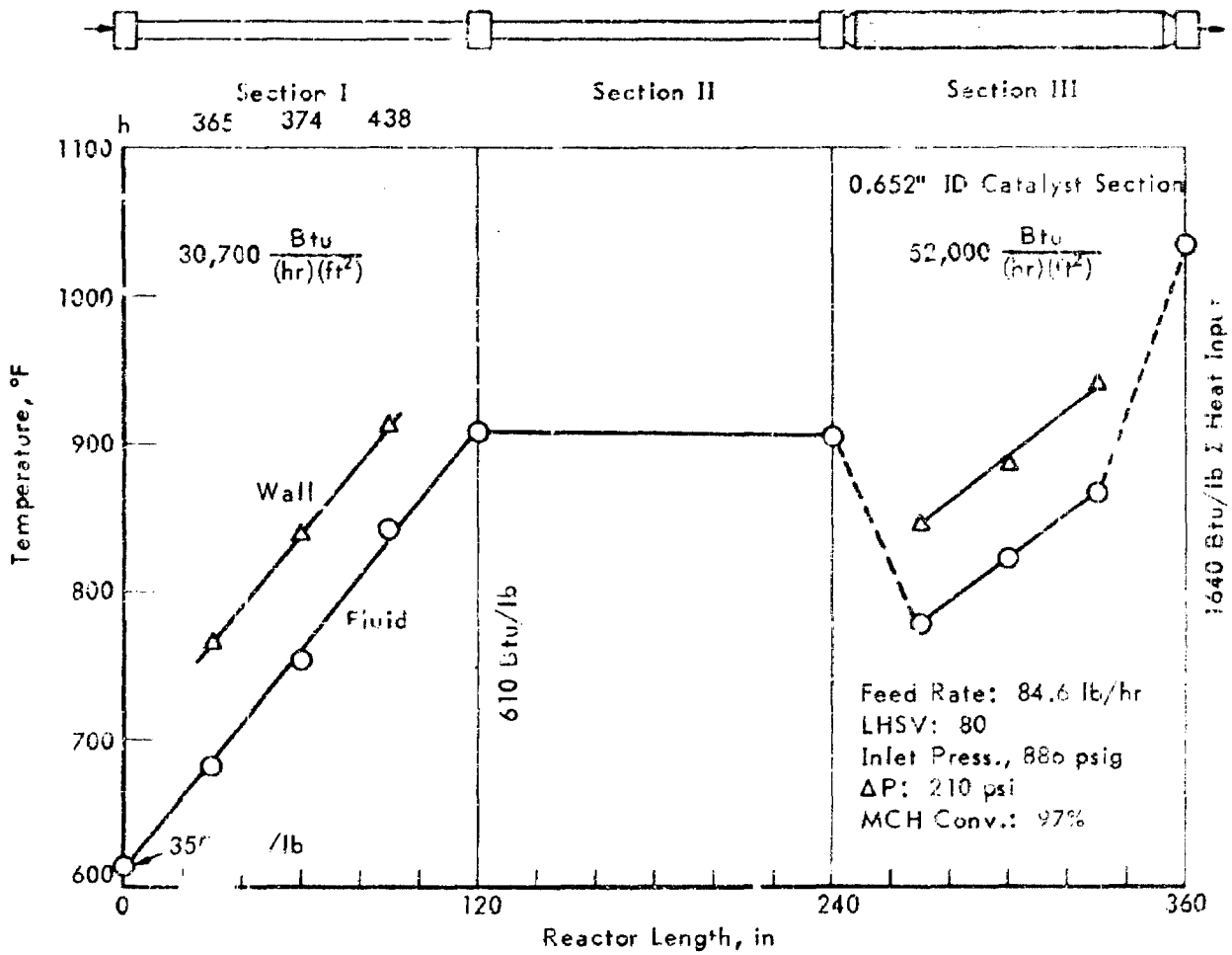


Figure 51. FSSTR - DEHYDROGENATION OF MCH OVER UOP-R8 IN A ¾-INCH REACTOR:
Temperature Profile for Run 10018-9-14:00

Table 58. FS-STR - DEHYDROGENATION OF MCH OVER UOP-R8 IN A 3/4-INCH REACTOR: HISTORY OF CATALYST CHARGE

Catalyst Charge 8915-195 (Charge I in 3/4-Inch Tube)

UOP-R8 (Pt/Al_2O_3) Platforming catalyst
Bed vol: 627 cc
Catalyst activated in place by heating at 1100°F in N_2 for 2 hours
Feed: 99.8% MCH, 0.1% toluene, 0.1% cyclohexane

Series	Run Time, hr	MCH Conversion, %	$\frac{\text{Vol Feed}}{\text{Vol Catalyst}}$	$\Sigma \frac{\text{Vol Feed}}{\text{Vol Catalyst}}$ (During Conv Runs Only)
	0.3	0	19	
8915-198	3.8	43-44	293	293
	0.8	0	28	
10018-5	7.3	62-98	366	659
	0.6	0	46	
10018-9	4.6	77-97	369	1028

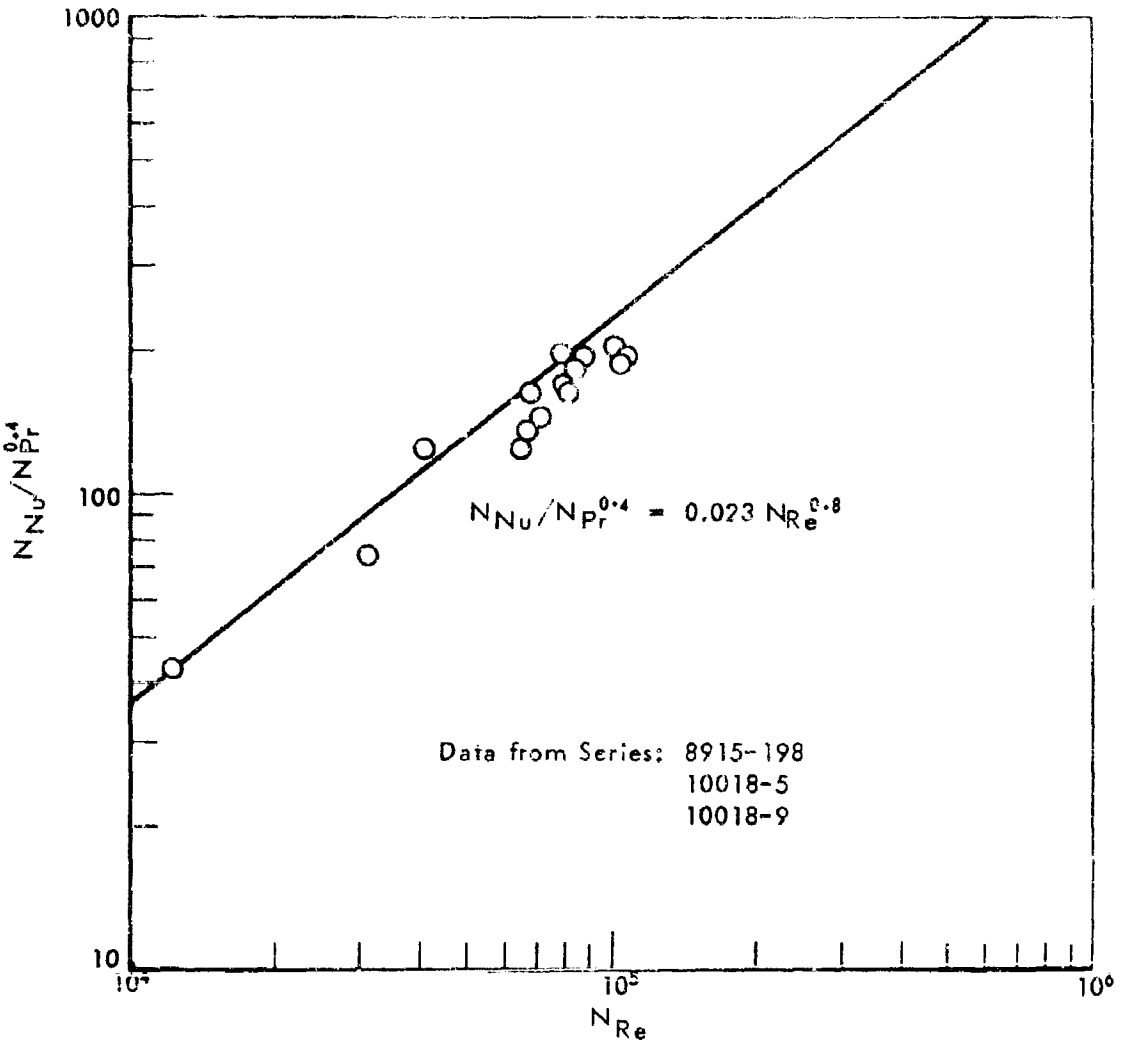


Figure 52. FSSTR - HEAT TRANSFER TO MCH IN EMPTY ⅜-INCH TUBE: Dittus-Boelter Correlation

Table . . FSSTR - HEAT TRANSFER CORRELATION: MCH IN EMPTY 3/8-INCH TUBE

Dimensionless numbers calculated for Dittus-Boelter correlation

Run	Temp, °F	Press., psig	N_{Re}	N_{Nu}	$N_{Pr}^{0.4}$	$N_{Nu}/N_{Pr}^{0.4}$
9815-198-13:00	698	900	68,500	172	1.03	163
	760	900	79,400	164	.98	168
	833	900	85,300	174	.95	184
8915-198-14:20	640	500	109,000	191	.98	195
	724	500	107,000	185	.98	189
	811	500	102,000	200	.98	204
10018-5-12:00 and 13:20	557	900	12,200	63	1.47	43
	679	900	31,300	78	1.05	74
	809	900	40,600	121	.96	126
10018-5-16:20	674	900	60,500	131	1.06	124
	748	900	71,800	145	.99	146
	835	900	79,900	185	.95	195
10018-9-13:00 and 14:00	681	900	66,800	143	1.05	136
	754	900	82,000	160	.99	162
	840	900	88,100	182	.95	192

Thermal Cracking of Propane

The Fuel System Simulation Test Rig (FSSTR) using the usual 3/8-in. (D x 0.049-in. wall x 10-ft long reactor tubes has been used to determine the heat sink capability of propane when subjected to temperatures which result in thermal cracking of the fuel. Two thirty-kva variable reactance continuously variable transformers have been installed giving much better control over the energy input to the FSSTR than was previously possible.

Feed rates corresponding to 100 and 400 LHSV (per 10-ft section) and pressures of 200 and 900 psig were selected as covering a range of conditions broad enough to demonstrate the characteristics of this fuel. The range of temperatures covered at each LHSV and pressure combination are outlined in Table 60. The procedure followed in these tests was to set the fuel flow rate and operating pressure and use Reactor Sections I and II to preheat the fuel to ca 1000°F at the entrance to Section III. Power was then supplied to Section III as necessary to raise the outlet temperature in about 50°F increments.

A summary of the operating data is presented in Table 61. Table 62 contains the product analyses for all runs. Depth of cracking is illustrated in Figure 53 as a function of temperature for the four pressure and feed rate combinations tested.

The heat sink capacity of propane at the various conditions tested is shown in Figure 54. Up to ca 1100°F the heat sink is provided only by latent and sensible heats. Above 1100°F the difference between the measured heat sink and the extrapolated heat content curve illustrates the contribution of the endothermic heat of reaction. Even under the most severe cracking conditions encountered (ca 65% of the propane reacting) the heat of reaction was only about 300 Btu/lb out of a total of 1400 Btu/lb. Also at this condition the endothermic reaction appears to be slowing and the heat sink capacity per degree is becoming smaller.

An example illustrating the temperature profile over the entire reactor is shown in Figure 55. Section III fluid temperatures for the five runs of Series 10018-27 are given in Figure 56. The effect of the reaction in flattening the temperature gradient is apparent.

As the temperature level was increased an upper limit was reached, for all except the shortest residence time condition, when pressure and flow fluctuations, probably caused by coke particles lodging against the pressure control valve, forced shutdown of the unit. The maximum heat sink attained without sign of operating difficulty was 1[illegible] Btu/lb (above liquid at 68°F) at 400 LHSV, 200 psig and 1392°F outlet temperature. No attempt was made to determine how long operation at these conditions could have been continued.

A few data points were obtained in Sections I and II for comparison with the Dittus-Boelter heat-transfer correlation:

$$N_{Nu} = 0.023\ N_{Re}^{0.8}\ N_{Pr}^{0.4}$$

This comparison is shown in Figure 57. Physical property data for propane used in calculating the Reynolds, Nusselt, and Prandtl numbers are given in Figure 58.

Table 60. FSSTR-THERMAL CRACKING OF PROPANE: RANGE OF OPERATING CONDITIONS

Section III inlet temperature 974-1014°F
LHSV based on Section III volume only

Nominal LHSV	Nominal Pressure, psig	Section III Exit Fluid Temp, °F
100	200	1143-1342[a]
100	900	1097-1373[a]
400	200	1093-1392
400	900	1104-1326[a]

a) Coke formation halted test at maximum listed temperatures for these series.

Table 61. FSSTR - THERMAL CRACKING OF PROPANE: DATA SUMMARY

Run No. 10018-	Propane Feed Rate		Pressure, psig		Reactor Section	Fluid Temp at Couplings, °F		Heat Transfer					Total Heat to Fluid, Btu/lb
								Temperature, °F					
	lb/hr	LHSV[a]	In	Out		In	Out	Fluid	Δt^{b}	Avg[b]			
21 - 13:40	14.7	111	800	800	I	60	512	110	19	120	8,000	440	
								167	154	264	8,000	52	
								360	113	417	8,000	71	592
					II	512	1011	641	91	687	8,200	90	
								907	71	943	8,200	115	788
					III	1011	1143	1036	15	1044	2,710	180	
								1075	15	1083	2,710	180	
								1111	15	1119	2,710	180	921
21 - 13:40	14.7	111	800	800	I	60	511	110	18	119	8,000	440	
								167	154	264	8,000	52	
								360	112	416	8,000	71	592
					II	511	987	633	86	676	7,630	89	
								887	68	921	7,630	112	767
					III	987	1186	1028	28	1042	5,580	146	
								1087	27	1101	5,920	145	
								1141	25	1154	5,920	157	958
21 - 14:20	14.7	111	800	800	I	60	515	110	19	120	8,000	420	
								169	156	247	8,000	52	
								365	114	421	8,000	71	592
					II	515	993	637	87	681	7,630	88	
								893	69	928	7,630	111	767
					III	993	1240	1050	40	1070	5,290	132	
								1127	36	1145	5,290	147	
								1194	34	1211	5,290	155	1024
21 - 15:10	14.7	111	201	201	I	60	521	110	18	119	8,000	440	
								174	155	252	8,000	52	
								369	114	426	8,000	71	592
					II	521	1002	645	86	688	7,630	89	
								901	71	937	7,630	108	767
					III	1002	1283	1079	50	1104	6,620	152	
								1171	47	1195	6,620	151	
								1246	42	1267	6,620	161	1091
21 - 16:00	14.7	111	800	800	I	60	518	111	18	120	8,000	440	
								170	157	249	8,000	51	
								362	115	421	8,000	71	592
					II	518	996	640	87	684	7,630	88	
								895	70	930	7,630	109	767
					III	996	1305	1108	68	1136	8,940	132	
								1222	59	1252	8,940	152	
								1297	52	1323	8,940	172	1177
21 - 16:40	14.7	111	200	800	I	60	508	110	18	119	8,000	440	
								163	155	241	8,000	52	
								357	214	414	8,000	71	592
					II	508	982	629	86	673	7,630	89	
								882	69	917	7,630	111	767
					III	982	1342	1108	79	1148	10,040	127	
								1241	67	1275	10,040	150	
								1516	62	1547	10,040	162	1268
Burned coke from reactor. Measured 0.3 g of carbon.													
24 - 12:50	13.8	104	902	902	I	68	547	213	54	240	7,570	131	
								292	82	333	7,570	90	
								443	65	476	7,570	113	304
					II	547	978	658	69	693	6,620	96	
								885	62	916	6,620	107	741
					III	978	1097	998	15	1008	2,300	150	
								1037	14	1044	2,300	160	
								1072	15	1079	2,300	180	660
24 - 13:30	13.8	104	901	901	I	68	554	215	53	242	7,390	139	
								297	81	338	7,390	91	
								450	66	483	7,390	112	384
					II	554	1012	674	75	712	6,970	93	
								914	64	946	6,970	109	750
					III	1012	1158	1041	22	1052	3,040	138	
								1089	21	1100	3,040	145	
								1130	19	1140	3,040	152	908
24 - 14:20	13.8	104	898	898	I	66	550	213	54	240	7,390	137	
								293	83	335	7,390	89	
								447	65	480	7,390	114	384
					II	550	1005	669	72	705	6,970	97	
								910	62	941	6,970	112	750
					III	1005	1198	1052	29	1067	4,320	149	
								1117	26	1130	4,320	166	
								1169	24	1181	4,320	180	968
24 - 15:10	13.8	104	900	900	I	67	558	215	53	242	7,390	139	
								294	83	336	7,390	89	
								450	66	484	7,390	109	384
					II	558	1012	674	71	610	6,970	98	
								914	63	946	6,970	111	750
					III	1012	1248	1067	46	1110	6,550	142	
								1173	41	1194	6,550	159	
								1226	37	1245	6,550	177	1079
24 - 16:00	13.8	104	906	906	I	67	550	216	53	241	7,390	139	
								291	80	331	7,390	92	
								443	69	480	7,390	107	384
					II	550	1000	668	71	705	6,970	98	
								911	64	943	6,970	104	750
					III	1000	1300	1120	64	1152	3,660	136	
								1220	57	1249	3,660	152	
								1273	54	1300	3,660	177	1240
24 - 16:40	13.8	104	904	908	I	67	560	216	53	243	7,390	139	
								297	81	338	7,390	91	
								452	70	487	7,390	105	384
					II	560	1014	678	74	714	6,970	97	
								915	65	947	6,970	111	750
					III	1014	1373	1170	05	1215	12,680	183	
								1268	78	1305	12,680	164	
								1338	69	1365	12,680	151	1392
Burned coke from reactor. Measured 0.0 g of carbon.													

a) LHSV based on single 15 ft long reactor section.
b) Δt and Avg temperatures use calculated inside tube wall temperatures (Tiw).

Table 61 (Contd). FSSTR - THERMAL CRACKING OF PROPANE: DATA SUMMARY

Run No. 10018-	Propane Feed Rate		Pressure, psig		Reactor Section	Fluid Temp at Couplings, °F		Heat Transfer					Total Heat to Fluid, Btu/lb
								Temperature, °F			Btu/(hr)(ft²)	Btu/(hr)(ft²)(°F)	
	lb/hr	LSHV[a]	In	Out		In	Out	Fluid	ΔT[b]	Avg[b]			
27 - 12:10	54.0	406	903	903	I	63	677	231	205	334	37,400	183	
								506	191	422	37,400	126	
								514	146	587	37,400	256	486
					II	677	1002	744	79	784	21,400	271	
								918	70	953	21,400	306	768
					III	1002	1104	1025	20	1033	7,350	370	
								1052	19	1062	7,350	390	
								1070	18	1088	7,350	410	866
27 - 13:00	54.0	406	905	905	I	64	675	231	199	331	37,400	188	
								346	188	420	37,400	199	
								513	146	596	37,400	256	486
					II	675	998	742	80	782	21,400	268	
								914	69	949	21,400	310	758
					III	998	1167	1035	36	1053	12,700	350	
								1082	33	1099	12,700	380	
								1127	51	1143	12,700	410	935
27 - 14:00	54.0	406	898	898	I	66	678	232	197	331	37,400	190	
								508	189	423	37,400	198	
								516	146	589	37,400	256	486
					II	678	999	745	78	784	21,400	274	
								914	68	948	21,400	315	768
					III	999	1229	1055	54	1080	18,350	340	
								1119	50	1144	18,350	370	
								1181	46	1204	18,350	400	1006
27 - 15:00	54.0	406	896	896	I	67	673	234	199	334	37,400	188	
								326	165	420	37,400	199	
								513	144	585	37,400	260	486
					II	673	996	741	78	780	21,400	274	
								910	68	944	21,400	315	768
					III	996	1292	1078	79	1118	26,800	340	
								1174	73	1211	26,800	368	
								1250	46	1293	26,800	406	1117
27 - 15:50	54.0	406	895	895	I	67	675	233	211	339	37,400	177	
(ΔP increasing: 18 psi at 16:16; 18 psi at 16:22)								446	187	420	37,400	200	
								513	145	595	37,400	258	486
					II	675	999	744	72	784	21,400	271	
								912	68	946	21,400	315	768
					III	999	1353	1116	112	1172	58,500	344	
								1259	101	1290	58,500	402	
								1310	41	1356	58,500	423	1871
Burned coke from reactor. Measured 0.6 g of carbon.													
30 - 12:30	53.0	399	197	194	I	62	672	174	39	119	36,900	1270	
								238	26	371	36,900	139	
								469	181	561	36,900	202	490
					II	672	995	743	76	781	20,100	265	
								914	67	943	20,100	300	759
					III	995	1095	1015	18	1024	6,780	380	
								1044	16	1052	6,780	420	
								1069	15	1077	6,780	450	851
30 - 13:40	53.0	399	197	194	I	65	677	106	51	120	36,900	1130	
								249	26	376	36,900	141	
								474	181	566	36,900	200	490
					II	677	1005	750	77	789	20,100	261	
								921	67	955	20,100	300	759
					III	1005	1149	1048	40	1068	13,700	380	
								1101	37	1120	13,700	420	
								1155	34	1172	13,700	400	941
30 - 14:20	53.0	399	197	192	I	65	659	103	27	117	36,900	1370	
								232	261	365	36,900	141	
								459	181	550	36,900	204	490
					II	659	981	730	76	768	20,100	265	
								901	67	935	20,100	300	759
					III	981	1250	1043	60	1073	19,500	325	
								1117	55	1145	19,500	355	
								1191	51	1217	19,500	383	1021
30 - 15:15	53.0	399	197	192	I	63	651	103	-5	116	36,900	1470	
								228	260	358	36,900	142	
								452	183	544	36,900	202	490
					II	651	974	724	76	762	20,100	265	
								893	67	927	20,100	300	759
					III	974	1314	1059	83	1101	26,900	317	
								1158	75	1196	26,900	351	
								1251	67	1289	26,900	392	1117
30 - 16:30	53.0	399	197	192	I	63	660	103	27	117	36,900	1370	
								232	261	365	36,900	141	
								459	181	550	36,900	204	490
					II	660	981	733	77	771	20,100	261	
								901	67	935	20,100	300	759
					III	981	1318	1045	64	1077	25,300	328	
								1123	58	1152	25,300	364	
								1199	52	1225	25,300	407	1209
30 - 17:45	53.0	399	197	192	I	63	659	103	27	117	36,900	1370	
								232	261	365	36,900	141	
								459	181	550	36,900	204	490
					II	659	981	730	76	768	20,100	265	
								901	67	935	20,100	300	759
					III	981	1250	1043	60	1073	19,500	325	
								1117	55	1145	19,500	355	
								1191	51	1217	19,500	383	1021
Burned coke from reactor. Measured [illegible] g of carbon.													

Table 62. FSSTR - THERMAL CRACKING OF PROPANE: PRODUCT ANALYSES

Run No. 10018-	Run Conditions				Product Gas Analyses, %m											Propane Conv., %
	LHSV[a]	Inlet Press., psig	Max. Fluid Temp, °F	Heat to Fuel, Btu/lb	H_2	CH_4	C_2H_4	C_2H_6	C_3H_6	C_3H_8	C_4	C_5	C_6	C_7	Average Mol wt	
21-12:40	111	200	1143	921	0.2	0.3		0.4	0.2	98.9					43.8	<1
13:40	"	"	1186	958	.3	.6	0.5	.4	.4	97.9					43.6	1
14:20	"	"	1240	1024	1.0	1.6	1.6	.5	1.1	94.2					42.8	3
15:10	"	201	1283	1091	2.4	3.9	3.6	.7	2.7	86.7					41.2	7
16:00	"	200	1326	1197	4.7	8.0	6.8	1.4	5.5	73.4			0.1		38.4	16
16:40	"	"	1342	1268	5.4	9.4	8.1	1.7	6.4	68.8			.1		37.4	19
24-12:30	104	902	1097	860	0.1	0.4	0.4	0.4		98.8					43.8	<1
13:30	"	901	1156	908	.4	1.5	1.4	.5	0.6	95.6					43.1	2
14:20	"	898	1198	988	.9	3.3	3.0	.7	1.3	90.8					42.1	5
15:10	"	900	1248	1079	2.4	9.4	7.0	2.0	3.8	74.7	0.5	0.3			37.7	16
16:00	"	906	1300	1230	3.8	19.3	10.6	5.4	7.3	51.1	1.3	.9	0.3		34.9	36
16:40[b]	"	904	1373	1392	5.	33.	12.	11.	9.	24.	2.	.5	1.2	0.2	29.0	64
27-12:10	406	903	1104	866		0.1		0.3		99.5					43.9	<1
13:00	"	905	1167	935	0.1	.5	0.4	.3		98.7					43.7	<1
14:00	"	898	1229	1006	.5	1.7	1.6	.4	0.6	95.2					43.0	2
15:00	"	896	1292	1117	2.0	6.4	5.3	1.2	2.8	82.1		0.1	0.1		40.4	10
15:50	"	895	1326	1271	3.9	13.8	9.8	3.2	5.9	62.3	0.7	0.2	.1		36.5	25
30-12:20	399	197	1093	851				0.3		99.7					44.0	<1
13:20	"	"	1199	941	0.2	0.3	0.3	.3	0.2	98.8					43.8	<1
14:20	"	"	1256	1021	.5	.7	.8	.3	.6	97.1					43.4	7
15:15	"	"	1314	1117	1.5	2.2	2.0	.4	1.6	92.2					42.3	4
16:30	"	"	1370	1209	3.7	5.5	4.9	.8	4.1	80.9	0.1				39.9	11
16:45	"	"	1392	1279	4.5	6.7	6.0	1.0	5.0	76.6	.1				39.0	13

a) LHSV based on single 10-ft reactor section.
b) Some liquid polymerization product during this run.

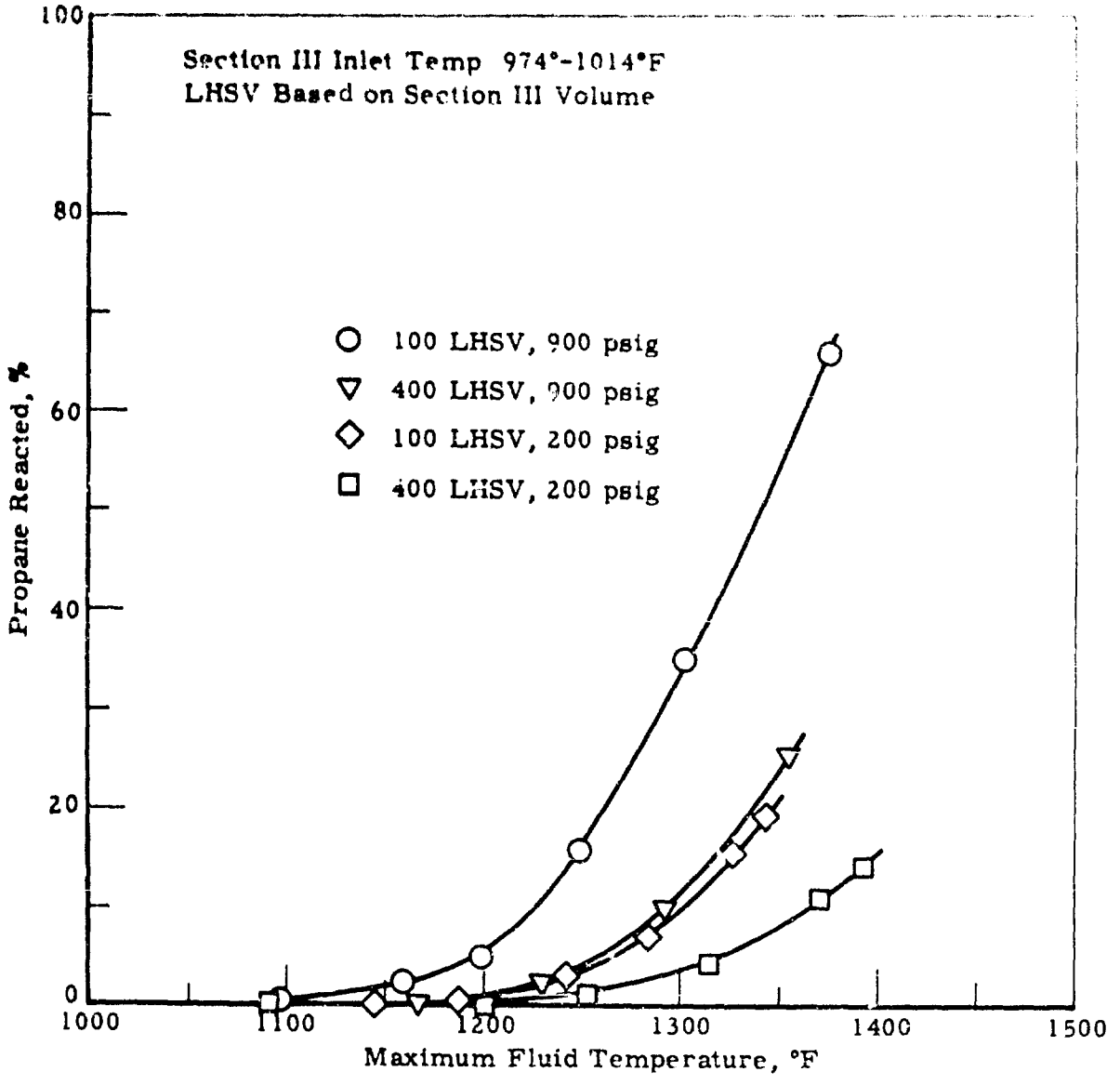


Figure 53. FSSTR-THERMAL CRACKING OF PROPANE
EFFECT OF REACTION CONDITIONS

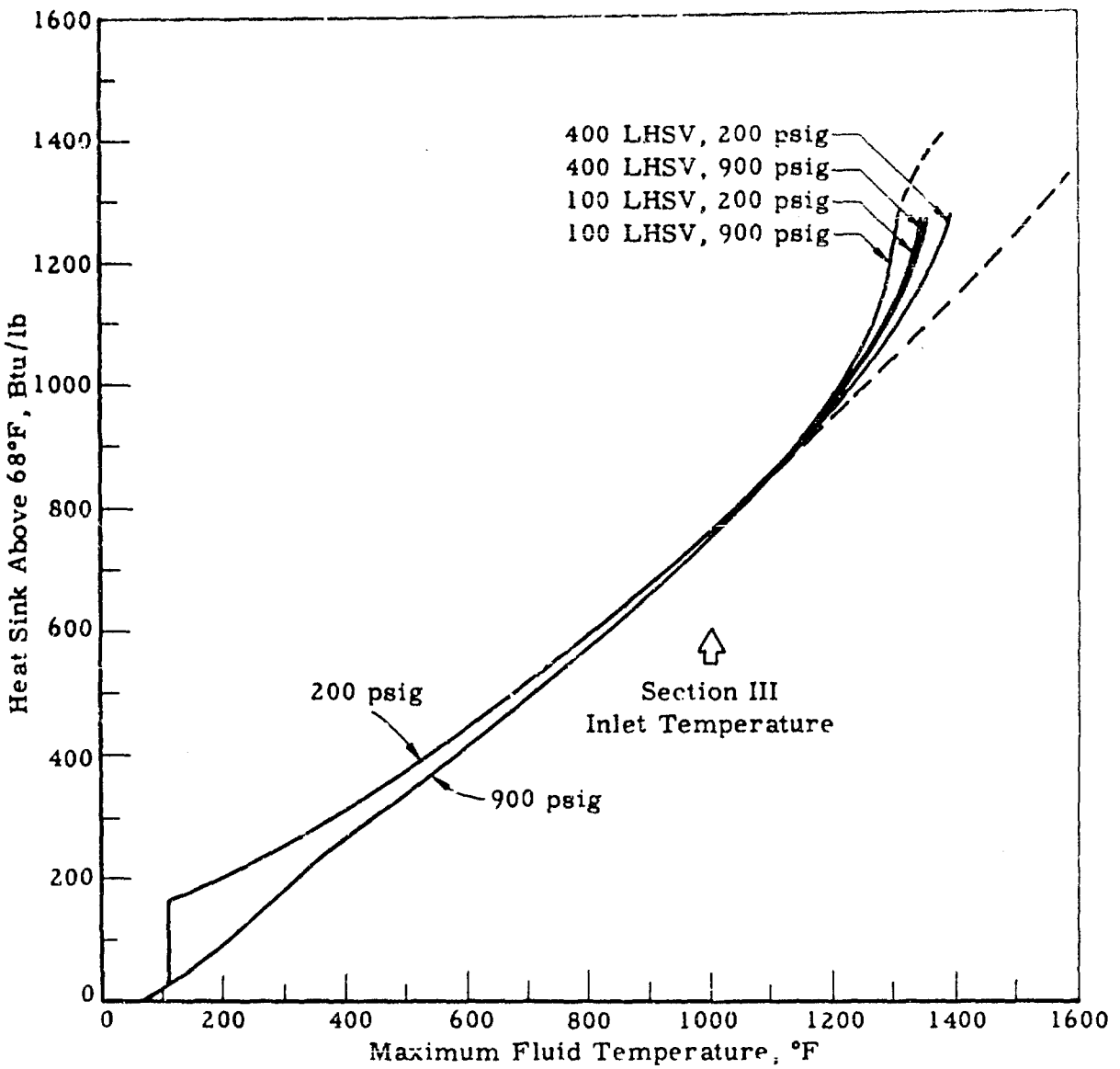


Figure 54. FSSTR-THERMAL CRACKING OF PROPANE: TOTAL HEAT SINK

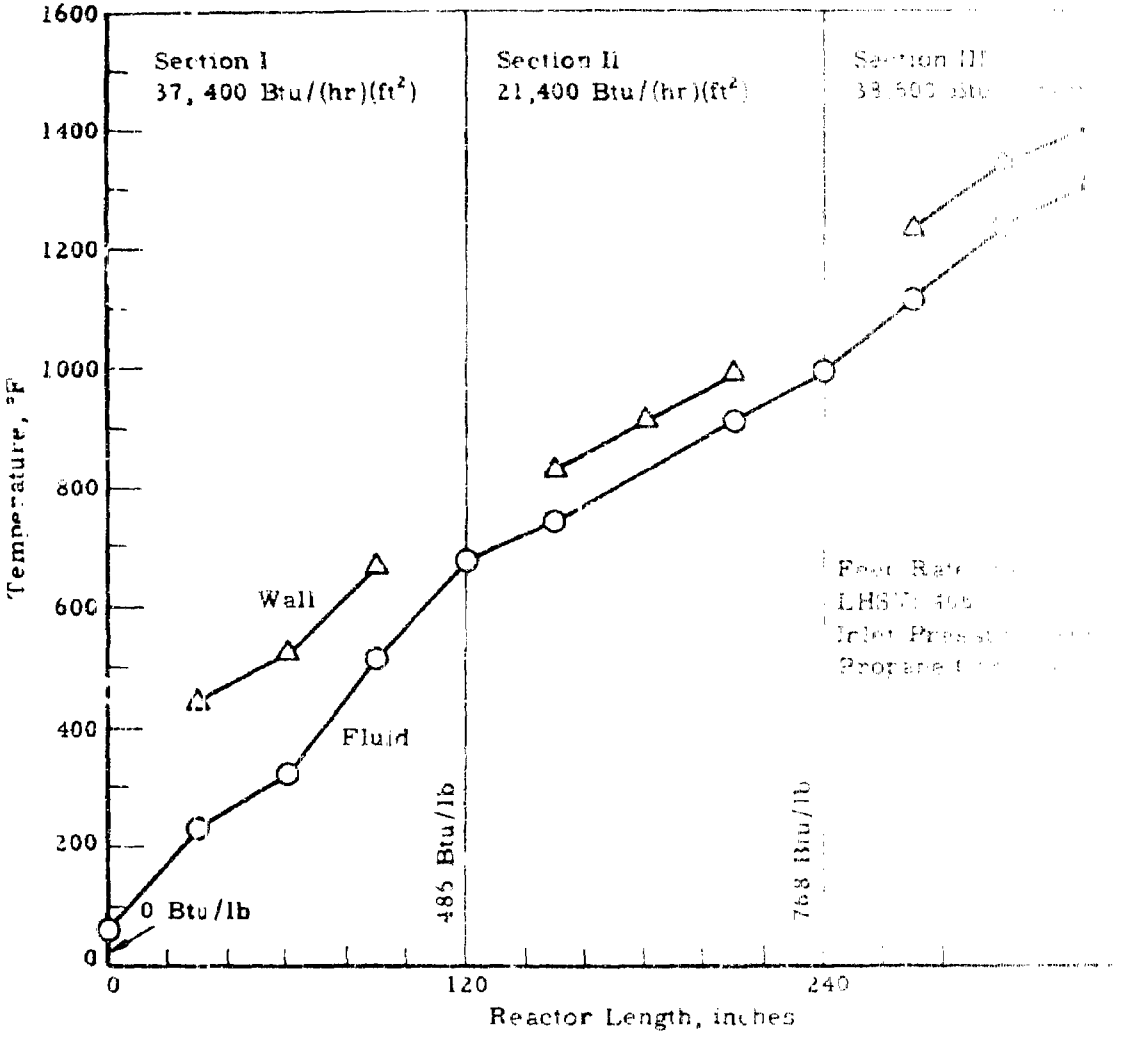


Figure 55. FSSTR-THERMAL CRACKING OF PROPANE.
Temperature Profile for Run 10018-27-[illegible]

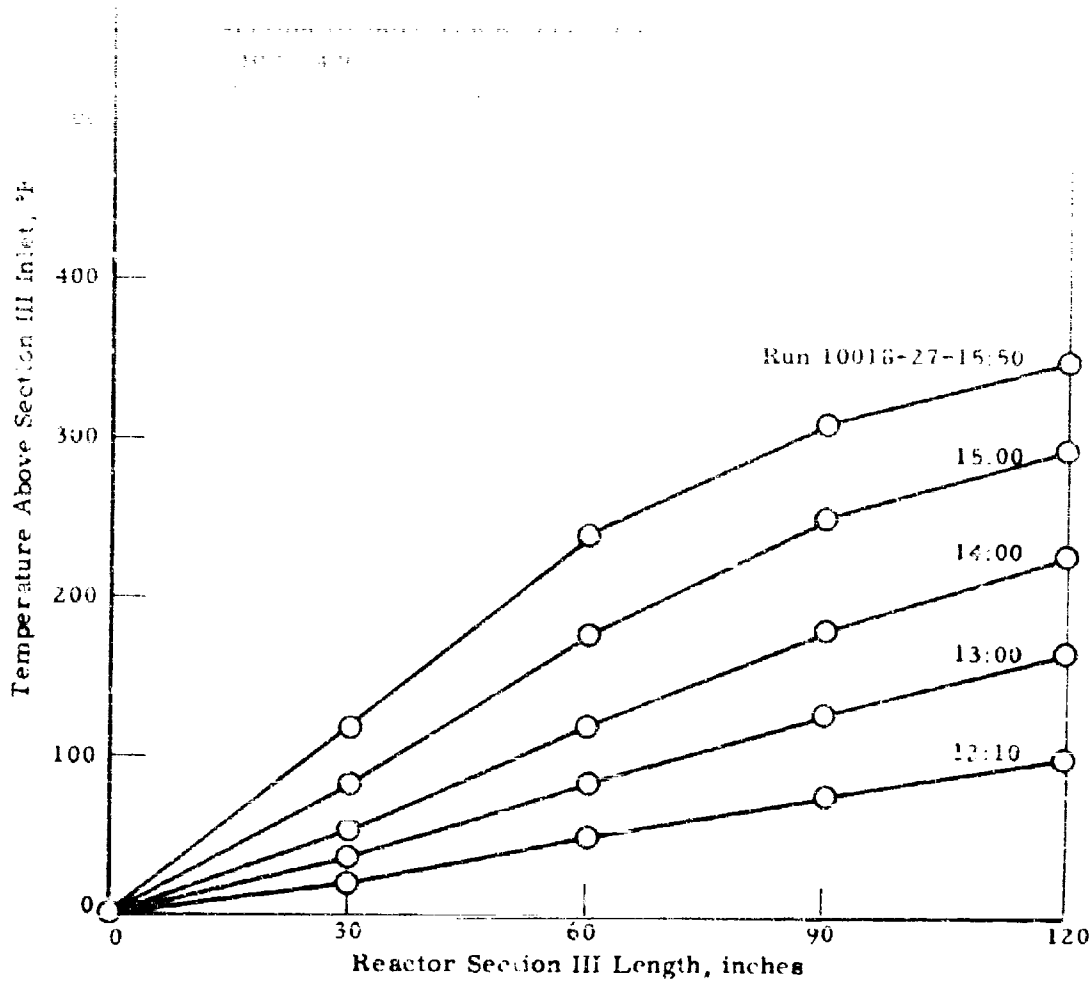


Figure 56. FSSTR - THERMAL CRACKING OF PROPANE
Section III, Temperature Profiles for Series 10018-27

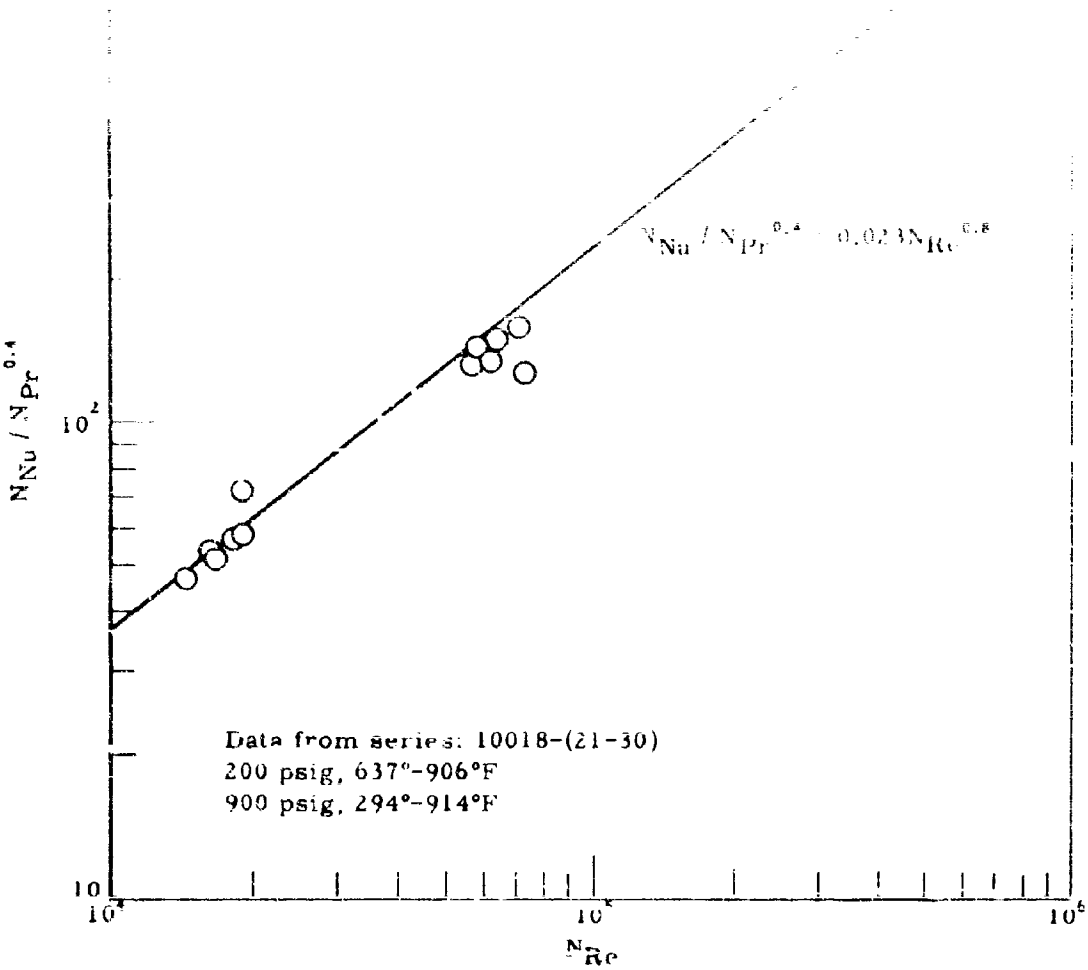


Figure 57. FSSTR - HEAT TRANSFER TO PROPANE IN EMPTY $\frac{5}{8}$ INCH TUBE: DITTUS-BOELTER CORRELATION

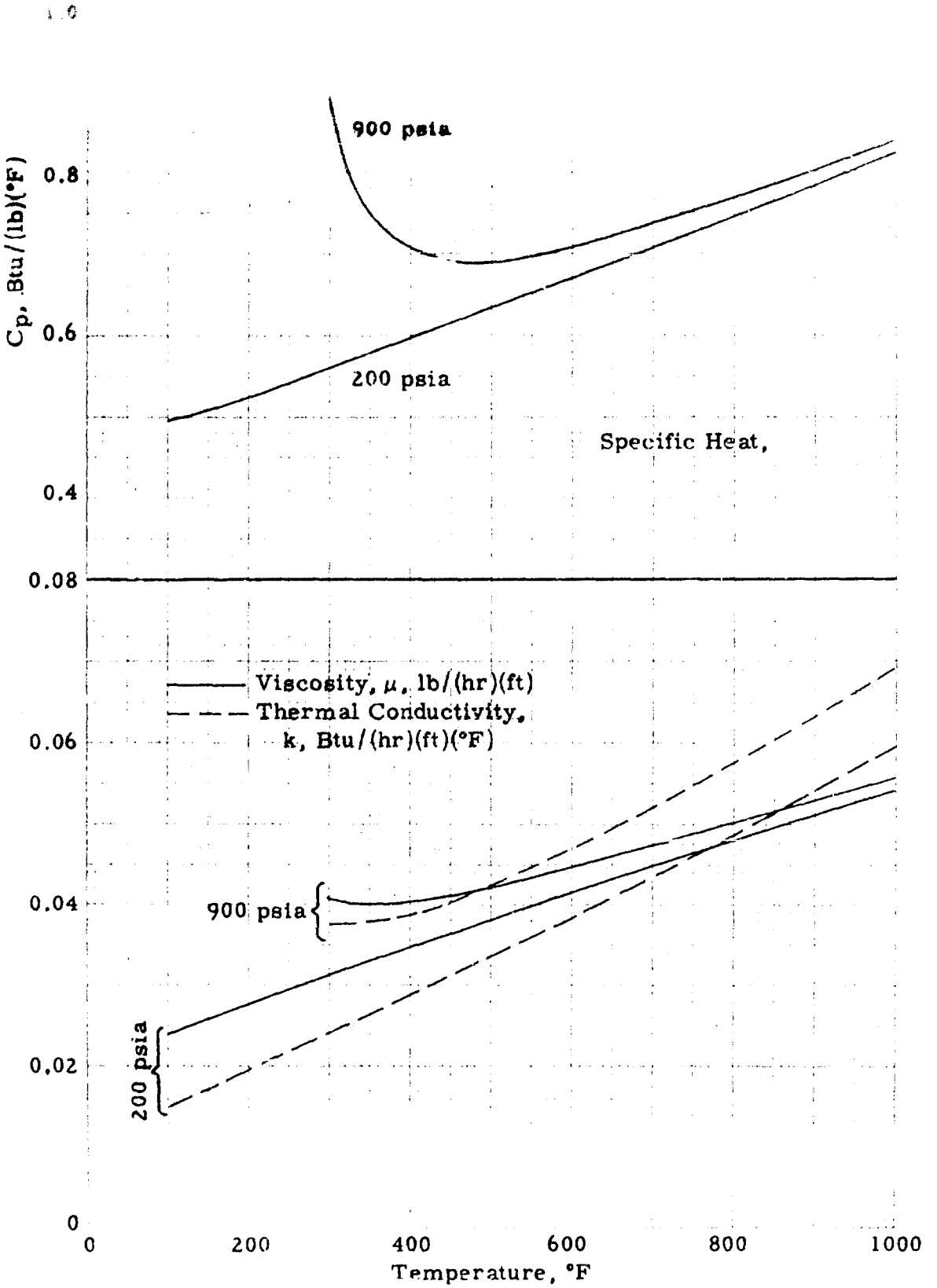


Figure 58. FSSTR-HEAT TRANSFER TO PROPANE: PHYSICAL PROPERTIES OF PROPANE

Catalytic Dehydrogenation of Propane

The catalytic dehydrogenation of propane was studied briefly in the FSSTR using a commercial catalyst (Catalysts and Chemicals, Inc., Catalyst C-94; 2% K_2O, 8% Cr_2O_3 on Al_2O_3). The as-received extruded pellets were crushed and screened 10-12 Tyler mesh prior to use. The usual 3/8" OD x 0.049" wall x 10 ft long Hastelloy C reactor tubes were used for this study with Reactor Section III being the catalyst section while Section I was used as a preheater. No power was supplied to Section II.

Two series of runs using a single catalyst charge of 64.8 g were made at a feed rate of 10 lb/hr (LHSV = 75 based on the catalyst section volume). Operating conditions, product analyses, and calculated values of heat sink are summarized in Table 63.

In the first series (10018-36) the fluid temperature at the catalyst section inlet was maintained at 900°F throughout the test period. Variables were inlet pressure of ca 430 and 590 psig and catalyst section exit fluid temperature of 1100° and 1200°F. The maximum conversion of propane measured during this run sequence was 7.7%. Conversion declined rapidly and after about 5 hours of operation the catalyst was almost completely deactivated. Following this test, coke containing 10.7 g of carbon was burned from the catalyst bed.

For the second test (Series 10018-40) nominal inlet and exit temperatures of 1000° and 1250°F, respectively, and an inlet pressure of ca 500 psig were maintained for the entire operating period. Conversion at the start of this test indicated that burning off the coke deposit following the previous run had restored normal catalyst activity. Propane conversions started at 22.5% and declined to 4.2% after 252 min of operations. Pressure drop increased from about 300 to 465 psi during the first 25 minutes, then increased at 5 psi per hour through the rest of the run to a maximum of 490 psi. Catalyst deactivation and pressure drop for this test are illustrated in Figure 59. Coke was not burned from the catalyst following this final run. However, a weight increase of 15 grams due to coke deposition was measured after dumping the catalyst charge.

The maximum heat sink attained during the propane dehydrogenation was 1205 Btu/lb (above liquid propane at 68°F). Of this, 217 Btu/lb was due to heat of reaction.

The short catalyst life and relatively low heat sink show little promise for this system. No further tests are planned for catalytic dehydrogenation of propane in the FSSTR unless a more stable catalyst is discovered.

High Heat Flux Section (in progress)

In order to permit investigation of heat flux conditions closer to those which might be encountered in combustion chamber cooling, a short reactor section has been constructed and installed in the FSSTR in place of the usual 10-ft long reactor section III. This reactor, a sketch of which is shown in Figure 60 is made up of a 2-ft long section of 3/8" OD x 0.049" wall Hastelloy C tube welded to Ni bus bars. 3/8" compression type fittings

Table 63. FBSTn - DEHYDROGENATION OF PROPANE OVER CHROMIA ON ALUMINA CATALYST: DATA SUMMARY

Catalyst = C-94

Run Time, min	Feed Rate		Fluid Press., psig[b]			Fluid Temp, °Fb)		Conv., %	Product Gas Composition, %m[c]							Heat Sink,[d] Btu/lb	
	lb/hr	LHSV[a]	In	Out	ΔP	In	Out		H_2	CH_4	C_2H_4	C_2H_6	C_3H_6	C_3H_8	Mol Wt	Total	Reaction
Series 10018-36 (Fresh Catalyst)																	
0	10.0	75	433	13	420	900	1100										
5								6.0	6.0	0.2		0.4	5.7	87.7	41.3	925	77
20								7.7	7.4	.2		.5	7.1	84.7	40.6	945	97
40								6.9	6.7	.3		.4	6.5	86.1	40.9	935	88
65								5.7	5.6	.2		.4	5.5	88.3	41.2	922	73
110								4.8	4.8	.3		.4	4.6	89.9	41.8	909	60
121	10.0	75	593	405	188	900	1100										
145								3.8	3.7	.4		.5	3.6	91.7	42.1	891	46
160								3.7	3.4	.4		.5	3.3	92.4	42.3	887	42
180								3.1	2.8	.4		1.1	2.6	93.0	42.5	876	32
200								3.2	2.7	.4	0.3	1.0	2.6	92.9	42.5	880	35
200	10.0	75	595	400	195	900	1200										
220								6.2	4.6	1.5	.7	1.3	4.4	87.5	41.3	996	60
240								5.1	3.7	1.5	.9	1.2	3.4	89.3	41.6	984	49
243	10.0	75	432	13	419	900	1200										
255								2.6	2.2	.5		1.1	2.1	94.1	42.7	963	24
260								2.4	2.2	.4		1.0	2.0	94.3	42.7	962	24
261	10.0	75	423	13	410	900	1100										
275								0.6	.6			.8	.5	98.1	43.6	855	6
285								0.7	.6			.9	.6	98.0	43.7	856	7
Series 10018-40 (Coke containing 10.79 carbon burned from catalyst following Series 10018-36)																	
5	9.7	73	478	170	308	1000	1255	22.5	14.6	3.5	0.9	3.1	13.7	63.2	36.0	1205	217
16			472	74	398			18.1	12.5	2.9	.9	2.4	12.3	69.0	37.2	1167	179
20			481	39	442												
26			485	21	464			17.1	11.5	3.4	1.5	2.3	11.0	70.3	37.4	1154	165
37			485	16	469												
47			483	14	469			9.5	7.1	1.9	1.1	1.2	6.8	81.8	40.0	1089	99
81			487	13	474			7.6	5.2	2.0	1.4	1.1	5.1	85.3	40.8	1067	78
131			493	13	480			5.7	3.6	1.9	1.5	.8	3.6	88.6	41.5	1048	58
192			498	13	485			4.4	2.6	1.6	1.3	.9	2.6	90.9	42.0	1032	43
252			503	13	490			4.2	2.4	1.6	1.4	.8	2.4	91.4	42.2	1031	42

15.0 g coke on catalyst.

a) LHSV based on 0.277" ID x 10 ft long catalyst section.
b) Across catalyst section.
c) Feed analysis; 99.4 %m C_3H_8, 0.6 %m C_2H_6.
d) Heat sink above liquid propane at 68°F (calculated).

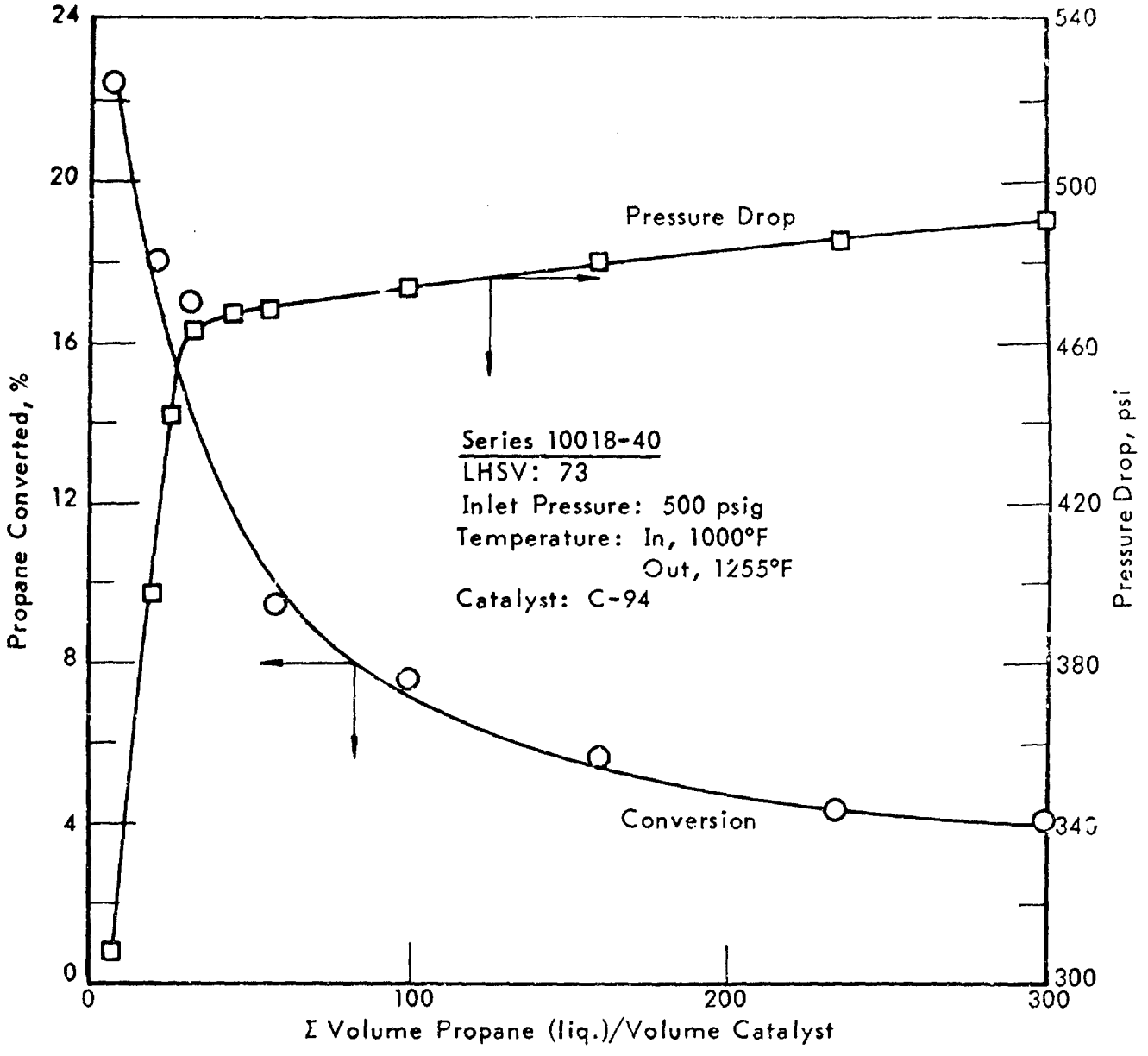


Figure 59. FSSTR - DEHYDROGENATION OF PROPANE OVER CHROMIA ON ALUMINA CATALYST: CATALYST DEACTIVATION

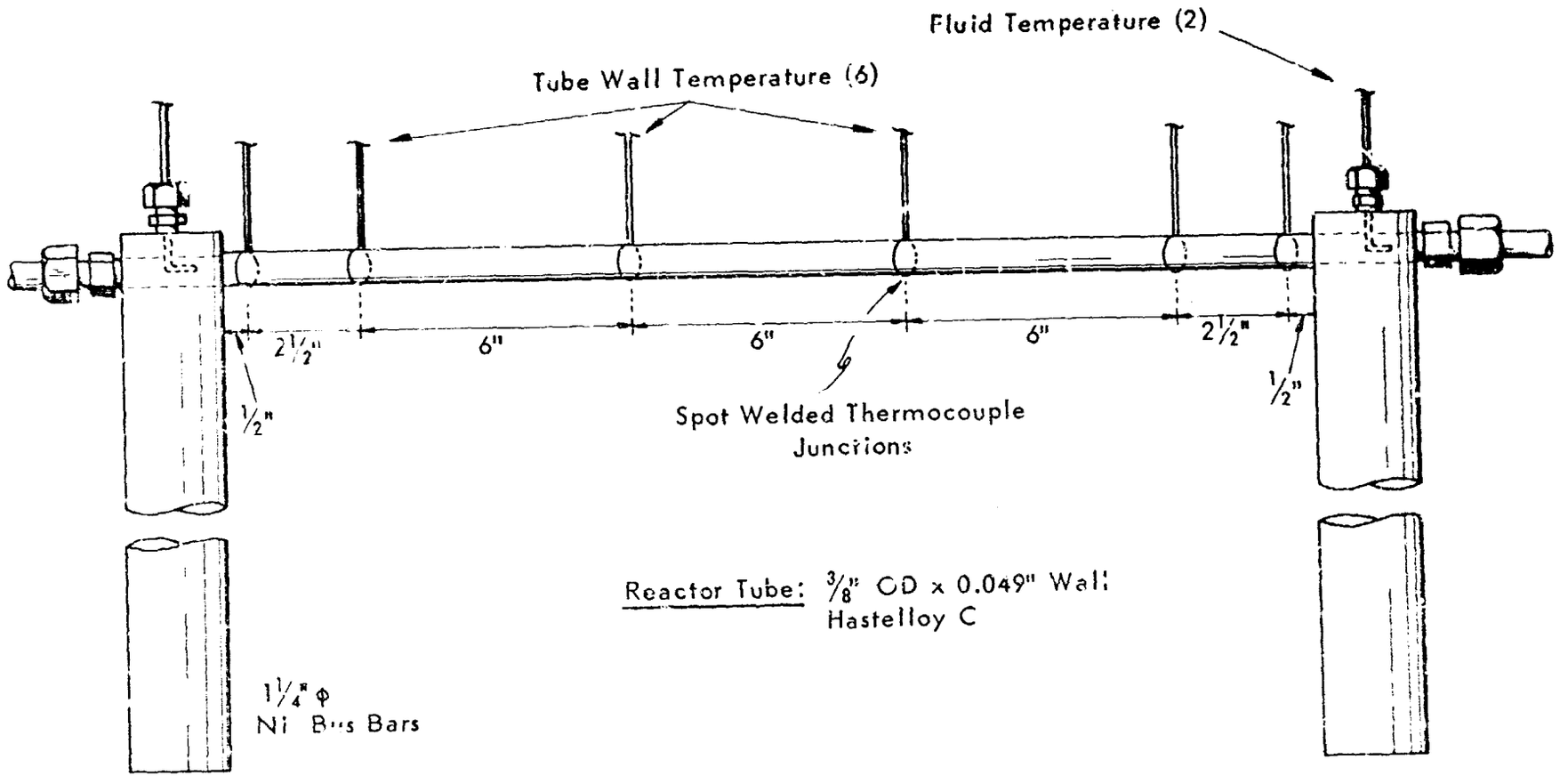


Figure 60. FSSTR - HIGH HEAT FLUX SECTION

provide inlet and outlet connections and 1/16" fittings are used as glands for inlet and outlet fluid temperature thermocouples. A 1/16" fitting is also provided in the exit end bus bar for sample withdrawal. Tube wall (external) temperatures are measured at six locations by thermocouples spot welded to the reactor tube. The two lead wires from each junction (insulated from direct contact with the tube by ceramic cement) are wrapped 1/2-turn each in opposite directions around the tube and then are led thru ceramic insulating tubes until well away from the high temperature area.

The electrical resistance of this reactor section is about 0.025 ohms. With the power supply presently in use, a maximum heat flux of ca 590,000 Btu/(hr)(ft^2) can be reached without exceeding the 1000 ampere rating of the transformer secondary.

No compensating heat is supplied around this reactor as with the 10-ft sections. However, a 2-in. layer of insulation surrounds the tube and at the high heat flux conditions to be studied heat losses will be a minor portion of the power supplied.

Dehydrogenation of MCH Over UOP-R8 in the High Heat Flux Reactor Section

12.9 grams of UOP-R8 Pt on Al_2O_3 catalyst in the form of 1/16" spheres was charged to the reactor and activated in place by heating in N_2. A series of eight tests has been completed covering the following range of condition:

Inlet Temperature, °F	900
Inlet Pressure, psig	885
Feed Rate, lb/hr	64.5
LHSV (for 2-ft section)	1600
Power to Catalyst Section, Btu/(hr)(ft^2)	0-359,000

Reactor sections I and II were used as preheaters for these runs.

A summary tabulation of the data obtained is presented in Table 64. Power to the reactor was increased in steps as shown until a point was reached when it became apparent that the catalyst bed was deactivating. This effect is shown in Figure 61 where exit fluid temperature is indicated. The continuing temperature rise shown in the final runs after a step increase in power indicates that the heat sink resulting from reaction is declining and a corresponding amount of power is going to heat the product. This is confirmed by the decline in conversion shown on the same figure.

In this series a maximum heat flux of 359,000 Btu/(hr)(ft^2) was attained which is higher by a factor of 10 than was previously reached in the 10-ft long 3/8"-diam catalyst section and 7 times higher than the maximum for the 3/4" diam tube (Reference 3 and preceding section this report).

Analysis of the data from these tests is still in progress. However, comparing the final run (10018-50-16:30) with the predicted performance

at similar conditions (Table 70 condition B) indicates that conversions higher than predicted were attained, resulting in higher pressure drop and lower exit temperature than predicted. Clarification of this point as well as investigation into reasons for the catalyst deactivation will require further effort.

Table 64. FSSTR - HIGH HEAT FLUX STUDY: DATA SUMMARY FOR SERIES 10018-50

Catalyst Section Inlet Conditions:

Feed: 99.7% MCH, 0.1% CH, 0.2% Toluene
Feed Rate: 64.5 lb/hr; 10.05 gph; 154,000 lb/(hr)(ft²)
LHSV: 1600 based on 2-ft catalyst section
Pressure: 885 psig

Properties	Run No. 10018-50-								
	12:30	13:10	13:50	14:30	15:10	15:40	16:05	16:30A[a]	16:30B[a]
Power Measurement									
Btu/hr x 10^{-3}	0	6.1	13.3	21.7	30.8	39.0	45.5	52.0	52.0
Btu/lb	0	96	210	342	485	615	717	820	820
Btu/(hr)(ft²) x 10^{-3}	0	42.1	91.7	150	212	269	314	359	359
Temperature, °F[a]									
Inlet Fluid	896	900	891	893	903	908	906	898	900
Wall at 1/2"	864	897	922	961	1009	1047	1072	1091	1094
Wall at 3"	800	839	880	931	988	1032	1067	1096	1100
Wall at 9"	737	787	841	901	963	1014	1054	1094	1099
Wall at 15"	713	773	836	902	968	1023	1069	1115	1122
Wall at 21"	701	771	841	913	988	1053	1115	1192	1212
Wall at 23 1/2"	699	770	840	913	990	1067	1141	1242	1266
Exit Fluid	699	745	788	831	880	936	1002	1100	1126
Exit Press., psig	700	671	645	604	548	505	466	436	436
MCH Conv, %	15	21	29	39	51	60	65	55	63

a) Temperatures are averaged over 15 min intervals except for Run 16:30 where two 7 min periods 20 min apart are indicated to show changing conditions.

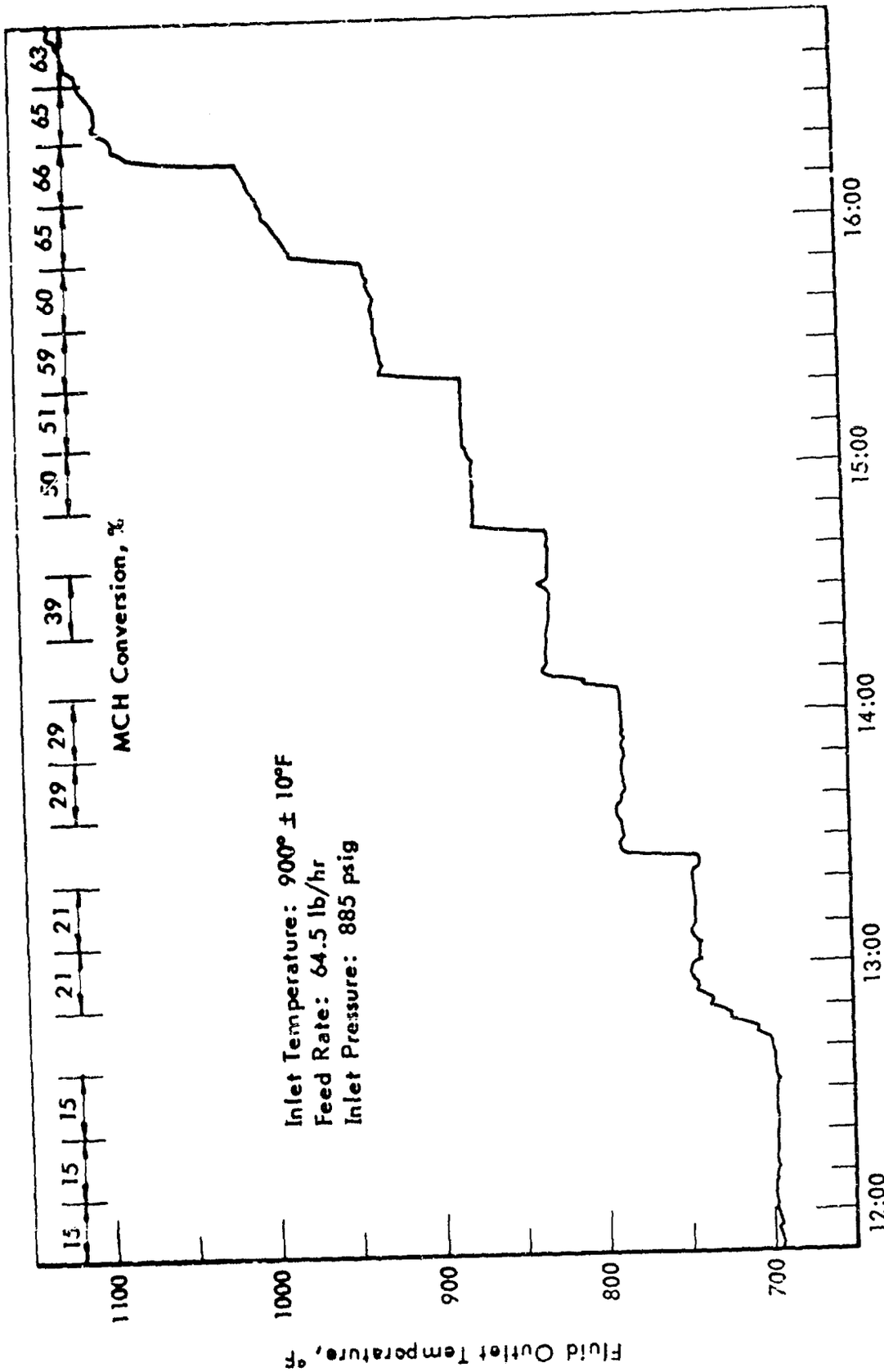


Figure 61. FSSTR - HIGH HEAT FLUX STUDY: CATALYST BED EXIT FLUID TEMPERATURE

Development of Analytical Models of Catalytic Reactors

Work has been concentrated on development of an improved version of the "Shell Packed Bed Reactor Program" for simulation of experiments which have been carried out in the FSSTR and for some exploration of the effects of reactor parameters on the performance of the reactor. A new version of the program has been written, tailored specifically to the requirements of calculations for endothermic fuel reactors.

The primary objective in undertaking a revision of the packed bed reactor program was to simplify input and output and reduce loading time and computer storage requirement in order to facilitate our own use of the program and to make it available for use by the Air Force and other Air Force Contractors on related contracts. The only significant feature of possible use, which was omitted, is the ability to represent a radial profile of mass velocity. This feature has not been used in past simulations of experimental work but could conceivably be of use in the future. Several additions have been made to allow coverage of a wider range of applications. These additions involve a revision of the available choices of the boundary conditions at the outer wall of the tube. In the new version: 1) the flux profile may be specified by a table of up to 10 values equally spaced along the length of the tube, or 2) the outside temperature of the tube may be similarly described by a table of up to 10 equally spaced points, or 3) the tube may be assumed heated by a secondary fluid flowing along the outside wall with constant mass velocity, heat capacity and heat transfer coefficient.

The basic equations representing the processes occurring within a single tube packed with catalyst and the logic of their solution remain the same as in the original version. A slight improvement in computation time is realized, 0.6 minutes of computer time on IBM 7040 compared with 0.7 minutes for the original version for a normal computation simulating a FSSTR run with 500 axial steps and two radical increments.

The rewriting was accomplished in two stages. In the first of these, the program was adapted to the requirements of calculations for endothermic fuels, but remained restricted to handling cylindrical, axisymmetric reactors. An addition to this version also allowed calculations for a sequence of adiabatic reactors, with reheating of the fluid between stages. Subsequently, in a second stage of modification, the program was adapted to also allow calculations for a packed bed in the configuration of a thin semi-infinite slab with heating on one face, and held adiabatic on the opposite face. Such a configuration is felt to be a reasonable approximation to the configuration which would be used for regenerative cooling of a combustion chamber. At the present time, MCH is the only fuel for which we have adequate thermodynamic and kinetic data to carry out calculations with the program. As experimental investigations of other fuels proceed and develop the required information, this can readily be incorporation into the program to allow the same types of calculations for these other fuels. Data for decalin to reaction products is now being assembled.

A listing of the current version of the program in FORTRAN IV language and memoranda describing each of these two stages of development

are contained in the Appendix. This program has been used for most of our own calculations and has been made available to the Air Force and other contractors.

Some work was also done on development of a one-dimensional program representing a single packed tube. In this program, radial temperature gradients are represented by approximations, and rates are calculated at an average (cross-sectional) temperature. Our present feeling is that such a representation cannot be made to function in a manner useful for design of equipment or refined calculations, but may be of value in early stages of attempting to develop reaction rate expressions for the endothermic reactions of other fuels. Such a program has a significant advantage in shorter computing time when a large number of cases must be run.

Simulations of FSSTR Experiments

The additional experiments carried out on dehydrogenation of MCH in the FSSTR using a 0.75" diameter tube were simulated in order to demonstrate the capability of the model for this wider range of conditions, and to assist in interpretation of heat transfer measurements made in these experiments. Substantially the same parameters were used in these simulations as had been used previously in simulation of experiments in the smaller diameter tube. Because of the larger ratio of tube diameter to particle diameter, two factors involved in calculation of pressure drop were adjusted. For the average fraction voids between particles, ϵ, a value of 0.415 was used rather than 0.432 which had been used for the smaller tube. The value of AF, the factor which corrects for a typical packing arrangement near the wall, was raised from 0.50 to 0.67. Both changes tend to make the calculated pressure drop larger in the larger tube. The rate expression used was the same as had been used previously. The parameters which are used to generate the equilibrium constant were adjusted slightly to bring the calculated value into better agreement with the tabulated values given by API 44 tables. The rate in lb-mole/hr-ft^3 of reactor volume is given by:

$$\text{Rate} = \frac{(1-\epsilon)A_1A_2C_{MCH}\exp[(B_1 + B_2)/R_gT_s]}{1 + A_2C_{MCH}\exp[B_2/R_gT_s]}\left[1 - \frac{P_{tol}P_{H_2}^3}{P_{MCH}A_3\exp[B_3/R_gT_s]}\right]$$

R_g = gas constant (Btu/lb mole-°R)

C_{MCH} = concentration of MCH (lb mole/ft^3)

T_s = surface temperature of catalyst (°R)

P_A = partial pressure of component A (atm)

ϵ = fraction voids in bed

A's and B's are reaction rate and equilibrium parameters.

$A_1 = 7.5 \times 10^{12}$ $\quad B_1 = -59,000$
$A_2 = 5.5 \times 10^{-8}$ $\quad B_2 = +54,000$
$A_3 = 4.0 \times 10^{20}$ $\quad B_3 = -92,500$

The run numbers and conditions for the seven runs simulated are given in the upper part of Table 65. The lower part of the table gives a

Table 65. COMPARISON OF COMPUTER CALCULATIONS WITH EXPERIMENTAL RESULTS FOR DEHYDROGENATION OF MCH IN 3/4-INCH TUBE

Run No.	8915-198		10018-5			10018-9	
	1300	1420	1200	1320	1620	1300	1400
Flux (Btu/hr-ft^2)	15700.	13300.	11740.	23100.	24080.	34500.	50000.
G (lb/hr-ft^2)	35500.	36800.	17200.	17200.	33200.	36700.	36700.
T_o, °F	895.	894.	898.	900.	900.	904.	905.
P_o, psig	911.	487.	901.	903.	903.	886.	886.
ΔP, psig[a]	109.	270.	30.	39.	113.	166.	207.
	102.	268.	30.	43.	113.	166.	210.
Temp on axis, °F							
2.5'	729.	684.	741.	774.	745.	756.	775.
	732.	687.	746.	773.	749.	758.	777.
5.0'	752.	694	776.	828.	779.	793.	823.
	750.	687.	777.	824.	777.	792.	822.
7.5'	771.	696.	804.	882.	805.	824.	875.
	764.	684.	800.	872.	798.	817.	866.
Outlet Temp (mean), °F	790.	695.	834.	1028.	834.	865.	1039.
	782.	682.	825.	1013.	838.	872.	1034.
Conversion	45	44	63	98	64	79	97
	43	44	64	98	62	77	97

a) Experimental values are underlined.

comparison of the calculated and observed values of pressure drop, conversion, outlet mean temperature, and values of the temperature at the axis of the reactor tube at three parts along its length. In this portion of the table the upper figure is the calculated, the lower (underlined) the experimental. These comparisons indicate a very satisfactory agreement between experiment and calculation. Calculations showed that the overall heat balance can be in error by up to about 4 percent. This is probably due to errors in experimental measurements of flow rate and heat flux. Figures 62, 63, and 64 show profiles of temperature at the tube axis and conversion calculated for three of the above experiments. Experimental points are shown for intermediate temperatures and overall conversion. These profiles demonstrate behavior typical of a constant-flux reactor. In Figure 62, it can be seen that the rate of reaction is nearly constant throughout the reactor (except for the first foot of length), the conversion increasing linearly with length. In this section nearly all of the added heat is utilized by the endothermic reaction, with only a small portion going to heat up the fluid. The temperature in this section rises as necessary to adjust the rate constant to maintain the chemical reaction rate at a level sufficient to absorb the heat being added. At the inlet, the feed was admitted at a temperature much higher than necessary to maintain a reaction rate capable of absorbing the heat added. Therefore, the temperature fell rapidly, with the sensible heat of the gas being absorbed by additional reaction in this section.

Explorations with the computer program have shown that the primary factors influencing the shape and location of such profiles are the rate of heat addition in B.t.u/lb of fluid flowing, and the inlet temperature; the actual heat flux and mass flow rate have only a minor influence upon these profiles.

Figure 63 shows profiles for a run in which the total heat addition was high enough to carry the conversion near to reactant exhaustion. Thus near the outlet, the rate of reaction declines and the rate of temperature increase turns up sharply, with sensible heat now absorbing a larger fraction of the heat input in this section.

Figure 64 shows profiles for a run made at lower pressure, with a high enough flow rate that the pressure drop seriously affects the pressure level in the reactor. The rapidly decreasing pressure shifts the equilibrium point of the reaction sufficiently that the reaction is maintained at a steady rate even though the temperature is nearly constant or declining throughout the reactor.

Heat Transfer to a Packed Bed Reactor

A second application of the packed bed computer program is in aiding analysis of rates of heat transfer to the FSSTR. In the experiments, the overall temperature difference is measured between a thermocouple on the outside wall of the reactor and a thermocouple at the centerline of the bed. Heat transfer between these two points occurs by a series of three consecutive processes: 1) generation of heat from electrical power and its transfer through the wall with an associated temperature drop Δt wall between outside and inside of the wall, 2) transport across a turbulent fluid film inside the wall, with an associated Δt film, 3) transport through the packed bed, radially, accompanied by absorption of heat by the fluid as sensible heat and

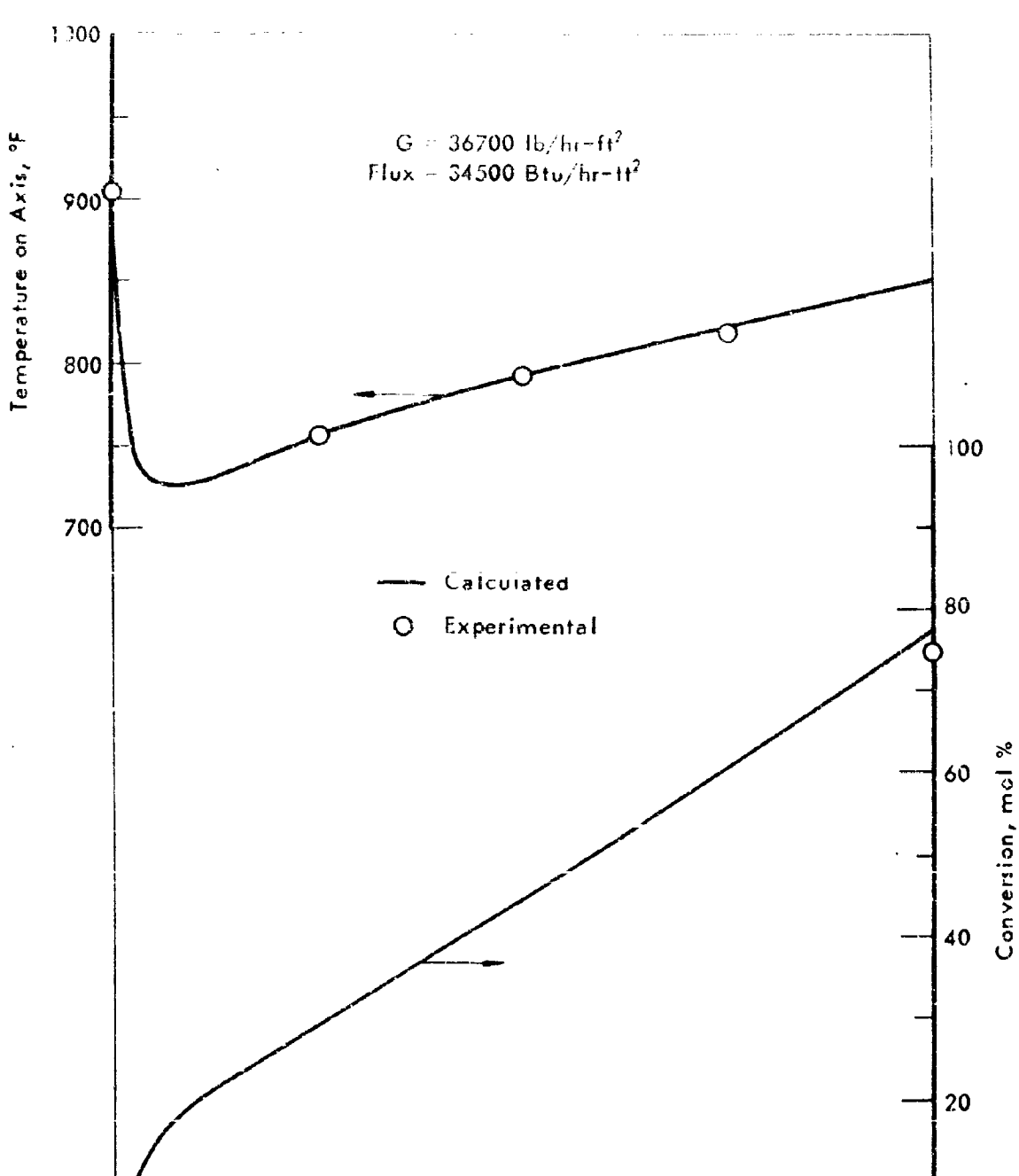


Figure 62. CALCULATED TEMPERATURE AND CONVERSION PROFILES FOR CONDITIONS OF RUN 10018-9-1300

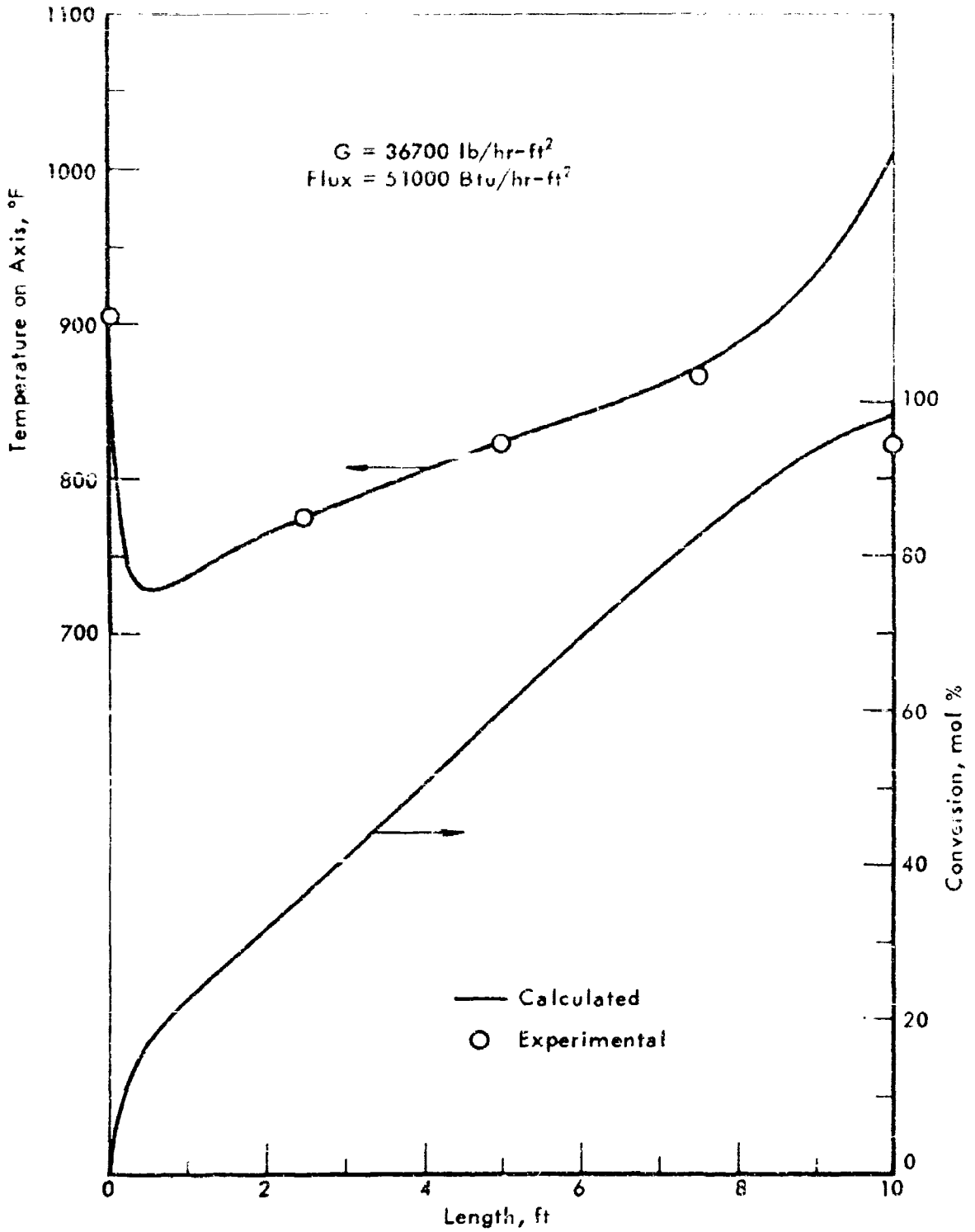


Figure 63. CALCULATED TEMPERATURE AND CONVERSION PROFILES FOR CONDITIONS OF RUN 10018-9-1400

62731

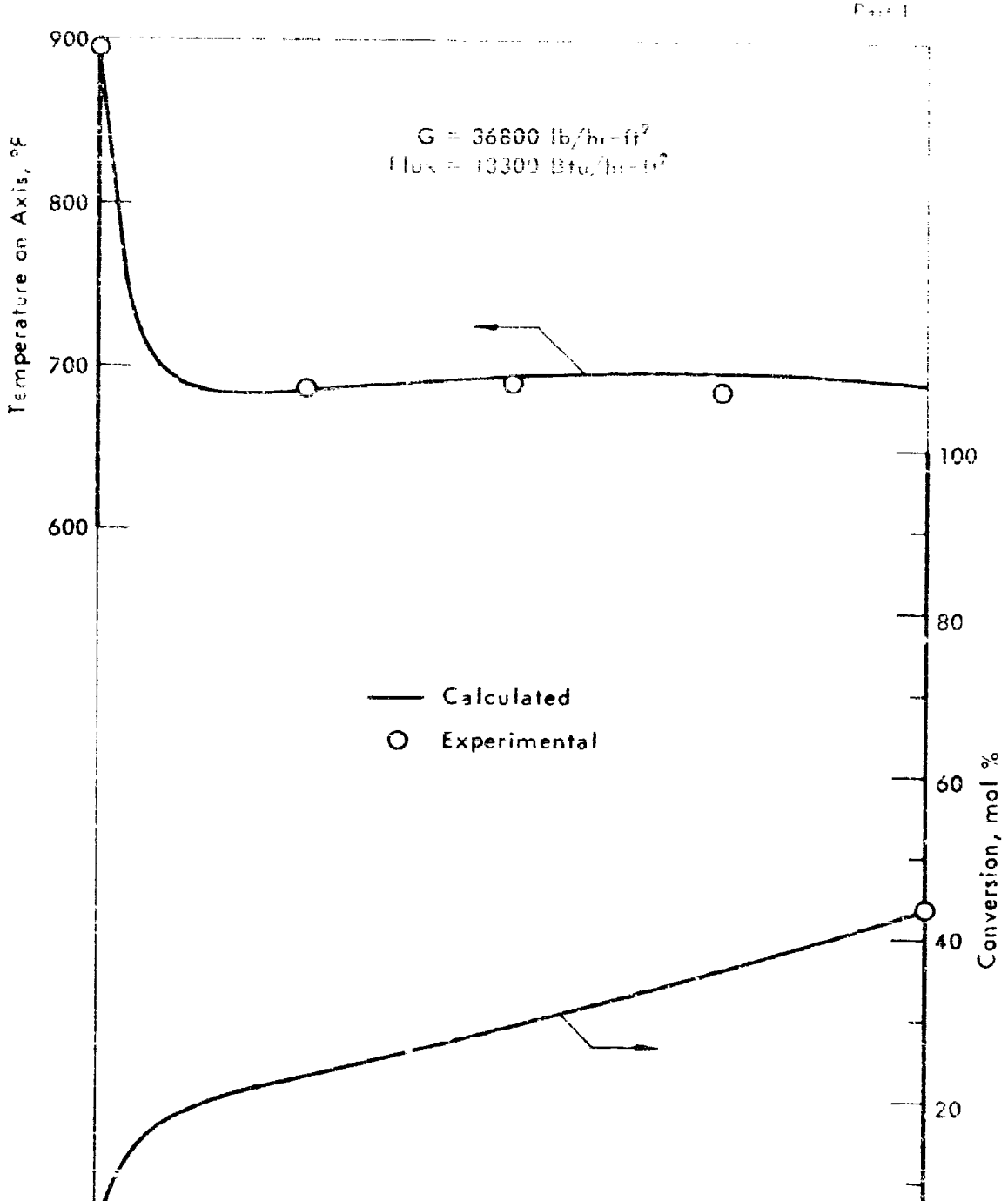


Figure 64. CALCULATED TEMPERATURE AND CONVERSION PROFILES FOR CONDITIONS OF RUN 8915-198-1420

endothermic heat of reaction, with an associated Δt packing. The measured temperature difference is the sum of these three. The first, Δt wall, may be simply calculated from the thermal conductivity and one half the thickness of the wall and the rate of heat generation. For the second, Δt film, correlations exist in the literature. However, these correlations are based on data at lower Reynolds' numbers. We are interested in demonstrating whether or not such correlations are applicable in our region of conditions. Therefore, we would like to be able to separate Δt film from the remaining processes. To do this, the computer program is used to calculate Δt packing, which allows calculation of Δt film by difference. The experimentally measured Δt's and the three component parts of each are given in Table 66 for the seven runs made with the 0.75-inch diameter tube. For each run, an average film heat-transfer coefficient calculated from the flux and the values of Δt_f is also given. A comparison of Nusselt numbers based upon wall heat-transfer coefficients calculated in this way, with a correlation based on that of Hanratty for heat-transfer to beds of spherical particles, is shown in Figure 65. The experimental results obtained in both the 3/8-inch and 3/4-inch tubes are in good agreement with this correlation and indicate its usefulness in predicting heat transfer coefficients at highly turbulent Reynolds' numbers.

Influence of Thermal Conductivity of Catalyst Particles

The radial temperature drop through the packing within the catalyst bed is a significant part of the overall radial temperature difference. In the past we have indicated that the major process influencing radial transport of heat within the bed was gas mixing. To assure ourselves that the parallel process of conduction of heat through the solid packing was not important in determining the radial temperature drop, exploratory runs were made with the computer program to determine the influence of the thermal conductivity of the catalyst.

Two pairs of runs were made for conditions representing two levels of flow conditions possible in our experimental apparatus; one pair at LHSV of 20, the other of LHSV of 100. In one run of each pair, the solid conductivity of the base run was taken as 0.130 Btu/hr-ft-°F, a value typical of our current catalyst. In the other run, a solid conductivity 10^3 times greater was taken. This value is arbitrarily high, but comes close to representing copper metal. To maximize the effect of radial conductivity, a total heat input of 1000 Btu/lb was taken for the 10-ft reaction section. In the higher space velocity pair, no significant difference between the two runs was observed, the largest difference being 0.5°F lower wall temperature at the outlet for the run with the higher conductivity. In the lower space velocity pair, differences were observable but still very small. A maximum difference of 3.5°F in the wall temperature at the outlet resulted.

From these explorations we conclude that any attempt to develop a catalyst supported on a base of higher thermal conductivity than the alumina we now use would clearly not be fruitful in terms of overall reactor performance.

Table 66. COMPONENTS OF MEASURED TEMPERATURE DIFFERENCES IN REACTION SECTION

Run No.	8915-198		10018-5			10018-9	
	1300	1420	1270	1320	1620	1300	1400
At 2.5'							
Measured Δt	28	26	29	57	42	56	81
Δt wall[a]	4	4	3	6	6	9	12
Δt film[b]	12.8	10.8	12.3	27.4	19.0	25.4	39.5
Δt packing[c]	11.2	11.2	13.7	23.6	17.0	21.6	29.5
At 5.0'							
Measured Δt	26	25	27	63	39	51	74
Δt wall[a]	4	4	3	6	6	8	12
Δt film[b]	12.0	10.2	12.1	25.2	18.1	23.6	33.2
Δt packing[c]	10.0	10.8	11.9	22.0	14.9	19.4	28.8
At 7.5'							
Measured Δt	28	28	30	58	41	55	84
Δt wall[a]	4	4	3	6	6	8	12
Δt film[b]	14.8	13.1	15.8	25.0	20.6	27.1	36.4
Δt packing[c]	9.2	10.9	11.2	27.0	14.4	19.9	35.6
Mean h_f (Btu/hr-ft^2)	1200	1190	900	900	1250	1360	1380

a) Determined from wall thickness, thermal conductivity of metal and flux, $\Delta t_w = \frac{q/A \cdot m}{2K_w}$.

b) By difference $\Delta t_f = \Delta t_m - \Delta t_w - \Delta t_p$.

c) Determined from computer program calculations.

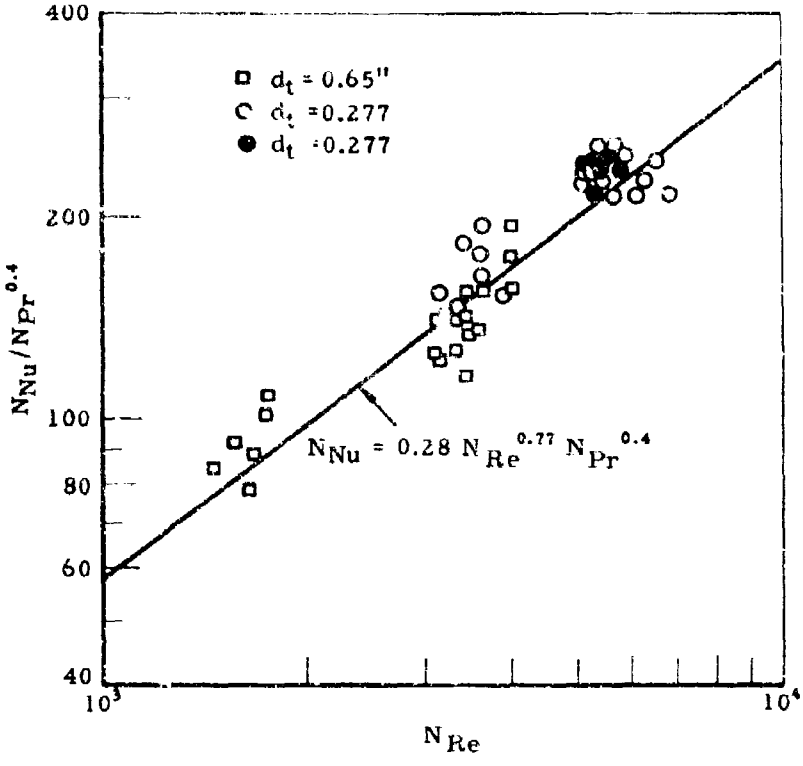


Figure 65. COMPARISON OF EXPERIMENTAL HEAT TRANSFER COEFFICIENTS AT TUBE WALL WITH CORRELATION

Exploratory Calculations

Further calculations have been carried out with the computer program to attempt to define, at least roughly, the upper limit conditions of mass velocity, heat flux, and endothermic capacity for MCH as an endothermic reacting fuel. For these calculations, which are specific to MCH fuel and R-8 catalyst, a reactor length of 2.0 ft and inlet fuel temperature of 900°F at 900 psig were selected as constant conditions.

Results shown in Table 67 indicate the effect of mass velocity and heat flux for a reactor tube 0.65-in. ID subject to a constant heat flux along its length. These calculations indicate moderately high but probably tolerable pressure drops of 250-400 psi over the two-foot length for mass velocities of 100,000-120,000 lb/hr-ft^2. Thus, 120,000 lb/hr-ft^2 is probably near the upper limit of mass velocity allowable by pressure drop at a constant heat flux of 0.5 x 10^6 Btu/hr-ft^2, maximum temperatures attained are probably within the permissible range. It should be noted that upper limit temperatures for this fuel and its reaction products have not been firmly established. However, our past experience with these hydrocarbons indicates that significantly above 1300°F the hydrocarbon will rapidly coke up the tube, and the fuel in contact with the catalyst will result in deactivation of the catalyst above some temperature in the range 1100-1200°F. At the higher flux level, 0.625 x 10^6 Btu/hr-ft^2, maximum temperatures are above these tentative upper limits. Thus, this level of heat flux is "too high". Figure 66 shows axial temperature profiles for three radial locations for the first set of conditions in Table 67. These show that although temperatures at the inlet end are well below stability limits; as reaction proceeds, the temperature of the fluid rises in order to maintain acceptance of the high rate of heat input. Even though the overall conversion attained is only 60%, the rate of the reaction is not sufficient at this conversion level to sustain this high level of heat input at the high space velocity (LHSV = 1250) for which the calculation was made.

In an attempt to obtain a high average heat input and keep temperatures below tolerable limits, calculations were made for reactors subject to tapered heat-flux profiles, with the maximum heat flux at the inlet (low-conversion end). Table 68 shows results of calculations where such a tapered flux profile was obtained by imposing the condition that the inside tube-wall temperature be 1225°F over the reactor length. For this condition with a tube diameter of 0.65 inches, the heat flux varies by a factor of three over the length; from nearly 10^6 Btu/hr-ft^2 at the inlet to 0.34 x 10^6 at the outlet end, with an average value of 0.62 x 10^6. The maximum temperature, both within the packing and at the wall remain within a safe range. The first three entries in this table show the effect of increasing the diameter of the reactor tube with space velocity held constant. The maximum and average heat fluxes increase as would be expected due to the decreased surface to volume ratio of the tube. However, the utilization of the endothermic capacity of the fluid, as indicated by the conversion attained and the total heat input in Btu/lb of fluid, decreases significantly with increased tube diameter. This decreased utilization of the endothermic capacity of the fluid together with the added weight and volume of larger diameter tubes, attaches a heavy penalty to the use of larger diameter tubes to increase permissible heat flux.

Table 67. PREDICTED EFFECT OF MASS VELOCITY AND HEAT FLUX IN CONSTANT FLUX REACTORS

Axisymmetric cylinder
L = 2 ft; d_t = 0.65 in. ID
Dehydrogenation of MCH over UOP R-8
Inlet pressure: 900 psig - total temp: 900°F
LHSV = 8/9

Mass Vel, lb/hr-ft², G	Flux, Btu/hr-ft² x 10⁶	ΔP, psig	Temp Out, °F	X_{out}	Btu/lb	Fluid Max Temp, °F	
						At Wall	In Packing
120,000	.625	396	1145	.61	768	1386	1223
100,000	.625	283	1234	.69	921	1513	1325
120,000	.50	348	1010	.56	615	1205	1075
100,000	.50	248	1065	.64	737	1293	1142

Table 68. COMPARISON OF PERFORMANCES CALCULATED FOR SEVERAL HIGH OUTPUT CONDITIONS FOR MCH DEHYDROGENATION

Axisymmetric cylinder
L = 2 ft; LHSV = 1250
G = 120,000 lbm/hr-ft²; t_w = 1225°F
P_{in} = 900 psig; T_{in} = 900°F

d_t, in.	Rel Rate, Constant	T_{max} in Packing	ΔP, psi	Temp Out, °F	X_{out}	Btu/lb	Heat Flux, Btu/hr-ft² x 10⁶		
							Inlet	Outlet	Average
0.277	1.0	1202	314	1198	.70	905	.89	.05	.31
0.65	1.0	1142	437	1100	.63	760	.95	.34	.625
1.32	1.0	1066	498	915	.48	460	1.1	.62	.76
0.65	2.0	1134	511	1086	.77	875	1.0	.37	.71

The basic barrier to attaining higher heat flux and higher utilization of endothermic capacity of the fuel is the slow rate of reaction at moderately high conversion. As an indication of the benefit which could be obtained from the use of a more active catalyst, the calculation summarized in the bottom line of Table 68 was carried out. Here, a reaction rate was assumed twice that obtained with our current catalysts. For the same configuration and conditions, this postulated increase in reaction rate resulted in an increase in conversion from 63% to 77% and of average heat flux from 0.625×10^6 to 0.71×10^6 Btu/hr-ft^2. Even this quite substantial increase in activity would leave nearly a quarter of the endothermic capacity of the fluid unused. Utilizing this remaining fraction would require a second stage catalytic reactor operated at lower space velocity, operating to extract heat from a load less intense than the combustor walls.

One Side Heating of Reactor Tubes

Although the preceding calculations have been discussed with reference to heat fluxes expected in regenerative cooling of the combustion chamber, these calculations were made for a cylindrical tube configuration uniformly heated around its periphery. In a regenerative application, the tube would in fact be largely heated from one side. A more realistic, simple approximation to this condition might be to consider the catalytic reactor as a flat plate of thickness t, length L, and indefinite extent (essentially infinite) in width, heated on one side of the thickness and adiabatic on the other. Using the version of the packed bed reactor program incorporating the most recent modifications, exploratory calculations were made for this configuration as well. Results obtained are illustrated by Table 69.

Table 69. EFFECT OF BED THICKNESS ON PERFORMANCE OF FLAT-PLATE CATALYTIC REACTOR FOR DEHYDROGENATION OF MCH

Length, ft	2	Mass Velocity, lb/hr-ft^2	100,000
Catalyst Pellet Diameter, in.	1/16	Inlet Temperature, °F	900
		Inlet Pressure, psig	900
		LHSV	1,000

Heated face of reactor maintained at 1225°F on inside of metal wall.

Thickness, in.	Heat Flux, Btu/hr-ft^2, x 10^6		Heat Input to Fluid, Btu/lb	Conversion of MCH	Outlet Temp, °F	Pressure Drop, psi
	Maximum	Average				
0.36	.93	.74	497	.528	900	240
0.24	.87	.69	685	.644	1000	240
0.18	.84	.61	808	.705	1084	215
0.144	.84	.52	874	.73	1133	210

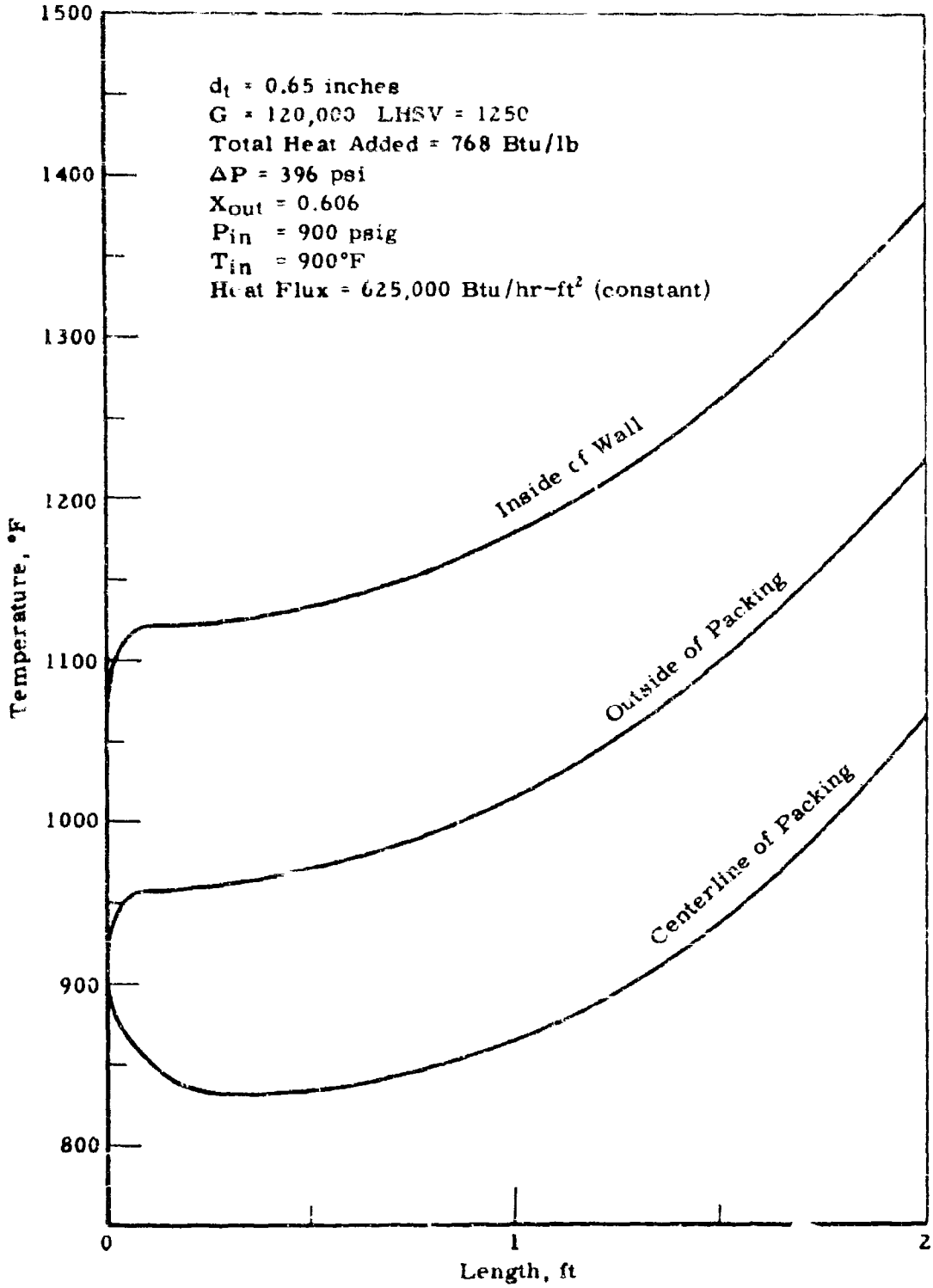


Figure 66. CALCULATED AXIAL TEMPERATURE PROFILES FOR DEHYDROGENATION OF METHYL CYCLOHEXANE AT HIGH HEAT FLUX

62925

The basic features of results with the flat plate configuration are similar to those with the axisymmetric cylinder. An average flux over a two-foot length of 0.5-0.7 x 10^6 Btu/hr-ft^2 can be attained with reasonable utilization of the endothermic capacity of the fuel. Some compromise between maximum heat flux and utilization of the available capacity of the fuel to take up heat must be made. With the flat plate configuration, the dimension of the layer compared to the particle diameter becomes more critical. The region of dimension which appears to be most favorable is a thickness of only two to four particle diameters.

High-Flux Test Section for FSSTR

Application of a catalytic, heat-exchanger reactor to regenerative cooling of the combustion chamber of a hydrocarbon-fueled scramjet would require that the reactor accept a heat flux of 10^6 Btu/hr-ft^2 or greater. In our experiments in the FSSTR, the highest heat flux employed in any experiment was 51,000 Btu/hr-ft^2, lower by twentyfold. Even in view of the success we have had simulating experiments with the mathematical model, we believe experiments at conditions nearer to those of application are desirable, before design of a practical system.

The equipment to be used for these experiments is described elsewhere in this report. Its design basis involves attempting to reach the highest possible heat flux input within the constraints of using the existing power supply, fuel feed system, and preheating arrangements. The computer-program model was used to predict the extreme conditions under which the experimental apparatus could be operated. Two examples of calculations for this equipment are given in Table 70. The fuel to be used is MCH. The conditions indicated for A in the table may be barely attainable due to the high pressure drop. However, maximum temperatures appear to be within reasonable upper limits. At the lower mass velocity and higher heat flux of conditions B, the pressure drop is reasonable but maximum temperatures predicted are probably above the upper limit tolerable by the hydrocarbon without significant coke formation. On the basis of such calculations the region to be investigated in this apparatus has been selected as:

$$1.5 \times 10^5 < G < 2.0 \times 10^5 \text{ lb/hr-ft}^2$$

$$2 \times 10^5 < q/A < 3\text{-}5 \times 10^5 \text{ Btu/hr-ft}^2$$

The upper limit of the heat flux is indefinite and will be approached gradually in the experiments. The heat flux which we expect to attain in these experiments is a factor of six greater than in our previous experiments, and should be within a factor of 2-3 of the maximum to be anticipated in practical application.

Shock Tube Studies of Ignition Delays of Hydrocarbons

Under the previous contract on this subject (AF 33(657)-11096) a program of measurement of ignition delays of hydrocarbon-oxygen inert mixtures was initiated. Experimental methods and equipment have been described in reports under that contract.[2)3)] Work in the same area has been carried out under the present contract with the general objective of providing information on the time required for ignition of hydrocarbon air mixtures in

Table 70. PREDICTED PERFORMANCE OF HIGH HEAT FLUX TEST SECTION FOR TWO SETS OF CONDITIONS

Length: 2 ft
Tube Diameter: 0.277-in. ID

Conditions	A	B
LHSV	2080	1500
Mass Velocity, lb/hr-ft^2	2 x 10^5	1.5 x 10^5
Heat Flux, Btu/hr-ft^2	3 x 10^5	3.5 x 10^5
Inlet		
Temp, °F	900	900
Pressure, psig	900	900
Heat Added, Btu/lb	520	810
Outlet		
Temp, °F	1073	1233
Pressure, psig	57	494
Conversion	0.41	0.57
Maximum Temp, °F		
Outside Tube Wall	1202	1402
Fluid at Wall	1142	1323
Fluid in Catalyst	1083	1248

the temperature range 1300-1800°F. Such information is being supplied to assist in screening hydrocarbon fuels for application to supersonic combustion systems and in the analysis of the supersonic combustion of hydrocarbons.

Using the same techniques described in previous reports, work was done on three high-boiling materials: n-dodecane, decalin, and α-methyl decalin, to extend the range of conditions under which they had been studied. Two new species, ethane and ethylene were investigated. A few additional experiments were done on methane and propane as fuels. Results are tabulated in Tables 76 through 82 in the Appendix.

Ethane and Ethylene

Our previous survey of ignition characteristics of hydrocarbons has not included the C_2's. They have not been seriously considered as potential heat sink fuels since they appear to offer no significant advantages over methane as cryogenic fuels. Furthermore, the highly refractory nature of methane led us to anticipate that the C_2's would also require at least somewhat more severe conditions for ignition than the higher molecular weight hydrocarbons and hence be no more attractive as potential fuels for supersonic combustion. However, recently White[34] reported that acetylene and ethylene have ignition delays similar to and in some cases shorter than hydrogen in very lean mixtures under low pressure conditions. It was therefore agreed to include ethane and ethylene in our experimental program; in these cases extending the range of conditions to leaner mixtures than we had studied with most other hydrocarbons in order to allow a cross comparison of our results for ethylene with those obtained by using a different experimental technique.

For ethylene, in lean and dilute mixtures, the results we obtained compared well with White's correlation. Figure 67 shows a comparison for a set of data obtained with a 1% ethylene plus oxygen mixture in argon at an equivalence ratio of 0.1. Our experimental points indicate ignition delays about 30% shorter than those given by White's correlation as shown in Figure 67, which he represented by

$$\log(\tau[O_2]^{1/3}[C_2H_4]^{2/3}) = -11.0 + \frac{17,900}{4.58T} .$$

It is significant that these data, in addition to agreeing reasonably well in magnitude, also support the low temperature coefficient of the correlation; viz., an activation energy for ignition of 17.9 kcal/mole.

At higher concentrations of fuel, our data indicate a radical change in the dominant ignition process, since the apparent activation energy increases to about 37 kcal/mole. In our experiments the boundary of the low activation energy region in which White's correlation applies appears to be set by the concentration of ethylene being less than about 10^{-5} moles/liter, rather than by a critical value of the fuel-oxygen ratio. At an equivalence ratio of 0.1, the low activation energy behavior was observed when the fuel plus oxygen concentration was 1%m but not when the fuel plus oxygen concentration was 10%m or 20%m.

In the region of more practical importance, with higher ethylene concentration, the ignition delay continues to decrease with the first power

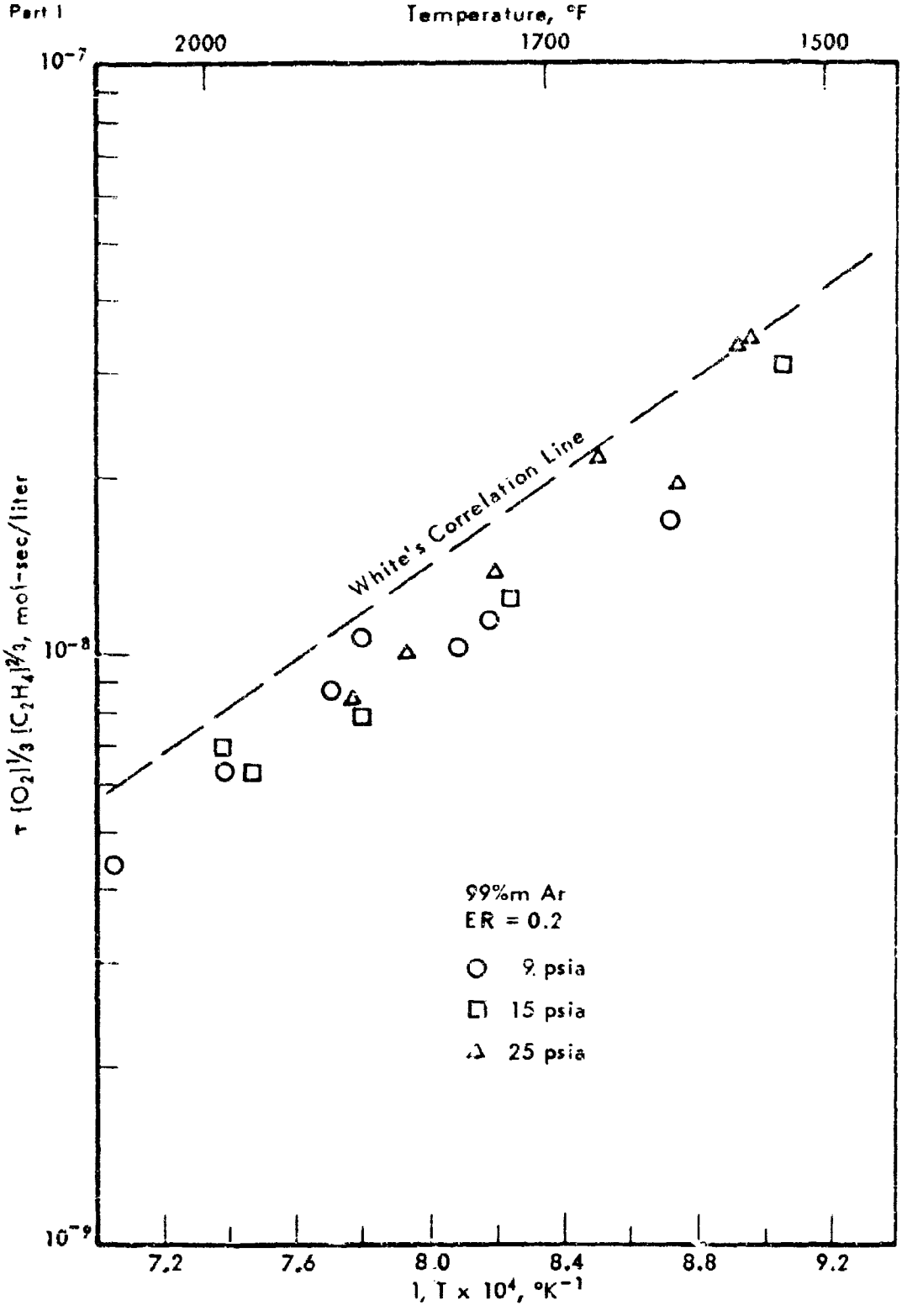


Figure 67. COMPARISON OF ETHYLENE IGNITION DATA WITH WHITE'S CORRELATION

of pressure. This pressure dependence appears to be due to dependence upon the concentration of reactants only (oxygen plus ethylene), not involving any dependence upon the concentration or partial pressure of the inert diluent. The ignition delay decreases almost proportionately to the concentration of total reactants from 1% to 20%m. This strong dependence upon concentration results in the lowest delays we have measured for any hydrocarbons in 20%m reactant mixtures. Figure 66 shows data obtained at this concentration with an equivalence ratio of 0.1.

A further difference between ethylene and the higher hydrocarbons we have studied previously is the occurrence of a minimum in ignition delay as a function of equivalence ratio. The form of White's correlation clearly shows the ignition delay decreasing with increasing fuel concentration (ca equivalence ratio) in the lean and dilute region. This pattern holds even in the more concentrated fuel mixtures (in which a stronger dependence of delay upon temperature was observed) up to an equivalence ratio of about 0.5. At this equivalence ratio a minimum delay time is reached; further increases in fuel-to-oxygen ratio increasing the delay. On the basis of the existence of this minimum delay region, we would predict by extrapolation that the ignition delays for stoichiometric ethylene in air would be about the same as those measured for equivalence ratios of 0.1 or 0.2 in the mixtures with 80%m argon; thus, at 1 atm, the anticipated temperature for a 1 millisecond delay would be 1400-1450°F (compared to 1550-1600 for MCH).

The quantitative ignition behavior of ethane was similar to that of ethylene. Ignition delays depended upon pressure to the inverse first power throughout the region studied. A minimum in ignition delay with equivalence ratio was observed centered about an equivalence ratio of 0.5, but this minimum was much broader and less marked than with ethylene. A low fuel concentration region in which the influence of temperature on ignition delay was lower than normal was also observed, bounded by an ethane concentration of about 10^{-5} moles/liter. However, the effect of reactant concentrations, in particular oxygen concentration on ignition delay was much less for ethane than for ethylene. Thus, although in very lean and dilute mixtures these two C_2's have about the same ignition delays, in mixtures of greater practical interest (i.e., 20% total reactant) ethane has ignition delays significantly larger than ethylene, and in fact these lie in the region characteristic of the higher molecular weight paraffins.

The data obtained for ethane ignitions have been divided into three regions of independent variables, and approximate correlations obtained for ignition delay in each region. The correlating equations are given:

1. Very lean and dilute mixtures with

$$(C_2H_6) < 10^{-5} \text{ m}/\ell$$

$$\log_{10} [\tau (C_2H_6)^{1/2} (M)^{1/2}] = -10.0 + \frac{18,000}{4.58T}$$

where τ is in seconds, (C_2H_6) in moles/liter and (M) represents the total concentration of all species including inerts.

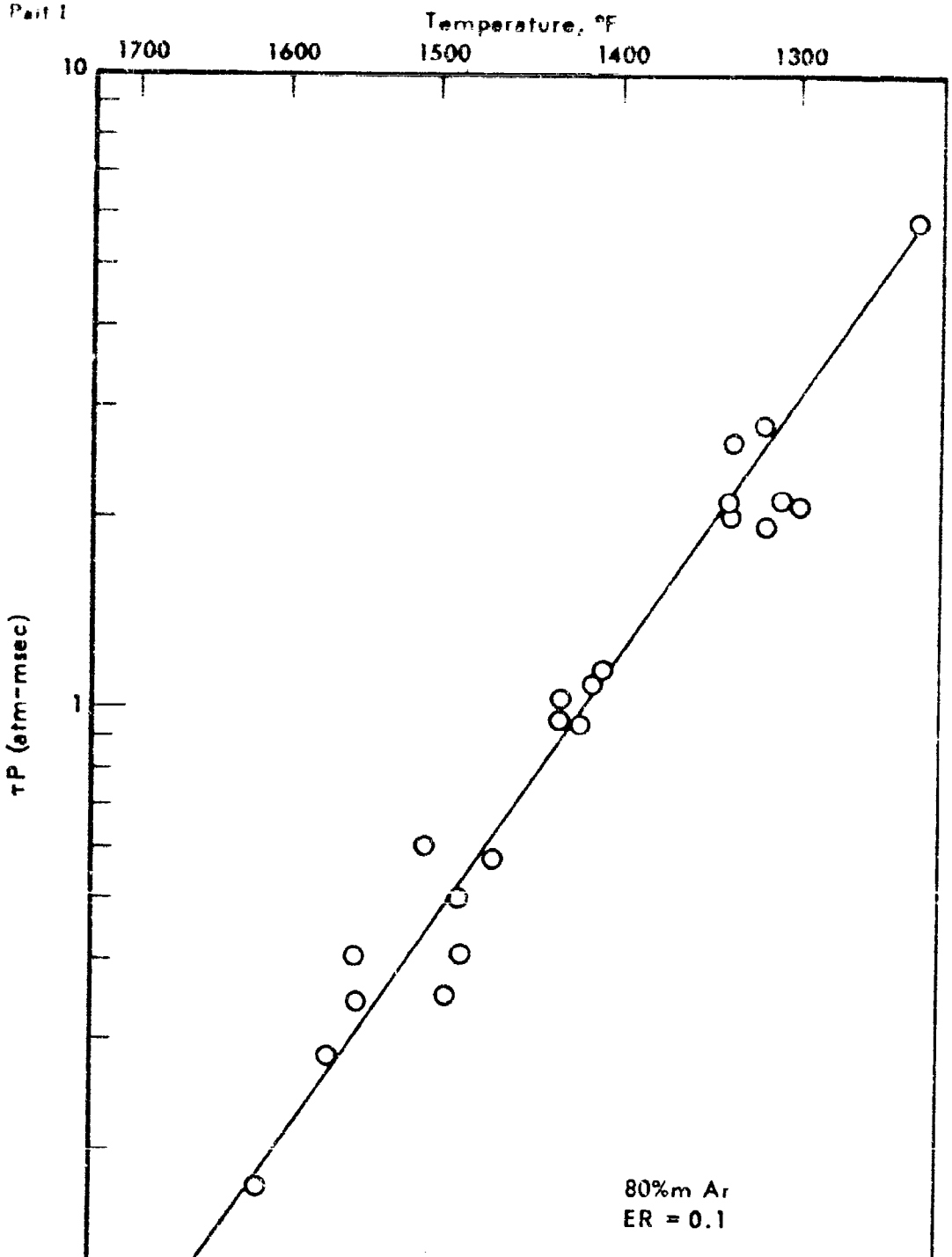


Figure 68. IGNITION DELAYS FOR ETHYLENE

62392

a. Lean, with $(C_2H_6) > 1 \times 10^{-5}$ m/l:

$$\log_{10} [\tau(M)] = -13.50 + \frac{35,000}{4.58T}$$

b. Near stoichiometric

$$\log_{10} [\tau(O_2)^{3/2}(M)^{1/2}/(C_2H_6)] = -10.56 + \frac{35,000}{4.58T}$$

These correlations are compared with the experimental data for the appropriate region in Figures 69, 70, and 71.

n-Dodecane

By modification of our procedure in making up the fuel-oxygen-inert premix, it was possible to extend the range of mixtures of n-dodecane studied to slightly higher fuel concentrations. The modification involved making the premix up to a lower total pressure; thus, only a few experiments could be made from each tank of premix. The maximum n-dodecane concentration obtained in this way allowed us to study 1%m fuel plus oxygen in argon at an equivalence ratio of 0.5 and a 5%m fuel plus oxygen at an equivalence ratio of 0.1.

Ignition delays for these mixtures showed close correspondence with those for n-octane under the same conditions both in absolute magnitude and in response of ignition delay to changes in experimental variables (i.e., temperature, equivalence ratio, concentration, and pressure). Thus, the results obtained with these additional mixtures offer support to our previous conclusion that n-octane can be used as a model compound for predicting the ignition delays of heavier n-paraffins.

Decalin and α-Methyldecalin

Similarly, the concentration range for decalin-oxygen argon mixtures was extended by making up the premixes to a lower total pressure. In this case, additional mixes of 10%m decalin plus oxygen with an equivalence ratio of 0.2 and 20%m fuel plus oxygen with 0.1 equivalence ratio were studied. Ignition delays measured for these mixtures followed the same pattern observed for the lower concentrations of decalin - the ignition delay for decalin was identical to that for methylcyclohexane at the same conditions (i.e., temperature, pressure, equivalence ratio, and concentration). Data for one of the mixtures studied are compared with those for MCH in Figure 72.

Two mixes with α-methyldecalin as fuel were made up to fairly low fuel concentrations (1% and 10%m fuel plus oxygen, both at 0.1 equivalence ratio) for exploratory determination of the ignition behavior of this bicyclic naphthene. Measurements with this fuel gave ignition delays which were indistinguishable from those of decalin (and MCH). Apparently the methyl substitution on the decalin has no significant influence on its ignition delay.

Methane

Ignition delays were measured for one additional methane mixture, 80%m argon, with an equivalence ratio of 0.1. We believe these data presented

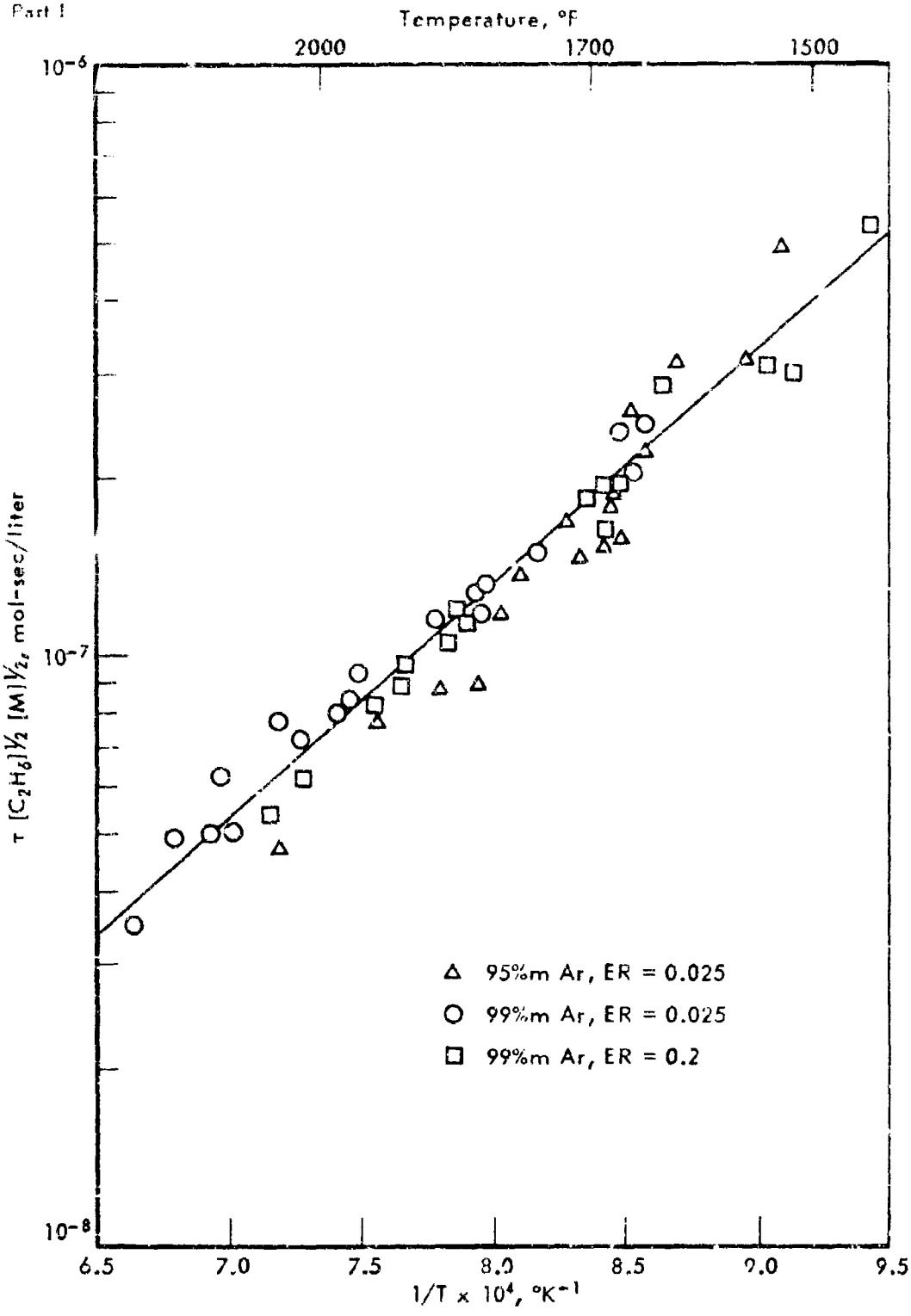


Figure 69. CORRELATION OF IGNITION DELAYS FOR VERY LEAN AND DILUTE ETHANE MIXTURES

62392

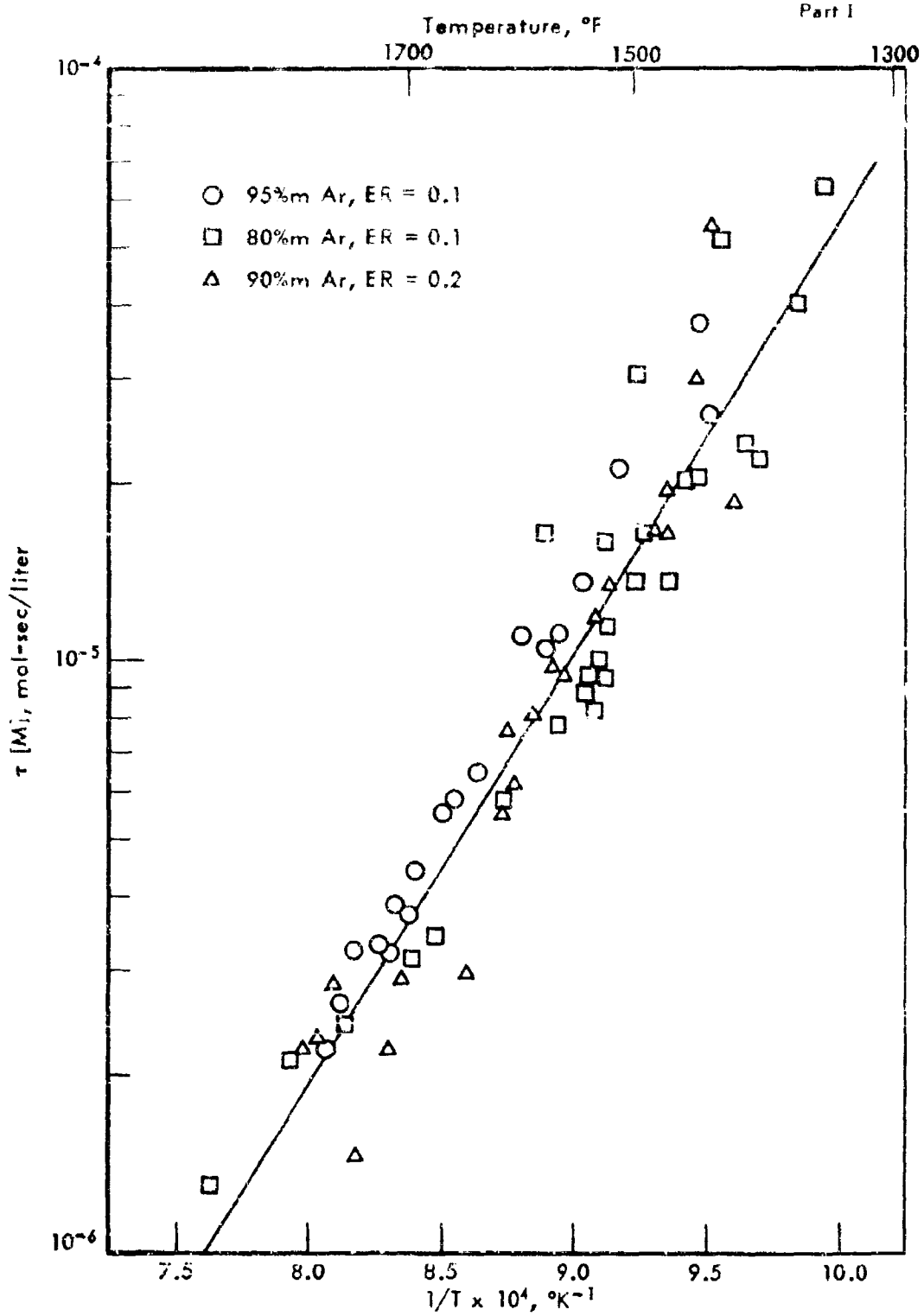


Figure 70. CORRELATION OF IGNITION DELAYS FOR LEAN ETHANE MIXTURES

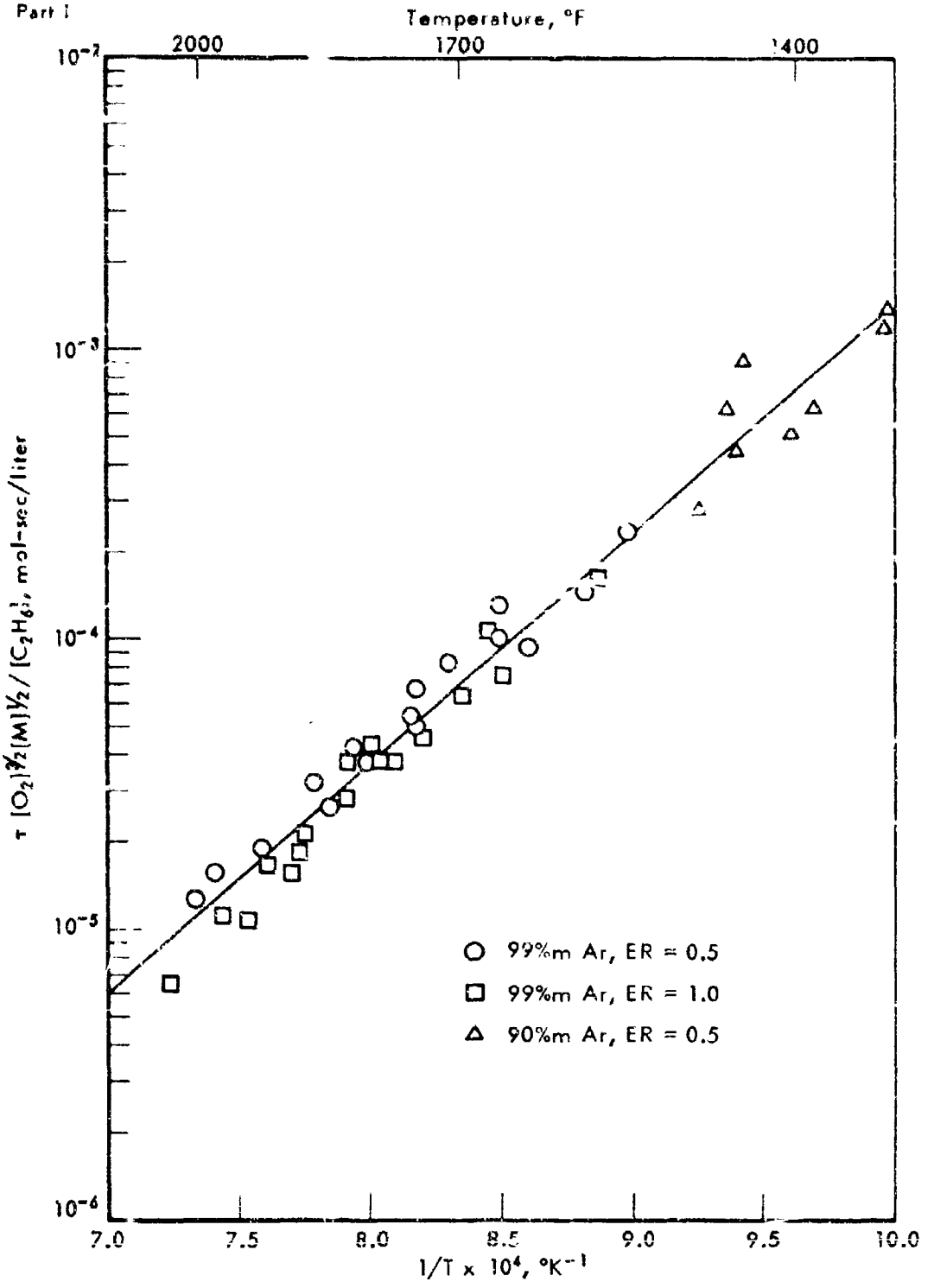


Figure 71. CORRELATION OF IGNITION DELAYS FOR NEAR STOICHIOMETRIC MIXTURES WITH ETHANE

62392

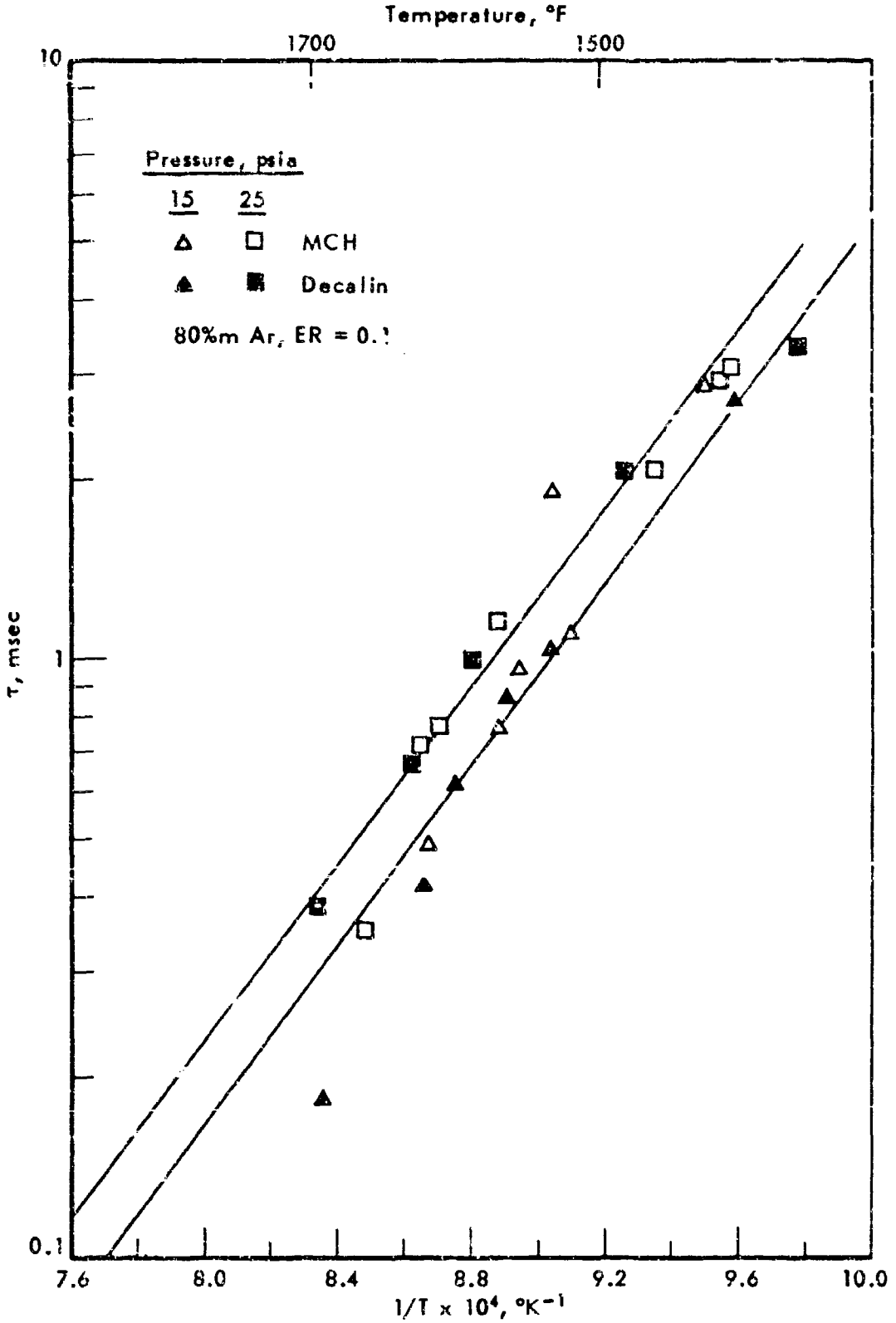


Figure 72. COMPARISON OF IGNITION DELAYS FOR MCH AND DECALIN

in Figure 72 give a realistic lower bound to the ignition delays which can be expected with methane-air mixtures at moderate pressures. These and previous data at somewhat richer but more dilute mixtures (APL-TDR 64-100 Pt II) indicate an inverse first order dependence of delay on total pressure and a temperature coefficient corresponding to an activation energy of about 25-30 kcal/mole for ignition of methane in lean mixtures. This is in contradistinction to the activation energy of 45-50 kcal/mole indicated by the data of Skinner and Ruehrwein[35] and Asaba et al.[36] [Ninth Symposium on Combustion, p. 195f (1963)] and our own earlier data for mixtures on the rich side of stoichiometric. The present body of data for lean mixtures is inadequate to define the dependence of ignition delay on the separate concentrations of oxygen and fuel. However, the data indicate that in the region studied delays decrease with increasing oxygen concentration and increase with increasing fuel concentration probably throughout the whole region. Thus increasing the equivalence ratio above the value of 0.1 at which the present measurements were made will certainly increase the delay above the measured value.

Examination of Experimental Method and Equipment

A second major area of work undertaken has been to determine experimentally the limitations of the present method and equipment (as used for the past two years) and to consider the capabilities of additional instrumentation for improving both the accuracy and kind of results obtained. Since these experiments were aimed at examination of experimental methods, they were restricted to fuels and mixture ratios which had been examined previously. Thus, the results presented in Tables 83 through 86 in the Appendix do not cover new fuels or wider ranges of conditions than those previously reported.[2,3] The conclusions based upon these experimental results may be grouped into three general categories: 1) those bearing upon limitations of our method for determining ignition delays; 2) the potentiality for improvement of detection of ignition delay by using observation of infrared emission from the igniting gas; and 3) the possibility of obtaining additional information on pre- and post-ignition phenomena by observing infrared emission as a function of time. Because the use of infrared detection equipment was an integral part of each of these categories, a brief description of the equipment used is given before further discussion of the conclusions reached.

Infrared Equipment

The additional equipment used allowed observation of infrared emission at specific wavelengths from the gas before, during, and after ignition. The observation of infrared emission is made in the same plane (approximately 17 feet from the diaphragm of the shock tubes) used for measurement of visible light emission and observation of pressure. The radiation is allowed to pass through a sodium chloride window into the monochromator of a Beckman IR-7 infrared spectrophotometer. The monochromatic radiation separated by this instrument is detected by either an indium antimonide detector cooled to liquid nitrogen temperature or a copper-doped germanium detector cooled to liquid helium temperature. The signal from the detector is amplified by a Tektronic type 122 low level preamplifier and then fed to an oscilloscope where the intensity of the

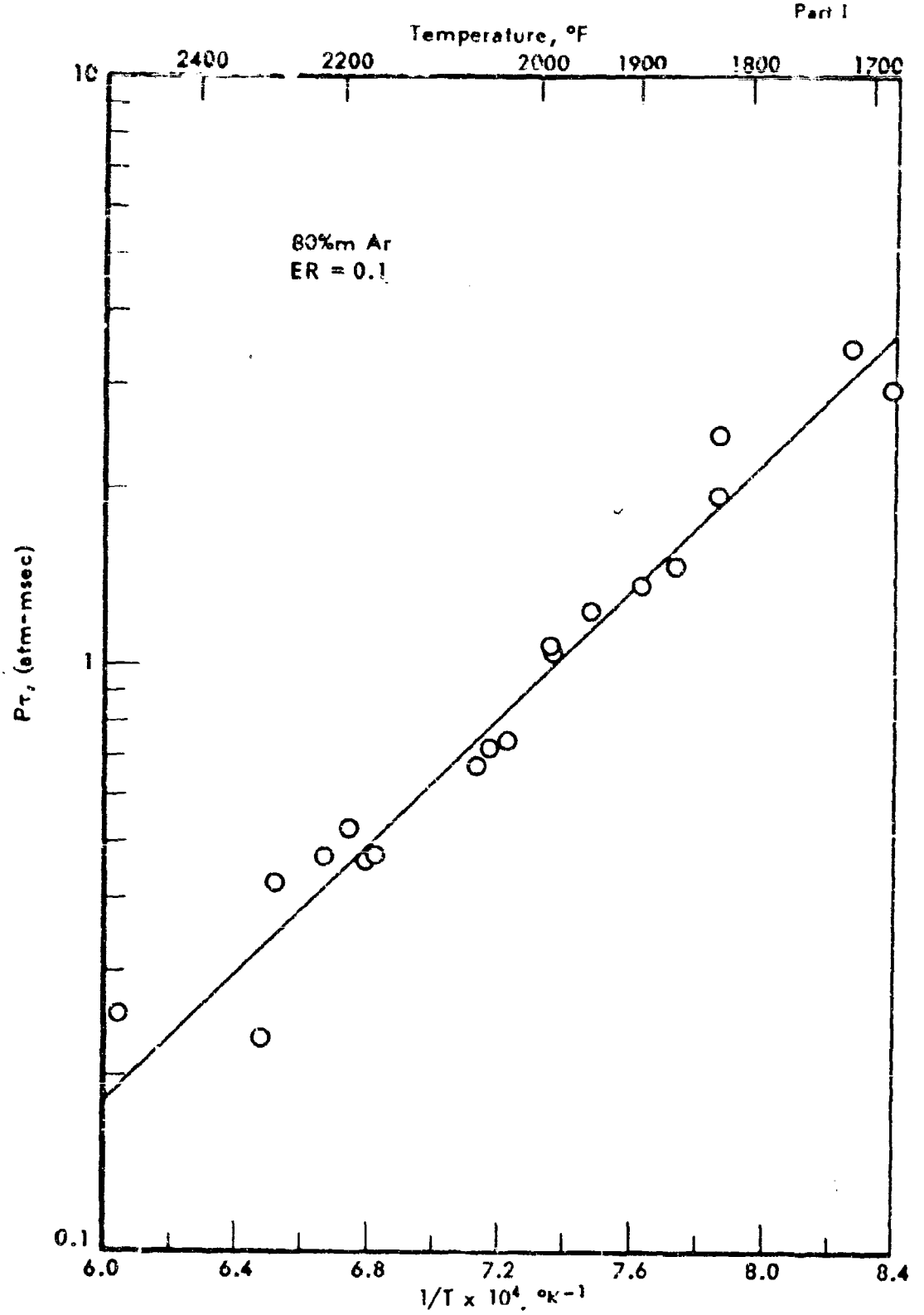


Figure 73. IGNITION DELAYS FOR METHANE-OXYGEN-ARGON

emission at the frequency set on the monochromator is displayed as a function of time. Several frequencies could be examined under the same conditions by repeating the experiment in the shock tube with the monochromator set for a different frequency for each run.

The principal advantage gained by observing infrared emission is the ability to detect the appearance and growth of concentration of particular molecular species. If the frequency observed is properly selected, it can be clearly associated with the presence of a particular molecular species (e.g., CO_2, H_2O, CO). Thus, the observed event of ignition using this method is the appearance of the species associated with the frequency being followed. Furthermore, since the intensity of emission is dependent upon the concentration of the emitting species, the possibility exists that the time histories of concentrations of particular species (during the combustion process) can be obtained from the infrared emission traces.

Limitations of the Experimental Method

The objective of the experiments in the shock tube is the measurement of the time between heating of the gas by the shock wave and the detectable onset of combustion. In our equipment, the measurement made at a given point along the tube is the time between passage of the shock wave and the combustion front (or wave). Fundamental to the interpretation of this measured quantity as proportional to the ignition delay is the assumption that both shock wave and combustion front are well-developed fronts moving along the tube at the same, constant velocity, with a fixed distance between them. This condition is approximately met in our apparatus except for mixtures in which it is possible for the flame front to develop into a detonation. Then, the first formation of the flame front occurs some distance behind the shock wave. However, the flame front accelerates, once formed, until it overtakes the original shock wave. In one limiting case, the detonation is fully developed before reaching the point at which it is observed. Then, the pressure and temperature rise and velocity of the wave are characteristic of a detonation in the mixture composition and not related to the shock wave parameters. Under somewhat less severe conditions the shock wave and flame front have merged but the detonation is not yet fully developed. These two cases yield no information from which a delay time could be calculated. They are easily recognized since the apparent delay time is zero (the flame front coincides with the shock front) and the pressure rise at the front is usually excessive for the conditions of the experiment. With slightly less severe conditions yet, the flame front has not yet merged with the shock front at the observation point. An apparent (but not physically meaningful) delay time is observed in such a case, and the fact that the flame front is accelerating is not readily detected. Fortunately, such behavior is observed only under conditions very near to those giving a more recognizable detonation and even then, the apparent delay is very sensitive to experimental conditions. The capability of detonation of certain mixture compositions places severe restrictions on the range of mixture ratios and concentrations for which we are able to study ignition delays with the method and equipment we have been using. For all of the hydrocarbons studied, no detonations have been observed for even stoichiometric mixtures containing one percent or less oxygen. At five percent oxygen, stoichiometric mixtures can no longer be studied and mixtures as lean as 0.5 stoichiometric have shown detonations. With increasing oxygen

concentration, the detonable region extends to even lower equivalence ratios. So long as the method used involves some lapse of time following the initial development of the ignition front in the apparatus, before the ignition delay is measured, there seems little possibility of removing this limitation on the composition of mixtures which can be studied.

A second apparatus factor which has not been taken into account up to the present time results from the fact that the shock wave velocity is attenuated by friction in the tube and moves at a velocity which decelerates slightly as the wave progresses down the tube. As a consequence of this attenuation, the pressure and temperature rises following the shock decrease as the wave progresses down the tube. The pressure profiles obtained in our experiments indicate a decrease in pressure following the shock of the order of 6-10% as the wave moves from the diaphragm end to the observation plane. The order of attenuation of shock strength is compatible with that found by others in studies of this phenomenon.[37] In itself, this pressure decrease is not very important because ignition delay is not very sensitive to pressure. However, this pressure decrease is accompanied by a corresponding drop in temperatures following the shock. Thus, gas compressed by the shock wave near the diaphragm end may be heated 50-75°C hotter than gas compressed by the same wave, later, at the observation plane. In all of the reported data, the temperature reported has been calculated from the shock velocity measured in the two-foot interval immediately upstream of the observation plane. This temperature is very nearly correct for short ignition delays (<600 μsec), since for these cases the gas observed igniting was shocked within this two-foot interval. For long ignition delays, the gas observed igniting was compressed much nearer the diaphragm and to a significantly higher temperature. A first-order correction for attenuation may be applied by adding to the reported temperature an increment proportional to the measured ignition delay, with a maximum correction of 50-75°C applied to the temperatures corresponding to observed delays of 3500 μsec. The effect of this correction on correlation of ignition delays is to raise the apparent temperature coefficient of ignition slightly and to bring the points corresponding to long ignition delays into better correlation with the remainder of the data. This is shown in Figures 74 and 75. The data are shown in Figure 74 without correction of the temperature for shock wave attenuation. In Figure 75 a maximum increment of 60°C was added to the point with longest delay and the temperatures for shorter delays were incremented proportionately. The dotted line in Figure 75 is the line from Figure 74 and the solid line is the new line of best fit for the corrected points. We have not yet attempted to review our earlier data to make corrections for shock wave attenuation. However, data obtained subsequently and discussed in the following sections have been corrected for this effect.

Detection of Ignition by Infrared Emission

A number of series of experiments were carried out using infrared detection equipment in order to determine whether this method could be used to determine the onset of combustion and whether it offered significant advantages over visible light detection. Observation of emitted radiation was concentrated on frequencies characteristic of two combustion products, CO_2 at 2300 cm^{-1} and CO at 2050 cm^{-1}. Of these two, because of the more intense emission by a given concentration and consequently higher potential

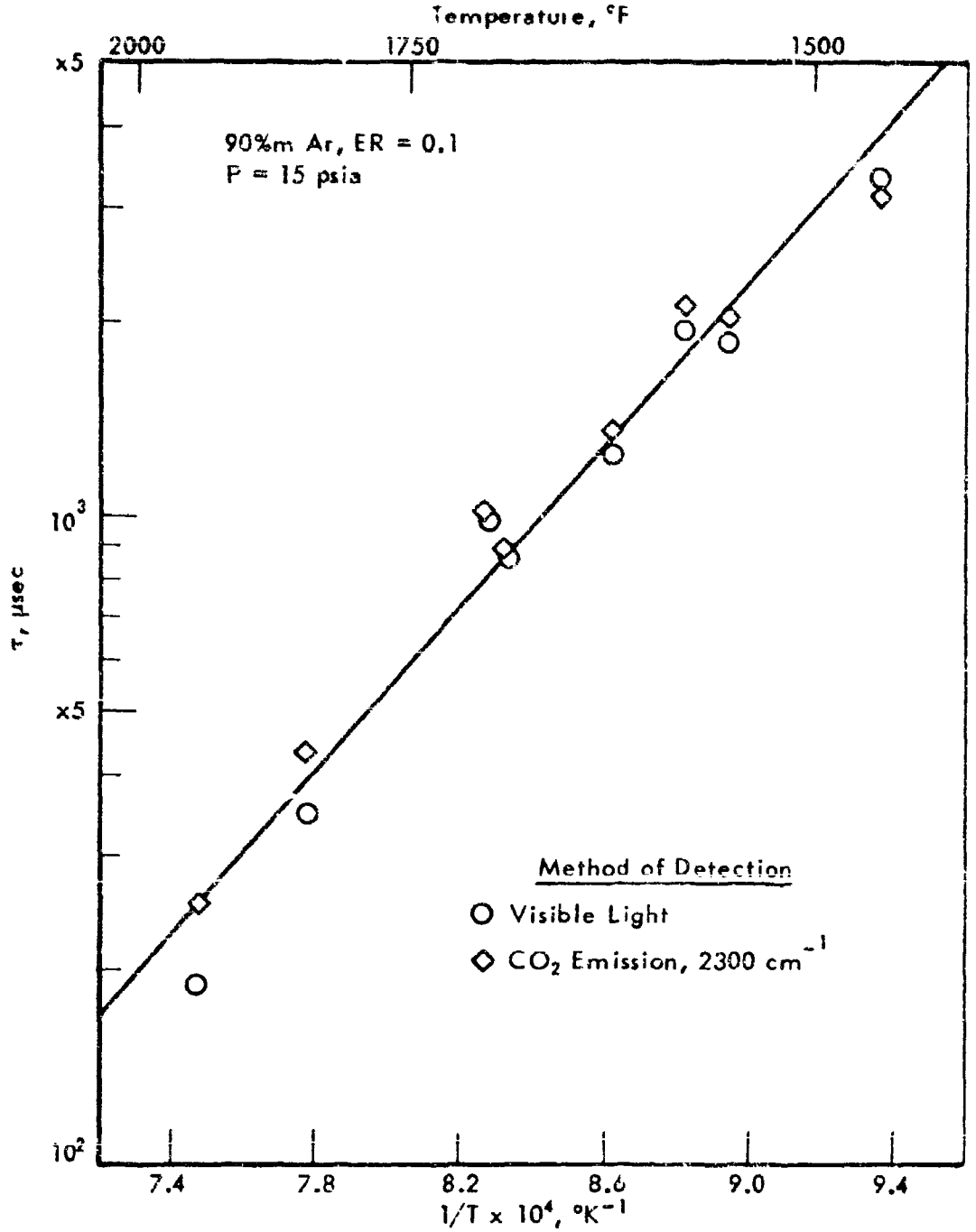


Figure 74. COMPARISON OF IGNITION DELAYS DETECTED BY TWO METHODS FOR A PROPANE-OXYGEN-ARGON MIXTURE

62731

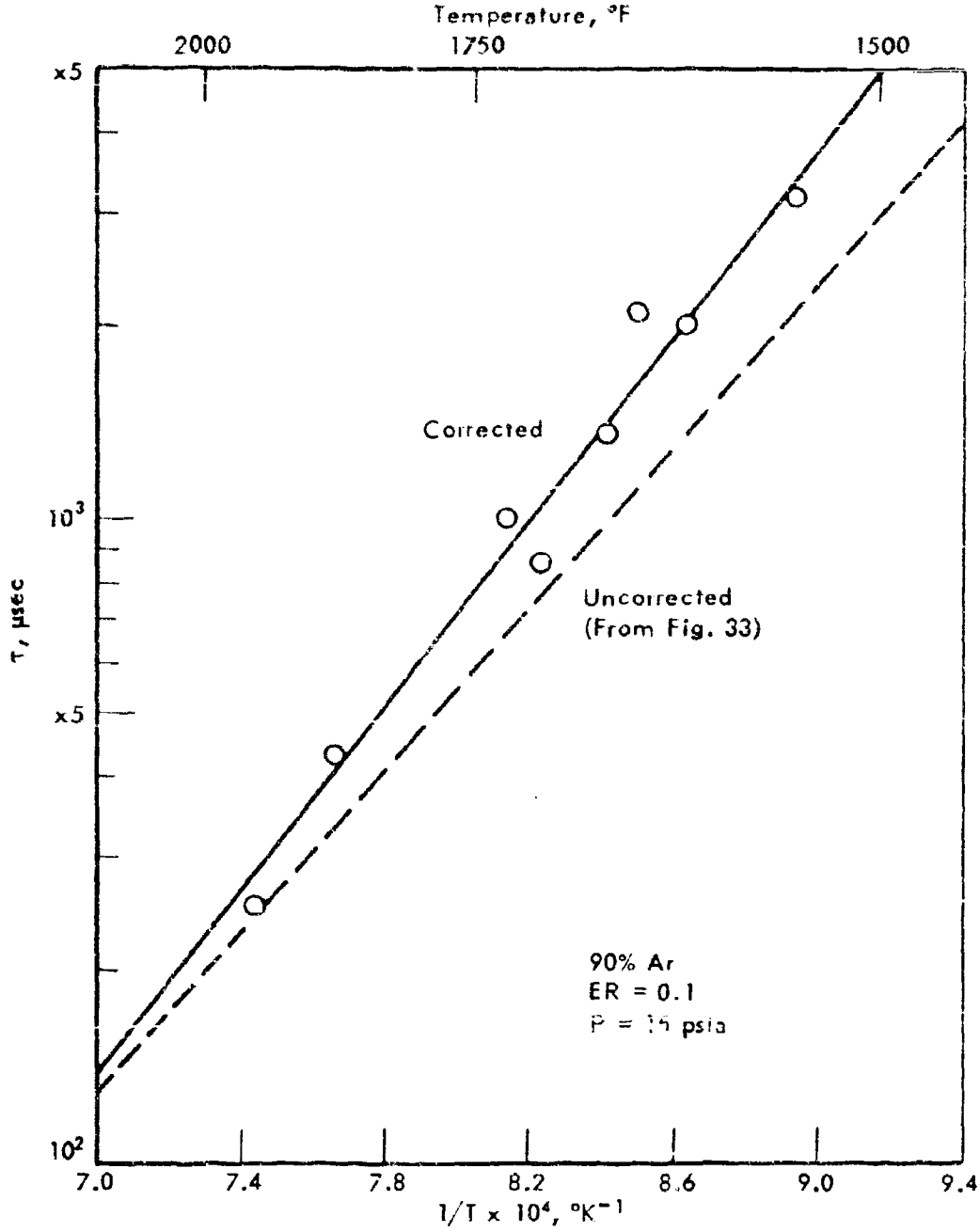


Figure 75. IGNITION DELAYS FOR PROPANE-OXYGEN-ARGON WITH TEMPERATURE CORRECTED FOR SHOCK WAVE ATTENUATION

signal-to-noise ratio in the recorded signal, CO_2 appeared to be the more promising combustion product to observe.

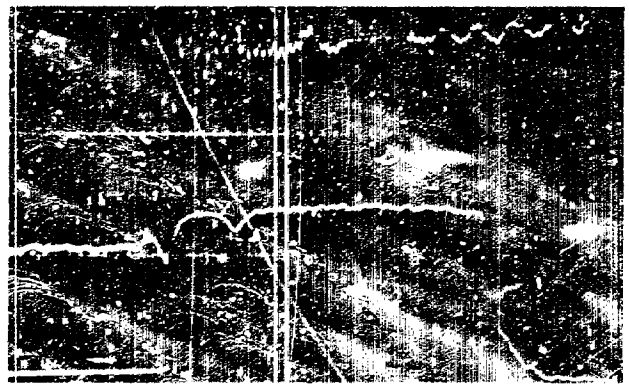
Figures 76a and 76b show calibrations obtained when 5%m CO_2 and 5%m CO in argon were shock-heated to a temperature of 1250°C. Although the gains used in amplifying the two signals were adjusted to give about the same maximum height of the trace, the higher signal to noise ratio obtained for CO_2 is apparent. For both species, the infrared emission (lower trace in each picture) begins to rise, very closely coincident with the pressure increase of the shock wave (upper trace in each picture). For CO_2, there is neither lag of emission behind the pressure trace which would indicate some additional relaxation process between forming heated molecules and their starting to emit, nor lead which would be a consequence of detection of light reflected ahead of the shock front. The CO emission builds up much more slowly to its maximum value.

With visible light detection, it has been observed under detonation or near detonation conditions that light is detected at the measurement station as much as 100 μsec ahead of the shock front pressure rise. Such a phenomenon can only be the result of detecting light reflected ahead of the actual combustion front. Thus, particularly for short ignition delays there has always been the question of whether the time of arrival of the combustion front was being taken erroneously from the detection of this reflected light. In the case of infrared detection, not only do the calibrations indicate no significant reflected radiation ahead of the front, but under detonation conditions, the delay observed goes to zero (emission coinciding with the pressure rise) as it should. This improvement in measurement of short ignition delays with the infrared equipment is probably due primarily to the superior inlet collimation system used with the monochromator.

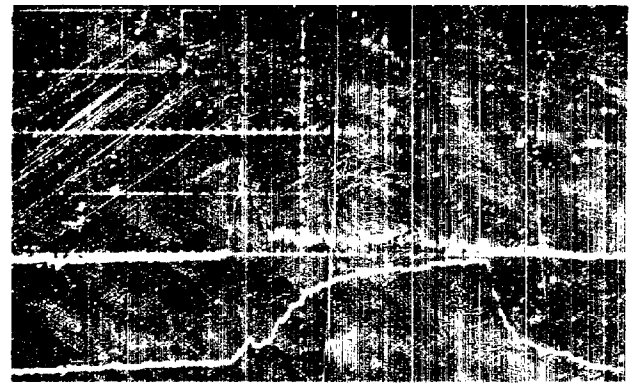
Figures 76c and 76d show comparisons of the CO_2 (lower) and visible light (upper) traces obtained in two experiments. These indicate CO_2 emission starting to rise very slightly after the first visible light is observed. From pictures such as these it appears that the onset of combustion can always (with hydrocarbons) be determined with at least as great precision from the CO_2 emission as from visible light, and in some cases (as in Figure 76c) with much better definition. Figure 77 shows a comparison of a series of ignition delays determined for a propane fuel mixture using both methods of detection. The agreement of the two methods is quite good down to delays of 500 μsec. Below this, visible light tends to indicate significantly shorter delay times, probably because of observation of light reflected ahead of the combustion zone. In this region delay times determined from CO_2 emission are of greater accuracy.

Figure 77 shows results from two sets of experiments. In each set (a and b or c and d), the IR emission was monitored first at 2300 cm^{-1} (CO_2) and then the experiment repeated monitoring at 2050 cm^{-1} (CO). These traces show the much better signal-to-noise ratio and clearer definition of ignition obtained by following CO_2 emission.

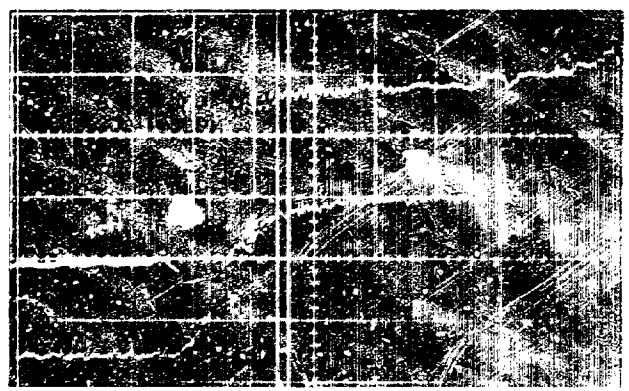
One further feature of the IR emission traces in Figures 76 and 77 which should be mentioned is the abrupt decrease in emission 1000-1200 μsec after the shock wave. This cessation of emission is due to the arrival of the contact surface between the driver gas (helium) and the fuel mixture at



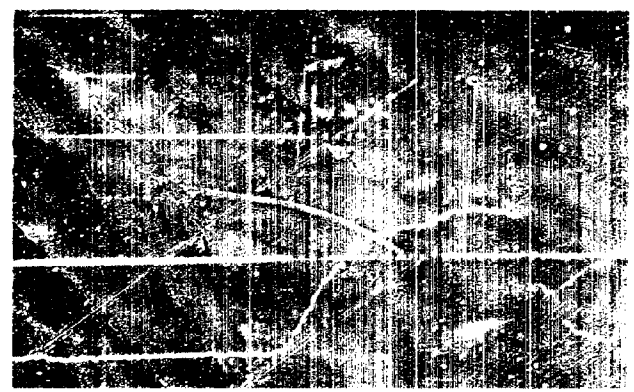
a) CO_2



c) Visible



b) CO

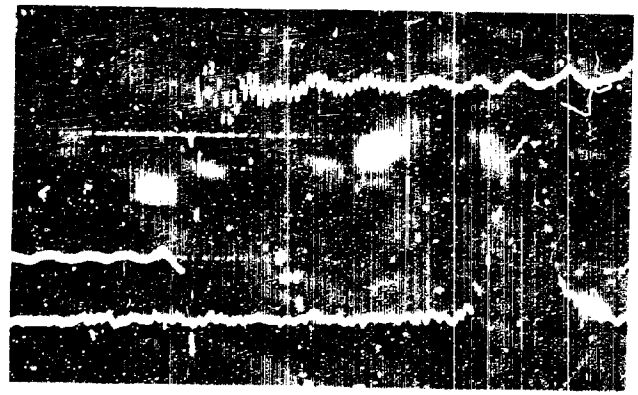


d) CO_2 IR

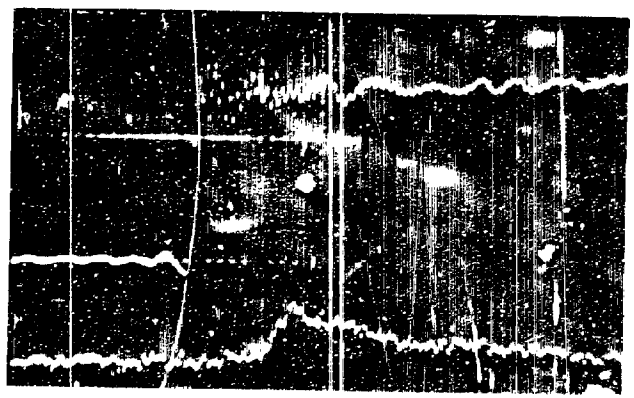
Figure 76. OSCILLOSCOPE TRACES SHOWING IR EMISSION FROM CO_2 AND CO CALIBRATION MIXTURES, AND COMPARISON OF CO_2 AND VISIBLE LIGHT EMISSION AT IGNITION



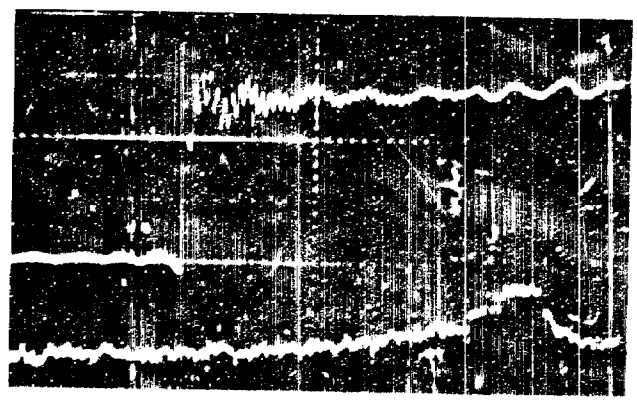
a) CO_2



c) CO_2



b) CO



d) CO

Figure 77. OSCILLOSCOPE TRACES SHOWING CO_2 AND CO IR EMISSION FOR IGNITION OF TWO PROPANE MIXTURES

this time. The arrival at 1000-1200 μsec of the contact surface at the observation window sets an upper limit of about 3500 μsec to the ignition delay times which can be measured in this apparatus.

With the more sensitive and accurate method of detection of ignition by emission from CO_2 in the 2350 cm^{-1} band of the infrared available, it appeared possible to reduce the lower limit of delay times which could be measured with confidence. Equipment was assembled to allow control of the triggering of the oscilloscope used to display the output from pressure transducer and IR detector, which enabled using a higher sweep rate on this oscilloscope to obtain a higher time resolution on the photographic record of the delay time data. While previously, sweep rates were limited to 100 μsec/cm or greater, with the additional control of triggering, sweep rates down to 10 μsec/cm have been used in recent experiments. With this increased resolution of data, delay times down to about 50 μsec have been measured; and we have reasonably high confidence in measurements down to about 100 μsec. This represents an increase of about a half-order of magnitude in the possible range of measurements.

A few measurements have been made of the initial rate of increase of CO_2 concentration following ignition of paraffins in lean mixtures. In these cases, a calibration for CO_2 concentration was obtained by running some auxilliary experiments with a mixture containing no fuel, but CO_2 equivalent to total combustion of the fuel in the mixture being studied. This gave a signal strength for maximum emission from the mixture following combustion. Signal strength from lower concentrations was assumed proportional to concentration. These measurements are discussed, together with ignition delay measurements for the compounds studied in the following section.

Determination of Concentration Histories of Molecular Species

As a reference for the development of analytical models of combustion of the fuels we have studied, it would be desirable to have not only the ignition delays for these fuels, but in addition measurements of concentration histories of at least some of the intermediates and combustion products during the course of combustion. Since the infrared monochromator and detector system which we have been using detects a signal whose intensity is dependent upon the concentration of the emitting species, it has a potentiality for providing this type of information. We have investigated both analytically and experimentally the problems involved in implementing this potentiality. The conclusion reached is that such information probably could be obtained for a limited range of fuel-oxygen-inert compositions. However, the effort required to obtain such information would be considerably greater than has been planned for combustion research under this contract. Whether this effort would be justified by the value of the data obtained is a matter that would have to be carefully studied before proceeding further.

The factors limiting compositions are the same for this case as for ignition delays. Thus, the region of most interest, near-stoichiometric mixtures containing about 20% oxygen, could not be investigated. In the study of ignition delays, the reaction follows a near isothermal course up to the point of ignition. However, if concentrations were followed beyond this point, through the exothermic combustion zone, the reaction course would

be nonisothermal and strongly dependent upon the mixture composition, and in particular the heat capacity of the inert diluent. The data obtained from the special compositions with which we work could nevertheless be used in testing analytical models of combustion kinetics, but not at their point of greatest interest.

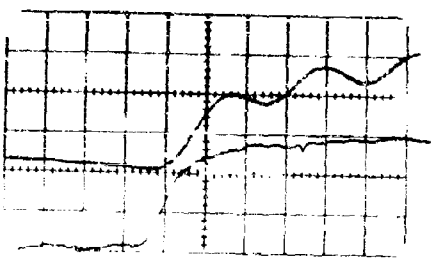
The major problems, however, relate to characteristics of the infrared emission. Except for CO_2, the signal-to-noise ratio of the detected signal for the species of interest does not allow a very precise determination of signal intensity. The intensity of emission is not in all cases linear in concentration of the species emitting, hence considerable calibration would be required to allow interpretation of data in terms of concentrations. Finally, in the case of CO, a strong time-dependence of the intensity of emission was observed in the few calibrations which were run. The separation of this inherent slow rate of rise of emission, from the true rate of change of concentration with time would probably present a formidable problem in interpretation.

Ignition Delays of Paraffins With Unusual Structures

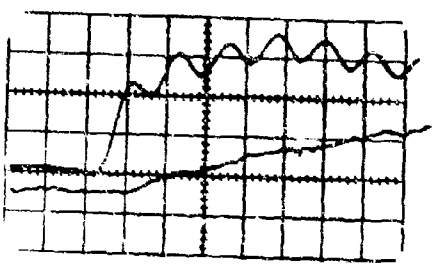
It was decided to reexamine structural effects on ignition delays and to a lesser extent post ignition increase of CO_2 concentration, for paraffins, using the newly available infrared detection techniques. Of particular interest were 2,2,3,3-tetramethyl butane and neopentane, two hydrocarbons of unusual structure in that they are totally branched and contain only primary hydrogens. Normal octane and 2,2,3-trimethyl butane were also incorporated in the experimental program for comparison purposes as more conventional paraffin structures. Experiments were concentrated in a fairly narrow range of operating conditions: 2-1/2 and 5% fuel plus oxygen and equivalence ratios of 0.1 and 0.2. Most experiments were done at 1 atmosphere pressure, but a few at 9 psia. Because of the decrease in the lower limit of measurable delays down to 50-100 μsec, these compounds could be studied over a wider temperature range than was previously possible.

Experimental results obtained are tabulated in the Appendix (Tables 87 through 90). In these tables, temperatures have been corrected for shock wave attenuation, by adding to the temperature obtained from shock wave velocity measurement, an increment proportional to delay time (17°C/ mill second).

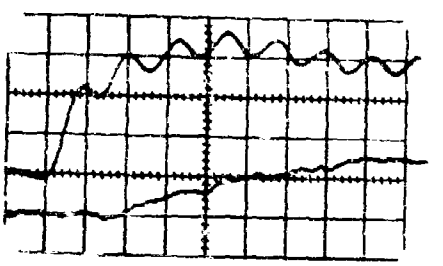
Figure 78 shows examples of oscilloscope traces obtained in various experiments. The upper trace in each case is the output from the pressure transducer and is used primarily to indicate the time of arrival of the shock wave at the measurement plane. (Oscillation superimposed on this trace is due to mechanical ringing.) The lower trace is output from the IR detector monitoring 2350 cm^{-1} and is approximately proportional to CO_2 concentration. Figure 78a was obtained in a calibration run with a mixture of CO_2, oxygen and argon containing CO_2 equivalent to that obtained in complete combustion of the fuel mixes. Observed at a sweep rate of 10 μsec/cm, these traces indicate that response of the CO_2 detector leads the pressure transducer by about 5 μsec. This lead is presumably due to imperfect alignment of the instruments. In subsequent experiments, delay times measured were corrected for this small offset. The trace also indicates rapid rise of CO_2 emission following the shock, and the level of emission to be expected from complete



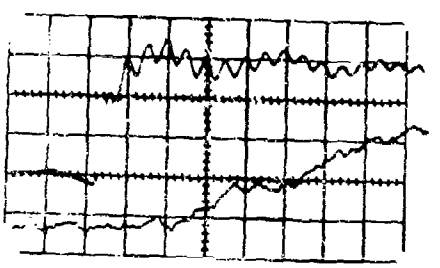
a)



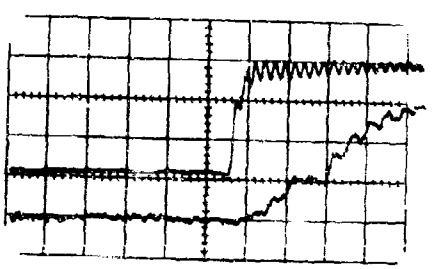
b)



c)



d)



e)

Figure 78. OSCILLOSCOPE TRACES AT HIGH SWEEP RATES FOR OBSERVATION OF IR EMISSION AT 2350 cm^{-1}

combustion. Results from the ignition experiments indicated an ultimate level of CO_2 emission corresponding to complete combustion of carbon in the fuel to CO_2 under all conditions studied. Figures 78b and c, observed at 20 μsec/cm, show results from ignition experiments resulting in fairly short ignition delays. The rise of CO_2 emission following ignition is nearly linear in time for the first 200 μsec, and much slower than the rise observed with the calibration mix, indicating that we are observing formation of CO_2 due to the combustion process. Figure 78d (at 50 μsec/cm) and Figure 78e (at 100 μsec/cm) show unusual behavior consistently observed with all of the hydrocarbons observed in these experiments under short delay conditions. CO_2 emission reaches a plateau level approximately 100 μsec after ignition, which persists until about 250 μsec after the shock wave passage. The level of the plateau is about half the level for complete combustion. No explanation for this behavior is offered. In subsequent interpretation of data, this behavior has not been taken into account.

Ignition delay results obtained with the paraffins followed the same general patterns observed previously. Delays at 9 psia were about 50-50-60% higher at 15 and 25 psia. No effect of pressure was observed between 15 and 25 psia. No significant effect of equivalence ratio was detected between 0.1 and 0.2. The effect of temperature is reasonably represented by an effective activation energy for ignition of about 40 kcal/mole. The effect of oxygen concentration is significant but indicates a dependence of ignition on oxygen concentration somewhat less than first order. These trends are indicated by the data shown in Figure 79 for ignition of n-octane under a variety of conditions. Delay times for the highly branched 2,2 3,3-tetramethyl butane and neopentane showed the same trends with pressure, temperature and concentrations, but were about a factor of two greater than those for n-octane. These are shown in Figure 80 and 81. Delays for less branched 2,2,3-trimethyl butane were only slightly shorter than those for 2,2,3,3-tetramethyl butane.

From these data it is concluded that ignition delay is not greatly influenced by the character of the hydrogens in the original fuel hydrocarbon. The highly branched neopentane and 2,2,3,3-tetramethyl butane contain only primary hydrogens, while n-octane contains predominantly secondary ones, and the intermediately-branched compounds contain tertiary hydrogens. However, this lack of influence of hydrogen character may be due to hydrocarbon cracking prior to ignition, which would cause the delay to be more dependent on the character of the cracking fragments than on the nature of the parent hydrocarbon. Tsang[38] has studied cracking behavior of these hydrocarbons and finds rate constants for cracking of 10^4 sec^{-1} or higher in the middle of the temperature range which we studied. However, since the activation energies for cracking are much higher than for ignition, Tsang's results would suggest that there may be a change in the character of the ignition process at lower temperatures where cracking is slow compared with ignition. On the other hand the difference in behavior of the two types of hydrocarbons (i.e., methane/ethane vs the highly branched ones) may simply be due to the fact that the more complex hydrocarbons have many more degrees of vibrational freedom and hence the chance of localizing sufficient energy in any one C-H bond coincident with a collision with an oxygen atom or molecule is very much greater. The shorter ignition delays and complex temperature response of ethane and ethylene would tend to support this suggestion.

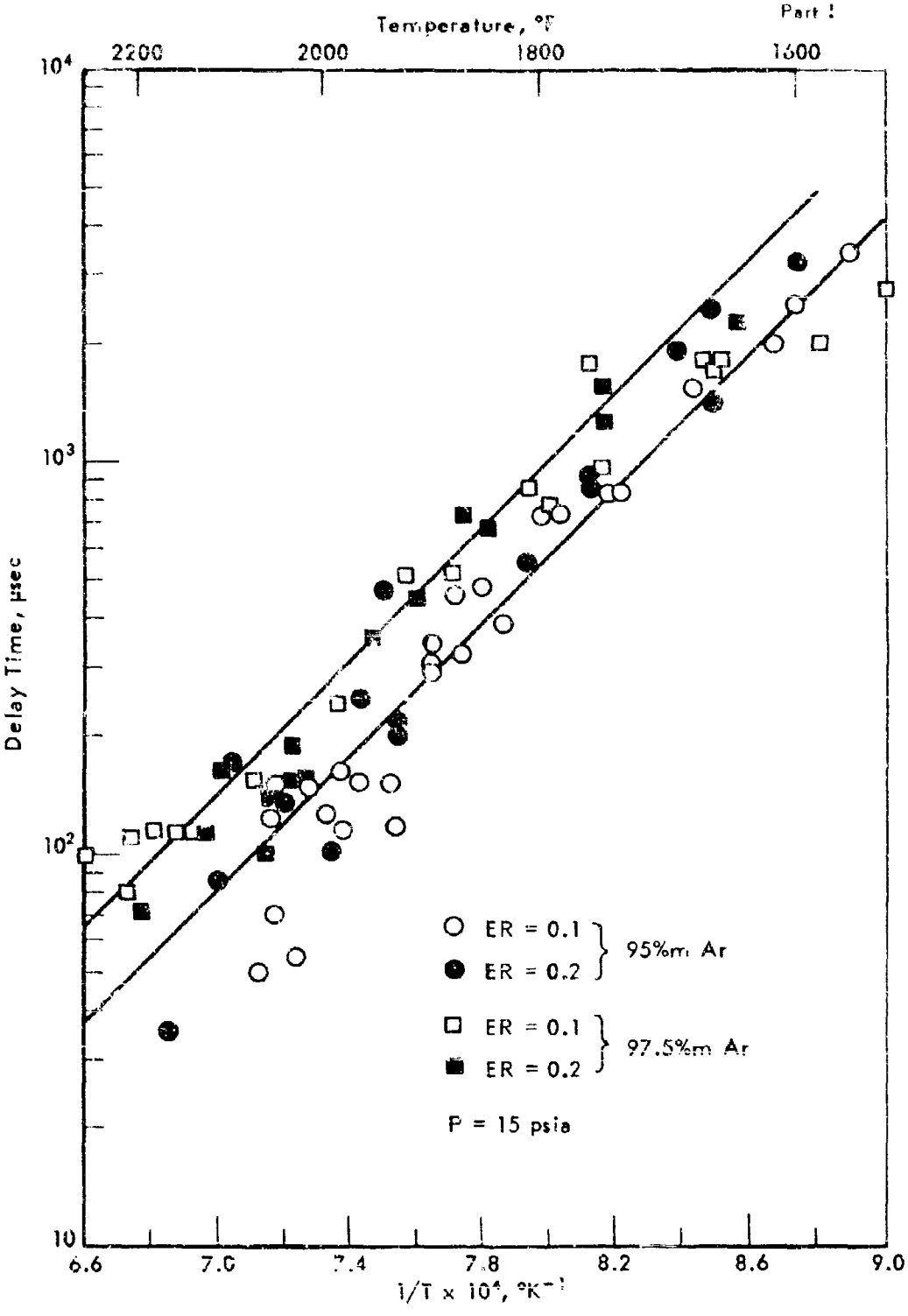


Figure 79. IGNITION DELAY TIMES FOR n-OCTANE

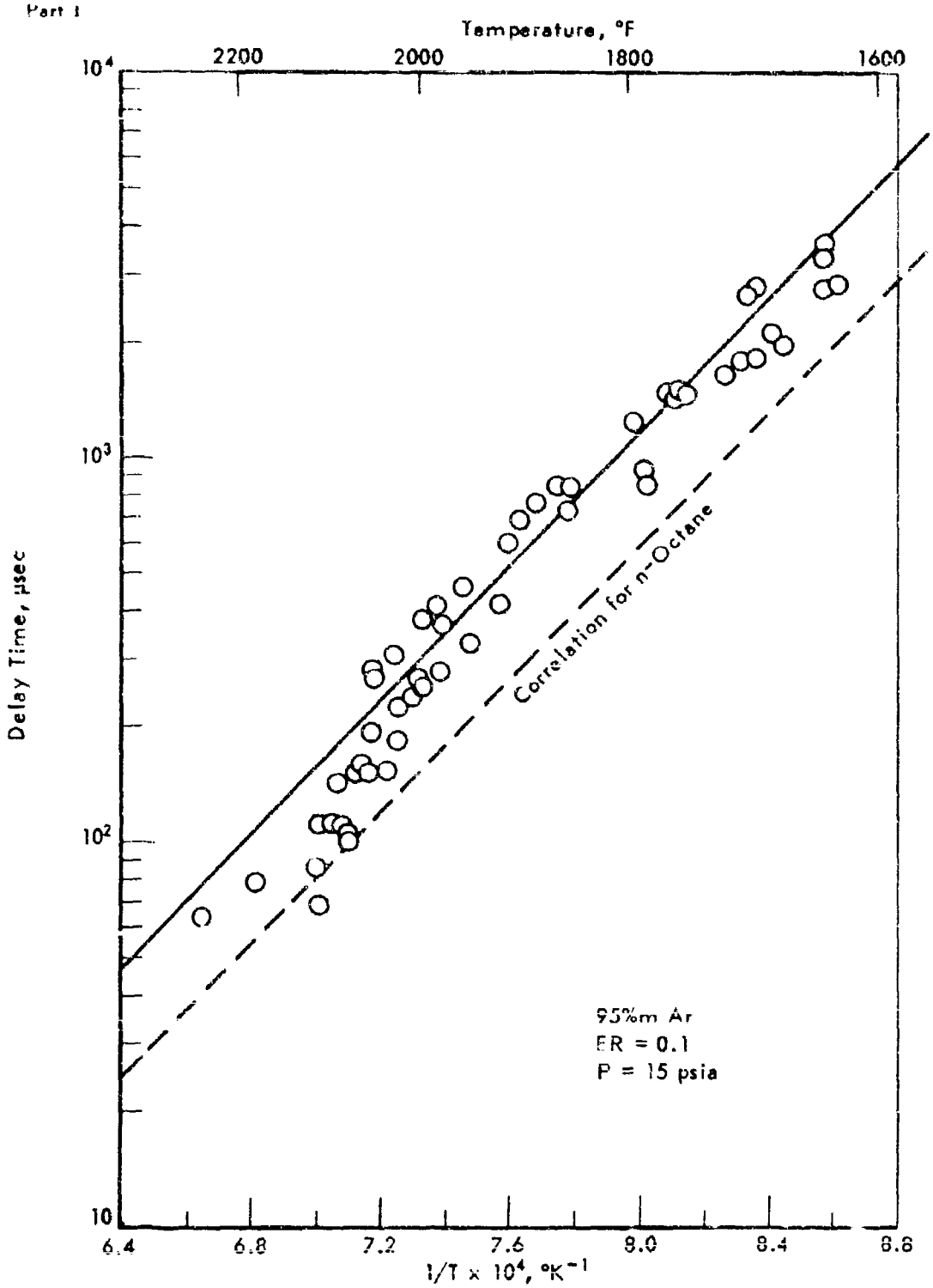


Figure 80. IGNITION DELAY TIMES FOR 2,2,3,3-TETRAMETHYLBUTANE

63294

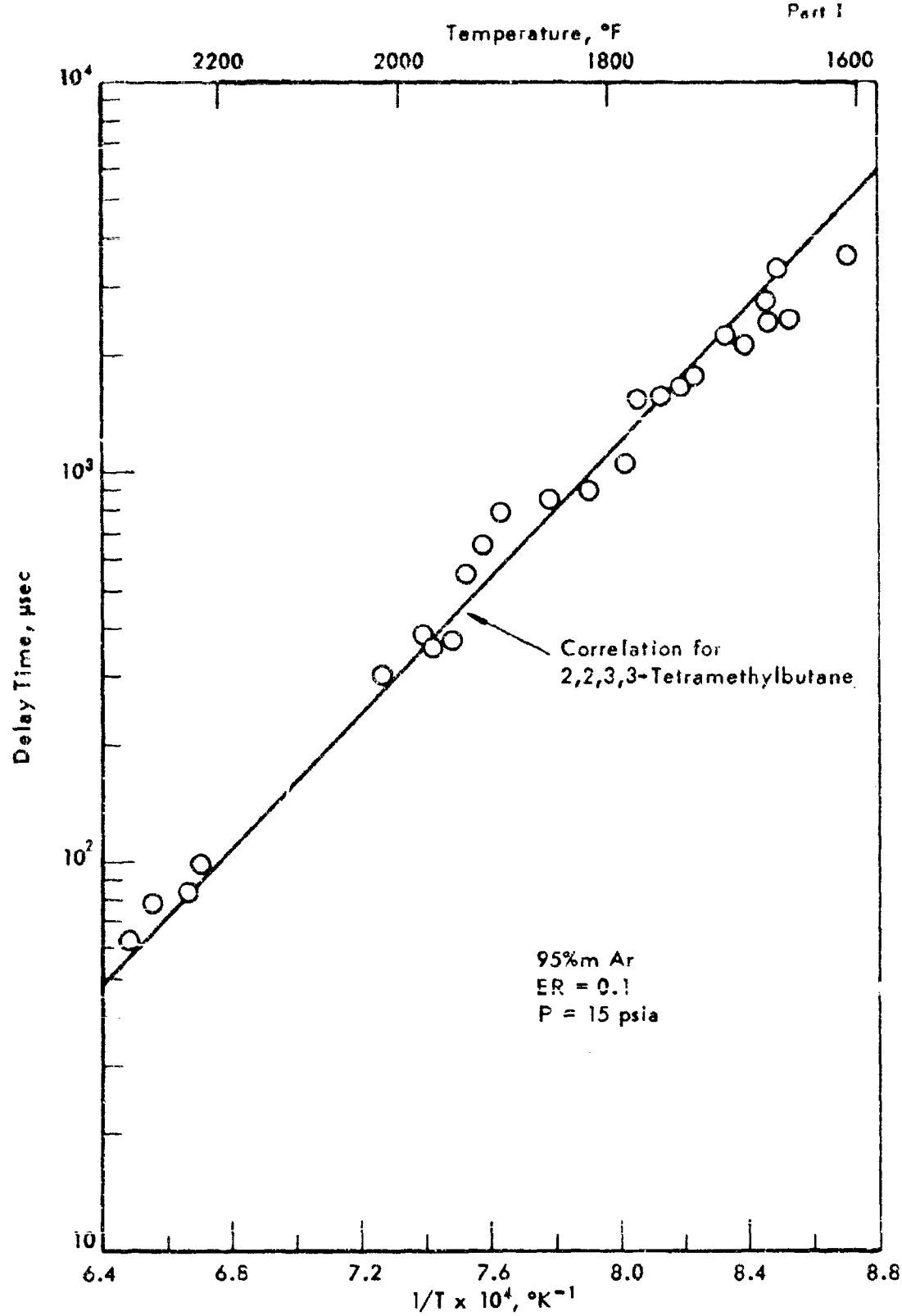


Figure 81. IGNITION DELAY TIMES FOR NEOPENTANE

In the examination of the post-ignition appearance of CO_2 it was found that the initial rate of appearance (over at least the first 100-300 μsec) following ignition may be described by:

$$R = k(C^* - C)$$

where C^* is the ultimate (total combustion) concentration of CO_2 and C, the current value. The rate constant, k, was found relatively insensitive to temperature, with an activation energy of about 7 kcal/mole or less; and has a value of 10^9 sec^{-1} in the middle of the temperature range studied (<1300°K). No significant effect of oxygen concentration on this rate was found. Data obtained for CO_2 formation from n-octane are shown in Figure 82. The most significant observation here is the low activation energy for post-ignition combustion. The indication is that combustion proceeds at a rate nearly independent of temperature, after ignition, and that a matter of several milliseconds will be required for relatively complete combustion. It should be pointed out that these results are limited to quite lean mixtures, however, hence the conclusion may not be safely extrapolated to near stoichiometric conditions.

Small-Scale Subsonic Combustion Tests

In order to study the combustion properties of endothermic fuels and reaction products under subsonic conditions, a small-scale combustor in which fuel can be burned over a wide range of operating conditions was designed and constructed. A first version of this equipment was constructed as a part of the previous contract. Its design and application to the burning of propane, MCH and toluene/$3H_2$ as fuels have been described.[1] Under the current contract a modification of this equipment was undertaken with the objectives of improving fuel-air mixing in the precombustion region, and of facilitating quantitative measurements of the radiant emission from flames.

An assembly drawing of the redesigned combustion chamber is shown in Figure 83. The major change for improvement in fuel-air mixing was in decreasing the area of the tangential slots by which air enters the mixer (part 22 in Figure 83). Decreasing this area by a factor of two raises the velocity of tangentially entering air to near sonic velocity. The remaining changes were made to facilitate viewing the flame radially through the window at part 15 with a radiometer in order to make quantitative measurements of flame radiation. The head end flange (23) was changed in order to bring the flame nearer to the viewing window. The combustion chamber was jacketed to allow water cooling of the metal walls. A target tube was installed opposite the viewing window to provide a cold background for viewing the flame, so that radiation seen is that from the flame gases only, with no significant contribution from the walls. To assure adequate cooling of the target, cooling water for the jacket is brought in directly behind this piece. Construction of redesigned parts for the combustor and assembly of these parts into the new configuration was completed.

Prior to installation of the radiometer, preliminary tests were undertaken to determine what effects these modifications might have had on the operability of the combustor. Two sets of tests were carried out; one with propane as the fuel, and one with toluene/$3H_2$ as fuel; both with a

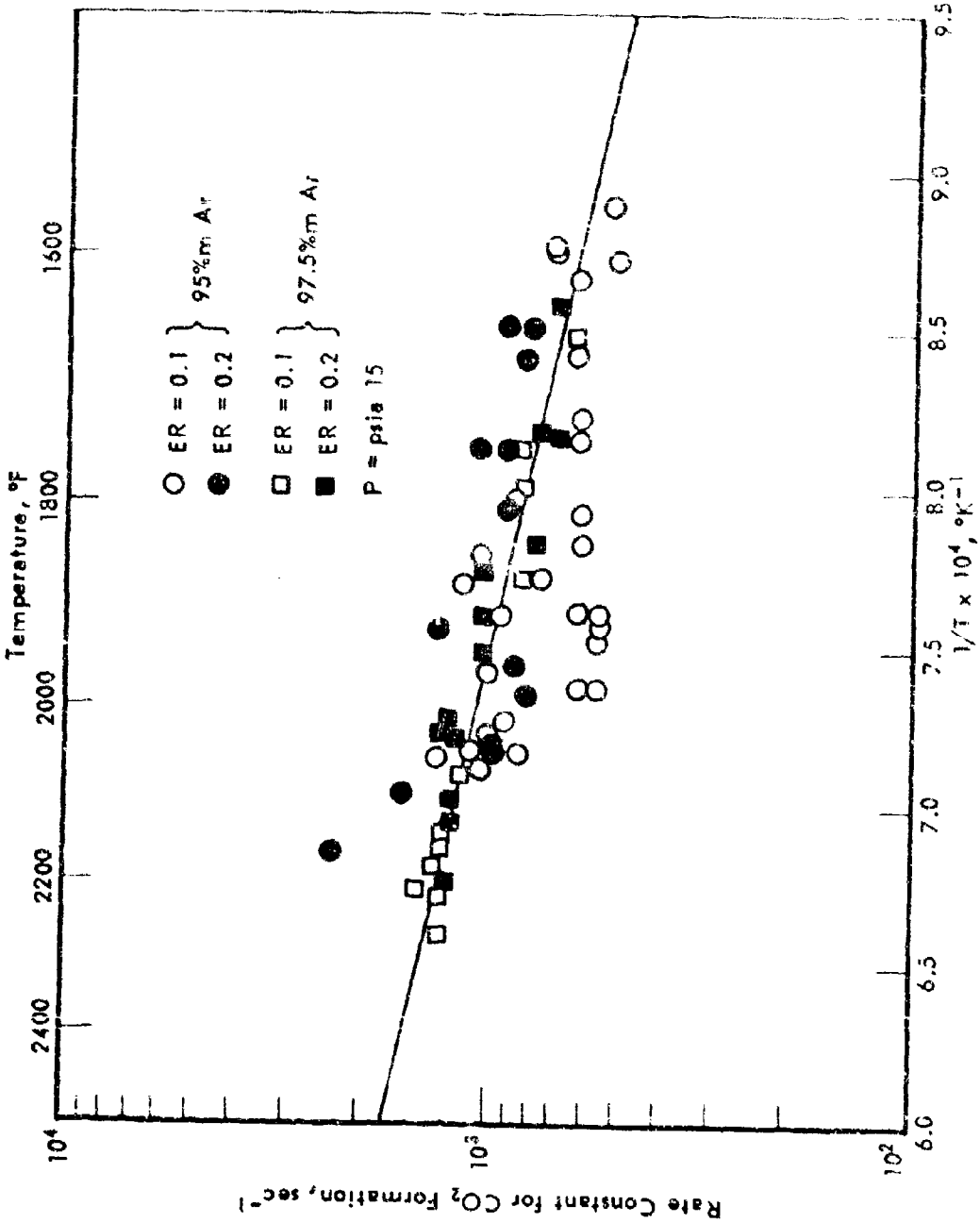


Figure 82. RATE CONSTANTS FOR POST-IGNITION APPEARANCE OF CO_2 FOR n-OCTANE MIXTURES

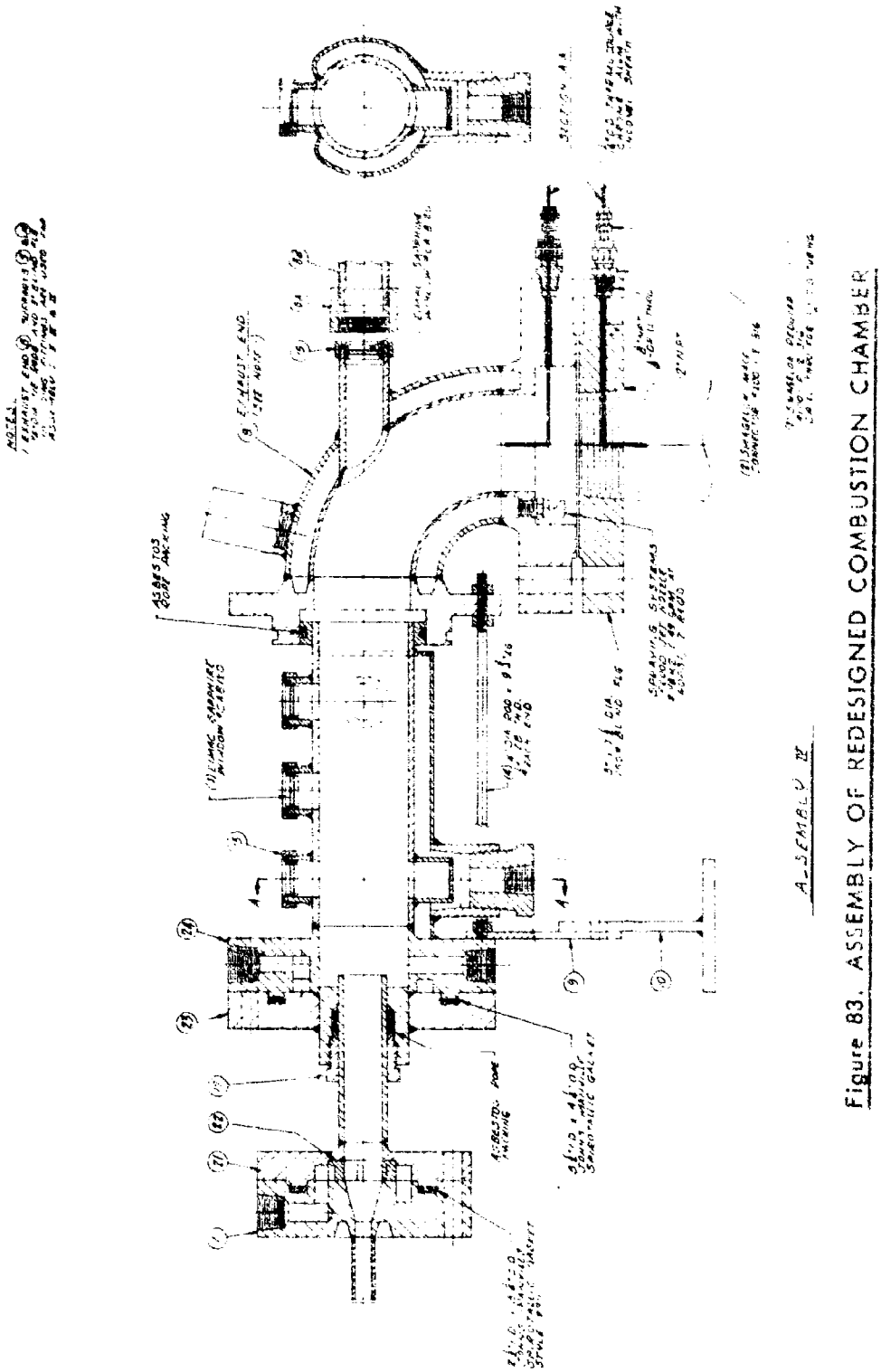


Figure 83. ASSEMBLY OF REDESIGNED COMBUSTION CHAMBER

62392

constant fuel flow of 5 lb/hr. The operable ranges found for these two fuels are given in Table 71. The only problem encountered in these tests was the inability to sustain combustion of the small pilot-ignition flame. However, it was possible to ignite the main flame with just the spark-ignition device, though less smoothly than with the pilot flame.

Table 71. STABILITY LIMITS IN MODIFIED SMALL-SCALE COMBUSTOR

Fuel Flow:	5 lb/hr
Fuel Preheat:	450°F
Air Preheat:	450°F
Combustor Pressure:	1 atm

Fuel	Equivalence Ratio	
	Lean Limit	Rich Limit
Propane	0.8	1.4
Toluene/$3H_2$	0.7	1.4[a)]

a) Blowoff not yet observed, but flame brightness indicated richer mixtures would not be of interest

The limits obtained for stability of propane flames were somewhat narrower than with the previous configuration. Part of this effect may be due to absence of the pilot flame, but it is probably due primarily to cooler combustor walls. No significant narrowing of limits was observed with the toluene/$3H_2$ fuel. Even in the new configuration, both fuels seem to have sufficiently broad stability limits on both sides of stoichiometric to accomodate our proposed test program.

No further modifications in the construction of the combustor have been undertaken to date. However, if further experimental work is to be carried out, it is recommended that: 1) the pilot flame holder be redesigned to provide greater shielding of this flame from the main air stream in the region of attachment, and 2) that a 1/4-inch diameter stainless steel rod, placed diametrically in the head end of the combustor be tried as a flame holder to given broader stability limits.

The radiometer acquired for use with the combustor is a Leeds and Northrup "Rayotube", with a short focal length and sapphire window (Model 8893-A48-K601-12-S). This has been installed on the subsonic combustor to view the interior of the combustor radially at the furthest upstream window. The instrument is essentially a thermopile with an optical system for focusing radiation from the small area viewed upon it. The output from the thermopile is dependent upon the radiant flux from the viewed area. With sapphire windows, the flux is not seriously attenuated at wave-lengths shorter than 4.5 microns. The manufacturers calibration for the instrument used indicates an output of 24.3 mv when viewing a blackbody at 1400°C (total flux, 1.4×10^5 Btu/hr-ft^2). In interpreting our measurements, we have assumed that the output from the "Rayotube" is proportional to the radiant flux down to the region of outputs encountered (at 1.0 mv). Thus, for each condition, a flux and equivalent backbody temperature are calculated:

$$\Sigma = \left(\frac{\text{mv out}}{24.3}\right)(1.4 \times 10^5)\ \text{Btu/hr-ft}^2$$

$$T_B = (3000)^4 \sqrt{\frac{\text{mv out}}{24.3}} - 460°F$$

Series of tests were carried out in the small-scale combustor (Table 72) with both propane and toluene/$3H_2$, using the "Rayotube" to monitor total radiation fluxes for propane of 5000-7000 Btu/hr-ft^2 and 6000-8000 for toluene/$3H_2$. The lowest fluxes were associated with the richest mixtures in both cases, presumably because of the lower flame temperature and lower production of the emitting species, CO_2 and H_2O. There was no indication of radiation from carbon particles with either fuel.

Table 72. RADIATION MEASUREMENTS FOR SMALL-SCALE COMBUSTOR

LR 9669-28

Fuel Flow: 5 lb/hr Pressure: 1 atm
Fuel Temp: 600-650°F Air Temp: 450°F

Equivalence Ratio	Rayotube Output (mv)	Σ (Btu/hr-ft^2)	T_B (°F)
	Propane Fuel		
0.86	1.118	6500	930
0.93	1.235	7250	970
0.975	1.185	6820	950
1.27	0.975	5720	888
1.45	0.75	4320	800
	Toluene/$3H_2$ Fuel		
0.95[a)]	1.18	6950	955
1.03	1.19	6950	955
1.15	1.28	7750	985
1.26	1.09	6380	925

a) Pure toluene fuel.

Physical Properties Program

Because of the need for the availability of the best possible physical properties data for endothermic fuel systems we have been engaged in assessing the merits of various methods of estimation and correlation. The objective is to make the data available generally to people associated with the present hydrocarbon scramjet effort. The study has involved mainly[39] two proprietary programs and the AIChE properties program and

attempting to select the best features of all three. All three are available as IBM 7040 computer programs. Output from the programs was cross compared with each other and with values hand calculated from selected literature data. As it turned out a considerable portion of our difficulties arose from "bugs" residing in the AIChE program and one of our own programs. These "bugs" have now been exterminated and the program we are now using we believe to be the best currently available. Data will be generated, using this system, for a number of the more promising candidate endothermic reaction systems. Results for the first of these, methylcyclohexane - toluene - hydrogen, are presented in the Appendix covering temperatures up to 1600°F and pressures to 3000 psia.

Because of its complexity, and, in part, its proprietary nature,[a] no attempt has been made to provide a complete description of the physical properties program used in this report. However, portions of the program are present in the AIChE Physical Property Estimation System, descriptions of which have been published by the American Institute of Chemical Engineers.[b][38] Moreover, literature references to the original methods of calculating physical properties are listed under a separate heading at the end of this report.

Mixture rules used were those recommended by either the API "Technical Data Book - Petroleum Refining[41] or by Reid and Sherwood.[42]

The internal program and the AIChE System now give essentially identical results and both have the desirable ability to utilize available experimental data to increase the accuracy of estimated properties. For our purposes, a disadvantage of the AIChE System is that it was intended to be used for equipment design and therefore generates irrelevant information and requires excessive computer time. The internal program gives desired properties only.

Methylcyclohexane-Toluene-Hydrogen System

The physical properties of MCH, toluene, and hydrogen are shown in the Appendix in Table 91 through 94. Properties of pure liquid MCH and toluene are presented in Tables 91 and 92. Properties of gaseous toluene, hydrogen, and MCH are to be found in Tables 91, 92, and 93. Table 94 contains properties data for the gaseous reaction system:

$$MCH \longrightarrow Toluene + 3H_2$$

for 0, 25, 50, 75, and 100 percent conversion. However, the mixtures are keyed in Table 94 headings by mole fraction composition as follows:

a) The proprietary program most relied on was the work of G. W. Lundberg and D. C. Whitney of our Physical Chemistry Dept.

b) An internal report by a contributor to the AIChE program (D. C. Whitney) was also used.[40]

% MCH Reacted	Table Headings (Mole Fractions in Mixture) MCH	Tol	H_2
0	1.0	-	-
25	0.429	0.143	0.429
50	0.2	0.2	0.6
75	0.077	0.231	0.692
100	-	0.25	0.75

Corresponding calculated weight fractions are also shown.

Estimated maximum errors for the program are shown in the following tabulation:

Physical Property	Percent Errors Estimated to be Less Than: For Pure Liquid	For Pure Real Gas	For Gaseous Mixtures
Density and/or Compressibility Factor	1	5	5-10
Thermal Conductivity	5	5	15
Heat Capacity	5	2-5	5
Enthalpy	5	2-5	5
Viscosity at High Temperature	5	5	15
Viscosity at Low Temperature	10	5	15
Latent Heat of Vaporization	3		
Vapor Pressure	1		
Surface Tension	3		

For gaseous mixtures, the indicated maximum errors apply generally in the pressure range to ca 1500 psia; above this probable errors may be as much as double those shown. The program does not provide an automatic method of including data through the critical region. This is of concern only for pure MCH in this case since the low critical temperature of MCH (570°F) makes the possibility of reaction occurring to produce toluene and H_2 extremely remote. To obtain properties through the critical region the appropriate liquid and vapor phase data should be plotted and the values estimated by interpolation.

Description of Methods Used for Extending or Estimating Pure Component Data

1. Compressibility Factor, $Z = \frac{PV}{RT}$, and Gas/Density calculated by the method of Redlich and Kwong, Ref. 43 and Ref. 52, Chapter 7.

2. Liquid Density, from

$$P = A-BT-C/(E-t), \qquad t \leq T_c-55°F$$

with constants from Ref. 41. Extrapolated to T_c by means of the Guggenheim relation,

$$P/P_c = 1 + a(T-T_R)^{1/3} + b(1-T_R), \text{ Ref. 44}$$

3. Gas Viscosity (Table 94) by the method of Wilke (low pressure) and Bear and Stiel (high pressure), Ref. 42, Chapter 9. Gas Viscosity (Tables 92 and 93), see Ref. 20, p. 528. When σ and ϵ/K (the Lennard Jones Force constants) are not known they are estimated by the method of Stiel and Thodos, Ref. 46. Experimentally derived constants are also given in this reference.

4. Liquid Viscosity, by extrapolating from two experimental data with

$$\log \mu = A - (B/T), \quad T_R = 0.7$$

Extrapolated to T_c by the method of Jossi, Stiel and Thodos, Ref. 47.

5. Gas Thermal Conductivity, by the methods of Chung-Bronile Welks (low pressure) and Stiel and Thodos (high pressure) Ref. 42, Chapter 10; Ref. 41, 48, 49.

6. Liquid Thermal Conductivity, extrapolated from a single datum or estimated by the method of Robbins and Kingrea. Ref. 50.

7. Gas Enthalpy, calculated from the Redlich-Kwong equation of state. Ref. 43 and 51. Pressure correction for the heat content is

$$H_T - H_T^\circ = PV - RT - \frac{3a}{2\sqrt{T_b}} \ln\left(1 \frac{b}{v}\right)$$

8. Liquid Enthalpy, found by adding the contributions of compression (to saturation pressure) and liquefaction to the ideal gas heat content. The Redlich-Kwong equation of state was used to estimate the effect of compression; the Watson correlation,

$$\Delta H_v = \Delta H_{v_1} \left[\frac{1 - T_R}{1 - T_{R1}}\right]^{0.38}$$

was used to extrapolate the heat of vaporization data.

9. Gas Heat Capacity, found by numerical differentiation (Lagrangian) of gas heat contents.

10. Liquid Heat Capacity, found by numerical differentiation of liquid heat content.

11. Freezing Point and Boiling Point, Ref. 51, 52.

12. Critical Properties, Ref. 53, 54.

13. Acentric Factor, calculated from vapor pressure tables,

$$\omega = -\log \frac{P_S^\circ}{P_C} - 1.000$$

where P_S° = vapor pressure at $T_R = 0.700$. Ref. 55, 56.

14. Heat of Vaporization at Boiling Point, Ref. 51, 57.

15. Heat of Formation at 77°F, Ref. 51.

16. Heat of Combustion at 77°F, Ref. 51.

17. Free Energy of Formation at 77°F, Ref. 51.

18. Fire-hazard properties, Ref. 58, 59.

Present Status and Future Projections

1. Information in the literature continues to indicate areas in which hydrocarbons would have a distinct advantage as fuels for high speed aircraft. A paper by Ashby and Stone points out the adverse effect on maximum L/D of increasing aircraft volume at Mach 6. Indications are that at this speed the lowering of L/D max could be reduced by about 40%. While it is true that this advantage will diminish with speed, it should remain an important factor over a considerable portion of the speed range up to Mach 12. It is anticipated that work by Marquardt Corporation and United Aircraft Research Laboratories will serve to more closely delineate the tradeoffs that can be expected.

2. Work by Marquardt Corporation has shown the effect of heat sink equivalence on the limiting Mach number obtainable with a scramjet engine. On this basis, significant benefits would accrue to increasing the presently obtainable heat sink available from naphthene dehydrogenation. This indicates that increased attention should be paid to the possibilities of dehydrocyclozation type reactions. This will be done with tailored type molecules such as bis-2,6-dimethylcyclohexyl and 1,4,5,8-tetramethyldecalin. Successful dehydrocyclization of these molecules should raise the reaction heat sink by about 50%. Other reaction types include dehydrogenation of polycyclic naphthenes, butadiene cracking, and dehydrogenation of methylamine to cyanogen.

3. Benefits in the handling and storage properties of fuels are possible by tailoring properties of the fuels by the use of mixtures. These could be very significant. Accordingly, we have continued to study the reactivity of binary mixtures over Pt/Al_2O_3; specifically, in this report, DCH with MDHN, DHN and MCH; DHN with MCH, and DCH with MCH. Although each component affects the reactivity of the other component no catastrophic effects have been observed and the overall reaction rate and heat sink are about maintained. However, we are concerned about the effect of various components on catalyst stability and we are continuing study of this aspect of the problem. It is anticipated that considerable flexibility will be possible in designing into the fuel and sort of volatility, viscosity, lubricity, freezing point, and other properties which will result in optimum engine and aircraft design.

4. We have finally arrived at a consistent method of calculating and extrapolating physical properties of the MCH-toluene/$3H_2$ system for various mixtures over the range from -200°F to 1600°F and pressures up to 3000 psi (although data around the critical region may still be uncertain). The method finally selected is based on the AIChE program plus two proprietary programs. We will now go on to determine the applicability of this program to other

fuel systems such as the decalin and DCH systems. These are considerably more complicated, in principle, than with MCH since the decalin system will have a minimum of five components and the DCH system a minimum of four. Also, less experimental data is available in the literature which may necessitate obtaining some in the laboratory.

5. We have re-examined the possibility of utilizing propane as a fuel from two different aspects based on the possibility of obtaining high conversion in a cracking reaction to methane and ethene. Two different approaches to a catalyst for this reaction are being examined. One involves the introduction of a highly dispersed or vaporized strongly acid catalyst such as an acid treated zeolite. The other involves the possibility of generating free radicals to act as catalysts for the cracking. High conversion in this reaction would give about the same total heat sink as would the MCH dehydrogenation but would have the advantage, if successful, of utilizing a low pressure drop throwaway type catalyst. So far, however, it has not been possible to develop a suitable catalyst.

6. A number of additional conventional type dehydrogenation type catalysts have been made in which a catalytic metal is placed on a suitable support and utilized as a bed. Variations in both the catalytic metal and the nature of the support have been investigated. Although several catalysts which are more active than our standard laboratory catalysts have resulted, nothing in the nature of a "breakthrough" has been achieved. So far relatively limited excursions from the presently active combination of platinum on alumina have been made. Work in the future in this area contemplates increasing the number of metallic components and also studying the incorporation of a wider variety of secondary elements in the support.

7. A desirable objective in the development of new catalysts is to modify the geometric arrangement of the catalyst in the bed to reduce pressure drop. In trying to achieve this objective we have been looking at the possibility of placing a catalyst on an open structure which will present less resistence to the flow of fluids. Such shapes are semicommercially available. However, depositing platinum on the surface, does not produce an active catalyst, probably because the low surface area of the shape. Attempts to increase the surface area by initially depositing a finely divided alumina (Baymal) has been tried and a reasonable level activity observed. Other possibilities of this general nature will be pursued in the future. Another method of reducing the pressure drop we are following is to utilize a disperse phase catalyst which will be carried along with the fuel through the reaction system into the engine. The most desirable type of catalysts have extremely high activity initially which rapidly drop off to the more usual level of catalysis. This type of catalyst we are studying in bed form but with primary interest in the very early stages of reaction. In application the catalyst would be introduced in fuel in the form of an extremely finely divided powder. Another method of introduction would involve incorporating a solid soluble metallic organic compound into the fuel and having it vaporize and proceed through the reaction zone unchanged as a vapor phase catalyst or decompose to a dispersed catalyst. This possibility is being investigated by heating MCH in an autoclave with various metal composites and observing if reaction occurs. Some indicates of reactive catalytic materials have been found, although conversions have not been

large. The most reactive material gave about 11% conversion. This approach will be explored further.

8. Modifications on the power input and temperature measurements on the FSSTR have been installed. These have improved the control and operating flexibility of the equipment as well as improving the precision of the data obtained. Studies on the thermal reaction of propane has been completed covering the range of space velocities up to 400, temperatures to 1400 and pressures to 900 psi. Results established that the highest temperature that can be tolerated in the reactor tube is about 1400°F under conditions that we have investigated to date and that the maximum reaction heat sink that can be achieved in thermal cracking is about 300 Btu/lb. Further work was done with propane using a chrome/alumina catalyst for dehydrogenation to propylene and hydrogen. This gave us an opportunity to investigate the effect of a different catalyst configuration on this reaction. Results were comparable to those obtained in the laboratory reactors; it was possible to achieve equipibrium conversion but activity decreased rapidly due to coke formation. If laboratory studies succeed in developing a satisfactory catalyst experiments utilizing a catalytic cracking catalyst in this equipment will be done in an attempt to bring about the conversion of propane to methane and ethane. The next fuel to be tested in the FSSTR will probably be decalin with the UOP R-8 catalyst.

9. One of the major objectives of the present contract has been to develop a satisfactory mathematical model for the reaction system in order to allow engine manufacturers and aircraft companies to utilize it in mating the reaction system to the heat sink requirements of a ramjet combustion chamber. The model under development during the last contract has now been brought to a more satisfactory state of development. It has been rewritten in a form less demanding in both machine and human time. With the program, we have not only been able to simulate the reactions taking place in the FSSTR in the MCH-Pt/Al_2O_3 system, but we have also been able to simulate operation under various conditions that we have not been able to achieve, as yet, experimentally. Thus we have been able to calculate the effect of very much higher flow rates, higher heat fluxes in terms of the temperature profile and pressure drop, to vary the bed length and to study the advantages and disadvantages of multiple adiabatic reaction sections. Though the program is giving some interesting insights in possible areas of experimentation, the heat fluxes are very much beyond those that we were able to investigate up to the middle of the year. Accordingly, we fabricated a short (2 foot) test section which was substituted for the third section of the FSSTR, allowing us to study heat fluxes approaching half a million Btu/hr/sq ft of tube surface. In the first series of runs with this section satisfactory operation was achieved at heat fluxes up to 300,000 Btu/hr/sq ft. However, as the flux increased the model results departed increasingly from experiment, in the direction of lower conversion. Reasons for this will be sought. Another modification of the model was accomplished to have it represent the case in which heat is being delivered to the reactor from only one side (slab geometry) a situation most apt to prevail in an actual use situation. This has yielded interesting results; however, it will be necessary to confirm them by experimental values. A possible convenient experimental setup has been devised and will be assembled and utilized in the next period.

10. One of the variables affecting the reaction of hydrocarbons to high temperature conditions is the amount of dissolved oxygen in the fuel at the time it is exposed to the thermal stress. However, the degree to which deoxygenation is beneficial appears to be an attribute of the particular fuel involved. With pure DHN little benefit is obtained, according to SD Coker recycle results, by reducing the O_2 content below about 8 ppm, whereas with MCH benefits accrue down to at least 1 ppm whilst with a mixed highly naphthenic jet fuel containing a broad mixture of components much lower and as yet incompletely defined limits appears to be operative. Whether this is a function of the types of compounds present or whether it is an attribute of the components mix will have to be determined in subsequent work. In the meantime we have completed a more comprehensive unit for determining thermal stability of fuels as well as catalytic activity and the thermal stability of reaction products. This is the CAFSTR, which has performed well at temperatures up to 1200°F at 1000 psi. However, with the material used in the rod heaters (Inconel), which provide the heat exchange surface, it is virtually impossible to rate the tubes by appearance as is done with cokers. Accordingly we are investigating the possibility of assessing the conditions of the tubes by determining the change in heat transfer characteristics calorimetrically, which of course, will yield a much more meaningful attribute.

11. We established, in an earlier contract, by analysis and by visual and photographic means, that the (simulated) products of endothermic reactions could be burned successfully in a small-scale subsonic burner if the hot products were initially mixed with air prior to being ignited. In order to establish this more firmly we obtained a radiometer to view the radiation more critically. The virtual equivalence of the radiation from propane and toluene under a variety of conditions we feel confirms this without fear of successful contradiction. It appears unnecessary to do additional work in this area except with fuels of higher molecular weight, unusual structure or following thermal cracking.

12. Our contribution to determining the supersonic combustion properties of our candidate fuels and their reaction products has been limited to determining ignition delay times in our single diaphragm shock tube. The results obtained have established that the ignition delay times observed with most hydrocarbons of carbon numbers above 2 are relatively indifferent to molecular weight, structure or to the presence of substantial amounts of H_2. This evidently stems from the fact that the primary step in the oxidation involves the removal of a proton by O_2 to form an O_2H or OH radical. The ignition delay then should be related to the weakest C-H bond which is ordinarily a tertiary or secondary one. This is borne out by the sluggishness of methane and to a somewhat lesser degree, ethane and ethylene. However, rather surprisingly, two other hydrocarbons, lacking secondary or tertiary hydrogen atoms, tetramethyl butane, and neopentane, had IDT's close to those shown by the majority of hydrocarbons. Not a great deal of additional work will be done with the shock tube as far as determining IDT's are concerned. Some work will be done with high density fuels such as Shelldyne which are of rather unusual structure. Another possibility not yet fully explored, would involve getting estimates of the rates of combustion from the rate of increase of the concentration of combustion products. Another area which has not been explored involves the use of additives to

reduce IDT's but whether this could lead to a practical application would have to be established before undertaking an investigation of this kind.

13. A bibliography of references of interest is included in the Appendix of this report. The present listing attempts to include all references published since the compilation of our previous literature survey[80] or which were overlooked at that time.

14. A "Fuels Evaluation Table" in the form of a summary table of the bench scale evaluation work done on various candidate fuels is included. This is an extension of a table previously published (Table 86, TDR-64-100, Part III, p. 255) and may be of interest in making a quick comparison of the reactivity and properties of different compounds. However, it does not include FSSTR data and should not be used in making definitive application evaluations.

APPENDIX

Page

Calculation of Contact Time 248

Pulse Reactor 248

Micro Catalyst Test Reactor 254

Tables 73-74. MCH Dehydrogenation With Various Catalysts in MICTR . . 261

CAFSTR Heat Exchanger Design 267

A Computer Program for Simulating Endothermic Fuel Reactions in a Packed Bed Reactor 270

Table 75. Shell Development Packed Bed Reactor Program 280

Tables 76-90. Ignition Delays From Shock Tube Experiments 297

Tables 91-94. Property Values for MCH/Toluene/H_2 317

Table 95. Summary Table: Evaluation of Vaporizing and Endothermic Fuels 336

Bench Scale Reactor - Description of the Apparatus, Procedure for the Experiments, Calculation of Heat Sinks 337

Table 96. Thermodynamic Heats of Reaction 342

Table 97. Latent Plus Sensible Heats of Various Naphthenes 343

Calculation of Contact Time

In our reports we have usually used either LHSV or the mass flow rate (G) to designate the feed rate. In order to facilitate an appreciation of the residence time in the reaction zone, we have expressed the relationship between these values and contact time under a variety of conditions.

Figures 84(a) through (e) give the relation between contact time and temperature for mass flow (G) of lb/hr/sq ft, length (L) of 1 foot and void fraction (ϵ) of 1 at 0, 25, 50, 75 and 100% conversion. In order to relate G and LHSV the length of the tube must be given. For example, for MCH in a 2-foot tube at a LHSV of 1600, with L = 2 feet, the contact time with R-8 catalyst (ϵ = 0.54) the nominal contact time (θ) at 50% conversion, 1000°F, 800 psi would be

$$\theta = t\,\frac{(L\epsilon)}{G} \quad \text{and} \quad G = \text{LHSV}\,(96)$$

$$= 7.2 \times 10^{3}\,\frac{(2 \times 0.54)}{96 \times 1600}$$

$$= 0.05 \text{ sec.}$$

This is only a nominal value since it assumes that the flowing mixture consists of a 50% converted MCH feed (i.e., 20%m MCH, 20%m toluene and 60%m H_2). Since the conversion actually increases from zero to 50% as the MCH proceeds through the tube, a point-to-point calculation would be necessary to obtain the true average contact time (this is an average contact time since some molecules will spend more time in pores than others).

Another example would be useful: MCH, P = 600, ϵ = 0.54, LHSV = 100, T = 900°F, 100% conversion in a 10-ft tube.

$$\theta = 3.6 \times 10^{3}\,\frac{(10 \times 0.54)}{480 \times 100}$$

$$= 0.41 \text{ sec}$$

Pulse Reactor

In a dispersed phase catalyst system the catalyst will be in contact with the reactants for about one second or less. Thus in this system the initial reactions that occur when the reactants first contact the catalyst surface will be more important in determining the product material composition than will the reactions that occur under steady-state conditions. One way of studying these initial reactions is by means of the pulse reactor technique. In such a system an inert carrier gas (e.g., helium) flows through the reactor continuously. At the desired time a small amount of feed is injected into the carrier gas stream and subsequently passes over the catalyst as a "pulse". The products, or a slip-stream sample thereof, are led directly into a GLC for analysis. This affords a rapid method of studying initial reactions under a variety of conditions. Other advantages of using a pulse reactor technique are that studies can be made: (a) at very high space velocities with small amounts of feed, and (b) also where only a small amount of feed is available. From the above considerations it appeared desirable to

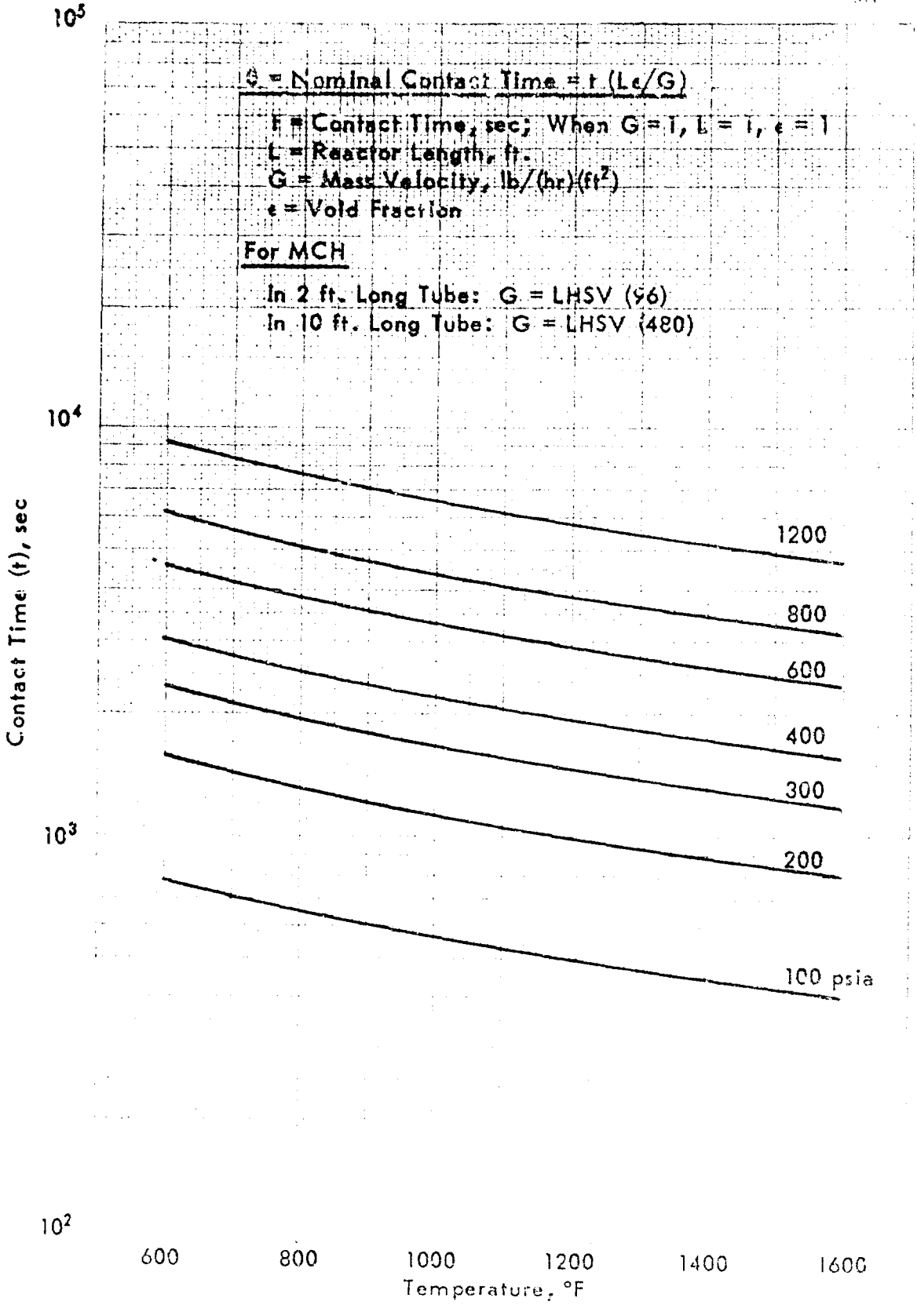


Figure 84a. CONTACT TIME FOR MCH DEHYDROGENATION: 100% CONVERSION

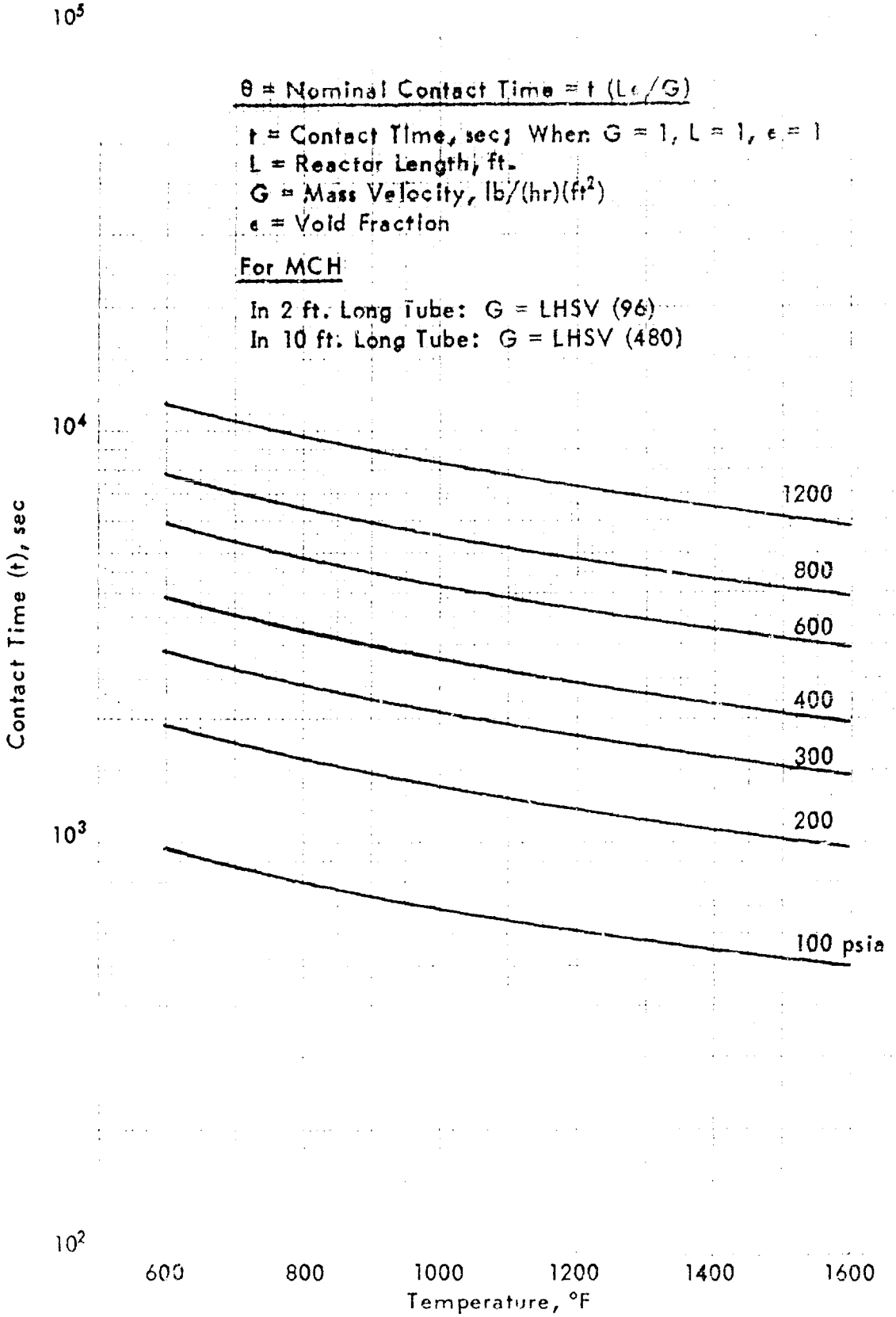


Figure 84b. CONTACT TIME FOR MCH DEHYDROGENATION: 75% CONVERSION

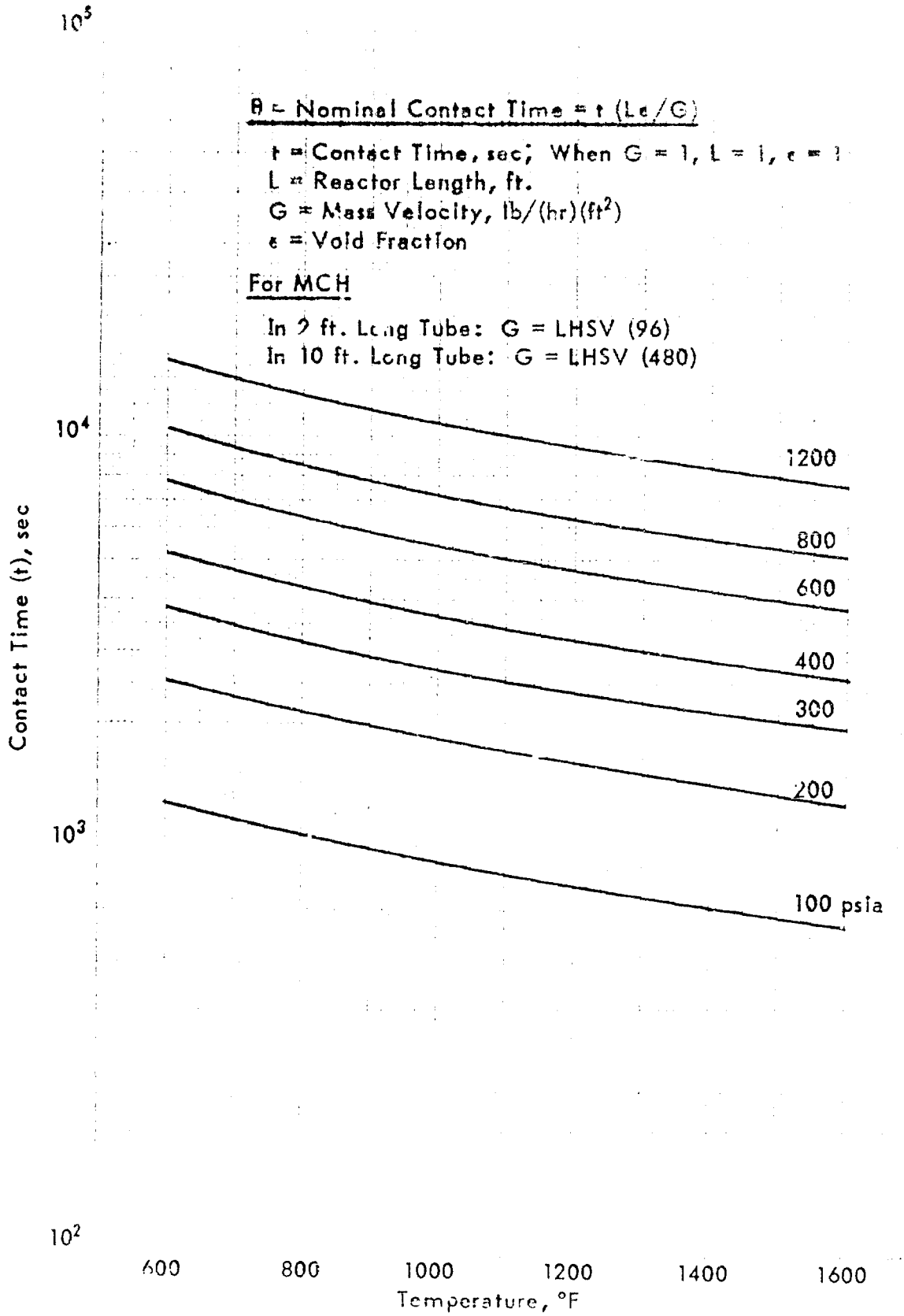
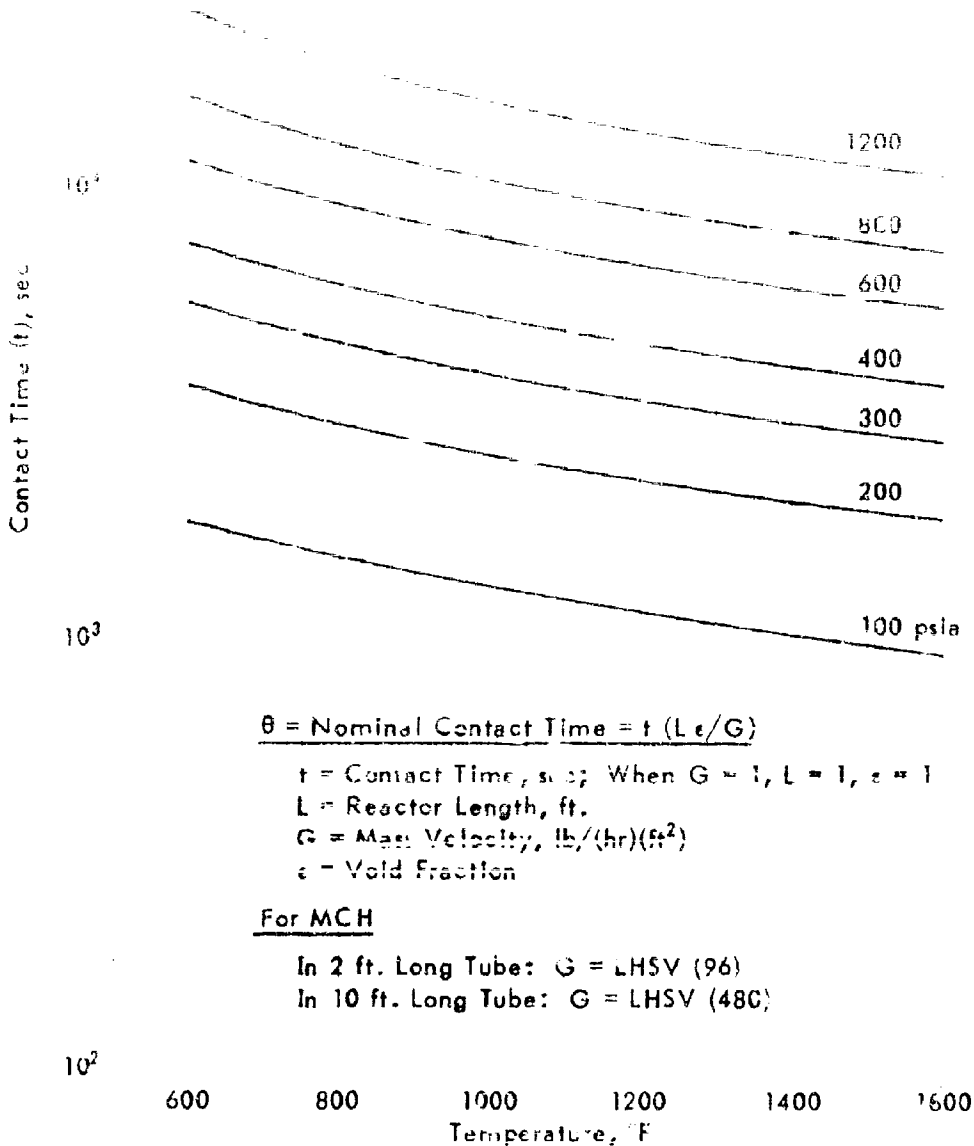


Figure 84c. CONTACT TIME FOR MCH DEHYDROGENATION: 50% CONVERSION



θ = Nominal Contact Time = t (L ε/G)

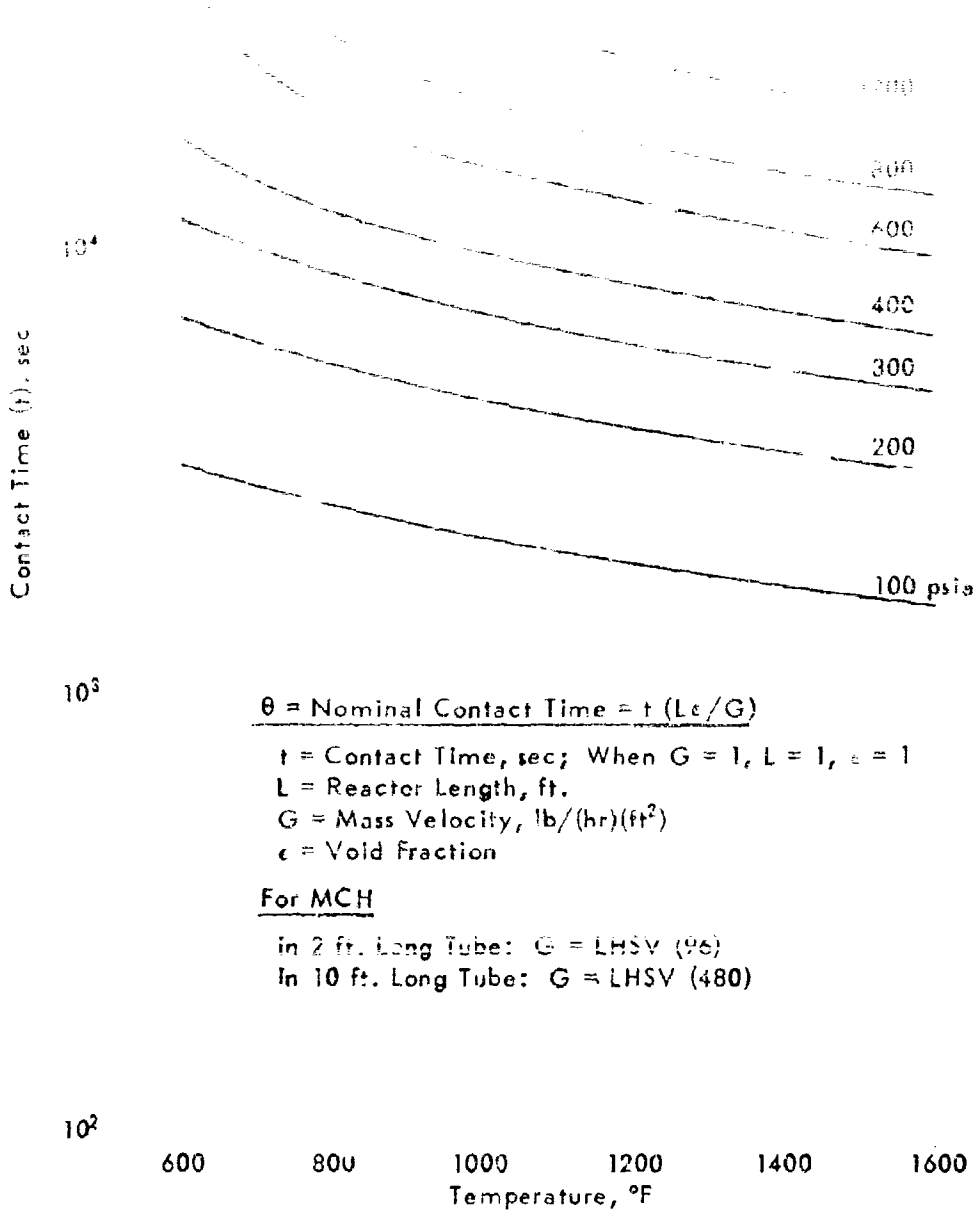
t = Contact Time, sec; When G = 1, L = 1, ε = 1
L = Reactor Length, ft.
G = Mass Velocity, lb/(hr)(ft²)
ε = Void Fraction

For MCH

In 2 ft. Long Tube: G = LHSV (96)
In 10 ft. Long Tube: G = LHSV (480)

Figure 84d. CONTACT TIME FOR MCH DEHYDROGENATION: 25% CONVERSION

63294



θ = Nominal Contact Time = t (Lε/G)

t = Contact Time, sec; When G = 1, L = 1, ε = 1
L = Reactor Length, ft.
G = Mass Velocity, lb/(hr)(ft^2)
ε = Void Fraction

For MCH

In 2 ft. Long Tube: G = LHSV (96)
In 10 ft. Long Tube: G = LHSV (480)

Figure 84e. CONTACT TIME FOR MCH DEHYDROGENATION: 0% CONVERSION

incorporate the pulse reactor technique into our catalytic program, even though with such a system the data is not necessarily obtained under steady-state conditions. Accordingly one section of our laboratory dual reactor system was modified in the following manner so that it could also be used as a pulse reactor system.

In our laboratory reactor system the furnace is 26 in. overall length and contains four heating elements of lengths 4", 8", 8", 4" located from top to bottom in that order. The outer shell of the furnace extends one inch beyond the top and bottom of the heating elements. The furnace consists of two hinged halves and opens lengthwise. Each half contains a heavy Meehanite liner with a groove down the center to hold the reactor tube. When closed the grooves form an opening 7/8 inch in diameter.

To modify the apparatus for use as a pulse reactor, a secondary furnace liner was fabricated from a 7/8-inch stainless steel rod (No. 416), 13 inches long. A 0.257-in. diameter hole was drilled down the center to accommodate a 1/4-in. OD reactor tube. Seven holes were drilled radially from the outside to the center hole in which thermocouples were cemented. The thermocouples were 1-1/2 inches apart and the top couple was 1-1/2 inches from the top of the liner. The thermocouples were situated so that they just touched the reactor wall. This secondary liner was placed in the Meehanite liners at the very bottom of the furnace and extended one inch below the bottom heating element. Figure 85 shows the construction of the secondary liner and its position in the furnace.

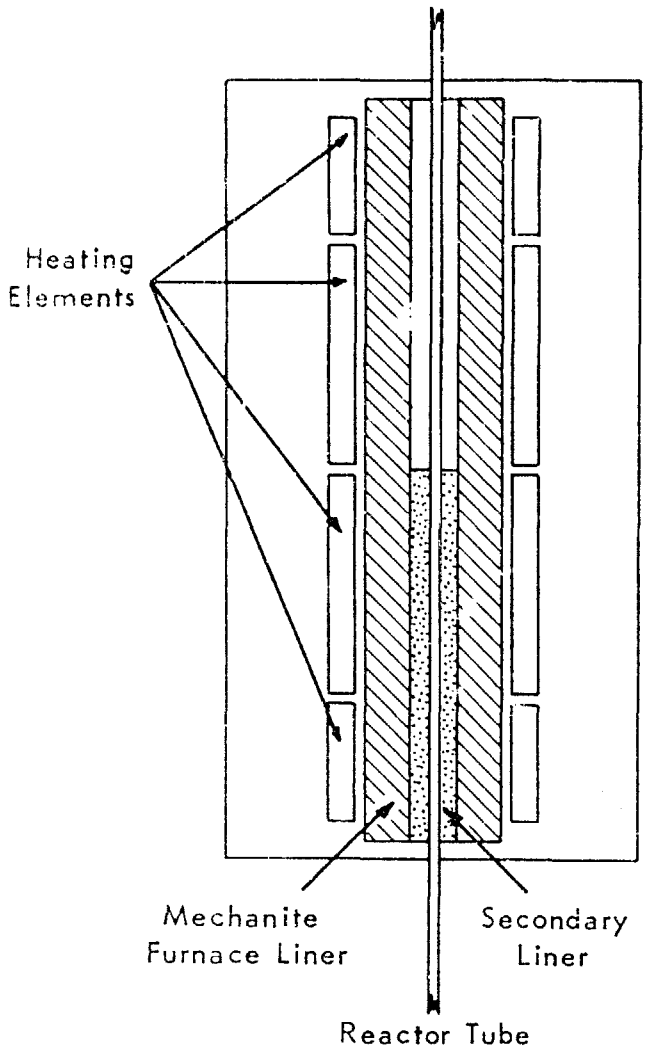
The reactor was a 1/4-in. OD stainless steel tube (No. 304) with 0.028-in. wall. An 1/8-in. OD thermowell can be fitted into the reactor at the bottom. Feed is injected into the carrier gas stream with a syringe pump. A slip-stream sample of the exit gas is led to the GLC via a heated lead. The pulse reactor system utilizes the same temperature and pressure controls and measuring devices as are used for the standard reactor tube. Thus the standard laboratory reactor can be converted to the pulse reactor by merely installing the secondary liner complete with thermocouples and reactor tube into the furnace, and connecting the syringe pump and the heated lead to the GLC. Figure 86 shows a schematic diagram of the pulse reactor system.

It should be noted that if desired this apparatus can be used as a small dimension continuous flow reactor and was actually used as such to study propane cracking.

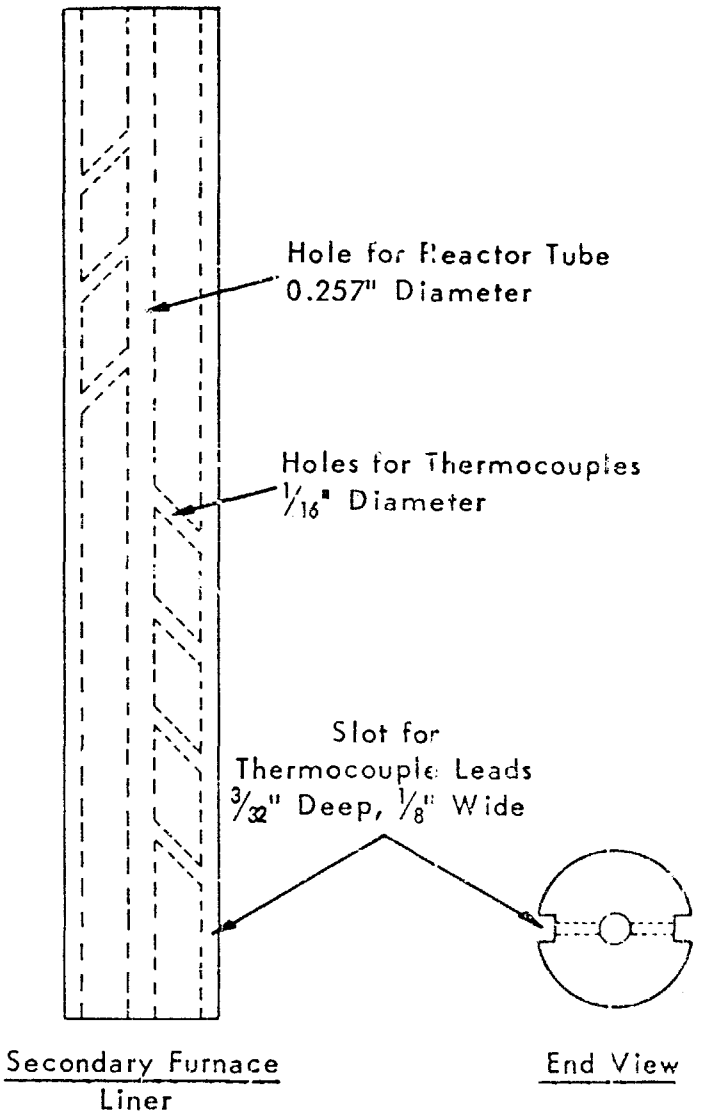
Micro Catalyst Test Reactor

The micro catalyst test reactor (MICTR) was completed and the first test run made with the reference catalyst (1% Pt/UOP R-8 Al_2O_3) at the end of October 1966. Since that time, 262 runs have been made with the MICTR. The design of the MICTR is shown in Figure 87. Figure 88 shows the layout of the overall apparatus and Figure 89 shows details of the furnace block and reactor tube construction. The feed line pressure gauge was eliminated to reduce feed holdup and a check valve was installed in the feed line to prevent "blow-back".

MICTR tests have been carried out at 662, 752, and 842°F block temperature, with MCH usually at LHSV 100, and 10 atm pressure. Hydrogen



Reactor Furnace with Secondary Furnace Liner in Position



Secondary Furnace Liner

End View

Figure 85. SECONDARY FURNACE LINER FOR PULSE REACTOR SYSTEM

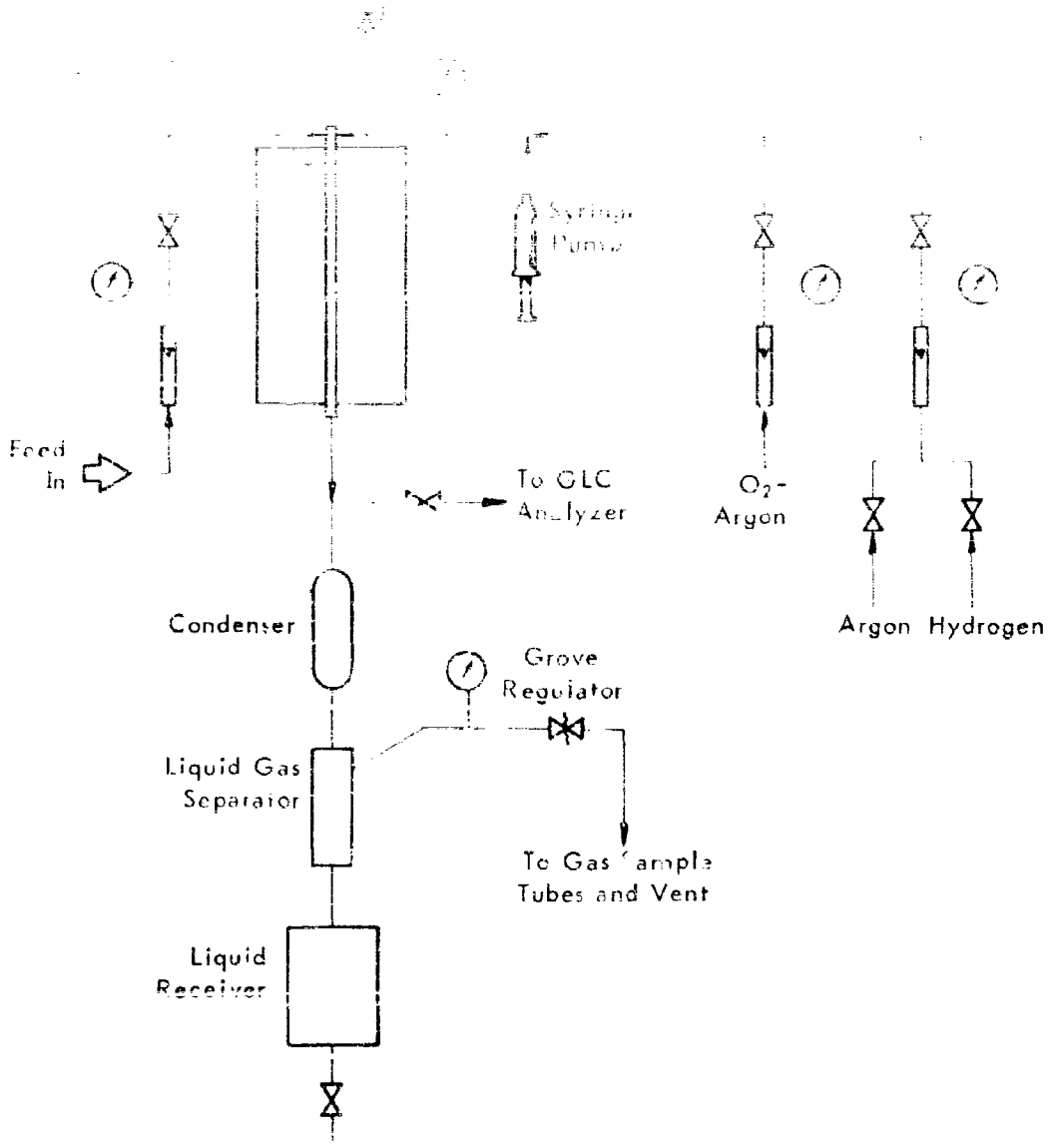


Figure 86. SCHEMATIC DIAGRAM OF PULSE REACTOR SYSTEM

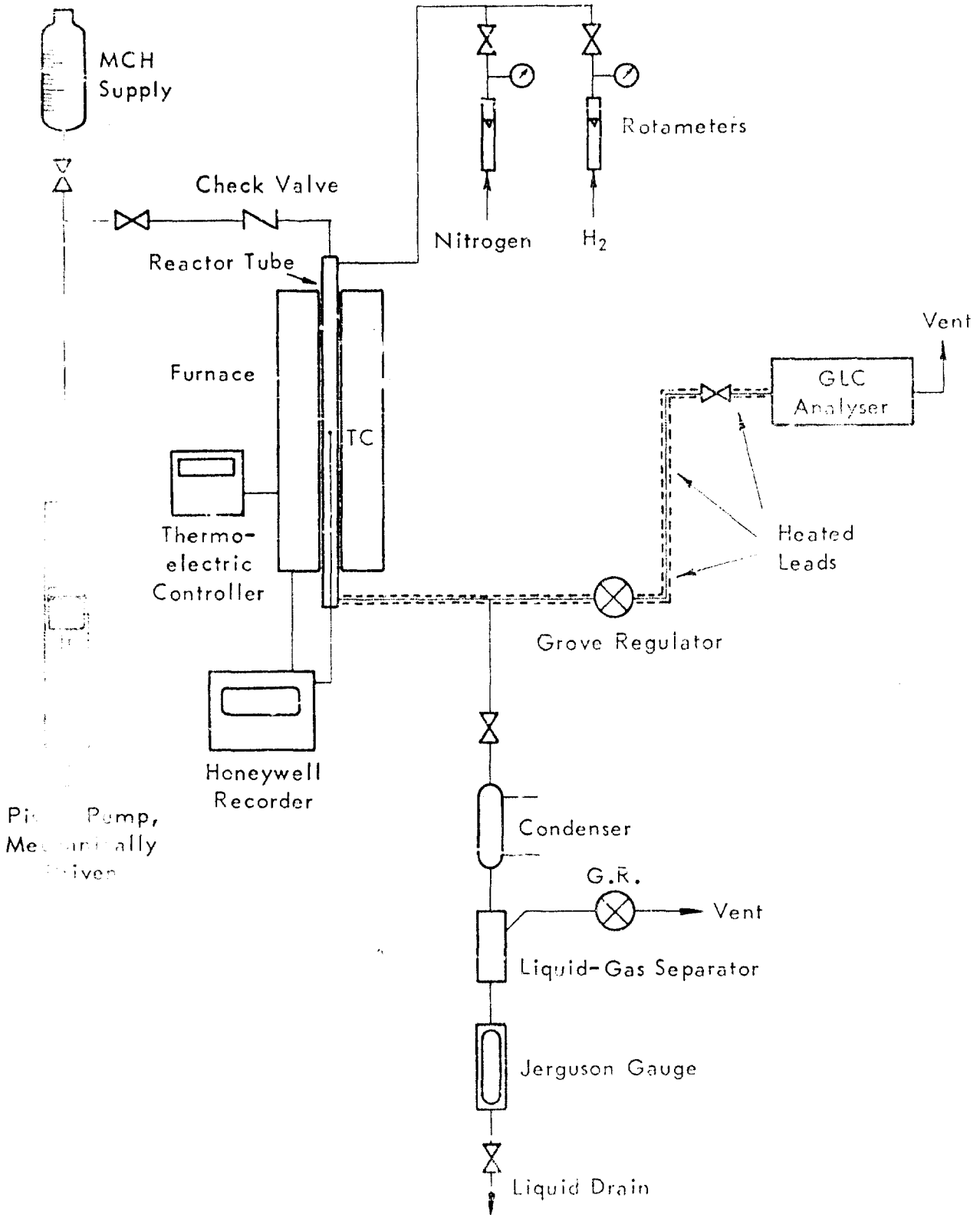


Figure 87. MICRO CATALYST TEST REACTOR (SCHEMATIC)
450 psig Pressure Rating

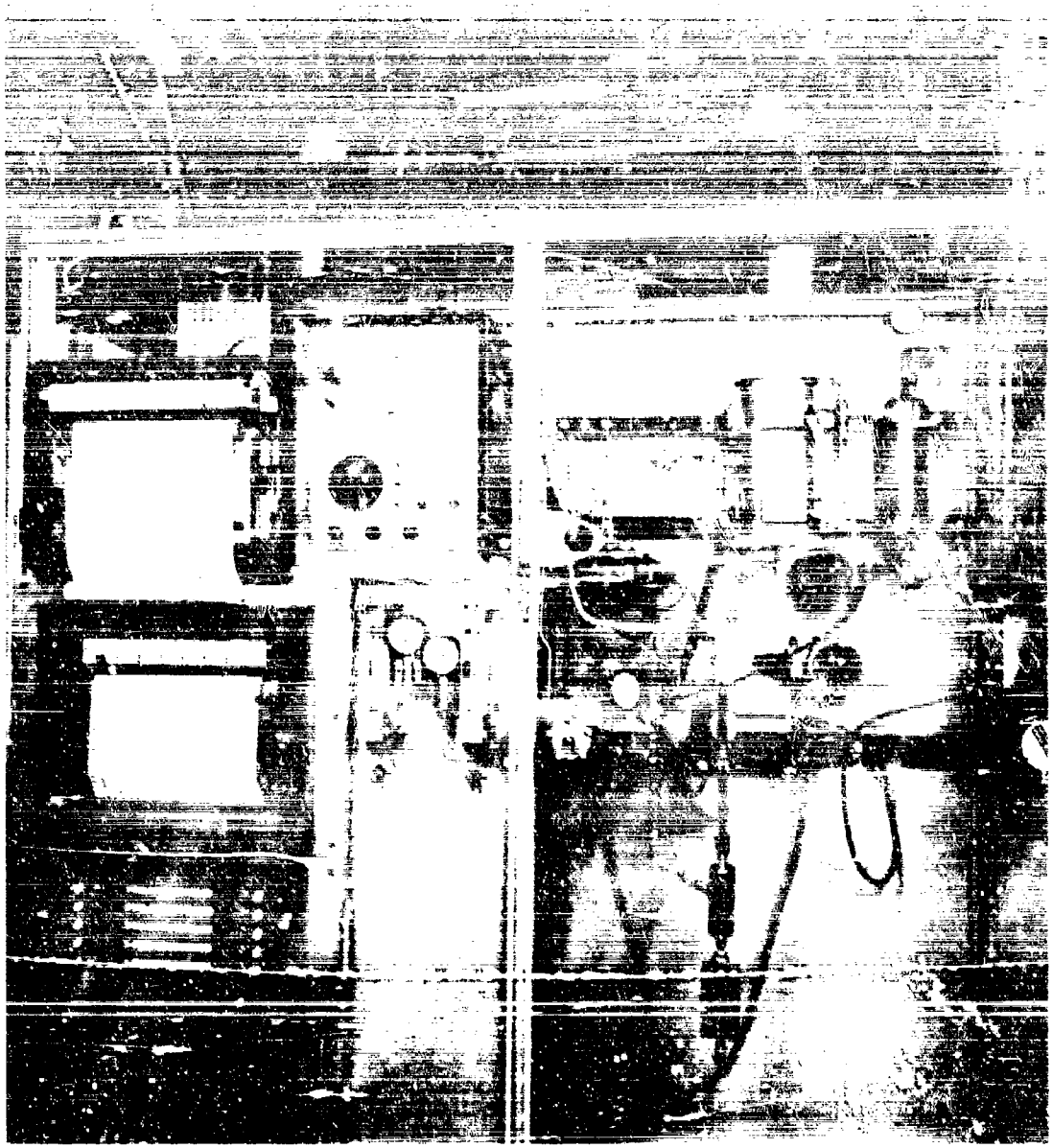


Figure 88. MICRO CATALYST TEST REACTOR
(General View)



Figure 69. MICRO CATALYST TEST REACTOR DETAIL -
Reactor Tube, Furnace and Stand

formed during the reaction is sufficient to maintain the pressure; no additional hydrogen is added. Samples at each temperature are bled at 3, 8, and 13 minute intervals into an Aerograph GLC unit, and the conversion of MCH to toluene determined from the ratio of the respective peak areas. It is necessary to recharge the piston pump after testing at each temperature. Catalysts (10-20 mesh granules) are diluted with 10-20 mesh quartz granules (0.9 ml:1.1 ml) before charging giving a bed length of 4-1/4 in. in the lower end of the 1/4-in. diameter thin walled stainless steel reactor tube. Catalysts are reduced 20 minutes at 797°F in hydrogen at 1 atm pressure before testing. Space velocity has been varied by changing catalyst volume, using a constant pump rate for MCH.

Temperatures have been measured at the outer skin of the reactor tube, 1 in. below the top and 1 in. below the bottom of the catalyst zone. An additional measurement is made in a thermowell at the very end of the catalyst bed. Up to run 140 the thermocouples were brought down parallel to the reactor tube via a closely adjacent slot in the block with the impinging bead held in place with Sauereisen cement. This proved mechanically unsatisfactory, however, and the couples were then brought in via a slot near the edge of the block and then by a right angle cut to the correct position; the couple beads were cemented so as to touch the reactor tube (cf Figure 89). Temperature drops of 30-40°F are observed with very active catalysts at 842°F block temperature.

The MICTR was operated in the catalyst preparation laboratory up to run 96 and then was moved to another location. Shortly after this, difficulty with the reproducibility of the activity of the reference catalyst (9874-24) was experienced. During about a month's period various possible refinements of procedure were made to obtain greater reproducibility. During this period 11 test runs were made and the following overall probable errors for the 8 and 13 minute samples results were calculated which are of consequence only when comparing candidate catalysts of high activity with the reference catalyst: 662°F, 29 ± 4% conversion; 752°F, 52 ± 3% conversion; and 842°F, 72 ± 7% conversion. Periodic checks for temperature calibration for both control and recording instruments have been found necessary. This was done after runs 105 and 220 which changed the base data for the reference catalyst. Values close to the above mean values are usually obtained if the flow of hydrogen gas used for catalyst reduction is not cut off until the pump is started (and a temperature drop observed), and the gas flow restarted just before the pump is stopped, during each test period. It seems best to retest the reference catalyst once a week for best data alignment with catalysts evaluated during this time interval.

All the results obtained at LHSV 100 are listed in sequence in Tables 73 and those at LHSV 200 in Table 74 of the Appendix. A few runs were left out where mechanical or instrumental problems occurred and the validity of the data obtained were in doubt. In such cases the catalysts were retested.

Table 73. MCH DEHYDROGENATION WITH VARIOUS CATALYSTS IN MICTR (LHSV = 100)

Period: December 1966 to February 1967

Conditions: 10 atm pressure. Catalysts reduced in H_2 for 20 min at 796°F. GLC samples normally taken at 3-, 8- and 13-min operation at each block temperature. Catalyst volume: 0.9 ml. Catalyst diluted with 1.1 ml quartz chips.

Run No.	Catalyst No. 9874-	Catalyst Description	% MCH Conversion		
			652°F	752°F	842°F
3	24	1% Pt/R-8 Al_2O_3 (Reference)	-, 28, 25	48, 43, 46 48,[a] 39,[a] -	72, 68, 60
19	24	1% Pt/R-8 Al_2O_3 (Reference)	23, 18, 18	-, 49, 47 -, 47, 52	60, 57, 58
6	90	2% Pt/R-8 Al_2O_3 (Reference)	31, 28, 28	57, 51, 47	60, 65, 63
7	180	2% Pt/R-8 Al_2O_3	27, 26, 34	54, 48, 46	70, 64, 64
4	41B	Expt'l. 1% metal	2, 1, -	23, 1, 05	5, 1, -
5	41C	Expt'l. 2% metal		59, 23, 1	15, 2, 0
8	19B	Expt'l. 1% metal	17, 9, 9	20, 18, 12	37, 29, 22
9	39B	Expt'l. 1% metal	20, 1, 3	34, 10, 1	4, 1,
10	56A	Expt'l. 1% metal	1, 0, -	0, -, -	0, 0, -
11	33	Bimetallic, 1 and 3%	20, 1, 1	2, 0, -	1, 0, -
12	22C	Expt'l. 5% metal	0, 0, -	0, 0, -	0, -, (932°F)
13	57A	Expt'l. 1% metal	0, 0, -	0, 0, -	0, 0, (932°F)
14	65B	Bimetallic, 1 and 1%	28, 26, 27	(33) 42, 45	-,
15	65A	Bimetallic, 0.5 and 0.5%	-, 27, 22	50, 46, 45	79, 72, 67
16	23	Expt'l. 1% metal	8, 6, -	9, 8, -	39, 13, 11
17	63B	Bimetallic, 1% and 1%	20, 18. 17	31, 30, 16	37, 7, 2
18	63A	Bimetallic, 0.5% and 0.5%	20, 16, 13	33, 28, 24	10, 3, 1
20	67B	Bimetallic, 1% and 1%	19, 20, 19	43, 37	73, 53, 50
21	94A	Expt'l. 2% metal	22, 17, 17	49, 27, 27	30, 25, 30

a) After 842°F run.

(Continued)

Table 73 (Contd-1). MCH DEHYDROGENATION WITH VARIOUS CATALYSTS IN MICTR (LHSV = 100)

Period: December 1966 to February 1967

Conditions: 10 atm pressure. Catalysts reduced in H_2 for 20 min at 796°F. GLC samples normally taken at 3-, 8- and 13-min operation at each block temperature. Catalyst volume: 0.9 ml. Catalyst diluted with 1.1 ml quartz chips.

Run No.	Catalyst No. 9874-	Catalyst Description	% MCH Conversion		
			662°F	752°F	842°F
Avg	24(ref)	1% Pt/R-8 Al_2O_3	28 ± 4	52 ± 3	72 ± 7
22	94B	4% metal/support #2	-, 20, 14	43, 39, 40	58, 57, 56
23	72	2% metal/support type #1	24, 25, -	54, 50, 48	71, 64, 63
24	73	2% metal/support type #1	25, 23, 22	50, 49, 48	80, 77, -
25	71	2% metal/support type #1	22, 18, 20	43, 43, 39	68, 72, 63
26	67A	Bimetallic; 0.5, 0.5% type #1	10, 13, 14	35, 31, 28	45, 37, 36
27	66B	Bimetallic; 1, 1%, type #1	22, 18, 18	37, 33, 33	50, 32, <1
28	58B	2% metal,[a] support type #1	-, 27, 28	47, 44, 42	75, 62, 66
29	95A	Bimetallic; 1, 1%, type #1	-, 27, 27	64, 56, 54	79, 80, 79
30	95B	Bimetallic, 0.5, 0.5%, type #1	37, 41, 37	52, 51, 49	74, 72, 73
31	96	2% metal, type #1	32, 29, 30	60, 57, 57	81, 74, 73
32	65B	Bimetallic, 1, 1% type #1	24, 28, 26	51, 54, 47	74, 69, 71
33	97	Bimetallic, 0.5, 0.5%	23, 24, 18	47, 42, 42	79, 50, 36
34	98	Bimetallic, 0.5, 0.5%, type #1	20, 22, 20	46, 43, 42	72, 62, 58
35	99	2% metal, support #3	-, -, -	-, 10, 0.7	0.5, -, -
36	103	2% metal, support #8	-	0, 0	0, 0
37	105	2% metal, support #8	-	0, 0	0, 0
38	58A	1% metal, support #1	29, 22, 30	47, 50, 43	61, 64, 68
39	95A	Bimetallic, 1%, 1% support type #1	35, 32, 28	57, 53, 54	85,(79),65
41	101	12% metal, support type #1	-	0, 0, 0	0, 0, 0
42	102	11% metal (sulfided), support type #1	-	15, 18, 16	15, 8, 10
43	107	2% metal, support type #1	33, 32, 32	60, 63, 63	87, 83,~79
44	108A	2% metal, support type #1	37, 30, 31	65, 65, 60	91, 82, 82
45	Shell 405	Classified	36, 42, 38	81,[b] 68,[b] 68[b]	85,[b] 80,[b] 80[b]
46	110	10% metal, support type #1	-	5, 4, 3	5, 3, 1
47	113	Bimetallic 1, 10%, support type #1	26, 25, -	56, 53, 51	78, 75, 73
48	112	2% metal,support type #1	31, 29, 31	50, 49, 48	(76),68, 55
49	111	1% metal, type #7	33, 36, 30	55, 56, 55	82, 75, 72
56	116	2% metal, type #1	0, 0, 0	0, 0, 1	3, 2, 0
58	Shell 405	Type classified	31, 31, 34	61, 59, 57	71,[b] 72,[b] 73[b]
59	117B	8% metal, support type #1	31, 30, 30	63, 65, 80	91, 89, 87
67	1118B	2% metal, support type #1, purif. dried (118°)	28, 33, 35	57, 53, 50	71, 71, 70
70	118A	2% metal, support type #1, purif. dried (500°)	-, 33, 34	62, 62, 59	76, 87, 88
71	120	Bimetallic, 2, 11%, support type #1	-, 29, 25	-, 45, 51	77, 78, 74
72	117A	4% metal, support type #1	33, 33, 33	59, 59, 60	90, 93, 89
74	124	10% metal, support type #1	-, 11, 11	19, 15, 12	18, ~3, 1
75	125	10% metal, support type #1	21, 21, 27	57, 57, 59	84, 81, 81
77	21C	2% metal, 2.7% Cl, support type #1	1, 0, 0	4, 1, 1	2, 1, 1
79	133	Bimetallic, 2, 5%, support type #1	29, 29, 26	52, 53, 53	57, 60, 57
80	131	4% metal, type #1	38, 34, 35	59, 58, 57	74, 73, 72
82	130	4% metal, type #1	42, 37, 36	69, 66, 65	85, 88, 85
83	132B	2% metal, type #1	38, 34, 35	62, 59, 58	85, 86, 80
84	132A	2% metal, type #1	40, 40, 36	70, 69, 64	88, 86, 86
85	13-270	Bimetallic, 2, 8%, support type #4	~1	-	~1
86	135	2% metal, support type #1	~1	~1	~1
87	136A	2% metal, support type #1	~1	~1	~1
88	137	Bimetallic, 2, 2%, support type #1	~1	~1	~1
89	140B	10% metal, support type #2	16, 14, 12	23, 20, 18	31, 16, 13
90	140A	10% metal, support type #2	29, 26, 26	44, 45, 44	70, 70, 70
91	140C	10% metal, support type #2	25, 25, 23	50, 46, 41	43, 38, 39
92	141A	Bimetallic, 1, 2% support type #1	~1	~1	~1
93	141B	Bimetallic, 1, 2% support type #1	~1	~1	~1
94	139	1% metal, support type #1	36, 35, 35	69, 60, 55	83, 75, -
95	141C	Bimetallic, 1, 1%, support type #1	25, 25, 22	49, 45, 45	60, 58, 54
96	142A	Bimetallic, 2, 11%, support type #1	-, 26, 30	47, 43, 41	38, 39, 38
		Moved MICTR to new location			
97	139	1% metal, support type #1	33,(43),40	62, 64, 65	83, 83, 84
98	142B	Bimetallic 4, 11% support type #1	37, 37, 37	60, 62, 60	85, 81, 68
100	-	Reactor tube filled with quartz only		-	0, 0, 0
101	24	1% metal, support type #1	32, 35, 32	60, 61, 59	79, 79, 78
102	140	8% metal, support type #1. (sulfided) 500	48, 44, 47	72, 70, 69	86, 84, 80
103	139	1% metal, support type #1	34, 31, 31	65, 65, 64	84, 83, 83
104	147A	2% metal, support type #4	<1	<1	<1
105	7	1% metal, support type #1	39, 38, 31	72, 69,(76)	91,(88),86
106	24[c]	1% metal, support type #1	32,(32),32	60, 60, 60	75, 70, 75
107	24	1% metal, support type #1	28, 25, 25	55, 49, 48	79, 68, 68
109	24	1% metal, support type #1	28, 25, 26	53, 49, 45	74, 65, 66

a) Impregnating solution different from that for catalyst #24.
b) Some benzene formed with additional conversion of MCH including toluene.
c) Indeterminate loading.

(Continued)

Table 73 (Contd-2). MCH DEHYDROGENATION WITH VARIOUS CATALYSTS IN MICTR (LHSV = 100)

Period: December 1966 to February 1967

Conditions: 10 atm pressure. Catalysts reduced in H_2 for 20 min at 796°F. GLC samples normally taken at 3-, 8- and 13-min operation at each block temperature. Catalyst volume: 0.9 ml. Catalyst diluted with 1.1 ml quartz chips.

Run No.	Catalyst No. 9874-	Catalyst Description	% MCH Conversion		
			662°F	752°F	842°F
110	139	1% metal, support type #1	32, 28, 28	45, 50, 44	80, 70, 69
111	7	1% metal, support type #1	36, 29, 28	64, 53, 52	89, 77, 76
112	152B	Bimetallic, 2, 2% type #1	22, 2, 2	28, 2, <1	10, 1, 2
113	130	4% metal, support type #1, purif., 932° muffled	28, 29, 28	62, 55, 51	89, 78, 78
114	142B	Bimetallic, 4%, 10%, type #1 (500°)	28, 31, 28	52, 55, 55	77, 82, 76
115	151A	Bimetallic, 2, 2%, type #1	25, 23, 27	43, 43, 38	60, 48, 45
116	24[a]	1% metal, support type #1	34, 27, 28	63, 56, 55	90, 80, 78
117	151B	Bimetallic, 2, 2%, type #1	28, 19, 9	43, 32, 27	79, 74, 68
118	151C[a]	Bimetallic, 2, 2%, type #1	18, 17, 16	38, 27, 23	49, 14, <1
119	152A[a]	Bimetallic, 2, 2%, type #1	0, 0, 0	<1	<1
120	152C	Bimetallic, 2, 2%, type #1	28, 18, (9)	44, <1	42, <1
121	148	5% metal, type #1	39, 32, 30	60, 57, 53	81, 85, 80
122	24[a]	1% metal, type #1	37, 30, 31	54, 58, 55	68, 64, 63
123	155C[b]	Bimetallic, 2, 10%, type #1	31, 32, 29	56, 55, 52	63, 67, 66
124	142[b]	10% metal, type #1	<1	2, 10, 17	21, 12, <1
125	100[b]	Metal + F, support type #9	0, 0, -	<1	<10
126	25B[b]	1% metal + F, support type #1	0	0	0
127	25A[b]	1% metal + Cl, support type #1	0	<1	<1
128	156A[b]	Bimetallic, 5, 5%, support type #1	30, 30, 27	53, 50, 49	70, 71, 69
129	HC577[b]	0.8% metal, support type #1	31, 33, 31	56, 54, 54	80, 77, 80, 85
130	24[b]	1% metal, support type #1	32, 34, 31	58, 56, 54	84, 81, 75, 75
131	24[b][c]	1% metal, support type #1	-	-	79, 75, 72
132	156B[b]	4% metal	37, 35, 34	61, 60, 57	80, 89, 85
134	24	1% metal, R-8, Al_2O_3	29, 29, 26	56, 50, 50	79, 72, 71, 70
135	157A	5% metal, R-8, Al_2O_3	23, 13, 6	1, 1, 1	24, 1, 0
136	24[d]	1% metal, R-8, Al_2O_3	28, (37), 30	50, 49, 47	75, 73, 70
137	139	1% metal, support, type #1	32, 33, 30	56, 54, 54	90, 79, 77
138	157B	Bimetallic, 5, 5%, support type #1	31, 29, 25	58, 50, 49	68, 64, 56
139	157C	Bimetallic, 5, 5%, support type #1	30, 32, 31	62, 57, 57	76, 78, 76
140	160B	4% metal, support type #5	33, 34, 23	56, 52, 49	78, 73, 73
143	160A	4% metal, support type #5	27, 28, 28	52, 52, 47	70, 70, 71
144	119A	2% metal, support type #7	33, 38, 37	64, 68, 64	89, 89, 88
145	119B	4% metal, support type #7	38, 32, 30	63, 59, 58	75, 67, 75
146	27	1% metal, 1% Cl, support type #1	7, 2, 1	5, <1, 1	1, <1
147	24	1% metal, support type #1	23, 40, 32	59, 57, 53	80, 78, 74
148	26A	1% metal, 1% F, type #1	20, 20, 35	46, 34, 27	45, 17, 8
149	161A	5% metal, support #6	28, 26, 23	37, 30, 30	45, 47, 37
150	161B	5% metal, support #6	36, 34, 33	61, 58, 56	79, 78, 85
151	161C	5% metal, support #6	28, 28, 24	47, 44, 43	57, 52, 55
152	155B	Bimetallic, 3, 2%, type #1	- 27, 25	44, 46, 43	55, 63, 59
153	155A	Bimetallic, 3, 2%, type #1	13, (22), 14	13, (11), 8	13, 11, 5
154	133	Bimetallic, 2, 5%, type #1	24, 29, 26	52, 51, 45	70, 64, 58
155	72	2% metal, support type #1	31, 30, 30	55, 53, 55	83, 77, 77
156	121A	10% metal, support type #1[e]	40, (26), 37	63, 64, 61	2[f]84; 2[f]81; 1[f]84
157	121B	30% metal, support type #1[e]	47, 41, 39	-, 8[f], 80; 3[f]71	2[f]; 70; 7[f]; 80; 4[f]; 75

a) New reactor tube.
b) Hydrogen flow left on until temp drop occurs, and hydrogen flow started before pump stopped after last sample taken.
c) After activation, tested directly at 450°F.
d) Reduced at 932°F instead of 796°F.
e) Reduced at 932°F before test.
f) Conversion to benzene.

(Continued)

Table 73 (Contd-3). MCH DEHYDROGENATION WITH VARIOUS CATALYSTS IN MCTR (LHSV = 100)

Period: March-May 1967

Conditions: 10 atm pressure. Catalysts reduced in H_2 for 20 min at 796°F. GLC samples normally taken at 5-, 8- and 13-min operation at each block temperature. Catalyst volume: 0.9 ml. Catalyst diluted with 1.1 ml quartz chips. LHSV = 100.

Run No.	Catalyst No. 9874-	Catalyst Description	% MCH Conversion		
			662°F	752°F	842°F
159	167A	0.76% metal, support type #1[a]	24,(42),30	61, 60, 56	87, 85, 80
160	24(ref)	1% Pt, R-8 Al_2O_3	26, 27, 27	49, 46, 48	72, 71, 64
161	105B	1% metal, R-8 Al_2O_3	33, 37, 35	62, 65, 60	82, 85, 85
162	165A	1% metal, R-8 Al_2O_3	18, 21, 23	47, 32, 30	51, 42, 8
163	111	1% metal, support type #7	42, 47, 39	57, 70, 61	86, 88, 81
164	168A	Bimetallic, 2, 2%, R-8 Al_2O_3	30, 37, 32	58, -, 56	83, 80, 79
165	168B	Bimetallic, 2, 2%, R-8 Al_2O_3	0, 0, -	<1	<1
166	169A	2.4% metal, support type #10	24, 20, 28	51, 51, 49	67, 70, 61
167	169B	2.4% metal, support type #10	22, 24, 22	37, 38, 32	44, 44, 42
168	171A	2.4% metal, support type #10	22, 18, 17	8, <1,( )	11, <1, -
169	171B	4.4% metal, support type #10	20, 15, 18	17, 26, 25	21, 14, -
170	24(ref)	1% Pt, R-8 Al_2O_3	27, 27, 29	49, 56, 54	76, 75, 70
171	171C	2.4% Pd, support type #10	-, 8, 7	14, <1	<1
172	173A	0.5% metal, support type #10	15, 10, <1	8, 5, <1	6, 3, 2
173	173B	0.5% metal, support type #10	<1, 2, -	6, 7, 5	8, 7, 6
174	173C	0.5% metal, support type #10	<1	2, 2, -	2, <1, -
175	173D	Bimetallic, 0.5, 0.5% support type #10	5, 3, 2	3, <1, -	2, 1, <1
176	183A	4% metal, support type #1	23, 31,(47)	78, 62, 56	88, 82, 79
177	183B	4% metal, support type #1	-, 26, 24	56, 50, 48	-, 73, 67
178	172A	6% metal, support type #1	0, 0,	0, 0,	
179	175A	2% metal, support type #1	35, 32, 28	56, 56, 52	74, 73, 65
180	24(ref)	1% Pt, R-8 Al_2O_3	29, 31, 19	54, 56, 52	80, 76, 72
181	175B	2% metal, support type #9	24, 26, 25	48, 41, 28	34, 20, -
182	172B	4.4% metal, support type #10	31, 34, 32	62, 63, 56	81, 82, 78
183	177B	Bimetallic, 5, 3%, R-8 Al_2O_3	28, 22, 21	50, 43, 40	58, 56, 52
184	181B	2% metal, support type #10	16, 15, 16	22, 14, 15	2, 1, 1
185	191	1% metal, R-8 Al_2O_3	27, 23, 26	52, 49, 56	79, 79, 73
186	24(ref)	1% Pt, R-8 Al_2O_3	21, 23, 18	46, 45, 41	69, 63, 58
187	177A	Bimetallic, 3, 4%, R-8 Al_2O_3	30, 23, 27	54, 49, 44	62, 63, 59
188	181A	1% metal, R-8 Al_2O_3	24, 24, 29	54, 57, 54	77, 80, 75
189	178A	5% metal, support type #10	0, 0,	0, 0	0, 0
190	178B	2% metal, support type #10	11, 14, 12	28, 17, 7	15, 11, 11
191	178C	2% metal, support type #10	19, 23, 26	45, 43, 43	67, 70, 63
192	24(ref)	1% Pt, R-8 Al_2O_3	25, 30, 27	55, 53, 50	75, 77, 72
193	183A	4% metal, support type #1[b]	39, 38, 36	71, 71, 67	83, 90, 88
194	183B	4% metal, support type #1[b]	28, 25, 16	46, 32, 47	65, 53, 34
195	179A	4% metal, support type #10	-, 27, 23	52, 38, 38	66, 62, 55
196	180A	5% metal, support type #10	0, 0	0, 0	0, 0
197	180B	5% metal, support type #10	0, 0	0, 0	0, 0
198	186	5% metal, R-8 Al_2O_3	0, 0	0, 0	0, 0
199	186A	Bimetallic, 2, 5%, Al_2O_3	26, 31, 32	48, 57, 54	81, 78, 74
200	186B	Bimetallic, 2, 5%, Al_2O_3	27, 30, 25	55, 49, 39	75, 53, 62
201	24(ref)	1% Pt, R-8 Al_2O_3	28, 30, 31	58, 54, 51	78, 75, 71
202	197B	4% metal, support type #1	32, 36, 36	68, 70, 67	94, 95, 90, 89
203	197A	4% metal, support type #1	35, 39, 36	70, 72, 66	95, 92, 89, 88
204	198A	4% metal, support type #1[c]	34, 27, 21	33, 34, 34	13, 12, 6
205	199A	4% metal, support type #1	26, 23, 24	54, 53, 54	84, 88, 84
206	199B	4% metal, support type #1[b]	38, 28, 32	63, 72, 68	92, 95, 91
207	199D	4% metal, support type #1[b]	27, 29, 28	57, 64, 60	86, 90, 87
208	199C	4% metal, support type #1	28, 37, 36	65, 66, 60	86, 90, 87

a) Pelleted powdered catalyst supplied to the United Aircraft Research Laboratory
b) Muffled at 1092°F for 1 hour in air.
c) Barium stabilized support.

(Continued)

Table 73 (Contd-4). MCH DEHYDROGENATION WITH VARIOUS CATALYSTS IN MICTR (LHSV = 100)

Period: March-May 1967

Conditions: 10 atm pressure. Catalysts reduced in H_2 for 20 min at 796°F. GLC samples normally taken at 3-, 8- and 13-min operation at each block temperature. Catalyst volume: 0.9 ml. Catalyst diluted with 1.1 ml quartz chips.

Run No.	Catalyst No.	Catalyst Description	% MCH Conversion		
			662°F	752°F	842°F
209	9874-24(ref)	1% Pt, R-8 Al_2O_3	22, 23, 23	56, 53, 49	79, 74, 70
210	9874-187C	4% metal, support type #9	26, 30, 29	57, 53, 50	61, 58, 56
211	9874-200A	4% metal, support type #1	37, 40, 36	69, 69, 66	93, 94, 90
212	9874-200B	4% metal, support type #1	34, 33, 35	57, 62, 58	87, 85, 81
213	9874-200C	4% metal, support type #1[a]	31, 35, 34	59, 63, 61	88, 88, 87
214	9874-200D	4% metal, support type #1[a]	29, 39, 36	73, 71, 66	96, 95, 91
215	10280- 5A	2% metal, support type #7	-, -, 33	58, 52, 54	85, 81, 75
216	10280- 5B	2% metal, support type #7	31, 37, 35	79, 68, 64	93, 91, 90
217	9874-24(ref)	1% Pt, R-8 support	23, 24, 24	46, 51, 52	87, 85, 80
218	9874-117A	4% metal, support type #1	-, -, 27	54, 57, 57	81, 82, 82
219	10280- 7A	Bimetallic (30:70 atom %), R-8 Al_2O_3	20, 15,(22)	31, 28, 28	32, 32, 25
222	9874-191	1% Pt, R-8 Al_2O_3	21, 23,(31)	48, 49, 50	78, 69, 76
223	9874-187A	Bimetallic, 2, 5%, support type #1	32, 27, 26	58, 56, 51	73, 74, 70
224	10280- 7B	Bimetallic (10:90 atom %), R-8 Al_2O_3	0, 0, -	0, 5, -	6, 0, -
225	9874-187B	Bimetallic, 2, 5%, R-8 Al_2O_3	19, 23, 24	45, 46, 47	65, 65, 62
226	9874-188A	Bimetallic, 2, 5%, R-8 Al_2O_3	-, 28, 27	61, 59, 57	79, 79, 77
227	10280- 9	Bimetallic, 2, 0.2%, R-8 Al_2O_3	23, 25, 25	46, 41, 37	57, 57, 56
228	9874-24(ref)	1% Pt, R-8 Al_2O_3	21, 27, 22	50, 45, 45	67, 70, 65
229	10280- 11B	Bimetallic, 2, 0.2%, R-8 Al_2O_3	-, 24, 18	30, 40, 34	45, 53, 49
230	10280- 11A	Bimetallic, 2, 0.6%, R-8 Al_2O_3	11, 11, 12	35, 25, 23	42, 35, 31
231	10280- 10	4% metal, support type #1	28, 33, 28	61, 53, 50	71, 77, 75
232	9874-188B	2% metal, 6% metal oxide-94% R-8 Al_2O_3	25, 20, 22	47, 48, 39	71, 59, 52
233	9874-189A	2% metal, 6% metal oxide-94% R-8 Al_2O_3	27, 32, 29	59, 57, 55	82, 80, 74
235	9874-190A	2% metal, 6% metal oxide-94% R-8 Al_2O_3	22, 22, 24	49, 58, 54	79, 82, 76
236	9874-190B	2% metal, 6% metal oxide-94% R-8 Al_2O_3	18, 20, 19	42, 29, 41	62, 49, 45
237	9874-189B	2% metal, 6% metal oxide-94% R-8 Al_2O_3	27, 23, 23	47, 43, 41	60, 60, 58
238	10280- 14	2% metal, 3% alkali carbonate, R-8 Al_2O_3	27, 25, 25	51, 53, 55	72, 71, 72
239	9874-24(ref)	1% Pt, R-8 Al_2O_3	23, 32, 28	54, 54, 52	77, 77, 70
240	10280- 13	4% metal, 5% metal oxide-94% R-8 Al_2O_3	26,(38),30	44, 46, 47	77, 71, 71
241	9874-192A	2% metal, 6% metal oxide-94% R-8 Al_2O_3	26, 34, 31	56, 56, 60	85, 85, 79
242	9874-192B	2% metal, 6% metal oxide-94% R-8 Al_2O_3	35, 28, 31	49, 49, 43	64, 66, 55
243	9874-200D[a]	4% metal, support type #1[a]	26, 23, 23	47, 48, 44	55, 69, 63
244	9874-24(ref)	1% Pt, R-8 Al_2O_3	35, 25, 23	48, 51, 47	76, 70, 67
245	9874-200A	4% metal, support type #1	30, 28, 32	63, 65, 61	90, 90, 84
246	9874-200A[b]	4% metal, support type #1	29, 32, 28	61, 53, 54	78, 70, 70
247	9874-200A[c]	4% metal, support type #1	39, 38, 36	71, 71, 67	96, 96, 92
248	9874-200D	4% metal, support type #1	25, 29, 29	63, 65, 61	87, 92, 88
249	10280- 16A	4% metal, 6% metal oxide-94% support type #1	23, 26, 28	69, 64, 62	93, 90, 87
250	10280- 16B[a]	4% metal, 6% metal oxide-94% support type #1[a]	29, 38, 36	66, 64, 61	92, 90, 86
251	10280- 22A	2% metal, support type #1	29, 35, 25	65, 57, 34	82, 83, 78
252	10280- 22B	4% metal, support type #1	31, 33, 30	68, 60, 58	86, 84, 80
253	9874-193A	2% Pt	24, 30, 29	59, 58, 54	84, 78, 74
254	9874-193B	2% metal, 6% metal oxide-94% R-8 Al_2O_3	30, 28, 25	50, 55, -	75, 68, 57
255	9874-24(ref)	1% Pt, R-8 Al_2O_3	26, 27, 24	47, 49, 49	75, 76, 69
256	9874-194A	2% metal, 5% metal (as oxide), R-8 Al_2O_3	23, 25, 24	53, 56, 54	73, 76, 70
257	9874-194B	2% metal, 6% metal oxide-94% R-8 Al_2O_3	31, 28, 21	48, 46, 45	67, 62, 52
258	10280- 24A	4% metal, support type #1	34, 29, 32	64, 68, 63	92, 92, 88
259	10280- 24B	4% metal, support type #1	48, 35, 33	62, 65, 61	92, 88, 85
260	10280- 15B	4% metal, 6% metal oxide-94% R-8 Al_2O_3	29, 33, 30	62, 59, 54	84, 85, 78
261	10280- 27	5% metal, R-8 Al_2O_3	0	0	<1
262	10280- 24C[a]	4% metal, support type #1[a]	39, 30, 28	60, 67, 64	94, 93, 88

a) Muffled at 1092°F for 1 hour in air.
b) LHSV = 200.
c) LHSV = 50.

Table 74. MCH DEHYDROGENATION WITH VARIOUS CATALYSTS IN MICTR (LHSV = 200)

Period: December 1966 to February 1967

Conditions: Same as given in Table 73
Catalyst Volume: 0.45 ml
Catalyst diluted with 1.55 ml quartz chips

Run No.	Catalyst No. 9874-	Catalyst Description	% MCH Conversion		
			662°F	752°F	842°F
51	24	1% Pt, R-8 Al_2O_3	23, 20, 20	33, 34, 30	55, 52, 5[illegible]
52	90	2% Pt, R-8 Al_2O_3	21, 22, 21	40, 43, 42	59, 58, 56
66	90	2% Pt, R-8 Al_2O_3	-	-	76, 80, 78, 70, 76[a]
68	90	2% Pt, R-8 Al_2O_3	21, (35), 24	43, 42, 42,	55, 55, 52
					71, 64, 64[a]
50	Shell 405	Classified	26, 27, 25	44, 46, 46	67, 65, 60
53	73	2% metal, support type no. 1	20, 20, 17	39, 39, 39	54, 56, 60
54	95A	Bimetallic 1, 1% support type no. 1	22, 22, -	40, 41, 38	58, 58, 58
55	108A	2% metal, support type no. 1	29, 30, 25	48, 48, 52	72, 67, 66
57	107	2% metal, support type no. 1	26, 25, 25	51, 51, 52	61, 61, 61
60	117B	8% metal, support type no. 1	26, 25, 23	52, 48, 59	78, 71, 71
61	119B	4% metal, support type no. 1	27, 29, 28	43, 45, 43	63, 62, 60
62	120	Bimetallic 2,11% support type no. 1	24, 32, 25	43, 46, 46	63, 65, 65
63	Shell 405	Classified	39, 25, 25	58, 50, 45	57, 57, 58
64	121A	10% metal, support type no. 1	25, 27, 23	51, 45, 45	59, 61, 55
65	121B	30% metal, support type no. 1	(50), 27, 25	47, 47, 46	67, 63, 63
69	108A	2% metal, support type no. 1			90, 91,[a]
73	117A	4% metal, support type no. 1	29, 29, 28	50, 46, (57)	64, 64, 60
					88, 84, 82[a]
76	125	10% metal, support type no. 1	-	55, 53, 52	75, 78, 79
					75, 75, 79[a]
78	118A	2% metal, support type no. 1	-	55, 57, 52	77, 74, 71
					87, 81, 80[a]
81	130	4% metal, support type no. 1 (purified, 932° muffled)	-	57, 55, 55	80, 77, 74
					87, 87, 83[a]

a) 932°F.

CAFSTR Heat Exchanger Design

All functional heat exchangers in the CAFSTR are identical, as shown in Figures 90 and 91.

Of particular importance is the annular design, permitting removal of the inner tube for inspection and plating, and for cleaning of the entire assembly. The inner tube is also the wall of the cartridge heating unit. A machine threaded header is welded to one end of the cartridge, which allows the rod to be removed after each test. The other end is positioned by a restricted portion of the annulus which centers the tube.

The outer heat exchanger shells are machined from Inconel Alloy 600 1-1/2" bar stock. The cartridge heater sheaths are also of Inconel 600, but other metals may be used for this purpose if desired.

To avoid fuel channeling, a circumferential distribution ring was provided at the inlet, while at the outlet, liquid flows without restriction through parallel slots positioned radially around the end of the heater.

The cartridge heaters for the annular heat exchangers are interchangeable and each is rated at 2000 watts, 220-vac. This represents two-fold or more the combined power requirement for heating fuel, heat losses, and rapid heatup of equipment on startup.

The exchangers for sensible heat were sized using the streamline flow equation of Sieder and Tate for heat-transfer coefficient,[11]

$$h = 2.0 \frac{k}{D} \left(\frac{wc_p}{kL} \right)^{1/3} \left(\frac{\mu}{\mu_s} \right)^{0.14},$$

where k = thermal conductivity of the fluid, Btu/hr ft°F,

D = annular width, ft,

w = mass rate of flow, lb/hr,

c_p = specific heat at constant pressure, Btu/lb°F,

L = length of the heat transfer surface, ft,

μ = absolute viscosity at bulk temperature, lb mass/hr ft,

μ_s = absolute viscosity at the surface temperature, lb mass/hr ft.

For a 13-inch long annular heated space, 5/8" x 11/16", and for MCH, calculated values of h ranged from 50 to 75 for the pressure range of 150 to 900 psia and temperature range of 600 to 1400°F. Calculated temperature differences between bulk fluid and wall varied from 65 to 170°F over these same sets of conditions.

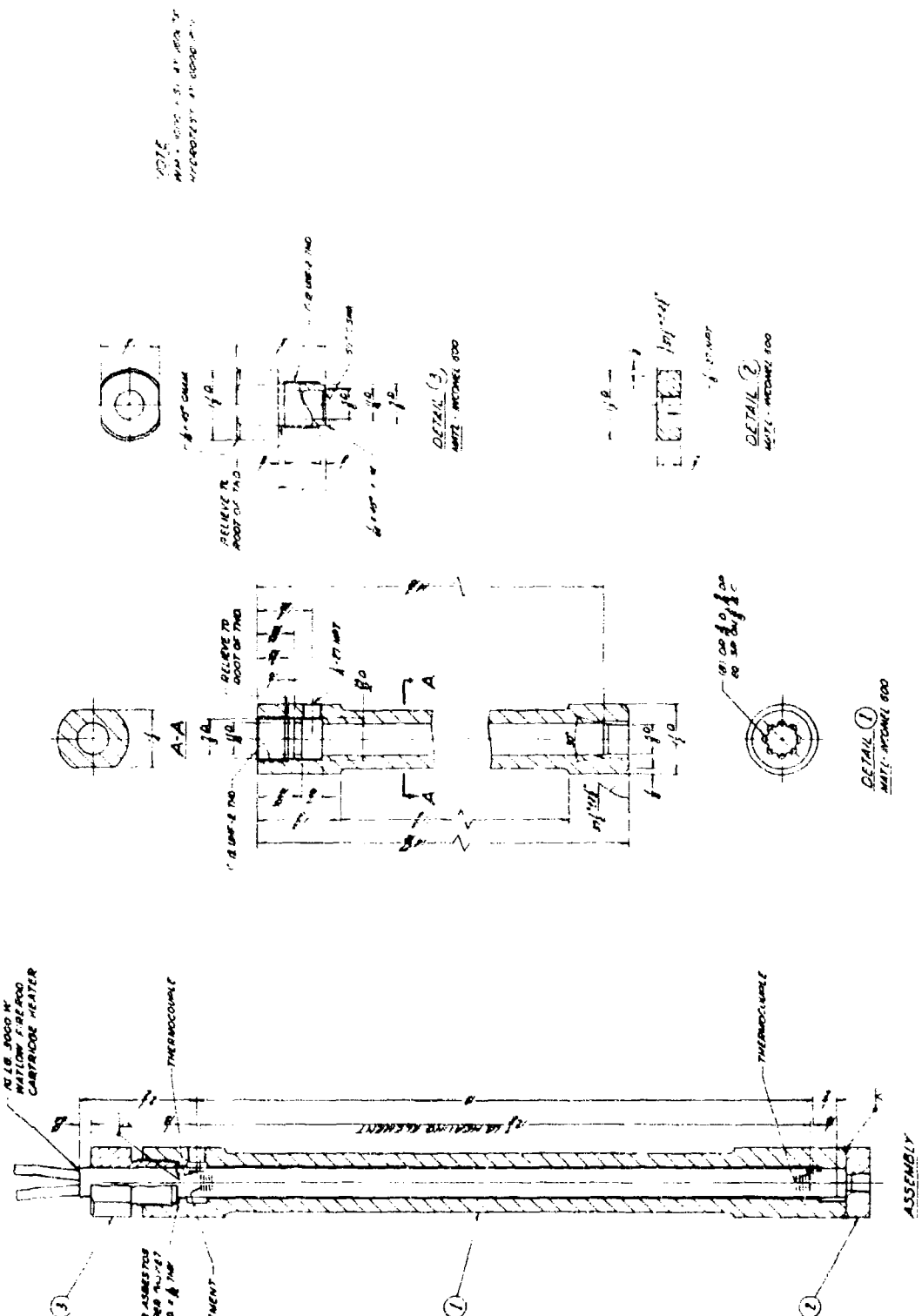


Figure 90. DETAILS OF HEAT EXCHANGER

62392

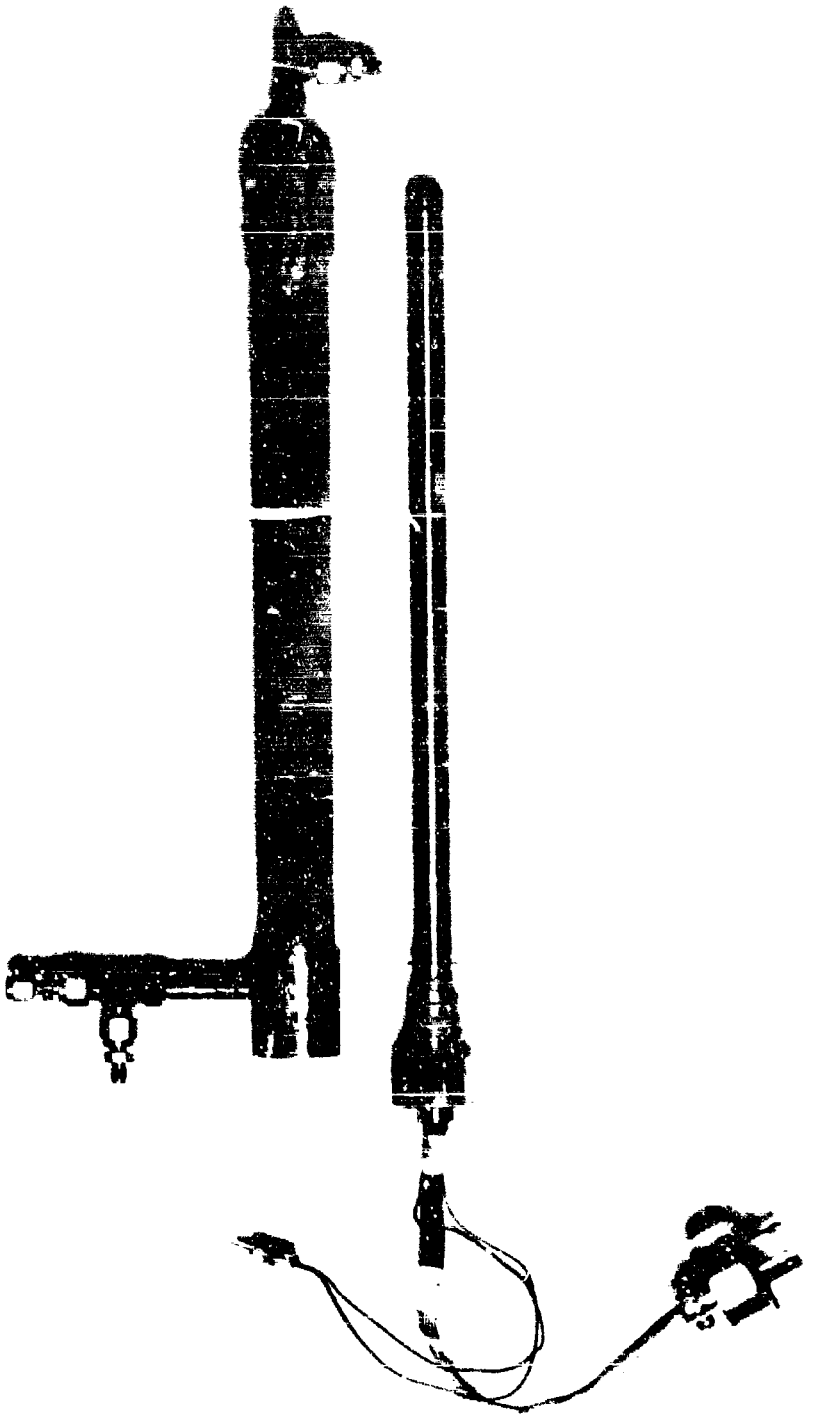


Figure 91. ANNULAR HEAT EXCHANGER FROM THE CAFSTR

AFAPL-TR-67-114
Part I

A Computer Program for Simulating Endothermic Fuel Reactions in a Packed Bed Reactor

The program described here was assembled to allow calculation of the amount of heat absorbed by a fluid passing through a single tube packed with catalyst. Calculations are made for the steady-state condition, with fluid flowing through the tube at constant mass velocity and undergoing endothermic reaction(s) when in contact with the catalyst. Heat is supplied to the fluid through the walls of the tube: 1) due to an axial profile of temperature imposed on the outside of the tube wall; 2) by flow of a secondary fluid outside the tube; or 3) due to an axial profile of heat flux imposed upon the tube wall. To calculate the extent of heat absorption, the program solves the set of partial differential equations describing the temperature and concentration distributions in the axial and radial directions within the symmetrical cylindrical tube. Thus, in addition to the heat absorption, these profiles of temperature and concentration and the axial profiles of pressure and tube wall temperature are also available from the program. An auxiliary portion of the program allows analogous calculations of conversion and temperature to be made for a series of adiabatic reactors with reheating of the fluid between stages.

In its present form the program makes calculations only for methyl cyclohexane as the fluid. This specificity is built into the program in two subprograms, REAX and RATE. As information becomes available for other endothermic fuels, alternates will be written for these two subprograms to allow calculations for other fluids. The remaining twelve subprograms are independent of the fluid used.

In the following sections, use of the program and a description of input and output formats are given. Subsequent sections contain a brief description of the equations integrated and their physical basis.

Input

Card 1. The first 72 columns comprise an alphanumeric field which will be printed out as a label for the problem at the top of the data printout. Column 75 (LIMIN) and column 80 (LAST) are control characters. LIMIN is set equal to zero for the first data deck loaded with the program. For subsequent decks, a 1 in LIMIN calls for card 6 as the next data card; a 2 calls for card 5 as the next data card; a blank or zero calls next for card 2. A

1 in LAST indicates the last set of data. The program will then not attempt to read another data deck following completion of the problem.

Card 2 - Six 12 character E format fields.

1-12: R, reactor radius in feet.
13-24: REACTR, reactor length in feet.
25-36: DP, catalyst particle diameter, in feet.
37-48: AF, a correction factor for the pressure drop calculation. (A function of DP/R, ranging from 0.5 for DP/R=0.45 to 0.67 for DP/R=0.19 to 1.0 for DP/R=0. Similar to Figure 35, Perry, Chemical Engineering Handbook, edition 3, page 394.)
49-60: EPSILN, fraction interparticular voids in bed.
61-72: PE, Peclet Number = 10.0

Card 3 - 5, 5 character I format fields followed by one 12 character E-format field.

1-5: JREACT, number of reactions for which calculations are to be made.
6-10: KC, number of components.
11-15: M, number of radial increments to be used in calculation. (2 has been adequate in our work). (2, 3, 4, 5, 6, 8, and 10 are permissible.)
21-25: IPSUP, a control character. If equal to 1 "intermediate printout" is suppressed and only the data printout and the final tabular printout will be obtained.
16-20: NPRI, number of axial points equally spaced axially along reactor for which results will be printed out either in intermediate printouts or in the final tabulation.
26-37: CROSKO, axial step length for integration in feet. This length will be shortened if necessary by the program to maintain stability in integration.

Card 4 - 5, 12 character E-format fields.

1-12: GAMA, compressibility factor of the fluid. (A constant value is used for the length of the reactor)
13-24: ZKF, thermal conductivity of the fluid (Btu/hr-ft-°F) (A constant value is used.)
25-36: ZMU, viscosity of the fluid (lb/hr-ft) (A constant value is used.)
37-48: HW, effective heat transfer coefficient through the wall of the tube. (Btu/hr-ft^2-°F).
49-60: HC, heat transfer coefficient outside tube wall (Btu/hr-ft^2-°F). If flux or outer tube wall temperature is to be specified supply a large number (e.g. 10^8) for HC.

Card 5 - 10 F5.4 fields giving the mole fractions of ten possible components in the fluid. For MCH fuels, the first six may be used. These are:

1-6, MCH; 7-12; H_2; 13-18, Toluene; 19-24, an isomer of MCH which will not undergo reaction to toluene; 25-30, cyclohexane; 31-36, benzene.

Card 6 - 6 E-format fields of 12 characters.

1-12: G, mass velocity of feed (lb/hr-ft^2)
13-24: P, inlet pressure (psig)
25-36: TBARE, inlet temperature (°F)
37-48: }
49-60: } Initial conversions of three possible reactions.
61-72: } These will normally be set equal to zero, except when calculating the second reactor in a series where it is desired to refer conversions to the feed composition to the first reactor. In this case the feed composition specified on Card 5 would be the initial feed to the first reactor. For the MCH system, the three possible reactions are: 1) MCH $\rightleftharpoons$ Toluene + $3H_2$, 2) MCH $\longrightarrow$ Isomer; 3) CH $\rightleftharpoons$ Benzene + $3H_2$.

Card 7 - 2I6, 5E 12.4

1-6 : INDEXT, a control character specifying the type of boundary condition to be used. The value of the control character also influences the interpretation of the data on this card and the following card (if used).
6-12: NPROP, specifies the number of E-format fields to be read on this card and the following. If NPROP is 5 or less, the following card will not be called for and should not be supplied except when calculating a series of adiabatic reactors in which case, Card 8 is always called for.
13-24: }
25-36: }
37-48: } Boundary condition information read under the name
49-60: } DATPRO (I), I = 1, 5
61-72: }

Card 8 - 5 E 12.4. These fields offer a continuation of boundary condition information read as DATPRO (I), I = 6, 11.

If INDEXT = 1, the boundary condition information (DATPRO) is treated as specified temperatures of the secondary fluid surrounding the reactor tube (°F). If HC is made very large, these temperatures are then effectively the outside wall temperatures of the tube. If NPROP = 1, this temperature is taken as a constant along the length of the tube with the value given by DATPRO (1), (Card 7, columns 13-24) If NPROP = 2, the temperature is taken to vary linearly along the length from an inlet end temperature of DATPRO (1) to an outlet end temperature of DATPRO (2). If NPROP = 3 or higher, (up to a maximum of 10), the DATPRO values are taken as equally spaced points on an axial temperature profile. In the program, these specified points are fit with a series of parabolas to obtain values for intermediate points along the reactor.

If INDEXT = 2, the boundary condition information is referred to a secondary fluid surrounding the tube. Only the first three values of DATPRO are used (NPROP should be set = 3, and Card 3 should be omitted). Reasonable values should be supplied for HC and HW in this case. DATPRO (1) is the inlet and temperature of the secondary fluid (°F). DATPRO (2) is the flow rate of the secondary fluid (lb/hr). For cocurrent flow this should have a positive sign and for countercurrent, a negative sign. DATPRO (3) is the heat capacity of the secondary fluid (Btu/lb-°F).

If INDEXT = 3, the boundary condition information is treated as a specified heat flux 1 Btu/hr-ft^2) to the tube. A single specified value for a constant flux or a sequence of values for a flux profile are treated in a manner analagous to that used for temperature profiles when INDEXT = 1. The value of NPROP should agree with the number of points specified and Card 8 omitted unless NPROP is 6 or greater. The flux values as well as HC and HW should be based on the inside wall area of the tube.

If INDEXT = 4, a one-dimensional calculation will be made for a series of adiabatic reactors. These reactors will all be of the same length specified by DATPRO (11) in feet. The number of reactors is given by NPROP and the separate feed temperatures to these are given by the first NPROP values of DATPRO in °F. The composition of the feed to each reactor after the first is given by the composition of the product leaving the preceding reactor. Card 8 is always required for this calculation.

Output

Three types of output printing are available from the program: 1) A first page repeating input data; 2) Intermediate printouts giving radial profile information at a selected number of points along the reactor; and 3) A final tabular printout listing heat transfer coefficients used and giving axial profiles of temperatures, pressure and conversion.

The printout of input data is reasonably self-explanatory. At the top is given the label from the first card of the input deck followed by the names of components and their mole fractions in the feed. The remaining input data is repeated below in the same units used in the input data deck. The portions labeled ARATE, BRATE, CRATE printout rate constant parameters which are built into the program in subprogram REAKN. The bottom portion of the page gives the boundary condition information.

The intermediate printout may be suppressed if not required as explained in the input section. Each intermediate printout occupies a separate page, giving the number of printout, pressure in psig, temperature of the "secondary fluid" in °F, mean conversion in each of the pertinent reactions, in moles/mole of feed and the mean temperature of the reacting fluid. This is followed by radial profiles of conversion and temperature. The radial profiles are at equal r^2 increments beginning at the centerline and ending at the outer limit of the packing. Then, the number of steps taken, the reactor length and heat added up to this length are given. Finally, the printout gives the mean fluid composition in both mole fraction and moles/mole of feed.

The final printout gives the heat-transfer coefficients used and a tabulation containing temperatures, pressure, conversions and heat added at NPRINT equally spaced points along the reactor length. H is the overall heat transfer coefficient from secondary fluid to the outside of the packing, HC and HW are as input, the coefficients across the secondary fluid and the metal wall. HF is the coefficient across the primary fluid film just inside the reactor wall. HP is the particle-to-fluid heat transfer coefficient inside the catalyst bed. The tabular part of the final printout lists: the length (in feet), heat added (Btu/lb), average fluid temperature (°F), centerline temperature of the reactor (°F), temperature at the outside of packing (°F), temperature on the hot side of reactor wall (°F), pressure (psig), and conversions by each of the three possible reactions (moles/mole of feed).

Numerical Integration Aspects of the Program

The program operates to solve the differential equations using a simple forward difference approximation in the axial direction and higher order approximations in the radial direction for temperature and conversions. The radial variable used is r^2, thus increments in the radial direction are of equal area. The radial increment is set by M, the number of radial increments data loaded. From the standpoint of computing time, it is desirable to use a minimum value for M. Our experience has been that the minimum value of M=2 has given satisfactory accuracy. Hence, a larger number of radial increments would be used only to obtain a more precise definition of radial profiles. The axial step is data loaded. However, for stability of integration, a relationship between the axial and radial step must be met:

$$k \leq \frac{0.3\ Pe}{4\ Dp}\left(\frac{R_t}{M}\right)^2$$

where: k is the axial step (ft)
Dp is the particle diameter (ft)
Pe is the Peclet Number
R_t is the tube radius (ft)

The program is arranged to automatically reduce the data loaded axial step size, if necessary, to meet this criterion. From the standpoint of accuracy we have found no benefit in reducing the axial step below the value required for stability. Of course, from the standpoint of computing time it is desired to use the largest possible axial step. Our experience with computation times is limited to those on an IBM 7040. Here, the compiled form of the program (object decks) require about 0.75 min for loading and 0.6-0.7 min for calculation of a ten foot reactor tube (500 axial steps) with one reaction. The inclusion of the second reaction adds about 0.1-0.2 min to this calculation. Our experimental results with the smaller diameter tube (R_t=1.15x10^{-2} ft) require a smaller axial step for stability (2000 axial steps for a 10 ft length) and take a proportionately longer calculation time. The calculation of the adiabatic reactors goes very much faster since no stability restriction is imposed and only one source term is required on each axial profile. For this type of calculation one is concerned only with the

effect of axial step size on accuracy. A step size of 0.02 ft has been satisfactory for the magnitude of rates and mass velocities for which we have been calculating up to this time.

Reactions in the MCH System

The portions of the program specific to the MCH fuel system have been set up to allow calculations for three possible reactions among six possible components. For a pure MCH feed, however, only the first two reactions and four components are necessary. The reactions in order are:

J	Reaction
1	MCH $\rightleftharpoons$ Toluene + $3H_2$
2	MCH $\rightarrow$ Isomer - not reversible
3	CH $\rightleftharpoons$ Benzene + $3H_2$

For most screening calculations, it will be sufficient to deal only with the first reaction (JREACT=1 and KC=3). For more refined calculations the formation of isomers (principally ethyl and dimethyl cyclopentanes) should be taken into account as well (JREACT=2, KC=4). Under extreme conditions of low space velocity and high temperature as much as five percent of the MCH feed may be diverted by this nearly isoenthalpic reaction and thus be unavailable for the primary endothermic reaction. The third reaction was included in the program only because some of our experiments were carried out with a feed containing about 3.5 mol % cyclohexane.

The first and primary reaction is treated as reversible. Both equilibrium and reaction rate parameters are built into subprogram REAXN. The rate of the reaction is calculated at each mesh point in the program by subroutine RATE, the reaction rate is calculated from the expression

$$R(\text{lb-mol/hr-ft}^3) = \frac{(1-\epsilon)\,(A_1 A_2)\exp\left(\frac{B_1+B_2}{R_g T_s}\right) C_{MCH}}{1 + A_2 \exp\left(B_2/R_g T_s\right) C_{MCH}} \left[1 - \frac{P_{tol} P_{H2}^3}{P_{MCH} K_{eq}}\right]$$

where: ϵ is the fraction voids in the bed.

C_{MCH} is the local concentration of MCH (lb mol/ft^3) in the gas phase.

P_{tol}, P_{H2} and P_{MCH} are the partial pressures of toluene, hydrogen and MCH (atm).

R_g is the gas constant (Btu/lb mol - °R).

T_s is the surface temperature of the catalyst pellet (°R).

K_{eq} is the equilibrium constant for the reaction (a function of temperature only).

A_1, A_2 and B_1, B_2 are rate parameters printed out with the input data as ARATES (1 and 2) and BRATES (1 and 2).

They have the values:

$A_1 = 7.5 \times 10^{12}$ $\quad B_1 = -59000$
$A_2 = 4.5 \times 10^{-8}$ $\quad B_2 = 54000$

K_{eq} for this reaction is calculated from the expression:

$$K_{eq} = 4.0 \times 10^{20} \exp\left(\frac{-92500}{R_g T_s}\right)$$

The surface temperature of the catalyst pellet is related to the fluid temperature by the equation:

$$T_s = T_g + \frac{R\Delta H_p}{6H_p}$$

This temperature and the reaction rate R, require an iterative calculation since each quantity depends on the other. They are calculated together in subroutine RATE.

The second reaction is treated as an irreversible first order catalytic reaction with the rate given by:

$$R_2 \text{ (lb-mol/hr-ft}^3\text{)} = (1-\epsilon)\, C_{MCH}\, A_3 \exp\left(B_3/R_g T_s\right)$$

This is obviously a simple approximation to the rate, but has proved satisfactory in reproducing experimental results when small conversions (5% or less) to isomer were observed. The values of the rate constant parameters: A_3 and B_3 are contained in subprogram REAX as ARATE (3) and BRATE (3). They have the values:

$A_3 = 1.4 \times 10^7$
$B_3 = -30,000$

The third reaction is also treated in a simplified manner suitable only for small concentraction of cyclohexane in the feed. The rate is given by:

$$R_3 \text{ (lb mol/ft}^3\text{-hr)} = (1-\epsilon)\, C_{CH}\, A_4 \exp\left(B_4/R_g T_s\right) \left\{1 - \frac{P_{BZ} P_{H_2}^3}{P_{CH} K'_{eq}}\right\}$$

where

$A_4 = 3.25 \times 10^8$
$B_4 = -27000$

Physical Basis of Computer Program for Simulating Packed Bed Reactor

Material and Energy Transport

The general equations describing material and energy transport within

a packed bed have been discussed in some detail previously[a] and will not be discussed here. We simplify the equations by making the following assumptions:

1. The flow is axially symmetric,
2. Axial diffusion and conduction may be neglected, and
3. Molecular diffusion may be neglected.

The last assumption is important. By imposing the same (eddy) diffusivity on all chemical species, it allows us to describe the material balance in terms of the conversion via each reaction rather than in terms of the concentration of each component. This reduces the number of equations from a maximum of ten to a maximum of three. In deriving the material-balance and associated equations the basis has been selected to be a "mass unit" of material equal to one mole of original feed. Conversions are thus expressed as moles of reaction per mole of original feed. Similarly mass velocities are expressed as these "mass units" per unit area per unit time.

The steady-state equations for material transport are written in terms of conversion, x_j, as follows:

$$0 = \left(\frac{\partial x_j}{\partial z}\right) - \frac{4d_p}{R^2 Pe}\left(u\frac{\partial^2 x_j}{\partial u^2} + \frac{\partial x_j}{\partial u}\right) - \frac{R_j}{G} \qquad j = 1 \text{ to JREACT} \qquad (1)$$

In simplified notation these are written:

$$0 = \dot{x}_j - \omega[ux'_j + x_j] - S_j \qquad (2)$$

where the dots signify differentiation axially and the primes signify differentiation radially. The quantity ω does not vary with axial position. There will be one such equation for each independent chemical reaction. All will have the same value of ω and will differ only in the "source term", S_j.

The steady-state equation for energy transport is written:

$$\begin{aligned} 0 = {} & \left(\frac{\partial T}{\partial z}\right) - \frac{4d_p}{R^2 Pe}\left(u\frac{\partial^2 T}{\partial u^2} + \frac{\partial T}{\partial u}\right) - \frac{4K}{GC_p R^2}\left(u\frac{\partial^2 T}{\partial u^2} + \frac{\partial T}{\partial u}\right) \\ & - \frac{4K}{GC_p R^2}\left[\frac{1}{K}\frac{\partial K}{\partial u}\right] u\left(\frac{\partial T}{\partial u}\right) - \frac{4d_p}{R^2 Pe}\left[\frac{\varepsilon}{C_p}\sum_{1}^{JREACT}\left(\frac{\partial C_p}{\partial x_j}\right)\left(\frac{\partial x_j}{\partial u}\right)\right] u\left(\frac{\partial T}{\partial u}\right) \\ & - \frac{4d_p}{R^2 Pe}\left(\frac{\partial C_p}{\partial T}\right)\left(\frac{\partial T}{\partial u}\right) u\left(\frac{\partial T}{\partial u}\right)\frac{1}{C_p} + \frac{1}{GC_p}\left[\sum_{1}^{JREACT} R_j Q_j\right] \end{aligned} \qquad (3)$$

The energy-transport equation has been written in such a form as to illustrate its similarity to the material-transport equation. In addition to the assumptions made for the material-transport equation, it has been assumed that the radial diffusivity for heat is the sum of an eddy diffusivity and a "non-eddy" diffusivity, K, the latter in turn being related in some manner to the transport

a) Beek, J., Advances in Chemical Engineering, Vol. 3, pp 203-271, New York, Academic Press, 1962.

of heat via conduction through the fluid, conduction through the packing, and radiation. In simplified notation equation (3) becomes:

$$0 = \dot{T} - \theta[uT'' + T'] - S_t \tag{4}$$

In general, since terms such as k, C_p, $\partial C_p/\partial T$, and $(\partial x_j/\partial u)$ vary axially as well as radially, it is convenient to lump all of the last five terms of equation (3) into the source term, S_T, when solving the problem on a computer. Equations (2) and (4) are then of the same general form.

The boundary conditions at the tube wall are:

$$x_j = \left(\frac{\partial x_j}{\partial u}\right) = 0 \qquad j = 1 \text{ to JREACT} \tag{5}$$

$$T' = \left(\frac{\partial T}{\partial u}\right) = -\frac{Rh(T - T_c)}{a\left(\frac{GC_p d_p}{Pe} + K\right)} = -H_T(T - T_c) \tag{6}$$

Average values of mass velocity, G, heat capacity, C_p^o, and thermal conductivity, K^o, are used in applying equation (6).

Coolant Temperatures

For a sensibly heated, cocurrent coolant the differential equation is:

$$\dot{T}_c = \left(\frac{\partial T_c}{\partial z}\right) = \frac{2\pi Rh}{WC}\ (T - T_c) \tag{7}$$

Pressure Drop

The differential equation for pressure drop is:

$$\dot{P} = \frac{\partial P}{\partial z} = \frac{fG^2 A_f}{\varepsilon_c \rho d_p} \tag{8}$$

For the friction factor the equation of Ergun[a] is used:

$$f = \frac{1 - \epsilon}{\epsilon^3}\left(1.75 + 150\,\frac{1 - \epsilon}{Re}\right) \tag{9}$$

For gases the specific volume will be of the form:

$$\frac{1}{\rho} = \frac{\gamma R_G T}{PM} \tag{10}$$

In terms of the conversion as defined in this report, the specific volume, averaged radially, becomes:

a) Ergun, S., Chem. Engr. Progress, 48, 89 (1952).

$$\frac{1}{\rho} = \frac{\gamma R_G T}{PM_o} \left[1 + \sum_{j=1}^{JREACT} \left(\sum_{k=1}^{KC} S_{k,j} \right) \bar{x}_j \right] \tag{11}$$

The variation of pressure within the bed has been included in the analysis because of its effect on the rate of gas phase reactions.

Heat-Transfer Coefficients

The heat-transfer coefficient from the fluid to the catalyst particles is that suggested by Beek[a] for

$$h_p = \frac{k_f}{d_p} \left[3.22 \, (Re)^{\frac{1}{3}} \, (Pr)^{\frac{1}{3}} + 0.117 \, (Re)^{0.8} \, (Pr)^{0.4} \right] \tag{12}$$

The heat transfer coefficient at the wall is given by:

$$h_w = \frac{k_f}{d_p} \left[0.203 \, (Re)^{\frac{1}{3}} \, (Pr)^{\frac{1}{3}} + 0.220 \, (Re)^{0.8} \, (Pr)^{0.4} \right] \tag{13}$$

Effective Thermal Conductivity Within the Bed

Radial transport of energy occurs by a variety of means, to wit: eddy conduction, conduction through the fluid, conduction through the catalyst and radiation. In equation (3), it is assumed that the conductivity is the sum of the eddy and "noneddy" conductivities. The latter includes all other forms of conduction and is treated by the method suggested by Beek.[a] The overall conductivity is:

$$K_{OVERALL} = \underbrace{\frac{C_p G d_p}{Pe}}_{\text{EDDY}} + \underbrace{\frac{0.5 \, h_p d_p k_s}{2k_s + 0.7 \, h_p d_p}}_{\text{PACKING}} + \underbrace{2\epsilon_r \sigma_r d_p T^3}_{\text{RADIATION}} \tag{14}$$

Note that no expression for molecular conductivity of the fluid has been included.

Heat Capacity

The heat capacity of each component is assumed to be of the form:

$$(C_p)_k = a_k + b_k T \tag{15}$$

The heat capacity of the mixture is assumed to be linear in composition.

Peclet Number

The Peclet number is assumed to be constant throughout the reactor.

---

a) Beek, J., Loc. cit.

```
C      SHELL DEVELOPMENT PACKED BED REACTOR PROGRAM   3/30/67
$IBFTC MAIN
C      MAIN  PROGRAM
       COMMON/ALL/ CROSSK, GBAR, HT, HM, JREACT, JRERUN, KC, KVPRIM, M,
      1MMINUS, MONE, MTWO, N, NPLUS, OMEGA, PHI(12), R, SIGMA(12),
      2TBARE(3,1), TREFR, TPRIME(3), TSUBE(12,3,1), V(13,3), UM(12,3),
      3UT(12,3), XBARM(3,3), XSUBM(12,3,3), Y, ZLENGT, ZM
       COMMON /XESEA/ AF, BARMC, BTUPPO, DP, E, EPSILN, EPSILR, FLARGE,
      1 G, GAMA, H, HC, HF, HP, HW, INDEXT, IPSUP, KINT, NPR, NPROC,
      2 NPROP, NSS, NSTEP, PE, REACTR, RGAS, ZKF, ZKS, ZMU
       COMMON/XFIND/ A(10), ANAME(2,10), ARATE(6), B(10), BRATE(6),
      1C(5,3), CRATE(6), DATPRO(11), DELTA(10), EQ(3,2), F(10), P(3),
      2 PROF(10,5), PSI(3), Q0(3), S(10,3), SR(12,3), ST(12,3),
      3 TPRINT(10,100), XI(3), ZBIGM(10)
       DIMENSION  SUBJEC(12)
C      START OF PROGRAM
       NRUN = 0
C      RETURN POINT FOR STACKED RUNS
C      READ AND WRITE TITLE OF RUN
   13  READ(5,1000)  (SUBJEC(I), I=1,12), LIMIN, LAST
C      LIMIN IS FLAG FOR ABBREVIATED DATA DECK
 1000  FORMAT (12A6, 2X, I1, 4X, I1)
       WRITE(6,1001) (SUBJEC(I) , I=1,12)
 1001  FORMAT (1H1 20X, 12A6)
C      ZERO SIGNIFICANT PARTS OF COMMON
       JRERUN = 0
       ZLENGT = 0.0
       CROSSK = 0.0
       NPR = 0
       DO 14 N=1,3
       P(N) = 0.0
       TBARE(N,1) = 0.0
       TPRIME(N) = 0.0
       XBARM(N,1) = 0.0
       XBARM(N,2) = 0.0
   14  XBARM(N,3) = 0.0
       KINT = 0
       NPROP = 0
       DO 15 I=1,10
   15  DATPRO(I) = 0.0
       NRUN = NRUN + 1
       JINPT = LIMIN + 1
C      COMPLETE DATA DECK REQUIRED FOR FIRST RUN
       IF(NRUN.EQ.1)  JINPT = 1
C      READ AND WRITE  INPUT DATA
       CALL INPUT(JINPT)
C      CALCULATE CONSTANT COEFFICIENTS
       CALL MISCEL
       IF(JRERUN.EQ.1)  GO TO 100
       CALL SRCOEF
       KVPRIM = 0
       CALL EXPCFC(UM)
       KVPRIM = 1
       CALL EXPCFC(UT)
       NSS = 0
       NP = 0
```

```
      NPLUS = 1
      KINT = 0
      ZLENGT = -CROSSK
      IF(I SUP) 42,41,42
C     PRINT OUT INITIAL PROFILE DATA
   41 CALL PRINT(1)
   42 CALL COMPOS
C     RETURN POINT FOR AXIAL STEP IN INTERGRATION
   50 ZLENGT = ZLENGT + CROSSK
   52 N = MOD(NSS,3) + 1
      NPLUS = MOD(NSS+1,3) + 1
      CALL RATE
      CALL SOURCE
      KVPRIM = 0
      CALL EXPLIC(XSUBM,UM,SR)
      KVPRIM = 1
      CALL EXPLIC(TSUBF,UT,ST)
      CALL COOLFX
      IF(JRERUN.EQ.1)  GO TO 100
      NSS = NSS+1
   53 NP = NP + 1
      IF(NP.LT.NPR)  GO TO 50
      KVPRIM = 0
      CALL AVERAG(XSUBM,XBARM)
      KVPRIM = 1
      CALL AVERAG(TSUBF, TBARF)
C     IPSUP SUPPRESSES INTERMEDIATE PRINT
      IF(IPSUP) 62,61,62
   61 CALL PRINT(1)
   62 CALL COMPOS
      NP = 0
      IF(NSS.LT.NSTEP)  GO TO 50
   71 CALL PRINT(2)
  100 IF(LAST.NE.1)  GO TO 13
  101 CALL EXIT
      END

$IBFTC INPU
      SUBROUTINE INPUT(JINPT)
      COMMON/ALL/ CROSSK, GBAR, HT, HM, JREACT, JRERUN, KC, KVPRIM, M,
     1MMINUS, MONE, MTWO, N, NPLUS, OMEGA, PHI(12), R, SIGMA(12),
     2TBARE(3,1), TREFR, TPRIME(3), TSUBF(12,3,1), V(13,3), UM(12,3),
     3UT(12,3), XBARM(3,3), XSUBM(12,3,3), Y, ZLENGT, ZM
      COMMON /XESFA/ AF, BARMO, BTUPPO, DP, E, EPSILN, EPSILR, FLARGE,
     1 G, GAMA, H, HC, HF, HP, HW, INDEXT, IPSUP, KINT, NPR, NPROC,
     2 NPROP, NSS, NSTEP, PE, REACTR, RGAS, ZKF, ZKS, ZMU
      COMMON/XFIND/ A(10), ANAME(2,10), ARATE(6), B(10), BRATE(6),
     1C(5,3), CRATE(6), DATPRO(11), DELTA(10), EQ(3,2), F(10), P(3),
     2 PROF(10,5), PSI(3), Q0(3), S(10,3), SR(12,3), ST(12,3),
     3 TPRINT(10,100), XI(3), ZBIGM(10)
      M = MSAVE
      REACTR = RESAVE
C     JINPT IS FLAG FOR ABBREVIATED DATA DECK
      GO TO (10,20,30), JINPT
C     FULL DATA DECK
   10 READ(5,1000) R, REACTR, DP, AF, EPSILN, PE
```

```
 1000 FORMAT(8F12.4)
      RESAVE = REACTR
      READ(5,1000) (ARATE(I), I=1,6)
      READ(5,1000) (BRATE(I), I=1,6)
      READ(5,1000) (CRATE(I), I=1,6)
      READ(5,1001) JREACT,KC,M,NPRI,IPSUP, CROSKO
 1001 FORMAT (5I5,F12.4)
      MSAVE = M
      READ(5,1000)  GAMA,ZKF, ZMU, HW, HC, DUM
C     4 OR 5 CARD INPUT DECK
   30 READ(5,1002)  (F(K), K=1,10)
 1002 FORMAT  (10F6.4)
C     3 OR 4 CARD DECK
   20 READ(5,1000) G, P(1), TBARE(1,1), (XBARM(1,I), I=1,3)
      READ(5,1003) INDEXT, NPROP, (DATPRO(I), I = 1,5)
 1003 FORMAT (2I6,5F12.4)
C     DUM IS USED TO LOAD 1.0 IF CARTESIAN COORDINATES
C     H USED TO TRANSMIT INDICATION OF CARTESIAN COORDINATES TO MISCEL
      H = DUM
      IF((NPROP.LE.5).AND.(INDEXT.NE.4))  GO TO 21
      READ(5,1000) (DATPRO(I), I=6,11)
      IF(INDEXT.EQ.4)  REACTR = DATPRO(11)
C     SECTION 2000 FOR PRINTOUT OF INPUT DATA
   21 WRITE(6,2000)
 2000 FORMAT (1H0, 55X, 10HINPUT DATA//)
      WRITE(6,2001) (ANAME(1,I), ANAME(2,I), I=1,5), (F(K),K=1,5)
 2001 FORMAT(1H , 16X, 9HCOMPONENT,4X,5(2A6,4X)/21X,1HF,8X,5(E12.4,4X))
      IF (KC.LT.6)  GO TO 22
      WRITE(6,2001) (ANAME(1,I), ANAME(2,I), I=6,10),(F(K),K=6,10)
   22 WRITE(6,2002) JREACT, R, GAMA, KC, REACTR, ZKF, M, DP, ZMU, NPRI,
     1 AF, HW, IPSUP, EPSILN, HC, CROSKO, PE
 2002 FORMAT(1H0//17X,9HJREACT = ,4X,I12,6X,3HR = ,10X,1PE12.4,6X,
     1 6HGAMA = ,7X, F12.4/17X,4HKC = 9X, I12, 6X,8HREACTR = ,5X,E12.4,
     26X, 5HZKF = ,8X,F12.4/17X,3HM = 10X,I12,6X,4HDP = 9X, F12.4,6X,
     35HZMU = 8X,E12.4/17X, 8HNPRINT = ,5X,I12,6X, 4HAF = 9X,E12.4,6X,
     4 4HHW =  9X, F12.4/17X, 7HIPSUP =  6X,I12,6X, 8HEPSILN = ,5X,
     5E12.4,6X,4HHC = 9X,E12.4/17X,8HCROSKO = 5X,F12.4,6X,4HPE = 9X,
     6 E12.4//)
      WRITE(6,2003) (ARATE(I),BRATE(I), CRATE(I), I=1,6)
 2003 FORMAT(1H , 33X,5HARATE,19X,5HBRATE,19X,5HCRATE/6(30X,1PE12.4,
     1 12X, E12.4, 12X, E12.4)//)
      WRITE(6,2004) G, P(1), TBARE(1,1),(XBARM(1,I), I=1,3)
 2004 FORMAT(1H /32X,4HG = 1PE12.4,7X,7HP(1) = 0PF6.1,10X,9HTINLET = ,
     1 F6.1/32X,7HX(1) =  F8.5,8X, 7HX(2) = F8.5, 9X,7HX(3) =  F8.5//)
C     FOLLOWING PRINT DEPENDS ON BOUNDARY CONDITION
      GO TO (41,42,43,44) , INDEXT
   41 WRITE(6,2011)  (DATPRO(I), I = 1,10)
 2011 FORMAT(1H0, 40X, 41HINDEXT = 1  COOLANT TEMPERATURE SPECIFIED/23X,
     1 4HDEGF, 4X, 5(4X,F8.2)/ 31X, 5(4X, F8.2))
      DO 51 I=1,10
   51 DATPRO(I) = DATPRO(I) +460. -TREFR
      GO TO 99
   42 WRITE(6,2012)  (DATPRO(I), I= 1,3)
 2012 FORMAT(1H0, 39X, 42HINDEXT = 2  CONSTANT HEAT CAPACITY COOLANT/
     1 18X, 14H INLET TEMP = ,F8.2,20H  DEGF, FLOW RATE = ,1PE12.4,
     2 14H  LB/HR, CP =  0PF8.4, 13H  BTU/LB-DEGF    )
```

```
      DATPRO(I) = DATPRO(I) +460. - TREFR
      GO TO 99
   43 WRITE (6,2013)  (DATPRO(I), I=1,10)
 2013 FORMAT(1HO, 42X, 35HINDEXT = 3  FLUX BOUNDARY CONDITION /12X,
     1 12HFLUX PROFILE, 5(4X,1PE12.4)/12X, 12H BTU/HR-FT2,5(4X,E12.4))
      GO TO 99
   44 WRITE(6,2014)  NPROP, (DATPRO(I), I=1,10)
 2014 FORMAT(1HO, 38X, 10HINDEXT = 4, 2X, I2,31H CONSECUTIVE ADIABATIC R
     1EACTORS / 17X, 14H INLET TEMP = ,5(4X,F8.2)/22X, 4HDEG, 3X,
     2 5(4X, F8.2))
      TBARE(1,1) = DATPRO(1)
      DO 61 I=1,10
   61 DATPRO(I) = DATPRO(I) + 460. - TREFR
C     SET INTERNAL VARIABLES
   99 NPR = NPRI
      CROSSK = CROSKO
      TBARE(1,1) = TBARE(1,1) +460. - TREFR
      P(1) = 144. * (P(1) + 14.7)
  100 RETURN
      END

$IBFTC PRIN
      SUBROUTINE PRINT(IDUM)
C     IDUM IS FLAG FOR INTERMEDIATE OR TABULAR PRINT
      COMMON/ALL/ CROSSK, GBAR, HT, HM, JREACT, JRERUN, KC, KVPRIM, M,
     1MMINUS, MONE, MTWO, N, NPLUS, OMEGA, PHI(12), R, SIGMA(12),
     2TBARE(3,1), TREFR, TPRIME(3), TSUBE(12,3,1), V(13,3), UM(12,3),
     3U1(12,3), XBARM(3,3), XSUBM(12,3,3), Y, ZLENGT, ZM
      COMMON /XESEA/ AF, BARMO, BTUPPO, DP, E, EPSILN, EPSILR, FLARGE,
     1 G, GAMA, H, HC, HF, HP, HW, INDEXT, IPSUP, KINT, NPR, NPROC,
     2 NPROP, NSS, NSTEP, PE, REACTR, RGAS, ZKF, ZKS, ZMU
      COMMON/XFIND/ A(10), ANAME(2,10), ARATE(6), B(10), BRATE(6),
     1C(5,3), CRATE(6), DATPRO(11), DELTA(10), EQ(3,2), F(10), P(3),
     2 PROF(10,5), PSI(3), QQ(3), S(10,3), SR(12,3), ST(12,3),
     3 TPRINT(10,100), XI(3), ZBIGM(10)
      DIMENSION  TCUR(12)
      GO TO (100,200), IDUM
C     SECTION 100 FOR INITIAL AND INTERMEDIATE PROFILES
  100 KPRINT = KINT + 1
      WRITE(6,1000) KPRINT
 1000 FORMAT(1H1 40X, 34H**** INTERMEDIATE PRINTOUT NUMBER I3,5H ****//)
      PCUR = P(NPLUS)/144. - 14.7
      TPCUR = TPRIME(NPLUS) + TREFR - 460.
      WRITE(6,1001)  NSS, PCUR, TPCUR
 1001 FORMAT(1H0 4X, 1HN 18X, 8HPRESSURE 27X, 20HHOT-SIDE TEMPERATURE //
     1 3X, I4,  9X, F15.2, 24X, F15.2)
      TBCUR = TBARE(NPLUS,1)  + TREFR - 460.
      WRITE(6,1002)
 1002 FORMAT(1HO 4X, 6HJREACT 7X, 4HXBAR 17X, 6HJREACT 7X, 4HXBAR 16X,
     1 6HJREACT 7X, 4HXBAR 20X, 4HTBAR //)
      WRITE(6,1003)  (J, XBARM(NPLUS,J) , J=1,JREACT)
 1003 FORMAT (1H 7X, I1, 4X, F15.8, 14X, I1, 4X, E15.8, 13X,I1,4X,E15.8)
      WRITE(6,1004)  TBCUR
 1004 FORMAT(1H+ 102X,F15.2)
      WRITE(6,1005)
 1005 FORMAT(3HO M15X,4HCONV30X,4HCONV 29X,4HCONV16X,11HTEMPERATURE//)
```

```
      DO 101 I=1,MONE
      WRITE(6,1006) I, (XSUBM(I,NPLUS,J), J=1,JREACT)
 1006 FORMAT(  1X, I2, 10X, E15.8, 10X, E15.8, 10X, E15.8)
      TCUR(I) = TSUBE(I, NPLUS,1) - TREFR - 460.
  101 WRITE(6,1007) TCUR(1)
 1007 FORMAT(1H+ 102X, E15.2)
      ZZELEN = ZLENGT + CROSSK
      WRITE(6,1008)  NSS, ZZELEN
 1008 FORMAT(1H0,40X,I5,22H STEPS HAVE BEEN TAKEN//41X,9HLENGTH = E15.8///)
      GO TO 5000
C     SECTION 200 FOR FINAL TABULAR PRINT
  200 WRITE (6,2000)
 2000 FORMAT(1H1 40X,24H**** FINAL PRINTOUT ****//)
      WRITE(6,2001) H, HC, HW, HF, HP
 2001 FORMAT (1H0 34X,50HHEAT TRANSFER COEFFICIENTS USED (BTU/HR-FTSQ-DE
     1GF)//36X, 4HH = E12.4, 2X,5HHC =  E12.4,2X, 5HHW = E12.4,2X,
     2 5HHF = E12.4,2X, 5HHP = E12.4///)
      WRITE(6,2002)
 2002 FORMAT (1H0 8X, 6HLENGTH 4X, 6HBTU/LB 6X, 4HTAVG 9X, 3HTCL 8X,
     1 3HTM1 8X, 3HTHS 8X, 3H P  9X, 2HX1 9X, 2HX2 9X, 2HX3)
      DO 201  I=1,KINT
  201 WRITE (6,2003)  (TPRINT(J,I), J=1,10)
 2003 FORMAT (1H 8X, F7.2, 6(4X,F7.1), 3(4X, F7.5))
 5000 RETURN
      END

$IBFTC MISC
      SUBROUTINE MISCEL
      COMMON/ALL/ CROSSK, GBAR, HT, HM, JREACT, JRERUN, KC, KVPRIM, M,
     1MMINUS, MONE, MTWO, N, NPLUS, OMEGA, PHI(12), R, SIGMA(12),
     2TBARE(3,3), TREFR, TPRIME(3), TSUBE(12,3,1), V(13,3), UM(12,3),
     3UT(12,3), XBARM(3,3), XSUBM(12,3,3), Y, ZLENGT, ZM
      COMMON /XESEA/ AF, BARMO, BTUPPO, DP, E, EPSILN, EPSILR, FLARGE,
     1 G, GAMA, H, HC, HF, HP, HW, INDEXT, IPSUP, KINT, NPR, NPROC,
     2 NPROP, NSS, NSTEP, PE, REACTR, RGAS, ZKF, ZKS, ZMU
      COMMON/XFIND/ A(10), ANAME(2,10), ARATE(6), B(10), BRATE(6),
     1C(6,3), CRATE(6), DATPRO(11), DELTA(10), EQ(3,2), F(10), P(3),
     2 PROF(10,5), PSI(3), QO(3), S(10,3), SR(12,3), ST(12,3),
     3 TPRINT(10,100), XI(3), ZBIGM(10)
      IF(INDEXT.EQ.4)  M=0
      ZM = M
      MONE = M + 1
      MMINUS = M - 1
      MTWO = M + 2
C     ADJUST AXIAL STEP SIZE TO MEET STABILITY CRITERION
      IF(INDEXT.EQ.4)  GO TO 42
      OMEGA = 4.0*DP/(R**2*PE)
      TESTK = 0.25*(1.0+3.0*H)/(OMEGA*ZM**2)
   43 IF(CROSSK.LE.TESTK)  GO TO 42
      CROSSK = CROSSK/2.0
      GO TO 43
C     MEAN MW AND MOLAL FLOW OF FEED
   42 BARMO = 0.0
      DO 41 I = 1,KC
   41 BARMO = BARMO + F(I)*ZBIGM(I)
      GBAR = G/BARMO
```

```
C       CALCULATE PRINT INTERVAL AND AXIAL STEP
        ZNP = NPR
        ZNSTEP = REACTR/CROSSK
        ZNPRT = ZNSTEP/ZNP
        ZNPRTA = ZNPRT + 0.5
        NPR = ZNPRTA
        ZNPRTA = NPR
        ZNSTEP = ZNPRTA * ZNP
        CROSSK = REACTR/ZNSTEP
        NSTEP = ZNSTEP
C       COEFFICIENTS FOR SIMPSONS RULE INTEGRATION
        IF(INDEXT.EQ.4)  GO TO 301
        GO TO(35,32,33,32,34,35,32,35,32), M
     32 SIGMA(1) = 1.0/(3.0*ZM)
        DO 3 0 I=2,M
        IEXP = I
    320 SIGMA (I) = (3.0+(-1.0)**IEXP)/(3.0*ZM)
        SIGMA(MONE) = SIGMA(1)
        GO TO 301
     33 SIGMA(1) = 0.125
        SIGMA (4) = SIGMA(1)
        SIGMA(2) = 0.375
        SIGMA(3) = SIGMA(2)
        GO TO 301
     34 SIGMA(1) = 0.06597222
        SIGMA(6) = SIGMA(1)
        SIGMA(2) = 0.26041667
        SIGMA(5) =  SIGMA(2)
        SIGMA(3) = 0.17361111
        SIGMA(4) = SIGMA(3)
        GO TO 301
C       M-VALUES OF 1, 7, AND 9 ARE FORBIDDEN
     35 WRITE(6,1000)  M
   1000 FORMAT (1H1 ,10X, 21H ERROR,MISCELLANEOUS,  , 4H M =  I5, 25HNOT A
       1 PERMISSIBLE VALUE.  / 10X, 41H THE NEXT SET OF DATA WILL BE PROCE
       2SSED.   )
        JRERUN = 1
        GO TO 100
C       COEFFICIENTS FOR HEAT CAPACITY AND ITS DERIVATIVES WITH TEMP AND
C        CONVERSION
    301 DO 333 ICT = 1,5
        DO 333 JCT = 1,JREACT
    333 C(ICT,JCT) = 0.0
        DO 10 K = 1,KC
        C(1,1) = C(1,1) + F(K)*A(K)
     10 C(2,1) = C(2,1) + F(K)*B(K)
        DO 12  J=1,JREACT
        DO 11 K=1,KC
        C(3,J) = C(3,J) + A(K)*S(K,J)
        C(4,J) = C(4,J) + B(K)*S(K,J)
     11 C(5,J) = 0.5*C(4,J)
     12 CONTINUE
        DO 500 I=1,MONE
        DO 501 J=1,JREACT
C       SET INITIAL FLAT PROFILES OF TEMP AND CONVERSION
    501 XSUBM(I,1,J) = XBARM(1,J)
```

```
      500 TSURF(I,1,1) = TBARE(I,1)
C         HEAT CAPACITY OF FEED AND INITIAL ENTHALPY
          C3JX = 0.0
          C4JX = 0.0
          ENTHO = 0.0
          DO 900 J=1,JREACT
          ENTHO = ENTHO + QO(J)*XBARM(1,J)
          C3JX = C3JX + C(3,J)*XBARM(1,J)
      900 C4JX = C4JX + C(4,J)*XBARM(1,J)
          CPO = C(1,1)+C3JX + (C4JX + C(2,1))*TBARE(1,1)
          BTUPPO = ENTHO/BARMO + (C(1,1)+C3JX+0.5*(C4JX+C(2,1))*TBARE(1,1))*
         1  TBARE(1,1)/BARMO
C         HEAT TRANSFER COEFFICIENTS AND PARAMETERS
       18 ZNPR = CPO*ZMU/(ZKF*BARMO)
          ZNRE = DP*G/ZMU
          HP=ZKF/DP*(3.22*(ZNRE*ZNPR)**0.333333+0.117*ZNRE**0.8*ZNPR**0.4)
          SIGMAR = 1.712E-9
          RGAS = 1544.0
          GC = 4.18*10.0**8
C         COEFFICIENTS FOR PRESSURE DROP CALCULATION
          FSMALL = (1.-EPSILN)/EPSILN**3*(1.75+150.0*(1.-EPSILN)/ZNRE)
          FLARGE = FSMALL*AF*GBAR**2*BARMO*GAMA*RGAS*CROSSK/GC/DP
C         DERIVATIVE OF VOLUME WITH CONVERSION
          DO 70 J=1,JREACT
          DELTA(J) = 0.0
          DO 69 K=1,KC
       69 DELTA(J) = DELTA(J) + S(K,J)
       70 CONTINUE
          SM = 0.0
          DO 72 J=1,JREACT
       72 SM=SM+DELTA(J)*XBARM(1,J)
          PSI(1) = (TBARE(1,1) +TREFR)*(1.0+SM)
          IF(INDEXT.EQ.4)  CALL ADIAID
          IF(INDEXT.EQ.4)  GO TO 100
          XI(1) = 0.6*HP*DP*ZKS/(2.0*ZKS+0.7*HP*DP)
          XI(2) = 2.0*EPSILR*SIGMAR*DP
          ZKO = XI(1) + XI(2)*(TO + TREFR)**3
          HM = 0.0
          HF=ZKF/DP*(0.203*(ZNRE*ZNPR)**0.333333+0.22*ZNRE**0.8*ZNPR**0.4)
          H = 1.0/(1.0/HW + 1.0/HC + 1.0/HF)
          HT = H*R*PF/(2.0*GBAR*DP)
          IF(INDEXT.EQ.2)  GO TO 23
          IF (NPROP.EQ.1) GO TO 23
C         COEFFICIENTS FOR AXIAL PROFILES OF FLUX OR TEMPERATURE
          FINK = NPROP -1
          NPROC = 1
          IF(NPROP.EQ.2)  GO TO 21
          RFINK = REACTR/FINK
          NQUAD = NPROP-2
          DO 22 I=1,NQUAD
          FI = I
          PROF(I,2) = DATPRO(I+1)
          PROF(I,3) = 0.5*(DATPRO(I+2)-DATPRO(I))/RFINK
          PROF(I,4) = (0.5*(DATPRO(I+2)+DATPRO(I))-DATPRO(I+1))/RFINK**2
          PROF(I,1) = RFINK*FI
       22 PROF(I,5) = PROF(I,1) + 0.5*RFINK
```

```
      PROF(NQUAD,5) = REACTR + 0.5
      GO TO 23
   21 PROF(1,1) = 0.0
      PROF(1,2) = DATPRO(1)
      PROF(1,3) = (DATPRO(2)-DATPRO(1))/REACTR
      PROF(1,4) = 0.0
      PROF(1,5) = REACTR + 0.5
   23 IF(INDEXT.EQ.3)  GO TO 26
      TPRIME(1) = DATPRO(1)
      IF(INDEXT.EQ.1)  GO TO 100
C     SENSIBLE COOLANT
   24 CCOOL = DATPRO(3)
      WCOOL = DATPRO(2)
      E = H*CROSSK/WCOOL/CCOOL
      GO TO 100
C     FLUX CONDITION
   26 TPRIME(1) = DATPRO(1)/H + TBARE(1,1)
  100 RETURN
      END

$IBFTC ADIA
      SUBROUTINE ADIAID
      COMMON/ALL/ CROSSK, GBAR, HT, HM, JREACT, JRERUN, KC, KVPRIM, M,
     1MMINUS, MONE, MTWO, N, NPLUS, OMEGA, PHI(12), R, SIGMA(12),
     2TBARE(3,1), TREFR, TPRIME(3), TSUBE(12,3,1), V(13,3), UM(12,3),
     3UT(12,3), XBARM(3,3), XSUBM(12,3,3), Y, ZLENGT, ZM
      COMMON /XESEA/ AF, BARMO, BTUPPO, DP, E, EPSILN, EPSILR, FLARGE,
     1 G, GAMA, H, HC, HF, HP, HW, INDEXT, IPSUP, KINT, NPR, NPROC,
     2 NPROP, NSS, NSTEP, PF, REACTR, RGAS, ZKF, ZKS, ZMU
      COMMON/XFIND/ A(10), ANAME(2,10), ARATE(6), B(10), BRATE(6),
     1C(5,3), CRATE(6), DATPRO(11), DELTA(10), EQ(3,2), F(10), P(3),
     2 PROF(10,5), PSI(3), Q0(3), S(10,3), SR(12,3), ST(12,3),
     3 TPRINT(10,100), XI(3), ZBIGM(10)
      IPSTOR = IPSUP
      NSECT = 1
      IPSUP = 1
      Y = CROSSK/GBAR
   40 NSS = 0
      NP = 0
      NPLUS = 1
      ZLENGT = -CROSSK
      CALL COMPOS
   50 ZLENGT = ZLENGT + CROSSK
      N = MOD(NSS,3) + 1
      NPLUS =  MOD(NSS+1,3) + 1
      CALL RATE
      TERM1 = 0.0
      TERM2 = 0.0
      TERMA = 0.0
      DO 29  J = 1,JREACT
      TERM1 = TERM1 + (C(3,J)*XSUBM(1,N,J))
      TERM2 = TERM2 + (C(4,J)*XSUBM(1,N,J))
   29 TERMA = TERMA+(SR(1,J)*(Q0(J)+TSUBE(1,N,1)*(C(3,J)+C(5,J)*
     1 TSUBE(1,N,1))))
      CP = C(1,1) + TERM1 + (TERM2 + C(2,1))*TSUBE(1,N,1)
   30 ST(1,1) = -TERMA/CP
```

```
      TSUBE(1,NPLUS,1) = TSUBE(1,N,1) + Y*ST(1,1)
      DO 31  J=1,JREACT
      XSUBM(1,NPLUS,J) = XSUBM(1,N,J) + Y*SR(1,J)
   31 XBARM(NPLUS,J) = XSUBM(1,NPLUS,J)
      TBARE(NPLUS,1) = TSUBE(1,NPLUS,1)
      CALL COOLFX
      IF(JRERUN.EQ.1)   GO TO 99
      NSS = NSS + 1
      NP = NP + 1
      IF(NP.LT.NPR)  GO TO 50
      CALL COMPOS
      NP = 0
      IF(NSS.LT.NSTEP)  GO TO 50
      IF(NSECT.EQ.NPROP)  GO TO 98
      NSECT = NSECT + 1
      KINT = KINT + 1
      DO 79  I=1,10
   79 TPRINT(I,KINT) = 0.0
      DO 80  J=1,JREACT
      XSUBM(1,1,J) = XSUBM(1,NPLUS,J)
   80 XBARM(1,J) = XSUBM(1,1,J)
      TBARE(1,1) = DATPRO(NSECT)
      TSUBE(1,1,1) = TBARE(1,1)
      P(1) = P(NPLUS)
      SM = 0.0
      DO 81  J=1, REACT
   81 SM = SM + DELTA(J)*XBARM(1,J)
      PSI(1) = (TBARE(1,1) + TREFR)*(1.0 + SM)
      GO TO 40
   98 H = 0.0
      HC = 0.0
      HW = 0.0
      HF = 0.0
      CALL PRINT(2)
   99 IPSUP = IPSTOR
      JRERUN = 1
  100 RETURN
      END

$IBFTC SRCO
      SUBROUTINE SRCOEF
C     CALCULATES CONSTANT COEFFICIENTS USED IN ENTHALPY SOURCE TERM
      COMMON/ALL/ CROSSK, GBAR, HT, HM, JREACT, JRERUN, KC, KVPRIM, M,
     1MMINUS, MONE, MTWO, N, NPLUS, OMEGA, PHI(12), R, SIGMA(12),
     2TBARE(3,1), TREFR, TPRIME(3), TSUBE(12,3,1), V(13,3), UM(12,3),
     3UT(12,3), XBARM(3,3), XSUBM(12,3,3), Y, ZLENGT, ZM
      COMMON /SORSOR/ VCO(13)
      DO 10 I=2,M
      FI = I
   10 PHI(I) = OMEGA*ZM*(FI-1.0)*GBAR/4.0
      PHI(MONE) = OMEGA*(HT**2)*GBAR
      ZMOR = 2.0*ZM/R**2
      V(1,1)= -3.0*ZMOR
      V(1,2) = 4.0*ZMOR
      V(1,3) = -ZMOR
      DO 11 I=2,M
```

```
      II=I
      V(I,1) = ZMOR*(2.0*FI - 3.0)
      V(I,2) = -4.0*ZMOR*(FI-1.0)
   11 V(I,3) = ZMOR*(2.0*FI-1.0)
      V(MONE,1) = -ZM*ZMOR
      V(MONE,2) = 8.0*ZM*ZMOR
      V(MONE,3) = -14.0*(ZM/R)**2
      V(MTWO,1) = HT*(4.0+12.0*ZM)/R**2
      DO 12 I=2,M
      FI = I
   12 VCO(I) = ZM/R**2*(FI-1.0)
      VCO(MONE) = 4.0*HT*ZM/R**2
  100 RETURN
      END

$IBFTC SOUR
      SUBROUTINE SOURCE
C     THIS ROUTINE CALCULATES ENTHALPY SOURCE TERM
      COMMON/ALL/ CROSSK, GBAR, HT, HM, JREACT, JRERUN, KC, KVPRIM, M,
     1MMINUS, MONE, MTWO, N, NPLUS, OMEGA, PHI(12), R, SIGMA(12),
     2TBARF(3,1), TREFR, TPRIME(3), TSUBF(12,3,1), V(13,3), UM(12,3),
     3UT(12,3), XBARM(3,3), XSUBM(12,3,3), Y, ZLENGT, ZM
      COMMON /XFSFA/ AF, BARMO, BTUPPO, DP, E, EPSILN, EPSILR, FLARGE,
     1 G, GAMA, H, HC, HF, HP, HW, INDEXT, IPSUP, KINT, NPR, NPROC,
     2 NPROP, NSS, NSTEP, PE, REACTR, RGAS, ZKF, ZKS, ZMU
      COMMON/XEIND/ A(10), ANAME(2,10), ARATE(6), B(10), BRATE(6),
     1C(5,3), CRATE(6), DATPRO(11), DELTA(10), EQ(3,2), F(10), P(3),
     2 PROF(10,5), PSI(3), Q0(3), S(10,3), SR(12,3), ST(12,3),
     3 TPRINT(10,100), XI(3), ZBIGM(10)
      DIMENSION  XISTAR(11), SPRIME(11), SPRIM2(11), SPRIM3(11),
     1 SPRIM4(11), CP(12)
      COMMON /FORSOR/ VCO(13)
      DO 30 I= 1,MONE
C     RADIAL THERMAL CONDUCTIVITY
      XISTAR(I) = XI(1) + XI(2)*(TSUBF(I,N,1)+TREFR)**3
C     EFFECT OF TEMP ON HEAT OF REACTION
      TERM1 = 0.0
      TERM2 = 0.0
      TERMA = 0.0
      DO 29 J=1,JREACT
      TERM1 = TERM1 + (C(3,J)*XSUBM(I,N,J))
      TERM2 = TERM2 + (C(4,J)*XSUBM(I,N,J))
C     REACTION CONTRIBUTION
   29 TERMA = TERMA + (SR(I,J)*(Q0(J) + TSUBF(I,N,1)*(C(3,J)+C(5,J)
     1 *TSUBF(I,N,1))))
C     LOCAL HEAT CAPACITY
      CP(I) = C(1,1) + TERM1 + (TERM2 + C(2,1))*TSUBF(I,N,1)
   30 SPRIME(I) = -TERMA
      DC = CP(MONE) + XISTAR(MONE) * PE/(GBAR*DP)
      UT(MTWO,1) = UT(MTWO,2) / DC
      FILDEL = TPRIME(N) -TSUBF(MONE,N,1)
C     RADIAL VARIATION IN HEAT CAPACITY
      SPRIM2(1) = 0.0
      DO 41 I= 2,M
      IPLUS = I + 1
      IMINUS = I - 1
```

```
      TERMC = 0.0
      DO 40 J=1,JREACT
   40 TERMC = TERMC+(C(3,J)+C(4,J)*TSUBE(I,N,1))*2.0*(XSUBM(IPLUS,N,J)
     1 -XSUBM(IMINUS,N,J))
   41 SPRIM2(I) = PHI(I)*(TSUBE(IPLUS,N,1)-TSUBE(IMINUS,N,1))*(CP(IPLUS)
     1 -CP(IMINUS) + TERMC)
      TERMD = 0.0
      DO 45 J=1,JREACT
   45 TERMD = TERMD + C(4,J)*XSUBM(MONE,N,J)
      SPRIM2(MONE) = PHI(MONE)*(FILDEL/DC)**2*(C(2,1) + TERMD)
C     NON-EDDY RADIAL CONDUCTIVITY
   50 SPRIM3 (1) = (V(1,1)*TSUBE(1,N,1)+V(1,2)*TSUBE(2,N,1)+V(1,3)*
     1 TSUBE(3,N,1))*XISTAR(1)
      DO 51 I=2,M
      IMINUS = I-1
      IPLUS = I+1
   51 SPRIM3(I) = (V(I,1)*TSUBE(IMINUS,N,1)+V(I,2)*TSUBE(I,N,1)+V(I,3)*
     1 TSUBE(IPLUS,N,1))*XISTAR(I)
   52 SPRIM3(MONE)= (V(MONE,1)*TSUBE(MMINUS,N,1)+V(MONE,2)*TSUBE(M,N,1)+
     1V(MONE,3)*TSUBE(MONE,N,1)+V(MTWO,1)/DC*FILDEL)*XISTAR(MONE)
C     RADIAL VARIATION IN CONDUCTIVITY
      SPRIM4(1) = 0.0
      DO 60 I=2,M
   60 SPRIM4(I) = VCO(I) *(TSUBE(I+1,N,1)-TSUBE(I-1,N,1))*(XISTAR(I+1)-
     1 XISTAR(I-1))
   61 SPRIM4(MONE) = VCO(MONE)*(1.5*XISTAR(MONE)- 2.0*XISTAR(M) +0.5*
     1XISTAR(MMINUS))*FILDEL/DC
      DO 70 I=1,MONE
C     FINAL SOURCE TERM
   70 ST(I,1) = (1.0/CP(I))*(SPRIME(I)+SPRIM2(I)+SPRIM3(I)+SPRIM4(I))
  100 RETURN
      END

$IBFTC RATE
      SUBROUTINE RATE
C     SUPPLIES REACTION RATE CALCULATIONS--SPECIFIC FOR FUEL.  THIS
C      ROUTINE FOR MCH.
      COMMON/ALL/ CROSSK, GBAR, HT, HM, JREACT, JRERUN, KC, KVPRIM, M,
     1MMINUS, MONE, MTWO, N, NPLUS, OMEGA, PHI(12), R, SIGMA(12),
     2TBARE(3,1), TREFR, TPRIME(3), TSUBE(12,3,1), V(13,3), UM(12,3),
     3UT(12,3), XBARM(3,3), XSUBM(12,3,3), Y, ZLENGT, ZM
      COMMON /XESEA/ AF, BARMC, BTUPPO, DP, E, EPSILN, EPSILR, FLARGE,
     1 G, GAMA, H, HC, HF, HP, HW, INDEXT, IPSUP, KINT, NPR, NPROC,
     2 NPROP, NSS, NSTEP, PE, REACTR, RGAS, ZKF, ZKS, ZMU
      COMMON/XFIND/ A(10), ANAME(2,10), ARATE(6), B(10), BRATE(6),
     1C(5,3), CRATE(6), DATPRO(11), DELTA(10), EQ(3,2), F(10), P(3),
     2 PROF(10,5), PSI(3), Q0(3), S(10,3), SR(12,3), ST(12,3),
     3 TPRINT(10,100), XI(3), ZBIGM(10)
      DIMENSION  CEE(10), YX(10), TSURF(11), TDELT(11)
      PAT = P(N) /2120.
C     CALCULATE MOLE FRACTIONS
      DO 9 I=1,MONE
      DO 10  K=1,KC
      XNUME = F(K)
      XDENO = 1.0
      DO 11  J=1,JREACT
```

```
      XNUME = XNUME + S(K,J)*XSUBM(I,N,J)
   11 XDENO = XDENO + DELTA(J)*XSUBM(I,N,J)
   10 YX(K) = XNUME/XDENO
      GROUP = (YX(2)**3)*(PAT**3)
      XKGR1 = YX(3)/YX(1)*GROUP
      XKGR2 = YX(6)/YX(5)*GROUP
C     BEGIN ITERATION FOR SURFACE TEMPERATURE
    8 TCOMP = (TDELT(I) + TCOMP)/2.0
      TSURF(I) = TREFR + TSUBE(I,N,1)  + TCOMP
      GR2 = P(N)/(GAMA*RGAS*TSURF(I))
      CEE(1) = GR2*YX(1)
      RT = 1.987*TSURF(I)
      RKRC = ARATE(2)*EXP(BRATE(2)/RT)*CEE(1)
      RATEK = ARATE(1)*EXP(BRATE(1)/RT)
      XKEQ1 = EQ(1,1)*EXP(EQ(1,2)/RT)
      REQ1 = 1.0 - XKGR1/XKEQ1
C     RATE OF MCH TO TOLUENE
      SR(I,1) = (1.0-EPSILN)*REQ1*RATEK*RKRC/(1.0+RKRC)
      TDELT(I) = -QO(1)*SR(I,1)*DP/((1.0-EPSILN)*HP*6.0)
      IF(ABS(TCOMP-TDELT(I)).GT.1.0)  GO TO 8
      IF(JREACT.EQ.1)  GO TO 22
C     RATE OF CRACKING
      SR(I,2) = (1.-EPSILN)*(CEE(1))*ARATE(3)*EXP(BRATE(3)/RT)
      IF(JREACT.EQ.2) GO TO 21
      XKEQ2 = EQ(3,1)*EXP(EQ(3,2)/RT  )
      REQ2 = 1.0 - XKGR2/XKEQ2
C     RATE OF CH TO BENZENE
      SR(I,3) = (1.-EPSILN)*GR2*YX(5)*ARATE(4)*EXP(BRATE(4)/RT)*REQ2
      GO TO 9
   22 SR(I,2) = 0.0
   21 SR(I,3) = 0.0
    9 CONTINUE
  100 RETURN
      END

$IBFTC REAX
C     SUPPLIES DATA PERTINENT TO REACTION AND REACTANTS--SPECIFIC FOR
C      FUEL.  THIS ROUTINE FOR MCH
      BLOCK DATA
      COMMON/ALL/ CROSSK, GBAR, HT, HM, JREACT, JRERUN, KC, KVPRIM, M,
     1MMINUS, MONE, MTWO, N, NPLUS, OMEGA, PHI(12), R, SIGMA(12),
     2TBARE(3,1), TREFR, TPRIME(3), TSUBE(12,3,1), V(13,3), UM(12,3),
     3UT(12,3), XBARM(3,3), XSUBM(12,3,3), Y, ZLENGT, ZM
      COMMON /XESEA/ AF, BARMO, BTUPPO, DP, E, EPSILN, EPSILR, FLARGE,
     1 G, GAMA, H, HC, HF, HP, HW, INDEXT, IPSUP, KINT, NPR, NPROC,
     2 NPROP, NSS, NSTEP, PE, REACTR, RGAS, ZKF, ZKS, ZMU
      COMMON/XEIND/ A(10), ANAME(2,10), ARATE(6), B(10), BRATE(6),
     1C(5,3), CRATE(6), DATPRO(11), DELTA(10), EQ(3,2), F(10), P(3),
     2 PROF(10,5), PSI(3), QO(3), S(10,3), SR(12,3), ST(12,3),
     3 TPRINT(10,100), XI(3), ZBIGM(10)
C     HEAT CAPACITIES AT TREFR
      DATA A/ 79.1, 7.099, 55.9, 79.1, 67.33, 45.41, 4*0.0/
C     TEMPERATURE COEFFICIENT OF CP
      DATA B/ 0.0363, 0.00272, 0.0238, 0.0363, 0.0302, 0.0169, 4*0.0/
C     MOLECULAR WEIGHTS
      DATA ZBIGM/98.189,2.016,92.141,98.189,84.162,78.114,4*0./
```

```
C       STOICHIOMETRIC FACTORS
        DATA S/-1.0, 3.0, 1.0, 7*0.0, -1.0, 2*0.0, 1.0, 6*0.0, 0.0, 3.0,
       1 2*0.0, -1.0, 1.0, 4*0.0/
C       EQUILIBRIUM  PARAMETERS
        DATA EQ/ 4.0E20, 0.0, 4.0E20, -92500.,  0.0, -93900./
C       HEATS OF REACTION
        DATA Q0/ 92500., 0.0, 93900./
        DATA ZKS, EPSILR, TREFR/ 0.130, 0.3, 1460./
C       NAMES OF COMPONENTS
        DATA ANAME/12OH    MCH        HYDROGEN    TOLUENE    C7 ISOMER  CYC
       1LOHEXANE    BENZENE
       2    /
        DATA ARATE/ 7.5 E12, 4.5 E-8, 1.4 E7, 3.25E8, 2*0.0/
        DATA BRATE/ -59000., 54000., -30000., -27000., 2*0.0/
        END

$IBFTC EXCO
        SUBROUTINE EXPCFO(UMUT)
C       CALCULATES CONSTANT COEFFICIENTS USED IN AXIAL STEP
        COMMON/ALL/ CROSSK, GBAR, HT, HM, JREACT, JRERUN, KC, KVPRIM, M,
       1MMINUS, MONE, MTWO, N, NPLUS, OMEGA, PHI(12), R, SIGMA(12),
       2TBARE(3,1), TREFR, TPRIME(3), TSUBE(12,3,1), V(13,3), UM(12,3),
       3UT(12,3), XBARM(3,3), XSUBM(12,3,3), Y, ZLENGT, ZM
        DIMENSION  UMUT(12,3)
        UMUT(1,1) = 1.0 - (1.5*OMEGA*ZM*CROSSK)
        UMUT(1,2) = 2.0*OMEGA*ZM*CROSSK
        UMUT(1,3) = -OMEGA*ZM*CROSSK/2.0
        DO 10 I=2,M
        FI = I
        UMUT(I,1) = CROSSK/2.0*ZM*(2.0*FI-3.0)*OMEGA
        UMUT(I,2) = 1.0 - 2.0*CROSSK*ZM*(FI-1.0)*OMEGA
   10   UMUT(I,3) = CROSSK/2.0*ZM*OMEGA*(2.0*FI-1.0)
   11   UMUT(MONE,1) = -OMEGA*CROSSK*(ZM**2)/2.0
        UMUT(MONE,2) = 4.0*OMEGA*CROSSK*(ZM**2)
        UMUT(MONE,3) = 1.0 - (CROSSK*OMEGA*3.5*(ZM**2))
   20   Y = CROSSK/GBAR
        IF(KVPRIM) 12,100,12
   12   UMUT(MTWO,2) = HT*CROSSK*OMEGA*(1.0 + 3.0*ZM)
  100   RETURN
        END

$IBFTC EXPL
        SUBROUTINE EXPLIC(YXT,UMUT,SRST)
C       AXIAL STEP - ARGUMENTS DISTINGUISH CONVERSION FROM ENTHALPY
        COMMON/ALL/ CROSSK, GBAR, HT, HM, JREACT, JRERUN, KC, KVPRIM, M,
       1MMINUS, MONE, MTWO, N, NPLUS, OMEGA, PHI(12), R, SIGMA(12),
       2TBARE(3,1), TREFR, TPRIME(3), TSUBE(12,3,1), V(13,3), UM(12,3),
       3UT(12,3), XBARM(3,3), XSUBM(12,3,3), Y, ZLENGT, ZM
        DIMENSION  YXT(12,3,3) , UMUT(12,3), SRST(12,3)
        IF(KVPRIM) 11,10,11
   10   LIMIT = JREACT
        WALL = 0.0
        GO TO 12
   11   LIMIT = 1
        WALL = UT(MTWO,1)*(TPRIME(N) - YXT(MONE,N,1))
   12   DO 13 J = 1,LIMIT
```

```
      YXT(I,NPLUS,J) = UMUT(I,1)*YXT(I,N,J) + UMUT(I,2)*YXT(2,N,J)
     1 +UMUT(I,3)*YXT(3,N,J) + Y*SRST(I,J)
      DO 14 I = 2,M
      IMINUS = I - 1
      IPLUS = I + 1
   14 YXT(I,NPLUS,J) = UMUT(I,1)*YXT(IMINUS,N,J) + UMUT(I,2)*YXT(I,N,J)
     1 +UMUT(I,3)*YXT(IPLUS,N,J) + Y*SRST(I,J)
   13 YXT(MONE,NPLUS,J) = UMUT(MONE,1)*YXT(MMINUS,N,J) + UMUT(MONE,2)*
     1 YXT(M,N,J) + UMUT(MONE,3)*YXT(MMINUS,N,J) + Y*SRST(MONE,J) + WALL
  100 RETURN
      END

$IBFTC COOL
      SUBROUTINE COOLEX
C     SUBROUTINE DOES ONE-DIMENSIONAL INTEGRATION OF P AND COOLANT TEMP
      COMMON/ALL/ CROSSK, GBAR, HT, HM, JREACT, JRERUN, KC, KVPRIM, M,
     1MMINUS, MONE, MTWO, N, NPLUS, OMEGA, PHI(12), R, SIGMA(12),
     2TBARE(3,1), TREFR, TPRIME(3), TSUBE(12,3,1), V(13,3), UM(12,3),
     3UT(12,3), XBARM(3,3), XSUBM(12,3,3), Y, ZLENGT, ZM
      COMMON /XESEA/ AF, BARMO, BTUPPO, DP, E, EPSILN, EPSILR, FLARGE,
     1 G, GAMA, H, HC, HF, HP, HW, INDEXT, IPSUP, KINT, NPR, NPROC,
     2 NPROP, NSS, NSTEP, PF, REACTR, RGAS, ZKF, ZKS, ZMU
      COMMON/XEIND/ A(10), ANAME(2,10), ARATE(6), B(10), BRATE(6),
     1C(5,3), CRATE(6), DATPRO(11), DELTA(10), EQ(3,2), F(10), P(3),
     2 PROF(10,5), PSI(3), Q0(3), S(10,3), SR(12,3), ST(12,3),
     3 TPRINT(10,100), XI(3), ZBIGM(10)
      ZZELEN = ZLENGT + CROSSK
      IF(INDEXT.EQ.4)  GO TO 15
C     COOLANT TEMPERATURE CALCULATION
      IF(INDEXT.EQ.2) GO TO 20
      IF(NPROP.EQ.1) GO TO 10
      PROLEN = ZZELEN - PROF(NPROC,1)
      FPROP=PROF(NPROC,2)+PROLEN*(PROF(NPROC,3)+PROF(NPROC,4)*PROLEN)
      IF(ZZELEN.GT.PROF(NPROC,5))  NPROC=NPROC+1
   12 IF(INDEXT.EQ.3) GO TO 30
   11 TPRIME(NPLUS) = FPROP
      GO TO 40
   10 FPROP = DATPRO(1)
      GO TO 12
   30 TPRIME(NPLUS) = FPROP/H + TSUBE(MONE,NPLUS,1)
      GO TO 40
   20 TPRIME(NPLUS) = TPRIME(N) + E*(TSUBE(MONE,N,1) -TPRIME(N))
C     CALCULATE MEAN TEMPERATURE AND CONVERSIONS
   40 KVPRIM = 0
      CALL AVERAG(XSUBM,XBARM)
      KVPRIM = 1
      CALL AVERAG(TSUBE,TBARE)
C     PRESSURE DROP CALCULATION
   15 SM = 0.0
      DO 14 J=1,JREACT
   14 SM= SM + DELTA(J)*XBARM(NPLUS,J)
      P(NPLUS) = P(N) - (FLARGE/P(N))*PSI(N)
C     TEST FOR PRESSURE - TERMINATION ON NEGATIVE PRESSURE
      IF(P(NPLUS).GT.0.0)  GO TO 60
      WRITE(6,1000)  ZZELEN
 1000 FORMAT(1HO,24X,8HZFAIL = E15.8/25X, 24HTHE PRESSURE IS NEGATIVE/
```


14

```
     1 25X, 38HTHIS PROBLEM ENDS IN SUBROUTINE COOLEX/25X, 38HTHE NEXT S
     2ET OF DATA WILL BE PROCESSED  )
       JRERUN = 1
       GO TO 100
    60 PSI(NPLUS) = (TBARE(NPLUS,1) + TREFR)*(1.0+SM)
   100 RETURN
       END

$IBFTC AVRG
       SUBROUTINE AVERAG(YXT,YXTBAR)
C      CALCULATES RADIAL AVERAGES .  ARGUMENTS DISTINGUISH TEMP FROM CONV
       COMMON/ALL/ CROSSK, GBAR, HT, HM, JREACT, JRERUN, KC, KVPRIM, M,
      1MMINUS, MONE, MTWO, N, NPLUS, OMEGA, PHI(12), R, SIGMA(12),
      2TBARE(3,1), TREFR, TPRIME(3), TSUBE(12,3,1), V(13,3), UM(12,3),
      3UT(12,3), XBARM(3,3), XSUBM(12,3,3), Y, ZLENGT, ZM
       DIMENSION  YXT(12,3,3), YXTBAR(3,3)
       IF(KVPRIM) 10,11,10
    10 YXTBAR(NPLUS,1) = 0.0
       DO 20 I= 1,MONE
    20 YXTBAR(NPLUS,1) = YXTBAR(NPLUS,1) + SIGMA(I)*YXT(I,NPLUS,1)
       GO TO 100
    11 DO 21 J=1,JREACT
       YXTBAR(NPLUS,J) = 0.0
       DO 21 I=1,MONE
    21 YXTBAR(NPLUS,J) = YXTBAR(NPLUS,J) + SIGMA(I)*YXT(I,NPLUS,J)
   100 RETURN
       END

$IBFTC COMP
       SUBROUTINE COMPOS
C      CALCULATES COMPOSITIONS AND ENTHALPIES FOR INTERMEDIATE PRINTOUT
       COMMON/ALL/ CROSSK, GBAR, HT, HM, JREACT, JRERUN, KC, KVPRIM, M,
      1MMINUS, MONE, MTWO, N, NPLUS, OMEGA, PHI(12), R, SIGMA(12),
      2TBARE(3,1), TREFR, TPRIME(3), TSUBE(12,3,1), V(13,3), UM(12,3),
      3UT(12,3), XBARM(3,3), XSUBM(12,3,3), Y, ZLENGT, ZM
       COMMON /XESEA/ AF, BARMO, BTUPPO, DP, E, EPSILN, EPSILR, FLARGE,
      1 G, GAMA, H, HC, HF, HP, HW, INDEXT, IPSUP, KINT, NPR, NPROC,
      2 NPROP, NSS, NSTEP, PE, REACTR, RGAS, ZKF, ZKS, ZMU
       COMMON/XEIND/ A(10), ANAME(2,10), ARATE(6), B(10), BRATE(6),
      1C(5,3), CRATE(6), DATPRO(11), DELTA(10), EQ(3,2), F(10), P(3),
      2 PROF(10,5), PSI(3), QO(3), S(10,3), SR(12,3), ST(12,3),
      3 TPRINT(10,100), X1(3), ZBIGM(10)
       DIMENSION  YBAR(10), ZBAR(10)
       SUM2 = 0.0
       DO 10 J=1,JREACT
    10 SUM2 = SUM2 + DELTA(J)*XBARM(NPLUS,J)
       PBAR = 1.0 + SUM2
       DO 12 K = 1,KC
       SUM1 = 0.0
       DO 11 J = 1,JREACT
    11 SUM1 = SUM1 + S(K,J)*XBARM(NPLUS,J)
       ZBAR(K) = F(K) + SUM1
    12 YBAR(K) = ZBAR(K)/PBAR
       ENTHO = 0.0
       C3JX = C(1,1)
       C4JX = C(2,1)
```

```
      DO 30 J=1,JREACT
      C3JX = C3JX + C(3,J)*XBARM(NPLUS,J)
      C4JX = C4JX + C(4,J)*XBARM(NPLUS,J)
   30 ENTHO = ENTHO + QO(J)*XBARM(NPLUS,J)
      BTUPP = ENTHO/BARMO + (C3JX+0.5*C4JX*TBARE(NPLUS,1))*TBARE(NPLUS,
     1 1)/BARMO - BTUPPO
      IF(IPSUP.EQ.1)  GO TO 99
      WRITE(6,1000) BTUPP
 1000 FORMAT(1HO,20X,20HPRINTOUT FROM COMPOS , 10X, 10HHEAT ADDED, 4X,
     1 F8.2, 2X, 6HBTU/LB )
      WRITE (6,1001)
 1001 FORMAT(1H  ,5X, 8HCOMPOUND ,12X,13HMOLE FRACTION, 7X, 19H MOLES/MO
     1LE OF FEED )
      DO 20 K = 1,KC
   20 WRITE (6,1002)  K, YBAR(K), ZBAR(K)
 1002 FORMAT (1H , 5X, I5, 7X, 2(6X, E15.8))
C     SETS UP DATA FOR FINAL TABULAR PRINT
   99 KINT = KINT+1
      J = KINT
      TPRINT(1,J) = ZLENGT + CROSSK
      TPRINT(2,J) = BTUPP
      TPRINT(3,J) = TBARE(NPLUS,1) + TREFR - 460.
      TPRINT(4,J) = TSUBE(1,NPLUS,1) + TREFR - 460.
      TPRINT(5,J) = TSUBE(MONE,NPLUS,1) + TREFR - 460.
      TPRINT(6,J) = TPRIME(NPLUS) + TREFR - 460.
      TPRINT(7,J) = P(NPLUS)/144. - 14.7
      TPRINT(8,J) = XBARM(NPLUS,1)
      TPRINT(9,J) = XBARM(NPLUS,2)
      TPRINT(10,J) = XBARM(NPLUS,3)
  100 RETURN
      END
```

```
$IBFTC EXCO
C       THIS VERSION FOR CARTESIAN COORDINATES
        SUBROUTINE EXPCOF(UMUT)
        CALCULATES CONSTANT COEFFICIENTS USED IN AXIAL STEP
        COMMON/ALL/ CROSSK, GBAR, HT, HM, JREACT, JRERUN, KC, KVPRIM, M,
       1MMINUS, MONE, MTWO, N, NPLUS, OMEGA, PHI(12), R, SIGMA(12),
       2TBARE(3,1), TREFR, TPRIME(3), TSUBE(12,3,1), V(13,3), UM(12,3),
       3UT(12,3), XBARM(3,3), XSUBM(12,3,3), Y, ZLENGT, ZM
        DIMENSION UMUT(12,3)
        ZMSQ = M**2
        UNIT = OMEGA*CROSSK*ZMSQ/4.0
        UMUT(1,1) = 1.0 - 3.5*UNIT
        UMUT(1,2) = 4.0*UNIT
        UMUT(1,3) = -0.5*UNIT
        DO 10 I=2,M
        UMUT(I,1) = UNIT
        UMUT(I,2) = 1.0 - 2.0*UNIT
     10 UMUT(I,3) = UNIT
        UMUT(MONE,1) = -UNIT/2.0
        UMUT(MONE,2) = 4.0*UNIT
        UMUT(MONE,3) = 1.0 - 3.5*UNIT
        Y = CROSSK/GBAR
        IF(KVPRIM) 12,100,12
     12 UT(MTWO,2) = 6.0*UNIT*HT/ZM
    100 RETURN
        END
$IBFTC SRCO
C       THIS VERSION FOR CARTESIAN COORDINATES
        SUBROUTINE SRCOEF
C       CALCULATES CONSTANT COEFFICIENTS USED IN ENTHALPY SOURCE TERM
        COMMON/ALL/ CROSSK, GBAR, HT, HM, JREACT, JRERUN, KC, KVPRIM, M,
       1MMINUS, MONE, MTWO, N, NPLUS, OMEGA, PHI(12), R, SIGMA(12),
       2TBARE(3,1), TREFR, TPRIME(3), TSUBE(12,3,1), V(13,3), UM(12,3),
       3UT(12,3), XBARM(3,3), XSUBM(12,3,3), Y, ZLENGT, ZM
        COMMON /FORSOR/ VCO(13)
        DO 10 I=2,M
     10 PHI(I) = OMEGA*ZM*ZM*GBAR/16.0
        PHI(MONE) = OMEGA*(HT**2)*GBAR
        ZMOR = (ZM/R)**2
        V(1,1) = -3.5*ZMOR
        V(1,2) = 4.0*ZMOR
        V(1,3) = -0.5*ZMOR
        DO 11 I=2,M
        V(I,1) = ZMOR
        V(I,2) = -2.0*ZMOR
     11 V(I,3) = ZMOR
        V(MONE,1) = -0.5*ZMOR
        V(MONE,2) = 4.0 *ZMOR
        V(MONE,3) = -3.5 * ZMOR
        V(MTWO,1) = 6.0*HT*ZMOR/ZM
        DO 12 I=2,M
     12 VCO(I) = ZMOR/4.0
        VCO(MONE) = 2.0*HT*ZM/R**2
    100 RETURN
        END
```

Table 76. IGNITION DELAYS FOR ETHYLENE-OXYGEN-ARGON MIXTURES

Note: ER is the equivalence ratio; the actual fuel/oxygen ratio divided by the stoichiometric fuel/oxygen ratio (taking H_2O and CO_2 as the products of combustion).

N = no ignition detected D = apparent detonation

Press, psia	Temp, °K	Delay, μsec	Press, psia	Temp, °K	Delay, μsec	Press, psia	Temp, °K	Delay, μsec
Argon, 99%; ER = 0.2								
9.2	1281	1162	15.0	1281	534	24.3	1218	558
8.3	1213	1295	15.6	1352	478	24.4	1258	401
8.8	1293	1005	14.9	1340	445	24.5	1281	345
9.6	1419	517	14.8	1213	804	26.5	1174	764
7.9	1235	1244	14.5	1141	1211	23.6	1114	1263
8.3	1146	1825	14.7	1104	1800	24.5	1119	1208
8.9	1352	767						
Argon, 99%; ER = 0.5								
9.0	1309	603	14.6	1263	472	24.6	1251	313
8.6	1303	632	14.9	1303	316	24.9	1234	375
9.2	1405	355	14.5	1206	712	24.0	1151	1159
8.8	1211	1395	14.5	1135	1818	24.4	1189	616
8.6	1173	1965	14.6	1167	1225	24.1	1102	2340
Argon, 99%; ER = 1.0								
8.5	1232	2120	15.0	1337	320	24.8	1255	754
8.4	1187	2720	15.1	1319	349	25.0	1295	349
8.6	1301	1172	14.9	1244	1000	24.9	1232	936
9.4	1421	325	15.0	1278	536	24.3	1171	1720
9.3	1397	387	14.6	1176	1730	24.1	1138	2500
9.1	1373	515	14.4	1144	2621			
Argon, 90%; ER = 0.1								
9.1	1152	3575	15.5	1126	387	25.0	1137	259
8.4	1066	2145	14.7	1091	956	25.5	1090	893
8.9	1121	1030	14.6	1086	1018	24.5	1091	957
8.8	1115	1063	15.3	1126	518	23.0	984	N
8.9	1126	1035	14.8	1056	1480	24.0	1032	2120
8.9	1106	1252	15.2	1032	2435	23.9	1046	1695
8.8	1071	2039				24.2	1081	1020
						24.1	1096	829

(Continued)

Table 76 (Contd). IGNITION DELAYS FOR ETHYLENE-OXYGEN-ARGON MIXTURES

Press, psia	Temp, °K	Delay, μsec	Press, psia	Temp, °K	Delay, μsec	Press, psia	Temp, °K	Delay, μsec
Argon, 90%m; ER = 0.2								
10.3	1174	264	16.0	1072	767	25.0	1077	448
9.2	1023	2755	15.9	1082	737	24.7	1052	606
8.4	981	N	15.9	1102	452	30.2	1195	D
9.1	1072	1658	15.0	995	2915	22.9	962	N
10.0	1163	461	15.8	1052	1015	26.0	1072	478
10.3	1184	264	18.6	1184	132	26.6	1004	2435
10.2	1153	394	15.6	1028	2165			
Argon, 90%m; ER = 0.5								
9.4	1077	D	14.7	968	3300	23.6	972	3030
8.2	959	3100	14.2	963	3360	24.3	991	2695
6.6	1005	2530	14.4	968	3045	24.2	996	2395
9.0	1014	2035				22.7	959	3350
9.0	1024	2170				22.2	950	3275
						24.6	1019	2420
Argon, 80%m; ER = 0.1								
9.4	1150	278	15.8	1125	277	25.0	1082	238
9.4	1115	552	15.[illegible]	1082	477	23.9	998	1318
9.6	1115	621	15.9	1072	542	24.3	1035	703
9.6	1091	924	14.8	998	2665	24.2	1039	670
8.1	945	N	15.6	1044	940	25.3	1086	204
8.5	985	3715	15.6	1049	908	22.6	949	3370
9.1	1049	1680	14.4	989	2880	23.5	989	1247
8.3	980	3730				24.1	998	1250
Argon, 80%m; ER = 0.2								
8.3	974	3035	14.2	951	3080	23.7	957	3400
8.7	1024	944	14.3	957	2720			
8.4	992	1660	14.8	961	3115			
8.3	948	3910						

Table 77. IGNITION DELAYS FOR ETHANE-OXYGEN-ARGON MIXTURES

Note: ER is the equivalence ratio; the actual fuel/oxygen ratio divided by the stoichiometric fuel/oxygen ratio (taking H_2O and CO_2 as the products of combustion).

N = no ignition detected D = apparent detonation

Press, psia	Temp, °K	Delay, μsec	Press, psia	Temp, °K	Delay, μsec	Press, psia	Temp, °K	Delay, μsec
Argon, 90%m; ER = 0.2								
9.9	1251	338	15.7	1224	134	25.4	1161	165
10.1	1235	438	15.1	1146	524	25.5	1140	328
8.9	1095	2005	15.8	1203	202	24.3	1075	900
9.0	1120	1370	15.4	1140	689	24.6	1100	648
8.1	1041	3170	16.0	1182	265	22.8	974	N
8.4	1070	2530	15.3	1120	315	24.0	1050	2365
8.8	1120	1500	15.2	1060	2550	24.5	1070	1025
9.9	1246	338	16.1	1130	687			
Argon, 80%m; ER = 0.2								
9.5	1156	D	19.2	1330	D	34.8	1319	D
8.7	1071	2560	15.1	1108	1192	25.0	980	3200
8.3	1025	N	17.0	1161	286	22.8	971	3450
8.3	1029	3530	14.7	1025	3030	24.7	1029	2075
9.0	1099	1995	15.2	1061	2380			
8.4	1057	2960						
Argon, 90%m; ER = 0.1								
9.0	1199	660	14.7	1204	331	24.2	1151	522
9.1	1236	367	15.3	1209	265	24.7	1183	329
8.8	1146	1235	15.2	1172	622	24.2	1125	807
8.7	1156	1175	14.8	1115	1290	23.7	1085	1468
8.8	1115	1675	14.7	1090	1463	23.9	1045	2515
8.5	1065	2540	14.7	1060	2370			
9.3	1231	433	14.8	1141	814			

(Continued)

Table 77 (Contd-1). IGNITION DELAYS FOR ETHANE-OXYGEN-ARGON MIXTURES

Press, psia	Temp, °K	Delay, μsec	Press, psia	Temp, °K	Delay, μsec	Press, psia	Temp, °K	Delay, μsec
Argon, 95%m; ER = 0.1								
8.7	1171	946	14.1	1193	381	24.3	1231	160
8.7	1204	636	14.7	1204	318	25.3	1220	192
8.4	1193	753	14.9	1160	598	24.8	1176	316
8.6	1242	385	14.8	1128	997	24.5	1139	626
7.9	1041	N	14.9	1108	1241	23.5	1061	2018
8.5	1118	1835	14.4	1051	2310	23.7	1092	1190
8.4	1209	574						
Argon, 80%m, ER = 0.1								
8.2	1033	3350	14.5	1099	860	24.0	1061	1085
8.7	1080	2520	14.3	1104	756	24.5	1099	516
10.2	1228	358	15.5	1182	317	24.2	1085	752
9.8	1193	460	14.8	1143	524	26.0	1099	585
11.2	1312	183	15.0	1118	693	23.4	983	3410
8.5	1056	3040	15.2	1099	825	23.7	1010	3520
8.3	1038	3495	16.2	1128	1385	25.7	1085	1538
11.2	1259	289	15.6	1109	759	25.1	1047	2700
8.8	1099	2410	14.3	1015	3460			
			15.0	1071	1088			
Argon, 95%m; ER = 0.025								
8.6	1189	1265	14.1	1200	633	24.4	1222	351
8.3	1184	1138	14.7	1267	387	24.7	1206	413
8.9	1278	646	14.6	1239	512	24.4	1167	628
8.9	1313	587	14.6	1189	758	24.5	1146	753
9.2	1383	363	14.8	1156	877	23.4	1088	1165
8.8	1189	1075	14.6	1114	1238			
Argon, 99%m; ER = 0.2								
8.8	1270	943	13.8	1179	921	23.9	1196	523
8.8	1304	822	14.4	1270	597	24.5	1281	314
8.7	1316	762	14.8	1328	413	24.0	1152	782
8.8	1376	544	15.0	1190	862	22.8	1062	1420
8.8	1401	483	14.5	1109	1320	22.8	1021	N
8.7	1185	1260	13.7	1036	2705			
8.2	1093	2270						

(Continued)

Table 77 (Contd-2). IGNITION DELAYS FOR ETHANE-OXYGEN-ARGON MIXTURES

Press, psia	Temp, °K	Delay, μsec	Press, psia	Temp, °K	Delay, μsec	Press, psia	Temp, °K	Delay, μsec
Argon, 99%m; ER = 0.025								
8.8	1276	1878	14.7	1265	1253	24.8	1259	812
8.5	1265	2000	15.0	1225	1365	24.0	1180	1318
6.8	1353	1468	13.7	1169	1950	24.5	1169	1342
9.1	1464	910	14.9	1341	822	25.0	1341	573
9.2	1554	462	14.6	1377	769	25.2	1390	482
8.8	1452	939	15.2	1502	392	25.9	1439	388
			14.5	1420	562			
Argon, 99%m; ER = 0.5								
8.4	1222	1492	14.7	1256	722	24.6	1250	375
8.8	1285	917	15.0	1314	318	24.5	1222	653
9.0	1350	448	14.7	1273	441	24.0	1177	1230
9.0	1362	353	14.9	1228	840	23.7	1113	2175
8.6	1200	1670	14.8	1177	1535	24.4	1205	806
8.6	1161	2445	14.8	1134	2190			
Argon, 99%m; ER = 1.0								
8.8	1294	1258	14.8	1265	1008	25.4	1254	856
8.7	1317	1055	14.9	1300	541	25.3	1294	381
9.0	1383	420	14.9	1329	384	25.0	1265	756
8.6	1347	706	14.7	1220	1590	26.8	1181	1855
8.8	1242	2135	14.8	1175	2465	24.3	1132	3050
9.1	1237	2075						
Argon, 90%m; ER = 0.5								
8.3	1078	2170	20.5	1452	D	37.0	1487	D
12.2	1452	D	23.7	1589	D	24.0	992	3455
14.3	1583	D	14.5	1030	2650	23.7	997	3375
8.4	1059	3730	17.3	1173	D	25.5	1063	2260
8.6	1063	3340	15.4	1068	2620	23.5	1001	3410
13.5	1505	D	18.8	1235	D			
8.2	1030	N						
8.0	1011	N						

Table 78. IGNITION DELAYS FOR DECALIN-OXYGEN-ARGON MIXTURES

Note: ER is the equivalence ratio; the actual fuel/oxygen ratio divided by the stoichiometric fuel/oxygen ratio (taking H_2O and CO_2 as the products of combustion).

N = no ignition detected D = apparent detonation

Press, psia	Temp, °K	Delay, μsec	Press, psia	Temp, °K	Delay, μsec	Press, psia	Temp, °K	Delay, μsec
Argon, 80% ; ER = 0.1								
8.6	1133	1540	15.0	1197	393	25.3	1197	143
8.7	1182	925	14.8	1162	670	25.2	1142	632
9.0	1233	505	15.2	1133	982	25.1	1157	423
8.9	1248	289	14.8	1080	2063	23.0	1042	2575
8.2	1061	3130	14.3	1024	3360	25.2	1123	774
						25.2	1108	1055
						22.8	1019	3360
Argon, 90% ; ER = 0.2								
9.5	1202	1142	15.6	1245	136	25.8	1181	367
9.2	1202	1176	15.4	1171	666	25.8	1155	597
9.3	1245	577	15.5	1202	533	25.0	1105	2150
9.7	1289	275	14.7	1075	3230			
8.5	1070	3870	16.0	1176	668			
8.5	1075	3880	14.1	1060	4170			
8.5	1100	3390	16.1	1181	635			
			14.6	1100	2675			

Table 79. IGNITION DELAYS FOR α-METHYL DECALIN-OXYGEN-ARGON MIXTURES

Note: ER is the equivalence ratio; the actual fuel/oxygen ratio divided by the stoichiometric fuel/oxygen ratio (taking H_2O and CO_2 as the products of combustion).

N = no ignition detected D = apparent detonation

Press, psia	Temp, °K	Delay, μsec	Press, psia	Temp, °K	Delay, μsec	Press, psia	Temp, °K	Delay, μsec
Argon, 99%; ER = 0.1								
8.8	1259	1035	14.6	1253	780	24.6	1253	842
8.7	1224	1363	14.8	1299	409	24.4	1276	440
8.9	1311	556	14.4	1202	1292	24.3	1264	720
9.0	1335	381	14.5	1174	1680	24.0	1174	1805
8.3	1141	3030	14.6	1141	2482	24.5	1169	1930
						24.3	1141	2600
Argon, 90%; ER = 0.1								
8.7	1246	336	14.9	1209	333	24.5	1172	593
8.8	1198	1030	14.9	1177	759	24.2	1125	1428
8.2	1090	2950	14.7	1115	1810	24.8	1193	364
8.8	1172	1250	14.8	1095	2440	24.6	1085	2560
9.1	1252	336	14.6	1135	1175	24.5	1110	1810
7.9	1115	2330						

Table 80. IGNITION DELAYS FOR n-DODECANE-OXYGEN-ARGON MIXTURES

Note: ER is the equivalence ratio; the actual fuel/oxygen ratio divided by the stoichiometric fuel/oxygen ratio (taking H_2O and CO_2 as the products of combustion).

N = no ignition detected D = apparent detonation

Press, psia	Temp, °K	Delay, μsec	Press, psia	Temp, °K	Delay, μsec	Press, psia	Temp, °K	Delay, μsec
Argon, 99%; ER = 0.5								
9.0	1248	1355	15.2	1288	794	24.8	1248	1198
8.8	1259	1390	15.1	1335	385	24.9	1323	320
8.7	1271	1205	14.6	1192	2020	25.2	1312	479
9.1	1389	30	15.0	1181	2358	25.1	1231	1444
8.5	1300	830						
8.8	1353	452						
8.7	1175	2910						
Argon, 95%; ER = 0.1								
8.5	1196	1152	14.7	1284	132	24.4	1158	1105
8.6	1228	775	14.7	1251	162	24.7	1196	480
8.7	1284	262	14.8	1234	323	24.9	1185	638
8.8	1279	262	14.9	1206	546	24.6	1131	1729
8.5	1228	807	15.0	1174	1113			
8.7	1251	518	14.5	1110	2248			
8.3	1126	2260						

Table 81. IGNITION DELAYS FOR PROPANE-OXYGEN-ARGON MIXTURES

Note: ER is the equivalence ratio; the actual fuel/oxygen ratio divided by the stoichiometric fuel/oxygen ratio (taking H_2O and CO_2 as the products of combustion).

N = no ignition detected D = apparent detonation

Press, psia	Temp, °K	Delay, μsec	Press, psia	Temp, °K	Delay, μsec	Press, psia	Temp, °K	Delay, μsec
Argon, 90%m; ER = 1.0								
10.1	1307	371	15.2	1134	2360	25.0	1110	2375
8.3	1124	4220	15.8	1163	1632	28.5	1203	432
8.8	1144	3885	14.9	1114	2585	24.3	1057	3420
9.9	1255	1460	14.6	1100	3470	27.0	1144	1520
9.0	1183	2760						
8.8	1173	2760						
Argon, 90%m; ER = 0.1								
9.1	1303	336	15.3	1274	397	26.9	1281	268
9.2	1281	434	15.5	1226	660	25.0	1188	750
9.0	1204	1315	14.7	1141	1450	25.3	1209	590
8.9	1226	1055	14.8	1161	1295	24.9	1130	1572
8.7	1209	1115	15.0	1120	1920	24.1	1059	3300
8.7	1135	2310				24.1	1079	3100
9.4	1314	337						
Argon, 99%m; ER = 1.0								
9.0	1242	2920	15.1	1341	706	25.0	1259	1638
8.3	1208	3370	15.1	1371	453	24.7	1208	2498
9.0	1335	1285	14.9	1271	1455	25.3	1335	706
8.6	1265	2455	14.5	1197	2800	25.6	1383	357
9.2	1377	840	14.9	1323	928			
8.8	1371	960						
8.8	1413	392						

Table 82. IGNITION DELAYS FOR METHANE-OXYGEN-ARGON MIXTURES

Note: ER is the equivalence ratio; the actual fuel/oxygen ratio divided by the stoichiometric fuel/oxygen ratio (taking H_2O and CO_2 as the products of combustion).

N = no ignition detected D = apparent detonation

Press, psia	Temp, °K	Delay, μsec	Press, psia	Temp, °K	Delay, μsec	Press, psia	Temp, °K	Delay, μsec
Argon, 80%; ER = 0.1								
8.4	1272	4250	15.0	1546	225	26.0	1482	295
9.8	1654	382	15.3	1470	444	24.9	1386	437
8.5	1336	2085	15.6	1465	444	26.5	1391	400
9.3	1499	744	15.1	1402	657	23.5	1210	216
9.3	1534	675	15.2	1358	1050	25.2	1310	787
8.8	1358	1810	14.8	1272	1915	25.3	1294	854
			14.3	1190	3060			

Table 83. IGNITION DELAYS FOR n-DODECANE-OXYGEN-ARGON MIXTURES

Argon, 90%m; ER = 0.1. Visible light used as criterion of ignition.

Press., psia	Temp, °K	Delay, μsec	Press., psia	Temp, °K	Delay, μsec	Press., psia	Temp, °K	Delay, μsec
8.8	1210	773	15.3	1226	337	24.0	1111	1400
8.5	1215	672	14.3	1121	1605	25.7	1231	135
6.6	1269	102	15.2	1188	569			
9.0	1291	136	15.1	1126	1440			
8.6	1226	574	14.8	1076	2640			
8.1	1076	3095	15.5	1215	269			
8.7	1162	1323						

Table 84. IGNITION DELAYS FOR TOLUENE/$2H_2$-OXYGEN-MIXTURES

Argon, 80%; ER = 0.1

Press., psia	Temp, °K	Delay, μsec	Press, psia	Temp, °K	Delay, μsec	Press., psia	Temp, °K	Delay, μsec
Ignition Detected From CO_2 Emission at 2300 cm^{-1}								
8.8	1052	3370	14.6	1071	3100	23.8	1038	2700
8.8	1114	2600	15.4	1129	1030	24.2	1043	2750
8.8	1139	2150	16.0	1214	460	25.7	1109	690
8.9	1158	1850	15.9	1219	360	24.9	1119	1000
9.6	1219	1280	16.0	1224	230	25.7	1124	660
9.9	1276	650	16.0	1239	320	25.1	1148	700
						25.4	1188	390
						25.7	1224	210
Ignition Detected From CO Emission at 2050 cm^{-1}								
			14.6	1028	2650			
			15.2	1090	1650			
			15.5	1134	830			
			15.7	1168	780			
			14.1	1214	390			
			14.3	1234	320			
			15.4	1301	250			

Table A5. IGNITION DELAYS FOR MeH-OXYGEN-ARGON MIXTURES

Argon, 99%m; ER = 0.1, Ignition Detected From CO_2 Emission at 2300 cm^{-1}			Argon, 99%m; ER = 0.1, Ignition Detected From CO Emission at 2050 cm^{-1}		
Press., psia	Temp, °K	Delay, μsec	Press., psia	Temp, °K	Delay, μsec
14.5	1125	2400	13.6	1213	1400
14.8	1180	2100	15.1	1288	900
14.6	1213	1260	15.0	1311	450
14.4	1247	940	14.5	1341	320
14.8	1300	750	14.9	1371	580
14.5	1316	640	(15)	1409	320
15.2	1323	470			
15.0	1377	320			
15.0	1230	2820	(15)	1180	3100
14.8	1264	2600	14.8	1219	2500
15.1	1340	1290	14.7	1275	1260
15.4	1394	620	15.6	1304	770
15.3	1418	560	15.3	1358	520
15.2	1449	560	15.2	1370	480
15.3	1480	460	15.3	1418	300
(15)	1556	330			
15.1	1133	2500	14.8	1107	2500
14.6	1171	1900	14.7	1149	1250
14.7	1231	748	15.0	1220	770
14.9	1276	740	14.9	1276	360
14.8	1299	390	(15.0)	1320	330
(15.0)	1343	360	(15.0)	1370	300
(15.0)	1355	300	(15.0)	1390	270
(15.0)	1410	270	(15.0)	1400	100
14.5	1130	N	14.3	1104	3430
14.7	1157	2600	15.1	1162	1910
15.0	1184	2000			
15.5	1205	2200	16.0	1238	780
15.4	1216	2000	15.7	1244	450
16.0	1249	700	17.4	1300	330
16.3	1294	460	16.2	1317	330
15.8	1300	430	16.5	1330	130
			17.3	1340	200

(Continued)

Table 85 (Contd). IGNITION DELAYS FOR MCH-OXYGEN-ARGON MIXTURES

Argon, 80%; ER = 0.1, Ignition Detected From CO_2 Emission at 2300 cm^{-1}								
Press., psia	Temp, °K	Delay, μsec	Press., psia	Temp, °K	Delay, μsec	Press., μsec	Temp, °K	Delay, μsec
8.6	1088	3120	14.1	1051	3000	24.1	1028	3370
8.6	1122	2240	15.1	1079	2780	25.2	1074	2460
9.1	1187	1570	14.7	1084	2540	24.8	1108	1180
9.7	1247	435	15.0	1088	2630	25.0	1118	700
9.7	1247	870	15.6	1132	1680	28.7	1167	1280
			15.9	1171	570	31.2	1294	400
Argon, 80%; ER = 0.1, Ignition Detected From CO Emission at 2050 cm^{-1}								
			14.3	1014	N			
			14.9	1061	2460			
			14.8	1065	2600			
			15.7	1122	1460			
			15.4	1122	810			
			15.3	1142	700			
			15.6	1147	850			

Table 86. IGNITION DELAYS FOR PROPANE-OXYGEN-ARGON MIXTURES

Argon, 90%m; ER = 0.1				
Press., psia	Temp, °K		Delay, μsec	
			Detection, CO_2 2300 cm^{-1}	Method Visible Light
14.4	1069		3150	3500
14.6	1120		2000	1850
14.3	1135		2100	1960
14.4	1161		1360	1230
14.1	1199		850	850
13.2	1209		1000	1000
14.6	1281		430	350
15.0	1337		250	190

Argon, 99%m; ER = 1.0				
Press., psia	Temp, °K		CO_2 Delay, μsec	Delay, μsec
14.2	1219		2310	2245
15.2	1317		1340	1180
14.8	1276		1460	1332
15.5	1377		775	646
15.2	1383		680	584
15.2	1413		619	489
16.8	1457		525	394
15.1	1507		433	298
15.2	1559		333	200

Argon, 99%m; ER = 1.0 Ignition Detected From CO_2 Emission at 2300 cm^{-1}			Argon, 99%m; ER = 1.0 Ignition Detected From CO Emission at 2050 cm^{-1}		
Press., psia	Temp, °K	Delay, μsec	Press., psia	Temp, °K	Delay, psia
15.3	1294	1650	(15)	1115	3020
15.0	1370	845	14.7	1214	2500
14.6	1407	555	14.5	1242	1630
15.6	1460	525	14.1	1271	820
(15)	1535	340	15.2	1407	325

(Continued)

Table 86 (Contd). IGNITION DELAYS FOR PROPANE-OXYGEN-ARGON MIXTURES

Argon, 99%m; ER = 0.1 Ignition Detected From CO_2 Emission at 2300 cm^{-1}			Argon, 99%m; ER = 0.1 Ignition Detected From CO Emission at 2050 cm^{-1}		
Press., psia	Temp, °K	Delay, µsec	Press., psia	Temp, °K	Delay, µsec
			(15.0)	1110	2200
13.8	1089	2800	13.6	1156	1230
14.1	1095	3300	15.0	1188	1050
14.2	1172	1230	14.6	1199	1700
13.9	1188	1180	14.0	1215	990
16.1	1204	1340	14.9	1269	530
14.0	1215	1220	14.8	1269	470
15.0	1275	610	15.0	1286	370
14.7	1292	440			

Table 87. IGNITION DELAYS FOR 2,2,3,3-TETRAMETHYL BUTANE-OXYGEN-ARGON MIXTURES

ER = 0.1, 97.5%m Argon		ER = 0.2, 97.5%m Argon		ER = 0.1, 95%m Argon					
P = 15 psia				P = 9 psia		P = 15 psia		P = 25 psia	
Temp, °K	Delay, μsec	Temp, °K	Delay, μsec	Temp, °K	Delay, μsec	Temp, °K	Delay, μsec	Temp, °K	Delay, μsec
1167	3050	1232	2500	1185	3700	1160	2700	1100	3700
1171	3300	1257	2360	1185	3550	1183	1900	1184	2440
1216	2050	1257	1700	1247	1410	1251	1225	1210	1400
1220	1650	1279	2050	1255	1850	1285	840	1225	1470
1262	1140	1321	730	1265	1290	1314	590	1237	925
1293	950	1346	775	1337	850	1345	460	1293	715
1313	860	1388	490	1372	430	1350	360	1307	560
1330	430	1388	475	1440	200			1326	460
1359	210	1394	500						
1365	180	1394	475						
1389	125	1416	330						
1401	35	1440	210						
1407	150	1485	200						
1407	100	1510	100						
1438	100	1516	115						
		1523	95						
		1536	120						
		1555	105						
		1562	60						

P = 15 psia, ER = 0.1, 95%m Argon

Temp, °K	Delay, μsec	Temp, °K	Delay, μsec	Temp, °K	Delay, μsec
1162	3530	1130	3700	1404	155
1162	3290	1160	2800	1404	150
1194	2015	1196	1800	1410	100
1196	2650	1200	2650	1410	100
1201	1770	1210	1650	1416	140
1227	1465	1235	1470	1416	110
1227	1405	1246	882	1422	110
1245	932	1288	730	1428	110
1250	966	1323	410	1428	85
1290	616	1338	329		
1300	782	1356	280		
1310	684	1363	370		
1352	410	1368	250		
1365	260	1374	230		
1383	300	1380	220		
1390	280	1380	180		
1390	270	1386	150		
1465	78	1398	190		
1503	64	1398	150		

Table 88. IGNITION DELAYS FOR NEOPENTANE-OXYGEN-ARGON MIXTURES

ER = 0.1, 9[illegible]m Argon

P = 9 psia		P = 15 psia		P = 2[illegible] psia	
Temp, °K	Delay, µsec	Temp, °K	Delay, µsec	Temp, °K	Delay, µsec
1215	3530	1147	3510	1179	3300
1239	1720	1170	2430	1181	2820
1284	1230	1180	2410	1191	2080
1337	825	1199	2270	1217	1770
1352	730	1220	1655	1240	1505
1374	540	1229	1510	1284	842
1406	340	1249	1028	1320	653
		1268	905	1341	360
		1312	783	1346	360
		1325	523		
		1352	390		
		1352	390		
		1377	300		
		1490	100		
		1503	81		
		1536	79		
		1545	62		
		1605	35		

Table 89. IGNITION DELAYS FOR 2,2,3-TRIMETHYL BUTANE-OXYGEN-ARGON MIXTURES

P = 15 psia, ER = 0.1, 95% Argon

Temp, °K	Delay, µsec	Temp, °K	Delay, µsec	Temp, °K	Delay, µsec
1161	3150	1360	200	1400	165
1187	2500	1366	200	1400	150
1203	1600	1374	160	1404	110
1230	1250	1380	200	1422	120
1245	1150	1380	195	1428	90
1264	950	1386	165	1459	70
1302	850	1392	150	1465	70
1316	320	1392	140	1471	35
1339	360	1398	100	1483	35

Table 20. IGNITION DELAYS FOR n-OCTANE-OXYGEN-ARGON MIXTURES

P = 15 psia

95% Argon				97.5% Argon			
ER = 0.1		ER = 0.2		ER = 0.1		ER = 0.2	
Temp, °K	Delay, μsec	Temp, °K	Delay, μsec	Temp, °K	Delay, μsec	Temp, °K	Delay, μsec
1126	3500	1140	3200	1107	2750	1165	2290
1152	2600	1176	1400	1134	2000	1223	1570
1160	2000	1177	2400	1177	1750	1223	1250
1187	1600	1190	1900	1178	1800	1275	682
1218	860	1231	900	1178	1800	1294	735
1224	860	1231	870	1225	950	1317	450
1255	740	1260	550	1230	870	1339	355
1262	850	1322	215	1250	760	1375	150
1274	390	1322	200	1263	850	1381	190
1284	490	1331	460	1297	510	1381	153
1293	325	1345	250	1319	510	1393	140
1300	470	1358	100	1356	240	1399	100
1315	310	1388	135	1401	155	1423	165
1315	300	1420	1170	1444	115	1435	115
1316	350	1426	85	1450	115	1473	73
1328	150	1460	35	1467	115		
1328	115			1481	110		
1345	150			1481	80		
1351	165			1513	100		
1357	125						
1357	115						
1386	55						
1392	150						
1392	70						
1397	125						
1404	50						

TABLE 91. PROPERTY VALUES FOR METHYLCYCLOHEXANE C7H14

MOLECULAR WEIGHT	98.18	HEAT, VAPORIZATION	138.72
BOILING POINT	213.68	HEAT, FUSION	29.6
FREEZING POINT	-195.87	HEAT, COMBUSTION	18797.
SPECIFIC GRAVITY	0.7753	FREE ENERGY, COMB.	138.6
CRITICAL TEMP.	570.5	HEAT, FORMATION	678.2
CRITICAL PRESSURE	504.	FREE ENERGY, FORM.	119.5
CRITICAL VOLUME	0.0561	FLASH POINT	25.
ACENTRIC FACTOR	0.257	AUTOIGNITION TEMP.	545.
LOWER EXPLO. LIMIT	1.2	UPPER EXPLO. LIMIT	

********** GAS PROPERTIES **********

TEMP.	PV/RT PRESSURE. 600	1200	VISCOS-ITY	THERMAL CONDUC-TIVITY	HEAT CAPAC-ITY	PRANDTL NUMBER	HEAT CONTENT PRESSURE. 0	600	1200
-200			0.0076	0.0009	0.087	0.712	-38.4		
-100			0.0106	0.0028	0.195	0.751	-24.1		
0			0.0136	0.0051	0.284	0.762	-0.0		
100			0.0165	0.0077	0.355	0.766	32.1		
200			0.0193	0.0105	0.420	0.769	70.9		
300			0.0220	0.0137	0.480	0.771	115.9		
400			0.0246	0.0170	0.536	0.773	166.7		
500			0.0270	0.0205	0.589	0.774	222.9		
600	0.343	0.408	0.0293	0.0242	0.638	0.775	284.3	231.2	210.7
700	0.656	0.477	0.0315	0.0279	0.685	0.776	350.5	323.4	290.9
800	0.760	0.589	0.0337	0.0316	0.728	0.776	421.2	400.4	375.5
900	0.823	0.692	0.0357	0.0354	0.769	0.777	496.1	479.0	460.2
1000	0.865	0.768	0.0377	0.0391	0.806	0.777	574.8	560.3	545.4
1100	0.895	0.822	0.0396	0.0428	0.840	0.778	657.1	644.6	632.3
1200	0.918	0.862	0.0415	0.0465	0.871	0.778	742.7	731.7	721.2

********** LIQUID PROPERTIES AT SATURATION PRESSURE **********

TEMP.	DENSITY	VISCOS-ITY	THERMAL CONDUC-TIVITY	HEAT CAPAC-ITY	HEAT CONTENT	HEAT OF VAPOR-IZATION	VAPOR PRESSURE	SURFACE TENSION
-150	53.97	33.029	0.113	0.227	-208.8	176.3	0.0000	0.0026
-100	52.68	12.328	0.097	0.282	-196.1	172.9	0.0004	0.0154
-50	51.37	5.853	0.085	0.334	-180.7	167.5	0.0078	0.0682
0	50.01	3.267	0.076	0.381	-162.8	162.8	0.0717	0.0612
50	48.62	2.045	0.069	0.424	-142.7	157.8	0.4011	0.0544
100	47.17	1.392	0.062	0.462	-120.5	152.4	1.5730	0.0478
150	45.67	1.009	0.057	0.499	-96.5	146.7	4.7485	0.0414
200	44.09	0.768	0.053	0.534	-70.6	140.5	11.7818	0.0352
250	42.43	0.607	0.049	0.569	-43.0	133.7	25.1844	0.0292
300	40.65	0.516	0.046	0.603	-13.8	126.2	47.9999	0.0235
350	38.73	0.446	0.043	0.638	17.2	117.7	83.6793	0.0181
400	36.60	0.386	0.041	0.677	50.1	107.9	136.0226	0.0130
450	34.14	0.334	0.038	0.726	85.1	95.8	209.2494	0.0083
500	31.07	0.283		0.808	123.2	79.8	308.2674	0.0042
550	26.26	0.222		1.118	168.7	52.4	439.3299	0.0009

SHELL DEVELOPMENT COMPANY

TABLE 92. PROPERTY VALUES FOR TOLUENE C7H8

MOLECULAR WEIGHT	92.14	HEAT, VAPORIZATION	156.28
BOILING POINT	231.12	HEAT, FUSION	41.5
FREEZING POINT	-138.98	HEAT, COMBUSTION	18433.
SPECIFIC GRAVITY	0.8735	FREE ENERGY, COMB.	4831.3
CRITICAL TEMP.	609.5	HEAT, FORMATION	233.4
CRITICAL PRESSURE	611.	FREE ENERGY, FORM.	571.0
CRITICAL VOLUME	0.0554	FLASH POINT	40.
ACENTRIC FACTOR	0.245	AUTOIGNITION TEMP.	1026.
LOWER EXPLO. LIMIT	1.3	UPPER EXPLO. LIMIT	7.0

********** GAS PROPERTIES **********

TEMP.	PV/RT ..PRESSURE. 600	1200	VISCOS -ITY	THERMAL CONDUC- TIVITY	HEAT CAPAC- ITY	PRANDTL NUMBER	HEAT CONTENT .....PRESSURE..... 0	600	1200
-200			0.0083	0.0007	0.054	0.665	-29.8		
-100			0.0113	0.0023	0.153	0.739	-19.3		
0			0.0145	0.0044	0.228	0.754	-0.0		
100			0.0177	0.0065	0.281	0.760	23.5		
200			0.0209	0.0091	0.332	0.764	56.1		
300			0.0241	0.0119	0.380	0.766	91.8		
400			0.0272	0.0150	0.423	0.768	131.9		
500			0.0302	0.0181	0.463	0.770	176.3		
600			0.0331	0.0214	0.498	0.771	224.3		
700	0.677	0.410	0.0359	0.0246	0.530	0.772	275.8	249.7	207.9
800	0.773	0.555	0.0386	0.0279	0.558	0.773	330.2	310.0	281.7
900	0.831	0.679	0.0412	0.0312	0.585	0.773	387.4	370.8	350.8
1000	0.870	0.760	0.0438	0.0344	0.609	0.774	447.2	433.0	417.4
1100	0.899	0.816	0.0462	0.0377	0.631	0.774	509.2	496.9	484.1
1200	0.920	0.857	0.0486	0.0409	0.651	0.775	573.3	562.5	551.7

********** LIQUID PROPERTIES AT SATURATION PRESSURE **********

TEMP.	DENSITY	VISCOS -ITY	THERMAL CONDUC- TIVITY	HEAT CAPAC -ITY	HEAT CONTENT	HEAT OF VAPOR- IZATION	VAPOR PRESSURE	SURFACE TENSION
-100	59.82	7.948	0.115	0.436	-216.6	197.3	0.0002	0.0873
-50	58.16	4.112	0.101	0.382	-202.6	192.0	0.0038	0.0799
0	56.49	2.455	0.090	0.341	-186.5	186.5	0.0394	0.0726
50	54.80	1.622	0.081	0.375	-168.5	180.7	0.2429	0.0655
100	53.08	1.154	0.074	0.405	-149.1	174.5	1.0320	0.0584
150	51.34	0.868	0.068	0.436	-128.0	167.9	3.3320	0.0515
200	49.55	0.682	0.063	0.466	-105.5	160.9	8.7492	0.0448
250	47.72	0.554	0.058	0.496	-81.4	153.3	19.6175	0.0383
300	45.81	0.456	0.055	0.524	-55.9	145.1	38.9319	0.0319
350	43.80	0.381	0.051	0.553	-29.0	135.9	70.2401	0.0258
400	41.62	0.328	0.048	0.584	-0.6	125.3	117.5735	0.0199
450	39.18	0.289	0.046	0.620	29.4	113.5	185.4601	0.0143
500	36.23	0.182	0.043	0.670	61.6	98.7	279.2389	0.0090
550	32.21	0.138		0.767	97.1	78.7	405.4143	0.0043
600	25.20	0.087		1.480	143.9	39.9	570.2360	0.0005

SHELL DEVELOPMENT COMPANY

TABLE 93. PROPERTY VALUES FOR HYDROGEN H2

MOLECULAR WEIGHT	2.02	HEAT, VAPORIZATION	194.39
BOILING POINT	-422.98	HEAT, FUSION	13.7
FREEZING POINT	-434.56	HEAT, COMBUSTION	60997.
SPECIFIC GRAVITY		FREE ENERGY, COMB.	33.0
CRITICAL TEMP.	-399.8	HEAT, FORMATION	
CRITICAL PRESSURE	188.	FREE ENERGY, FORM.	
CRITICAL VOLUME	0.5159	FLASH POINT	
ACENTRIC FACTOR	-0.230	AUTOIGNITION TEMP.	1085.
LOWER EXPLO. LIMIT	4.0	UPPER EXPLO. LIMIT	75.0

********** GAS PROPERTIES **********

TEMP.	PV/RT ..PRESSURE.		VISCOS -ITY	THERMAL CONDUC- TIVITY	HEAT CAPAC- ITY	PRANDTL NUMBER	HEAT CONTENT .....PRESSURE.....		
	600	1200					0	600	1200
-200	1.034	1.076	0.0129	0.0638	3.432	0.695	-683.1	-686.9	-687.0
-100	1.032	1.068	0.0162	0.0771	3.412	0.719	-341.1	-337.4	-331.8
0	1.028	1.058	0.0192	0.0912	3.413	0.717	-0.0	7.5	16.0
100	1.025	1.050	0.0218	0.1081	3.433	0.693	342.3	352.0	362.3
200	1.022	1.044	0.0243	0.1237	3.447	0.678	686.2	697.3	708.8
300	1.020	1.039	0.0267	0.1389	3.459	0.665	1031.6	1043.6	1056.0
400	1.018	1.035	0.0290	0.1519	3.464	0.660	1377.9	1390.7	1403.7
500	1.016	1.032	0.0311	0.1648	3.469	0.655	1724.5	1737.8	1751.3
600	1.015	1.029	0.0332	0.1768	3.472	0.652	2071.7	2085.4	2099.3
700	1.013	1.027	0.0352	0.1895	3.479	0.645	2419.2	2433.3	2447.4
800	1.012	1.025	0.0370	0.2028	3.487	0.637	2767.5	2781.8	2796.2
900	1.012	1.023	0.0389	0.2171	3.499	0.627	3116.8	3131.3	3145.9
1000	1.011	1.022	0.0407	0.2328	3.512	0.615	3467.3	3482.0	3496.8
1100	1.010	1.020	0.0425	0.2496	3.529	0.601	3819.3	3834.2	3849.1
1200	1.010	1.019	0.0443	0.2677	3.547	0.587	4173.1	4188.1	4203.1

SHELL DEVELOPMENT COMPANY

UNITS FOR PROPERTY VALUES IN TABLES 91 - 93

MOLECULAR WEIGHT	POUNDS/MOLE	HEAT, VAPORIZATION, BOIL. PT.		BTU/LB
BOILING POINT	DEGREES F.	HEAT, FUSION		BTU/LB
FREEZING POINT	DEGREES F.	HEAT, COMBUSTION	25 DEG. C.	BTU/LB
SPECIFIC GRAVITY	(A)	FREE ENERGY, COMB.	25 DEG. C.	BTU/LB
CRITICAL TEMP.	DEGREES F.	HEAT, FORMATION	25 DEG. C.	BTU/LB
CRITICAL PRESSURE	PSIA	FREE ENERGY, FORM.	25 DEG. C.	BTU/LB
CRITICAL VOLUME	CUFT/LB	FLASH POINT		DEG. F.
ACENTRIC FACTOR	(A)	AUTOIGNITION TEMP.		DEG. F.
EXPLOSIVE LIMITS	PERCENT BY VOLUME IN AIR			

********** GAS PROPERTIES **********

TEMP	PV/RT ..PRESSURE. 100	200	VISCOS -ITY	THERMAL CONDUC- TIVITY	HEAT CAPAC- ITY	PRANDTL NUMBER	HEAT CONTENT .....PRESSURE..... 0	100	200
DEG. F	(A)	(B)	LB(MASS) /FT/HR	(D)	BTU/LB /DEG.F	(A)	BTU/POUND	(B)	(C)

********** LIQUID PROPERTIES AT SATURATION PRESSURE **********

TEMP.	DENSITY	VISCOS -ITY	THERMAL CONDUC- TIVITY	HEAT CAPAC -ITY	HEAT CONTENT	HEAT OF VAPOR- IZATION	VAPOR PRESSURE	SURFACE TENSION
DEG. F	LB/ CUFT	LB(MASS)/ FT/HR	(D)	BTU/LB/ DEG. F	BTU/LB (C)	BTU/LB	PSIA	POUNDALS/ FOOT

(A) DIMENSIONLESS UNITS (LIQUID SP. GR. AT 60/60°F)
(B) PRESSURE IN PSIA
(C) REFERENCE STATE -- GAS AT 0 DEGREES F.
(D) BTU/HR/FT/DEG. F

Table 94.

TABLE V4. PHYSICAL PROPERTIES OF METHYLCYCLOHEXANE-TOLUENE-HYDROGEN MIXTURES — SHELL DEVELOPMENT COMPANY

	COMPONENT MCH	TOLUENE	HYDROGEN
MOLE FRACTION	1.00000	0.	0.
WEIGHT FRACTION	1.00000	0.	0.

GAS VISCOSITY (POUNDS/FOOT/HOUR)

TEMP DEG.F	PRESSURE (PSIA) 0.	100.	200.	300.	400.	500.	600.	700.	800.	900.	1200.	1500.	1800.	2100.	2400.	2700.	3000.
600.	0.0307	0.0314	0.0325	0.0340	0.0343	0.0407	0.0584	0.0739	0.0823	0.0887	0.1034	0.1148	0.1245	0.1332	0.1412	0.1486	0.1555
650.	0.0320	0.0328	0.0337	0.0350	0.0349	0.0396	0.0442	0.0531	0.0641	0.0726	0.0897	0.1019	0.1122	0.1211	0.1293	0.1368	0.1438
700.	0.0334	0.0341	0.0350	0.0361	0.0377	0.0397	0.0427	0.0469	0.0530	0.0602	0.0780	0.0909	0.1014	0.1106	0.1188	0.1264	0.1334
750.	0.0347	0.0354	0.0362	0.0373	0.0386	0.0403	0.0425	0.0454	0.0492	0.0538	0.0691	0.0819	0.0924	0.1015	0.1098	0.1173	0.1243
800.	0.0361	0.0367	0.0375	0.0384	0.0396	0.0411	0.0429	0.0451	0.0478	0.0511	0.0631	0.0748	0.0850	0.0940	0.1020	0.1095	0.1164
850.	0.0374	0.0380	0.0388	0.0398	0.0407	0.0420	0.0435	0.0453	0.0475	0.0500	0.0585	0.0697	0.0792	0.0878	0.0956	0.1028	0.1096
900.	0.0388	0.0393	0.0400	0.0408	0.0418	0.0430	0.0443	0.0459	0.0477	0.0497	0.0574	0.0661	0.0748	0.0828	0.0903	0.0972	0.1038
950.	0.0401	0.0407	0.0413	0.0421	0.0430	0.0440	0.0452	0.0466	0.0481	0.0499	0.0563	0.0638	0.0715	0.0789	0.0860	0.0926	0.0989
1000.	0.0414	0.0420	0.0426	0.0433	0.0441	0.0451	0.0462	0.0474	0.0488	0.0503	0.0558	0.0623	0.0691	0.0760	0.0825	0.0888	0.0948
1050.	0.0428	0.0433	0.0439	0.0446	0.0453	0.0462	0.0472	0.0483	0.0495	0.0509	0.0557	0.0614	0.0675	0.0737	0.0798	0.0858	0.0914
1100.	0.0441	0.0446	0.0452	0.0458	0.0465	0.0473	0.0483	0.0493	0.0504	0.0516	0.0559	0.0609	0.0665	0.0721	0.0778	0.0833	0.0887
1150.	0.0453	0.0457	0.0463	0.0469	0.0476	0.0483	0.0492	0.0501	0.0512	0.0523	0.0561	0.0607	0.0656	0.0708	0.0760	0.0812	0.0863
1200.	0.0464	0.0468	0.0474	0.0480	0.0486	0.0493	0.0501	0.0510	0.0519	0.0530	0.0565	0.0606	0.0651	0.0699	0.0747	0.0796	0.0843
1250.	0.0475	0.0480	0.0485	0.0490	0.0496	0.0503	0.0511	0.0519	0.0528	0.0537	0.0570	0.0607	0.0649	0.0692	0.0737	0.0782	0.0827
1300.	0.0486	0.0490	0.0495	0.0501	0.0507	0.0513	0.0520	0.0528	0.0536	0.0545	0.0575	0.0610	0.0648	0.0688	0.0730	0.0772	0.0815
1350.	0.0497	0.0501	0.0506	0.0511	0.0517	0.0523	0.0530	0.0537	0.0545	0.0553	0.0581	0.0613	0.0648	0.0686	0.0725	0.0765	0.0805
1400.	0.0508	0.0512	0.0516	0.0521	0.0527	0.0533	0.0539	0.0546	0.0553	0.0561	0.0587	0.0617	0.0650	0.0685	0.0722	0.0759	0.0797
1450.	0.0519	0.0522	0.0527	0.0532	0.0537	0.0542	0.0548	0.0555	0.0562	0.0569	0.0594	0.0622	0.0653	0.0686	0.0720	0.0755	0.0791
1500.	0.0529	0.0533	0.0537	0.0542	0.0547	0.0552	0.0558	0.0564	0.0571	0.0578	0.0601	0.0627	0.0656	0.0687	0.0719	0.0753	0.0786
1550.	0.0539	0.0543	0.0547	0.0552	0.0556	0.0562	0.0567	0.0573	0.0579	0.0586	0.0608	0.0633	0.0660	0.0689	0.0720	0.0751	0.0783
1600.	0.0550	0.0553	0.0557	0.0562	0.0566	0.0571	0.0577	0.0582	0.0588	0.0595	0.0616	0.0639	0.0665	0.0692	0.0721	0.0751	0.0781

GAS THERMAL CONDUCTIVITY (BTU/FOOT/HOUR/DEG.F)

TEMP DEG.F	PRESSURE (PSIA) 0.	100.	200.	300.	400.	500.	600.	700.	800.	900.	1200.	1500.	1800.	2100.	2400.	2700.	3000.
600.	0.0254	0.0259	0.0263	0.0268	0.0272	0.0287	0.0336	0.0374	0.0392	0.0406	0.0447	0.	0.	0.	0.	0.	0.
650.	0.0277	0.0280	0.0284	0.0288	0.0290	0.0299	0.0314	0.0340	0.0369	0.0389	0.0446	0.	0.	0.	0.	0.	0.
700.	0.0298	0.0301	0.0305	0.0309	0.0309	0.0317	0.0327	0.0340	0.0357	0.0376	0.0448	0.	0.	0.	0.	0.	0.
750.	0.0320	0.0323	0.0326	0.0324	0.0329	0.0336	0.0343	0.0353	0.0364	0.0378	0.0454	0.	0.	0.	0.	0.	0.
800.	0.0341	0.0344	0.0347	0.0345	0.0349	0.0355	0.0361	0.0369	0.0377	0.0387	0.0464	0.	0.	0.	0.	0.	0.
850.	0.0363	0.0366	0.0369	0.0366	0.0370	0.0375	0.0381	0.0387	0.0394	0.0402	0.0478	0.	0.	0.	0.	0.	0.
900.	0.0385	0.0388	0.0391	0.0388	0.0392	0.0396	0.0401	0.0407	0.0413	0.0419	0.0495	0.	0.	0.	0.	0.	0.
950.	0.0408	0.0410	0.0413	0.0410	0.0413	0.0417	0.0422	0.0427	0.0432	0.0438	0.0514	0.	0.	0.	0.	0.	0.
1000.	0.0431	0.0433	0.0436	0.0432	0.0435	0.0439	0.0443	0.0448	0.0452	0.0458	0.0534	0.	0.	0.	0.	0.	0.
1050.	0.0453	0.0454	0.0458	0.0454	0.0457	0.0461	0.0465	0.0469	0.0473	0.0478	0.0555	0.	0.	0.	0.	0.	0.
1100.	0.0474	0.0478	0.0481	0.0477	0.0480	0.0483	0.0487	0.0491	0.0495	0.0499	0.0576	0.	0.	0.	0.	0.	0.
1150.	0.0497	0.0499	0.0502	0.0497	0.0500	0.0504	0.0507	0.0510	0.0514	0.0518	0.0595	0.	0.	0.	0.	0.	0.
1200.	0.0518	0.0520	0.0522	0.0518	0.0521	0.0524	0.0527	0.0530	0.0534	0.0537	0.0615	0.	0.	0.	0.	0.	0.
1250.	0.0539	0.0541	0.0543	0.0539	0.0541	0.0544	0.0547	0.0550	0.0553	0.0557	0.0635	0.	0.	0.	0.	0.	0.
1300.	0.0559	0.0561	0.0563	0.0559	0.0561	0.0564	0.0567	0.0570	0.0573	0.0576	0.0654	0.	0.	0.	0.	0.	0.
1350.	0.0579	0.0581	0.0583	0.0579	0.0581	0.0583	0.0586	0.0589	0.0592	0.0595	0.0673	0.	0.	0.	0.	0.	0.
1400.	0.0599	0.0601	0.0604	0.0598	0.0600	0.0603	0.0605	0.0608	0.0611	0.0614	0.0692	0.	0.	0.	0.	0.	0.
1450.	0.0618	0.0620	0.0622	0.0617	0.0619	0.0621	0.0624	0.0627	0.0629	0.0632	0.0711	0.	0.	0.	0.	0.	0.
1500.	0.0637	0.0639	0.0641	0.0635	0.0638	0.0640	0.0642	0.0645	0.0648	0.0650	0.0730	0.	0.	0.	0.	0.	0.
1550.	0.0655	0.0657	0.0659	0.0654	0.0656	0.0658	0.0661	0.0663	0.0665	0.0668	0.0748	0.	0.	0.	0.	0.	0.
1600.	0.0674	0.0675	0.0677	0.0672	0.0674	0.0676	0.0678	0.0681	0.0683	0.0685	0.0765	0.	0.	0.	0.	0.	0.

Table 94 (CONT'D 1)

TABLE 94. PHYSICAL PROPERTIES OF METHYLCYCLOHEXANE-TOLUENE-HYDROGEN MIXTURES — SHELL DEVELOPMENT COMPANY

	COMPONENT MCH	TOLUENE	HYDROGEN
MOLE FRACTION	1.00000	0.	0.
WEIGHT FRACTION	1.00000	0.	0.

GAS DENSITY (POUNDS/CUBIC FOOT)

TEMP DEG.F	PRESSURE (PSIA) 0.	100.	200.	300.	400.	500.	600.	700.	800.	900.	1200.	1500.	1800.	2100.	2400.	2700.	3000.
600.	0.	0.923	1.998	3.302	5.007	7.656	15.031	19.476	21.438	22.776	25.402	27.141	28.465	29.542	30.453	31.244	31.942
650.	0.	0.873	1.856	3.022	4.421	6.218	8.764	12.640	16.424	18.806	22.689	24.939	26.559	27.836	28.893	29.798	30.588
700.	0.	0.829	1.754	2.901	4.011	5.448	7.210	9.423	12.078	14.711	19.841	22.676	24.623	26.114	27.327	28.351	29.237
750.	0.	0.790	1.657	2.619	3.697	4.923	6.334	7.958	9.834	11.852	17.107	20.434	22.699	24.405	25.774	26.917	27.899
800.	0.	0.755	1.572	2.464	3.444	4.527	5.729	7.065	8.536	10.116	14.796	18.332	20.845	22.742	24.255	25.512	26.586
850.	0.	0.723	1.497	2.332	3.233	4.211	5.271	6.420	7.656	8.967	13.011	16.476	19.120	21.159	22.795	24.153	25.311
900.	0.	0.693	1.430	2.218	3.054	3.949	4.906	5.925	7.004	8.135	11.661	14.909	17.566	19.688	21.414	22.854	24.084
950.	0.	0.666	1.370	2.112	2.898	3.728	4.604	5.526	6.492	7.495	10.470	13.615	16.202	18.348	20.128	21.628	22.916
1000.	0.	0.642	1.314	2.020	2.760	3.536	4.348	5.194	6.073	6.980	9.795	12.549	15.022	17.145	18.946	20.484	21.814
1050.	0.	0.619	1.264	1.937	2.638	3.368	4.126	4.911	5.721	6.553	9.122	11.662	14.007	16.076	17.870	19.424	20.782
1100.	0.	0.598	1.218	1.861	2.528	3.219	3.931	4.666	5.420	6.190	8.561	10.917	13.131	15.130	16.897	18.450	19.821
1150.	0.	0.578	1.175	1.792	2.429	3.085	3.759	4.450	5.157	5.876	8.082	10.281	12.373	14.293	16.020	17.559	18.930
1200.	0.	0.560	1.136	1.729	2.338	2.963	3.604	4.258	4.924	5.601	7.669	9.731	11.710	13.552	15.230	16.745	18.108
1250.	0.	0.542	1.099	1.670	2.255	2.853	3.464	4.085	4.717	5.357	7.306	9.250	11.128	12.892	14.519	16.002	17.349
1300.	0.	0.526	1.065	1.616	2.178	2.752	3.336	3.929	4.531	5.138	6.985	8.826	10.611	12.302	13.876	15.324	16.650
1350.	0.	0.511	1.033	1.565	2.107	2.659	3.219	3.787	4.361	4.941	6.697	8.447	10.149	11.772	13.293	14.704	16.006
1400.	0.	0.497	1.003	1.518	2.041	2.573	3.112	3.656	4.207	4.761	6.437	8.106	9.734	11.292	12.763	14.136	15.411
1450.	0.	0.483	0.975	1.474	1.980	2.493	3.012	3.536	4.065	4.596	6.202	7.798	9.358	10.857	12.279	13.615	14.862
1500.	0.	0.470	0.948	1.432	1.923	2.419	2.920	3.425	3.934	4.445	5.986	7.518	9.016	10.460	11.836	13.134	14.353
1550.	0.	0.458	0.923	1.393	1.869	2.349	2.833	3.321	3.812	4.305	5.788	7.261	8.703	10.096	11.428	12.691	13.881
1600.	0.	0.447	0.899	1.356	1.818	2.284	2.753	3.225	3.699	4.175	5.605	7.024	8.415	9.761	11.052	12.280	13.442

GAS COMPRESSIBILITY FACTOR

TEMP DEG.F	PRESSURE (PSIA) 0.	100.	200.	300.	400.	500.	600.	700.	800.	900.	1200.	1500.	1800.	2100.	2400.	2700.	3000.
600.	0.	0.9353	0.8643	0.7944	0.6807	0.5638	0.3446	0.3103	0.3222	0.3612	0.4079	0.4772	0.5460	0.6137	0.6804	0.7461	0.8109
650.	0.	0.9440	0.8838	0.8184	0.7459	0.6629	0.5645	0.4566	0.4016	0.3946	0.4361	0.4959	0.5588	0.6220	0.6848	0.7471	0.8086
700.	0.	0.9512	0.8997	0.8451	0.7868	0.7240	0.6545	0.5861	0.5225	0.4827	0.4771	0.5219	0.5767	0.6344	0.6929	0.7513	0.8095
750.	0.	0.9573	0.9128	0.8665	0.8183	0.7682	0.7165	0.6645	0.6152	0.5743	0.5305	0.5552	0.5998	0.6508	0.7043	0.7587	0.8133
800.	0.	0.9624	0.9238	0.8841	0.8436	0.8023	0.7607	0.7197	0.6807	0.6462	0.5890	0.5943	0.6272	0.6707	0.7187	0.7687	0.8196
850.	0.	0.9668	0.9330	0.8988	0.8642	0.8295	0.7951	0.7618	0.7299	0.7011	0.6443	0.6360	0.6577	0.6933	0.7355	0.7809	0.8280
900.	0.	0.9707	0.9410	0.9112	0.8814	0.8519	0.8229	0.7949	0.7685	0.7444	0.6924	0.6770	0.6895	0.7177	0.7541	0.7949	0.8382
950.	0.	0.9739	0.9478	0.9217	0.8959	0.8705	0.8458	0.8221	0.7998	0.7794	0.7333	0.7150	0.7210	0.7428	0.7739	0.8102	0.8496
1000.	0.	0.9768	0.9537	0.9308	0.9082	0.8862	0.8650	0.8447	0.8257	0.8082	0.7679	0.7492	0.7510	0.7677	0.7940	0.8262	0.8620
1050.	0.	0.9793	0.9588	0.9386	0.9188	0.8997	0.8813	0.8638	0.8474	0.8324	0.7972	0.7795	0.7788	0.7917	0.8139	0.8424	0.8749
1100.	0.	0.9815	0.9633	0.9454	0.9280	0.9113	0.8952	0.8801	0.8659	0.8529	0.8223	0.8060	0.8041	0.8142	0.8332	0.8584	0.8879
1150.	0.	0.9835	0.9672	0.9514	0.9361	0.9213	0.9073	0.8941	0.8818	0.8705	0.8439	0.8293	0.8269	0.8351	0.8515	0.8740	0.9007
1200.	0.	0.9852	0.9707	0.9566	0.9431	0.9301	0.9178	0.9063	0.8955	0.8857	0.8626	0.8497	0.8473	0.8552	0.8687	0.8889	0.9133
1250.	0.	0.9868	0.9738	0.9613	0.9493	0.9378	0.9270	0.9169	0.9075	0.8990	0.8789	0.8678	0.8656	0.8717	0.8846	0.9029	0.9253
1300.	0.	0.9881	0.9765	0.9654	0.9547	0.9446	0.9351	0.9263	0.9181	0.9107	0.8933	0.8837	0.8820	0.8875	0.8993	0.9161	0.9368
1350.	0.	0.9894	0.9790	0.9691	0.9596	0.9507	0.9423	0.9345	0.9274	0.9209	0.9059	0.8978	0.8966	0.9019	0.9128	0.9283	0.9475
1400.	0.	0.9905	0.9812	0.9723	0.9639	0.9560	0.9487	0.9418	0.9356	0.9300	0.9171	0.9103	0.9097	0.9149	0.9251	0.9397	0.9577
1450.	0.	0.9915	0.9832	0.9753	0.9678	0.9608	0.9544	0.9484	0.9429	0.9381	0.9270	0.9215	0.9215	0.9267	0.9364	0.9501	0.9671
1500.	0.	0.9923	0.9849	0.9779	0.9713	0.9651	0.9594	0.9542	0.9495	0.9453	0.9359	0.9315	0.9321	0.9373	0.9467	0.9597	0.9758
1550.	0.	0.9932	0.9865	0.9803	0.9744	0.9690	0.9640	0.9595	0.9554	0.9517	0.9439	0.9405	0.9416	0.9469	0.9561	0.9686	0.9839
1600.	0.	0.9939	0.9880	0.9824	0.9773	0.9725	0.9681	0.9642	0.9606	0.9576	0.9510	0.9486	0.9502	0.9557	0.9646	0.9767	0.9913

Table 94 (CONT'D 2)

TABLE 94. PHYSICAL PROPERTIES OF METHYLCYCLOHEXANE-TOLUENE-HYDROGEN MIXTURES — SHELL DEVELOPMENT COMPANY

	COMPONENT MCH	TOLUENE	HYDROGEN
MOLE FRACTION	1.00000	0.	0.
WEIGHT FRACTION	1.00000	0.	0.

GAS HEAT CONTENT (BTU/POUND)

TEMP DEG.F	PRESSURE (PSIA) 0.	100.	200.	300.	400.	500.	600.	700.	800.	900.	1200.	1500.	1800.	2100.	2400.	2700.	3000.
600.	282.	278.	273.	268.	261.	252.	229.	219.	215.	212.	209.	207.	206.	205.	205.	205.	205.
650.	315.	311.	307.	302.	301.	292.	271.	261.	257.	254.	248.	245.	244.	242.	242.	242.	242.
700.	349.	346.	342.	338.	338.	330.	314.	305.	301.	297.	290.	285.	283.	281.	280.	280.	279.
750.	384.	381.	378.	378.	373.	367.	357.	350.	346.	342.	332.	325.	323.	321.	319.	319.	318.
800.	421.	418.	414.	411.	408.	404.	400.	396.	391.	387.	375.	368.	364.	361.	360.	359.	358.
850.	458.	455.	452.	449.	446.	443.	441.	438.	434.	429.	417.	410.	405.	402.	401.	399.	399.
900.	496.	493.	491.	488.	485.	[illegible]	483.	480.	476.	471.	460.	452.	447.	444.	442.	441.	440.
950.	535.	533.	530.	528.	525.	523.	524.	521.	518.	514.	502.	495.	490.	487.	485.	483.	482.
1000.	575.	573.	570.	568.	564.	564.	565.	563.	559.	556.	545.	538.	534.	530.	528.	526.	525.
1050.	616.	614.	611.	609.	607.	606.	606.	604.	601.	598.	589.	582.	578.	575.	572.	570.	569.
1100.	657.	655.	653.	651.	649.	648.	648.	646.	643.	640.	633.	627.	622.	619.	616.	614.	613.
1150.	700.	698.	696.	694.	692.	690.	689.	688.	686.	683.	677.	671.	667.	664.	661.	659.	658.
1200.	743.	741.	739.	737.	735.	734.	732.	730.	728.	726.	721.	717.	713.	710.	707.	705.	703.
1250.	787.	785.	783.	781.	780.	778.	775.	773.	771.	770.	766.	762.	759.	756.	753.	751.	749.
1300.	831.	829.	828.	826.	824.	822.	818.	816.	815.	814.	812.	809.	805.	802.	800.	798.	796.
1350.	876.	874.	873.	871.	869.	867.	863.	861.	860.	859.	858.	855.	852.	849.	847.	845.	843.
1400.	922.	920.	919.	917.	915.	913.	908.	906.	906.	905.	904.	902.	899.	896.	894.	892.	890.
1450.	968.	966.	965.	963.	962.	959.	955.	953.	952.	952.	951.	949.	947.	944.	942.	940.	938.
1500.	1014.	1013.	1012.	1010.	1009.	1007.	1003.	1001.	1000.	1000.	999.	997.	994.	992.	990.	988.	986.
1550.	1061.	1060.	1059.	1058.	1056.	1055.	1052.	1050.	1049.	1049.	1047.	1045.	1042.	1040.	1038.	1036.	1035.
1600.	1109.	1108.	1107.	1105.	1104.	1103.	1102.	1101.	1100.	1099.	1096.	1093.	1090.	1088.	1086.	1085.	1083.

GAS HEAT CAPACITY (BTU/POUND/DEG.F)

TEMP DEG.F	PRESSURE (PSIA) 0.	100.	200.	300.	400.	500.	600.	700.	800.	900.	1200.	1500.	1800.	2100.	2400.	2700.	3000.
600.	0.6460	0.6534	0.6659	0.8148	0.8135	0.8163	0.8397	0.8416	0.8318	0.8193	0.7830	0.7602	0.7469	0.7384	0.7325	0.7282	0.7249
650.	0.6702	0.6765	0.6860	0.7813	0.7808	0.7806	0.8494	0.8695	0.8634	0.8513	0.8114	0.7856	0.7707	0.7613	0.7548	0.7501	0.7465
700.	0.6932	0.6987	0.7056	0.7045	0.7220	0.7545	0.8563	0.8839	0.8872	0.8760	0.8351	0.8080	0.7923	0.7825	0.7757	0.7708	0.7670
750.	0.7159	0.7198	0.7247	0.6747	0.6971	0.7380	0.8603	0.9028	0.9030	0.8833	0.8541	0.8275	0.8119	0.8020	0.7952	0.7902	0.7864
800.	0.7349	0.7387	0.7443	0.7517	0.7624	0.7807	0.8335	0.8531	0.8550	0.85[illegible]0	0.8409	0.8301	0.8219	0.8155	0.8103	0.8062	0.8028
850.	0.7537	0.7577	0.7626	0.7688	0.7774	0.7911	0.8275	0.8465	0.8464	0.8477	0.8462	0.8415	0.8361	0.8310	0.8266	0.8228	0.8196
900.	0.7724	0.7760	0.7802	0.7854	0.7921	0.8018	0.8238	0.8319	0.8403	0.844[illegible]	8519	0.8525	0.8496	0.8458	0.8420	0.8386	0.8357
950.	0.7904	0.7935	0.7972	0.8014	0.8065	0.8127	0.8226	0.8302	0.8368	0.84[illegible]	[illegible]501	0.8631	0.8624	0.8597	0.8566	0.8536	0.8509
1000.	0.8075	0.8104	0.8135	0.8169	0.8206	0.8239	0.8237	0.8294	0.8359	0.84[illegible]	[illegible]448	0.8733	0.8745	0.[illegible]29	0.8704	0.8678	0.8653
1050.	0.8240	0.8265	0.8292	0.8319	0.8344	0.8354	0.8272	0.8295	0.8376	0.847[illegible]	0.8719	0.8831	0.8859	0.8852	0.8833	0.8811	0.8790
1100.	0.8396	0.8419	0.8442	0.8463	0.8479	0.8471	0.8332	0.8336	0.8419	0.8521	0.8795	0.8926	0.[illegible]946	0.8967	0.8954	0.8936	0.8918
1150.	0.8545	0.8565	0.8585	0.8603	0.8611	0.8591	0.8415	0.8436	0.8488	0.8591	0.8876	0.9017	0.[illegible]065	0.9074	0.9067	0.9054	0.9039
1200.	0.8688	0.8705	0.8722	0.8736	0.8740	0.8713	0.8522	0.8505	0.8582	0.8683	0.8961	0.9104	0.[illegible]158	0.9173	0.9171	0.9163	0.9151
1250.	0.8820	0.8837	0.8852	0.8864	0.8866	0.8838	0.8653	0.8633	0.8703	0.8794	0.9050	0.9187	0.[illegible]244	0.9264	0.9268	0.9264	0.9256
1300.	0.8946	0.8962	0.8976	0.8987	0.8990	0.8966	0.8808	0.8791	0.8850	0.8927	0.9145	0.9257	0.[illegible]323	0.9347	0.9356	0.9356	0.9353
1350.	0.9065	0.9079	0.9093	0.9105	0.9110	0.9096	0.8987	0.8978	0.9022	0.9079	0.9243	0.9343	0.[illegible]395	0.9422	0.9435	0.9441	0.9441
1400.	0.9178	0.9190	0.9204	0.9217	0.9227	0.9230	0.9190	0.9194	0.9221	0.9253	0.9347	0.9435	0.9459	0.9489	0.9507	0.9517	0.9522
1450.	0.9279	0.9293	0.9308	0.9324	0.9342	0.9365	0.9417	0.9439	0.9445	0.9447	0.9455	0.9483	0.9517	0.9547	0.9570	0.9586	0.9595
1500.	0.9374	0.9389	0.9405	0.9425	0.9453	0.9504	0.9668	0.9714	0.9695	0.9661	0.9568	0.9547	0.9568	0.9598	0.9625	0.9646	0.9660
1550.	0.9462	0.9477	0.9496	0.9521	0.9561	0.9645	0.9943	1.0038	0.9972	0.9896	0.9685	0.9608	0.9612	0.9641	0.9672	0.9698	0.9717
1600.	0.9542	0.9559	0.9580	0.9612	0.9667	0.9788	1.0242	1.0301	1.0274	1.0152	0.9807	0.9665	0.9648	0.9674	0.9710	0.9741	0.9766

Table 94 (CONT'D 3)

TABLE 94. PHYSICAL PROPERTIES OF METHYLCYCLOHEXANE-TOLUENE-HYDROGEN MIXTURES — SHELL DEVELOPMENT COMPANY

	COMPONENT MCH	TOLUENE	HYDROGEN
MOLE FRACTION	0.42900	0.14300	0.42900
WEIGHT FRACTION	0.75000	0.23400	0.01500

GAS VISCOSITY (POUNDS/FOOT/HOUR)

TEMP DEG.F	PRESSURE (PSIA) 0.	100.	200.	300.	400.	500.	600.	700.	800.	900.	1200.	1500.	1800.	2100.	2400.	2700.	3000.
600.	0.0336	0.0338	0.0337	0.0341	0.0345	0.0351	0.0356	0.0363	0.0369	0.0377	0.0403	0.0435	0.0469	0.0506	0.0544	0.0582	0.0618
650.	0.0344	0.0347	0.0351	0.0355	0.0359	0.0363	0.0369	0.0374	0.0380	0.0387	0.0410	0.0437	0.0467	0.0499	0.0532	0.0565	0.0599
700.	0.0359	0.0361	0.0365	0.0368	0.0372	0.0376	0.0381	0.0385	0.0392	0.0398	0.0418	0.0442	0.0468	0.0496	0.0525	0.0555	0.0586
750.	0.0373	0.0376	0.0379	0.0382	0.0386	0.0390	0.0394	0.0399	0.0404	0.0409	0.0427	0.0448	0.0472	0.0497	0.0523	0.0550	0.0577
800.	0.0387	0.0390	0.0392	0.0396	0.0399	0.0403	0.0407	0.0411	0.0416	0.0421	0.0437	0.0456	0.0477	0.0500	0.0523	0.0548	0.0573
850.	0.0401	0.0404	0.0406	0.0409	0.0413	0.0416	0.0420	0.0424	0.0428	0.0433	0.0443	0.0465	0.0484	0.0505	0.0526	0.0549	0.0571
900.	0.0415	0.0417	0.0420	0.0423	0.0426	0.0429	0.0433	0.0437	0.0441	0.0445	0.0459	0.0475	0.0492	0.0511	0.0531	0.0551	0.0572
950.	0.0429	0.0431	0.0434	0.0437	0.0440	0.0443	0.0446	0.0450	0.0453	0.0457	0.0470	0.0485	0.0501	0.0518	0.0537	0.0555	0.0575
1000.	0.0443	0.0445	0.0448	0.0450	0.0453	0.0456	0.0459	0.0463	0.0466	0.0470	0.0482	0.0496	0.0511	0.0527	0.0543	0.0561	0.0579
1050.	0.0457	0.0459	0.0461	0.0464	0.0467	0.0470	0.0473	0.0475	0.0479	0.0483	0.0494	0.0507	0.0521	0.0535	0.0551	0.0568	0.0585
1100.	0.0471	0.0473	0.0475	0.0478	0.0480	0.0483	0.0486	0.0489	0.0492	0.0495	0.0506	0.0518	0.0531	0.0545	0.0560	0.0575	0.0591
1150.	0.0483	0.0485	0.0488	0.0490	0.0492	0.0495	0.0498	0.0501	0.0504	0.0507	0.0517	0.0528	0.0540	0.0554	0.0567	0.0582	0.0597
1200.	0.0495	0.0497	0.0499	0.0502	0.0504	0.0507	0.0509	0.0512	0.0515	0.0518	0.0527	0.0538	0.0550	0.0562	0.0575	0.0589	0.0603
1250.	0.0507	0.0509	0.0511	0.0513	0.0516	0.0518	0.0520	0.0523	0.0526	0.0529	0.0538	0.0548	0.0559	0.0571	0.0583	0.0596	0.0609
1300.	0.0519	0.0521	0.0523	0.0525	0.0527	0.0529	0.0532	0.0534	0.0537	0.0540	0.0548	0.0558	0.0568	0.0579	0.0591	0.0603	0.0616
1350.	0.0530	0.0532	0.0534	0.0536	0.0538	0.0540	0.0543	0.0545	0.0548	0.0550	0.0559	0.0568	0.0578	0.0588	0.0599	0.0611	0.0623
1400.	0.0542	0.0544	0.0545	0.0547	0.0549	0.0551	0.0554	0.0556	0.0558	0.0561	0.0569	0.0578	0.0587	0.0597	0.0608	0.0619	0.0630
1450.	0.0553	0.0555	0.0556	0.0558	0.0560	0.0562	0.0565	0.0567	0.0569	0.0572	0.0579	0.0588	0.0597	0.0606	0.0616	0.0627	0.0638
1500.	0.0564	0.0566	0.0567	0.0569	0.0571	0.0573	0.0575	0.0577	0.0580	0.0582	0.0589	0.0598	0.0606	0.0615	0.0625	0.0635	0.0646
1550.	0.0575	0.0577	0.0578	0.0580	0.0582	0.0584	0.0586	0.0588	0.0590	0.0592	0.0600	0.0607	0.0616	0.0624	0.0634	0.0643	0.0653
1600.	0.0586	0.0587	0.0589	0.0591	0.0593	0.0594	0.0596	0.0598	0.0601	0.0603	0.0610	0.0617	0.0625	0.0634	0.0642	0.0652	0.0661

GAS THERMAL CONDUCTIVITY (BTU/FOOT/HOUR/DEG.F)

TEMP DEG.F	PRESSURE (PSIA) 0.	100.	200.	300.	400.	500.	600.	700.	800.	900.	1200.	1500.	1800.	2100.	2400.	2700.	3000.
600.	0.0381	0.0383	0.0385	0.0381	0.0384	0.0387	0.0390	0.0393	0.0396	0.0400	0.0471	0.	0.	0.	0.	0.	0.
650.	0.0403	0.0405	0.0407	0.0403	0.0405	0.0408	0.0411	0.0414	0.0417	0.0420	0.0491	0.	0.	0.	0.	0.	0.
700.	0.0426	0.0428	0.0429	0.0425	0.0427	0.0430	0.0432	0.0435	0.0438	0.0441	0.0512	0.	0.	0.	0.	0.	0.
750.	0.0448	0.0450	0.0452	0.0447	0.0449	0.0452	0.0454	0.0457	0.0459	0.0462	0.0534	0.	0.	0.	0.	0.	0.
800.	0.0470	0.0472	0.0474	0.0469	0.0471	0.0473	0.0475	0.0478	0.0480	0.0483	0.0555	0.	0.	0.	0.	0.	0.
850.	0.0493	0.0494	0.0496	0.0491	0.0493	0.0495	0.0497	0.0500	0.0502	0.0504	0.0577	0.	0.	0.	0.	0.	0.
900.	0.0516	0.0517	0.0519	0.0514	0.0516	0.0518	0.0520	0.0522	0.0524	0.0526	0.0599	0.	0.	0.	0.	0.	0.
950.	0.0538	0.0540	0.0541	0.0536	0.0538	0.0540	0.0542	0.0544	0.0546	0.0548	0.0621	0.	0.	0.	0.	0.	0.
1000.	0.0561	0.0563	0.0564	0.0559	0.0561	0.0563	0.0564	0.0566	0.0568	0.0570	0.0644	0.	0.	0.	0.	0.	0.
1050.	0.0584	0.0586	0.0587	0.0582	0.0584	0.0585	0.0587	0.0589	0.0591	0.0593	0.0666	0.	0.	0.	0.	0.	0.
1100.	0.0607	0.0609	0.0610	0.0605	0.0606	0.0608	0.0610	0.0611	0.0613	0.0615	0.0689	0.	0.	0.	0.	0.	0.
1150.	0.0629	0.0630	0.0632	0.0626	0.0628	0.0629	0.0631	0.0633	0.0634	0.0636	0.0710	0.	0.	0.	0.	0.	0.
1200.	0.0650	0.0651	0.0653	0.0647	0.0649	0.0650	0.0652	0.0653	0.0655	0.0657	0.0731	0.	0.	0.	0.	0.	0.
1250.	0.0671	0.0672	0.0673	0.0668	0.0669	0.0671	0.0672	0.0674	0.0675	0.0677	0.0751	0.	0.	0.	0.	0.	0.
1300.	0.0691	0.0693	0.0694	0.0688	0.0690	0.0691	0.0692	0.0694	0.0695	0.0697	0.0772	0.	0.	0.	0.	0.	0.
1350.	0.0712	0.0713	0.0714	0.0708	0.0710	0.0711	0.0712	0.0714	0.0715	0.0717	0.0792	0.	0.	0.	0.	0.	0.
1400.	0.0732	0.0733	0.0734	0.0728	0.0730	0.0731	0.0732	0.0734	0.0735	0.0736	0.0812	0.	0.	0.	0.	0.	0.
1450.	0.0751	0.0753	0.0754	0.0749	0.0749	0.0751	0.0752	0.0753	0.0755	0.0756	0.0831	0.	0.	0.	0.	0.	0.
1500.	0.0771	0.0772	0.0773	0.0767	0.0769	0.0770	0.0771	0.0772	0.0774	0.0775	0.0850	0.	0.	0.	0.	0.	0.
1550.	0.0790	0.0791	0.0792	0.0786	0.0788	0.0789	0.0790	0.0791	0.0793	0.0794	0.0869	0.	0.	0.	0.	0.	0.
1600.	0.0809	0.0810	0.0811	0.0805	0.0806	0.0808	0.0809	0.0810	0.0811	0.0812	0.0888	0.	0.	0.	0.	0.	0.

Table 94 (CONT'D 4)

TABLE 94. PHYSICAL PROPERTIES OF METHYLCYCLOHEXANE-TOLUENE-HYDROGEN MIXTURES — SHELL DEVELOPMENT COMPANY

	COMPONENT MCH	TOLUENE	HYDROGEN
MOLE FRACTION	0.42900	0.14300	0.42900
WEIGHT FRACTION	0.75000	0.23400	0.01500

GAS DENSITY (POUNDS/CUBIC FOOT)

TEMP DEG.F	PRESSURE (PSIA) 0.	100.	200.	300.	400.	500.	600.	700.	800.	900.	1200.	1500.	1800.	2100.	2400.	2700.	3000.
600.	0.	0.502	1.071	1.558	2.112	2.684	3.273	3.879	4.499	5.133	7.093	9.075	10.985	12.756	14.355	15.783	17.055
650.	0.	0.478	0.970	1.476	1.995	2.528	3.073	3.630	4.198	4.776	6.550	8.340	10.084	11.731	13.251	14.636	15.889
700.	0.	0.457	0.924	1.403	1.902	2.391	2.900	3.419	3.944	4.477	6.104	7.742	9.346	10.880	12.317	13.646	14.867
750.	0.	0.437	0.883	1.338	1.800	2.271	2.749	3.234	3.725	4.221	5.729	7.242	8.730	10.162	11.519	12.790	13.971
800.	0.	0.419	0.845	1.279	1.718	2.164	2.616	3.072	3.533	3.998	5.406	6.817	8.205	9.549	10.833	12.045	13.182
850.	0.	0.403	0.811	1.225	1.644	2.068	2.496	2.928	3.364	3.802	5.126	6.449	7.752	9.019	10.235	11.392	12.485
900.	0.	0.387	0.779	1.176	1.576	1.981	2.389	2.799	3.212	3.627	4.878	6.126	7.356	8.554	9.710	10.815	11.866
950.	0.	0.373	0.750	1.131	1.515	1.902	2.291	2.682	3.076	3.470	4.658	5.840	7.006	8.144	9.244	10.302	11.312
1000.	0.	0.360	0.723	1.089	1.458	1.829	2.202	2.576	2.952	3.328	4.459	5.585	6.693	7.777	8.829	9.842	10.814
1050.	0.	0.348	0.698	1.051	1.406	1.762	2.120	2.479	2.839	3.199	4.280	5.354	6.412	7.448	8.455	9.427	10.364
1100.	0.	0.337	0.675	1.015	1.357	1.701	2.045	2.390	2.735	3.081	4.117	5.145	6.158	7.150	8.116	9.051	9.954
1150.	0.	0.326	0.653	0.982	1.312	1.643	1.975	2.307	2.640	2.972	3.967	4.954	5.926	6.878	7.807	8.709	9.580
1200.	0.	0.316	0.633	0.951	1.270	1.590	1.910	2.231	2.551	2.871	3.829	4.778	5.713	6.630	7.525	8.394	9.237
1250.	0.	0.307	0.614	0.922	1.231	1.540	1.850	2.160	2.469	2.778	3.702	4.616	5.517	6.401	7.265	8.105	8.921
1300.	0.	0.298	0.596	0.895	1.194	1.494	1.794	2.093	2.392	2.691	3.583	4.467	5.337	6.190	7.025	7.838	8.628
1350.	0.	0.289	0.579	0.870	1.160	1.450	1.741	2.031	2.321	2.610	3.473	4.327	5.169	5.994	6.802	7.590	8.357
1400.	0.	0.282	0.563	0.845	1.128	1.409	1.691	1.973	2.254	2.534	3.371	4.197	5.012	5.812	6.595	7.359	8.104
1450.	0.	0.274	0.548	0.823	1.097	1.371	1.645	1.918	2.191	2.463	3.274	4.076	4.866	5.642	6.402	7.144	7.868
1500.	0.	0.267	0.534	0.801	1.068	1.334	1.601	1.866	2.131	2.396	3.184	3.962	4.729	5.482	6.221	6.943	7.647
1550.	0.	0.260	0.521	0.781	1.041	1.300	1.559	1.817	2.075	2.332	3.098	3.855	4.601	5.333	6.051	6.753	7.439
1600.	0.	0.254	0.508	0.761	1.015	1.267	1.520	1.771	2.022	2.273	3.018	3.754	4.479	5.192	5.891	6.575	7.244

GAS COMPRESSIBILITY FACTOR

TEMP DEG.F	PRESSURE (PSIA) 0.	100.	200.	300.	400.	500.	600.	700.	800.	900.	1200.	1500.	1800.	2100.	2400.	2700.	3000.
600.	0.	0.9834	0.9670	0.9509	0.9352	0.9200	0.9053	0.8914	0.8782	0.8659	0.8355	0.8163	0.8[illegible]	0.8[illegible]	0.8256	0.8448	0.8687
650.	0.	0.9859	0.9721	0.9586	0.9455	0.9329	0.9208	0.9094	0.8987	0.8887	0.8640	0.8482	0.8418	0.8442	0.8541	0.8700	0.8904
700.	0.	0.9880	0.9763	0.9649	0.9540	0.9435	0.9335	0.9241	0.9153	0.9072	0.8871	0.8743	0.8691	0.8710	0.8793	0.8929	0.9106
750.	0.	0.9898	0.9799	0.9703	0.9611	0.9524	0.9441	0.9363	0.9291	0.9225	0.9062	0.8960	0.8920	0.8940	0.9013	0.9132	0.9290
800.	0.	0.9914	0.9829	0.9748	0.9671	0.9598	0.9530	0.9465	0.9406	0.9352	0.9221	0.9142	0.9114	0.9136	0.9204	0.9312	0.9455
850.	0.	0.9927	0.9855	0.9787	0.9722	0.9661	0.9604	0.9552	0.9503	0.9459	0.9355	0.9294	0.9278	0.9304	0.9370	0.9470	0.9601
900.	0.	0.9938	0.9877	0.9820	0.9766	0.9715	0.9668	0.9625	0.9585	0.9550	0.9468	0.9424	0.9418	0.9449	0.9513	0.9609	0.9731
950.	0.	0.9947	0.9896	0.9848	0.9803	0.9761	0.9723	0.9688	0.9656	0.9628	0.9565	0.9535	0.9538	0.9573	0.9638	0.9733	0.9845
1000.	0.	0.9956	0.9913	0.9873	0.9836	0.9801	0.9770	0.9741	0.9716	0.9694	0.9647	0.9630	0.9641	0.9681	0.9746	0.9835	0.9946
1050.	0.	0.9963	0.9927	0.9894	0.9864	0.9836	0.9811	0.9788	0.9769	0.9752	0.9719	0.9710	0.9731	0.9774	0.9840	0.9928	1.0035
1100.	0.	0.9969	0.9940	0.9913	0.9888	0.9866	0.9846	0.9829	0.9814	0.9802	0.9781	0.9783	0.9808	0.9855	0.9922	1.0009	1.0112
1150.	0.	0.9975	0.9951	0.9929	0.9909	0.9892	0.9877	0.9864	0.9853	0.9845	0.9835	0.9845	0.9876	0.9926	0.9994	1.0080	1.0181
1200.	0.	0.9980	0.9961	0.9943	0.9928	0.9915	0.9904	0.9895	0.9888	0.9883	0.9882	0.9899	0.9934	0.9987	1.0057	1.0142	1.0241
1250.	0.	0.9984	0.9969	0.9956	0.9945	0.9935	0.9928	0.9922	0.9918	0.9917	0.9923	0.9946	0.9986	1.0042	1.0112	1.0197	1.0294
1300.	0.	0.9988	0.9977	0.9967	0.9959	0.9953	0.9948	0.9946	0.9945	0.9946	0.9959	0.9988	1.0031	1.0089	1.0161	1.0245	1.0340
1350.	0.	0.9991	0.9983	0.9977	0.9972	0.9969	0.9967	0.9967	0.9968	0.9972	0.9991	1.0024	1.0071	1.0131	1.0203	1.0287	1.0381
1400.	0.	0.9994	0.9989	0.9985	0.9983	0.9982	0.9983	0.9985	0.9989	0.9994	1.0019	1.0056	1.0106	1.0168	1.0241	1.0324	1.0417
1450.	0.	0.9997	0.9995	0.9993	0.9993	0.9995	0.9998	1.0002	1.0008	1.0015	1.0044	1.0085	1.0137	1.0200	1.0274	1.0357	1.0449
1500.	0.	1.0000	0.9999	1.0000	1.0002	1.0006	1.0011	1.0017	1.0024	1.0033	1.0066	1.0110	1.0164	1.0229	1.0303	1.0386	1.0477
1550.	0.	1.0002	1.0003	1.0004	1.0010	1.0016	1.0022	1.0030	1.0038	1.0048	1.0085	1.0132	1.0189	1.0254	1.0329	1.0411	1.0501
1600.	0.	1.0004	1.0007	1.0012	1.0017	1.0024	1.0032	1.0041	1.0051	1.0063	1.0103	1.0152	1.0210	1.0277	1.0351	1.0433	1.0522

Table 94 (CONT'D 5)

TABLE 94. PHYSICAL PROPERTIES OF METHYLCYCLOHEXANE-TOLUENE-HYDROGEN MIXTURES

SHELL DEVELOPMENT COMPANY

	COMPONENT MCH	TOLUENE	HYDROGEN
MOLE FRACTION	0.42900	0.14300	0.42900
WEIGHT FRACTION	0.75000	0.23400	0.01600

GAS HEAT CONTENT (BTU/POUND)

TEMP DEG.F	PRESSURE (PSIA) 0.	100.	200.	300.	400.	500.	600.	700.	800.	900.	1200.	1500.	1800.	2100.	2400.	2700.	3000.
600.	295.	293.	291.	290.	288.	286.	284.	282.	280.	278.	273.	268.	263.	259.	256.	253.	251.
650.	328.	327.	325.	323.	322.	320.	318.	316.	315.	313.	308.	304.	300.	296.	293.	290.	288.
700.	363.	361.	360.	358.	356.	355.	353.	352.	350.	349.	345.	341.	337.	334.	331.	328.	326.
750.	398.	397.	395.	394.	392.	391.	389.	388.	387.	385.	382.	378.	374.	371.	369.	366.	364.
800.	434.	433.	432.	430.	429.	428.	426.	425.	424.	423.	419.	416.	413.	410.	407.	405.	403.
850.	471.	470.	469.	468.	466.	465.	464.	463.	462.	461.	457.	454.	452.	449.	447.	445.	443.
900.	509.	508.	507.	506.	505.	504.	503.	502.	501.	500.	497.	494.	491.	489.	487.	485.	483.
950.	548.	547.	546.	545.	544.	543.	542.	541.	540.	539.	536.	534.	532.	529.	528.	526.	524.
1000.	588.	587.	586.	585.	584.	583.	582.	581.	580.	579.	577.	575.	573.	571.	569.	567.	566.
1050.	628.	627.	626.	626.	625.	624.	623.	622.	621.	621.	618.	616.	614.	612.	611.	609.	608.
1100.	669.	669.	668.	667.	666.	665.	664.	664.	663.	662.	660.	658.	656.	655.	653.	652.	650.
1150.	711.	711.	710.	709.	708.	707.	707.	706.	705.	705.	703.	701.	699.	697.	696.	695.	693.
1200.	754.	753.	752.	752.	751.	750.	749.	749.	748.	747.	746.	744.	742.	741.	739.	738.	737.
1250.	797.	796.	796.	795.	794.	794.	793.	792.	792.	791.	789.	788.	786.	785.	783.	782.	781.
1300.	841.	840.	839.	839.	838.	838.	837.	836.	836.	835.	833.	832.	830.	829.	828.	827.	826.
1350.	885.	884.	884.	883.	883.	882.	881.	881.	880.	880.	878.	877.	875.	874.	873.	872.	871.
1400.	930.	929.	929.	928.	928.	927.	927.	926.	925.	925.	923.	922.	921.	920.	919.	918.	917.
1450.	975.	975.	974.	974.	973.	973.	972.	972.	971.	971.	969.	968.	967.	966.	965.	964.	963.
1500.	1021.	1021.	1020.	1020.	1019.	1019.	1018.	1018.	1017.	1017.	1015.	1014.	1013.	1012.	1011.	1011.	1010.
1550.	1067.	1067.	1066.	1066.	1065.	1065.	1065.	1064.	1064.	1063.	1062.	1061.	1060.	1059.	1058.	1058.	1057.
1600.	1114.	1114.	1113.	1113.	1112.	1112.	1111.	1111.	1111.	1110.	1109.	1108.	1107.	1107.	1106.	1105.	1105.

GAS HEAT CAPACITY (BTU/POUND/DEG.F)

TEMP DEG.F	PRESSURE (PSIA) 0.	100.	200.	300.	400.	500.	600.	700.	800.	900.	1200.	1500.	1800.	2100.	2400.	2700.	3000.
600.	0.6536	0.6563	0.6598	0.6636	0.6676	0.6719	0.6764	0.6813	0.6863	0.6916	0.7074	0.7206	0.7291	0.7337	0.7359	0.7364	0.7361
650.	0.6751	0.6780	0.6810	0.6842	0.6876	0.6911	0.6948	0.6986	0.7025	0.7066	0.7187	0.7293	0.7374	0.7428	0.7462	0.7481	0.7489
700.	0.6961	0.6987	0.7013	0.7040	0.7068	0.7097	0.7126	0.7156	0.7186	0.7216	0.7306	0.7391	0.7466	0.7526	0.7569	0.7598	0.7616
750.	0.7162	0.7184	0.7207	0.7230	0.7253	0.7276	0.7299	0.7322	0.7345	0.7367	0.7431	0.7498	0.7567	0.7630	0.7680	0.7717	0.7741
800.	0.7337	0.7358	0.7379	0.7402	0.7424	0.7448	0.7472	0.7496	0.7520	0.7544	0.7616	0.7683	0.7742	0.7790	0.7826	0.7852	0.7871
850.	0.7515	0.7534	0.7554	0.7574	0.7594	0.7615	0.7636	0.7657	0.7678	0.7699	0.7762	0.7820	0.7872	0.7915	0.7949	0.7975	0.7994
900.	0.7688	0.7704	0.7721	0.7738	0.7757	0.7775	0.7794	0.7812	0.7831	0.7849	0.7904	0.7954	0.8000	0.8039	0.8070	0.8098	0.8115
950.	0.7851	0.7867	0.7882	0.7898	0.7914	0.7930	0.7947	0.7963	0.7979	0.7995	0.8041	0.8085	0.8125	0.8160	0.8190	0.8214	0.8234
1000.	0.8006	0.8023	0.8037	0.8051	0.8065	0.8079	0.8094	0.8108	0.8121	0.8135	0.8175	0.8213	0.8248	0.8279	0.8307	0.8330	0.8350
1050.	0.8160	0.8172	0.8185	0.8198	0.8210	0.8223	0.8235	0.8247	0.8259	0.8271	0.8305	0.8337	0.8368	0.8396	0.8421	0.8444	0.8464
1100.	0.8304	0.8315	0.8326	0.8338	0.8349	0.8360	0.8370	0.8381	0.8391	0.8402	0.8431	0.8459	0.8485	0.8510	0.8534	0.8556	0.8576
1150.	0.8441	0.8451	0.8461	0.8471	0.8481	0.8491	0.8500	0.8510	0.8519	0.8528	0.8553	0.8577	0.8600	0.8623	0.8645	0.8668	0.8685
1200.	0.8571	0.8580	0.8590	0.8599	0.8608	0.8615	0.8625	0.8633	0.8641	0.8649	0.8671	0.8692	0.8712	0.8733	0.8753	0.8773	0.8791
1250.	0.8694	0.8703	0.8711	0.8720	0.8728	0.8736	0.8743	0.8751	0.8758	0.8765	0.8785	0.8803	0.8822	0.8841	0.8860	0.8878	0.8895
1300.	0.8811	0.8819	0.8827	0.8834	0.8842	0.8849	0.8856	0.8863	0.8870	0.8876	0.8895	0.8912	0.8929	0.8947	0.8964	0.8981	0.8997
1350.	0.8920	0.8928	0.8935	0.8943	0.8950	0.8957	0.8964	0.8970	0.8977	0.8983	0.9001	0.9017	0.9034	0.9050	0.9066	0.9082	0.9097
1400.	0.9023	0.9030	0.9036	0.9045	0.9052	0.9058	0.9065	0.9072	0.9078	0.9084	0.9103	0.9120	0.9136	0.9152	0.9166	0.9181	0.9194
1450.	0.9119	0.9126	0.9133	0.9140	0.9147	0.9154	0.9161	0.9168	0.9175	0.9181	0.9201	0.9219	0.9235	0.9251	0.9264	0.9277	0.9288
1500.	0.9208	0.9215	0.9222	0.9229	0.9237	0.9244	0.9251	0.9259	0.9266	0.9273	0.9295	0.9315	0.9332	0.9348	0.9360	0.9371	0.9380
1550.	0.9290	0.9297	0.9305	0.9312	0.9320	0.9328	0.9336	0.9344	0.9352	0.9360	0.9385	0.9407	0.9427	0.9442	0.9454	0.9463	0.9470
1600.	0.9366	0.9373	0.9380	0.9389	0.9397	0.9406	0.9415	0.9424	0.9433	0.9443	0.9471	0.9497	0.9519	0.9535	0.9546	0.9553	0.9557

Table 94 (CONT'D 6)

TABLE 94. PHYSICAL PROPERTIES OF METHYLCYCLOHEXANE-TOLUENE-HYDROGEN MIXTURES — SHELL DEVELOPMENT COMPANY

	COMPONENT MCH	TOLUENE	HYDROGEN
MOLE FRACTION	0.20000	0.20000	0.60000
WEIGHT FRACTION	0.50000	0.46900	0.03100

GAS VISCOSITY (POUNDS/FOOT/HOUR)

TEMP DEG.F	PRESSURE (PSIA) 0.	100.	200.	300.	400.	500.	600.	700.	800.	900.	1200.	1500.	1800.	2100.	2400.	2700.	3000.
600.	0.0345	0.0347	0.0349	0.0352	0.0354	0.0357	0.0360	0.0363	0.0366	0.0369	0.0380	0.0393	0.0407	0.0422	0.0438	0.0454	0.0471
650.	0.0360	0.0362	0.0364	0.0366	0.0368	0.0371	0.0373	0.0376		0.0382	[illegible]	[illegible]	0.0416	0.0430	0.0444	0.0459	0.0475
700.	0.0375	0.0376	0.0378	0.0380	0.0382	0.0385	0.0387	0.0390		0.0395	0.0406	0.0415	0.0427	0.0439	0.0452	0.0466	0.0480
750.	0.0389	0.0391	0.0393	0.0394	0.0397	0.0399	0.0401	0.0403		0.0409	0.0417	0.0427	0.0438	0.0449	0.0461	0.0473	0.0486
800.	0.0404	0.0405	0.0407	0.0409	0.0411	0.0413	0.0415	0.0417	0.0420	0.0422	0.0430	0.0439	0.0449	0.0459	0.0470	0.0482	0.0494
850.	0.0419	0.0419	0.0421	0.0423	0.0425	0.0427	0.0429	0.0431	0.0433	0.0435	0.0443	0.0451	0.0460	0.0470	0.0480	0.0491	0.0502
900.	0.0432	0.0433	0.0435	0.0437	0.0439	0.0441	0.0443	0.0445	0.0447	0.0449	0.0456	0.0464	0.0472	0.0481	0.0491	0.0501	0.0511
950.	0.0447	0.0448	0.0449	0.0451	0.0453	0.0455	0.0456	0.0458	0.0460	0.0462	0.0469	0.0477	0.0484	0.0493	0.0502	0.0511	0.0521
1000.	0.0461	0.0462	0.0464	0.0465	0.0467	0.0468	0.0470	0.0472	0.0474	0.0476	0.0482	0.0489	0.0497	0.0505	0.0513	0.0522	0.0531
1050.	0.0475	0.0476	0.0478	0.0479	0.0481	0.0482	0.0484	0.0486	0.0488	0.0489	0.0496	0.0502	0.0509	0.0517	0.0525	0.0533	0.0541
1100.	0.0489	0.0490	0.0492	0.0493	0.0495	0.0496	0.0498	0.0499	0.0501	0.0503	0.0509	0.0515	0.0522	0.0529	0.0536	0.0544	0.0552
1150.	0.0502	0.0504	0.0505	0.0506	0.0508	0.0509	0.0511	0.0512	0.0514	0.0516	0.0521	0.0527	0.0534	0.0540	0.0547	0.0555	0.0563
1200.	0.0515	0.0516	0.0517	0.0518	0.0520	0.0521	0.0523	0.0524	0.0526	0.0528	0.0533	0.0538	0.0545	0.0551	0.0558	0.0565	0.0572
1250.	0.0527	0.0528	0.0529	0.0530	0.0532	0.0533	0.0535	0.0536	0.0538	0.0539	0.0544	0.0550	0.0556	0.0562	0.0568	0.0575	0.0582
1300.	0.0539	0.0540	0.0541	0.0542	0.0544	0.0545	0.0546	0.0548	0.0549	0.0551	0.0556	0.0561	0.0566	0.0572	0.0578	0.0585	0.0591
1350.	0.0550	0.0552	0.0553	0.0554	0.0555	0.0556	0.0558	0.0559	0.0561	0.0562	0.0567	0.0572	0.0577	0.0583	0.0589	0.0595	0.0601
1400.	0.0562	0.0563	0.0564	0.0565	0.0567	0.0568	0.0569	0.0571	0.0572	0.0573	0.0578	0.0583	0.0588	0.0593	0.0599	0.0605	0.0611
1450.	0.0574	0.0575	0.0576	0.0577	0.0578	0.0579	0.0581	0.0582	0.0583	0.0585	0.0589	0.0594	0.0598	0.0604	0.0609	0.0615	0.0621
1500.	0.0585	0.0586	0.0587	0.0588	0.0589	0.0591	0.0592	0.0593	0.0594	0.0596	0.0600	0.0604	0.0609	0.0614	0.0619	0.0625	0.0630
1550.	0.0596	0.0597	0.0598	0.0599	0.0600	0.0602	0.0603	0.0604	0.0605	0.0607	0.0611	0.0615	0.0619	0.0624	0.0629	0.0635	0.0640
1600.	0.0607	0.0608	0.0609	0.0610	0.0611	0.0613	0.0614	0.0615	0.0616	0.0617	0.0621	0.0625	0.0630	0.0634	0.0639	0.0644	0.0650

GAS THERMAL CONDUCTIVITY (BTU/FOOT/HOUR/DEG.F)

TEMP DEG.F	PRESSURE (PSIA) 0.	100.	200.	300.	400.	500.	600.	700.	800.	900.	1200.	1500.	1800.	2100.	2400.	2700.	3000.
600.	0.0487	0.0489	0.0490	0.0485	0.0487	0.0489	0.0491	0.0493	0.0496	0.0498	0.0574	0.	0.	0.	0.	0.	0.
650.	0.0511	0.0512	0.0514	0.0509	0.0510	0.0512	0.0514	0.0516	0.0518	0.0520	0.0597	0.	0.	0.	0.	0.	0.
700.	0.0534	0.0535	0.0537	0.0532	0.0533	0.0535	0.0537	0.0539	0.0541	0.0543	0.0620	0.	0.	0.	0.	0.	0.
750.	0.0558	0.0559	0.0560	0.0555	0.0557	0.0558	0.0560	0.0562	0.0564	0.0566	0.0643	0.	0.	0.	0.	0.	0.
800.	0.0581	0.0582	0.0584	0.0578	0.0580	0.0581	0.0583	0.0585	0.0586	0.0588	0.0666	0.	0.	0.	0.	0.	0.
850.	0.0605	0.0606	0.0607	0.0601	0.0603	0.0605	0.0606	0.0608	0.0609	0.0611	0.0689	0.	0.	0.	0.	0.	0.
900.	0.0628	0.0629	0.0631	0.0625	0.0626	0.0628	0.0629	0.0631	0.0633	0.0634	0.0712	0.	0.	0.	0.	0.	0.
950.	0.0652	0.0653	0.0654	0.0648	0.0650	0.0651	0.0653	0.0654	0.0656	0.0657	0.0736	0.	0.	0.	0.	0.	0.
1000.	0.0676	0.0677	0.0678	0.0672	0.0674	0.0675	0.0676	0.0678	0.0679	0.0681	0.0759	0.	0.	0.	0.	0.	0.
1050.	0.0700	0.0701	0.0702	0.0696	0.0697	0.0699	0.0700	0.0701	0.0703	0.0704	0.0783	0.	0.	0.	0.	0.	0.
1100.	0.0724	0.0725	0.0726	0.0720	0.0721	0.0722	0.0724	0.0725	0.0726	0.0728	0.0807	0.	0.	0.	0.	0.	0.
1150.	0.0747	0.0748	0.0749	0.0743	0.0744	0.0745	0.0746	0.0748	0.0749	0.0750	0.0829	0.	0.	0.	0.	0.	0.
1200.	0.0768	0.0769	0.0770	0.0764	0.0766	0.0767	0.0768	0.0769	0.0770	0.0772	0.0851	0.	0.	0.	0.	0.	0.
1250.	0.0790	0.0791	0.0792	0.0786	0.0787	0.0788	0.0789	0.0791	0.0792	0.0793	0.0872	0.	0.	0.	0.	0.	0.
1300.	0.0812	0.0813	0.0813	0.0807	0.0808	0.0809	0.08[illegible]	0.0812	0.0813	0.0814	0.0894	0.	0.	0.	0.	0.	0.
1350.	0.0833	0.0834	0.0835	0.0829	0.0830	0.0831	0.0832	0.0833	0.0834	0.0835	0.0915	0.	0.	0.	0.	0.	0.
1400.	0.0854	0.0855	0.0856	0.0849	0.0850	0.0852	0.0853	0.0854	0.0855	0.0856	0.0936	0.	0.	0.	0.	0.	0.
1450.	0.0875	0.0876	0.0877	0.0870	0.0871	0.0872	0.0873	0.0874	0.0875	0.0876	0.0956	0.	0.	0.	0.	0.	0.
1500.	0.0895	0.0896	0.0897	0.0891	0.0892	0.0893	0.0894	0.0895	0.0896	0.0897	0.0977	0.	0.	0.	0.	0.	0.
1550.	0.0916	0.0917	0.0918	0.0911	0.0912	0.0913	0.0914	0.0915	0.0916	0.0917	0.0997	0.	0.	0.	0.	0.	0.
1600.	0.0936	0.0937	0.0938	0.0931	0.0932	0.0933	0.0934	0.0935	0.0936	0.0937	0.1017	0.	0.	0.	0.	0.	0.

Table 94 (CONT'D 7)

TABLE 94. PHYSICAL PROPERTIES OF METHYLCYCLOHEXANE-TOLUENE-HYDROGEN MIXTURES — SHELL DEVELOPMENT COMPANY

	COMPONENT MCH	TOLUENE	HYDROGEN
MOLE FRACTION	0.20000	0.20000	0.60000
WEIGHT FRACTION	0.50000	0.44900	0.03100

GAS DENSITY (POUNDS/CUBIC FOOT)

TEMP DEG.F	PRESSURE (PSIA) 0.	100.	200.	300.	400.	500.	600.	700.	800.	900.	1200.	1500.	1800.	2100.	2400.	2700.	3000.
600.	0.	0.347	0.699	1.054	1.413	1.775	2.139	2.506	2.876	3.247	4.365	5.481	6.583	7.660	8.701	9.700	10.652
650.	0.	0.331	0.666	1.003	1.343	1.685	2.029	2.375	2.722	3.070	4.118	5.161	6.191	7.199	8.177	9.120	10.024
700.	0.	0.317	0.636	0.957	1.280	1.605	1.931	2.258	2.586	2.915	3.901	4.882	5.851	6.799	7.722	8.615	9.476
750.	0.	0.303	0.609	0.915	1.223	1.533	1.843	2.153	2.465	2.776	3.710	4.637	5.551	6.448	7.323	8.171	8.992
800.	0.	0.291	0.584	0.877	1.172	1.467	1.763	2.059	2.355	2.651	3.538	4.418	5.286	6.137	6.969	7.778	8.561
850.	0.	0.280	0.561	0.842	1.124	1.407	1.690	1.973	2.256	2.539	3.384	4.222	5.048	5.859	6.652	7.425	8.175
900.	0.	0.269	0.540	0.810	1.081	1.352	1.623	1.894	2.165	2.436	3.244	4.045	4.834	5.609	6.367	7.107	7.827
950.	0.	0.260	0.520	0.780	1.041	1.302	1.562	1.822	2.082	2.342	3.117	3.883	4.639	5.382	6.109	6.819	7.511
1000.	0.	0.251	0.502	0.753	1.004	1.255	1.506	1.756	2.006	2.255	3.000	3.736	4.461	5.174	5.873	6.556	7.223
1050.	0.	0.242	0.485	0.727	0.970	1.212	1.453	1.695	1.935	2.176	2.892	3.600	4.298	4.984	5.657	6.315	6.958
1100.	0.	0.235	0.469	0.703	0.938	1.171	1.405	1.638	1.870	2.102	2.792	3.475	4.147	4.809	5.458	6.093	6.715
1150.	0.	0.227	0.454	0.681	0.908	1.134	1.359	1.584	1.809	2.033	2.700	3.359	4.008	4.647	5.274	5.888	6.489
1200.	0.	0.220	0.440	0.660	0.880	1.099	1.317	1.535	1.752	1.969	2.614	3.251	3.879	4.497	5.103	5.698	6.280
1250.	0.	0.214	0.427	0.641	0.853	1.066	1.277	1.488	1.699	1.909	2.533	3.150	3.758	4.357	4.944	5.521	6.086
1300.	0.	0.208	0.415	0.622	0.829	1.035	1.240	1.445	1.649	1.852	2.458	3.056	3.646	4.226	4.796	5.355	5.904
1350.	0.	0.202	0.404	0.605	0.805	1.005	1.205	1.404	1.602	1.799	2.387	2.968	3.540	4.103	4.657	5.200	5.734
1400.	0.	0.197	0.393	0.588	0.783	0.978	1.172	1.365	1.558	1.750	2.321	2.885	3.441	3.988	4.526	5.055	5.574
1450.	0.	0.191	0.382	0.573	0.763	0.952	1.141	1.329	1.516	1.703	2.258	2.807	3.347	3.880	4.403	4.918	5.423
1500.	0.	0.186	0.372	0.558	0.743	0.927	1.111	.294	1.476	1.658	2.199	2.733	3.259	3.778	4.288	4.789	5.281
1550.	0.	0.182	0.363	0.544	0.724	0.904	1.083	1.261	1.439	1.616	2.143	2.663	3.176	3.681	4.178	4.667	5.147
1600.	0.	0.177	0.354	0.531	0.7[illegible]	0.882	1.056	1.230	1.403	1.576	2.090	2.597	3.097	3.590	4.075	4.551	5.020

GAS COMPRESSIBILITY FACTOR

TEMP DEG.F	PRESSURE (PSIA) 0.	100.	200.	300.	400.	500.	600.	700.	800.	900.	1200.	1500.	1800.	2100.	2400.	2700.	3000.
600.	0.	0.9941	0.9884	0.9830	0.9778	0.9730	0.9680	0.9645	0.9607	0.9573	0.9494	0.9451	0.9442	0.9468	0.9526	0.9613	0.9726
650.	0.	0.9953	0.9907	0.9864	0.9823	0.9786	0.9752	0.9720	0.9692	0.9667	0.9611	0.9585	0.9588	0.9621	0.9680	0.9764	0.9870
700.	0.	0.9962	0.9926	0.9892	0.9861	0.9832	0.9806	0.9782	0.9762	0.9744	0.9707	0.9695	0.9709	0.9747	0.9808	0.9890	0.9991
750.	0.	0.9971	0.9942	0.9916	0.9892	0.9870	0.9851	0.9834	0.9820	0.9808	0.9786	0.9787	0.9809	0.9852	0.9915	0.9996	1.0094
800.	0.	0.9977	0.9956	0.9938	0.9918	0.9903	0.9889	0.9878	0.9868	0.9861	0.9853	0.9863	0.9893	0.9941	1.0005	1.0085	1.0180
850.	0.	0.9983	0.9967	0.9953	0.9940	0.9930	0.9921	0.9914	0.9909	0.9908	0.9909	0.9928	0.9963	1.0015	1.0081	1.0161	1.0254
900.	0.	0.9988	0.9977	0.9967	0.9959	0.9953	0.9948	0.9945	0.9944	0.9944	0.9956	0.9982	1.0023	1.0077	1.0145	1.0225	1.0316
950.	0.	0.9992	0.9985	0.9979	0.9975	0.9972	0.9971	0.9972	0.9973	0.9977	0.9996	1.0028	1.0073	1.0130	1.0199	1.0279	1.0369
1000.	0.	0.9996	0.9992	0.9990	0.9989	0.9989	0.9991	0.9994	0.9999	1.0004	1.0030	1.0067	1.0116	1.0175	1.0245	1.0325	1.0413
1050.	0.	0.9999	0.9998	0.9999	1.0001	1.0004	1.0008	1.0013	1.0020	1.0028	1.0059	1.0100	1.0152	1.0214	1.0284	1.0364	1.0451
1100.	0.	1.0002	1.0004	1.0007	1.0011	1.0016	1.0022	1.0030	1.0039	1.0048	1.0084	1.0129	1.0183	1.0246	1.0318	1.0397	1.0483
1150.	0.	1.0004	1.0008	1.0013	1.0020	1.0027	1.0035	1.0044	1.0054	1.0066	1.0105	1.0153	1.0210	1.0274	1.0346	1.0425	1.0510
1200.	0.	1.0006	1.0012	1.0019	1.0027	1.0036	1.0046	1.0056	1.0068	1.0081	1.0124	1.0174	1.0232	1.0298	1.0370	1.0448	1.0533
1250.	0.	1.0008	1.0016	1.0024	1.0034	1.0044	1.0055	1.0067	1.0080	1.0094	1.0139	1.0192	1.0252	1.0319	1.0390	1.0468	1.0552
1300.	0.	1.0010	1.0019	1.0029	1.0039	1.0051	1.0063	1.0076	1.0090	1.0105	1.0153	1.0208	1.0268	1.0335	1.0408	1.0485	1.0568
1350.	0.	1.0011	1.0021	1.0032	1.0044	1.0057	1.0070	1.0084	1.0099	1.0114	1.0165	1.0221	1.0283	1.0350	1.0422	1.0499	1.0581
1400.	0.	1.0012	1.0024	1.0036	1.0049	1.0062	1.0076	1.0091	1.0107	1.0123	1.0175	1.0232	1.0295	1.0362	1.0434	1.0511	1.0592
1450.	0.	1.0013	1.0025	1.0039	1.0052	1.0067	1.0081	1.0097	1.0113	1.0130	1.0183	1.0242	1.0305	1.0373	1.0445	1.0521	1.0601
1500.	0.	1.0014	1.0027	1.0041	1.0055	1.0070	1.0086	1.0102	1.0119	1.0136	1.0191	1.0250	1.0314	1.0381	1.0453	1.0529	1.0608
1550.	0.	1.0015	1.0029	1.0043	1.0058	1.0074	1.0090	1.0106	1.0124	1.0141	1.0197	1.0257	1.0321	1.0389	1.0460	1.0535	1.0613
1600.	0.	1.0015	1.0030	1.0045	1.0061	1.0077	1.0093	1.0110	1.0128	1.0146	1.0202	1.0263	1.0327	1.0395	1.0466	1.0540	1.0618

Table 94 (CONT'D 8)

TABLE 94. PHYSICAL PROPERTIES OF METHYLCYCLOHEXANE-TOLUENE-HYDROGEN MIXTURES — SHELL DEVELOPMENT COMPANY

	COMPONENT MCH	TOLUENE	HYDROGEN
MOLE FRACTION	0.20000	0.20000	0.60000
WEIGHT FRACTION	0.50000	0.44900	0.05100

GAS HEAT CONTENT (BTU/POUND)

TEMP DEG.F	PRESSURE (PSIA) 0.	100.	200.	300.	400.	500.	600.	700.	800.	900.	1200.	1500.	1800.	2100.	2400.	2700.	3000.
600.	310.	309.	308.	307.	306.	305.	304.	303.	302.	301.	298.	296.	293.	291.	289.	287.	286.
650.	344.	343.	342.	341.	340.	339.	338.	337.	337.	336.	333.	331.	329.	327.	325.	323.	322.
700.	379.	378.	377.	376.	375.	374.	374.	373.	372.	371.	369.	367.	365.	363.	361.	360.	359.
750.	414.	414.	413.	412.	411.	410.	410.	409.	408.	407.	405.	404.	402.	400.	399.	397.	396.
800.	451.	450.	449.	449.	448.	447.	447.	446.	445.	445.	443.	441.	439.	438.	437.	435.	434.
850.	488.	488.	487.	486.	486.	485.	484.	484.	483.	482.	481.	479.	478.	476.	475.	474.	473.
900.	526.	526.	525.	524.	524.	523.	523.	522.	522.	521.	519.	518.	517.	516.	514.	514.	513.
950.	565.	565.	564.	563.	563.	562.	562.	561.	561.	560.	559.	558.	556.	555.	554.	554.	553.
1000.	605.	604.	604.	603.	603.	602.	602.	601.	601.	600.	599.	598.	597.	596.	595.	594.	593.
1050.	645.	644.	644.	644.	643.	643.	642.	642.	641.	641.	640.	639.	638.	637.	636.	635.	635.
1100.	686.	685.	685.	685.	684.	684.	683.	683.	683.	682.	681.	680.	679.	679.	678.	677.	677.
1150.	727.	727.	727.	726.	724.	726.	725.	725.	724.	724.	723.	722.	721.	721.	720.	720.	[illegible]
1200.	770.	769.	769.	769.	768.	768.	768.	767.	767.	767.	766.	765.	764.	764.	763.	762.	[illegible]
1250.	812.	812.	812.	811.	811.	811.	810.	810.	810.	810.	809.	808.	807.	807.	806.	806.	806.
1300.	856.	855.	855.	855.	855.	854.	854.	854.	853.	853.	852.	852.	851.	851.	850.	850.	850.
1350.	900.	899.	899.	899.	898.	898.	898.	898.	897.	897.	897.	896.	895.	895.	895.	894.	894.
1400.	944.	944.	943.	943.	943.	943.	942.	942.	942.	942.	941.	941.	940.	940.	939.	939.	939.
1450.	989.	988.	988.	988.	988.	988.	987.	987.	987.	987.	986.	986.	985.	985.	985.	984.	984.
1500.	1034.	1034.	1034.	1033.	1033.	1033.	1033.	1033.	1032.	1032.	1032.	1032.	1031.	1031.	1031.	1030.	1030.
1550.	1080.	1079.	1079.	1079.	1079.	1079.	1079.	1078.	1078.	1078.	1078.	1078.	1077.	1077.	1077.	1077.	1076.
1600.	1126.	1125.	1125.	1125.	1125.	1125.	1125.	1124.	1124.	1124.	1124.	1124.	1124.	1123.	1123.	1123.	1123.

GAS HEAT CAPACITY (BTU/POUND/DEG.F)

TEMP DEG.F	PRESSURE (PSIA) 0.	100.	200.	300.	400.	500.	600.	700.	800.	900.	1200.	1500.	1800.	2100.	2400.	2700.	3000.
600.	0.6640	0.6662	0.6684	0.6704	0.6728	0.6750	0.6773	0.6795	0.6817	0.6839	0.6904	0.6965	0.7020	0.7068	0.7109	0.7144	0.7171
650.	0.6840	0.6859	0.6878	0.6897	0.6916	0.6936	0.6955	0.6974	0.6993	0.7012	0.7067	0.7118	0.7166	0.7208	0.7245	0.7276	0.7303
700.	0.7036	0.7047	0.7064	0.7080	0.7097	0.7114	0.7130	0.7147	0.7163	0.7179	0.7225	0.7269	0.7310	0.7346	0.7379	0.7408	0.7433
750.	0.7212	0.7227	0.7241	0.7254	0.7271	0.7285	0.7299	0.7313	0.7327	0.7340	0.7380	0.7417	0.7451	0.7483	0.7513	0.7539	0.7563
800.	0.7371	0.7385	0.7396	0.7413	0.7427	0.7441	0.7454	0.7468	0.7481	0.7494	0.7533	0.7569	0.7602	0.7632	0.7660	0.7684	0.7706
850.	0.7534	0.7546	0.7559	0.7571	0.7584	0.7596	0.7609	0.7621	0.7633	0.7645	0.7679	0.7711	0.7741	0.7769	0.7794	0.7816	0.7836
900.	0.7690	0.7701	0.7713	0.7724	0.7735	0.7746	0.7757	0.7768	0.7779	0.7790	0.7820	0.7849	0.7876	0.7901	0.7923	0.7944	0.7962
950.	0.7840	0.7850	0.7860	0.7871	0.7881	0.7891	0.7901	0.7910	0.7920	0.7929	0.7957	0.7983	0.8007	0.8029	0.8049	0.8068	0.8085
1000.	0.7984	0.7993	0.8002	0.8011	0.8020	0.8029	0.8038	0.8047	0.8056	0.8064	0.8088	0.8111	0.8133	0.8153	0.8172	0.8189	0.8204
1050.	0.8121	0.8130	0.8138	0.8146	0.8155	0.8163	0.8170	0.8178	0.8186	0.8193	0.8215	0.8238	0.8255	0.8273	0.8290	0.8305	0.8320
1100.	0.8252	0.8261	0.8268	0.8276	0.8283	0.8290	0.8297	0.8304	0.8311	0.8318	0.8337	0.8356	0.8373	0.8389	0.8404	0.8419	0.8432
1150.	0.8378	0.8385	0.8392	0.8399	0.8405	0.8412	0.8418	0.8425	0.8431	0.8437	0.8454	0.8471	0.8486	0.8501	0.8515	0.8528	0.8540
1200.	0.8498	0.8504	0.8510	0.8516	0.8522	0.8528	0.8534	0.8540	0.8545	0.8551	0.8567	0.8582	0.8596	0.8609	0.8622	0.8634	0.8645
1250.	0.8611	0.8617	0.8622	0.8628	0.8633	0.8639	0.8644	0.8649	0.8655	0.8660	0.8675	0.8689	0.8701	0.8713	0.8725	0.8736	0.8747
1300.	0.8718	0.8723	0.8729	0.8734	0.8739	0.8744	0.8749	0.8754	0.8759	0.8763	0.8777	0.8789	0.8802	0.8813	0.8824	0.8835	0.8845
1350.	0.8819	0.8824	0.8829	0.8834	0.8839	0.8843	0.8848	0.8853	0.8857	0.8862	0.8874	0.8887	0.8898	0.8909	0.8920	0.8929	0.8939
1400.	0.8913	0.8918	0.8923	0.8928	0.8933	0.8937	0.8942	0.8946	0.8951	0.8955	0.8967	0.8979	0.8990	0.9001	0.9011	0.9021	0.9030
1450.	0.9002	0.9007	0.9012	0.9016	0.9021	0.9025	0.9030	0.9034	0.9039	0.9043	0.9053	0.9067	0.9078	0.9089	0.9099	0.9108	0.9117
1500.	0.9084	0.9089	0.9094	0.9099	0.9103	0.9108	0.9113	0.9117	0.9122	0.9126	0.9139	0.9151	0.9162	0.9173	0.9183	0.9192	0.9200
1550.	0.9161	0.9166	0.9171	0.9175	0.9180	0.9185	0.9190	0.9194	0.9199	0.9204	0.9217	0.9230	0.9242	0.9253	0.9263	0.9272	0.9280
1600.	0.9231	0.9236	0.9241	0.9246	0.9251	0.9256	0.9261	0.9266	0.9271	0.9276	0.9291	0.9304	0.9317	0.9328	0.9339	0.9348	0.9356

Table 94 (CONT'D 9)

TABLE 94. PHYSICAL PROPERTIES OF METHYLCYCLOHEXANE-TOLUENE-HYDROGEN MIXTURES — SHELL DEVELOPMENT COMPANY

	COMPONENT		
	MCH	TOLUENE	HYDROGEN
MOLE FRACTION	0.07700	0.23100	0.69200
WEIGHT FRACTION	0.25000	0.70400	0.04600

GAS VISCOSITY (POUNDS/FOOT/HOUR)

TEMP DEG.F	PRESSURE (PSIA)															
	0.	100.	200.	300.	400.	500.	600.	700.	800.	900.	1200.	1500.	1800.	2100.	2400.	2700.	3000.
600.	0.0356	0.0357	0.0358	0.0360	0.0362	0.0363	0.0365	0.0367	0.0369	0.0372	0.0379	0.0386	0.0393	0.0404	0.0413	[illegible]	[illegible]
650.	0.0370	0.0372	0.0373	0.0374	0.0376	0.0378	0.0380	0.0381	0.0383	0.0385	0.0392	0.0399	0.0407	0.0415	0.0424	[illegible]	[illegible]
700.	0.0386	0.0386	0.0389	0.0390	0.0390	0.0392	0.0394	0.0395	0.0397	0.0399	0.0405	0.0412	0.0419	0.0427	0.0435	[illegible]	[illegible]
750.	0.0400	0.0401	0.0402	0.0403	0.0405	0.0406	0.0408	0.0410	0.0411	0.0413	0.0419	0.0425	0.0432	0.0439	0.0446	[illegible]	[illegible]
800.	0.0414	0.0415	0.0416	0.0418	0.0419	0.0421	0.0422	0.0424	0.0425	0.0427	0.0433	0.0438	0.0444	0.0451	0.0458	[illegible]	[illegible]
850.	0.0429	0.0430	0.0431	0.0432	0.0433	0.0435	0.0436	0.0438	0.0439	0.0441	0.0446	0.0451	0.0457	0.0463	0.0470	[illegible]	[illegible]
900.	0.0443	0.0444	0.0445	0.0446	0.0448	0.0449	0.0450	0.0452	0.0453	0.0455	0.0459	0.0464	0.0470	0.0476	0.0482	[illegible]	[illegible]
950.	0.0457	0.0458	0.0459	0.0461	0.0462	0.0463	0.0464	0.0466	0.0467	0.0468	0.0473	0.0478	0.0483	0.0489	0.0494	[illegible]	[illegible]
1000.	0.0472	0.0473	0.0474	0.0475	0.0476	0.0477	0.0478	0.0480	0.0481	0.0482	0.0487	0.0491	0.0496	0.0501	0.0506	[illegible]	[illegible]
1050.	0.0484	0.0487	0.0488	0.0489	0.0490	0.0491	0.0492	0.0493	0.0495	0.0496	0.0500	0.0505	0.0509	0.0514	0.0518	[illegible]	[illegible]
1100.	0.0500	0.0501	0.0502	0.0503	0.0504	0.0505	0.0506	0.0507	0.0509	0.0510	0.0514	0.0518	0.0522	0.0527	0.0531	[illegible]	[illegible]
1150.	0.0514	0.0515	0.0516	0.0517	0.0518	0.0519	0.0520	0.0521	0.0522	0.0523	0.0527	0.0531	0.0535	0.0540	0.0544	[illegible]	[illegible]
1200.	0.0528	0.0527	0.0528	0.0529	0.0530	0.0531	0.0532	0.0533	0.0534	0.0535	0.0539	0.0543	0.0547	0.0551	0.0555	[illegible]	[illegible]
1250.	0.0538	0.0539	0.0540	0.0541	0.0542	0.0543	0.0544	0.0545	0.0546	0.0547	0.0551	0.0554	0.0558	0.0562	0.0567	[illegible]	[illegible]
1300.	0.0551	0.0551	0.0552	0.0553	0.0554	0.0555	0.0556	0.0557	0.0558	0.0559	0.0562	0.0566	0.0570	0.0574	0.0578	[illegible]	[illegible]
1350.	0.0563	0.0563	0.0564	0.0565	0.0566	0.0567	0.0568	0.0569	0.0570	0.0571	0.0574	0.0577	0.0581	0.0585	0.0589	[illegible]	[illegible]
1400.	0.0574	0.0575	0.0576	0.0577	0.0578	0.0578	0.0579	0.0580	0.0581	0.0582	0.0585	0.0589	0.0592	0.0596	0.0600	[illegible]	[illegible]
1450.	0.0584	0.0587	0.0587	0.0588	0.0589	0.0590	0.0591	0.0592	0.0593	0.0594	0.0597	0.0600	0.0603	0.0607	0.0610	[illegible]	[illegible]
1500.	0.0597	0.0598	0.0599	0.0600	0.0601	0.0601	0.0602	0.0603	0.0604	0.0605	0.0608	0.0611	0.0614	0.0618	0.0621	[illegible]	[illegible]
1550.	0.0606	0.0610	0.0610	0.0611	0.0612	0.0613	0.0613	0.0614	0.0615	0.0616	0.0619	0.0622	0.0625	0.0628	0.0632	[illegible]	[illegible]
1600.	0.0620	0.0621	0.0621	0.0622	0.0623	0.0624	0.0625	0.0625	0.0626	0.0627	0.0630	0.0633	0.0636	0.0639	0.0642	[illegible]	[illegible]

GAS THERMAL CONDUCTIVITY (BTU/FOOT/HOUR/DEG.F)

TEMP DEG.F	PRESSURE (PSIA)															
	0.	100.	200.	300.	400.	500.	600.	700.	800.	900.	1200.	1500.	1800.	2100.	2400.	2700.	3000.
600.	0.0571	0.0577	0.0579	0.0573	0.0575	0.0576	0.0578	0.0580	0.0582	0.0584	0.0666	0.	0.	0.	0.	0.	0.
650.	0.0601	0.0602	0.0604	0.0598	0.0599	0.0601	0.0603	0.0604	0.0606	0.0608	0.0690	0.	0.	0.	0.	0.	0.
700.	0.0626	0.0627	0.0628	0.0622	0.0624	0.0625	0.0627	0.0628	0.0630	0.0632	0.0714	0.	0.	0.	0.	0.	0.
750.	0.0650	0.0652	0.0653	0.0647	0.0648	0.0650	0.0651	0.0653	0.0654	0.0656	0.0739	0.	0.	0.	0.	0.	0.
800.	0.0673	0.0674	0.0677	0.0671	0.0672	0.0674	0.0675	0.0677	0.0678	0.0680	0.0763	0.	0.	0.	0.	0.	0.
850.	0.0700	0.0701	0.0702	0.0695	0.0697	0.0698	0.0700	0.0701	0.0703	0.0704	0.0787	0.	0.	0.	0.	0.	0.
900.	0.0724	0.0725	0.0727	0.0720	0.0721	0.0723	0.0724	0.0725	0.0727	0.0728	0.0812	0.	0.	0.	0.	0.	0.
950.	0.0749	0.0750	0.0751	0.0745	0.0746	0.0747	0.0749	0.0750	0.0751	0.0753	0.0836	0.	0.	0.	0.	0.	0.
1000.	0.0774	0.0775	0.0776	0.0770	0.0771	0.0772	0.0773	0.0774	0.0776	0.0777	0.0861	0.	0.	0.	0.	0.	0.
1050.	0.0799	0.080	0.0801	0.0794	0.0796	0.0797	0.0798	0.0799	0.0800	0.0801	0.0885	0.	0.	0.	0.	0.	0.
1100.	0.0824	0.0825	0.0826	0.0819	0.0820	0.0821	0.0823	0.0824	0.0825	0.0826	0.0910	0.	0.	0.	0.	0.	0.
1150.	0.0848	0.0849	0.0850	0.0844	0.0845	0.0846	0.0847	0.0848	0.0849	0.0850	0.0934	0.	0.	0.	0.	0.	0.
1200.	0.0871	0.0872	0.0873	0.0868	0.0867	0.0868	0.0870	0.0871	0.0872	0.0873	0.0957	0.	0.	0.	0.	0.	0.
1250.	0.0894	0.0895	0.0896	0.0889	0.0890	0.0891	0.0892	0.0893	0.0894	0.0895	0.0980	0.	0.	0.	0.	0.	0.
1300.	0.0917	0.0917	0.0918	0.0912	0.0913	0.0914	0.0915	0.0916	0.0917	0.0918	0.1002	0.	0.	0.	0.	0.	0.
1350.	0.0939	0.0940	0.0941	0.0934	0.0935	0.0936	0.0937	0.0938	0.0939	0.0940	0.1025	0.	0.	0.	0.	0.	0.
1400.	0.0961	0.0962	0.0963	0.0956	0.0957	0.0958	0.0959	0.0960	0.0961	0.0962	0.1047	0.	0.	0.	0.	0.	0.
1450.	0.0983	0.0984	0.0985	0.0978	0.0979	0.0980	0.0981	0.0982	0.0983	0.0984	0.1069	0.	0.	0.	0.	0.	0.
1500.	0.1005	0.1006	0.1007	0.1000	0.1001	0.1002	0.1003	0.1004	0.1005	0.1090	0.	0.	0.	0.	0.	0.	0.
1550.	0.1027	0.1028	0.1029	0.1022	0.1023	0.1023	0.1024	0.1025	0.1026	0.1027	0.1112	0.	0.	0.	0.	0.	0.
1600.	0.1049	0.1050	0.1050	0.1043	0.1044	0.1045	0.1046	0.1047	0.1048	0.1048	0.1134	0.	0.	0.	0.	0.	0.

Table 94 (CONT'D 10)

TABLE 94. PHYSICAL PROPERTIES OF METHYLCYCLOHEXANE-TOLUENE-HYDROGEN MIXTURES — SHELL DEVELOPMENT COMPANY

	COMPONENT MCH	TOLUENE	HYDROGEN
MOLE FRACTION	0.07700	0.23100	0.69200
WEIGHT FRACTION	0.25000	0.70400	0.04600

GAS DENSITY (POUNDS/CUBIC FOOT)

TEMP DEG.F	0.	100.	200.	300.	400.	500.	600.	700.	800.	900.	1200.	1500.	1800.	2100.	2400.	2700.	3000.
							PRESSURE (PSIA)										
600.	0.	0.264	0.534	0.807	1.071	1.341	1.611	1.881	2.152	2.422	3.230	4.032	4.823	5.599	6.357	7.095	7.811
650.	0.	0.254	0.507	0.765	1.021	1.277	1.533	1.789	2.045	2.301	3.066	3.823	4.570	5.309	6.020	6.720	7.400
700.	0.	0.243	0.487	0.731	0.975	1.219	1.463	1.706	1.950	2.193	2.919	3.637	4.345	5.041	5.722	6.387	7.035
750.	0.	0.233	0.466	0.699	0.933	1.166	1.399	1.631	1.864	2.095	2.788	3.470	4.144	4.806	5.455	6.090	6.709
800.	0.	0.224	0.447	0.671	0.894	1.118	1.341	1.563	1.785	2.006	2.667	3.319	3.963	4.595	5.215	5.822	6.415
850.	0.	0.215	0.430	0.645	0.859	1.073	1.287	1.500	1.713	1.925	2.558	3.182	3.798	4.404	4.998	5.580	6.149
900.	0.	0.207	0.414	0.621	0.827	1.033	1.238	1.443	1.647	1.851	2.458	3.057	3.648	4.229	4.800	5.359	5.906
950.	0.	0.200	0.399	0.598	0.797	0.995	1.193	1.390	1.587	1.783	2.366	2.942	3.510	4.069	4.618	5.156	5.684
1000.	0.	0.193	0.385	0.577	0.769	0.960	1.151	1.341	1.530	1.719	2.281	2.836	3.383	3.922	4.451	4.970	5.479
1050.	0.	0.186	0.372	0.558	0.743	0.928	1.112	1.295	1.478	1.660	2.203	2.738	3.266	3.784	4.296	4.798	5.290
1100.	0.	0.180	0.360	0.540	0.719	0.898	1.075	1.253	1.430	1.606	2.130	2.647	3.157	3.659	4.153	4.638	5.115
1150.	0.	0.175	0.349	0.523	0.696	0.869	1.041	1.213	1.384	1.555	2.062	2.562	3.056	3.542	4.020	4.490	4.951
1200.	0.	0.170	0.339	0.507	0.675	0.843	1.010	1.176	1.342	1.507	1.998	2.483	2.961	3.432	3.895	4.351	4.799
1250.	0.	0.165	0.329	0.492	0.655	0.818	0.980	1.141	1.302	1.462	1.938	2.409	2.874	3.329	3.779	4.222	4.656
1300.	0.	0.160	0.319	0.478	0.636	0.794	0.952	1.108	1.264	1.420	1.882	2.339	2.789	3.233	3.670	4.100	4.523
1350.	0.	0.155	0.310	0.465	0.619	0.772	0.925	1.077	1.229	1.380	1.830	2.273	2.711	3.142	3.567	3.985	4.397
1400.	0.	0.151	0.302	0.453	0.604	0.751	0.900	1.048	1.196	1.342	1.780	2.211	2.637	3.057	3.470	3.878	4.278
1450.	0.	0.147	0.294	0.440	0.586	0.731	0.876	1.020	1.164	1.307	1.733	2.153	2.568	2.976	3.377	3.776	4.166
1500.	0.	0.144	0.287	0.430	0.571	0.713	0.854	0.994	1.134	1.273	1.688	2.098	2.502	2.900	3.293	3.680	4.061
1550.	0.	0.140	0.279	0.418	0.557	0.695	0.832	0.969	1.106	1.242	1.646	2.045	2.439	2.828	3.211	3.588	3.960
1600.	0.	0.137	0.273	0.409	0.543	0.678	0.812	0.946	1.079	1.211	1.606	1.995	2.380	2.759	3.133	3.502	3.865

GAS COMPRESSIBILITY FACTOR

TEMP DEG.F	0.	100.	200.	300.	400.	500.	600.	700.	800.	900.	1200.	1500.	1800.	2100.	2400.	2700.	3000.
							PRESSURE (PSIA)										
600.	0.	0.9980	0.9961	0.9943	0.9928	0.9915	0.9903	0.9894	0.9886	0.9881	0.9878	0.9892	0.9924	0.9974	1.0039	1.0119	1.0213
650.	0.	0.9984	0.9973	0.9959	0.9953	0.9945	0.9939	0.9934	0.9932	0.9931	0.9939	0.9963	1.0002	1.0056	1.0123	1.0201	1.0295
700.	0.	0.9987	0.9984	0.9979	0.9978	0.9970	0.9968	0.9968	0.9969	0.9972	0.9990	1.0021	1.0066	1.0123	1.0191	1.0271	1.0361
750.	0.	0.9988	0.9988	0.9980	0.9980	0.9980	0.9982	0.9985	1.0000	1.0006	1.0031	1.0069	1.0118	1.0178	1.0247	1.0327	1.0416
800.	0.	1.0000	1.0000	1.0001	1.0003	1.0007	1.0012	1.0018	1.0025	1.0034	1.0066	1.0109	1.0161	1.0223	1.0294	1.0373	1.0460
850.	0.	1.0003	1.0006	1.0010	1.0015	1.0021	1.0029	1.0037	1.0046	1.0057	1.0094	1.0141	1.0196	1.0260	1.0332	1.0411	1.0497
900.	0.	1.0006	1.0011	1.0017	1.0025	1.0033	1.0042	1.0053	1.0064	1.0076	1.0118	1.0168	1.0226	1.0291	1.0363	1.0441	1.0526
950.	0.	1.0008	1.0015	1.0024	1.0033	1.0043	1.0054	1.0066	1.0079	1.0092	1.0138	1.0190	1.0250	1.0316	1.0388	1.0466	1.0550
1000.	0.	1.0010	1.0019	1.0029	1.0040	1.0051	1.0064	1.0077	1.0091	1.0106	1.0154	1.0209	1.0270	1.0337	1.0409	1.0487	1.0570
1050.	0.	1.0011	1.0022	1.0033	1.0046	1.0059	1.0072	1.0088	1.0101	1.0117	1.0168	1.0224	1.0286	1.0354	1.0426	1.0503	1.0586
1100.	0.	1.0013	1.0025	1.0037	1.0051	1.0064	1.0079	1.0094	1.0110	1.0127	1.0179	1.0237	1.0300	1.0368	1.0440	1.0516	1.0597
1150.	0.	1.0014	1.0027	1.0040	1.0055	1.0069	1.0085	1.0101	1.0117	1.0134	1.0189	1.0249	1.0311	1.0379	1.0451	1.0527	1.0608
1200.	0.	1.0015	1.0029	1.0043	1.0058	1.0074	1.0090	1.0106	1.0123	1.0141	1.0197	1.0256	1.0320	1.0388	1.0460	1.0535	1.0615
1250.	0.	1.0015	1.0030	1.0045	1.0061	1.0077	1.0094	1.0111	1.0128	1.0146	1.0203	1.0264	1.0328	1.0395	1.0467	1.0541	1.0618
1300.	0.	1.0016	1.0031	1.0047	1.0063	1.0080	1.0097	1.0115	1.0133	1.0151	1.0208	1.0269	1.0334	1.0401	1.0472	1.0545	1.0622
1350.	0.	1.0017	1.0032	1.0048	1.0065	1.0082	1.0100	1.0118	1.0136	1.0155	1.0213	1.0274	1.0338	1.0405	1.0475	1.0548	1.0624
1400.	0.	1.0017	1.0033	1.0050	1.0067	1.0084	1.0102	1.0120	1.0139	1.0158	1.0216	1.0277	1.0342	1.0409	1.0478	1.0550	1.0624
1450.	0.	1.0017	1.0034	1.0051	1.0068	1.0086	1.0104	1.0122	1.0141	1.0160	1.0219	1.0280	1.0344	1.0411	1.0480	1.0551	1.0624
1500.	0.	1.0018	1.0035	1.0052	1.0070	1.0087	1.0106	1.0124	1.0143	1.0162	1.0221	1.0282	1.0346	1.0412	1.0480	1.0551	1.0623
1550.	0.	1.0018	1.0035	1.0053	1.0070	1.0088	1.0107	1.0125	1.0144	1.0163	1.0222	1.0283	1.0347	1.0413	1.0480	1.0550	1.0621
1600.	0.	1.0018	1.0036	1.0053	1.0071	1.0089	1.0108	1.0126	1.0145	1.0164	1.0223	1.0284	1.0347	1.0412	1.0479	1.0548	1.0618

Table 94 (CONT'D 11)

TABLE 94. PHYSICAL PROPERTIES OF METHYLCYCLOHEXANE-TOLUENE-HYDROGEN MIXTURES — SHELL DEVELOPMENT COMPANY

	COMPONENT MCH	TOLUENE	HYDROGEN
MOLE FRACTION	0.07700	0.27100	0.65200
WEIGHT FRACTION	0.25600	0.70400	0.04600

GAS HEAT CONTENT (BTU/POUND)

TEMP DEG.F	PRESSURE (PSIA) 0.	100.	200.	300.	400.	500.	600.	700.	800.	900.	1200.	1500.	1800.	2100.	2400.	2700.	3000.
600.	324.	323.	322.	322.	321.	320.	320.	319.	319.	318.	316.	314.	313.	312.	310.	309.	308.
650.	359.	357.	357.	356.	355.	355.	354.	354.	353.	352.	351.	349.	348.	347.	346.	345.	344.
700.	393.	392.	392.	391.	390.	390.	389.	389.	388.	388.	387.	385.	384.	383.	382.	381.	381.
750.	428.	428.	427.	427.	426.	426.	425.	425.	425.	424.	423.	422.	421.	420.	419.	419.	418.
800.	465.	464.	464.	464.	463.	463.	462.	462.	462.	461.	460.	459.	458.	457.	457.	456.	455.
850.	502.	502.	501.	501.	501.	500.	500.	499.	499.	499.	498.	497.	496.	495.	495.	494.	494.
900.	540.	540.	539.	539.	539.	538.	538.	538.	537.	537.	536.	536.	535.	534.	534.	533.	533.
950.	579.	578.	578.	578.	577.	577.	577.	577.	576.	576.	575.	575.	574.	574.	573.	573.	573.
1000.	618.	618.	617.	617.	617.	617.	616.	616.	616.	616.	615.	615.	614.	614.	613.	613.	613.
1050.	658.	658.	657.	657.	657.	657.	657.	656.	656.	656.	656.	655.	655.	654.	654.	654.	653.
1100.	699.	698.	698.	698.	698.	697.	697.	697.	697.	697.	696.	696.	696.	695.	695.	695.	695.
1150.	740.	739.	739.	739.	739.	739.	739.	736.	738.	738.	738.	737.	737.	737.	737.	737.	736.
1200.	781.	781.	781.	781.	781.	780.	780.	780.	780.	780.	780.	779.	779.	779.	779.	779.	779.
1250.	824.	823.	823.	823.	823.	823.	823.	823.	822.	822.	822.	822.	822.	822.	822.	821.	821.
1300.	866.	866.	866.	866.	866.	866.	866.	865.	865.	865.	865.	865.	865.	865.	865.	865.	865.
1350.	909.	909.	909.	909.	909.	909.	909.	909.	909.	909.	908.	908.	908.	908.	908.	908.	909.
1400.	953.	953.	953.	953.	953.	953.	953.	952.	952.	952.	952.	952.	952.	952.	952.	952.	952.
1450.	997.	997.	997.	997.	997.	997.	997.	997.	997.	997.	997.	996.	997.	997.	997.	997.	997.
1500.	1041.	1041.	1041.	1041.	1041.	1041.	1041.	1041.	1041.	1041.	1041.	1041.	1041.	1041.	1041.	1042.	1042.
1550.	1086.	1086.	1086.	1086.	1086.	1086.	1086.	1086.	1086.	1086.	1086.	1086.	1086.	1086.	1087.	1087.	1087.
1600.	1131.	1131.	1131.	1131.	1131.	1131.	1131.	1131.	1131	1131.	1132.	1132.	1132.	1132.	1132.	1132.	1133.

GAS HEAT CAPACITY (BTU/POUND/DEG.F)

TEMP DEG.F	PRESSURE (PSIA) 0.	100.	200.	300.	400.	500.	600.	700.	800.	900.	1200.	1500.	1800.	2100.	2400.	2700.	3000.
600.	0.6714	0.6732	0.6746	0.6764	0.6780	0.6796	0.6812	0.6827	0.6843	0.6858	0.6901	0.6942	0.6980	0.7016	0.7046	0.7074	0.7098
650.	0.6894	0.6908	0.6923	0.6937	0.6951	0.6965	0.6978	0.6992	0.7005	0.7018	0.7056	0.7092	0.7125	0.7155	0.7183	0.7208	0.7231
700.	0.7064	0.7077	0.7090	0.7103	0.7114	0.7127	0.7138	0.7150	0.7162	0.7173	0.7206	0.7237	0.7266	0.7293	0.7318	0.7340	0.7360
750.	0.7227	0.7238	0.7250	0.7261	0.7271	0.7282	0.7292	0.7303	0.7313	0.7323	0.7351	0.7378	0.7404	0.7427	0.7449	0.7469	0.7488
800.	0.7371	0.7382	0.7392	0.7402	0.7413	0.7423	0.7433	0.7443	0.7452	0.7462	0.7489	0.7515	0.7539	0.7562	0.7584	0.7602	0.7619
850.	0.7517	0.7527	0.7536	0.7546	0.7555	0.7564	0.7573	0.7582	0.7591	0.7600	0.7624	0.7648	0.7670	0.7690	0.7709	0.7726	0.7742
900.	0.7658	0.7667	0.7675	0.7684	0.7692	0.7701	0.7709	0.7717	0.7725	0.7732	0.7755	0.7775	0.7796	0.7814	0.7831	0.7847	0.7862
950.	0.7793	0.7801	0.7809	0.7817	0.7824	0.7832	0.7839	0.7846	0.7853	0.7860	0.7881	0.7900	0.7918	0.7934	0.7950	0.7965	0.7978
1000.	0.7923	0.7930	0.7937	0.7944	0.7951	0.7958	0.7964	0.7971	0.7977	0.7984	0.8002	0.8019	0.8035	0.8051	0.8065	0.8079	0.8091
1050.	0.8048	0.8054	0.8060	0.8067	0.8073	0.8079	0.8085	0.8091	0.8097	0.8102	0.8119	0.8134	0.8149	0.8163	0.8176	0.8188	0.8199
1100.	0.8167	0.8173	0.8178	0.8184	0.8190	0.8195	0.8200	0.8205	0.8211	0.8216	0.8231	0.8245	0.8258	0.8271	0.8283	0.8294	0.8304
1150.	0.8280	0.8286	0.8291	0.8296	0.8301	0.8306	0.8311	0.8316	0.8321	0.8325	0.8339	0.8351	0.8364	0.8375	0.8386	0.8396	0.8404
1200.	0.8386	0.8394	0.8398	0.8403	0.8408	0.8412	0.8417	0.8421	0.8425	0.8430	0.8442	0.8454	0.8465	0.8475	0.8485	0.8494	0.8504
1250.	0.8492	0.8496	0.8500	0.8505	0.8509	0.8513	0.8517	0.8521	0.8525	0.8529	0.8541	0.8551	0.8561	0.8571	0.8580	0.8589	0.8598
1300.	0.8589	0.8593	0.8597	0.8601	0.8605	0.8609	0.8613	0.8617	0.8620	0.8624	0.8635	0.8645	0.8654	0.8663	0.8672	0.8680	0.8688
1350.	0.8681	0.8685	0.8689	0.8693	0.8696	0.8700	0.8704	0.8707	0.8711	0.8714	0.8724	0.8734	0.8743	0.8751	0.8760	0.8768	0.8775
1400.	0.8768	0.8772	0.8775	0.8779	0.8783	0.8786	0.8790	0.8793	0.8796	0.8800	0.8809	0.8819	0.8827	0.8836	0.8843	0.8851	0.8858
1450.	0.8849	0.8853	0.8856	0.8860	0.8864	0.8867	0.8870	0.8874	0.8877	0.8880	0.8890	0.8899	0.8907	0.8916	0.8923	0.8931	0.8938
1500.	0.8925	0.8929	0.8932	0.8936	0.8939	0.8943	0.8946	0.8950	0.8953	0.8956	0.8966	0.8975	0.8984	0.8992	0.8999	0.9007	0.9013
1550.	0.8994	0.8999	0.9003	0.9007	0.9010	0.9014	0.9017	0.9021	0.9024	0.9028	0.9037	0.9047	0.9056	0.9064	0.9072	0.9079	0.9086
1600.	0.9061	0.9065	0.9069	0.9072	0.9076	0.9080	0.9083	0.9087	0.9091	0.9094	0.9104	0.9114	0.9123	0.9132	0.9140	0.9147	0.9154

Table 94 (CONT'D 12)

TABLE 94. PHYSICAL PROPERTIES OF METHYLCYCLOHEXANE-TOLUENE-HYDROGEN MIXTURES — SHELL DEVELOPMENT COMPANY

		COMPONENT	
	MCH	TOLUENE	HYDROGEN
MOLE FRACTION	0.	0.25000	0.75000
WEIGHT FRACTION	0.	0.93800	0.06200

GAS VISCOSITY (POUNDS/FOOT/HOUR)

TEMP DEG.F	PRESSURE (PSIA) 0.	100.	200.	300.	400.	500.	600.	700.	800.	900.	1000.	1500.	1800.	2100.	2400.	2700.	3000.
600.	0.0362	0.0363	0.0364	0.0366	0.0367	0.0368	0.0370	0.0371	0.0373	0.0374	0.0390	0.0385	0.0391	0.0398	0.0405	0.0411	0.0419
650.	0.0377	0.0378	0.0379	0.0380	0.0382	0.0383	0.0384	0.0386	0.0387	0.0388	0.0393	0.0398	0.0404	0.0410	0.0416	0.0423	0.0429
700.	0.0392	0.0393	0.0394	0.0395	0.0396	0.0397	0.0399	0.0400	0.0401	0.0403	0.0407	0.0412	0.0417	0.0423	0.0428	0.0434	0.0441
750.	0.0406	0.0407	0.0408	0.0409	0.0410	0.0412	0.0413	0.0414	0.0415	0.0417	0.0421	0.0425	0.0430	0.0436	0.0441	0.0446	0.0452
800.	0.0421	0.0422	0.0423	0.0424	0.0425	0.0426	0.0427	0.0428	0.0429	0.0431	0.0435	0.0439	0.0444	0.0448	0.0453	0.0459	0.0464
850.	0.0435	0.0436	0.0437	0.0438	0.0439	0.0440	0.0441	0.0442	0.0443	0.0445	0.0448	0.0452	0.0457	0.0461	0.0466	0.0471	0.0476
900.	0.0450	0.0451	0.0451	0.0452	0.0453	0.0454	0.0455	0.0456	0.0457	0.0459	0.0462	0.0466	0.0470	0.0474	0.0479	0.0484	0.0488
950.	0.0464	0.0465	0.0466	0.0467	0.0467	0.0468	0.0469	0.0470	0.0471	0.0473	0.0476	0.0480	0.0483	0.0486	0.0490	0.0494	0.0501
1000.	0.0478	0.0479	0.0480	0.0481	0.0482	0.0482	0.0483	0.0484	0.0485	0.0486	0.0490	0.0493	0.0497	0.0501	0.0505	0.0510	0.0514
1050.	0.0492	0.0493	0.0494	0.0495	0.0496	0.0496	0.0497	0.0498	0.0499	0.0500	0.0503	0.0507	0.0510	0.0514	0.0518	0.0522	0.0526
1100.	0.0506	0.0507	0.0508	0.0509	0.0510	0.0510	0.0511	0.0512	0.0513	0.0514	0.0517	0.0520	0.0524	0.0527	0.0531	0.0534	0.0538
1150.	0.0521	0.0521	0.0522	0.0523	0.0524	0.0524	0.0525	0.0526	0.0527	0.0528	0.0531	0.0534	0.0537	0.0540	0.0544	0.0547	0.0551
1200.	0.0533	0.0534	0.0534	0.0535	0.0536	0.0537	0.0538	0.0538	0.0539	0.0540	0.0543	0.0546	0.0549	0.0553	0.0556	0.0559	0.0563
1250.	0.0544	0.0544	0.0547	0.0547	0.0548	0.0549	0.0550	0.0551	0.0551	0.0552	0.0555	0.0558	0.0561	0.0564	0.0567	0.0570	0.0574
1300.	0.0555	0.0555	0.0556	0.0560	0.0560	0.0561	0.0562	0.0563	0.0563	0.0564	0.0567	0.0569	0.0572	0.0575	0.0578	0.0581	0.0585
1350.	0.0566	0.0567	0.0571	0.0571	0.0572	0.0573	0.0574	0.0574	0.0575	0.0576	0.0578	0.0581	0.0583	0.0587	0.0590	0.0593	0.0596
1400.	0.0581	0.0582	0.0583	0.0583	0.0584	0.0585	0.0585	0.0586	0.0587	0.0588	0.0590	0.0592	0.0595	0.0598	0.0601	0.0604	0.0607
1450.	0.0593	0.0594	0.0594	0.0595	0.0595	0.0596	0.0597	0.0597	0.0598	0.0599	0.0601	0.0604	0.0606	0.0609	0.0612	0.0615	0.0618
1500.	0.0605	0.0605	0.0606	0.0606	0.0607	0.0608	0.0608	0.0609	0.0610	0.0610	0.0613	0.0617	0.0617	0.0620	0.0623	0.0626	0.0629
1550.	0.0616	0.0617	0.0617	0.0618	0.0618	0.0619	0.0620	0.0620	0.0621	0.0622	0.0624	0.0626	0.0628	0.0631	0.0634	0.0637	0.0639
1600.	0.0627	0.0628	0.0628	0.0629	0.0629	0.0630	0.0631	0.0631	0.0632	0.0633	0.0635	0.0637	0.0639	0.0642	0.0644	0.0647	0.0649

GAS THERMAL CONDUCTIVITY (BTU/FOOT/HOUR/DEG.F)

TEMP DEG.F	PRESSURE (PSIA) 0.	100.	200.	300.	400.	500.	600.	700.	800.	900.	12..	15 0.	1800.	2100.	2400.	2700.	3000
600.	0.0653	0.0654	0.0655	0.0656	0.0656	0.0652	0.0653	0.0655	0.0657	0.0658	0.0746	0.	0.	0.	0.	0.	0.
650.	0.0670	0.0680	0.0681	0.0674	0.0675	0.0677	0.0679	0.0681	0.0682	0.0684	0.0771	0.	0.	0.	0.	0.	0.
700.	0.0705	0.0706	0.0707	0.0708	0.0702	0.0703	0.0705	0.0706	0.0708	0.0709	0.0797	0.	0.	0.	0.	0.	0.
750.	0.0730	0.0732	0.0733	0.0724	0.0727	0.0729	0.0730	0.0732	0.0733	0.0734	0.0822	0.	0.	0.	0.	0.	0.
800.	0.0754	0.0757	0.0758	0.0751	0.0752	0.0754	0.0755	0.0757	0.0758	0.0760	0.0848	0.	0.	0.	0.	0.	0.
850.	0.0782	0.0783	0.0784	0.0777	0.0778	0.0780	0.0781	0.0782	0.0784	0.0785	0.0873	0.	0.	0.	0.	0.	0.
900.	0.0808	0.0809	0.0810	0.0803	0.0804	0.0805	0.0807	0.0808	0.0809	0.0810	0.0899	0.	0.	0.	0.	0.	0.
950.	0.0834	0.0835	0.0836	0.0829	0.0830	0.0831	0.0832	0.0833	0.0834	0.0836	0.0924	0.	0.	0.	0.	0.	0.
1000.	0.0856	0.0860	0.0861	0.0854	0.0855	0.0857	0.0858	0.0859	0.0860	0.0861	0.0950	0.	0.	0.	0.	0.	0.
1050.	0.0884	0.0886	0.0887	0.0880	0.0881	0.0882	0.0883	0.0884	0.0886	0.0887	0.0976	0.	0.	0.	0.	0.	0.
1100.	0.0911	0.0912	0.0913	0.0906	0.0907	0.0908	0.0909	0.0910	0.0911	0.0912	0.1002	0.	0.	0.	0.	0.	0.
1150.	0.0937	0.0938	0.0939	0.0932	0.0933	0.0934	0.0935	0.0936	0.0937	0.0938	0.1027	0.	0.	0.	0.	0.	0.
1200.	0.0961	0.0962	0.0963	0.0956	0.0957	0.0958	0.0959	0.0960	0.0961	0.0962	0.1051	0.	0.	0.	0.	0.	0.
1250.	0.0985	0.0986	0.0987	0.0980	0.0981	0.0981	0.0982	0.0983	0.0984	0.0985	0.1075	0.	0.	0.	0.	0.	0.
1300.	0.1006	0.1010	0.1011	0.1003	0.1004	0.1005	0.1006	0.1007	0.1008	0.1009	0.1089	0.	0.	0.	0.	0.	0.
1350.	0.1033	0.1033	0.1034	0.1027	0.1028	0.1029	0.1030	0.1030	0.1031	0.1032	0.1122	0.	0.	0.	0.	0.	0.
1400.	0.1054	0.1057	0.1058	0.1050	0.1041	0.1052	0.1053	0.1056	0.1055	0.1056	0.1145	0.	0.	0.	0.	0.	0.
1450.	0.1080	0.1080	0.1081	0.1074	0.1074	0.1075	0.1076	0.1077	0.1078	0.1079	0.1169	0.	0.	0.	0.	0.	0.
1500.	0.1103	0.1104	0.1104	0.1097	0.1098	0.1098	0.1099	0.1100	0.1101	0.1102	0.1192	0.	0.	0.	0.	0.	0.
1550.	0.1126	0.1127	0.1127	0.1120	0.1121	0.1121	0.1122	0.1123	0.1124	0.1125	0.1215	0.	0.	0.	0.	0.	0.
1600.	0.1149	0.1150	0.1150	0.1143	0.1144	0.1144	0.1145	0.1146	0.1147	0.1148	0.1236	0.	0.	0.	0.	0.	0.

Table 94 (CONT'D 13)

TABLE 94. PHYSICAL PROPERTIES OF METHYLCYCLOHEXANE-TOLUENE-HYDROGEN MIXTURES — SHELL DEVELOPMENT COMPANY

	COMPONENT MCH	TOLUENE	HYDROGEN
MOLE FRACTION	0.	0.25000	0.75000
WEIGHT FRACTION	0.	0.99300	0.00700

GAS DENSITY (POUNDS/CUBIC FOOT)

TEMP DEG.F	PRESSURE (PSIA) 0.	100.	200.	300.	400.	500.	600.	700.	800.	900.	1200.	1500.	1800.	2100.	2400.	2700.	3000.
600.	0.	0.216	0.432	0.648	0.864	1.079	1.295	1.510	1.724	1.939	2.577	3.208	3.838	4.461	5.080	5.626	6.197
650.	0.	0.204	0.412	0.618	0.824	1.029	1.234	1.438	1.642	1.846	2.452	3.051	3.641	4.222	4.791	5.349	5.892
700.	0.	0.197	0.394	0.591	0.787	0.983	1.179	1.374	1.568	1.762	2.340	2.910	3.472	4.025	4.567	5.099	5.619
750.	0.	0.188	0.376	0.564	0.754	0.941	1.128	1.315	1.501	1.684	2.238	2.782	3.319	3.847	4.366	4.877	5.372
800.	0.	0.181	0.362	0.542	0.723	0.903	1.082	1.261	1.439	1.617	2.145	2.666	3.180	3.684	4.183	4.671	5.146
850.	0.	0.174	0.348	0.522	0.695	0.868	1.040	1.212	1.383	1.553	2.060	2.560	3.053	3.539	4.018	4.484	4.943
900.	0.	0.168	0.336	0.503	0.669	0.835	1.001	1.166	1.330	1.494	1.982	2.463	2.937	3.404	3.863	4.313	4.756
950.	0.	0.162	0.324	0.485	0.645	0.805	0.965	1.124	1.282	1.440	1.910	2.373	2.830	3.279	3.722	4.154	4.578
1000.	0.	0.156	0.312	0.468	0.623	0.777	0.931	1.085	1.238	1.390	1.843	2.290	2.730	3.164	3.591	4.011	4.424
1050.	0.	0.151	0.302	0.452	0.602	0.751	0.900	1.048	1.196	1.343	1.781	2.212	2.638	3.057	3.470	3.876	4.276
1100.	0.	0.146	0.292	0.438	0.583	0.727	0.871	1.014	1.157	1.299	1.723	2.140	2.552	2.958	3.358	3.751	4.138
1150.	0.	0.142	0.283	0.424	0.565	0.704	0.844	0.983	1.121	1.259	1.668	2.073	2.472	2.865	3.252	3.634	4.009
1200.	0.	0.138	0.275	0.411	0.547	0.683	0.818	0.953	1.087	1.220	1.618	2.010	2.397	2.778	3.154	3.524	3.889
1250.	0.	0.134	0.267	0.399	0.531	0.663	0.794	0.925	1.055	1.185	1.570	1.951	2.326	2.695	3.062	3.421	3.776
1300.	0.	0.130	0.259	0.388	0.516	0.644	0.772	0.898	1.025	1.151	1.525	1.895	2.260	2.620	2.975	3.325	3.669
1350.	0.	0.126	0.252	0.377	0.502	0.626	0.750	0.874	0.996	1.119	1.483	1.843	2.198	2.548	2.893	3.234	3.569
1400.	0.	0.123	0.245	0.367	0.488	0.609	0.730	0.850	0.970	1.089	1.443	1.793	2.139	2.480	2.816	3.148	3.474
1450.	0.	0.120	0.239	0.357	0.476	0.593	0.711	0.828	0.944	1.060	1.405	1.746	2.083	2.415	2.743	3.066	3.385
1500.	0.	0.116	0.233	0.349	0.463	0.578	0.693	0.807	0.920	1.033	1.370	1.702	2.030	2.354	2.674	2.989	3.300
1550.	0.	0.114	0.227	0.340	0.452	0.564	0.675	0.787	0.897	1.007	1.336	1.660	1.980	2.296	2.608	2.916	3.220
1600.	0.	0.111	0.221	0.331	0.441	0.550	0.659	0.767	0.875	0.983	1.303	1.620	1.932	2.241	2.546	2.846	3.143

GAS COMPRESSIBILITY FACTOR

TEMP DEG.F	PRESSURE (PSIA) 0.	100.	200.	300.	400.	500.	600.	700.	800.	900.	1200.	1500.	1800.	2100.	2400.	2700.	3000.
600.	0.	0.9998	0.9996	0.9994	0.9992	0.9989	1.0002	1.0007	1.0013	1.0020	1.0050	1.0091	1.0143	1.0204	1.0278	1.0359	1.0448
650.	0.	1.0002	1.0004	1.0007	1.0011	1.0017	1.0023	1.0031	1.0040	1.0050	1.0087	1.0133	1.0188	1.0253	1.0326	1.0407	1.0495
700.	0.	1.0005	1.0010	1.0016	1.0023	1.0032	1.0041	1.0051	1.0062	1.0074	1.0116	1.0166	1.0225	1.0291	1.0364	1.0444	1.0531
750.	0.	1.0004	1.0015	1.0024	1.0033	1.0043	1.0055	1.0067	1.0079	1.0093	1.0139	1.0193	1.0254	1.0321	1.0395	1.0474	1.0559
800.	0.	1.0010	1.0020	1.0030	1.0041	1.0053	1.0066	1.0080	1.0094	1.0109	1.0159	1.0215	1.0277	1.0345	1.0419	1.0498	1.0583
850.	0.	1.0012	1.0023	1.0035	1.0048	1.0061	1.0075	1.0090	1.0106	1.0122	1.0174	1.0232	1.0295	1.0364	1.0438	1.0516	1.0598
900.	0.	1.0013	1.0026	1.0039	1.0053	1.0068	1.0083	1.0099	1.0115	1.0132	1.0186	1.0246	1.0310	1.0379	1.0452	1.0530	1.0611
950.	0.	1.0014	1.0028	1.0043	1.0058	1.0073	1.0089	1.0104	1.0123	1.0140	1.0196	1.0257	1.0322	1.0391	1.0464	1.0540	1.0620
1000.	0.	1.0015	1.0030	1.0045	1.0061	1.0077	1.0094	1.0111	1.0129	1.0147	1.0204	1.0266	1.0331	1.0400	1.0471	1.0548	1.0628
1050.	0.	1.0016	1.0032	1.0048	1.0064	1.0081	1.0098	1.0118	1.0134	1.0153	1.0211	1.0273	1.0339	1.0406	1.0478	1.0553	1.0630
1100.	0.	1.0017	1.0033	1.0049	1.0066	1.0084	1.0101	1.0120	1.0138	1.0157	1.0216	1.0278	1.0343	1.0411	1.0482	1.0556	1.0632
1150.	0.	1.0017	1.0034	1.0051	1.0068	1.0086	1.0104	1.0122	1.0141	1.0160	1.0220	1.0282	1.0347	1.0415	1.0485	1.0558	1.0633
1200.	0.	1.0018	1.0035	1.0052	1.0070	1.0088	1.0106	1.0125	1.0144	1.0163	1.0222	1.0285	1.0350	1.0417	1.0486	1.0558	1.0632
1250.	0.	1.0018	1.0035	1.0053	1.0071	1.0089	1.0108	1.0126	1.0145	1.0165	1.0224	1.0287	1.0351	1.0418	1.0487	1.0557	1.0630
1300.	0.	1.0018	1.0036	1.0054	1.0072	1.0090	1.0109	1.0128	1.0147	1.0166	1.0226	1.0288	1.0352	1.0419	1.0487	1.0556	1.0627
1350.	0.	1.0019	1.0036	1.0054	1.0072	1.0091	1.0110	1.0128	1.0148	1.0167	1.0227	1.0288	1.0352	1.0417	1.0484	1.0553	1.0624
1400.	0.	1.0019	1.0037	1.0055	1.0073	1.0091	1.0110	1.0129	1.0148	1.0168	1.0227	1.0288	1.0351	1.0416	1.0482	1.0550	1.0620
1450.		1.0019	1.0037	1.0055	1.0073	1.0092	1.0110	1.0129	1.0148	1.0168	1.0227	1.0288	1.0350	1.0414	1.0480	1.0547	1.0615
1500.		1.0019	1.0037	1.0055	1.0073	1.0092	1.0110	1.0129	1.0148	1.0168	1.0226	1.0287	1.0349	1.0412	1.0477	1.0543	1.0610
1550.	0.	1.0019	1.0037	1.0055	1.0073	1.0092	1.0110	1.0129	1.0148	1.0167	1.0226	1.0286	1.0347	1.0409	1.0473	1.0538	1.0605
1600.	0.	1.0019	1.0037	1.0055	1.0073	1.0092	1.0110	1.0129	1.0148	1.0167	1.0225	1.0284	1.0345	1.0406	1.0470	1.0534	1.0599

Table 94 (CONT'D 14)

TABLE 94. PHYSICAL PROPERTIES OF METHYLCYCLOHEXANE-TOLUENE-HYDROGEN MIXTURES — SHELL DEVELOPMENT COMPANY

	MCH	COMPONENT TOLUENE	HYDROGEN
MOLE FRACTION	0.	0.25000	0.75000
WEIGHT FRACTION	0.	0.93800	0.06200

GAS HEAT CONTENT (BTU/POUND)

TEMP DEG.F	PRESSURE (PSIA) 0.	100.	200.	300.	400.	500.	600.	700.	800.	900.	1200.	1500.	1800.	2100.	2400.	2700.	3000.
600.	339.	338.	338.	337.	337.	337.	336.	336.	335.	335.	334.	333.	332.	331.	330.	336.	329.
650.	373.	373.	373.	372.	372.	371.	371.	371.	370.	370.	369.	368.	367.	367.	366.	366.	365.
700.	409.	408.	408.	408.	407.	407.	407.	406.	406.	406.	406.	405.	404.	403.	402.	402.	402.
750.	445.	444.	444.	444.	443.	443.	443.	443.	442.	442.	441.	441.	440.	440.	439.	439.	439.
800.	481.	481.	481.	481.	480.	480.	480.	480.	479.	479.	479.	478.	478.	477.	477.	477.	477.
850.	519.	518.	518.	519.	518.	518.	517.	517.	517.	517.	516.	516.	516.	515.	515.	515.	515.
900.	557.	556.	556.	556.	556.	556.	556.	555.	555.	555.	555.	555.	554.	554.	554.	554.	554.
950.	595.	595.	595.	595.	595.	594.	594.	594.	594.	594.	594.	594.	593.	593.	593.	593.	593.
1000.	634.	634.	634.	634.	634.	634.	634.	634.	633.	633.	633.	633.	633.	633.	633.	633.	633.
1050.	674.	674.	674.	674.	674.	674.	674.	674.	673.	673.	673.	673.	673.	673.	673.	673.	673.
1100.	714.	714.	714.	714.	714.	714.	714.	714.	714.	714.	714.	714.	714.	714.	714.	714.	714.
1150.	755.	755.	755.	755.	755.	755.	755.	755.	755.	755.	755.	755.	755.	755.	755.	755.	755.
1200.	797.	796.	797.	796.	796.	796.	796.	796.	796.	796.	796.	796.	797.	797.	797.	797.	797.
1250.	838.	838.	838.	838.	838.	838.	838.	838.	838.	838.	838.	838.	838.	839.	839.	839.	840.
1300.	881.	881.	881.	881.	881.	881.	881.	881.	881.	881.	881.	881.	881.	881.	882.	882.	882.
1350.	923.	923.	923.	923.	923.	923.	923.	923.	923.	923.	924.	924.	924.	924.	925.	925.	925.
1400.	966.	966.	966.	966.	966.	66.	966.	966.	967.	967.	967.	967.	967.	968.	968.	968.	969.
1450.	1010.	1010.	1010.	1010.	1010.	1010.	1010.	1010.	1010.	1010.	1010.	1011.	1011.	1011.	1012.	1012.	1013.
1500.	1054.	1054.	1054.	1054.	1054.	1054.	1054.	1054.	1054.	1054.	1054.	1055.	1055.	1055.	1056.	1056.	1057.
1550.	1098.	1098.	1098.	1098.	1098.	1098.	1098.	1098.	1098.	1098.	1099.	1099.	1099.	1100.	1100.	1101.	1101.
1600.	1142.	1142.	1142.	1142.	1142.	1143.	1143.	1143.	1143.	1143.	1143.	1144.	1146.	1145.	1145.	1146.	1146.

GAS HEAT CAPACITY (BTU/POUND/DEG.F)

TEMP DEG.F	PRESSURE (PSIA) 0.	100.	200.	300.	400.	500.	600.	700.	800.	900.	1200.	1500.	1800.	2100.	2400.	2700.	3000.
600.	0.6821	0.6834	0.6846	0.6861	0.6873	0.6886	0.6898	0.6911	0.6923	0.6935	0.6969	0.7001	0.7031	0.7058	0.7083	0.7106	0.7128
650.	0.6979	0.6989	0.7001	0.7014	0.7024	0.7035	0.7046	0.7057	0.7067	0.7078	0.7108	0.7136	0.7162	0.7187	0.7210	0.7232	0.7249
700.	0.7128	0.7138	0.7149	0.7159	0.7169	0.7179	0.7188	0.7198	0.7207	0.7216	0.7243	0.7267	0.7291	0.7312	0.7332	0.7351	0.7368
750.	0.7272	0.7281	0.7290	0.7299	0.7308	0.7317	0.7325	0.7333	0.7342	0.7350	0.7373	0.7395	0.7415	0.7434	0.7451	0.7469	0.7485
800.	0.7400	0.7408	0.7416	0.7424	0.7434	0.7443	0.7451	0.7459	0.7466	0.7474	0.7496	0.7517	0.7535	0.7555	0.7572	0.7588	0.7602
850.	0.7518	0.7528	0.7536	0.7546	0.7554	0.7561	0.7569	0.7576	0.7583	0.7590	0.7597	0.7617	0.7634	0.7648	0.7670	0.7686	0.7701
900.	0.7634	0.7643	0.7652	0.7660	0.7677	0.7683	0.7690	0.7697	0.7703	0.7710	0.7726	0.7734	0.7751	0.7767	0.7783	0.7797	0.7810
950.	0.7746	0.7752	0.7760	0.7768	0.7775	0.7781	0.7787	0.7793	0.7798	0.7804	0.7818	0.7831	0.7847	0.7863	0.7877	0.7891	0.7904
1000.	0.7845	0.7852	0.7858	0.7865	0.7871	0.7877	0.7883	0.7888	0.7894	0.7900	0.7915	0.7930	0.7936	0.7941	0.7956	0.7970	0.7984
1050.	0.7935	0.7940	0.7946	0.7951	0.7957	0.7962	0.7967	0.7972	0.7977	0.7982	0.7996	0.8009	0.8021	0.8033	0.8045	0.8057	0.8068
1100.	0.8019	0.8024	0.8029	0.8034	0.8039	0.8044	0.8049	0.8054	0.8059	0.8063	0.8078	0.8091	0.8103	0.8115	0.8126	0.8137	0.8147
1150.	0.8098	0.8103	0.8108	0.8113	0.8118	0.8123	0.8128	0.8133	0.8137	0.8142	0.8156	0.8169	0.8181	0.8193	0.8204	0.8215	0.8224
1200.	0.8172	0.8176	0.8181	0.8186	0.8190	0.8195	0.8199	0.8204	0.8208	0.8213	0.8226	0.8239	0.8251	0.8262	0.8273	0.8284	0.8294
1250.	0.8240	0.8244	0.8249	0.8253	0.8257	0.8262	0.8266	0.8270	0.8274	0.8279	0.8291	0.8303	0.8314	0.8325	0.8336	0.8346	0.8356
1300.	0.8302	0.8306	0.8310	0.8314	0.8318	0.8322	0.8326	0.8330	0.8334	0.8338	0.8350	0.8361	0.8372	0.8383	0.8393	0.8403	0.8413
1350.	0.8359	0.8363	0.8367	0.8371	0.8375	0.8379	0.8383	0.8387	0.8391	0.8394	0.8406	0.8416	0.8426	0.8436	0.8445	0.8455	0.8464
1400.	0.8411	0.8415	0.8419	0.8423	0.8427	0.8431	0.8434	0.8438	0.8442	0.8446	0.8457	0.8467	0.8476	0.8486	0.8495	0.8504	0.8513
1450.	0.8459	0.8463	0.8467	0.8470	0.8474	0.8478	0.8481	0.8485	0.8488	0.8492	0.8503	0.8512	0.8522	0.8531	0.8540	0.8549	0.8558
1500.	0.8504	0.8508	0.8512	0.8515	0.8519	0.8522	0.8526	0.8529	0.8533	0.8536	0.8547	0.8556	0.8565	0.8574	0.8583	0.8592	0.8600
1550.	0.8547	0.8551	0.8554	0.8558	0.8561	0.8565	0.8568	0.8572	0.8575	0.8579	0.8589	0.8598	0.8607	0.8616	0.8624	0.8633	0.8641
1600.	0.8589	0.8593	0.8596	0.8600	0.8603	0.8607	0.8610	0.8614	0.8617	0.8621	0.8630	0.8639	0.8648	0.8656	0.8665	0.8673	0.8681
1650.	0.8630	0.8634	0.8637	0.8641	0.8644	0.8648	0.8651	0.8655	0.8658	0.8661	0.8671	0.8680	0.8688	0.8697	0.8705	0.8713	0.8721
1700.	0.8670	0.8674	0.8677	0.8681	0.8684	0.8688	0.8691	0.8694	0.8698	0.8701	0.8711	0.8720	0.8728	0.8736	0.8744	0.8752	0.8760
1750.	0.8710	0.8713	0.8717	0.8720	0.8723	0.8727	0.8730	0.8733	0.8737	0.8740	0.8749	0.8758	0.8766	0.8774	0.8782	0.8790	0.8797
1800.	0.8749	0.8753	0.8756	0.8759	0.8763	0.8766	0.8769	0.8772	0.8776	0.8779	0.8788	0.8796	0.8804	0.8812	0.8819	0.8827	0.8834
1850.	0.8788	0.8791	0.8795	0.8798	0.8801	0.8804	0.8807	0.8810	0.8813	0.8816	0.8825	0.8833	0.8841	0.8848	0.8856	0.8863	0.8870
1900.	0.8826	0.8829	0.8832	0.8835	0.8838	0.8841	0.8844	0.8847	0.8850	0.8853	0.8862	0.8870	0.8877	0.8885	0.8892	0.8899	0.8906
1950.	0.8863	0.8866	0.8869	0.8872	0.8875	0.8877	0.8880	0.8883	0.8886	0.8889	0.8897	0.8905	0.8912	0.8919	0.8926	0.8933	0.8940
2000.	0.8900	0.8903	0.8906	0.8909	0.8912	0.8914	0.8917	0.8920	0.8923	0.8926	0.8934	0.8941	0.8948	0.8955	0.8962	0.8969	0.8975
2050.	0.8936	0.8939	0.8942	0.8945	0.8947	0.8950	0.8953	0.8956	0.8958	0.8961	0.8969	0.8976	0.8983	0.8990	0.8997	0.9003	0.9010
2100.	0.8972	0.8975	0.8978	0.8980	0.8983	0.8986	0.8988	0.8991	0.8994	0.8996	0.9004	0.9011	0.9018	0.9024	0.9031	0.9037	0.9044
2150.	0.9007	0.9010	0.9013	0.9015	0.9018	0.9020	0.9023	0.9026	0.9028	0.9031	0.9038	0.9045	0.9052	0.9058	0.9065	0.9071	0.9077
2200.	0.9042	0.9045	0.9047	0.9050	0.9052	0.9055	0.9057	0.9060	0.9062	0.9065	0.9072	0.9079	0.9085	0.9091	0.9098	0.9104	0.9110
2250.	0.9076	0.9079	0.9081	0.9084	0.9086	0.9089	0.9091	0.9093	0.9096	0.9098	0.9105	0.9112	0.9118	0.9124	0.9130	0.9136	0.9142
2300.	0.9110	0.9113	0.9115	0.9118	0.9120	0.9122	0.9125	0.9127	0.9129	0.9132	0.9138	0.9145	0.9151	0.9157	0.9163	0.9169	0.9174
2350.	0.9144	0.9146	0.9149	0.9151	0.9153	0.9156	0.9158	0.9160	0.9162	0.9165	0.9171	0.9177	0.9183	0.9189	0.9195	0.9200	0.9206
2400.	0.9177	0.9180	0.9182	0.9184	0.9186	0.9189	0.9191	0.9193	0.9195	0.9197	0.9204	0.9210	0.9215	0.9221	0.9227	0.9232	0.9237
2450.	0.9211	0.9213	0.9215	0.9217	0.9219	0.9221	0.9223	0.9225	0.9227	0.9229	0.9235	0.9241	0.9246	0.9252	0.9257	0.9262	0.9267
2500.	0.9244	0.9246	0.9248	0.9250	0.9252	0.9254	0.9256	0.9258	0.9260	0.9262	0.9267	0.9272	0.9277	0.9282	0.9287	0.9292	0.9297
2550.	0.9276	0.9278	0.9280	0.9282	0.9284	0.9286	0.9288	0.9289	0.9291	0.9293	0.9298	0.9303	0.9308	0.9313	0.9317	0.9322	0.9326
2600.	0.9308	0.9310	0.9312	0.9314	0.9316	0.9317	0.9319	0.9321	0.9323	0.9325	0.9329	0.9334	0.9338	0.9343	0.9347	0.9351	0.9356
2650.	0.9340	0.9342	0.9343	0.9345	0.9347	0.9349	0.9350	0.9352	0.9354	0.9355	0.9360	0.9364	0.9368	0.9372	0.9376	0.9380	0.9384
2700.	0.9371	0.9373	0.9374	0.9376	0.9378	0.9379	0.9381	0.9382	0.9384	0.9386	0.9390	0.9394	0.9398	0.9402	0.9406	0.9410	0.9413
2750.	0.9402	0.9403	0.9405	0.9406	0.9408	0.9409	0.9411	0.9412	0.9414	0.9415	0.9419	0.9423	0.9427	0.9430	0.9434	0.9437	0.9441
2800.	0.9432	0.9433	0.9435	0.9436	0.9438	0.9439	0.9440	0.9442	0.9443	0.9445	0.9448	0.9452	0.9455	0.9459	0.9462	0.9465	0.9468
2850.	0.9461	0.9462	0.9464	0.9465	0.9466	0.9468	0.9469	0.9470	0.9472	0.9473	0.9477	0.9480	0.9483	0.9486	0.9489	0.9492	0.9495
2900.	0.9490	0.9491	0.9492	0.9494	0.9495	0.9496	0.9497	0.9499	0.9500	0.9501	0.9504	0.9507	0.9510	0.9513	0.9516	0.9519	0.9521
2950.	0.9518	0.9519	0.9520	0.9521	0.9523	0.9524	0.9525	0.9526	0.9527	0.9528	0.9531	0.9534	0.9537	0.9540	0.9542	0.9545	0.9548
3000.	0.9545	0.9546	0.9547	0.9548	0.9549	0.9550	0.9551	0.9552	0.9553	0.9554	0.9557	0.9559	0.9562	0.9564	0.9567	0.9569	0.9572

AFAPL-TR-65-114 Part I

Table 95. SUMMARY TABLE: EVALUATION OF VAPORIZING AND ENDOTHERMIC FUELS[d]

Values in parentheses are estimated
Catalyst: 1% Pt/Al_2O_3

Report and Page	Flash Point, °F	Vapor Press., psia, °F		Freezing Point, °F	Boiling Point, °F	Viscosity, cs at -30°F	Net Heat of Combustion, Btu/lb	Specific Heat, Btu/lb/°F	Thermal Stability (N_2), Tmax, °F	Density, lb/gal at 60°F	Mol wt	Hydrocarbon	Basis Type	Basis
		300	500											
III,[a] [illegible]	(90)	(19)	(148)	(-64)	(285)	(1.59)	18,697	(0.424[60])	(700)	(7.042)	124.2	1,[illegible]-Trimethyl CH 1,[illegible]-, [illegible]- 1,[illegible]-,trans-[illegible]	CH	[illegible]
III,[a] 55	(90)	(13)	(120)	(-122) -122	(287)	(1.59)	(18,659) (18,659)	(0.41[60]) (0.41[60])	700	(7.08)	124.2	1,[illegible]-Trimethyl CH 1,trans-,trans-[illegible] = 0.7% 1,trans-,cis-4 = 1.6% 1,cis-,cis-[illegible] = 97.7% 1,cis-2,trans-[illegible]	CH	[illegible]
III,[a] 55	(86)	(10.4)	(128)	(-92)	(2[illegible]) 2)[illegible]	(1.59)	18,545	(.422[60])	(700)	[illegible]	126.2	1,2,5-Trimethyl CH 1,trans-2,cis-[illegible] = 1.0% 1,trans-,trans-[illegible] = 99.0% 1,cis-2,cis-[illegible]	CH	[illegible]
(b)	(113)	10	(157)	-120	351	4.54	18,470	.45[100])	(750)	6.668	140.3	Tetramethyl CH	CH	[illegible] 98.1
III,[a] 47	210	1.2	23.5	35	401	Solid	18,400	0.381[68]	695	7.435	140.3	Dimethylhexyl	CH	[illegible] 98%
III,[a] 47	(170)	(4.3)	(48)	-67[c])	(34[illegible])	(16.5)	(18,210)	(0.[illegible][60])	725	7.574	138.2	Decalin (F-11) 84.5% cis-DHN 15.1% trans-DHN 0.4% THN	CH	[illegible]
III,[a] 47												Decalin (MKP-1005)	CH	[illegible]
III,[a] 89	(180)	(4)	(50)	-8	466	(16.5)	(18,300)	(.43[60])	(775-800)	7.509	132.5	1-Methyldecalin	CH	MCH (80% [illegible])
III,[a] 89	(200)	(4)	(50)	55	468	(16.5)	(18,200)	(.43[60])	(775-800)	7.215	132.5	2-Methyldecalin	CH	MCH (80% [illegible])

Report and Page	Endothermic Capacity, Btu/lb: Reaction	Latent + Sensible Heat	Total at 1340°F	Total, Btu/ft³	Total as % OH	Catalytic: Temperature, °F: Block	Wall	Catalyst	LHSV	Reaction 10 Min Program: Conversion, %	Heat Sink, Btu/lb: Reaction	Total at Block Temp.	Total at 1340°F	Rate [illegible]	[illegible]	Relative Ref [illegible]: [illegible]	Rate
III,[a] 55	685	950	1635	78.4	[illegible]	[illegible]	715	596	100	64.3	360	710	1210	0.7	[illegible]	[illegible]	[illegible]
III,[a] 55	685	950	1635	78.4	[illegible]	492	754	653	100	67.3	414	1004	1364	-	1.0	-	-
III,[a] 55	685	950	1635	78.4	[illegible]	[illegible]	714	594	100	56.3	369	745	1314	0	-	[illegible]	-
						[illegible]	784	660	100	64.5	419	1057	1364	-	-	-	-
III,[a] 55	685	950	1635	78.4	5.8	[illegible]	727	619	100	60.3	322	[illegible]	1257	3.1	-	[illegible]	-
						1022	897	759	100	77.5	391	1041	1364	-	-	-	-
(b)	615	950	1565	75.1	-	842		618	100	68.3	275	693	1358	9.1	-	-	-
						942	810	687	100	75.3	429	1044	1357	-	-	-	-
III,[a] 47	1058	950	1968	94.4	10.7	842	754	601	100	58.2	406	966	1334	-	-	-	-
						1022	891	680	100	65.4	[illegible]	1111	1357	-	[illegible]	-	-
						1022	903	756	50	89.8	938	1235	1344	-	-	-	-
III,[a] 47	950	1100	2050	98.4	11.2	842	742	632	100	40.2	351	1071	1418	0.1	-	-	-
						1022	877	716	100	56.6	520	1170	1555	-	-	-	-
III,[a] 47	950	1100	2050	98.4	11.2	1022	914	719	50	89.3	452	1268	1307	-	-	-	-
III,[a] 5,	900	1100	2000	96.0	11.0	842	732	629	100	35.4	312	1082	1412	0.1	-	[illegible]	-
						842	800	678	100	43.0	390	1170	1490	-	-	-	-
III,[a] 89	900	1100	2000	96.0	11.0	842	730	650	100	36.2	309	1010	1490	0.9	-	[illegible]	-
						1022	867	719	100	53.9	463	1315	1541	-	-	-	-

a) Reference 1.
b) This report
c) 932°F.
d) Combination of Table 89, reference 5.

Bench-Scale Reactor - Description of the Apparatus, Procedure for the Experiments, Calculation of Heat Sinks

The apparatus used for the reaction studies consisted of two identical reactor units, each with a hot tube reactor and with conventional devices for measuring feed flow rates and for collecting and measuring reaction products. A schematic of one reactor unit is shown in Figure 92; photographs of the complete dual reactor assembly are shown in Figures 93 and 94.

The reactor was a furnace-heated stainless steel tube (1/2-inch IPS) 33 inches long. The catalyst bed (ca 5 inches long) was located in the lower portion of the tube; the top portion served as a preheater. For thermal reaction studies, a bed of quartz was used instead of catalyst. The non-hydrocarbon gases (used for catalyst regeneration), were metered through conventional rotameters and entered the reactor at the top. Liquid hydrocarbon feed was forced from a liquid reservoir through a rotameter by means of argon pressure. The feed was then vaporized in a heated line and entered the reactor as a vapor through a separate tube that terminated just above the catalyst bed. The hot exit gases from the reactor passed through a condenser and then a liquid-gas separator. The liquid was collected in a Jerguson gauge; the gas products were passed through a Grove pressure regulator, a wet test meter and then were vented. Gas samples were taken upstream from the wet-test meter. A thermowell entered the reactor from the bottom end and served to contain the thermocouples used for measuring bed temperatures.

The platinum catalyst was stored in the unreduced form and sieved before charging. It was reduced with hydrogen just before starting the experiment. The reduction was carried out as follows. After loading and pressure testing the reactor was brought to 572°F in argon and then hydrogen flow started. The catalyst was held at this temperature in hydrogen for 30 minutes and then brought to reaction temperature. The flow was maintained and the catalyst held at the reaction temperature for one hour after which the hydrogen was shut off and the feed flow started. After catalyst reduction the catalyst was always cooled to below 572°F or brought up to reaction temperature in an atmosphere of hydrogen.

Calculation of Conversions, Selectivities and Coke Formed

The conversions and selectivities were calculated on the basis of gas phase (at reaction temperature) product material only; any coke or polymer formed did not enter into the calculations. Thus, conversions are minimum and selectivities are maximum values.

Calculation of Heat Sinks and Heats of Reaction

Endothermic heats of reaction were calculated from the conversion, selectivity for a given product and the thermodynamic heat of reaction at 100% conversion. Thus, the contribution to the total heat of reaction by any given reaction is given by Hp = CpxSpxHp where

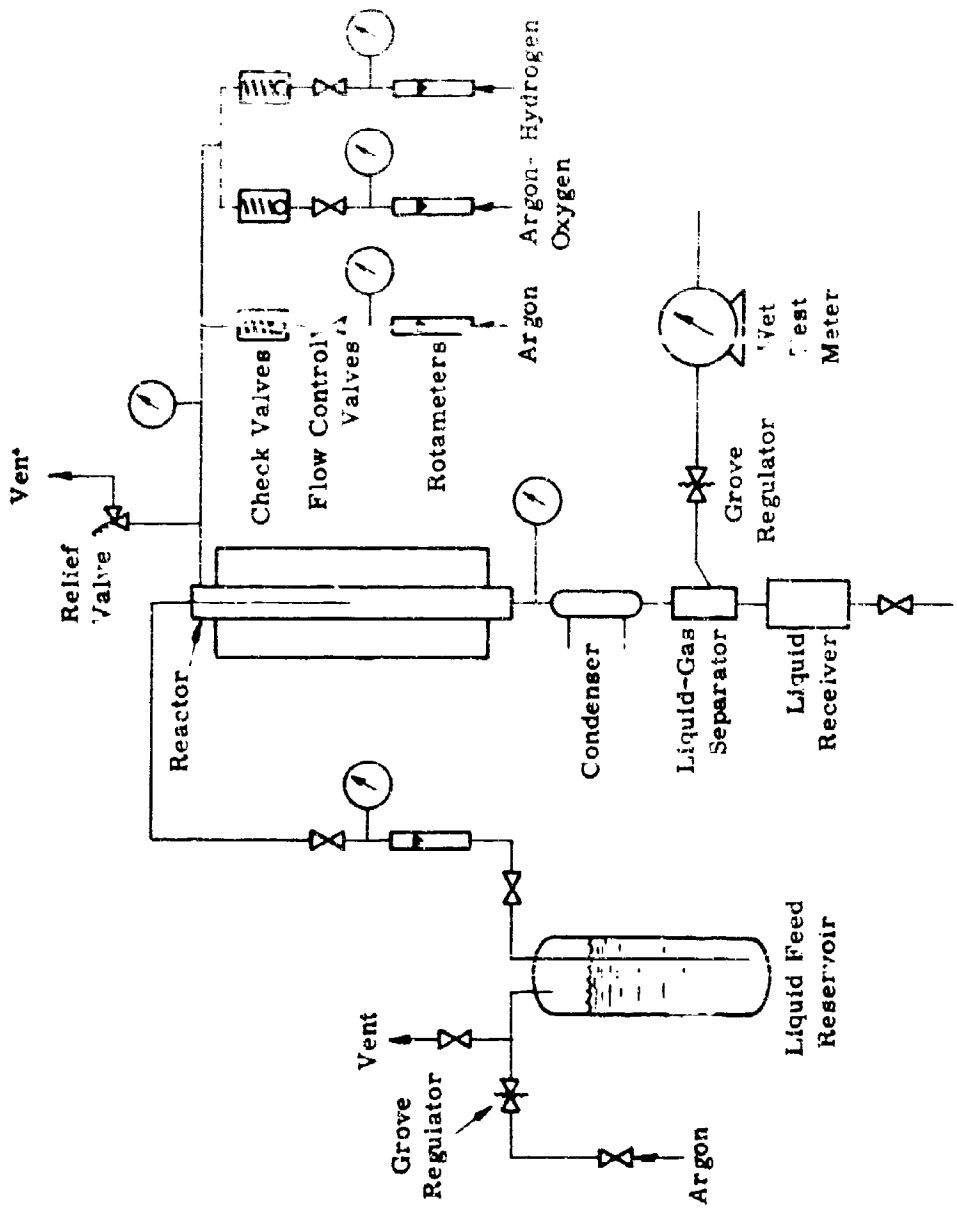


Figure 92. BENCH-SCALE REACTOR SYSTEM (SCHEMATIC)

59003

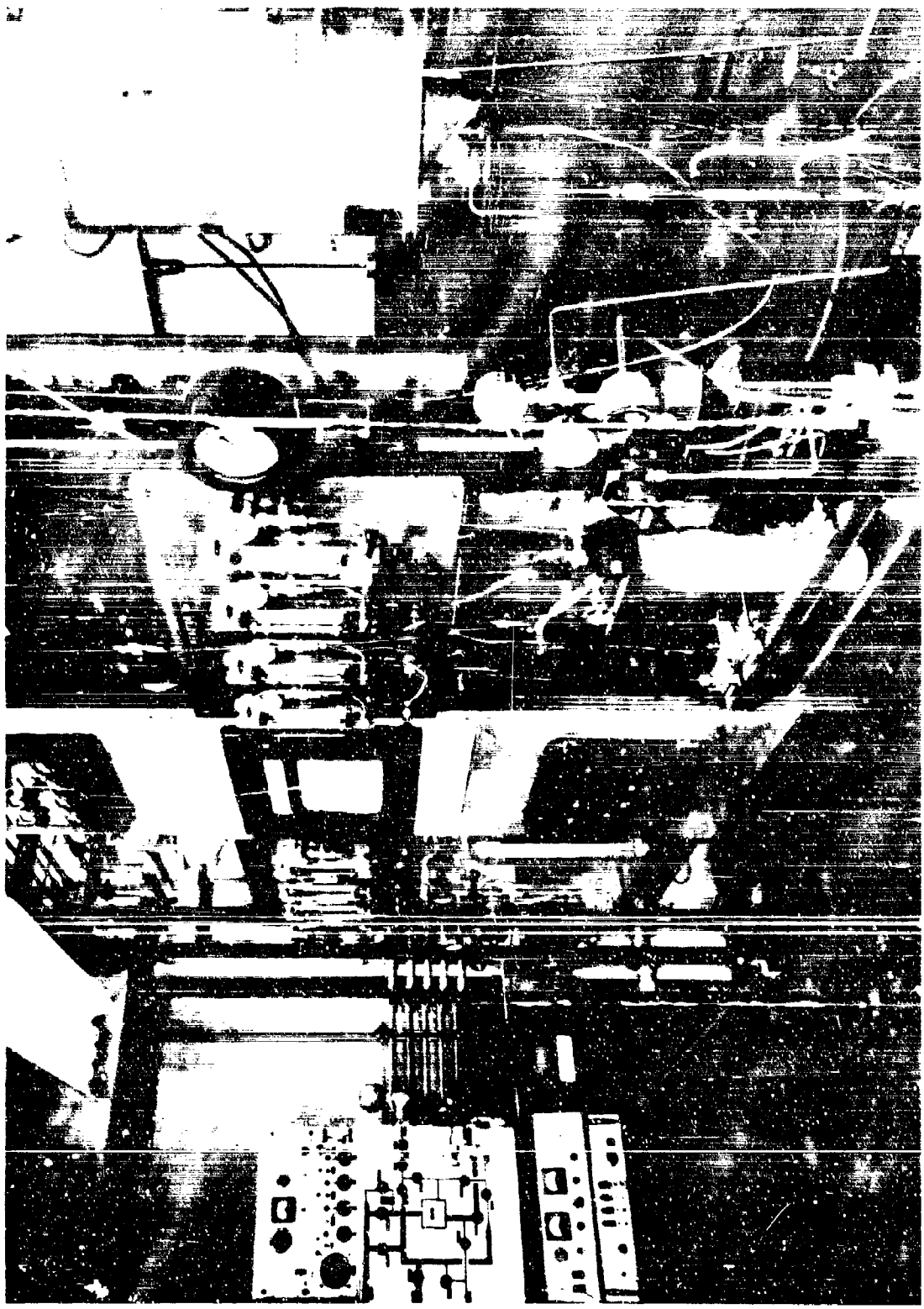


Figure 93. DUAL CATALYTIC REACTOR

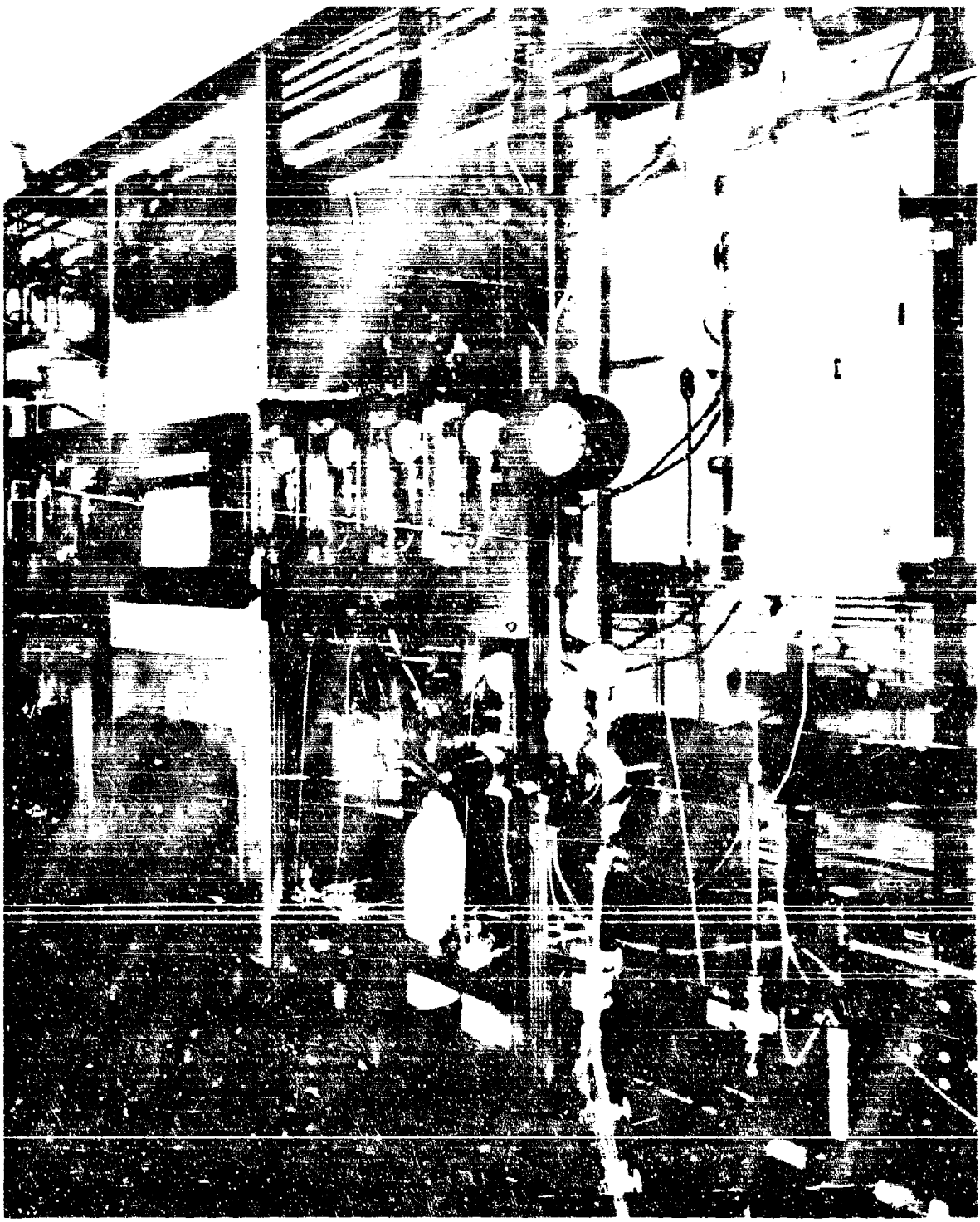


Figure 94. DUAL CATALYTIC REACTOR SHOWING REACTOR NO. 2 AND PRODUCT SAMPLING SYSTEM

Y_p = [illegible]

S_p = Selectivity for product P

ΔH_p = Thermodynamic heat of reaction to form product P

Thermodynamic heats of reaction ΔH_p for the various [illegible] are tabulated in Table 9a. Latent and sensible heats for various substances at various temperatures are shown in Table 9b.

Table 96. THERMODYNAMIC HEATS OF REACTION

Naphthene	Reaction Products	$\Delta H_{R\mu}$, Btu/lb
Diethylcyclohexane	DEB, H_2	622
	Light gas	-600[a]
Dicyclohexyl	Benzene, H_2	1038
	Toluene, pentane	325
	Cyclohexane	-94[a]
	Hexane	-322[a]
	MCH, pentane	-231[a]
	Light gas	22
	Diphenyl, H_2	1080
	Phenylcyclohexane, H_2	540
Decalin	Naphthalene, H_2	950
	Tetralin, H_2	670
	CH + olefin	143
	MCH + olefin	143
	DMCH + olefin	143
	DECH	-110[a]
	Benzene + olefin	800
	Toluene + olefin	800
	EB + olefin	800
	DEB	~700
	Alkyl aromatics	~400
Methyldecalin	Methylnaphthalene, H_2	900
	Methyltetralin, H_2	600
	MCH, olefin	130
	DMCH olefin	130
	DECH, CH_4	-240[a]
	Benzene, olefin + CH_4	600
	Toluene, olefin	730
	DEB, CH_4	550
	Xylene, olefin	700
	Light gas	-230[a]

Table 97. LATENT PLUS SENSIBLE HEATS OF VARIOUS NAPHTHENES

Naphthene	Latent Plus Sensible Heat, Btu/lb[a]						
	Temperature, °F						
	842	932	1022	1112	1202	1293	1340
MCH[b]	707	772	847	920	995	1070	1120
DCH	560	620	687	742	839	891	930
DHN	710	780	850	920	990	1065	1100
MDHN	710	780	850	920	990	1065	1100

a) From 70°F to temperature indicated.
b) From freezing point (-196°F); to convert to 70°F subtract 163 Btu/lb.

REFERENCES

1. "Vaporizing and Endothermic Fuels for Advanced Engine Application", Technical Documentary Report No. APL TDR 64-100 Part I. Contract No. AF 33(657)-11096, Shell Development Company, September 1964.

2. Ibid. Part II, September 1965.

3. Ibid, Part III, September 1966.

4. Allam, U. I. and Vlugter, J. C., J. Inst. of Pet. 52, 385 (1966).

5. Aeronautics and Astronautics, October, 1966, "Case for the Hypersonic Transport".

   a) Miller, Rene H., "HST-Developing the Foundation", p. 30.

   b) Ferri, Antonio, "Goals of Hypersonic", p. 34.

   c) Laidlaw, W. R. and Johnston, E. W., "Developing HST Structural", p. 40.

   d) Simpson, Robert W. and Hursch, John W., "Guiding the Hypersonic Transport", p. 44.

   e) Weber, Richard J., Dugan, James F., Jr., and Luidens, Roger W., "Methane-Fueled Propulsion Systems", p. 48.

   f) Goethert, Bernard H., "Hypersonic Cruise Vehicles in the 'World of Tomorrow'", p. 56.

6. Stroud, J. F. and Miller, L. D., J. Aircraft 3, 548 (1966).

7. Kaufman, L. G., Meckler, L., and Hartofilis, S. A., J. Aircraft 3, 555 (1966).

8. Petersen, R. H., Gregory, T. J., and Smith, C. L., J. Aircraft 3, 398 (1966).

9. Du Pont Fact Sheet, A-51424.

10. Ashby, G. C. and Stone, D. R., J. Spacecraft 4, 277 (1967).

11. Campell, J. B., "The Hypersonic Era", Space/Aeronautics, p. 53, November 1966.

12. Delberger, L. H., "Advanced Interceptor Aircraft", Space/Aeronautics, p. 54, November 1966.

13. Ferri, A., "Review of Scramjet Propulsion Technology", AIAA Third Annual Meeting, Boston, Massachusetts, November 29, 1966. Paper No. 66-286.

14. Kirkwood, T. F., Comments on Future Air Transportation Systems, The Rand Corporation, Santa Monica, Calif., May 1966, (AD 633023).

REFERENCES (CONTD-1)

15. Froment, G. F., "Fixed Bed Catalytic Reactors - Current Design Status", Industrial Engineering Chemistry 59, 18 (1967).

16. Kittrell, J. R. and Mezaki, R., "Reaction Rate Modeling in Heterogeneous Catalysis", Industrial Engineering Chemistry 59, 28 (1967).

17. Rubins, P. M. and Bauer, R. C., Astronautics and Aeronautics, p. 17. May 1967.

18. Wheeler, A., "Advances in Catalysis", III, Academic Press, New York, pp. 249-329 (1951).

19. M[illegible]awa, T. and Pitzer, K. S., J. Am. Chem. Soc. 80, 60 (1958).

20. Benson, "Foundations of Chemical Kinetics", McGraw-Hill, New York, pp. 27-28, 1960.

21. Monsanto Research Corporation, Contract No. AF 33(616)-5799 and AF 33(657)-8193.

22. Fabuss, B. M., Borsanyi, A. S., Duncan, D. A., Kafesjian, R. and Smith, J. O. (Monsanto Research Corp.), "Research on the Mechanism of Thermal Decomposition of Hydrocarbon Fuels", U.S. Air Force, ASD TDR 63-102, Part 2, Contract AF 33(657)-8193, August 1964.

23. Lundberg, W. N., ed. "Antioxidation and Antioxidants", Interscience, New York, Chapter 3, p. 108, (1961).

24. Nixon, A. C. and Henderson, H. T., "Thermal Stability of Endothermic Heat-Sink Fuels", Industrial Engineering Chemistry Product Research and Development 5, 87, March 1966.

25. Bagnetto, L., Phillips Petroleum Company, Technical Documentary Report No. APL-TDR-64-89, Part II, August 1965.

26. McKeown, A. B. and Hibbard, R. B., U.S. NACA RM E 55128, December 28, 1965.

27. Shuler, R. L., Krynitski, J. A., and Carhart, H. W., U.S. Naval Research Laboratory, NRL Report No. 10, September-November 1965.

28. Bially, J. J., Norris, T. A., and Frascati, F. P., Texaco Inc., USAF ASD-TDR-64-83, July 1964.

29. Elsey, P. G., Anal. Chem. 31, 869-, (1959).

30. Zengel, A. E., "A Comparison of the Capabilities of a Fuel Coker and the Minex Heat Exchanger of Determining Hydrocarbon Fuel Thermal Stability", Technical Report AFAPL-TR-64-154, Air Force Aero Propulsion Laboratory Research and Technology Division, Air Force Systems Command, Wright-Patterson Air Force Base, Ohio, March 1965.

REFERENCES (CONTD-2)

31. Lusebrink, T. R. and Sorem, S. S., "Symposium on Jet Fuels", ACS Division of Pet. Chem. Preprints, New York Meeting, September 1960.

32. Lusebrink, T. R., Shell Development Company, ASD-TR-61-687, Contract No. AF 33(616)-7667.

33. Kutzko, G., TDR ASD-TDR, Part II, pp. 62-920, General Electric Company, January 1964.

34. White, D. R., "Density Induction Times Behind Shock Waves in Very Lean Mixtures of D_2, H_2, C_2H_2, and C_2H_4 with O_2", ARL 65-274, Contract AF 33(657)-7945, 26 pp., December 1965.

35. Skinner, G. B. and Ruehrwein, R. A., J. Phys. Chem. 63, 1736-42 (1959).

36. Asaba, T., et al, "Ninth Symposium on Combustion" Academic Press, New York, p. 193, 1963.

37. Bradley, V. N., "Shock Waves in Chemistry and Physics", John Wiley, New York, pp. 88-89, 1962.

38. Tsang, W., J. Chem. Phys. 44, 4283 (1966).

39 "A.I.Ch.E. Physical Property Estimation System", Volume I: Report, 1965, American Institute of Chemical Engineers, 345 East 47 Street, New York, New York 10017.

40. Whitney, D. C., Shell Development Company, Technical Report No. 363-66.

41. "Technical Data Book - Petroleum Refining", American Petroleum Institute, Division of Refining, 1271 Avenue of the Americas, New York, 1966.

42. Reid, R. C. and Sherwood, T. K., "The Properties of Gases and Liquids", Second Edition, McGraw-Hill, New York, 1966.

43. Redlich, O. and Kwong, J. N. S., Chem. Rev. 44, 233 (1949).

44. Guggenheim, E. A., J. Chem. Phys. 13, 253 (1935).

45. Hirschfelder, J. O., Curtiss, C. F., and Bird, R. , "Molecular Theory of Gases and Liquids", John Wiley and Sons, Inc., New York, 1954. (Also notes added in second printing, 1963.)

46. Stiel, L. I. and Thodos, G., J. Chem. Eng. Data 7, 234 (1962).

47. Jossi, J. A., Stiel, L. I., and Thodos, G., A.I.Ch.E. Journal 8, (1), 59 (1962).

48. Hirschfelder, J. O., J. Chem. Phys. 26, 282 (1957).

REFERENCES (CONTD-3)

49. Lambert, J. D., et al, Proc. Royal Soc. 231, 280 (1955).

50. Robbins, L. A. and Kingrea, C. L., Proc. API, 42, (III), 52 (1962).

51. American Petroleum Institute Research Project 44, "Selected Values of Properties of Hydrocarbons and Related Compounds", Agricultural and Mechanical College of Texas, College Station, Texas.

52. "Selected Values of Properties of Chemical Compounds", Manufacturing Chemists Association Research Project, Texas A and M University, College Station, Texas, 1965.

53. "Technical Data Book: Petroleum", Shell Development Company, 1945.

54. Kobe, K. A. and Lynn, K. E., Jr., Chem. Rev. 52, 117 (1953).

55. Lewis, G. N., Randall, M., Pitzer, K. S., and Brewer, L., "Thermodynamics", Second Edition, McGraw-Hill Book Co., Inc. New York, 1961.

56. Edminister, W. C., "Applied Hydrocarbon Thermodynamics", Gulf Publishing Company, Houston, Texas, Chapter 4, 1961.

57. "Technical Data Book: Chemical", Shell Development Company, 1947.

58. "Safety Manual", Second Edition, Shell Development Company, 1962.

59. "Fire-Hazard Properties of Flammable Liquids, Gases and Volatile Solids", NFPA No. 325M-1965 in "National Fire Codes", Vol. 1, 1965-66.

60. "Literature Survey on Vaporizing and Endothermic Fuels for Advanced Engine Application", Shell Development Company, Report S-13979.

BIBLIOGRAPHY[a)]

1. Agapov, G. I., CALCULATION OF THE COEFFICIENTS IN THE G. M. PANCHENKOV EQUATION. Tr., Mosk. Inst. Neftekhim. i Gaz. Prom. No. 51, 186-8 (1964).

2. Agapov, G. I. and Levinter, M. E., CALCULATION OF COEFFICIENTS IN THE EQUATION OF COKE FORMATION ON CATALYSTS. Tr., Mosk. Inst. Neftekhim. i Gaz. Prom, No. 51, 126-8 (1964).

3. Ahern, J. E. and Yankura, G. A., ADVANCED RAMJET CONCEPTS PROGRAM. 1965 VOLUME V - LIQUID METAL FILM COOLED NOZZLE STUDY. Marquardt Corp. Final Report 1 March 31 November 1965, Report No. 25188-Vol-5, AF APL TR-66-49-Vol-5, U.S. Air Force Contract AF 33(615)-2399, June 1966, 60 pp. (AD 3730596). CONFIDENTIAL.

4. Akhmedov, Sh. T., Guseinov, D. A., Mirzoev, B. M., DEHYDROGENATION OF CYMENES TO ISOPROPENYL TOLUENES. Uch. Zap. Azerb. Gos. Univ., Ser. Fiz.-Mat. i Khim. Navk 1961 (6), 59-75; L. A. 61, 1777 (1964); Ref. Zh., Khim. 1963, Abstr. No. 22N60.

5. Aladiev, I. T., HEAT TRANSFER TO LIQUIDS BOILING IN PIPES AND DURING BULK BOILING. Teploenergetika (USSR) 10, 57-61 (1963); Redstone Scientific Information Center Report No. RSIC-530, TT 66-61387, March 1966, 16 pp. (AD 633583).

6. Alchudzhan, A. A., Mantikyan, M. A., Aikazyan A. M., MIXED ADSORPTION CATALYSTS FOR DEHYDROGENATION. III. Pd, Au/SiO_2 AS A CATALYST FOR CYCLOHEXANE DEHYDROGENATION. Izv. Akad. Nauk Arm. SSR, Khim. Nauki 17 (4), 363-74 (1964) (Russ.).

7. Alm, J., THE TRANSFORMATION OF NAPHTHENES ON NICKEL-ZINC OXIDE-TUNGSTEN OXIDE CATALYSTS. Monatsber. Deut. Akad. Wiss. Berlin 6 (1), 18-22 (1964).

8. Amirkhanov, Kh. I., Alibekov, B. G., Vikhrov, D. I., Kerimov, A. M., ISOCHORIC HEAT CAPACITIES OF SOME ALKANES. Teploenergetika 11 (3), 81-6 (1964).

9. Appeldoorn, J. K., Campion, R. J., Dukek, W. G. Furry, M. J., Tao, F. F., LUBRICITY PROPERTIES OF HIGH-TEMPERATURE JET FUELS. Esso Research and Engineering Co. Quarterly Progress Report No. 1, 15 May-15 August 1965, U.S. Air Force Contract AF 33(615)-2828, August 1965, 43 pp. (AD 472 148).

10. Appeldoorn, J. K., Campion, R. J., Read, C. L., Tao, F. F., LUBRICITY PROPERTIES OF HIGH-TEMPERATURE JET FUELS. Esso Research and Engineering Co. Quarterly Progress Report No. 2, 15 August-15 November 1965, U. S. Air Force Contract AF 33(615)-2828, November 1965, 46 pp. (AD 480 825).

a) This extends the survey of the literature presented in reference 60 (cf preceding page).

11. Appeldoorn, J. K., Campion, R. J., Feng, I-M., Tao, F. F., LUBRICITY PROPERTIES OF HIGH-TEMPERATURE JET FUELS. Esso Research and Engineering Co. Quarterly Progress Report No. 3, 15 November 1965-15 February 1966, U.S. Air Force Contract AF 33(615)-2828, February 1966, 49 pp. (AD 481 937).

12. Allam, M. I. and Vlugter, J. C., AROMATIZATION OF KEROSINE FRACTIONS CONTAINING BICYCLONAPHTHENES. Part I. Thermodynamics Considerations. J. Inst. Pet. 52, 385 (1966). Part II. Conversions of Decalin and Tetralin Over a Platinum Reforming Catalyst, ibid 53, 43, 1967.

13. Ashby, G. C. and Stone, D. R., (NASA Langley Research Center, Hampton, Va.) AERODYNAMIC EFFECT OF VOLUME ADDITION TO A HIGH L/D WING/BODY AT MACH 6.0., J. Spacecraft 4, 277 (1967).

14. Aucoin, P. J., Jr., FUNDAMENTAL RELATIONS IN THE SUPERSONIC FLOW OF A PERFECT GAS AND THE METHOD OF CHARACTERISTICS CALCULATIVE TECHNIQUE. Marquardt Corp. Report No. 5278, U.S. Air Force Contract AF 33(657)-10796, March 1963, 54 pp. (AD 481 391).

15. Avbel, J. A., PROPOSED REVISION TO MIL-E-5007B AND MIL-E-5009B STANDARDIZED METHOD OF CONDUCTING CONTAMINATED FUEL TESTS. U.S. Naval Air Engineering Center, Aeronautical Engine Laboratory. Final Report. Report No. NAEC-AEL-1791 February 1965, 13 pp. (AD 456 891).

16. Aviatsionnyi Institut, Moscow. Trudy (USSR) No. 157, 102 pp. 1964; Parandjuk, S., AIRBREATHING PROPULSION TECHNOLOGY: COMPILATION OF ABSTRACTS. U.S. Library of Congress, Aerospace Technology Division Report No. 2, Report No. ATD-U-64-116, TT 66-61113, December 1964, 40 pp. (AD 631 642).

17. Backman, K. C., TEST RESULTS FROM THE ESSO HEAT TRANSFER UNIT FOR FA-S-1, FA-S-2A AND RAF 176-64. Esso Research and Engineering Co., Products Research Division Final Report, SST 65-6, U.S. Federal Aviation Agency Contract FA-SS-65-5, May 1965, 123 pp. (AD 4792812).

18. Bader, F. and Bunt, E. A., RAMJET TECHNOLOGY. SECTION ON FLOW PROCESSES AND ENGINE PERFORMANCE. CHAPTER 5. COMBUSTOR FLOW AND ENGINE PERFORMANCE. Johns-Hopkins University, Applied Physics Laboratory Technical Memo, Report No. TG-610-5, U.S. Navy Contract NOw-62-0604-C, November 1964, 90 pp. (AD 631 817).

19. Badger, G. M., Jolad, S. D., Spotswood, T. M., FORMATION OF AROMATIC HYDROCARBONS AT HIGH TEMPERATURES. XX. PYROLYSIS OF NAPHTHALENE-1-"C. Australian J. Chem. 17 (7), 771-7 (1964).

20. Badger, G. M., Donnelly, J. K., Spotswood, T. M., FORMATION OF AROMATIC HYDROCARBONS AT HIGH TEMPERATURES. XXII. PYROLYSIS OF PHENANTHRENE. Australian J. Chem. 17 (10), 1138-46 (1964).

21. Badger, G. M., Kimber, R. W. L., Nowotny, J., THE FORMATION OF AROMATIC HYDROCARBONS AT HIGH TEMPERATURES. XVI. THE PYROLYSIS OF TETRALIN-1-^{14}C. Australian J. Chem. 15, 616-25 (1962).

22. Bagretto, L., THERMAL STABILITY OF HYDROCARBON FUELS. Phillips Petroleum Co. Quarterly Progress Report No. 7, 1 June-31 August 1965, Report No. 4236-65A, U.S. Navy Contract AF 33(657)-10639, September 1965, 64 pp. (AD 475 006).

23. Bagnetto, L. and Schirmer, R. M., THERMAL STABILITY OF HYDROCARBON FUELS. Phillips Petroleum Co. Progress Report No. 9, 1 December 1965-28 February 1966, Report No. 43 90-66R, U.S. Air Force Contract AF 33(657)-10639, March 1966, 81 pp. (AD 485 292).

24. Balenkova, E. S., Alybina, A. Yu., Kochnova, G. P., Khromov, S. I., Kazanskii, B. A., CATALYTIC CONVERSIONS OF CYCLO UNDECANE IN THE PRESENCE OF NICKEL CATALYSTS. Nefte-Khimiya 4 (1), 16-20 (1964).

25. Barningham, R. C., COMPONENT PROPULSION PROGRAM FOR FUTURE HIGH-PERFORMANCE STRATEGIC AIRCRAFT. VOLUME II. ENGINE/AIRFRAME INTEGRATION STUDIES. Pratt and Whitney Aircraft Semiannual Report No. 1, 1 August 1965-31 January 1966, Report No. PWA-2767-Vol-2, U.S. Air Force Contract AF 33(657)-14903, February 1966, 33 pp. (AD 369 613) (REPORT CLASSIFIED SECRET).

26. Barningham. R. C., COMPONENT PROPULSION PROGRAM FOR FUTURE HIGH-PERFORMANCE STRATEGIC AIRCRAFT* VOLUME XI. TURBINE COOLING. Pratt and Whitney Aircraft Co. Semi-annual Report No. 1, 1 August 1965-31 January 1966, Report No. PWA-2767-Vol-11, U.S. Air Force Contract AF 33(657)-14903, February 1966, 16 pp. (AD 369 517) (CONFIDENTIAL).

27. Barningham, R. C., COMPONENT PROPULSION PROGRAM FOR FUTURE HIGH-PERFORMANCE STRATEGIC AIRCRAFT. VOLUME I. SUMMARY. Pratt and Whitney Aircraft Semi-annual Report No. 2, 1 February-31 July 1966, Report No. PWA-2863-Vol-1, U.S. Air Force Contract AF 33(657)-14903, August 1966, 61 pp. (AD 375 350 L) (CONFIDENTIAL).

28. Barningham, R. C., COMPONENT PROPULSION PROGRAM FOR FUTURE HIGH-PERFORMANCE STRATEGIC AIRCRAFT. VOLUME II. ENGINE/AIR FRAME INTEGRATION STUDIES. Pratt and Whitney Aircraft Semi-annual Report No. 2, 1 February-3 July 1966 Report No. PWA-2863-Vol-2, U.S. Air Force Contract AF 33(657)-14903, August 1966, 42 pp. (AD 375 351 L) (SECRET).

29. Barningham, R. C., COMPONENT PROPULSION PROGRAM FOR FUTURE HIGH-PERFORMANCE STRATEGIC AIRCRAFT. VOLUME IV. ENGINE DESIGN STUDIES. Pratt and Whitney Aircraft Semi-annual Report No. 2, 1 February-31 July 1966, Report No. PWA-2863-Vol-4, U.S. Air Force Contract AF 33(657)-14903, August 1966, 32 pp. (AD 375 353 L) (CONFIDENTIAL).

30. Barningham, R. C., COMPONENT PROPULSION PROGRAM FOR FUTURE HIGH-PERFORMANCE STRATEGIC AIRCRAFT. VOLUME IX. BURNERS. Pratt and Whitney Aircraft Semiannual Report No. 2, 1 February-31 July 1966, Report No. PWA-2863, Vol. 9, U.S. Air Force Contract AF 33(657)-14903, August 1966, 54 pp. (AD 375 557L) (REPORT CLASSIFIED CONFIDENTIAL).

31. Barningham, R. C., COMPONENT PROPULSION PROGRAM FOR FUTURE HIGH-PERFORMANCE STRATEGIC AIRCRAFT. VOLUME XI. TURBINE COOLING. Pratt and Whitney Aircraft Semiannual Report No. 2, 1 February - 31 JULY 1966, Report No. PWA-2863-Vol. 11, U.S. Air Force Contract AF 33(657)-14903, August 1966, 10 pp. (AD 375 359L) (REPORT CLASSIFIED CONFIDENTIAL).

32. Barningham, R. C., COMPONENT PROPULSION PROGRAM FOR FUTURE HIGH-PERFORMANCE STRATEGIC AIRCRAFT. VOLUME XIV. INFRARED SUPPRESSION. Pratt and Whitney Aircraft Semiannual Report No. 2, 1 February - 31 July 1966, Report No. PWA-2863, Vol. 14, U.S. Air Force Contract AF 33(657)-14903, August 1966, 24 pp. (AD 375 362L) (REPORT CLASSIFIED SECRET).

33. Barningham, R. C., COMPONENT PROPULSION PROGRAM FOR FUTURE HIGH-PERFORMANCE STRATEGIC AIRCRAFT. VOLUME XVIII. DEMONSTRATOR ENGINE. Pratt and Whitney Aircraft Semiannual Report No. 2, 1 February-31 July 1966, Report No. PWA-2863, Vol. 18, U.S. Air Force Contract AF 33(657)-14903, August 1966, 100 pp. (AD 375 366L) (REPORT CLASSIFIED CONFIDENTIAL).

34. Barusch, M. R. and MacPherson, J. H. (California Research Corp.), ENGINE FUEL ADDITIVES. Advan. Petrol. Chem. Refining 10, 456-546 (1965).

35. Beech, J. C. and Ziebland, H., HEAT TRANSFER TO KEROSINE, D. ENG. R.D. 2495, AT SUPERCRITICAL AND SUBCRITICAL PRESSURES. Explosives Research and Development Establishment, Waltham Abbey (England) Report ERDE-5R63, May 1963, 1 Vol. (AD 420 775).

36. Begg, H. A., Chapman, C. E., Brady, J. F., SPACEPLANE. PROPULSION AND PROPULSION DESIGN. General Development Corp., Technical Status Report No. ZPM59-011, February 1961, 1 Vol. (AD 342 997L) (REPORT CLASSIFIED SECRET).

37. Bergles, A. E. and Rohsenow, W. M. (Massachusetts Inst. of Technology), THE DETERMINATION OF FORCED-CONVECTION SURFACE-BOILING HEAT TRANSFER. J. Heat Transfer 86, (3), 365-72 (1964); C.A. 61, 10332 (1964).

38. Bernstein, T. N., Maddux, G. E., Engle, R. M., Jr., THE ANALYTICAL DETERMINATION OF THE THERMAL RESPONSE OF A TYPICAL AIRCRAFT STRUCTURE SUBJECTED TO TRANSIENT EXTERNAL HEATING AND COOLING. U.S. Air Force Flight Dynamics Laboratory, Wright-Patterson A.F.B., Final Report 1 July 1964-30 June 1965, Report No. AFFDL-TR-65-219, February 1966, 60 pp. (AD 480 622).

39. Bert, J. A. and Porter, H. R. (California Research Corp.), SURFACTANTS IN JET FUELS - SYMPTOMS, SOURCES, AND SOLUTIONS. Proc. Am. Petrol. Inst. Sect. III 43, 165-72 (1963); C. A. 61, 118-23 (1964).

40. Billig, F. S., A REVIEW OF EXTERNAL BURNING RAMJETS. Johns Hopkins University, Applied Physics Laboratory Final Report No. TG-801, U.S. Navy Contract NOw-62-0604, December 1965, 133 pp. (AD 370 639L) (REF AT CLASSIFIED CONFIDENTIAL).

41. Bishop, P. H. H., Rogers, K. F., Gilbey, D. M., A NEW METHOD FOR THE MEASUREMENT OF HEAT TRANSFER. Great Britain Royal Aircraft Establishment Technical Report No. TR-66040, February 1966, 23 pp. (AD 634 158).

42. Blanchard, G. C., MECHANISM OF MICROBIOLOGICAL CONTAMINATION OF JET FUEL AND DEVELOPMENT OF TECHNIQUES FOR DETECTION OF MICROBIOLOGICAL CONTAMINATION. Melpar, Inc., Final Technical Report, 1 March 1963 - 31 January 1966, Report No. 4019, AFD TDR-64-70-Pt-3, U.S. Air Force Contract AF 33(657)-9186, January 1966, 212 pp. (AD 637 876).

43. Blouri, B., Nubaui, R., Rumpt, P., Padzerski, A., PYROLYSIS OF LONG CHAIN ALIPHATIC HYDROCARBONS. I. THERMAL DECOMPOSITION OF DODECANE WITH FORMATION OF 1-ALKENES. Bull. Soc. Chim. France 1965 (2), 336-41; C. A. 62, 14471 (1965).

44. Bluston, H. S., AN EXPERIMENTAL STUDY OF THE TURBULENT MIXING OF A SUBSONIC AND A SUPERSONIC JET IN A CLOSED DUCT. Polytechnic Institute of Brooklyn, Department of Aerospace Engineering and Applied Mechanics Report No. pibal - 868, AF OSR 65-1794, U.S. Air Force Office of Scientific Research Contract AF-AF OSR-1-63, May 1965, 56 pp. (AD 624 551)

45. Bolshakov. G. F., INSOLUBLE RESIDUES FORMING DURING THE HEATING OF JET FUELS. Khimiya i Tekhnologiya Topliv i Masel (USSR) 8, No. 5, 55-7 (1963) (U.S. Air Force Translation No. ftd-TT-65-1064; TT 66-600004) (AD 625 143).

46. Borne, U., Homann, K. A. and Wagner, H. G. (Gottingen University), CARBON FORMATION IN PREMIXED FLAMES. Tenth Sumposium (Intl) on Combustion, Pittsburgh: The Combustion Institute, 1965, pp. 503-512.

47. Botteri, B. P., Cretcher, R. E., Fultz, J. R., Lander, H. R., A REVIEW AND ANALYSIS OF THE SAFETY OF JET FUEL. U.S. Air Force Aero Propulsion Laboratory, Wright-Patterson AFB Technical Report June-October 1965, Report No. AF APL-TR-66-9, March 1966, 63 pp. (AD 373 633) (REPORT CLASSIFIED CONFIDENTIAL).

48. Bollinger, L. E. (Ohio State University), DETONABILITY OF COMBUSTIBLE MIXTURES. Presented at the Annual National Conference on Environmental Effects on Aircraft and Propulsion Systems (5th), Princeton, N.J., 20-22 September 1965; AFOSR 66-0342, U.S. Air Force Office of Scientific Research Contract AF-AFOSR-203-65, 1965, 34 pp. (AD 630 641).

49. Boreskova, E. G., Topchieva, K. V., Piguzova, L. I., CATALYTIC ACTIVITY OF SYNTHETIC ZEOLITES IN THE CRACKING OF CUMENE. Kinetika i Kataliz 5 (5), 903-9 (1964); C. A. 62, 9036 (1965).

50. Boreskova, E. G., Lygin, V. I., Topchieva, K. V., NATURE OF ACTIVE CENTERS IN THE CRACKING OF CUMENE CATALYZED BY DECATIONIZED ZEOLITES. Kinetika i Kataliz 5 (6), 11 15-8 (1964); C. A. 62, 9037 (1965).

51. Brizendine, J. C., FUTURE TRANSPORTS. Douglas Aircraft Company, AIAA Paper No. 66-820, AIAA Third Annual Meeting, Boston, Massachusetts, November 29-December 2, 1966.

52. Brodskii, A. M., Lavrovskii, K. P., Rumyantsev, A. N., Timkin, V. N., Fish, Yu. L., PRODUCTION OF HIGHER α-OLEFINS BY HIGH-SPEED CONTACT CRACKING OF PARAFFINIC PETROLEUM PRODUCTS. Neftekhimiya 4 (6), 880-7 (1964); C. A. 62, 8906 (1965).

53. Brossard, J., DETONATION AS A SHOCK WAVE FOLLOWED BY A COMBUSTION WAVE. Compt. Rend. Congr. Natl. Soc. Savantes, Sect. Sci. 87, 339-51 (1962) (Pub. 1963) (in French); C. A. 61, 14456 (1964).

54. Brown, M. L. and Campbell, R. C., APPLIED RESEARCH INVESTIGATION OF THE SUPERSONIC/HYPERSONIC COMBUSTION RAMJET ENGINE. Marquardt Corp. Final Summary Report, 1 January - 31 December 1962, A SD-TDR63-590, U.S. Air Force Contract AF 33(657)-8491, December 1963, 480 pp. (AD 345 914) (REPORT CLASSIFIED SECRET).

55. Brown, M. L., SUPERSONIC COMBUSTION RAMJET ENGINE PROGRAM. Marquardt Corp. Monthly Letter Progress Report for January 1965, Report No. LR-275-10M, U. S. Air Force Contract AF 33(657)-8491, February 1965, 11 pp. (AD 363649)(REPORT CLASSIFIED CONFIDENTIAL).

56. Brown, M. L. Woodgritt, K. E., Ozawa, R. I., APPLIED RESEARCH AND ADVANCED TECHNOLOGY FOR THE SUPERSONIC COMBUSTION RAMJET FOR 1964. PART I. DESIGN AND ANALYSIS, FUEL INJECTION AND COMBUSTION, NOZZLES, STRUCTURES, AND CONTROL SYSTEM STUDIES. Marquardt Corp. Final Report No. 6087, APL-TR-65-15-Pt. 1, U.S. Air Force Contract AF 33(615)-1469, April 1965, 615 pp. (AD 359 464) (REPORT CLASSIFIED CONFIDENTIAL).

57. Buchmann, O. A., EXPLORATORY DEVELOPMENT OF HIGH-TEMPERATURE HEAT EXCHANGERS. Garrett Corp. AiResearch Mfg. Division Interim Engineering Progress Report No. 3. 1 January-31 March 1966, Report No. 66-0482, RTDIR-3084, Vol. 3, U.S. Air Force Contract AF 33(615)-2753, March 1966, 95 pp. (AD 485 344).

58. BUNT, E. A., RAMJET TECHNOLOGY, SECTION ON FLOW PROCESSES AND ENGINE PERFORMANCE. CHAPTER 2, BASIC ADIABATIC THEORY. Applied Physics Laboratory, Johns Hopkins University, TG-610-2, U.S. Navy Contract NOw-62-0604c, October 1964, 92 pp. (AD 607 979).

59. Burnette, T. D., Campbell, R. C., Woodgrift, K. E. (Marquardt Corp.), TEST RESULTS ON SCRAMJETS. Presented at the AIAA/ASD (AFSC) Vehicle Design and Propulsion Meeting on November 5, 1963 at Dayton Ohio; Marquardt Corp. Report No. 6015, U.S. Air Force Contract AF 33(657)-10795, December 1963, 22 pp. (AD 345 763) (REPORT CLASSIFIED CONFIDENTIAL).

60. Campbell, E. S., Heinen, F. J., Schalit, L. M. (New York Univ.), A THEORETICAL STUDY OF FLAME PROPERTIES AS A FUNCTION OF THE CHARACTERISTICS OF FLAME GASES. Philosophical Transactions of the Royal Society of London ser. A, 259, No. 1101, 355-89, (April 21 1966); AFOSR-66-1728, U.S. Air Force Contract AF 49(638)-169, July 1965, 38 pp. (AD 638 707).

61. Caras, G. J., SUPERSONIC COMBUSTION: A BIBLIOGRAPHY. Redstone Scientific Information Center Report No. RSIC-520, February 1966, 54 pp. (AD 375 627) (REPORT CLASSIFIED SECRET).

62. Chaulin, P., Ravel, M., Gozlan, A., EXPERIMENTAL AND DESIGN STUDIES FOR TURBO-RAMJET COMBINATION ENGINE. VOLUME 1 - SPECIFICATIONS AND PERFORMANCE. Polarid Electronics Corp. Final Report No. 5147/NIOBE-4/29/Z, AF APL TR-66-34-Vol-1, U.S. Air Force Contract AF 61(052)-750, January 1966, 50 pp. (AD 486 375).

63. Chaulin, P., Ravel, M., Gozlan, A., EXPERIMENTAL AND DESIGN STUDIES FOR TURBO-RAMJET COMBINATION ENGINE. VOLUME II - CALCULATION ANALYSIS. Nord Aviation (France) Final Report nos. 5148/NIOBE-4/30/Z, 5149/NIOBE-4/31/Z, AF APL TR-66-34-Vol. 2, U.S. Air Force Contract AF 61(052)-750, January 1966, 138 pp. (AD 486 376).

64. Chaulin, P., Ravel, M., Gozlan, A., EXPERIMENTAL AND DESIGN STUDIES FOR TURBO-RAMJET COMBINATION ENGINE. VOLUME III - DATA. Nord Aviation (France) Final Report nos. 5150/NIOBE-4/32/Z, 5151/NIOBE-4/33/Z, AFAPL TR-66-Vol. 3, U.S. Air Force Contract AF 61(052)-750, January 1966, 80 pp. (AD 486 377).

65. Chaulin, P., Ravel, M., Gozlan, A., EXPERIMENTAL AND DESIGN STUDIES FOR TURBO-RAMJET COMBINATION ENGINE. VOLUME IV - CALCULATED RESULTS. Nord Aviation (France) Final Report nos. 5152/NIOBE-4/34/Z, 5153/NIOBE-4/35/Z, AFAPL TR-66-34-Vol. 4, U.S. Air Force Contract AF 61(052)-750, January 1966, 175 pp. (AD 486 378)

66. Chaulin, P., Ravel, M., Gozlan, A., EXPERIMENTAL AND DESIGN STUDIES FOR TURBO-RAMJET COMBINATION ENGINE. VOLUME V - COMBUSTION-TEST INSTALLATION. Nord Aviation (France) Final Report no. 5154/NIOBE-4/36/Z, AFAPL TR-66-34-Vol. 5, U.S. Air Force Contract AF 61(052)-750, January 1966, 66 pp. (AD 484 774).

67. Chaulin, P., Ravel, M., Gozlan, A., EXPERIMENTAL AND DESIGN STUDIES FOR TURBO-RAMJET COMBINATION ENGINE. VOLUME VI - COMBUSTION TESTS AT LES GATINES. Nord Aviation (France) Final Report no. 5155/NIOBE-4/37/Z, AFAPL TR-66-34-Vol. 6, U.S. Air Force Contract AF 61(052)-750, January 1966, 127 pp. (AD 484 775).

68. Chaulin, P., Ravel, M., Gozlan, A., EXPERIMENTAL AND DESIGN STUDIES FOR TURBO-RAMJET COMBINATION ENGINE. VOLUME VII - COMBUSTION TESTS AT SACLAY. Nord Aviation (France) Final Report no. 5156/NIOBE-4/38/Z, AFAPL TR-66-34-Vol. 7, U.S. Air Force Contract AF 61(052)-750, January 1966, 90 pp. (AD 484 776).

69. Chertkov, Ya. B., Marinchenko, N. I., Zrelov, V. N., A METHOD FOR THE ANALYSIS OF MICROIMPURITIES AND DEPOSITS IN FUELS OF THE MEDIUM BOILING RANGE. Neftepererabotka i Neftekhim., Nauchn.-Tekhn. Sb. 1963 (11), 16-18; C. A. 61, 1680 (1964).

70. Cheng, H., INTENSIFICATION EFFECT OF ULTRASONIC WAVES ON THE HEAT TRANSFER PROCESS BETWEEN LIQUIDS OUTSIDE AND INSIDE THE TUBES. Wu Li Hsueh Pao (Chinese People's Republic) 20, 368-73 (1964); U.S. Air Force Translation Report No. FTD-TT-65-1766, TT 66-62287 (AD 639 162).

71. Churchill, A. V., Hagar, J. A., Zengel, A. E., Foster, R. P., Sutphin, E. M., ECONOMICAL FUEL FOR BOTH SST AND SUBSONIC AIRCRAFT IS HERE NOW. SAE Journal, 74, No. 6, 82 (1966).

72. Congelliere, J. T., Frank, H., Odegaard, E. A., 1965 ADVANCED RAMJET CONCEPTS PROGRAM FINAL REPORT. VOLUME III. EJECTOR SCRAMJET ANALYSIS. Marquardt Corp. Technical Report, 1 March 1965 - 1 April 1966, Report No. 25188-Vol. 3, AF APL TR-66-49-Vol. 3, U.S. Air Force Contract AF 33(615)-2399, August 1966, 268 pp. (AD 375 125L) (REPORT CLASSIFIED CONFIDENTIAL).

73. Copley, J. A., A SCALING TECHNIQUE FOR INVESTIGATING HEAT TRANSFER FROM LUMINOUS FLAMES. U.S. Naval Weapons Laboratory Technical Report No. NWL-TR-2058, August 1966, 29 pp. (AD 488 832).

74. Crunnet, J. L., RESULTS OF RAMJET FACILITY MODEL TESTS AT MACH 11. Fluidyne Engineering Corp. Technical Report, AEDC TR-66-138, U.S. Air Force Contract AF 40(600)-1132, July 1966, 50 pp. (AD 484 824).

75. Curran, E. T. and Stull, F. D., THE UTILIZATION OF SUPERSONIC COMBUSTION RAMJET SYSTEMS AT LOW MACH NUMBERS. Research and Technology Division, Air Force Systems Command Report RTD-TDR 63-4097, January 1964, 40 pp. (AD 348 073) (REPORT CLASSIFIED CONFIDENTIAL).

76. Curran, E. T. and Swithenbank (Sheffield University, England), REALLY HIGH SPEED PROPULSION BY SCRAMJETS. Aircraft Engineering (citation incomplete); Sheffield University (England) Scientific Report No. MIC-67, AFOSR 66-1861, U.S. Air Force European Office of Aeronautical Research Contract AF-EOAR-23-65, October 1965, 35 pp. (AD 638 520).

77. Danchevskaya, M. N., Kobozev, N. I., Pankroshev, Yu. A., CATALYSIS WITH METAL VAPORS. III. CATALYTIC CRACKING OF HYDROCARBONS IN ZINC VAPORS. Zh. Fiz. Khim. 38 (2), 442-8 (1964); C. A. 61, 72 (1964).

78. Da Riva, I., DIFFUSION FLAMES AND SUPERSONIC COMBUSTION. Instituto Nacional de Technica Aerospacial, Madrid (Spain) Final Report for 1 April 1963 - 1 April 1965, AFOSR 65-1604, U.S. Air Force European Office for Air Research Contract AF-EOAR-43-63, April 1965, 23 pp. (AD 622 581).

79. Da-Riva, I., Linan, A., Fraga, E., SOME RESULTS IN SUPERSONIC COMBUSTION. Instituto Nacional de tecnica Aerospacial, Madrid. U.S. Air Force Grant AF-EOAR-63-43, 1964, 28 pp. (AD 451 191).

80. Davies, R. A. and Scully, D. B. (Manchester), CARBON FORMATION FROM AROMATIC HYDROCARBONS. II - COMBUSTION AND FLAME 10, No. 2, 165-70 (1966). See also C and F 9, 185 (1965).

81. DeJarnette, H., BIBLIOGRAPHY ON RADIANT HEAT TRANSFER. Martin Co. Report No. ER-13490, May 1964, 24 pp. (AD 459 685).

82. Defense Documentation Center, REACTION KINETICS IN FLAMES. A DDC REPORT BIBLIOGRAPHY. Bibliography for 1959-May 1962, Report No. ARB-10375, May 1962, 62 pp. (AD 446 776).

83. Dobrowolski, A., ANALYSIS OF NONCONSTANT AREA COMBUSTION AND MIXING IN RAMJET AND ROCKET-RAMJET HYBRID ENGINES, Lewis Research Center, Cleveland, Ohio, NASA TN D-3626, October 1966.

84. Doebler, R. L. and Hinton, M. G., Jr., CURRENT STATUS AND CHALLENGE OF AIRBREATHING PROPULSION FOR LAUNCH VEHICLE SYSTEMS. Aerospace Corp. Technical Documentary Report No. TDR-669(6520-10)-1, SSD TR-66-56, U.S. Air Force Contract AF 04(695)-669, March 1966, 33 pp. (AD 372 320) (REPORT CLASSIFIED CONFIDENTIAL).

85. Donovan, A. F., Lawrence, H. R., Goddard, F. E., Gilroth, R. R., HIGH SPEED AERODYNAMICS AND JET PROPULSION. VOLUME VIII. HIGH SPEED PROBLEMS OF AIRCRAFT AND EXPERIMENTAL METHODS. Princeton University Press, Princeton, N.J., 1961, 1013 pp., U.S. Navy Contract Nonr-03201 (AD 638986).

86. Donovan, M. B., A SURVEY OF STAGNATION POINT HEATING. Boeing Co. Document No. D2-22050, rev. A, January 1963, 75 pp. (AD 444 657).

87. Douglas Aircraft Co., DESIGN CONCEPTS FOR MINIMUM WEIGHT, HIGH PERFORMANCE SUPERSONIC AIRCRAFT STRUCTURES. Monthly letter progress report No. C-25-3273, U.S. Air Force Contract AF 33(657)-8541, September 1962, 11 pp. (AD 458 691L).

88. Douglas Aircraft Co., Inc., DESIGN CONCEPTS FOR MINIMUM WEIGHT HIGH PERFORMANCE SUPERSONIC AIRCRAFT STRUCTURES, VOLUME II. MANUFACTURING. ASD-TDR-63-871, Vol. 2, U.S. Air Force Contract AF 33(657)-8541, September 1963, 170 pp. (AD 454 415L).

89. Douglas Aircraft Co., Inc., DESIGN CONCEPTS FOR MINIMUM WEIGHT HIGH PERFORMANCE SUPERSONIC AIRCRAFT STRUCTURES, VOLUME I. STRUCTURAL DESIGN AND ANALYSIS. Report for 1 April 1962 - 20 November 1963, ASD-TDR-63-871, Vol. 1, U.S. Air Force Contract AF 33(657)-8541, September 1963, 395 pp. (AD 424 377L).

90. Douglas Aircraft Co., DESIGN CONCEPTS FOR MINIMUM WEIGHT, HIGH PERFORMANCE SUPERSONIC AIRCRAFT STRUCTURES. Monthly letter progress report No. C1-25-5207, U.S. Air Force Contract AF 33(657)-8541, November 1963, 3 pp. (AD 458 692L).

91. Douglas Aircraft Co., Inc., DESIGN CONCEPTS FOR MINIMUM WEIGHT HIGH PERFORMANCE SUPERSONIC AIRCRAFT STRUCTURES. VOLUME III. TESTING. Final Report ASD-TDR-63-871, Vol. 3, U.S. Air Force Contract AF 33(657)-8541, May 1964, 379 pp. (AD 444 219L).

92. Drabkina, I. E., Orechkin, D. B., Popova, T. S., EFFECT OF ELEMENTAL SULFUR ON THE STABILITY OF DISTILLATE FUELS. Neftepererabotka i Neftekhim., Nauchn.-Tekhn. Sb. 1964 (2), 14-17; C.A. 61, 9337 (1964).

93. Dugger, G. L., A SUPERSONIC COMBUSTION RAMJET MISSILE (SCRAM) FOR NAVAL MISSIONS. Applied Physics Laboratory, Johns Hopkins University Report No. TG-640, U.S. Navy Contract NOw-62-0604c, January 1965, 137 pp. (AD 364 465) (REPORT CLASSIFIED CONFIDENTIAL).

94. Dwyer, O. E. (Brookhaven National Laboratory), TRANSFER OF HEAT TO FLUIDS FLOWING THROUGH PIPES, ANNULI AND PARALLEL PLATES. Nucl. Sci. Eng. 17, 336-44 (1963); C.A. 61, 2741 (1964).

95. Dukek, W. G. (Esso Research and Engineering Co.), FUELS AND LUBRICANTS FOR THE NEXT GENERATION AIRCRAFT - THE SUPERSONIC TRANSPORT. J. Inst. Petrol. 50 (491), 273-96 (1964); C. A. 62, 12949 (1965).

96. Eglinton, G., Raphael, R. A., Willis, R. G., Zabkiewicz, J. A., REARRANGEMENT OF DIACETYLENES TO AROMATIC COMPOUNDS. J. Chem. Soc. 1964 (August), 2597-603; C.A. 61, 10620 (1964).

97. Erickson, W. D., Williams, G. C., Hottel, H. C., LIGHT-SCATTERING MEASUREMENTS ON SOOT IN A BENZENE-AIR FLAME. Combust. Flame 8 (2), 127-32 (1964); C. A. 61 11474 (1964).

98. Fabuss, B. M., Duncan, D. A., Smith, J. O. (Monsanto Research Corp.) and Satterfield, C. N., EFFECT OF ORGANOSULFUR COMPOUNDS ON THE RATE OF THERMAL DECOMPOSITION OF SELECTED SATURATED HYDROCARBONS. Ind. Eng. Chem., Process Design Develop. 4 (1), 117-22 (1965); C.A. 62, 2697 (1965).

99. Fabuss, B. M., Katesjian, R., Smith, J. O. (Monsanto Research Corp.), THERMAL DECOMPOSITION RATES OF SATURATED CYCLIC HYDROCARBONS. Ind. Eng. Chem., Process Design Develop. 3 (3), 248-54 (1964); C.A. 61, 1731 (1964).

100. Fabuss, B. M., Smith, J. O., Satterfield, C. N. (Monsanto Research Corp.), THERMAL CRACKING OF PURE SATURATED HYDROCARBONS. Advan. Petrol. Chem. Refining 9, 157-201 (1964); C.A. 62, 3863 (1965).

101. Fagan, W. and Leipziger, S., NONUNIFORM COOLING OF A HEAT-GENERATING CYLINDER OR SPHERE, Journal of Heat Transfer, 88C, 257-264 (No. 3), 1966.

102. Faro, I. D. V. and Keirsey, J. L., RAMJET TECHNOLOGY, SECTION ON FLOW PROCESSES AND ENGINE PERFORMANCE. CHAPTER 3B. SUPERSONIC INLETS. Johns Hopkins University, Applied Physics Laboratory Technical Memo, Report No. TG-610-3B, U.S. Navy Contract NOw-62-0604-c, March 1965, 70 pp. (AD 631 872).

103. Faro, I. D. V., RAMJET TECHNOLOGY. SECTION ON FLOW PROCESSES AND ENGINE PERFORMANCE. CHAPTER FOUR. PROPULSION NOZZLES. Johns Hopkins University, Applied Physics Laboratory Technical Memo, Report No. TG-610-4, U.S. Navy Contract NOw-62-0604-c, February 1965, 57 pp. (AD 631 715).

104. Favin, S., IBM 7090 PROGRAM FOR COMPLEX CHEMICAL KINETIC FLOW COMBUSTION. John Hopkins University, Applied Physics Laboratory Report No. TG-456, U.S. Navy Contract NOw-62-0604-c, December 1962, 40 pp. (AD 631 721).

105. Federal Aviation Agency, UNITED STATES SUPERSONIC TRANSPORT PROGRAM. CHRONOLOGY. BRIEF HISTORY RESEARCH CONTRACT SUMMARY. Report No. SST-65-10, July 1965, 48 pp. (AD 468 505).

106. Feldman, L., SOME PRELIMINARY DESIGN APPROACHES TO THE APPLICATION OF THE SUPERSONIC COMBUSTION RAMJET TO THE LOW ALTITUDE RUN-IN PROBLEM. General Applied Science Laboratories, Inc. Technical Report No. TR-579, U.S. Navy Contract SD-149, January 1966, 54 pp. (AD 370 142) (REPORT CLASSIFIED SECRET).

107. Ferri, A., REVIEW OF SCRAMJET PROPULSION TECHNOLOGY, AIAA Paper No. 66-826, AIAA Third Annual Meeting, Boston, Massachusetts, November 29 - December 2, 1966.

108. Ferri, A. and Vaglio-Laurin, R., A REVIEW OF THE WORK PERFORMED AT THE POLYTECHNIC INSTITUTE OF BROOKLYN AEROSPACE INSTITUTE. Polytechnic Institute of Brooklyn Report for 1 September 1957 - 31 August 1963, No. PIB AL-809, AFOSR-5428, U.S. Air Force Contract AF 49(638)-217, September 1963, 34 pp. (AD 621 162).

109. Finefrock, V. H., MICROBIAL CONTAMINATION OF USAF JP-4 FUELS. Air Force Aero Propulsion Laboratory, Research and Technology Division, Air Force Systems Command, Technical Report AFAPL-TR-66-91, August 1966, Wright Patterson Air Force Base, Ohio.

110. Fitch, R. E., SUPERSONIC COMBUSTION EXPERIMENTS IN THE BOEING 44-INCH HOTSHOT WIND TUNNEL. Boeing Company Report No. DN-D2-22125, February 1963, 20 pp. (AD 354 623) (REPORT CLASSIFIED CONFIDENTIAL).

111. Flornes, B. J. and Stroup, K. E., 1964 ADVANCED RAMJET CONCEPTS PROGRAM. VOLUME I. ADVANCED JET COMPRESSION CONCEPTS. Marquardt Corporation Final Report No. 25155, APL-TR-65-32-Vol. 1, U.S. Air Force Contract AF 33(615)-1581, March 1965, 232 pp. (AD 360 320L) (REPORT CLASSIFIED CONFIDENTIAL).

112. Fristrom, R. M., MEASUREMENT OF BURNING VELOCITY A SURVEY. Esso Development Co. Ltd., England Report No. TG-481, U.S. Nave Contract NOw-62-0604-c, April 1963, 50 pp. (AD 631 638).

113. Frolova, V. S., Polataiko, R. I., Skarchenko, V. K., Musienko, V. P., Galich, R. I., DEHYDROGENATION OF HEXANE ON CHROMIA-ZINC OXIDE CATALYSTS. Neft. i Gaz. Prom., Inform. Nauchn.-Tekhn. Sb. 1964 (3), 54-5; C.A. 62, 2647 (1965).

114. Fromm, E. A., Quigg, H. T., Schirmer, R. M., EFFECT OF JP-5 SULFUR CONTENT ON HOT CORROSION OF SUPERALLOYS IN MARINE ENVIRONMENT. Phillips Petroleum Co., Research Division Progress Report No. 2, Report No. 4319-66R, U.S. Navy Contract Now-65-0310, January 1966, 62 pp. (AD 479 488).

115. Froning, H.D., SCRAM PROPULSION STUDY. VOLUME I. (SUMMARY). Douglas Aircraft Company Final Report No. SM-47718-Vol. 1, U.S. Navy Contract NOw-64-0434F, September 1964, 79 pp. (AD 364 498) (REPORT CLASSIFIED CONFIDENTIAL).

116. Galich, P. N., Gutyrya, V. S., Neimark, I. E., Egorov, Yu. P., Ilin, V. G., Golubchenko, I. T., Frolova, V. S., CATALYTIC REACTIONS ON ZEOLITES. Neftekhim., Akad. Nauk Ukr. SSR, Inst. Khim. Vysokomolekul. Soedin. 1964, 13-24; C.A. 62, 8905 (1965).

117. Gazley, C., Jr., Hartnett, J. P., Eckert, E. R. G., PROCEEDINGS OF THE ALL-SOVIET UNION CONFERENCE ON HEAT AND MASS TRANSFER (2D), VOLUME I. Rand Corporation Report No. R-451-PR-Vol. 1, U.S. Air Force Contract AF 49(638)-1700, August 1966, 377 pp. (AD 637 690).

118. General Applied Science Laboratories, Inc., ANALYTICAL AND EXPERIMENTAL EVALUATION OF HYPERSONIC RAMJET. Final Summary Report, No. TR 355, January 1962-March 1963, ASD-TDR-63-591, U.S. Air Force Contract AF 33(657)-7911, April 1963, 255 pp. (AD 345 944) (REPORT CLASSIFIED CONFIDENTIAL).

119. General Applied Science Laboratories, Inc., ANALYTICAL AND EXPERIMENTAL EVALUATION OF THE SUPERSONIC COMBUSTION RAMJET. Final Summary Report No. TR 435, APL-TDR 64-68, U.S. Air Force Contract AF 33(657)-10463, May 1964, 226 pp. (AD 352 049) (REPORT CLASSIFIED CONFIDENTIAL).

120. General Applied Science Laboratories, ANALYTICAL AND EXPERIMENTAL INVESTIGATION OF ADVANCED AIR-BREATHING ENGINES. Final Summary Report No. GASL-TR-479, U.S. Air Force Contract AF 33(615)-1575, April 1965, 164 pp. (AD 360 045) (REPORT CLASSIFIED CONFIDENTIAL).

121. General Dynamics Astronautics, AEROSPACEPLANE PROPULSION SYSTEM/VEHICLE INTEGRATION STUDY. EVALUATION OF PRATT AND WHITNEY AIRCRAFT TURBORAMJET ENGINES. Final Report No. 63-1069, Volume 4, U.S. Air Force Contract AF 33(657)-10162, October 1963, 234 pp. (AD 345 604L) (REPORT CLASSIFIED SECRET).

122. General Dynamics Astronautics, AEROSPACEPLANE PROPULSION SYSTEM/VEHICLE INTEGRATION STUDY. EVALUATION OF THE GENERAL ELECTRIC COMPANY TURBO-RAMJET ENGINES. Final Report No. 63-1069, Volume 5, U. S. Air Force Contract AF 33(657)-10162, October 1963, 126 pp. (AD 345 603L) (REPORT CLASSIFIED SECRET).

123. General Electric Co., ANALYTICAL AND EXPERIMENTAL EVALUATION OF THE SUPERSONIC COMBUSTION RAMJET ENGINE. VOLUME III. COMPONENT EVALUATION. Final Technical Report June 1964-June 1965, Report No. R65FPD184-Vol. 3, AF APL TR-65-103-Vol. 3, U.S. Air Force Contract AF 33(615)-1586, December 1965, 272 pp. (AD 367 775L) (REPORT CLASSIFIED CONFIDENTIAL).

124. General Electric Co., ANALYTICAL AND EXPERIMENTAL EVALUATION OF THE SUPERSONIC COMBUSTION RAMJET ENGINE. VOLUME I. PROPULSION SYSTEM AND APPLICATIONS INVESTIGATIONS. Final Technical Report June 1964-June 1965, Report No. R65FPD184-Vol. 1, AF APL TR-65-103-Vol. 1, U.S. Air Force Contract AF 33(615-1586, December 1965, 160 pp. (AD 367 773L) (REPORT CLASSIFIED CONFIDENTIAL).

125. General Electric Co., ANALYTICAL AND EXPERIMENTAL EVALUATION OF THE SUPERSONIC COMBUSTION RAMJET ENGINE. VOLUME II. COMPONENT EVALUATION. Final Technical Report June 1964-June 1965, Report No. 65FPD-184-Vol. 2, AF APL TR-65-103-Vol. 2, U.S. Air Force Contract AF 33(615)-1586, December 1965, 370 pp. (AD 367 774L) (REPORT CLASSIFIED CONFIDENTIAL).

126. Germain, J. E., Ostyn, M., Beufils, J. P., TEXTURE OF CATALYSTS BY GAS ABSORPTION. II. Pt-Al_2O_3 CATALYSTS, J. Chim. Phys. 62 (1), 32-6 (1965). C.A. 62, 15471 (1965).

127. Gilks, J. H. (I.C.I. Ltd), ANTIOXIDANTS FOR PETROLEUM PRODUCTS. J. Inst. Petrol. 50 (491), 309-18 (1964); C.A. 62, 12950 (1965).

128. Glenny, R. J. E., SOME MATERIALS AND COOLING TECHNIQUES APPLICABLE TO AIR-BREATHING ENGINES AT HIGH FLIGHT SPEEDS. American Institute of Aeronautics and Astronautics Paper No. 65-743, New York, 1965.

129. Gluckstein, M. E., Hu, J., Lehikoinen, U.A., IMPROVED HEAT FLUX HYDROCARBON FUELS. Ethyl Corp. Quarterly Progress Report No. 3, Report No. GR-65-60, U.S. Army Contract DA-18-035-AMC-285(A), April 1966, 52 pp. (AD 372 019) (REPORT CLASSIFIED CONFIDENTIAL).

130. Gordon, J. S., COMBUSTION GAS EMITTED RADIATION AND CHEMILUMINESCENCE PHENOMENA. Astrosystems International, Inc. Annual Technical Status Report 15, April 1965-15 April 1966, Report No. TR-64002-F2, AFOSR 66-1366, U.S. Air Force Contract AF 49(638)-1400, May 1966, 52 pp. (AD 635 161).

131. Hamelin, G. L., INVESTIGATION OF THE MIXING OF COAXIAL HETEROGENEOUS GAS JETS AS APPLIED TO SUPERSONIC COMBUSTION. Master's Thesis, U. S. Air Force Institute of Technology, Wright-Patterson AFB School of Engineering Report No. GA/ME/65-2, August 1965, 78 pp. (AD 622035).

132. Hartill, W. R. (Marquardt Corp.), DESIGN TECHNIQUE AND TEST RESULTS OF A QUADRIFORM LOW DRAG SCRAMJET INLET. Presented at the AIAA Propulsion Specialists Conference U. S. Air Force Academy, Colorado Springs, Colo., 15 June 1965; Marquardt Corp. Report No. MP-1334, U. S. Air Force Contract AF 33(657)-8491, 1965, 21 pp. (AD 372899) (REPORT CLASSIFIED CONFIDENTIAL).

133. Hartill, W. R., ANALYTICAL AND EXPERIMENTAL INVESTIGATION OF A SCRAMJET INLET OF QUADRIFORM SHAPE. Marquardt Corp. Technical Report No. 6096, APL-TR-65-74, U. S. Air Force Contract AF 33(657)-8491, August 1965, 109 pp. (AD 364159L)(REPORT CLASSIFIED CONFIDENTIAL).

134. Hawkins, R. and Fox, M. D., REAL GAS EFFECTS RELEVANT TO THE PERFORMANCE OF A KEROSINE FUELLED RAMJET. Supersonic Flow, Chem. Process. Radiative Transfer., 1964, 113-36.

135. Hawthorn, R. D. and Nixon, A. C. (Shell Development) SHOCK TUBE IGNITION DELAY STUDIES OF ENDOTHERMIC FUELS, AIAA Journal, 4, 513-20, March 1966.

136. Hayek, A. J., CRITICAL AREA COOLING INVESTIGATIONS. Marquardt Corp. Final Report No. 6085, Contract AF 33(657)-11754, December 1964, 87 pp. (AD 355867)(REPORT CLASSIFIED CONFIDENTIAL).

137. Heller, J. and Greensfelder, B. S., A STUDY OF ANTICATALYTIC MATERIALS. Stanford Research Institute Final Report 5 March 1964-31 January 1966, Report No. SRI-66-1508, U. S. Army Contract DA-18-064-AMC-209(A), May 1966, 67 pp. (AD 373035)(REPORT CLASSIFIED CONFIDENTIAL).

138. Herbst, W. A., ENDOTHERMIC REACTIONS FOR COOLING AND PROVIDING FUEL IN SUPERSONIC COMBUSTION, U. S. Patent 3,263,414, 2 August 1966, assigned to Esso Research and Engineering Co.

139. Hibbard, R. R. and Olson, W. I. (Lewis Research Center), FUELS FOR TURBOJETS AND RAMJETS. Combust. Propellenti Nuovi, Atti Conv., Milan 1963, 217-36 (Pub. 1964)(Eng.)

140. Hightower, J. W. and Emmett, P. H. (Johns Hopkins University), CATALYTIC CRACKING OF n-HEXADECANE. IV. THE FORMATION AND BEHAVIOR OF AROMATICS OVER A SILICA-ALUMINA CATALYST, J. Am. Chem. Soc., 87 (5), 939-49 (1965).

141. Hube, F. K., PRESSURE DISTRIBUTION AND MASS FLOW IN A HYPERSONIC INLET CONFIGURATION AT MACH NUMBERS 3 THROUGH 8. Arnold Engineering Development Center, Arnold Air Force Station Technical Report No. AEDC-TR-66-90 prepared in cooperation with ARO, Inc., U. S. Air Force Contract AF 40(600)-1200, April 1966, 16 pp. (AD 371751L)(REPORT CLASSIFIED CONFIDENTIAL).

142. Huybregtse, R. and van der Linder, A. C. (Koninklijke/Shell Lab.), THE OXIDATION OF α-OLEFINS BY A PSEUDOMANAS. REACTIONS INVOLVING THE DOUBLE BOND. Antonie van Leeuwenhoek J. Microbiol. Serol., 30 (2), 185-96 (1964).

143. Jacobs, H. R. and Woodcock, G. R., HEAT TRANSFER IN RAMJETS AND LIQUID ROCKETS. Boeing Co. Report No. DN-D2-12041, March 1962, 149 pp. (AD 450927).

144. Johnston, R. K. and Monita, C. M., EVALUATION OF A DETECTOR FOR FREE WATER IN FUEL. Southwest Research Institute Summary Report March 1965-March 1966, Report No. RS-481, AFAPL TR-66-39, U. S. Air Force Contract AF 33(615)-2327, April 1966, 43 pp. (AD 481506).

145. Johnston, R. K., Tyler, J. C., and Weichlein, R. G., FUEL CONTAMINATION SURVEY AT AIR FORCE BASES. Southwest Research Institute Final Technical Report 11 July 1963-30 September 1964, Report No. RS-429, SEG TR-65-7, U. S. Air Force Contract AF 33(657)-11362, March 1965, 339 pp. (AD 480436).

146. Jost, F. and Bazant, V., CATALYTIC DEALKYLATION OF ALKYL AROMATIC COMPOUNDS. X. INFLUENCE OF PREPARATIVE PROCEDURES ON PROPERTIES OF NICKEL-ALUMINA CATALYST. Collection Czech. Chem. Commun., 30 (3), 853-61 (1965) (Eng.).

147. Kaliko, M. A., Pelevina, R. S., Pervushina, M. N., and Fedotova, T. V., PRODUCTION OF HIGHER NORMAL α-OLEFINS BY THE CATALYTIC CONVERSIONS OF PARAFFINS. Neftekhimiya, 5 (1), 24-32 (1965).

148. Kamberov, Yu. G., Kakhramanova, A. T., and Mekhtiev, S. D., THERMODYNAMIC CALCULATIONS OF THE n-OCTANE PRESSURE PYROLYSIS. Azerb. Khim. Zh., 1964 (3), 111-8.

149. Kaplan, B., VISIBLE RADIATION FROM A STREAM OF REACTING CHAR PARTICLES. General Applied Science Laboratories, Inc. Technical Memo. Renport No. GA SL-TM-140, U. S. Supersonic Development Contract SD-149, April 1966, 50 pp. (AD 374669)(REPORT CLASSIFIED SECRET).

150. Keough, A. H. (Norton Co.), CATALYTIC CRACKING OF HYDROCARBONS WITH OPEN SYNTHETIC MORDENITES. Am. Chem. Soc., Div. Petrol. Chem., Preprints 8 (1), 65-8 (1963).

151. Kim, S. K., Flynn, G. P., and Ross, J., THERMAL CONDUCTIVITY OF MODERATELY DENSE GASES. University of Virginia Technical Report on Project Squid, Report No. BRN-15-P, U. S. Navy Contract Nonr-362300, September 1965, 16 pp.; Prepared in cooperation with Brown University. (AD 471864).

152. Kirk, H. F., RAMJET TECHNOLOGY. CHAPTER 13. FACILITIES AND TESTING. Johns Hopkins University, Applied Physics Laboratory Technical Memo, Report No. TG-610-13, U. S. Navy Contract NOW-62-0604-C, May 1965, 42 pp. (AD 630826).

153. Kirkegaard, P. M. and Waite, H. R., IGNITION SENSITIZATION OF GELLED JP-5 FUEL. Atlantic Research Corp. Final Report, U. S. Naval Ordnance Test Station Report NOTS TP 4113, U. S. Navy Contract N60530-11071. April 1966, 12 pp. (AD 483275).

154. Kirkwood, T. F., COMMENTS ON FUTURE AIR TRANSPORTATION SYSTEMS. Rand Corp. Report No. P-3362, May 1966, 9 pp. (AD 633023).

155. Kistiakowsky, G. B. and Smith, W. R., THE KINETICS OF CIS-TRANS ISOMERIZATION. IV. J. Am. Chem. Soc., 57, 269 (1935).

156. Klimov, K. I., Vilenkin, A. V., and Kichkin, G. I., NEW METHOD OF EVALUATING THE EFFECTIVENESS OF ACTION OF ANTI-SCORING ADMIXTURES TO OILS AND FUELS. Vsyesoiuznoe Navchno Tekhnicheskoz Soveshchanie po Prisadkam K Maslam i Toplivam Trudy (USSR) 1960-1, 273-8; U. S. Air Force Translation FTD-TT-65-1491, TT66-61131, March 1966, 15 pp. (AD 631838).

157. Kolesnikova, T. A. and Sadyrina, N. A., PREPARATION AND ACTIVATION OF CATALYSTS FOR THE DEPOLYMERIZATION OF HYDROCARBONS. Tr. Bashkirsk. Nauchn.-Issled. Inst. po Pererabotke Nefti No. 7, 97-101 (1964).

158. Knecht, A. T., Jr., Kools, J. W., Muhbaler, D. J., and Rizzuto, A. R., MICROBIAL UTILIZATION OF HYDROCARBON FUEL FORMULATIONS WITH THE PRODUCTION OF GUMS, SLIMES, SLUDGE AND SURFACE ACTIVE COMPONENTS. Sinclair Research Inc. Final Report 1 April 1963-28 September 1965, U. S. Army Contract DA-19-129-AMC-88(N), October 1965, 185 pp. (AD 476174L).

159. Kobayashi, K. and Yumada, K., OXIDATIVE DECOMPOSITION OF HYDROCARBONS BY MICROORGANISMS. I. DECOMPOSITION OF STRAIGHT-CHAIN HYDROCARBONS. Hakko Kyokaishi, 21 (10), 407-14 (1963).

160. Kobayashi, K. and Yamada, K., OXIDATIVE DECOMPOSITION OF HYDROCARBONS BY MICROORGANISMS. II. DECOMPOSITION OF CYCLIC HYDROCARBONS. Hakko Kyokaishi, 21 (1), 453-8 (1963).

161. Konovalchikov, O. D., Galich, P. N., Petrov, A. A., and Skarchenko, V. K., DEHYDROGENATION OF n-HEXANE ON ACTIVATED CARBON AND Cr_2O_3 - CARBON CATALYSTS. Kinetika i Kataliz, 5 (3), 561-3 (1964).

162. Konovalchikov, O. D., Galich, P. N., Musienko, V. P., Skarchenko, V. K., and Petrov, A. A., EFFECT OF THE PORE STRUCTURE OF AN ALUMINOCHROME CATALYST ON THE CONVERSION OF n-HEXANE. Kinetika i Kataliz, 5 (2), 350-4 (1964).

163. Krakow, B. (Warner and Swasey Co.), DETERMINATION OF HOT-GAS TEMPERATURE PROFILES FROM INFRARED EMISSION AND ABSORPTION SPECTRA. AIAA Journal, 3, No. 7, 1359-60 (1965); Revised edition, AFOSR 66-0352, U. S. Air Force Contract AF 49(638)-1132, March 1965, 3 pp. (AD 631616).

164. Krohn, N. A. and Wymer, R. G. (Oak Ridge National Laboratory), EFFECTS OF INCORPORATED RADIOACTIVITY AND EXTERNAL RADIATION ON HETEROGENEOUS CATALYSIS. Ind. Uses Large Radiation Sources, Proc. Cont. Sulzburg, Austria, 1963, 2, 25-39, discussion 39-40.

165. Kuchta, J. M., Cato, R. J., Martindill, G. H., and Gilbert, W. H. (U. S. Bureau of Mines), IGNITION CHARACTERISTICS OF FUELS AND LUBRICANTS. U. S. Air Force, AFAPL TR-66-21 , March 1966, 83 pp. (AD 632730).

166. Kuchta, J. M., Spolan, I., and Zubetakis, M. G. (U. S. Bureau of Mines), FLAMMABILITY CHARACTERISTICS OF METHYLACETYLENE, PROPADIENE (ALLENE), AND PROPYLENE MIXTURES. J. Chem. Eng. Data, 9 (5), 467-72 (1964).

167. Kushida, R., Falconer, F., and Seiveno, D., ADVANCED AIR-BREATHING ENGINE STUDY. National Engineering Science Co. Report No. SN 129. U. S. Air Force Contract AF 33(657)-10794. November 1964, 93 pp. (AD 355503)(REPORT CLASSIFIED CONFIDENTIAL).

168. Kushida, R., Seiveno, D., and Troblay, J., ADVANCED AIR-BREATHING ENGINE STUDY. National Engineering Science Co. Quarterly Report No. SN 129, APL-TDR-64-16, U. S. Air Force Contract AF 33(657)-10794, April 1964, 71 pp. (AD 349675)(REPORT CLASSIFIED CONFIDENTIAL).

169. Langenbeck, W. and Grimm, H., THE SELECTIVITY OF ZINC-DOPED NICKEL CATALYST DURING THE DEHYDROGENATION OF CYCLOHEXANE. Z. Anorg. Allgem. Chem., 332 (1-2), 55-62 (1964).

170. Laster, M. L., THERMODYNAMIC FACTORS AFFECTING THE PERFORMANCE OF SUPERSONIC COMBUSTORS. Arnold Engineering Development Center, Arnold Air Force Station Technical Report No. AEDC-TR-65-252, prepared in cooperation with ARO, Inc. Presented at the 12th Annual Air Force Science and Engineering Symposium, 12-14 October 1965, Brooks AFB, U. S. Air Force Contract AF 40(600)-1200, December 1965, 28 pp. (AD 367800)(REPORT CLASSIFIED CONFIDENTIAL).

171. Lebedev, W. P., THE THEORY OF THE CATALYTICAL ACTIVITY OF MIXING CATALYSTS. THE COMPOSITION OF THE CATALYTICALLY ACTIVE CENTERS OF Ni-Mg MIXING CATALYSTS. Zeitschrift fur Physikalische Chemie, 225, No. 1, 101-15 (1965) (U. S. Air Force Translation FTD-TT-65-221)(HP 466258).

172. Lettler, A. J., RADIATION ACTIVATION OF PARA-ORTHO HYDROGEN CATALYSTS. Arthur D. Little, Inc. Report No. C64814, RTD-TDR63-4106, Suppl. 1, U. S. Air Force Contract AF 33(657)-8878, December 1963, 21 pp. (AD 345789)(REPORT CLASSIFIED CONFIDENTIAL).

173. Lettler, A. J., RADIATION ACTIVATION OF PARA-ORTHO HYDROGEN CATALYSTS. Arthur D. Little, Inc. Report No. C64814, RTD-TDR63-4106, U. S. Air Force Contract AF 33(657)-8878, December 1963, (no. of pages not legible)(AD 425799).

174. Lettler, A. J., RADIATION ACTIVATION OF PARA-ORTHO HYDROGEN CATALYSTS. Arthur D. Little, Inc. Quarterly Progress Report No. 2, U. S. Air Force Contract AF 33(615)-1362, June 1964, 17 pp. (AD 449210).

175. Levinson, G. S. (Shell Development Company), HIGH TEMPERATURE PREFLAME REACTIONS OF n-HEPTANE. Combustion and Flame, 9 (1), 63-72 (1965).

176. Lewis, B., Pease, R. N., and Taylor, H. S., HIGH SPEED AERODYNAMICS AND JET PROPULSION. VOLUME II. COMBUSTION PROCESSES. Princeton University Press, Princeton, N. J., 1956, 662 pp. U. S. Navy Contract Nonr-03201 (AD 638982).

177. Lewis, G. O. and Kah, C. L., HIGH CHAMBER PRESSURE STAGED COMBUSTION RESEARCH PROGRAM. Pratt and Whitney Aircraft Final Report, 19 October 1964-18 October 1965, Report No. PWA-FR-1676, AFRPL TR-66-70, U. S. Air Force Contract AF 04(611)-10372, June 1966, 149 pp. (AD 374697) (REPORT CLASSIFIED CONFIDENTIAL).

178. Lin, C. C., HIGH SPEED AERODYNAMICS AND JET PROPULSION. VOLUME V. TURBULENT FLOWS AND HEAT TRANSFER. Princeton University Press, Princeton, N. J., 1959, 563 pp., U. S. Navy Contract Nonr-03201 (AD 638983).

179. Liptert, F. W. and O'Neill, J. E., FEASIBILITY STUDY OF A SUPERSONIC COMBUSTION TURBOJET ENGINE. General Applied Science Laboratories Inc. Final Technical Report 1 August 1964-9 August 1965, Report No. TR-545, APL-TR-65-102, U. S. Air Force Contract AF 33(615)-2119, August 1965, 175 pp. (AD 366972)(REPORT CLASSIFIED CONFIDENTIAL).

180. Lodwick, J. R. (British Petroleum Co.), CHEMICAL ADDITIVES IN PETROLEUM FUELS: SOME USES AND ACTION MECHANISMS. J. Inst. Petrol, 50 (491), 297-308 (1964).

181. Lopatik, M. D., HYDROCARBON-OXIDIZING CAPACITY OF MYCOBACTERIA. Mikrobiologiya, 33 (2), 236-8 (1964); C. A. 61, 4736 (1964).

182. Lyster, W. N. (Univ. of Houston), KINETICS OF CHEMICAL REACTIONS - DEHYDROCYCLIZATION OF n-HEPTANE. Univ. Microfilms (Ann Arbor, Mich.), Order No. 64-7594, 374 pp.

183. MacFarlane, J. J., Holderness, F. H., and Whitcher, F. S. E (N.G.T.E.), SOOT FORMATION IN PREMIXED C_3 AND C_6 HYDROCARBON - AIR FLAMES AT PRESSURES UP TO 20 ATMOSPHERES. Combustion and Flame, 8, 215-29 (1964). (Similar to AD 411328 listed in literature survey as 0572.)

184. Malone, E. W., HEAT FLUX MEASUREMENT. Boeing Co. Document No. D2-35057, January 1963, 33 pp. (AD 467835).

185. Mamedaliev, Yu. G., Ismailov, R. G., Mamedaliev, G. M., Aliev, S. M., Gustinov, N. I., and Akhmed-Zade, Z. A., DEHYDROGENATION OF ALKYL AROMATIC HYDROCARBONS IN THE FLUIDIZED BED OF VARIOUS OXIDE CATALYSTS. Dokl. Akad. Nauk. Azerb. SSR, 20 (5), 7-10 (1964).

186. Mamedaliev, Yu. G. and Mamedaliev, G. M., DEALKYLATION AND TRANSALKYLATION OF AROMATIC HYDROCARBONS IN THE PRESENCE OF ALUMINOSILICATE CATALYSTS. Ichrannye Proizvedeniya, Adad. Nauk. Azerb. SSR, Inst. Neftekhim. Protsessov, 1, 524-67 (1965).

187. Marquardt Corp., SUPERSONIC COMBUSTION RAMJET ENGINE PROGRAM. Monthly Letter Progress Report No. LR-344-6M, U. S. Air Force Contract AF 33(615)-1469, September 1964, 1 vol. (AD 361127)(REPORT CLASSIFIED CONFIDENTIAL).

188. Marquardt Corp., LACE-ACES HEAT EXCHANGER DESIGN STUDY. Final Report, U. S. Air Force Contract AF 33(657)-11754, November 1964, 1 vol. (AD 346416L)(REPORT CLASSIFIED CONFIDENTIAL).

189. Marquardt Corp., SUPERSONIC COMBUSTION RAMJET ENGINE PROGRAM, Monthly Letter Progress Report for October 1964, Report No. LR-344-8M, U. S. Air Force Contract AF 33(615)-1469, November 1964, 24 pp. (AD 364471) (REPORT CLASSIFIED CONFIDENTIAL).

190. Marquardt Corp., HYPERSONIC RAMJET PROGRAM. Monthly Letter Progress Report for October 1964, Report No. LR 343-8, U. S. Force Contract AF 33(615)-1467, November 1964, 37 pp. (AD 364468)(T CLASSIFIED CONFIDENTIAL).

191. Marquardt Corp., SUPERSONIC COMBUSTION ENGINE PROGRAM (INLET). Monthly Letter Progress Report No. LR-275-7M, U. S. Air Force Contract AF 33(657)-8491, November 1964, 3 pp. (AD 359843)(REPORT CLASSIFIED CONFIDENTIAL).

192. Marquardt Corp., SUPERSONIC COMBUSTION RAMJET PROGRAM. Monthly Letter Progress Report for December 1964, Report No. LR-344-10M, U. S. Air Force Contract AF 33(615)-1469, January 1965, 7 pp. (AD 364470)(REPORT CLASSIFIED CONFIDENTIAL).

193. Marquardt Corp., SUPERSONIC COMBUSTION RAMJET ENGINE PROGRAM (INLET). Monthly Progress Report for December 1964, Report No. LR-275-9M, U. S. Air Force Contract AF 33(657)-8491, January 1965, 6 pp. (AD 364473) (REPORT CLASSIFIED CONFIDENTIAL).

194. Martin, E. C., A RESEARCH AND DEVELOPMENT STUDY OF FUEL AND OIL CONTAMINANTS. Southwest Research Institute Monthly Progress Report, 1 October-1 November 1963, U. S. Army Contract DA23-072-AMC-128, November 1962, 56 pp. (AD 345314)(REPORT CLASSIFIED CONFIDENTIAL).

195. Maslyanskii, G. N., Rabinovich, G. L., and Avtonomova, N. Kh., CATALYTIC DEALKYLATION OF ETHYLBENZENE. Neftekhimiya, 4 (3), 421-5 (1964); C. A. 61, 6832 (1964).

196. Maslyanskii, G. N., Rabinovich, G. L., and Brisker, K. L., CATALYTIC DEALKYLATION OF XYLENE ISOMERS. Neftekhimiya, 4 (3), 426-30 (1964); C. A. 61, 6832 (1964).

197. Maurel, R. and Saudemont, G., CERTAIN TRANSITORY PHENOMENA IN HETEROGENEOUS CATALYSIS. Bull. Soc. Chim. France 1964 (10), 2435-6.

198. Maxim, R. E., CONVECTIVE HEAT TRANSFER AND FLOW FRICTION CHARACTERISTICS OF COMPACT HEAT EXCHANGER SURFACES. U. S. Naval Postgraduate School Master's Thesis, 1962, 47 pp. (AD 482250).

199. Mazitova, F. N., Durova, O. S., and Bukhryakova, V. V., SYNTHESIS OF MULTIFUNCTIONAL FUEL OXIDATION INHIBITORS. Neftekhimiya, 4 (2), 323-8 (1964); C. A. 61, 4127 (1964).

200. McGinley, L. AUTOXIDATION AND ANTIOXIDANTS. Rept. Progr. Appl. Chem., 48, 149-56 (1963).

201. McKee, D. W. and Norton, F. J. (General Electric Research Laboratory), CATALYTIC ACTIVITY OF NOBLE METAL ALLOYS. METHANE-DEUTERIUM EXCHANGE AND PROPANE CRACKING ON PLATINUM-PALLADIUM AND PALLADIUM-RHODIUM ALLOYS. J. Catalysis, 3 (3), 252-67 (1964); C. A. 61, 3729 (1964).

202. McLaren, G. W., Krynitsky, J. A., and Hazlett, R. N., EFFECT OF CORROSION INHIBITORS ON JET FUEL FILTRATION. U. S. Naval Research Laboratory Final Report No. NRL-MR-1660, November 1965, 18 pp. (AD 474875L).

203. Meguerian, G. H., Hillstrom, W., Hirschberg, E. H., Rakowsky, F. W. and Zletz, A., FUNDAMENTAL INVESTIGATION OF THE CATALYTIC DEGRADATION OF HYDROCARBON FUELS. American Oil Co. Final Report, U. S. Army Contract DA-18-108-AMC-198A, January 1965, 1 vol. (AD 461420).

204. Melnikova, N. P., Fedorov, A. P., and Kuleshova, A. N., REACTIONS OF INDIVIDUAL HYDROCARBONS IN CATALYTIC REFORMING. Khim. i Tekhnol. Topliv i Masel, 9 (7), 24-8 (1964).

205. Melvin, A. SPONTANEOUS IGNITION OF METHANE-AIR MIXTURES AT HIGH PRESSURE. I and II. Combustion and Flame, 10, No. 2, 120-134 (1966).

206. Merkulov, I. A., PROBLEMS OF SPACE AIR-BREATHING JET ENGINES. Izvestiya Akademiya Nauk SSSR, Energetika i Transport 1965, No. 5, 159-72; U. S. Library of Congress, Aerospace Technology Division ATD Work Assignment No. 76, Report No. ATD-66-8, TT66-6D934, January 1966, 23 pp. (AD 630764).

207. Michels, H. H., THEORETICAL RESEARCH ON THERMODYNAMIC AND TRANSPORT PROPERTIES OF GASES AT HIGH TEMPERATURES. United Aircraft Corp. Final Report No. UACRL-E9 10004-12, AFOSR-66-0407, U. S. Air Force Contract AF 49(638)-1133, January 1966, 15 pp. (AD 628911).

208. Mickley, H. S., Nestor, J. W., Jr., and Gould, L. A. (Massachusetts Institute of Technology), A KINETIC STUDY OF THE REGENERATION OF A DEHYDROGENATION CATALYST. Can. J. Chem. Eng., 43 (2), 61-8 (1965).

209. Mirzaeva, A. K., Elagina, N. V., Sterin, Kh. E., Bobrov, A. V., and Kazanskii, B. A., THE CATALYTIC CONVERSION OF AMYLBENZENE ON A PLATINUM CATALYST. Neftekhimiya, 4 (3), 417-20 (1964).

210. Morgan, J. E. and Schiff, H. I. (McGill University), ATOM RECOMBINATION ON SURFACES. Montreal, Canada, November 1965.

211. Mosely, R. B. and Good, J. M. (Shell Development Co.), EFFECTS OF INERT SOLIDS ON HETEROGENEOUS REACTIONS. J. Catalysis, 4 (1), 85-9 (1965).

212. Mullaney, G. J., Ku, P. S., and Botch, W. D. (Boeing), DETERMINATION OF INDUCTION TIMES IN ONE-DIMENSIONAL DETONATIONS (H_2, C_2H_2 and C_2H_4). AIAA Journal, 3 No. 5, May 1965, pp. 873-75.

213. Murzinov, I. N., TEMPERATURE PROFILES IN BODIES TRAVELING AT HIGH ALTITUDES AT HYPERSONIC SPEED. Akad. Nauk SSSR, Izvestiya. Mekhanika i Mashinostroenie, 1964, No. 4, 148-50; U. S. Air Force Translation Report No. TT-65-1478; TT65-61414 (AD 633713).

214. Musienko, V. P., Polatalko, R. I., Skarchenko, V. K., Frolova, V. S., and Galich, P. N., CONVERSION OF n-HEXANE ON CHROMIUM-MAGNESIUM OXIDE CATALYSTS. Ukr. Khim. Zh., 30 (9), 915-8 (1964).

215. Nardo, S. V. and Brown, L. D., EXPERIMENTAL HEAT TRANSFER AND TEMPERATURE DISTRIBUTION IN A HOLLOW TUBE WITH INTERNAL AIRFLOW AT HIGH TEMPERATURE AND PRESSURE. NASA Doc. N62-12031, 42 pp. (1962); C.A. 61, 9183 (1964).

216. Nixon, A. C., Bjorklund, I. S., Hawthorn, R. D., Henderson, H. T., Ritchie, A. W., LITERATURE SURVEY ON VAPORIZING AND ENDOTHERMIC FUELS FOR ADVANCED ENGINE APPLICATIONS. Shell Development Co. Special Report No. S-13979, U.S. Air Force Contract AF 33(657)-11096, November 1965, 362 pp. (AD 476611).

217. Nixon, A. C. et al, VAPORIZING AND ENDOTHERMIC FUELS FOR ADVANCED ENGINE APPLICATION. Shell Development Co. Report No. S-14007, for Aeronautical Systems Division, Wright-Patterson Air Force Base, Ohio, Contract No. AF 33(615)-3789 Quarterly Progress Report No. 1, June 1966 - August 1966.

218. Nixon A. C. et al, VAPORIZING AND ENDOTHERMIC FUELS FOR ADVANCED ENGINE APPLICATION. Shell Development Company Report S-14014 for Aeronautical Systems Division, Wright-Patterson Air Force Base, Ohio, Contract No. AF 33(615)-3789 Quarterly Progress Report No. 2, Sept. 1966 - Nov. 1966.

219. Nixon, A. C., Ackerman, G. H., Bjorklund, I. S., Hawthorn, R. D., Henderson, H. T., Ritchie, A. W., VAPORIZING AND ENDOTHERMIC FUELS FOR ADVANCED ENGINE APPLICATION. PART II. STUDIES OF THERMAL AND CATALYTIC REACTIONS, THERMAL STABILITIES AND COMBUSTION PROPERTIES OF HYDROCARBON FUELS. June 1964-June 1965 (APL TDR 64-100).

220. Nixon, A. C., Ackerman, G. H., Hawthorn, F. D., Henderson, H. T., and Ritchie, A. W., VAPORIZING AND ENDOTHERMIC FUELS FOR ADVANCED ENGINE APPLICATION. PART III. FURTHER STUDIES OF THERMAL AND CATALYTIC REACTIONS, THERMAL STABILITIES AND COMBUSTION PROPERTIES OF HYDROCARBON FUELS, September 1966, APL-TDR-64-100.

221. Munn, D., MICROBIOLOGICAL INVESTIGATIONS. Dayton University Research Institute RTD-TDR-63-4118-Part 2, U.S. Air Force Contract AF 33(657)-9175, February 1965, 40 pp. (AD 464158).

222. Omilian, B., A PARAMETRIC STUDY AND SURVEY OF THE THEORETICAL PERFORMANCE OF THE SUPERSONIC COMBUSTION RAMJET. Flight Sciences Laboratory, Inc. Report for June 1962-May 1963, AFOSR-5351-2, U.S. Air Force Contract AF 49(638)-1173, October 1963, 56 pp. (AD 348072) (REPORT CLASSIFIED CONFIDENTIAL).

223. Osgerby, I. A., AN INVESTIGATION OF SUPERSONIC COMBUSTION AND HETEROGENEOUS TURBULENT JET MIXING RELATED TO THE DESIGN/OPERATION OF SCRAMJETS. Doctoral Thesis Sheffield University (England), AFOSR 66-1855, U.S. Air Force European Office of Aeronautical Research Contract AF-EOAR-23-65, October 1965, 235 pp. (AD 638665).

224. Panchenkov. G. M., Kuznetsov, I. I., Bazilevich, V. V., Bessmertnaya, E. K., Zhorov, Yu. M., THE EFFECT OF KINETIC FACTORS ON THE YIELD, FRACTIONAL COMPOSITION, AND STRUCTURE OF OLEFINS IN THE THERMAL CRACKING OF n-HEXADECANE. Tr., Mosk. Inst. Neftekhim. i Gaz. Prom. No. 51, 142-7 (1964); C.A. 62, 14474 (1965).

225. Panchenkov, G. M., Venkatachalam, K. A., Zhorov, Yu. M., THE KINETICS OF THE DEHYDROCYCLIZATION OF PARAFFIN HYDROCARBONS ON OXIDE CATALYSTS. Neftekhimiya 4 (1), 30-6 (1964); C.A. 61, 500 (1964).

226. Panchenkov, G. M., Zhorov, Yu. M., Kazunskaya, A. S., Kolesnikov, I. M., Venkatachalam, K. A., THE KINETICS OF DEHYDROCYCLIZATION AND DEHYDROGENATION OF HYDROCARBONS IN CONTINUOUS PROCESSES. Tr., Mosk. Inst. Neftekhim. i Gaz. Prom. No. 51, 154-70 (1964); C.A. 62, 14399 (1965).

227. Pansing, W. F. (American Oil Co.), THE CATALYTIC CRACKING OF HEXADECANE-EFFECTS OF IMPURITIES, OLEFINS, AND STEAM. J. Phys. Chem. 69 (2), 392-9 (1965); C.A. 62, 7555 (1965).

228. Pansing, W. F. and Malloy, J. B. (American Oil Co.), CHARACTERIZING CRACKING CATALYSTS BY THE KINETICS OF CUMENE CRACKING. Ind. Eng. Chem., Process Design Develop. 4 (2), 181-7 (1965); C.A. 62, 11596 (1965).

229. Parker, K. O., EXPLORATORY DEVELOPMENT OF HIGH-TEMPERATURE HEAT EXCHANGERS. Garrett Corp., AiResearch Mfg. Division Interim Engineering Progress Report 1 July-30 September 1965, Report No. L-9578, RTD IR-3084-Vol. 1, U.S. Air Force Contract AF 33(615)-2753, September 1965, 82 pp. (AD 369380) (REPORT CLASSIFIED CONFIDENTIAL).

230. Peskin, R. L., A THEORETICAL INVESTIGATION OF AEROSOL FLASHING. Rutgers-The State University New Jersey Annual Progress Report, 1 February 1965-31 January 1966, EA 66-4, U.S. Army Contract DA-AMC-18-035-80(A), February 1966, 65 pp. (AD 482569).

231. Phillips, D. C. (Marquardt Corp.) and Unterberg, W., HIGH-SPEED HYDROCARBON-AIR MIXTURE IGNITION BEHIND BLUFF BODIES. Pyrodynamics 1 (1-2), 41-60 (1964); C.A. 61, 4139 (1964).

232. Pichtelberger, J. R., SMOKE SUPPRESSANT FUEL ADDITIVES RESULTS OF TESTS OF ETHYL CORPORATION COMBUSTION IMPROVER NO. 2. U.S. Naval Air Engineering Center, Aeronautical Engine Laboratory Phase Report No. NAEC-AEL-1827, March 1966, 54 pp. (AD 478876L)

233. Plank, C. J., Rosinski, E. J., Hawthorne, W. P. (Socony Mobil Oil Co., Inc), ACIDIC CRYSTALLINE ALUMINOSILICATES. NEW SUPERACTIVE, SUPERSELECTIVE CRACKING CATALYSTS. Ind. Eng. Chem., Prod. Res. Develop. 3 (3), 165-9 (1964); C.A. 61, 9336 (1964).

234. Plank, P. P. and MacMiller, C. J., ANALYTICAL INVESTIGATION OF CANDIDATE THERMAL-STRUCTURAL CONCEPTS APPLICABLE TO WING, FUSELAGE AND INLET STRUCTURE OF A MANNED HYPERSONIC VEHICLE. North American Aviation Inc. Final Technical Report 15 June-5 December 1965, Report No. NA-65-1061, AFFDL TR-66-15, U.S. Air Force Contract AF 33(615)-2996, February 1966, 478 pp. (AD 370 834) (REPORT CLASSIFIED SECRET).

235. Pluchery, M. and Germi, P., OBSERVATION OF PYROCARBONS DEPOSITED ON VARIOUS SUBSTRATES AT INTERMEDIATE TEMPERATURES BY MEANS OF ELECTRON MICROSCOPY, ELECTRON AND X-RAY DIFFRACTION. Proc. European Reg. Conf., Electron Microscopy, 3rd, Prague 1964 (A), 405; C.A. 62, 11597 (1965).

236. Pratt and Whitney Aircraft, COMPARISON OF AIR-BREATHING PROPULSION SYSTEMS FOR SCRAMJET CRUISE VEHICLES. Report for 1 July 1964-1 March 1965, Report No. PWA-2596, U.S. Air Force Contract AF 33(615)-1305, May 1965, 188 pp. (AD 373608L) (REPORT CLASSIFIED CONFIDENTIAL) Re-issue of Report No. PWA-2559 without section VII.

237. Pratt and Whitney Aircraft, AMSA PROPULSION STUDY. Final Report No. PWA-2510, December 1964. 1 vol. (AD 358464L) (REPORT CLASSIFIED SECRET).

238. Quigg, H. T., HIGH PRESSURE COMBUSTOR STUDIES OF DOWNSTREAM METAL TEMPERATURE AS RELATED TO HYDROCARBON STRUCTURE. Progress Report No. 1, Report No. 4240-65R, U.S. Navy Contract NOw-65-0310-d, November 1965, 88 pp. (AD 476160).

239. Rachinskii, A. V., ENERGY AND FLOW RATE OF A GAS WITH SUSPENDED PARTICLES MOVING THROUGH IT. Tr. Vses. Zaochn. Energ. Inst. 1962 (20), 44-54; C.A. 61, 7713 (1964); Ref. Zh., Khim. 1964, Abstr. No. 11 14.

240. Rachinskii, F. Yu., Bruk, Yu. A., Bolshakov, G. F., METHOD OF IMPROVING THE THERMOXIDATION STABILITY OF HYDROCARBON FUELS. USSR Patent 159,591, Appl. No. 805093/23-4, 29 Novembe[illegible] (U.S. Air Force Translation ttd-TT-65-1127; TT 66-60053) (AD 625247).

241. Rackley, D. H. and Asbury, D. F., COMPONENT PROPULSION PROGRAM FOR FUTURE HIGH PERFORMANCE STRATEGIC AIRCRAFT. General Electric Co., Advanced Engine and Technology Dept. Report No. R66 FPD 14, U.S. Air Force Contract AF 33(657)-14902, January 1966, 172 pp. (AD 371521L) (REPORT CLASSIFIED CONFIDENTIAL).

242. Rakovskii, V. E., Orshanskii, R. B., Parnov, E. I., Volgina, I. V., Zhirnova, V. M., Topuneva, A. I., Basharin, I. E., THERMAL DECOMPOSITION OF CERTAIN HYDROCARBONS IN THE PRESENCE OF FERRIC OXIDE. Tr. Kalininsk. Tort. Inst. 1963 (13), 140-3; C.A. 62, 5114 (1965); Ref. Zh., Khim. 1964, Abstr. No. 13B604.

243. Raymond, A. E., OVER THE HORIZON IN AIR TRANSPORTATION. RAND Corp. Report No. P-3396, August 1966, 17 pp.; Published in Astronautics and Aeronautics, September 1966 (AD 638031).

244. Rieche, A., Seeboth, H., Wolf, H., DEALKYLATION OF TOLUENE, XYLENE, ETHYLBENZENE, AND CUMENE, AND FORMATION OF TOLUENE FROM BENZENE AND METHANE ON A TECHNICAL NICKEL CATALYST UNDER NORMAL PRESSURE. Monatsber., Deut. Akad. Wiss. Berlin 6 (5), 364-70 (1964); C.A. 61, 15993 (1964).

245. Rigdon, W. S. and Thomas, M., STAGNATION POINT HEAT TRANSFER IN AIR, CONSIDERING SIMULTANEOUS CHEMICAL REACTIONS. Douglas Aircraft Co. Report No. SM-45730, September 1963, 47 pp. (AD 464586).

246. Rosner, D. E. (Aerochem Research Laboratories, Inc.), EFFECTS OF CONVECTIVE DIFFUSION ON THE APPARENT KINETICS OF ZEROTH ORDER SURFACE-CATALYZED CHEMICAL REACTIONS. Chemical Engineering Science 21, 223-39 (1966); Revised ed., AFOSR 66-1804, U.S. Air Force Contract AF 49(638)-1138, August 1965, 19 pp. (AD 638704).

247. Rozengart, M. I., Gitis, K. M., Kazanskii, B. A., DEVELOPMENT OF AN ALUMINA-CHROMIUM OXIDE-POTASSIUM OXIDE CATALYST IN THE DEHYDROCYCLIZATION OF PARAFFIN HYDROCARBONS. Neftekhimiya 4 (3), 406-12 (1964); C.A. 61, 8101 (1964).

248. Rozengart, M. I., Mortikov, E. S., Kazanskii, B. A., DEHYDROCYCLIZATION OF n-HEPTENES ON ALUMINUM-CHROMIUM-POTASSIUM OXIDE CATALYSTS. Dokl. Akad. Nauk SSSR 158 (4), 911-4 (1964); C.A. 62, 2697 (1965).

249. Rozengart, M. I., Kuznetsova, Z. F., Gitis, K. M., ROLE OF POTASSIUM OXIDE IN THE ALUMINA-CHROMIA CATALYST FOR AROMATIZATION OF HEPTANE. Neftekhimiya 5 (1), 17-23 (1965); C.A. 62, 12948 (1965).

250. Rubinshtein, I. A. and Sobolev, E. P., ANTIOXIDATION PROPERTIES OF ORGANO-SULFUR COMPOUNDS AND A CRITERION FOR THEIR EVALUATION. Khim. i Tekhnol. Topliv i Masel 10 (1), 45-9 (1965); C.A. 62, 11597 (1965).

251. Ruhnke, L. H., Will, E., Pederson, P., ELECTRO-HYDRODYNAMIC REMOVAL OF MICROORGANISMS FROM HYDROCARBON FUELS. Litton Systems, Inc., Applied Science Division Final Report 25 June 1963-20November 1965, Report No. ASD-2905, U.S. Army Contract DA-19-129-AMC-141(N), November 1965, 138 pp. (AD 630889).

252. Ryashentseva, M. A., Minachev, Kh. M., Atanaseva, Yu. A., (DEHYDROGENATION) OF CYCLOHEXANE IN THE PRESENCE OF ALUMINA-PALLADIUM CATALYSTS CONTAINING NEODYMIUM OXIDE. Neftekhimiya 2 (1), 41-3 (1962); C.A. 61, 2934 (1964).

253. Ryashentseva, M. A. and Minachev, Kh. M., CATALYTIC PROPERTIES OF RHENIUM CATALYSTS IN THE CONVERSION OF HYDROCARBONS AND THEIR MIXTURES. Renii, Akad. Nauk SSSR, Inst. Met., Tr. 2-go (Vtorogo) Vses. Soveshch., Moscow 1962, 226-30 (Pub. 1964); C.A. 62, 11707 (1965).

254. Ryley, M. O., Jr., SKIN FRICTION, HEAT TRANSFER, AND PRESSURE MEASUREMENTS ON HYPERSONIC INLET COMPRESSION SURFACES IN THE MACH NUMBER RANGE 7.5 to 16. Cornell Aeronautical Laboratory Inc. Final Report May 1964-December 1965, Report No. AA-1948-Y-3, AFFDL TR-65-199, U.S. Air Force Contract AF 33(615)-1845, December 1965, 93 pp. (AD 627798).

255. Sanlorenzo, E. and Kush, E. (General Applied Science Laboratories, Inc.), GROUND TESTING OF A MODEL INTEGRATED SCRAMJET ENGINE SYSTEM. Presented at the AIAA Propulsion Joint Specialist Meeting, Colorado Springs, Colorado, 14-18 June 1965; General Applied Science Laboratories Summary Technical Report No. GASL-TR-540, U.S. Air Force Contract AF 33(615)-2436, June 1965, 30 pp. (AD 370709) (REPORT CLASSIFIED CONFIDENTIAL).

256. Sato, T. and Matsumoto, R., RADIANT HEAT TRANSFER FROM LUMINOUS FLAME. Proc. Heat Transfer Conf., 1961-62, Univ. Colo. 1961 (and) London 1962, 804-11 (Pub. 1963); C.A. 61, 11633 (1964).

257. Sedgwick, T. A. and Rose, A., LACE/ACES HEAT EXCHANGER DESIGN AND TEST SITE PREPARATION. Marquardt Corp. Final Report, U.S. Air Force Contract AF 33(657)-11754, May 1964, 35 pp. (AD 356417) (REPORT CLASSIFIED CONFIDENTIAL).

258. Seemann, V., SOME ASPECTS OF COMBUSTION KINETICS: ANALYTICAL SURVEY. U.S. Library of Congress, Aerospace Technology Division Report No. 1 on ATD work assignment No. 68, Report No. ATD-65-100, TT66-60153, December 1965, 136 pp. (AD 625832).

259. Sergienko, S. R., Medredeva, V. D., Garbalinskii, V. A., SELECTIVITY OF CATALYSTS FOR DEHYDROGENATION OF PARAFFINIC HYDROCARBONS. Izv. Akad. Nauk. Turkm. SSR, Ser. Fiz.-Tekhn., Khim. i Geol. Nauk 1964 (3), 25-31; C.A. 61, 10516 (1964).

260. Scheitz, J. A. and Jannone, J. (General Applied Science Laboratories), THE IGNITION OF FLOWING HYDROCARBON/AIR MIXTURES BY A HYDROGEN PILOT FLAME. Pyrodynamics 2, 1-14 (1965); AFOSR 64-2008, U.S. Air Force Contracts AF 49(638)-1503 and AF 49(638)-991, 1964, 14 pp. (AD 626243).

261. Schirmer, R. M. and Quigg, H. T., EFFECT OF JP FUEL COMPOSITION ON FLAME RADIATION AND HOT CORROSION. Phillips Petroleum Co. Summary Report 1 April 1964-31 March 1965, Report No. 4230-65R, U.S. Navy Contract NOw 64-0443d, October 1965, 122 pp. (AD 474003).

262. Schleicher, A. R., RAPID GELLING OF AIRCRAFT FUEL. Western Co. of North America, Research Division Final Report. USA AVLABS TR-65-18, U.S. Army Contract DA-44-177-AMC-112(T), February 1966, 34 pp. (AD 629765).

263. Schribner, W. G., Warren, J. H., Zengel, A. E., Lander, H. R. (Wright-Patterson AFB), AN EXAMINATION OF METHODS FOR CALCULATING VAPOR PRESSURES OF PETROLEUM HYDROCARBONS. NASA Accession No. N64-19653 (AD 437285); C.A. 61, 15897 (1964).

264. Schuster, F., THE IGNITION VELOCITY OF GAS MIXTURES. Gas-Wasserfach 105 (35), 951-3 (1964); C.A. 61, 14427 (1964).

265. Scipioni, A. and Simioni, F. (University of Padua, Italy), ACTIVITY OF MOLYBDENUM CATALYSTS IN AROMATIZATION PROCESSES. Atti Ist. Veneto Sci., Lettere Arti, Classe Sci. Mat. Nat. 121, 83-107 (1962-1963); C.A. 62, 7554 (1965).

266. Shiba, T., Aonuma, T., Yoshida, K., Hattori, H., Sato, M., ACIDITY AND ACTIVITY OF SILICA-ALUMINA CATALYSTS. Shokubai (Tokyo) 6 (3), 176-81 (1964); C. A. 62, 8985 (1965).

267. Shimulis, V. I. and Zemanek, F., KINETICS OF THE DEHYDROGENATION OF CYCLOHEXENE ON A PALLADIUM FILM. I. LOCALIZED ADSORPTION. Kinetika i Kataliz 5 (5), 898-902 (1964); C.A. 62, 2690 (1965).

268. Shopov, D. and Andreev, A., KINETICS OF CATALYTIC CRACKING OF TETRALIN. Compt. Rend. Acad.Bulgare Sci. 16 (6), 625-8 (1963) (in English); C.A. 61, 4999 (1964).

269. Shuikin, N. I., Hofman, Kh., Erivanskaya, L. A., DEHYDROGENATION OF 1-METHYLCYCLOPENTENE IN THE PRESENCE OF OXIDE CATALYSTS. Izv. Akad. Nauk SSSR, Ser. Khim. 1964 (5), 912-4; C.A. 61, 5525 (1964).

270. Shuikin, N. I., Naryshkina, T. I., Kashchupkina, Z. A., SUPPRESSION OF COKE FORMATION ON ALUMINA-POTASSIA CATALYST DURING THE DEHYDROCYCLIZATION OF PIPERYLENE INTO CYCLOPENTADIENE. Kinetika i Kataliz 5 (5), 950-2 (1964); C.A. 62, 456 (1965).

271. Singleton, A. H., Kinard, G., Schmauch, G. E., Waring, R. W., Jr., Lapin, A., APPLICATION OF THE PARAORTHO CONVERSION REACTION OF HYDROGEN TO ORBITAL SYSTEMS. Air Products and Chemicals, Inc. Final Report November 1962-February 1964, U.S. Air Force Contract AF 33(657)-10057, (AD 350-603) (REPORT CLASSIFIED SECRET). APL-TDR-64-43.

272. Skarchenko, V. K., Frolova, V. S., Golubchenko, I. T., Musienko, V. P., Galich, P. N., IRON OXIDE-ALUMINUM OXIDE CATALYSTS IN THE DEHYDROGENATION OF NORMAL ALKANES. Kinetika i Kataliz 5 (5), 932-5 (1964); C.A. 62, 2647 (1965).

273. Skarchenko, V. K., THE SELECTIVITY OF CATALYSTS FOR THE DEHYDROGENATION OF PARAFFIN HYDROCARBONS. Neftekhim., Akad. Nauk Ukr. SSR, Inst. Khim. Vysokomolekul. soedin. 1964, 5-12; C.A. 62 8906 (1965).

274. Skarchenko, V. K., Galich, P. N., Golubchenko, I. T., Frolova, V. S., Musienko, V. P., CHROMIUM-IRON-ALUMINUM OXIDES AS CATALYSTS OF THE DEHYDROGENATION OF n-HEXANE. Kinetika i Kataliz 5 (3), 548-9 (1964); C.A. 61, 8207 (1964).

275. Skarchenko, V. K., Galich, P. N., Musienko, V. P., Frolova, V. S., Golubchenko, I. T., CATALYTIC INFLUENCE OF IRON OXIDE ON THE DEHYDROGENATION REACTION OF n-HEXANE. Neftekhim., Akad. Nauk Turkm. SSR 1963, 76-8 C.A. 61, 15961 (1964).

276. Sklyar, V. T., Lebedev, E. V., Zakupra, V. A., DEHYDROCRACKING OF PARAFFIN HYDROCARBONS OVER OXIDE CATALYSTS. Neftekhimiya 4 (2), 209-14 (1964); C.A. 61, 2879 (1964).

277. Sklyar, V. T., Lebedev, E. V., Zakupra, V. A., DEHYDROCRACKING OF ALKANES ON SULFIDE CATALYSTS. Neftekhimiya 4 (2), 200-8 (1964); C.A. 61, 1678 (1964).

278. Snyder, A. D., Robertson, J., Zanders, D. L. and Skinner, G. B. (Monsanto Research Corp.), SHOCK TUBE STUDIES OF FUEL-AIR IGNITION CHARACTERISTICS", AFAPL-TR-65-93 August, 1965, Contract AF 33(615)-1317 44 pp.

279. Sokulik, A. S., SELF-IGNITION, FLAME AND DETONATION IN GASES. TRANSLATED FROM THE RUSSIAN. Jerusalem: Israel Program for Scientific Translations, 1963, 458 pp.; C.A. 61, 2512 (1964).

280. Southwest Research Institute, EVALUATION OF FUEL ADDITIVES CAUSING ENGINE MALPERFORMANCE. Summary Report, U.S. Army Contract DA-23-072-ORD-1766(X), November 1965, 9 pp. (AD 482170) (REPORT CLASSIFIED CONFIDENTIAL).

281. Starshov, I. M. and Syrmolaeva, G. P., THE CATALYTIC INFLUENCE OF METALS ON COKE FORMATION DURING THE PYROLYSIS OF PROPANE. Neftepererabotka i Neftekhim., Nauchn.-Tekhn. Sb. 1964 (2), 26-9; C.A. 61, 5429 (1964).

282. Sterligov, O. D. and Eliseev, N. A., DEHYDROGENATION OF ISOPENTANE ON ALUMINA-CHROMIA-POTASSIUM OXIDE CATALYSTS. EFFECT OF CHROMIA CONTENTS IN THE CATALYST. Neftekhimiya 5 (1), 10-16 (1965); C.A. 62, 12-953 (1965).

283. Sterman, L. S. and Mikhailov, V. D., INVESTIGATION OF CRITICAL HEAT FLUXES FOR SURFACE BOILING OF ORGANIC LIQUIDS IN TUBES. Inzh.-Fiz. Zh., Akad. Nauk Belorussk. SSR 7 (2), 10-14 (1964); C.A. 61, 317 (1964).

284. Samsonov, G. V., SOME PROBLEMS OF SURFACE ACTIVITY OF METAL AND NONMETAL ALLOYS IN REGARD TO THEIR ELECTRONIC STRUCTURE. Poverkhn. Yavleniya v. Rasplavakh i Protsessakh Poroshkovoi Met., Akad. Nauk Ukr. SSR, Inst. Metallokeram. i Spets. Splavov 1963, 90-6; C.A. 61, 6727 (1964).

285. Surber, L. E., EFFECTS OF EXIT FLOW NONUNIFORMITY ON SCRAM AIR INDUCTION SYSTEM PERFORMANCE DETERMINATION. Air Force Flight Dynamics Laboratory, Wright-Patterson A.F.B. Technical Report No. AFFDL-TR-65-231, March 1966, 94 pp. (AD 372481L) (REPORT CLASSIFIED CONFIDENTIAL).

286. Tager, S. A. and Smirnov, A. S., CONSTRUCTING I-THETA DIAGRAMS OF COMBUSTION PRODUCTS TAKING INTO ACCOUNT THE DISSOCIATION OF CO_2 AND H_2O. Teploenergetika (USSR) 1965, No. 5, p. 94; U.S. Air Force Translation No. FTD-TT-65-1457, March 1966, 5 pp. (AD 631 577).

287. Tamagno, J., Fructman, I., and Slutsky, S., SUPERSONIC COMBUSTION IN PREMIXED HYDROCARBON-AIR FLOW, GASL TR No. 602, Contract AF 49(638)-1503 AFOSR, 55 pp.; May 1966, AFOSR 66-0872.

288. Tamagno, J., Fruchtman, I., Slutsky, S., SUPERSONIC COMBUSTION IN PREMIXED HYDROCARBON-AIR FLOW. General Applied Science Laboratories Final Report No. tr-602, U.S. Air Force Contract AF 49(638)-1503, May 1966, 64 pp. (AD 633977).

289. Tamagno, J. and Trentacoste, N. (General Applied Science Laboratories, Inc.), IGNITION AND AXI-SYMMETRIC TURBULENT FLAME PROPAGATION IN HYDROGEN-AIR MIXTURES AT SUPERSONIC SPEEDS. 104 pp. (1964) (AD 604429); C.A. 62, 2661 (1965); U.S. Govt. Res. Rept. 39 (20), 41 (1964).

290. Tanatarov, M. A. and Levinter, M. E., MECHANISM OF COKE FORMATION. Khim. i Tekhnol. Topliv i Masel 10 (1), 29-32 (1965); C.A. 62, 11196 (1965).

291. Tarasenkova, E. M., Abarenkova, E. A., Manzon, F. A., Vagner, V. V., CATALYTIC CONVERSION OF HEPTANE ON MANGANESE OXIDES. Tr. Leningr. Inzh.-Ekon. Inst. No. 46, 96-102 (1964); C.A. 61, 8171 (1964).

292. Taylor, W. F. and Wallace, T. J., THE STUDY OF HYDROCARBON FUEL VAPOR PHASE DEPOSITS. Esso Research and Engineering Co. Quarterly Progress Report No. 1, 16 May-16 August 1966, U.S. Air Force Contract AF 33(615)-3575, August 1966, 27 pp. (AD 489416).

293. Tetenyi, P. (Inst. Isotopes, Budapest), KINETICS OF THE CATALYTIC DEHYDROGENATION OF HYDROAROMATIC COMPOUNDS. VII. ROLE OF THE DEHYDROGENATION OF CYCLOHEXANE IN THE KINETICS OF THE REACTION. Acta Chim. Acad. Sci. Hung. 40 (2), 157-66 (1964); C.A. 61, 9375 (1964).

294. Tetenyi, P., Babernics, L., Guczi, L., Schachter, K., EFFECT OF THE METHOD OF PREPARATION ON THE ADSORPTIVE AND CATALYTIC PROPERTIES OF Ni. I. Acta Chem. Acad. Sci. Hung. 40 (4), 387-9 (1964); C.A. 62, 3446 (1965).

295. Tetenyi, P., Schachter, K., Babernics, L., EFFECT OF THE METHOD OF PREPARATION ON THE ABSORPTIVE AND CATALYTIC PROPERTIES OF NICKEL. III. KINETICS OF THE DEHYDROGENATIONS OF CYCLOHEXANE. Acta Chim. Acad. Sci. Hung. 42 (3), 227-41 (1964) (Eng.); C.A. 62, 11655 (1965).

296. Tetenyi, P., Schachter, K., Holly, S. (Inst. Isotopes, Budupest), KINETICS OF THE CATALYTIC DEHYDROGENATION OF HYDROAROMATIC COMPOUNDS. VI. INVESTIGATION OF THE ADSORPTION OF METHYLCYCLOHEXANE ON NICKEL CATALYSTS BY A KINETIC METHOD. Acta Chim. Acad. Sci. Hung. 40 (2), 145-55 (1964); C.A. 61, 9375 (1964).

297. Thring, M. W., LUMINOUS RADIATION FROM FLAMES. Chemical and Process Engineering 46 No. 10 pp. 544-51, October 1965.

298. Thring, M. W., Foster, P. J., McGrath, I. A., Ashton, J. S., PREDICTION OF THE EMISSIVITY OF HYDROCARBON FLAMES. Proc. Heat Transfer Conf. 1961-62, Univ. Colorado 1961, (and) London 1962, 796-803 (Pub. 1963); C.A. 61, 11640 (1964).

299. Tong, L. S., BOILING HEAT TRANSFER AND TWO-PHASE FLOW, John Wiley and Sons, Inc. New York.

300. Townend, L. H. and Reid, J. (Royal Aircraft Establishment), SOME EFFECTS OF STABLE COMBUSTION IN WAKES FORMED IN A SUPERSONIC STREAM. Supersonic Flow, Chem Process. Radiative Transfer 137-55 (1964); C.A. 62, 6161.

301. Traver, R. H. and Porter, H. O., COMPARISON OF ADVANCED RAMJET ENGINES. U.S. Naval Ordnance Plant Technical Publication Report No. NOTS-TP-3766, NAVWEPS 8719, January 1965, 40 pp. (AD 375709L) (REPORT CLASSIFIED CONFIDENTIAL).

302. Treccani, V., MICROBIAL DEGRADATION OF HYDROCARBONS. Progr. Ind. Microbiol. (D.J.D. Hockenhull, editor. Fordon and Breach, Sci. Publ., Inc. New York) 4, 1-33 (1964); C.A. 62, 5843 (1965).

303. Tung, S. E. and Mcinich, E. (Continental Oil Co.), HIGH-PURITY ALUMINA. I. THE NATURE OF ITS SURFACE ACID SITES AND ITS ACTIVITY IN SOME HYDROCARBON CONVERSION REACTIONS. J. Catalysis 3 (3), 229-38 (1964); C.A. 61, 3730 (1964).

304. Ulery, H. E. and Richards, J. H. (California Institute of Technology), THE ACID-CATALYZED CYCLIZATION OF ACYCLIC DIENES. J. Am. Chem. Soc. 86 (15), 3113-17 (1964); C.A. 61, 6879 (1964).

305. U.S. Air Force, THERMOPHYSICAL PROPERTIES OF CERTAIN AVIATION FUELS IN THE LIQUID AND GASEOUS STATE, FTD-TT-61-81/1+2, 3 April 1962, 201 pp. (English) (AD 274116).

306. Uselton, B. L., DYNAMIC STABILITY TESTS ON THE SNAP-27 FUEL CASK CONFIGURATION AT MACH NUMBERS 6 and 10. Arnold Engineering Development Center, Arnold Air Force Station Technical Report No. AEDC-TR-66-154 prepared in cooperation with ARO, Inc., U.S. Air Force Contract AF 40(600)-1200, August 1966, 11 pp. (AD 487030).

307. Usov, Yu. N., Kuvshinova, N. I., Shestova, L. S., KINETICS OF DEHYDROCYCLIZATION OF n-HEPTANE AND n-OCTANE ON AN Al_2O_3-Pt CATALYST. Neftekhimiya 4 (5), 700-6 (1964); C.A. 62, 3899 (1965).

308. Van Tiggelen, A., THEORETICAL AND EXPERIMENTAL STUDY OF REACTION KINETICS IN FLAMES. Louvain University, Belgium, Final Technical Report, AFOSR 65-2240, U.S. Air Force European Office of Air Research Contract AF-EOAR-42-63, October 1965, 16 pp. (AD 628144).

309. Venkatachalam, K. A., Panchenkov, G. M., Zhorov, Yu. M., THE STABILITY OF AN ALUMINUM-CHROMIUM-POTASSIUM CATALYST IN THE DEHYDROCYCLIZATION OF PARAFFIN HYDROCARBONS. Tr., Mosk. Inst. Neftekhim. i Gaz. Prom. No. 51, 136-41 (1964); C.A. 62, 14399 (1965).

310. Voevodskii, V. V., INHIBITION OF PARAFFIN CRACKING IN THE GAS PHASE. Kinetika i Kataliz 5 (4), 603-8 (1964); C.A. 62, 2647 (1965).

311. Vorogushin, V. T., SELECTION OF THE OPTIMUM PARAMETERS OF A SUPERSONIC RAMJET ENGINE WITH A HEAT EXCHANGER. Izv. VUZ Aviats. Tekh. (4), 75-81, 1961, U.S.S.R.

312. Vorogushin, V. T., SELECTION OF THE OPTIMUM PARAMETERS OF A SUPERSONIC RAMJET ENGINE WITH A HEAT EXCHANGER. Izv. Vyssh. Uchenb. Zaved. Ser. Aviats. Tekh. 1961, No. 4, 75-81 (Great Britain Ministry of Aviation Translation MOA-TIL-T5396) (AD 441158).

313. Vybihal, J., PRODUCTION OF BENZENE BY CATALYTIC AROMATIZATION OF GASOLINE. Sb. Praci Vyzhomu Chem. Vyuziti Uhli, Dehtu Ropy No. 3, 34-51 (1964); C.A. 62, 7556 (1965).

314. Walker, J. H., RAMJET TECHNOLOGY. CHAPTER 10. PRELIMINARY DESIGN FOR SUPERSONIC FLIGHT. Johns Hopkins University, Applied Physics Laboratory Technical Memo, Report No. TG-610-10, U.S. Navy Contract NOw-62-0604-c, February 1966, 100 pp. (AD 630 827).

315. Wallace, T. J. (Esso Research and Engineering Co.), CHEMISTRY OF FUEL INSTABILITY. Advan. Petrol. Chem. Refining 9, 353-407 (1964), C.A. 62, 3877 (1965).

316. Wallace, T. J. and Friedman, R., FUNDAMENTAL INVESTIGATION OF THE CATALYTIC DEGRADATION OF HYDROCARBON FUELS. Process Research Division, Esso Research and Engineering Co. Quarterly Progress Report No. PaRD.3M. 65, U.S. Army Contract DA-18-035-AMC-330A, May 19[illegible], 31 pp (AD 464454).

317. Wallace, T. J. and Friedman, R., FUNDAMENTAL INVESTIGATION OF THE DEGRADATION OF HYDROCARBON FUELS. Esso Research and Engineering Co. Quarterly Progress Report No. 2, Report No. PaRD.3M.65, U.S. Army Contract DA-18-035AMC-330A, August 1965, 41 pp. (AD 468552).

318. Wallace, T. J., Vogelfanger, E., Friedman, R., FUNDAMENTAL INVESTIGATION OF THE DEGRADATION OF HYDROCARBON FUELS. Esso Research and Engineering Co. Quarterly Progress Report No. 3, 16 August-16 November 1965, Report No. PaRD.7M.65, U.S. Army Contract DA-18 035-AMC-330(A), November 1965, 87 pp. (AD 474 453).

319. Wallace, T. J., Friedman, R., Vogelfanger, E., Weiss, M. A., FUNDAMENTAL INVESTIGATION OF THE DEGRADATION OF HYDROCARBON FUELS. Process Research Division, Esso Research and Engineering Co. Progress Report No. 4 (Final) February 1965-June 1966, Report No. PaRD-3M-666R, U.S. Army Contract DA-18-035-AMC-330(A), July 1966, 315 pp. (AD 373805) (REPORT CLASSIFIED CONFIDENTIAL).

320. Watton, A., RECENT STUDIES OF AIR-BREATHING LAUNCH VEHICLES AND THEIR PROPULSION IMPLICATIONS. Systems Engineering Group, Research and Technology Division, Wright-Patterson A.F.B. Technical Report No. SEG-TR-65-65, February 1966, 48 pp. (AD 372217) (REPORT CLASSIFIED SECRET).

321. Weiss, M. A. and Morgenthaler, J. H., RAMJET TECHNOLOGY. CHAPTER 3. AIR-FUEL MIXTURE PREPARATION. Johns Hopkins University Technical Memo, Report No. TG-610-3, U.S. Navy Contract NOw-62-0604-c, January 1966, 91 pp. (AD 630828).

322. W[illegible]er, E., AN INVESTIGATION OF CARBON DEPOSITION. Washington University Dept. of Chemical Engineering Progress Report No. 3, 1 November 65 - 31 January 66, U.S. Air Force Contract AF 04(694)-695, February 1966, 3 pp. (AD 627813).

323. Whisman, M. L. and W[illegible]rd, C. [illegible], STORAGE STABILITY OF HIGH TEMPERATURE FUELS. U.S. Bureau of Mines Report for February 1965-February 1966, AFAPL TR-65-13-P[illegible], II. Air Force Contract AF 33(615)-64-1009, February 1966, 18[illegible] pp [illegible] 6307-3).

324. White D. R. (General Electric Research Lab.), DENSITY INDUCTION TIMES BEHIND SHOCK WAVES IN VERY LEAN MIXTURES OF D_2, H_2, C_2H_2, AND C_2H_4 WITH O_2, ARL 65-274, December 1965; 26 pp. Contract AF 33(657)-7945; also presented at 11th Intl. Symposium on Combustion, August 1966.

325. White, D. R., A STUDY OF SHOCK WAVE INDUCED REACTIONS. U. S. Air Force, Office of Aerospace Research, ARL 66-0177, September 1966, 37 pp.

326. Williams, F. A., COMBUSTION THEORY; THE FUNDAMENTAL THEORY OF CHEMICALLY REACTING FLOW SYSTEMS. (Addison-Wesley Series in Engineering Science). Reading, Massachusetts, Addison-Wesley, 1965, 477 pp.; C.A. 62, 8699 (1965).

327. Wilson, D. M. and Fisher, P. D., EFFECT OF A HIGHLY COOLED WALL ON HYPERSONIC TURBULENT HEAT TRANSFER. U.S. Naval Ordnance Laboratory Report No. NOL TR-65-153, Aerodynamics Research - 250, June 1966, 49 pp. (AD 638232)

328. Wilson, G. R., Smith, J. O., Martin, H. F., Klein, D., Harrington, E. C., EFFECTS OF SELECTED STRAINS OF MICROORGANISMS ON THE COMPOSITION OF FUELS AND LUBRICANTS. Monsanto Research Corp. Final Report, 1 September 1962-27 November 1964, Report No. MRB-2023F, RTD TDR-63-4117-Pt. 2, U.S. Air Force Contract AF 33(657)-9814, January 1966, 154 pp. (AD 628673).

329. Wilson, W. E., Jr. and Berl, W. G., RAMJET TECHNOLOGY. CHAPTER 6. FUELS. Johns Hopkins University, Applied Physics Laboratory Technical Memo, Report No. TG-610-6, U.S. Navy Contract NOw-62-0604-c, July 1965, 54 pp. (AD 631673).

330. Witte, R. and Pechtold, N., THE BEHAVIOR OF HYDROCARBONS IN HIGH-TEMPERATURE PYROLYSIS. Erdoel Kohle 15, 977-82 (1962); C.A. 61, 10512 (1964); C.Z. 1964 (12), Abstr. No. 2182.

331. Worley, W. E., RAMJET TECHNOLOGY. CHAPTER 7. FUEL SYSTEMS. Johns Hopkins University in Cooperation with Bendix Mishawaka Division, Bendix Corporation Technical Memo, Report No. TG-610-7, U.S. Navy Contract NOw-62-0604-c, March 1966, 156 pp. (AD 630330).

332. Yantovskii, S. A., TWO-STAGE COMBUSTION OF EXPLOSIVE MIXTURES. II. RATES OF THE FIRST AND SECOND STAGES OF IGNITION OF n-HEPTANE-AIR MIXTURES AT PRESSURES ABOVE ONE ATMOSPHERE. Kinetika i Kataliz 5 (3), 399-406 (1964) C.A. 61, 8121.

333. Zhabrova, G. M., Kazanskii, V. B., Vlasimirova, V. I., Kadenatsi, B. M., Pariiskii, G. B., RADIATION-CATALYTIC CONVERSIONS OF CYCLOHEXANE. Neftekhimiya 4 (5), 755-62 (1964); C.A. 62, 3564 (1965).

334. Zhorov, A. K., Kholdyarov, M. I., Petina, V. V., Butyagin, S. M., DEHYDROCYCLIZATION OF A LOW-OCTANE FRACTION OF KOROBKOV PETROLEUM ON AN ALUMINA-CHROMIA CATALYST LOW IN CHROMIUM OXIDE. Izv. Vysshikh Uchebn. Zavedenii Neft i Gaz. [illegible], 51-4 (1964), C.A. 62, 3804 (1965).

335. Zhorov, Yu. M., Tsenchenkov, S. M., Kuznetsov, O. L., Bazilevich, V. V., THE STRUCTURE OF OLEFINS FORMED BY CATALYTIC TRANSFORMATION OF n-HEXADECANE. Tr., Mosk. Inst. Neftekhim. i Gaz. Prom. No. 51, 146-53 (1964); C.A. 62, 14474 (1965).

336. Zimmerman, C. C. and York, R. (Cornell University), THERMAL DEMETHYLATION OF TOLUENE. Ind. Eng. Chem., Process Design Develop. 3 (3), 254-8 (1964); C.A. 61, 1730 (1964).

337. Zrelov, U. N. and Rybakov, K. V., THAT THE FUEL BE PURE. Vestnik Protivovozdushnoi Oborony (USSR) 1966, No. 1, 83-4; Institute of Modern Languages Translation, AERDLT-1843-66, TT 61378, U.S. Army Contract DA-44-009-AMC-363(T), May 1966, 7 pp. (AD 633413).

SUBJECT INDEX FOR BIBLIOGRAPHY

Supersonic Aircraft
13, 16, [illegible], 26, 27, 28, 29, 30, 31, 32, 33, 36, 38, 44, 51, 71, 85, 86, 87, 88, 89, 90, 91, 95, 105, 135, 154, 213, 234, 241, 243, 254, 306, 320

Vaporizing and Endothermic Fuels
129, 130, 139, 216, 217, 218, 219, 220

Thermal Reaction
43, 82, 98, 99, 100, 148, 175, 224, 235, 242, 281, 290, 308, 322, 330, 336

Catalysis and Catalytic Reactions
1, 2, 4, 5, 7, 12, 19, 20, 21, 24, 49, 50, 52, 77, 96, 113, 116, 126, 137, 140, 142, 146, 147, 150, 155, 157, 159, 160, 161, 162, 164, 169, 171, 172, 173, 174, 181, 182, 185, 186, 195, 196, 197, 201, 203, 204, 208, 209, 210, 211, 214, 225, 226, 227, 228, 233, 242, 244, 246, 247, 248, 249, 252, 253, 259, 265, 266, 267, 268, 269, 270, 271, 272, 273, 274, 275, 276, 277, 281, 282, 283, 284, 290, 291, 293, 294, 295, 296, 302, 303, 304, 307, 309, 310, 313, 333, 334, 335

High Temperature Stability
22, 23, 34, 39, 240, 250, 292, 315, 316, 317, 318, 319, 323

Fuel Contaminants
15, 39, 42, 45, 47, 69, 92, 95, 109, 114, 144, 145, 153, 158, 181, 194, 202, 221, 251, 280, 302, 337

Fuel Additives
34, 39, 95, 127, 156, 180, 199, 200

Combustion Characteristics
18, 46, 47, 48, 53, 60, 61, 66, 67, 68, 78, 79, 80, 83, 97, 104, 110, 112, 130, 131, 135, 149, 163, 167, 168, 170, 176, 177, 179, 187, 190, 205, 212, 231, 232, 238, 256, 257, 260, 261, 264, 278, 279, 286, 287, 288, 289, 297, 298, 300, 308, 322, 324, 325, 326, 328, 332

Physical and Chemical Properties
8, 9, 10, 11, 151, 207, 262, 263, 305

Heat Transfer and Flow Behavior
5, 14, 17, 18, 35, 38, 41, 57, 70, 73, 81, 94, 101, 117, 132, 133, 136, 141, 143, 173, 183, 184, 189, 198, 213, 215, 229, 230, 239, 245, 254, 285, 299, 311, 312, 327

Advanced Engines
3, 16, 40, 54, 55, 56, 58, 59, 62, 63, 64, 65, 66, 67, 68, 72, 74, 75, 76, 84, 93, 102, 103, 106, 107, 108, 111, 115, 118, 119, 120, 121, 122, 123, 124, 125, 128, 132, 133, 134, 149, 152, 167, 168, 187, 190, 191, 192, 193, 206, 222, 223, 236, 237, 255, 285, 301, 311, 312, 314, 321, 329, 331